ELASTODYNAMICS OF FAILURE IN A CONTINUUM

Thesis by

Jean-Bernard Minster

In Partial Fulfillment of the Requirements

for the Degree of

Doctor of Philosophy

California Institute of Technology

Pasadena, California

1974

(Submitted December 4, 1973)

... à mes parents,

pour leur confiance inébranlable.

ACKNOWLEDGMENTS

Professor Charles Archambeau has exerted a profound influence on my education at the California Institute of Technology. This thesis owes a lot to his continuing enthusiasm and his unwaivering confidence in the outcome. For his inspiration, criticism and friendship I express here my deep and lasting gratitude.

I am indebted to many colleagues for numerous discussions about this work. I wish to thank particularly Dr. Thomas Hanks, who read critically the entire text, and Dr. Thomas Jordan who also read portions of it. Their comments and suggestions were both helpful and instructive.

I am grateful to the professors, staff and students of the Seismological Laboratory for providing me with the exciting and friendly environment which made my work so enjoyable.

To my friend Carol Jean Ruiz, I owe a special word of gratitude, for she did an outstanding job of typing a very difficult manuscript.

Mr. Laszlo Lenches prepared the figures, and I thank him for their quality and clarity. Some of the numerical calculations were performed with the help of geophysicists from Systems, Science and Software, Inc.

This research was supported by the Advanced Research Projects Agency of the Department of Defense and was monitored by the Air Force Office of Scientific Research under Contracts nos. F44620-72-C-0078 and F44620-72-C-0083.

ABSTRACT

A general treatment of the elastodynamics of failure in a prestressed elastic continuum is given, with particular emphasis on the geophysical aspects of the problem. The principal purpose of the study is to provide a physical model of the earthquake phenomenon, which yields an explicit description of the radiation field in terms of source parameters.

The Green's tensor solution to the equations of motion in a medium with moving boundaries is developed. Using this representation theorem, and its specialization to the scalar case by means of potentials, it is shown that material failure in a continuum can be treated equivalently as a boundary value problem or as an initial value problem. The initial value representation is shown to be preferable for geophysical purposes, and the general solution for a growing and propagating rupture zone is given.

The energy balance of the phenomenon is discussed with particular emphasis on the physical source of the radiated energy. It is also argued that the flow of energy is the controlling factor for the propagation and growth of a failure zone. Failure should then be viewed as a generalized phase change of the medium.

The theory is applied to the simple case of a growing and propagating spherical failure zone. The model is investigated in detail both analytically and numerically. The analysis is performed in the frequency domain and the radiation fields are given in the form of multipolar expansions. The necessary theorems for the manipulation of

such expansions for seismological purposes are proved, and their use discussed on the basis of simple examples.

The more realistic ellipsoidal failure zone is investigated. The static problem of an arbitrary ellipsoidal inclusion under homogeneous stress of arbitrary orientation is solved. It is then shown how the analytical solution can be combined with numerical techniques to yield more realistic models.

The conclusion is that this general approach yields a very flexible model which can be adapted to a wide variety of physical circumstances. In spite of the simplicity of the model, the predicted radiation field is rather complex; it is discussed as a function of source parameters, and scaling laws are derived which ease the interpretation of observed spectra. Preliminary results in the time domain are also shown. It is concluded that the model can be compared favorably both with the observations, and with results obtained from purely numerical models.

TABLE OF CONTENTS

Page

GENERAL INTRODUCTION

The branch of Seismology covered by the general denomination of "earthquake modeling" has received considerable impetus during the last decade. The reasons are several. One of the principal reasons is that the earthquake phenomenon, although not yet thoroughly understood, has lost a lot of the aura of mystery which surrounded it in the past. In particular, the theory of plate tectonics provides a broad frame in which earthquakes find a natural place. Except for some intraplate events, and for those events which are associated with volcanism, most shallow earthquakes can be explained in a gross sense as a manifestation of the relative motions of the plates. Similarly deep focus earthquakes may, in general, be associated with downgoing slabs at trenches.

Another impetus was given to this line of research by the advent of underground nuclear explosions, and the possibility that such tests might trigger a seismic event. Also, the necessity of being able to discriminate between underground explosions and spontaneous seismic events made it necessary to try and characterize earthquakes more completely than by their magnitude only. Finally, the more accurately earthquakes are modeled, the better we understand their mechanism, and thus the greater our chances are to eventually predict their occurrence.

Because earthquakes occur spontaneously, they should give us some information about the physical conditions under which they occur. This includes, for example, information about the thermodynamic state of earth materials, and about the state of stress of the Earth in earthquake zones. How much of this information can be retrieved from

observations of the radiation field depends on how well parameters such as rupture size, rupture velocity, etc., can be estimated. It also depends on how well the rupture phenomenon is understood. For that reason, it is desirable to construct a model of an earthquake which depends explicitly on the parameters of interest, and which is flexible enough to be adaptable to a wide range of situations. Two main classes of models can be found in the seismological literature: kinematic models and dynamic models.

The most popular of the kinematic models is the dislocation model (e.g., Haskell, 1964; Savage, 1966): a displacement dislocation is created along the rupture surface, with a time history which is arbitrarily chosen and is hopefully at least approximately correct. Although very convenient to use, these models lack what may be the most fundamental property of an earthquake: its spontaneity. In addition, they lead to a representation in which the energy radiated emanates from a surface (the rupture boundary). The same is true of the widely used two dimensional model of Brune (1970), wherein a stress dislocation is created along the fault surface.

In contrast, elastodynamic relaxation models (e.g., Archambeau, 1964) take full advantage of the spontaneity of the phenomenon. The only assumption is then that the material is in an initial state of stress, and that rupture takes place in a given region. Such models lead to a representation where the radiated energy comes explicitly from where it was stored in the first place, that is, from the stressed material surrounding the rupture zone. Because elastodynamic models lead to a more complicated mathematical formulation, their development

has not been as rapid as for simpler models, and their use is not as widely spread.

In the present study we shall investigate some fundamental properties of the various models, with particular emphasis on elasto-dynamic relaxation models.

The principal contribution of this work to the field of earthquake seismology is that a general, self-consistent formulation of the seismic source problem is constructed which encompasses all of the general model classes (Chapter I). We can then compare the various models, and show in what sense they are fundamentally equivalent, in spite of their different mathematical treatments (Chapter II). We can further assess the trade-off between the degree of convenience offered by these models, and the capability that they possess to approximate various realistic physical situations, and also give a precise evaluation of the approximations involved.

The question of the energy released by an earthquake is discussed in detail, and, more specifically, we discuss the problem of where this energy finds its source (Chapter III). The energetics of the failure phenomenon are introduced as particularly important to a more profound understanding of the physical processes involved. We propose that material failure can be regarded as a generalized phase transformation of the medium, so that rupture propagation is essentially controlled by the conservation equations of continuum mechanics, suitably generalized to allow for the presence of discontinuities. We also suggest that the problem of incipient failure in a continuum could be treated in a similar frame.

A complete treatment of the elastodynamic source model is then given for a particular geometry--that of a spherical rupture (Chapter IV). This includes an extensive investigation of the properties of the radiation field predicted by this model. The analysis is performed in the spectral domain, and the dependence of the radiation spectra on the source parameters is obtained on the basis of both analytical and numerical results (Chapters IV and VII). It is argued that, in spite of the particular geometry that we adopted, this model provides us with a "standard" against which observations can be compared and thus interpreted, and also against which other models can be tested. These include, for example, simpler models of the dislocation type, as well as more realistic models derived by a combination of analytical and numerical techniques. To obtain such a "standard" model constitutes, of course, the principal motivation for a thorough investigation. The attractiveness of analytical solutions, especially for the study of the most general properties of the model, leads us to justify sacrificing geometrical realism for a greater mathematical tractability. The spherical model also serves to illustrate the use of general multipolar representations of the radiation field. A special effort is made to develop the necessary mathematical tools for the manipulation of multipolar fields in seismological applications, and we also indicate how time domain information (e.g., synthetic seismograms) can be retrieved from them (Chapter V).

The model is generalized to include a more realistic geometry--that of an ellipsoidal rupture zone (Chapter VI). Particularly interesting in this respect is the illustration of how the analytical

approach may be combined with numerical techniques, both by necessity and for reasons of convenience. This combination opens the possibility of constructing very sophisticated models, which might take into account some of the complications encountered in physical situations (e.g., geological structure, complicated rupture geometries, etc.).

The final contribution of this study consists of a number of useful results which were proved in the context of this particular problem, but possess greater generality. Such results include the Green's tensor solution to the equations of motion of an elastic continuum with moving boundaries, and transformation theorems for multipolar expansions under rotation and translation of the coordinate system. Further, the complete static solution to the problem of an arbitrary ellipsoidal inclusion embedded in a matrix subjected to a uniform stress of arbitrary orientation is given in Chapter VI. The results should find applications in fields other than geophysics as well. In this context a large number of identities between ellipsoidal harmonics and elliptic functions were proved and are given in Appendices.

Of course, such a work cannot be expected to be the final word on the problem. Indeed, as usual, it seems that more questions are raised for each question which is answered, more doors opened for each door closed. In view of the results that we obtained in this study, let us briefly focus on some of the issues raised which would constitute a natural extension of our research.

The most challenging, because the least understood, of these problems is to try and develop a fairly general theory of material failure valid for phenomena on a scale comparable to that of an

earthquake. We suggest that an approach using the thermodynamic theory of materials with memory of Coleman (1964) might be quite fruitful, when combined with the ideas presented in Chapter III. At the same time, one should keep in mind that such a continuum theory should be tied with the observations of rock mechanics, in particular, concerning rock dilatancy in the context of earthquake prediction (e.g., Whitcomb et al., 1973)

Another promising aspect of elastodynamic source theory is concerned with the further construction of realistic models obtained by coupling numerical near-source calculations with the analytical treatment. This can be done by the methods proposed in the present study. Comparison of the theoretically predicted radiation field with the observations, both in the spectral domain and in the time domain, should yield invaluable information on the physical processes involved in an earthquake. The recovery of this information need not be done by trial and error, since a number of inversion techniques have been developed in geophysics (e.g., Jordan, 1972). However, the "seismic source inverse problem" has yet to be formulated in the general case.

Only by combining a better understanding of the failure phenomenon with a realistic modeling method can we hope to sort out the complex information hidden in the observed radiation field. Of critical importance in the long range is the determination of the absolute state of stress of the Earth. Possible applications to the seismic prediction problem, to the driving mechanism of plate tectonics, etc., come to mind immediately and need not be discussed here. The literature quoted here, altough by no means comprehensive, should be helpful in that respect.

Chapter I

GREEN'S TENSOR SOLUTIONS IN ELASTODYNAMICS

Introduction

The equations controlling the flow of a continuum--in particular the conservation equations--are nonlinear. In fact most materials, especially those commonly encountered in Earth Sciences, do not behave linearly. For example, many of the phenomena associated with the theory of Plate Tectonics are anelastic, and diastrophic phenomena can hardly be described by a linear mechanism. On the other hand, the fact remains that when undergoing small strains, the rocks constituting the crust and mantle of the Earth behave elastically to a good approximation. This prompted Sir Harold Jeffreys to challenge the suggestion that mantle rocks behave viscously:

> "I am not suggesting that rocks behave as perfectly elastic even under small stresses; it appears that under any stress some elastic afterworking and hysteresis occur. What I say is that 1) at numerous points the facts are contrary to what we should expect if viscous flow was of dominating importance; 2) they are at no point contrary to what we should expect if the rocks at great depths have a non-zero strength and flow is negligible unless the stress-differences exceed the strength; and 3) the latter hypothesis leads directly to explanations of many of the outstanding facts." (The Earth, 5th edition, 1970, p.431).

Thus, whereas the very phenomenon of rock fracture is not elastic, its effects on the surrounding material and, in particular, the radiation of seismic waves can be adequately described within the framework of linearized elasticity.

Furthermore, because of the difficulties usually met in solving

nonlinear problems, and because the mathematical theory of linear equations is well developed, one tries in general to linearize a complex problem in order to obtain at least approximate solutions. Certainly the advent of high speed digital computers, in association with the development of sophisticated numerical techniques gives us now the capability of finding solutions to very nonlinear problems; but these methods provide the investigator with the numerical answer to a specific question. The dependence of this answer on the various parameters of the problem must then be found through a tedious, and often costly, parameter study. Linear problems are more likely to lend themselves to analytical investigations. One of their major advantages is that the principle of superposition of solutions can often be applied in one form or another.

The concept of Green's tensor solutions (or Green's function solutions in the scalar case) is a mere generalization of the principle of superposition for linear problems. Morse and Feshbach (1953) use the terminology of influence function, in analogy with electrostatic theory. The analog in filter theory is the impulse response of a filter. The basic idea is as follows: If a fixed observer knows the effect of an impulsive point source as a function of the position of this source, he can evaluate the effect of a distributed source by decomposing it into a juxtaposition (in space and time) of weighted impulsive point sources, and then superposing their effects. The superposition will be done by a summation in the discrete case, and an integration in the continuous case.

Green's tensor solutions have been widely used in elastostatics and

elastodynamics (e.g., Love, 1927). Their introduction in seismology has been mainly associated with the application of dislocation theory to the modelling of earthquakes (e.g., Stekete, 1958; Maruyama, 1963; Haskell, 1964). We shall show in this chapter how this formalism permits us to isolate the effects of driving forces, of boundary conditions, and of initial values. The case of moving boundaries with known evolution is a generalization of the classical treatment. This extension will be found particularly useful in the subsequent chapters for the description of a growing rupture zone. For this purpose it was necessary to generalize Reynolds' transport theorem in a continuum to the case of moving boundaries. This is done in Appendix 1, and the results are given in the first section of this chapter.

From the generalized transport theorem we first obtain the usual conservation equations of continuum mechanics. Conservation conditions at flow discontinuities are also obtained in this manner for moving discontinuities. These conditions reduce to the Rankine-Hugoniot equations when the discontinuity is a shock front in a fluid. The conservation equations are generally nonlinear and can be satisfied by very general flows in the continuum. Their linearization in the case of a linearly elastic material is a well known procedure and will not be dwelt upon.

The remainder of the chapter is devoted to the development of Green's tensor solutions in elastodynamics. It is shown how the generalized Green's theorem for the theory of elasticity--proved in section I-2--leads to a formal Green's tensor solution, and how initial and boundary conditions are then explicitly used in this solution

(section I-3). Finally, the scalar case (wave equation) is briefly discussed.

Cartesian tensor notation is used throughout; so is Einstein's summation convention. Conservation equations will be given both in vector and in component form.

The proof of Green's theorem, in section I-2, is carried out in what may seem superfluous detail: The rationale behind this is that we hope to be able to generalize these results in future work, to include more complex geometries such as Riemanian geometry. However, this does not appear to be very easy, and lies beyond the scope of the present work. We hope that the details presented here may provide some insight into the difficulties ahead.

I-1 Transport theorem and conservation equations

Reynolds' transport theorem, proved in Appendix 1, furnishes an expression for the material time derivative of the volume integral of a flow function. Given a continuous flow in a continuum, of velocity $\mathbf{V}$, and a continuous function of the flow $F(\mathbf{x},t)$-- F can be any tensorial function--then we have

$$\frac{d}{dt}\int_{V(t)} F\, dv = \int_{V(t)} \left[\frac{dF}{dt} + F\, \nabla \cdot \mathbf{V}\right] dv$$

$$= \int_{V(t)} \left[\frac{\partial F}{\partial t} + \nabla \cdot (F\mathbf{V})\right] dv \quad . \qquad \text{(I-1-1)}$$

Here $V(t)$ is an arbitrary volume of the continuum moving with the flow. $V(t)$ is bounded by a closed surface $S(t)$, which is a material surface (see Appendix 1), and we may apply Gauss' theorem and write

$$\frac{d}{dt}\int_{V(t)} F\, dv = \int_{V(t)} \frac{\partial F}{\partial t}\, dv + \int_{S(t)} F\ \mathbf{V} \cdot \hat{n}\, da \quad . \qquad \text{(I-1-2)}$$

Here $\hat{n}$ is the outward unit normal vector to $S(t)$.

The theorem (I-1-2) is generalized in Appendix 1 to the case where the flow and the function F have a discontinuity across an internal boundary of the medium moving with the velocity $\mathbf{U}$. If $\Sigma(t)$ denotes the portion of this internal boundary lying within $V(t)$, the generalized transport theorem reads

$$\frac{d}{dt}\int_{V(t)} F\, dv = \int_{V(t)} \left[\frac{\partial F}{\partial t} + \nabla \cdot (F\mathbf{V})\right] dv + \int_{\Sigma(t)} \left[\!\left[F(\mathbf{V}-\mathbf{U}) \cdot \hat{n}_\Sigma\right]\!\right]_\Sigma da \quad . \tag{I-1-3}$$

The notation $[\![F]\!]_\Sigma$ is used to represent the jump of the function F across $\Sigma(t)$. The boundary $\Sigma(t)$ may represent a shock front or a phase boundary, and a positive unit normal $\hat{n}_\Sigma$ may be defined arbitrarily. We shall assume without loss of generality that $\mathbf{U} \cdot \hat{n}_\Sigma$ is positive. The jump $[\![F]\!]_\Sigma$ is then the difference between the limiting values of F when Σ is approached from its positive and negative sides successively.

Note that the presence of the third term in (I-1-3) is required in order to satisfy boundary conditions on Σ . This term disappears if Σ is not a discontinuity, for the jump appearing in the integrand vanishes in that case. This term also disappears if on both sides of $\Sigma(t)$ the vector $\mathbf{V}-\mathbf{U}$ is tangential to Σ : in this circumstance there is no transport of F across the discontinuity.

The transport theorem can then be used to derive the conservation equations. It is shown in Appendix 1 that if a quantity F is conserved, then at all points of the continuum where the flow is regular we have

$$\frac{dF}{dt} + F\, \nabla_x \cdot \mathbf{V} = k(\mathbf{x},t) \quad , \tag{I-1-4}$$

or, equivalently

$$\frac{\partial F}{\partial t} + \nabla \cdot (F\mathbf{V}) = k(\mathbf{x},t) \quad . \tag{I-1-5}$$

Here $k(\mathbf{x},t)$ is the (local) rate of production (or destruction) of F. It is thus a volumic source density of F and represents the effects of sources or sinks of F present in the medium.

In addition, along surfaces of discontinuity, the conservation theorem takes the form of the jump condition

$$\left[\!\left[F(\mathbf{V}-\mathbf{U}) \cdot \hat{n}_\Sigma \right]\!\right]_\Sigma = k_\Sigma(\mathbf{x}_\Sigma,t) \quad . \tag{I-1-6}$$

Here $k_\Sigma(\mathbf{x}_\Sigma,t)$ is a surficial density of source of F on the discontinuity. Note that if the volumic source density is of the form $k = \nabla \cdot \kappa$ then at a discontinuity Σ the surficial density k_Σ must include a term of the form $\left[\!\left[\kappa \cdot \hat{n}_\Sigma \right]\!\right]_\Sigma$ (see Appendix 1). The source terms on the right-hand sides of equations (I-1-4) to (I-1-5) are additive and thus when several mechanisms occur which generate F, their effects can be considered separately. We now turn to some special forms taken by these equations in particular cases. In all cases we shall formulate the conservation equations so that they may be directly compared to the general forms (I-1-4) to (I-1-6).

I-1-a) Conservation of mass

Since one always assumes in continuum mechanics that no mass is either created or destroyed, the conservation of mass may be expressed

by direct application of (I-1-4) . If ρ is the density of the material, we have, away from discontinuity

$$\frac{d\rho}{dt} + \rho \nabla \cdot \mathbf{V} = \frac{\partial \rho}{\partial t} + \nabla \cdot (\rho \mathbf{V}) = 0 \quad . \tag{I-1-7}$$

This is the continuity equation. At a discontinuity, (I-1-6) becomes

$$\left[\!\left[\rho(\mathbf{V}-\mathbf{U}) \cdot \hat{n}_\Sigma \right]\!\right]_\Sigma = 0 \quad , \tag{I-1-8}$$

which is the standard jump condition of shock wave theory.

Note that, by virtue of (I-1-7) , if the quantity F is of the form $F = \rho G$, where G is termed the "density of F ," then

$$\frac{dF}{dt} + F \nabla \cdot \mathbf{V} = \frac{d(\rho G)}{dt} + \rho G \nabla \cdot \mathbf{V} = \rho \frac{dG}{dt} \quad ,$$

and (I-1-4) becomes

$$\rho \frac{dG}{dt} = k(\mathbf{x},t) \quad . \tag{I-1-9}$$

This relation will prove useful in many cases.

I-1-b) Conservation of linear momentum

Here we assume that Cauchy's stress principle holds: The interaction of the material lying outside a volume V with the material within V may be represented by the tractions acting on the boundary

S of V , with outer normal $\hat{n}$. Thus if $\mathbf{T}$ is the stress tensor, the tractions acting on S are $\mathbf{t} = \mathbf{T} \cdot \hat{n}$, where the dot product on the right-hand side is taken to mean the contraction $T_{ij}n_j$. The conservation of linear momentum is expressed by equating the rate of change of ρ to the forces acting upon the material. Using the form of equation (I-1-4) we have

$$\rho \frac{d}{dt} \mathbf{V} = \frac{\partial(\rho \mathbf{V})}{\partial t} + \nabla \cdot (\rho \mathbf{V} \otimes \mathbf{V}) = \rho \mathbf{f} + \nabla \cdot \mathbf{T} \quad . \text{(I-1-10)}$$

Here $\mathbf{f}$ is the body force density, and the symbol $\otimes$ is used to denote the tensorial outer product, so that $\mathbf{V} \otimes \mathbf{V}$ is a symmetric dyadic. In component form, (I-1-10) reads

$$\rho \frac{dV_i}{dt} = \frac{\partial(\rho V_i)}{\partial t} + (\rho V_i V_j)_{,j} = \rho f_i + T_{ji,j} \quad . \qquad \text{(I-1-11)}$$

This is the equation of motion for a continuum.

At a discontinuity $\Sigma(t)$ carrying no externally applied surficial force density, (I-1-6) yields

$$\left[\!\left[\rho \, \mathbf{V}[(\mathbf{V}-\mathbf{U}) \cdot \hat{n}_\Sigma] \right]\!\right]_\Sigma = \left[\!\left[\mathbf{T} \cdot \hat{n}_\Sigma \right]\!\right]_\Sigma \quad , \qquad \text{(I-1-12)}$$

or, in component form

$$\left[\!\left[\rho V_i (V_j - U_j) \, n_j \right]\!\right]_\Sigma = \left[\!\left[T_{ij} n_j \right]\!\right]_\Sigma \quad . \qquad \text{(I-1-13)}$$

For the case of a fluid $T_{ij} = -p\delta_{ij}$, where δ_{ij} is the Kronecker delta, and (I-1-13) reduces to the usual jump condition encountered in shock wave theory in fluids.

I-1-c) Conservation of angular momentum

We are only concerned here with non-polar media, for which Newton's third law holds in its strong form. In other words, we assume that no body couples are present. If this were the case, the medium would have to be treated as a Cosserat continuum, (see, e.g., Malvern, 1969, for a more extensive discussion and a bibliography on the theory of multipolar media). Then we express the conservation of angular momentum by equating the rate of change of $\rho\, \mathbf{r}\times\mathbf{V}$ to the moment of all the forces present, with respect to the origin -- $\mathbf{r}$ is the position vector . We write, away from discontinuities

$$\rho \frac{d}{dt}(\mathbf{r}\times\mathbf{V}) = \frac{\partial}{\partial t}(\rho\, \mathbf{r}\times\mathbf{V}) + \nabla\cdot[\rho(\mathbf{r}\times\mathbf{V})\otimes\mathbf{V}] = \rho\mathbf{r}\times\mathbf{f} + \nabla\cdot(\mathbf{r}\times\mathbf{T}) \quad , \tag{I-1-14}$$

where, by a slight abuse of notation, we define by $\mathbf{r}\times\mathbf{T}$ the antisymmetrized tensor product $\varepsilon_{ijk}\, x_j\, T_{\ell k}$, since no confusion can arise. The symbol ε_{ijk} represents the usual permutation tensor defined by

$\varepsilon_{ijk} = 0$ if any two of (i,j,k) are equal

$\quad\quad 1$ if (i,j,k) is an even permutation of $(1,2,3)$

$\quad -1$ if (i,j,k) is an odd permutation of $(1,2,3)$.

In component form (I-1-14) becomes

$$\rho \frac{d}{dt} (\varepsilon_{ijk} x_j V_k) =$$

$$\frac{\partial}{\partial t} (\rho \varepsilon_{ijk} x_j V_k) + (\rho \varepsilon_{ijk} x_j V_k V_\ell)_{,\ell} = \rho \varepsilon_{ijk} x_j f_k + (\varepsilon_{ijk} x_j T_{\ell k})_{,\ell} \qquad \text{(I-1-15)}$$

Noting that $\frac{d\mathbf{r}}{dt} = \mathbf{V}$, and $\mathbf{V} \times \mathbf{V} \equiv 0$, we can write the left-hand side of (I-1-14) as $\rho\, \mathbf{r} \times \frac{d\mathbf{V}}{dt}$, and replace it by use of the equation of motion (I-1-10) . (I-1-14) becomes then

$$\mathbf{r} \times (\nabla \cdot \mathbf{T}) = \nabla \cdot (\mathbf{r} \times \mathbf{T}) \quad ,$$

or, in component form

$$\varepsilon_{ijk} x_j T_{\ell k,\ell} = (\varepsilon_{ijk} x_j T_{\ell k})_{,\ell} \quad .$$

But, because $x_{j,\ell} = \delta_{j\ell}$, this reduces to $\varepsilon_{ijk} T_{jk} = 0$ or

$$T_{[jk]} = 0 \quad . \qquad \text{(I-1-16)}$$

This is the usual result for non-polar media: the conservation of angular momentum, away from discontinuities, requires the skew-symmetric part of the stress tensor to vanish. The stress tensor is thus symmetric.

At a discontinuity $\Sigma(t)$, carrying no externally applied surface force density or surface couple density, we have, by direct comparison with (I-1-6)

$$\left[\!\left[\rho(\mathbf{r}\times\mathbf{V})[(\mathbf{V}-\mathbf{U})\cdot\hat{\mathbf{n}}_\Sigma] \right]\!\right]_\Sigma = \left[\!\left[(\mathbf{r}\times\mathbf{T})\cdot\hat{\mathbf{n}}_\Sigma \right]\!\right]_\Sigma \qquad \text{(I-1-17)}$$

or

$$\left[\!\left[\rho\varepsilon_{ijk}x_j V_k (V_\ell - U_\ell)\, n_\ell \right]\!\right]_\Sigma = \left[\!\left[\varepsilon_{ijk}x_j T_{\ell k} n_\ell \right]\!\right]_\Sigma \quad . \qquad \text{(I-1-18)}$$

This condition has to be satisfied at discontinuities of the flow if angular momentum is to be conserved.

I-1-d) Conservation of energy

The kinetic energy density is $\frac{1}{2}\rho\mathbf{V}\cdot\mathbf{V}$; we denote the internal energy density by ρu , where u is the specific internal energy of the medium (per unit mass). The total energy density $\rho E = \rho u + \frac{1}{2}\rho\mathbf{V}\cdot\mathbf{V}$ is conserved. This is expressed by use of the first law of thermodynamics. Casting the equation in the general form (I-1-4) , we have, away from discontinuities,

$$\rho\frac{dE}{dt} = \frac{\partial}{\partial t}(\rho E) + \nabla\cdot(\rho E\mathbf{V}) = \rho\,\mathbf{f}\cdot\mathbf{V} + \rho h + \nabla\cdot(\mathbf{V}\cdot\mathbf{T} - \mathbf{q}) \quad . \qquad \text{(I-1-19)}$$

Here h is the heat source density, $\mathbf{q}$ is the heat flux vector, and $\mathbf{V}\cdot\mathbf{T}$ indicates the contraction $V_j T_{ij}$. In component form,

$$\rho\frac{dE}{dt} = \frac{\partial}{\partial t}(\rho E) + (\rho E V_i)_{,i} = \rho f_i V_i + \rho h + (V_j T_{ij} - q_i)_{,i} \qquad \text{(I-1-20)}$$

At a discontinuity Σ devoid of any externally applied surface forces and of surface heat source density, (I-1-6) specializes to

$$\left[\!\left[\rho E(\mathbf{V}-\mathbf{U})\cdot \hat{n}_\Sigma\right]\!\right]_\Sigma = \left[\!\left[(\mathbf{V}\cdot\mathbf{T}-\mathbf{q})\cdot \hat{n}_\Sigma\right]\!\right]_\Sigma \qquad \text{(I-1-21)}$$

or

$$\left[\!\left[\rho E(V_i - U_i)\, n_i\right]\!\right]_\Sigma = \left[\!\left[(V_j T_{ij} - q_i)\, n_i\right]\!\right]_\Sigma \quad . \qquad \text{(I-1-22)}$$

This is the condition prevalent across discontinuities of the flow. It allows for transformation of internal energy into kinetic energy across the boundary and vice versa. In fact the quantities h and $\mathbf{q}$ may be generalized to include other forms of energy as well (e.g., electromagnetic energy; see Malvern, 1969). The condition (I-1-22) prevails even if energy is transformed from one form into another across Σ .

If the state of the material is known, along with the flow, within two regions of the medium separated by a discontinuity Σ , and if the conditions are satisfied for the conservation of mass and momentum, then equations (I-1-19) and (I-1-21) can be (theoretically) solved for $\mathbf{U}$, the velocity of the boundary. One has to know the quantity of ρE liberated (or absorbed) at the crossing of Σ . This is the generalized form of the problem of Stephan, discussed by Carslaw and Jaeger (1959, Chapter XI). The problem is greatly simplified if the medium is at rest. O'Connell and Wasserburg (1972) solve an analogous problem. We shall come back to this particular problem in Chapter III.

If we isolate the kinetic energy term on the left-hand side of (I-1-19) we get $\frac{1}{2}\rho\frac{d}{dt}(\mathbf{V}\cdot\mathbf{V}) = \rho\mathbf{V}\cdot\frac{d\mathbf{V}}{dt}$. By use of the equation

of motion (I-1-11) this reduces to $\mathbf{V} \cdot [\rho \mathbf{f} + \nabla \cdot \mathbf{T}]$. It is more convenient to evaluate this quantity in component form. We have

$$\rho V_i f_i + V_j T_{ij,i} = \rho V_i f_i + (V_j T_{ij})_{,i} - D_{ij} T_{ij} \qquad \text{(I-1-23)}$$

where D_{ij} is the deformation tensor defined by $D_{ij} = V_{(i,j)}$. D_{ij} is thus the symmetric part of $V_{i,j}$ and if we write

$$V_{i,j} = D_{ij} + \Omega_{ij} \quad , \qquad \text{(I-1-24)}$$

then the skew symmetric tensor Ω_{ij} is the vorticity tensor.

By combination of (I-1-19) and (I-1-23) and using the definition of total energy, we obtain

$$\rho \frac{du}{dt} = \frac{\partial(\rho u)}{\partial t} + \nabla \cdot (\rho u \mathbf{V}) = \mathbf{D} : \mathbf{T} + \rho h - \nabla \cdot \mathbf{q} \qquad \text{(I-1-25)}$$

or

$$\rho \frac{du}{dt} = \frac{\partial(\rho u)}{\partial t} + (\rho u V_i)_{,i} = D_{ij} T_{ij} + \rho h - q_{i,i} \quad . \qquad \text{(I-1-26)}$$

This is the usual "energy equation" (e.g., Malvern, 1969). We must note, however, that this is not a conservation equation because ρu , the internal energy, is not a conserved quantity. Therefore, we cannot write a jump condition analogous to (I-1-6) in that case. Carslaw and Jaeger point out that (I-1-26) is merely the differential equation of conduction of heat in a moving medium (Carslaw and Jaeger, 1959, p. 13). The appropriate equation to be used at discontinuities is

(I-1-22) , because the total energy is indeed a conserved quantity. The term $D_{ij}T_{ij}$ on the right-hand side of (I-1-26) represents the energy dissipated by internal deformation of the medium. It can be evaluated if a specific constitutive equation is assumed to hold for the medium under consideration. For example, in the case of a viscous fluid $T_{ij} = -p\delta_{ij} + \eta_{ij}$, where η_{ij} is the viscous stress, then

$$D_{ij}T_{ij} = D_{ij}\eta_{ij} = \Phi \quad , \tag{I-1-27}$$

the dissipation function. We shall not discuss here the forms of various constitutive equations of interest.

Let us consider the jump condition (I-1-22) in greater detail. If the flow velocity $\mathbf{V}$ is continuous, then by (I-1-8) the density ρ is continuous, and by (I-1-13) the tractions across Σ are continuous. Then the kinetic energy terms on the right-hand sides of (I-1-22) do not give any contribution to the jump, and we get

$$\rho \left[\!\left[u \right]\!\right]_\Sigma (\mathbf{V}-\mathbf{U}) \cdot \hat{n}_\Sigma = - \left[\!\left[\mathbf{q} \cdot \hat{n}_\Sigma \right]\!\right]_\Sigma \quad .$$

But because the specific volume is continuous across Σ , the jump in the internal energy reduces to the jump in enthalpy. The interpretation is clear if Σ is a phase boundary: $\left[\!\left[u \right]\!\right]_\Sigma$ is then the latent heat of transformation (per unit mass) ℓ . This latent heat is understood in an algebraic sense, and corresponds to the transformation of material from the state on the positive side to the state on the

negative side of Σ . We write

$$\rho \ell (\mathbf{V}-\mathbf{U}) \cdot \hat{n}_\Sigma = - \left[\!\left[\mathbf{q} \cdot \hat{n}_\Sigma \right]\!\right]_\Sigma \quad . \tag{I-1-28}$$

This reduces to the boundary condition use by Carslaw and Jaeger for the solution of Stephan's problem. For a medium at rest, and in the one dimensional case, (I-1-28) reduces indeed to

$$q_1 - q_2 = \rho \ell U \quad . \tag{I-1-29}$$

Another special case of interest is that where $\mathbf{V}-\mathbf{U}$ is tangent to the surface Σ . Then (I-1-22) yields

$$\left[\!\left[V_i t_i \right]\!\right]_\Sigma = \left[\!\left[q_i n_i \right]\!\right]_\Sigma \tag{I-1-30}$$

where the t_i's are the components of traction on Σ . The obvious interpretation is that the jump in the normal heat flux balances the work done by the tractions on Σ --in particular, frictional work.

I-1-e) <u>The entropy equation</u>

Let us assume that the continuum admits a caloric equation of state of the form

$$u = u(s, y_i) \quad , \tag{I-1-31}$$

where u is the specific internal energy, s the specific entropy,

and the y_i's are a set of thermodynamic state variables. We assume that the medium is homogeneous, so that the functional dependence (I-1-31) is the same for all particles. Defining the thermodynamic temperature by $T = \left(\frac{\partial u}{\partial s}\right)_y$ and the thermodynamic tensions by $Y_i = \left(\frac{\partial u}{\partial y_i}\right)_s$, then for reversible processes we have the Gibbs relation

$$du = T\, ds + Y_i dy_i \quad . \tag{I-1-32}$$

The Y_i's are sometimes referred to as generalized forces, and dy_i as generalized displacements.

Of special interest to us will be the case of the elastic solid, then

$$du = T\, ds + \sigma_{ij} de_{ij} \quad , \tag{I-1-33}$$

where σ_{ij} is the elastic stress tensor, and where e_{ij} is the infinitesimal strain tensor. For an inviscid fluid, this reduces to

$$du = T\, ds - p\, dv \quad , \tag{I-1-34}$$

where p is the pressure and v the specific volume.

The general theory can be found for example in Truesdell and Toupin (1960), and a succinct exposition in Malvern (1969). In the absence of viscosity or any nonlinear phenomena, elimination of u between (I-1-33) and (I-1-25) yields

$$\rho T \frac{ds}{dt} = \rho h - \nabla \cdot \mathbf{q} \qquad \text{(I-1-35)}$$

away from discontinuities.

For the case of a viscous fluid the dissipation function Φ (defined in I-1-27) appears on the right-hand side and we have

$$\rho T \frac{ds}{dt} = \Phi + \rho h - \nabla \cdot \mathbf{q} \quad . \qquad \text{(I-1-36)}$$

This is the entropy equation.

However, the second law of thermodynamics yields the Clausius - Duhem inequality

$$\frac{ds}{dt} \geq \frac{h}{T} - \frac{1}{\rho} \nabla \cdot \frac{\mathbf{q}}{T} \quad . \qquad \text{(I-1-37)}$$

This inequality means that the rate of increase of entropy is greater than or equal to its rate of input in any arbitrary volume (see Malvern, 1969). Combining (I-1-36) and (I-1-37) we get

$$\Phi - \frac{1}{T} \mathbf{q} \cdot \nabla T \geq 0 \quad , \qquad \text{(I-1-38)}$$

for which it is sufficient to assume (Truesdell and Noll, 1965)

$$\left.\begin{aligned} \Phi &\geq 0 \\ \mathbf{q} \cdot \nabla T &\leq 0 \end{aligned}\right\} \qquad \text{(I-1-39)}$$

In order to satisfy the second of these inequalities, we shall assume a constitutive equation of the form

$$q_i = - \chi_{ij} T_{,j} \quad . \tag{I-1-40}$$

This is the law of heat conduction in an anisotropic medium (Carslaw and Jaeger, 1959). We shall further assume that the conductivity tensor χ_{ij} satisfies the Onsager reciprocal relation $\chi_{ij} = \chi_{ji}$ (e.g., Malvern, 1969) and that the matrix χ_{ij} is positive (Landau and Lifchitz, 1967).

If we go back to the caloric equation of state, it follows from (I-1-31) and the definitions leading to (I-1-32) that the temperature is a function of the thermodynamic state $T = T(s,y_i)$. If we assume that this relation is invertible, then $s = s(T,y_i)$. Thus

$$\frac{ds}{dt} = \left(\frac{\partial s}{\partial T}\right)_{y_i} \frac{dT}{dt} + \left(\frac{\partial s}{\partial y_i}\right)_T \frac{dy_i}{dt} \quad .$$

As an example, we treat the case of an elastic solid, then

$$\frac{ds}{dt} = \left(\frac{\partial s}{\partial T}\right)_{e_{ij}} \frac{dT}{dt} + \left(\frac{\partial s}{\partial e_{ij}}\right)_T \frac{de_{ij}}{dt} \quad . \tag{I-1-41}$$

But

$$\left(\frac{\partial s}{\partial T}\right)_{e_{ij}} = \frac{C_v}{T} \quad ; \quad \left(\frac{\partial s}{\partial e_{ij}}\right)_T = \frac{\alpha}{K_T} \delta_{ij} \quad ,$$

where C_v is the specific heat at constant volume, α the coefficient

of thermal expansion, and K_T the isothermal compressibility coefficient (e.g. Landau and Lifchitz, 1967) Further $\frac{de_{ij}}{dt}\delta_{ij} = V_{i,i}$, so that the combination of (I-1-35) , (I-1-40) and (I-1-41) yields

$$\rho C_v \frac{dT}{dt} + \frac{\alpha T}{K_T} V_{i,i} = \rho h + (\chi_{ij} T_{,j})_{,i} \quad , \qquad \text{(I-1-42)}$$

the equation of heat conduction in an elastic solid. This equation takes various forms when derived for different materials (Stokesian fluids, etc...) and when different state variables are chosen. We shall refer the reader to the literature for the various cases usually encountered, since the example (I-1-42) suffices for our present purposes.

Similarly we shall not discuss here the equations of thermo-elasticity, since they require a choice of constitutive equations and thus a specialization of the material.

I-2 Green's theorem and the elastic operator

The general equation of motion in a continuum (equation I-1-11) exhibits a nonlinear term of the form $(\rho V_i V_j)_{ij}$ --the convective term. For that reason, flow solutions to boundary value and initial value problems cannot be expressed by superposition of a particular solution to the inhomogeneous equation and the general solution of the homogeneous equation, a fortiori by a Green's function or a Green's tensor solution. In the other hand, for the case of an elastic continuum undergoing infinitesimal strains, equation (I-1-11) is usually linearized. The (vector) wave equation so obtained can then be solved by determining its Green's tensor for the problem at hand.

Discussion of Green's tensor and Green's tensor solution will be the object of section I-3. However, we need before hand to derive the generalized Green's theorem for the elastic operator.

Let us denote the cartesian coordinates of a particle in an elastic medium with respect to an arbitrary (cartesian) reference frame by x_i, $i = 1,2,3,$. The displacement of this particle away from its reference--in general, equilibrium--position is represented by the vector $\mathbf{u}(\mathbf{x},t)$, of components $u_i(\mathbf{x},t)$, $i = 1,2,3$.

By linearization of the equation of motion (I-1-11) we obtain

$$\frac{\partial}{\partial t}\left(\rho \frac{\partial u_i}{\partial t}\right) = T_{ij,i} + \rho f_i \quad . \tag{I-2-1}$$

Since we want to solve (I-2-1) for the u_i's , we must relate the stress tensor T_{ij} to the displacement through some constitutive equation. The infinitesimal strain tensor is given by

$$e_{ij} = u_{(i,j)} = \frac{1}{2}\,(u_{i,j} + u_{j,i}) \quad , \tag{I-2-2}$$

and the generalized Hooke's law then reads

$$T_{ij} = \sigma_{ij} = C_{ijk\ell}e_{k\ell} = C_{ijk\ell}u_{(k,\ell)} \quad , \tag{I-2-3}$$

where σ_{ij} denotes the elastic stress tensor.

If the cartesian tensor $C_{ijk\ell}$ --the elastic tensor--satisfies the symmetry conditions

$$C_{ijk\ell} = C_{jik\ell} = C_{ij\ell k} = C_{k\ell ij} \quad , \tag{I-2-4}$$

then (I-2-3) reduces to

$$\sigma_{ij} = C_{ijk\ell}u_{k,\ell} \quad . \tag{I-2-5}$$

We can therefore rewrite (I-2-1) as

$$\frac{\partial}{\partial t}\left(\rho\,\frac{\partial u_i}{\partial t}\right) = (C_{ijk\ell}u_{k,\ell})_{,j} + \rho f_i \quad . \tag{I-2-6}$$

If we now consider the time t as a fourth coordinate, so that the ordered couple $(\mathbf{x},t)$ is in fact the order quadruplet (x_1,x_2,x_3,x_4), we can extend the three dimensional Euclidean space in which

displacements are measured into a four-dimensional Euclidean space. We should note here that we are not defining a space-time in the relativistic sense, that is, we do not assume a Lorentz metric. Time is still considered in a Newtonian sense.

We shall make the convention that Latin indices $(i,j,...)$ take values $1,2,3$, while Greek indices $(\alpha,\beta,...)$ take values $1,2,3,4$.

By keeping a Newtonian notion of time, we cannot allow any arbitrary transformation of the coordinate system. In fact, time has to be independent of the spatial coordinates and we must restrict the orthogonal coordinate transformations to those of the form

$$x'_\alpha = A_{\alpha\beta}x_\beta + B_\alpha \quad . \tag{I-2-7}$$

Here the space-like part A_{ij} of the matrix $A_{\alpha\beta}$ is orthogonal and represents an orthogonal transformation of the space coordinates, but $A_{\alpha 4} = A_{4\alpha} = a\,\delta_{\alpha 4}$, where a is a scalar and $\delta_{\alpha 4}$ the Kronecker delta. In other words, the only time transformations allowed here are translations of the origin and changes of scale. Under these specific restrictions we seek to rewrite (I-2-6) in the form

$$(C_{\alpha\beta\gamma\delta}u_{\gamma,\delta})_{,\beta} = \rho f_\alpha \quad . \tag{I-2-8}$$

It is sufficient for this purpose to define $u_4 = f_4 = 0$, and the array $C_{\alpha\beta\gamma\delta}$ by

$$\left.\begin{aligned} C_{\alpha\beta\gamma\delta} &= -\, C_{ijk\ell} && \text{for } \alpha,\beta,\gamma,\delta = 1,2,3 \\ C_{i4k4} &= C_{4i4k} = \rho\, \delta_{ik} && \\ C_{\alpha\beta\gamma\delta} &= 0 && \text{otherwise} \end{aligned}\right\} \qquad \text{(I-2-9)}$$

Thus $C_{\alpha\beta\gamma\delta}$ possesses the symmetries

$$C_{\alpha\beta\gamma\delta} = C_{\beta\alpha\gamma\delta} = C_{\alpha\beta\delta\gamma} = C_{\gamma\delta\alpha\beta} \qquad \text{(I-2-10)}$$

similar to (I-2-4) . The arrays $C_{\alpha\beta\gamma\delta}$, u_α, f_α , will transform as cartesian tensors under transformations of the type (I-2-7) . But we must emphasize again that these are not the most general orthogonal coordinate transformations on the four-dimensional Euclidean space that we have just constructed, and $C_{\alpha\beta\gamma\delta}$ will not be a cartesian tensor on that space in general.

Except for the fact that (I-2-8) has to be linear, there are no restrictions on the $C_{\alpha\beta\gamma\delta}$ and they may be functions of the coordinates. Equation (I-2-8) is a very compact form for the equations of motion, we rewrite it as

$$\frac{\partial}{\partial x_\beta}\left(C_{\alpha\beta\gamma\delta}\,\frac{\partial u_\gamma}{\partial x_\delta}\right) = \rho f_\alpha \quad . \qquad \text{(I-2-11)}$$

This defines a vector valued, second order linear differential operator,

which, when applied to a space-like vector $\mathbf{u}$ yields a space-like vector $\rho\mathbf{f}$. Defining

$$\mathscr{L}_{\alpha\gamma} \equiv \frac{\partial}{\partial x_\beta}\left(C_{\alpha\beta\gamma\delta}\frac{\partial}{\partial x_\delta}\right) \quad , \tag{I-2-12}$$

we have

$$\mathscr{L}_{\alpha\gamma}u_\gamma = \rho f_\alpha \quad , \tag{I-2-13}$$

or

$$\mathscr{L}\,\mathbf{u} = \rho\,\mathbf{f} \quad . \tag{I-2-14}$$

We shall henceforth call $\mathscr{L}$ the elastic operator. (Kupradze, 1963, defines the "elastic operator" in an analogous fashion in the frequency domain). Stakgold (1968) shows how the definition of such operators can be extended to include differentiations in a distributional sense. In fact, one can define the operation of $\mathscr{L}$ on a space-like tensor. If $\mathbf{W}$ is a space-like tensor (i.e., without any time-like component), it satisfies

$$W_{\alpha\ \beta\ \ldots\ \lambda} \equiv W_{\alpha\ \beta\ \ldots\ \lambda}(1-\delta_{\alpha 4})\ldots(1-\delta_{\lambda 4}) \tag{1-2-15}$$

Then $\mathscr{L}\mathbf{W}$ is a space-like tensor given by the contraction $\mathscr{L}_{\mu\alpha}W_{\alpha\ \beta\ \ldots\ \lambda}$, where other conventions can be chosen as to which subscript is to be contracted.

Now, given a time-dependent spatial volume $V(t)$ bounded by a surface $S(t)$, and a time interval $[t_1,t_2]$, we can define a four-volume Ω in the space-time. Given two space-like vectors $\mathbf{u}(x_\alpha)$

and $\mathbf{v}(x_\alpha)$, the integral

$$(\mathbf{u}\,,\mathbf{v})_\Omega = \int_\Omega u_i v_i \, d^4x = \int_{t_1}^{t_2} dt \int_{V(t)} u_i v_i \, d^3x \qquad \text{(I-2-16)}$$

defines an inner product of the two vectors. Further $(\mathbf{u}\,,\mathbf{u})_\Omega$ is positive and vanishes only with $\mathbf{u} = 0$, and the triangular inequality holds

$$(\mathbf{u}+\mathbf{v}\,,\mathbf{u}+\mathbf{v})_\Omega \leq (\mathbf{u}\,,\mathbf{u})_\Omega + (\mathbf{v}\,,\mathbf{v})_\Omega \quad , \qquad \text{(I-2-17)}$$

so that this inner product may be used to define a norm on the space.

In addition, because the space is flat, the integral of a tensor is a tensor, and we can define the quantity

$$(\mathbf{G},\mathbf{u})_\Omega = \int_\Omega G_{ik} u_i \, d^4x \quad , \qquad \text{(I-2-18)}$$

where G_{ik} is a space-like tensor, so that the quantity defined is a space-like vector. If G_{ik} is a two-point tensor $G_{ik}(\mathbf{x},\mathbf{x}')$, we have to specify the variable of integration on the right-hand side of (I-2-18):

$$\begin{aligned} (\mathbf{G},\mathbf{u})_\Omega^{\mathbf{x}'} &= \int_\Omega G_{ik}(\mathbf{x},\mathbf{x}')\, u_i(\mathbf{x}')\, d^4x' \\ (\mathbf{G},\mathbf{u})_\Omega^{\mathbf{x}} &= \int_\Omega G_{ik}(\mathbf{x},\mathbf{x}')\, u_i(\mathbf{x})\, d^4x \quad . \end{aligned} \qquad \text{(I-2-19)}$$

The first definition yields a vector function of $\mathbf{x}$, and the second one a vector function of $\mathbf{x}'$. If $G(\mathbf{x},\mathbf{x}')$ is symmetric in $\mathbf{x}$ and $\mathbf{x}'$, then clearly both definitions are completely equivalent.

To define the formal adjoint $\mathscr{L}^*$ of the operator $\mathscr{L}$, we proceed as in the scalar case (e.g., Stakgold, 1968), and compute $(\mathscr{L}\mathbf{u},\mathbf{v})_\Omega$ by an integration by parts. We have

$$(\mathscr{L}\mathbf{u},\mathbf{v})_\Omega = \int_\Omega v_\alpha (C_{\alpha\beta\gamma\delta} u_{\gamma,\delta})_{,\beta} \, d^4x \quad . \tag{I-2-20}$$

To integrate by parts, we simply note that,

$$v_\alpha (C_{\alpha\beta\gamma\delta} u_{\gamma,\delta})_{,\beta} = (v_\alpha C_{\alpha\beta\gamma\delta} u_{\gamma,\delta})_{,\beta} - v_{\alpha,\beta} C_{\alpha\beta\gamma\delta} u_{\gamma,\delta} \tag{I-2-21}$$

But because of the symmetry properties (I-2-10)

$$- v_{\alpha,\beta} C_{\alpha\beta\gamma\delta} u_{\gamma,\delta} = - v_{\alpha,\beta} C_{\gamma\delta\alpha\beta} u_{\gamma,\delta} \tag{I-2-22}$$

However, the indices $\alpha \ldots \delta$ are dummy indices and can be renamed, thus

$$- v_{\alpha,\beta} C_{\gamma\delta\alpha\beta} u_{\gamma,\delta} = - u_{\alpha,\beta} C_{\alpha\beta\gamma\delta} v_{\gamma,\delta} \quad . \tag{I-2-23}$$

But by simple comparison with (I-2-21)

$$- u_{\alpha,\beta} C_{\alpha\beta\gamma\delta} v_{\gamma,\delta} = u_\alpha (C_{\alpha\beta\gamma\delta} v_{\gamma,\delta})_{,\beta} - (u_\alpha C_{\alpha\beta\gamma\delta} v_{\gamma,\delta})_{,\beta} \tag{I-2-24}$$

Combining equations (I-2-21) through (I-2-24) we finally get

$$v_\alpha (C_{\alpha\beta\gamma\delta} u_{\gamma,\delta})_{,\beta} = u_\alpha (C_{\alpha\beta\gamma\delta} v_{\gamma,\delta})_{,\beta} + (v_\alpha C_{\alpha\beta\gamma\delta} u_{\gamma,\delta} - u_\alpha C_{\alpha\beta\gamma\delta} v_{\gamma,\delta})_{,\beta} \tag{I-2-25}$$

and, by replacing (I-2-25) in (I-2-20)

$$(\mathscr{L}\mathbf{u},\mathbf{v})_\Omega = \int_\Omega \left[u_\alpha (C_{\alpha\beta\gamma\delta} v_{\gamma,\delta})_{,\beta} + (v_\alpha C_{\alpha\beta\gamma\delta} u_{\gamma,\delta} - u_\alpha C_{\alpha\beta\gamma\delta} v_{\gamma,\delta})_{,\beta} \right] d^4x \tag{I-2-26}$$

Therefore we can define the formal adjoint $\mathscr{L}^*$ by rewriting this as

$$(\mathscr{L}\mathbf{u},\mathbf{v})_\Omega = (\mathbf{u}, \mathscr{L}^*\mathbf{v})_\Omega + \int_\Omega J_{\beta,\beta}\, d^4x \quad . \tag{I-2-27}$$

J_β is the bilinear concomitant of $\mathbf{u}$ and $\mathbf{v}$, and (I-2-27) is the sought generalization of Green's theorem. From (I-2-26) it is evident that $\mathscr{L}^* \equiv \mathscr{L}$: we say that $\mathscr{L}$ is formally self adjoint.

It is important at this point to note that J_β has a time-like component. We recall that in (I-2-7) we had to restrict the allowable coordinate transformations on our space-time. In fact, the array J_β would not in general transform as the components of a vector under the most general orthogonal mapping in the four-dimensional space-time. For this reason, we shall treat time as a special coordinate, and write

$$\int_{\Omega} J_{\beta,\beta}\, d^4x = \int_{\Omega} J_{i,i}\, d^4x + \int_{\Omega} J_{t,t}\, d^4x \qquad \text{(I-2-28)}$$

Gauss' theorem is readily applicable to the first integral on the right-hand side of this equation, we have

$$\int_{\Omega} J_{i,i}\, d^4x = \int_{t_1}^{t_2} \int_{V(t)} J_{i,i}\, d^3x$$

$$= \int_{t_1}^{t_2} \int_{S(t)+\Sigma(t)} J_i n_i\, da \quad . \qquad \text{(I-2-29)}$$

Here we have distinguished between $S(t)$, the external boundary of $V(t)$, and $\Sigma(t)$, representing all internal boundaries. If $\Sigma(t)$ presents a surface of discontinuity of the fields $\mathbf{u}$ and $\mathbf{v}$, or of the operator $\mathscr{L}$, then the integration will have to be taken on both sides of this discontinuity. In such a case jumps can be defined in the same manner as in Appendix 1 or in section I-1. The array n_i represent the components of the (space-like) outer unit normal to the various boundaries. The geometry is described on figure I-2-1.

We can expand the product $J_j n_j$ and write

$$\begin{aligned} J_j n_j &= - v_i C_{ijk\ell} u_{k,\ell} n_j + u_i C_{ijk\ell} v_{k,\ell} n_j \\ &= u_i t_i^{(v)} - v_i t_i^{(u)} \quad , \end{aligned} \qquad \text{(I-2-30)}$$

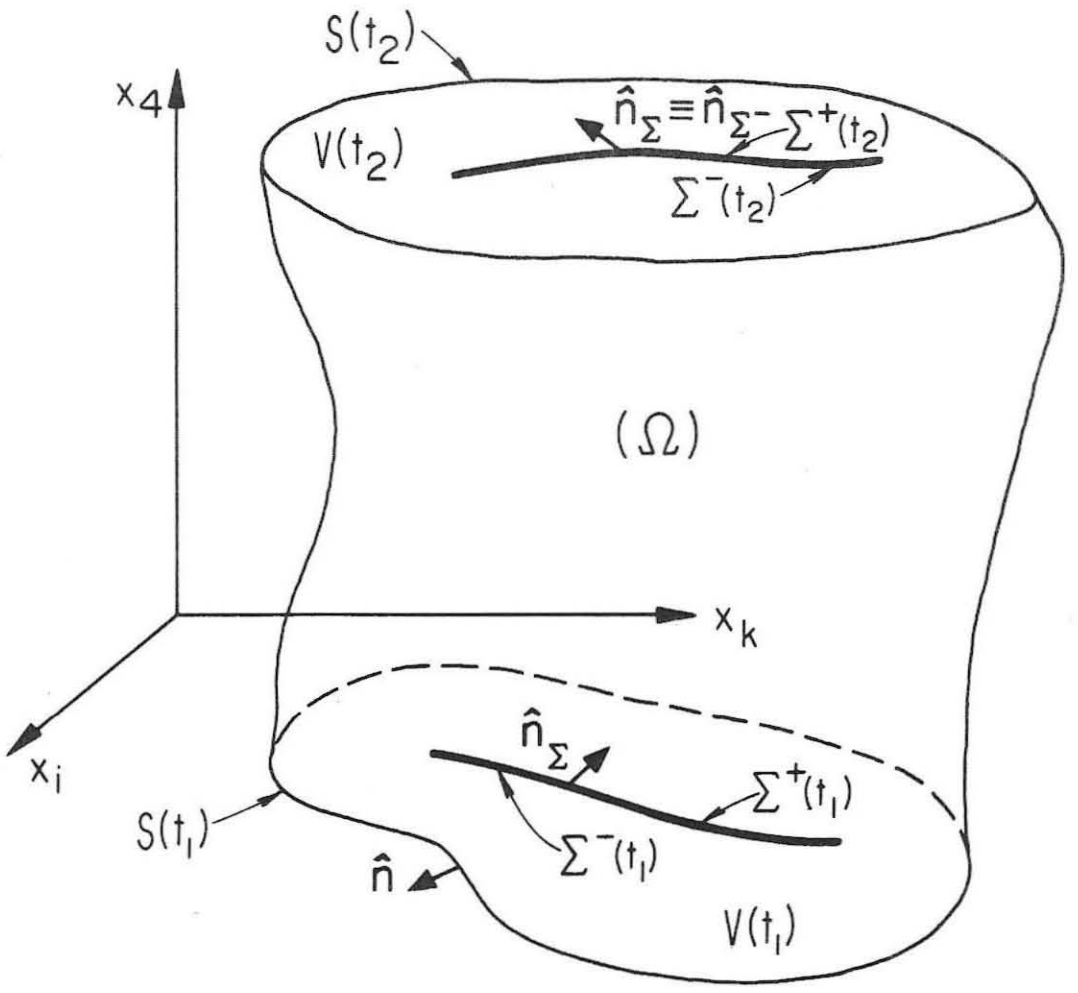

Figure I-2-1. Geometry of the four-volume Ω . x_i and x_k are spatial coordinates, x_4 is the time coordinate. The geometry is shown (in two dimensions) at times t_1 and t_2 .

where $t_i^{(u)}$, $t_i^{(v)}$ are the tractions on the boundaries associated with the displacement fields $\mathbf{u}$ and $\mathbf{v}$ respectively. With reference to figure (I-2-1) we may thus write

$$\int_{\Omega} J_{i,i}\, d^4x = \int_{t_1}^{t_2} dt \int_{S(t)} \left(u_i t_i^{(v)} - v_i t_i^{(u)} \right) da$$

$$+ \int_{t_1}^{t_2} dt \int_{\Sigma(t)} \left[\!\left[u_i t_i^{(v)} - v_i t_i^{(u)} \right]\!\right] da \qquad .(I\text{-}2\text{-}31)$$

The last term in (I-2-28) can be evaluated separately. Using the definition (I-2-9) for the coefficients $C_{\alpha\beta\gamma\delta}$ we have

$$\int_{\Omega} J_{t,t}\, d^4x = \int_{t_1}^{t_2} dt \int_{V(t)} \frac{\partial}{\partial t} \left[\rho v_i \frac{\partial u_i}{\partial t} - \rho u_i \frac{\partial v_i}{\partial t} \right] d^3x \qquad . \quad (I\text{-}2\text{-}32)$$

The volume integral may now be evaluated by using the generalized transport theorem proved in Appendix 1 (equation A-1-14), conveniently recast in the form

$$\int_{V(t)} \frac{\partial}{\partial t} [\ ]\, d^3x = \frac{d}{dt} \int_{V(t)} [\ ]\, d^3x - \int_{S(t)+\Sigma(t)} [\ ]\, \mathbf{U} \cdot \hat{n}\, da \qquad .$$

(I-2-33)

Here the bracket is the same as the one appearing in the integrand on the right-hand side of (I-2-32) , and can be thought of as a function

of the flow since it is a function of both position and time which can be attached to each particle in the medium. $\mathbf{U}$ is the velocity of the boundary over which the surface integral is taken.

Combining (I-2-27) , (I-2-31) , (I-2-32) , and (I-2-33) , we have the generalization of Green's theorem in the form

$$(\mathscr{L}\mathbf{u},\mathbf{v})_\Omega = (\mathbf{v},\mathscr{L}^*\mathbf{u})_\Omega + \int_{t_1}^{t_2} dt \int_{S(t)+\Sigma(t)} \left[\!\left[u_i t_i^{(v)} - v_i t_i^{(u)} \right]\!\right] da$$

$$- \int_{t_1}^{t_2} dt \int_{S(t)+\Sigma(t)} \left[\!\left[\rho v_i \frac{\partial u_i}{\partial t} - \rho u_i \frac{\partial u_i}{\partial t} \right]\!\right] \mathbf{U}\cdot\hat{n}\, da$$

$$+ \int_{t_1}^{t_2} \frac{d}{dt} \int_{V(t)} \left(\rho v_i \frac{\partial u_i}{\partial t} - \rho u_i \frac{\partial v_i}{\partial t} \right) d^3x\, dt \quad . \tag{I-2-34}$$

Here we have extended the definition of a jump to the case of external boundaries, where the value of a jump is simply the limiting value of the quantity under consideration when the boundary is approached from the inner side.

Equation (I-2-34) can be compacted by noting that the linearized form of the jump condition (I-1-13) is

$$\left[\!\left[\rho \frac{\partial u_i}{\partial t} U_j n_j + t_i^{(u)} \right]\!\right]_\Sigma = 0 \quad . \tag{I-2-35}$$

Making use of this relation in (I-2-34) yields

$$(\mathscr{L}\mathbf{u},\mathbf{v})_\Omega = (\mathbf{u},\mathscr{L}^*\mathbf{v})_\Omega$$

$$+\int_{t_1}^{t_2} dt \int_{S(t)+\Sigma(t)} \left[\left(\rho \frac{\partial v_i}{\partial t} U_j n_j + t_i^{(v)} \right) [\![u_i]\!] - \left(\rho \frac{\partial u_i}{\partial t} U_j n_j + t_i^{(u)} \right) [\![v_i]\!] \right] da$$

$$+\int_{t_1}^{t_2} \frac{d}{dt} \int_{V(t)} \left(\rho v_i \frac{\partial u_i}{\partial t} - \rho u_i \frac{\partial v_i}{\partial t} \right) d^3x \, dt \qquad \text{(I-2-36)}$$

The last integral in this equation has to be understood as a Stieltjes integral, that is, it is of the form $\int_{t_1}^{t_2} dF$, where

$$F = F(t) = \int_{V(t)} \left(\rho v_i \frac{\partial u_i}{\partial t} - \rho u_i \frac{\partial v_i}{\partial t} \right) d^3x \quad .$$

If the functional F is continuous, the last term reduces to $F(t_2) - F(t_1)$.

We shall see in the next section that the terms involving surface integrals on the right-hand side of (I-2-34) are useful in solving boundary value problems. Similarly the last term, involving a volume integral is particularly useful in solutions to initial value problems.

In elastostatics, time is absent from equation (I-2-34) and

this equation reduces to Betti's formula (e.g., Kupradze, 1968, or Ben-Menahem and Singh, 1968).

In concluding this section, we note that the time coordinate could be handled in the same way as spatial coordinates up to equation (I-2-27) . The reasons why we subsequently gave it as separate treatment stem mainly from the Newtonian notion of time that we kept throughout. The analysis presented here can undoubtedly be extended to other geometries (e.g., possibly to relativistic problems), for linearized problems. There are, however, theoretical subtleties and difficulties: for instance, how should one define the time-like components of the strain tensor? These problems lie outside the scope of the present work; attempts at their solutions will be undertaken in the future.

I-3 Green's tensor solutions to the linearized equation of motion in an elastic medium

The linearized equation of motion in an elastic medium, which we wrote in the last section as

$$\mathscr{L}_{\alpha\gamma} u_\gamma = \rho f_\alpha \quad , \tag{I-3-1}$$

is to be solved for $\mathbf{u}(x_\alpha)$, if the operator $\mathscr{L}$ and the body force density $\mathbf{f}$ are known. In addition to satisfying equation (I-3-1) , the solution $\mathbf{u}$ will, in general, be required to satisfy boundary conditions and initial conditions. We shall denote symbolically these conditions by

$$\mathscr{B}\mathbf{u} = \mathbf{b} \quad . \tag{I-3-2}$$

This equation is to be satisfied on the boundary $\partial\Omega$ of the domain Ω . $\mathscr{B}$ is an operator, $\mathbf{b}$ is a given vector function on $\partial\Omega$. We shall represent symbolically homogeneous conditions by

$$\mathscr{B}\mathbf{u} = 0 \quad . \tag{I-3-3}$$

We shall always assume that (I-3-2) and (I-3-3) represent proper conditions and that no incompatibility arises from them.

Because of the linearity of the problem, the general solution to equation (I-3-1) can be written as the sum of any particular solution

and of the general solution to the homogeneous equation

$$\mathscr{L}_{\alpha\gamma} u_\gamma = 0 \quad . \tag{I-3-4}$$

We shall show in this section that the Green's tensor solution achieves precisely that goal. In a first step we shall define Green's tensor and show the system it satisfies ; then by recasting (I-3-1) in integral form we shall derive the Green's tensor solution formally, and last we shall discuss it. For simplicity we assume the coefficients $C_{\alpha\beta\gamma\delta}$ to be independent of time.

i) Green's tensors

We suppose that equation (I-3-1) is to be solved within a four-dimensional volume Ω . Given an arbitrary point $\mathbf{x}_o$ within the domain Ω , we say that the space-like tensor

$$g_{\alpha\beta}(\mathbf{x};\mathbf{x}_o) \equiv g_{\alpha\beta}(\mathbf{x};\mathbf{x}_o)(1 - \delta_{\alpha 4})(1 - \delta_{\beta 4}) \quad ,$$

is a fundamental solution of the operator $\mathscr{L}$, with pole at $\mathbf{x}_o$ if it is any solution of the equation

$$\mathscr{L}_{\alpha\gamma} g_{\gamma\beta} = \Delta_{\alpha\beta} \quad , \tag{I-3-5}$$

where the space-like tensor $\Delta_{\alpha\beta}$ is given by

$$\Delta_{\alpha\beta} = 4\pi\, \delta_{\alpha\beta}(1 - \delta_{\alpha 4})(1 - \delta_{\beta 4})\, \delta(\mathbf{x} - \mathbf{x}_o) \quad . \qquad \text{(I-3-6)}$$

Here $\delta(\mathbf{x} - \mathbf{x}_o)$ is the (four-dimensional) Dirac delta distribution. Clearly $g_{\alpha\beta}$ will present a singularity at $\mathbf{x} = \mathbf{x}_o$, and therefore will have to satisfy (I-3-5) in a distributional sense, (see e.g., Stakgold, 1968, for a more complete discussion of distributional solutions). The normalization factor 4π was introduced because it is convenient in the scalar case of potential theory (see e.g., Morse and Feshbach, 1953, chapter 7; see also Courant and Hilbert, 1966, for a discussion of the scalar case).

But for boundary conditions requirements, $g_{\alpha\beta}(\mathbf{x};\mathbf{x}_o)$ is the α component of displacement in the medium at $\mathbf{x}$ caused by an impulsive force in the β direction at $\mathbf{x}_o$. For this reason we shall call $\mathbf{x}_o$ the source point and $\mathbf{x}$ the receiver (or observer's) point.

In a similar fashion one defines fundamental solutions of the adjoint operator $\mathscr{L}^*$ by

$$\mathscr{L}^*_{\alpha\gamma} h_{\gamma\beta} = \Delta_{\alpha\beta} \quad . \qquad \text{(I-3-7)}$$

In order to generalize the notion of adjointness, we have to discuss the effects of initial and boundary conditions. Morse and Feshbach (chapter 7) give a general discussion of the problem; we shall restrict ourselves to the essential points.

Consider the system

$$\begin{cases} \mathscr{L}_{\alpha\gamma} u_\gamma = \rho f_\alpha & , \\ \mathscr{B}\,\mathbf{u} = 0 & , \end{cases} \qquad \text{(I-3-8)}$$

with homogeneous boundary conditions. (This system is to be distinguished from equation (I-3-1) .) Following Stakgold (1968), we call $\mathcal{D}$ the set of all twice differentiable functions $\mathbf{u}$ that satisfy the conditions $\mathscr{B}\mathbf{u} = 0$. Let $\mathcal{D}^*$ be the set of all twice differentiable functions $\mathbf{v}$ such that

$$\forall_{\mathcal{D}}\, \mathbf{u} \ , \ (\mathscr{L}\mathbf{u}, \mathbf{v}) = (\mathbf{u}, \mathscr{L}^*\mathbf{v}) \quad . \qquad \text{(I-3-9)}$$

Then from the results of section I-2, the fields $\mathbf{v}$ have to satisfy a set of conditions $\mathscr{B}^*\mathbf{v} = 0$ termed the adjoint conditions. The adjoint system is then

$$\begin{cases} \mathscr{L}^*_{\alpha\gamma} v_\gamma = \rho f_\alpha & , \\ \mathscr{B}^*\mathbf{v} = 0 & . \end{cases} \qquad \text{(I-3-10)}$$

We saw earlier that if $\mathscr{L}^* \equiv \mathscr{L}$, the operator $\mathscr{L}$ is formally self-adjoint. If, furthermore, $\mathcal{D} = \mathcal{D}^*$ and $\mathscr{B} = \mathscr{B}^*$, then the <u>system</u> (I-3-8) is said to be self-adjoint.

We can now define the Green's tensor $G_{\alpha\beta}(\mathbf{x}; \mathbf{x}_o)$ for the completely inhomogeneous problem

$$\begin{cases} \mathscr{L}_{\alpha\gamma} u_\gamma = \rho f_\alpha \\ \mathscr{B}\, \mathbf{u} = \mathbf{b} \end{cases} ; \qquad \text{(I-3-11)}$$

it is the fundamental solution of $\mathscr{L}$ satisfying the corresponding homogeneous conditions, that is

$$\begin{cases} \mathscr{L}_{\alpha\gamma} G_{\gamma\beta} = \Delta_{\alpha\beta} \\ \mathscr{B}\, \mathbf{G} = 0 \end{cases} . \qquad \text{(I-3-12)}$$

Similarly the adjoint Green's tensor is defined by

$$\begin{cases} \mathscr{L}^*_{\alpha\gamma}\ G^*_{\alpha\beta} = \Delta_{\alpha\beta} \\ \mathscr{B}^*\ \mathbf{G}^* = 0 \end{cases} . \qquad \text{(I-3-13)}$$

The most fundamental property of the Green's tensor is the reciprocity relation which we now prove.

From the definitions (I-3-12) and (I-3-13) we have

$$(\mathscr{L}\, \mathbf{G} ,\ \mathbf{G}^*)^{\mathbf{x}}_{\Omega} - (\mathbf{G} ,\ \mathscr{L}^* \mathbf{G}^*)^{\mathbf{x}}_{\Omega} = 0 \qquad \text{(I-3-14)}$$

where the inner product is taken with respect to $\mathbf{x}$ (cf. section I-2). But if we write

$$\mathscr{L}_{\alpha\gamma} G_{\alpha\beta}(\mathbf{x}\,;\,\mathbf{x}_o) = \Delta_{\alpha\beta}(\mathbf{x}\,;\,\mathbf{x}_o) \quad ,$$

$$\mathscr{L}^{*}_{\alpha\gamma} G^{*}_{\alpha\beta}(x ; x_1) = \Delta_{\alpha\beta}(x ; x_1) \quad .$$

and use the definition of $\Delta_{\alpha\beta}$ given by (I-3-6) , we can rewrite (I-3-14) as

$$G^{*}_{\alpha\beta}(x_o ; x_1) = G_{\alpha\beta}(x_1 ; x_o) \quad .$$

Since x_1 is arbitrary, we have

$$G_{\alpha\beta}(x ; x_o) = G^{*}_{\alpha\beta}(x_o ; x) \quad . \qquad \text{(I-3-15)}$$

This is the reciprocity relation. If the system (I-3-12) is self-adjoint, we have

$$G_{\alpha\beta}(x ; x_o) = G_{\alpha\beta}(x_o ; x) \qquad \text{(I-3-16)}$$

and, in that case, Green's tensor is symmetric in x and x_o .

In the general case, physical problems are not self-adjoint, and symmetry relation (I-3-16) is not satisfied. One has then to use the general reciprocity relation (I-3-15) . However, for problems in the mechanics of continuous media, it is customary to make an additional physical assumption, namely that the causality principle has to be satisfied. The effect of this assumption is to reduce the class of acceptable solutions to those for which time flows in a particular

direction. We shall now see how it affects the Green's tensor: The Green's tensor is usually required to be "causal" (e.g., Morse and Feshbach, 1953). For macroscopic events it is reasonable to assume that the flow of time is unidirectional, so that if an impulse source occurs at t_o no effect should be felt anywhere at an earlier time $t < t_o$. Here again time plays a special role, and we write $\boldsymbol{x} = (\mathbf{r}, t)$, where $\mathbf{r}$ is the spacelike part of the vector position $\boldsymbol{x}$. Then for a causal Green's tensor

$$G_{\alpha\beta}(\mathbf{r}, t; \mathbf{r}_o, t_o) \equiv 0 \quad \text{for} \quad t < t_o \quad . \tag{I-3-17}$$

We observe immediately that the causal Green's tensor does not satisfy (I-3-16) since one side of the equation or the other vanishes identically if $t \neq t_o$. However, since we assumed the coefficients $C_{\alpha\beta\gamma\delta}$ to be independent of time, equation (I-3-1) does not imply any directionality of time. Therefore, by reversing the flow of time while exchanging source and receiver, we can obtain a reciprocity relation of the form

$$G_{\alpha\beta}(\mathbf{r}, t; \mathbf{r}_o, t_o) = G_{\alpha\beta}(\mathbf{r}_o, -t_o; \mathbf{r}, -t) \quad . \tag{I-3-18}$$

By comparison of (I-3-18) and (I-3-15), one sees therefore that the causal Green's tensor satisfies

$$G^{*}_{\alpha\beta}(\mathbf{r}, t; \mathbf{r}\ t_o) = G_{\alpha\beta}(\mathbf{r}, -t; \mathbf{r}_o, -t_o) \quad , \tag{I-3-19}$$

which is the result of Morse and Feshbach (1953).

One sees at this point that the causality requirement has rather profound consequences on the nature of the Green's tensor (and thus on the solution). Its symmetry in the time coordinate is fundamentally different from its symmetry in the space coordinates. This means that when a condition is imposed upon a solution along a time-like part of $\partial\Omega$ (such as an initial value condition), then since (I-3-16) cannot be satisfied, the problem is not self-adjoint. Stakgold (1968) points out that initial value problems are never self-adjoint.

The general reciprocity relation (I-3-15) is very useful for the solution of source problems. So far we have always assumed that the operator $\mathscr{L}$ was applied at the receiver point $\boldsymbol{x}$. All operations were carried with respect to the coordinates x_α. However, the intuitive notion of a Green's function solution, as expressed in the introduction to this chapter, calls for the superposition of the effects of all sources. One thus expects to integrate these effects over the source coordinates. For this reason we wish to find the equations satisfied by $G_{\alpha\beta}(\boldsymbol{x}; \boldsymbol{x}_o)$ and $G^*_{\alpha\beta}(\boldsymbol{x}; \boldsymbol{x}_o)$ as a function of the source coordinates. If we define

$$\mathscr{L}^{o}_{\alpha\gamma} u_\gamma = \frac{\partial}{\partial x^o_\beta}\left(C_{\alpha\beta\gamma\delta} \frac{\partial u_\gamma}{\partial x^o_\delta} \right) \qquad \text{(I-3-20)}$$

as the operation of $\mathscr{L}$ over $\mathbf{u}$ at $\boldsymbol{x}_o$, then from (I-3-15) we see that

$$\begin{cases} \mathscr{L}^{*o}_{\alpha\gamma} G_{\gamma\beta} = \Delta_{\alpha\beta} \\ \mathscr{B}^{*o} G = 0 \end{cases} \qquad \text{(I-3-21)}$$

and

$$\begin{cases} \mathscr{L}^{o}_{\alpha\gamma} G^{*}_{\alpha\beta} = \Delta_{\alpha\beta} \\ \mathscr{B}^{o} G^{*} = 0 \end{cases} \qquad \text{(I-3-22)}$$

are the systems satisfied, where all operations are carried on the source coordinates.

The system (I-3-21) is that needed for a formal derivation of the Green's tensor solution, which we present next.

ii) Green's tensor solution

The system (I-3-11) must be satisfied everywhere in Ω ; in particular, at any point $\mathbf{x}_o$ we have

$$\begin{cases} \mathscr{L}^{o}_{\alpha\gamma} u_\gamma = \rho f_\alpha(\mathbf{x}_o) & \text{in } \Omega, \\ \mathscr{B}^{o} \mathbf{u} = \mathbf{b}(\mathbf{x}_o) & \text{on } \partial\Omega. \end{cases} \qquad \text{(I-3-23)}$$

Further the Green's tensor $G_{\gamma\beta}(\mathbf{x};\mathbf{x}_o)$ satisfies (I-3-21) as shown above. We wish to apply the generalized Green's theorem (I-2-36) to the solution $\mathbf{u}(\mathbf{x}_o)$ and the fundamental solution $G_{\gamma\beta}(\mathbf{x};\mathbf{x}_o)$. For this purpose we need a few preliminary remarks.

First, just as $G_{km}(\mathbf{x};\mathbf{x}_o)$ is the k^{th} component of displacement generated at $\mathbf{x}$ by an impulsive force acting at $\mathbf{x}_o$ in the m^{th} direction, similarly the space-like tensor

$$G_{ijm}(\mathbf{x};\mathbf{x}_o) = C_{ijk\ell}G_{km,\ell} \qquad \text{(I-3-24)}$$

will be the (i,j) component of stress associated with this displacement.

Next, if we assume that the Green's tensor is causal--that is, $G_{\alpha\beta}(\mathbf{r},t;\mathbf{r}_o,t_o) \equiv 0$ for $t < t_o$ -- then the upper limit on the time integrals appearing in (I-2-36) can be changed to $t^+ > t$. An upper bound t^+ is used instead of t to insure that the integration be performed over the closed interval $[t_1,t]$, in particular allowing $t_o = t$. (Clearly all operations will be carried with respect to the source coordinates, the receiver coordinates acting as parameters.) For simplicity we shall assume that $t_1 = 0$.

Third, by reference to the systems (I-3-21) and (I-3-23) , and by the definition of the tensor $\Delta_{\alpha\beta}$ given in (I-3-6) we have

$$\int_\Omega u_\alpha \left(\mathscr{L}^{*o}_{\alpha\gamma} G_{\gamma\beta}\right) d^4x(o) = \begin{cases} 0 & \text{if } \mathbf{x} \notin \Omega \\ 4\pi u_\beta(\mathbf{x}) & \text{if } \mathbf{x} \subset \Omega \end{cases}$$

and

$$\int_\Omega \left(\mathscr{L}^{o}_{\alpha\gamma} u_\gamma\right) G_{\alpha\beta}\, d^4x(o) = \int_\Omega \rho f_\alpha G_{\alpha\beta}\, d^4x(o) \qquad \text{. (I-3-25)}$$

Last, because the tensor $G_{\alpha\beta}$ and the vectors u_α and f_α are all purely space-like, we may now restrict the range of the indices to (1,2,3) and thus use Latin subscripts.

Then, applying Green's theorem in the form (I-2-36), we obtain in component form

$$4\pi u_m(\mathbf{x}) = \int_\Omega \rho f_i(\mathbf{x}_o)\, G_{im}(\mathbf{x};\mathbf{x}_o)\, d^4x^{(o)}$$

$$+\int_o^{t^+} dt_o \int_{S(t_o)+\Sigma(t_o)} \left\{ \left(\sigma_{ij} + \rho \frac{\partial u_i}{\partial t_o} U_j\right) n_j [\![G_{im}]\!] - \left(G_{ijm} + \rho \frac{\partial G_{im}}{\partial t_o} U_j\right) n_j [\![u_i]\!] \right\} da^{(o)}$$

$$+\int_o^{t^+} \frac{d}{dt_o} \int_{V(t_o)} \left(\rho u_i \frac{\partial G_{im}}{\partial t_o} - \rho G_{im} \frac{\partial u_i}{\partial t_o}\right) d^3x^{(o)}\, dt_o$$

(I-3-26)

Here according to the conventions of section I-2, $S(t_o)$ represents the external boundary of $V(t_o)$ and $\Sigma(t_o)$ an internal surface of discontinuity oriented by an arbitrary choice of its unit normal direction. The jump notation $[\![F]\!]_\Sigma$ represents the difference between the limiting values of F when Σ is approached from the positive and negative side successively. On an external boundary the jump will be taken as the value of F when S is approached from within V. We must emphasize again that all operations appearing in the various integrands of (I-3-26), including the computation of the stress

tensor, are performed with respect to the source coordinates.

For convenience let us rewrite (I-3-26) as

$$4\pi u_m(\mathbf{x}) = 4\pi u_m^{(p)} + 4\pi u_m^{(b)} + 4\pi u_m^{(i)} \quad . \qquad \text{(I-3-27)}$$

We shall refer to (I-3-26) as the formal Green's tensor solution to the elastic problem. At this point we have not made explicit use of the boundary conditions in systems (I-3-21) and (I-3-23) , and (I-3-26) is an integral equation in $\mathbf{u}$ if $\mathbf{G}$ is given as a fundamental solution.

To understand the nature and mechanics of Green's tensor solutions, we shall now analyze the formal equation (I-3-26) in greater detail. Two important questions are raised: 1) if $\mathbf{u}$ satisfies (I-3-26) , does it satisfy the linearized equation of motion (I-3-1) ? and 2) how are the boundary conditions satisfied by use of this formalism?

To answer these questions, let us operate with $\mathscr{L}$ <u>at the receiver point</u> $\mathbf{x}$ on both sides of (I-3-27) . Because in (I-3-26) $\mathbf{x}$ is treated as a parameter, the operation of the elastic operator can be carried directly on the integrands. The only function depending on $\mathbf{x}$ is the Green's tensor and we know that

$$\mathscr{L}_{\alpha\gamma}\, G_{\gamma\beta} = \Delta_{\alpha\beta}(\mathbf{x}; \mathbf{x}_o) \quad .$$

Thus we can operate with $\mathscr{L}$ successively on the three terms that make up the right-hand side of (I-3-27). Operating on the first term,

one gets immediately

$$\mathscr{L}\mathbf{u}^{(p)} = \rho \mathbf{f} \quad . \tag{I-3-28}$$

This shows that $u_m^{(p)}$ is a particular solution of the inhomogeneous equation. We therefore expect the additional terms to satisfy the homogeneous equation. From equation (I-3-26) it is clear that $u_m^{(p)}$ is a weighted superposition of fundamental solutions, or impulse responses, where the weighting function is the body force distribution. This observation has led in various cases to the terminology of "influence function" to denote the Green's function, in particular in connection with electrostatic theory (e.g., Morse and Feshbach, 1953).

We may note at this point that if the boundary conditions imposed upon the solution in system (I-3-23) are homogeneous, then since the Green's tensor satisfies the adjoint system, by definition $u_m^{(b)}$ and $u_m^{(i)}$ vanish identically and $u_m(\boldsymbol{\chi}) = u_m^{(p)}(\boldsymbol{\chi})$. Their presence is thus intimately related to the presence of inhomogeneous conditions. Furthermore, when the body force density $\mathbf{f}$ vanishes identically, only $u_m^{(b)}$ and $u_m^{(i)}$ are present, and must therefore satisfy the homogeneous equation.

We now turn our attention to the second term in (I-3-27) , namely $u_m^{(b)}$. From equation (I-3-26) we see that the application of $\mathscr{L}$ at the point $\boldsymbol{\chi}$ upon $u_m^{(b)}$ will yield a non-zero answer only if $\boldsymbol{\chi}$ belongs to a boundary (external or internal) of the volume $V(t_o)$. Thus $u_m^{(b)}$ satisfies the homogeneous equation $\mathscr{L}\mathbf{u}^{(b)} = 0$ at every point within the valume $V(t_o)$. Since the integration is

performed over all the boundaries of $V(t_o)$, the boundary conditions imposed on u and on the Green's tensor can be used explicitly to compute $u_m^{(b)}$. For brevity we shall confine our discussion to the two fundamental kinds of boundary conditions usually encountered in elastic problems. We shall use the terminology of Kupradze (1963).

For boundary value problems of the first kind, the displacement jump $\left[\!\left[u_i(\mathbf{r}_o, t_o) \right]\!\right]_{S(t_o)+\Sigma(t_o)}$ is specified. The Green's tensor then satisfies the adjoint homogeneous condition

$$\left[\!\left[G_{im}(\mathbf{x}\,;\,\mathbf{x}_o) \right]\!\right]_{S(t_o)+\Sigma(t_o)} = 0 \quad ,$$

and we have

$$4\pi u_m^{(b)}(\mathbf{x}) = -\int_o^{t^+} dt_o \int_{S(t_o)+\Sigma(t_o)} \left(G_{ijm} + \rho \frac{\partial G_{im}}{\partial t_o} U_j \right) n_j \left[\!\left[u_i \right]\!\right] da^{(o)} \qquad \text{(I-3-29)}$$

where the integrand is known, so that we can compute $u_m^{(b)}(\mathbf{x})$. Similarly for boundary value problems of the second kind, the quantity $\left(\sigma_{ij} + \rho \frac{\partial u_i}{\partial t_o} U_j \right) n_j$ is to be specified on the boundary. Then the Green's tensor satisfies the adjoint homogeneous condition $\left(G_{ijm} + \rho \frac{\partial G_{im}}{\partial t_o} U_j \right) n_j = 0$ on the boundary and we have in that case

$$4\pi u_m^{(b)} = \int_o^{t^+} dt_o \int_{S(t_o)+\Sigma(t_o)} \left(\sigma_{ij} + \rho \frac{\partial u_i}{\partial t_o} U_j \right) n_j \left[\!\left[G_{im} \right]\!\right] da^{(o)} \qquad \text{(I-3-30)}$$

Here again the integrand is known.

Thus we see that by using the boundary conditions imposed upon the Green's tensor we have deleted all unknown quantities from the integrand in the second term of (I-3-26) . (Mixed boundary conditions can be handled in an identical fashion.) However, this does not furnish a complete answer to the question raised above. Does the field $u_m^{(b)}(\mathbf{x})$ take the correct boundary value as the point $\mathbf{x}$ approaches the boundary? The answer to this question is difficult to obtain. Morse and Feshbach (1953) present a rather heuristic discussion for the scalar case. Kupradze (1963), working in the frequency domain, proves that it is true for the elastic equation in the case of stationary boundaries and of an homogeneous isotropic matrix with homogeneous isotropic inclusions. He uses the theory of multidimensional singular integral equations, and obtains the answer as a consequence of generalized Tauberian theorems. For our present purposes we shall assume the answer to be true, without proof. A complete proof for the case of growing boundaries remains an outstanding problem of the theory.

In a last step we discuss the last term $u_m^{(i)}$. It was pointed out in section I-2 that this term is to be understood in the sense of a Stieltjes integral, that is

$$4\pi u_m^{(i)} = \int_o^{t^+} dF_m(t_o) \quad ,$$

where

$$F_m(t_o) = \int_{V(t_o)} \left(\rho u_i \frac{\partial G_{im}}{\partial t_o} - \rho G_{im} \frac{\partial u_i}{\partial t_o} \right) d^3x(o) \quad ,$$

so that we need only take into account such times t_o where $F(t_o)$ presents a discontinuous behavior. For the sake of simplicity we shall assume that F_m is continuous on $[o,t^+]$, so that

$$4\pi u_m^{(i)}(\mathbf{x}) = F_m(t^+) - F_m(0) \quad . \qquad \text{(I-3-31)}$$

However, we assumed the Green's tensor to be causal so that it vanishes at $t_o = t^+$ along with its derivative. Thus

$$4\pi u_m^{(i)}(\mathbf{x}) = \int_{V(o)} \left[\rho G_{im} \frac{\partial u_i}{\partial t_o} - \rho u_i \frac{\partial G_{im}}{\partial t_o} \right]_{t_o=0} d^3x(o) \quad . \qquad \text{(I-3-32)}$$

It is now apparent that $u_m^{(i)}$ depends explicitly on the initial conditions of the problem. Furthermore, if we apply the operator $\mathscr{L}$ at $\mathbf{x}$ throughout, it can be applied directly on the integrand on the right-hand side, and operates only upon the Green's tensor. The delta function $\delta(t - t_o)$ and its derivative $\frac{\partial}{\partial t_o}\delta(t - t_o)$ are thus generated, and $u^{(i)}$ is a solution of the homogeneous equation

$\mathscr{L}\mathbf{u}^{(i)} = 0$ except at $t = t_o = 0$. Here again, when the initial conditions are specified, the integrand of (I-3-32) is known.

Thus, whereas the formal Green's function solution (I-3-26) is in the form of an integral equation in $\mathbf{u}$ (multidimensional, and singular, as pointed out by Kupradze, 1963), when boundary and initial conditions are specified, all unknown terms disappear from the various integrands. Then the solution $u_m(\mathbf{x})$ is obtained by simple evaluation of the integrals; this combination of the formal Green's tensor solution with the limiting conditions is called the Green's tensor solution of the problem.

iii) Discussion

Having just derived the formal Green's tensor solution, we are now faced with the next logical step which is to construct the Green's tensor itself. Unfortunately, in most cases we shall not be able in general to take that step!

The existence and the dyadic nature of the Green's tensor are discussed, for example, by Morse and Feshbach (1953, chapters 7 and 11). But because there are two wave velocities in an homogeneous isotropic elastic medium--the compressional and shear wave velocities--the determination of the Green's tensor for particular problems is often extremely arduous, or impossible. Morse and Feshbach (chapter 11) present a general formalism by which the Green's tensor can theoretically be obtained. In practice, even if it can be found, its use in computing the solution is often cumbersome and will necessitate numerical integration techniques.

For inhomogeneous media, the questions of existence and uniqueness of the solution to elastic problems have been investigated by Kupradze (1963). Working in the frequency domain, this author shows that the elastic boundary value problem has a unique solution in a composite medium (made up of an homogeneous isotropic matrix containing homogeneous isotropic inclusions). This is done for a variety of boundary conditions at the boundary between matrix and inhomogeneities. By use of the Green's tensor formulation he shows the complete equivalence of the elastic boundary value problem with the solution of a multidimensional singular integral equation analogous to (I-3-26) . Finally, he describes how to obtain the solution by a numerical scheme. Kupradze restricts himself to monochromatic stationary sources. Thus for separable sources (Archambeau, 1968), the transient problem can be solved by a simple convolution in the time domain, or a multiplication in the frequency domain. For nonseparable sources, such as the sources presented in Chapter IV, one has to expand the radiation field in multipolar form and use a different excitation function for each multipole, since the multipole coefficients are independent functions of frequency (Archambeau, 1968).

For the case of anisotropic media the problem becomes even more complex. There are three real wave velocities in aeolotropic media (e.g., Love, 1927). Further, these wave velocities are functions of the direction of propagation. Lifchitz and Rosentsveig (1947) derive the Green's tensor for the equations of static equilibrium in an aeolotropic medium and point out that even in this particular case, the result is very complicated.

A large number of questions, on the other hand, can be answered without specific knowledge of the Green's tensor. In Chapter II, we shall show how the formalism leading to the formal Green's tensor solution permits us to investigate general, but fundamental, properties of the radiation field generated by a seismic source. However, a few additional properties of the Green's tensor can be discussed now. Because it is the only practical case of interest, we shall assume for the remainder of this section that the material within $V(t_o)$ is homogeneous. In that case the Green's tensor satisfies

$$C_{\alpha\beta\gamma\delta} \frac{\partial}{\partial x_\beta} \frac{\partial}{\partial x_\delta} G_{\gamma\mu} = \Delta_{\alpha\mu} \quad . \qquad \text{(I-3-33)}$$

Two observations can be made about (I-3-33). First, we note that for the infinite domain the equation is invariant under translation and the Green's tensor is function only of $(\boldsymbol{\chi} - \boldsymbol{\chi}_o)$. We can thus choose the origin of coordinates at the source point $\boldsymbol{\chi}_o$. The second observation is then that the right-hand side is an homogeneous function of the receiver's coordinates, of degree -4, since $\delta(a\boldsymbol{\chi}) = a^{-4}\delta(\boldsymbol{\chi})$. Thus since the left-hand side is a linear combination of second derivatives of $G_{\alpha\mu}$, we can state that: for the infinite homogeneous domain, the Green's tensor is a homogeneous function of degree -2 of the relative coordinates $x^*_\alpha = x_\alpha - x^{(o)}_\alpha$.

Now the Green's tensor for the infinite domain and that for any particular problem both are fundamental solutions of the elastic operator with pole at $\boldsymbol{\chi}_o$. Therefore, they differ only by a regular

solution of the homogeneous equation. This means in particular that for a homogeneous medium, any Green's tensor behaves asymptotically as the Green's tensor for the infinite domain as $|\mathbf{x} - \mathbf{x}_o| \to 0$.

One especially important case is that where the medium is further simplified and is assumed to be homogeneous and isotropic. We shall denote the Green's tensor for the infinite domain in that case by $\Gamma_{\alpha\beta}(\mathbf{x}; \mathbf{x}_o)$ and because of its particular importance, we shall often refer to it as the fundamental solution for the unlimited isotropic homogeneous medium. In view of the foregoing discussion, it is worthwhile to enumerate several particular properties of $\Gamma_{\alpha\beta}$, in particular:

1) Γ is a homogeneous function of degree -2 of the relative coordinates $x^*_\alpha = x_\alpha - x^{(o)}_\alpha$.

2) Because of the isotropy, Γ depends, in fact, on $r^* = |r - r_o|$ and on $t^* = t - t_o$; furthermore, $\Gamma_{\alpha\beta} = \Gamma_{\beta\alpha}$ (e.g., Maruyama, 1963).

3) Any Green's tensor in a homogeneous isotropic medium may be written

$$G_{\alpha\beta} = \Gamma_{\alpha\beta} + g_{\alpha\beta} \quad , \tag{I-3-34}$$

where $g_{\alpha\beta}$ is a regular solution of the homogeneous equation (e.g., Morse and Feshbach, chapter II, 1953).

4) Any Green's tensor in a homogeneous isotropic medium will

behave asymptotically as $\Gamma_{\alpha\beta}$ in the vicinity of the pole $\boldsymbol{\chi}_o$ (e.g., Kupradze, 1963).

5) When expressed in the frequency domain, it reduced in the limit of zero frequency to the classical Somigliana tensor of elastostatics (e.g., Ben Menahem and Singh, 1968).

For completeness, let us give Γ_{mk} explicitly (e.g., Maruyama, 1963).

$$\Gamma_{mk}(r^*,t^*) = \frac{1}{\rho}\left\{\left(\frac{1}{r^*}\right)_{,mk} \int_{r^*/V_p}^{r^*/V_s} \tau\, \delta(t^* + \tau)\, d\tau \right.$$

$$+ \frac{1}{r^*} r^*_{,m} r^*_{,k} \left[\frac{1}{V_p^2}\, \delta\left(t^* + \frac{r^*}{V_p}\right) - \frac{1}{V_s^2}\, \delta\left(t^* + \frac{r^*}{V_s}\right)\right]$$

$$\left. + \delta_{mk} \frac{1}{r^*}\left[\frac{1}{V_s^2}\, \delta\left(t^* + \frac{r^*}{V_s}\right)\right]\right\} \qquad \text{(I-3-35)}$$

where V_p and V_s are the P-wave and S-wave velocities respectively.

The most important of the properties enumerated above is the third one. Indeed, $\Gamma_{\alpha\beta}$ represents the impulse response of the unlimited medium, and in any limited domain, for $|\boldsymbol{\chi} - \boldsymbol{\chi}_o|$ small enough, the response is intuitively expected to be the same (cf. property 4). However, $\Gamma_{\alpha\beta}$ will not satisfy the proper boundary conditions to qualify as a Green's tensor. The perturbation $g_{\alpha\beta}$ is introduced precisely so that $G_{\alpha\beta}$ should satisfy the required boundary conditions. Since $\Gamma_{\alpha\beta}$ is known, the perturbation can be obtained for geometries

with sufficient symmetry as an eigenfunction expansion. If the perturbation can be shown to be small, it can also be obtained by a perturbation series (see any textbook on scattering theory for that purpose).

In seismic source theory we shall be concerned with an infinite medium containing an internal boundary of small dimensions, such as a small cavity. If $\mathbf{x}_o$ is not on this boundary, $g_{\alpha\beta}$ then represents the field superposed onto $\Gamma_{\alpha\beta}$ to account for the presence of the boundary; it represents the scattered field.

Methods for constructing the Green's tensor $G_{\alpha\beta}$ largely depend on the particular problem at hand. We shall enumerate a few:

1) Solution of an integral equation
2) Method of images
3) Eigenfunction expansion
4) Transform methods
5) Mapping in the complex plane
6) Perturbation methods

A description of these various techniques would obviously take us too far from the goals of this discussion. We shall, therefore, refer the reader to the literature, where abundant examples can be found for scalar cases in particular (e.g., Stakgold, 1968; Morse and Feshbach, 1953; Courant and Hilbert, 1937; Maruyama, 1963; Haskell, 1964). A large number of solutions to the elastic problem in a half-space have also been compiled by Johnson (1973).

I-4 Green's function solution to the scalar wave equation - Potentials.

We shall consider in this section the particular case of a homogeneous isotropic elastic medium. In this case, the tensor $C_{ijk\ell}$ depends only on the Lamé constants λ and μ. The equation of motion (I-2-11) becomes then

$$\rho \frac{\partial^2 u_i}{\partial t^2} = (\lambda + \mu)\, u_{k,ki} + \mu\, u_{i,kk} + \rho f_i \qquad \text{(I-4-1)}$$

We now define four scalar potentials χ_α, $\alpha = 1,\ldots,4$ in the usual fashion

$$\chi_i = \frac{1}{2}\, \varepsilon_{ijk}\, u_{k,j} \quad ; \quad \chi_4 = u_{\ell,\ell} \qquad \text{(I-4-2)}$$

so that χ_i, $i = 1,2,3$ are the cartesian components of the rotation vector potential, and χ_4 is the dilatation. Then, by taking successively the curl and the divergence of (I-4-1), we find that these potentials satisfy the scalar wave equations

$$\frac{1}{c_\alpha^2} \frac{\partial^2 \chi_\alpha}{\partial t^2} - \nabla^2 \chi_\alpha = q_\alpha \quad , \qquad \text{(I-4-3)}$$

where $c_i = V_s$, $i = 1,2,3$, and $c_4 = V_p$, -- V_s and V_p are the S- and P-wave velocities. The forcing term is given by

$$q_i = \frac{\rho}{2V_s^2} \varepsilon_{ijk} f_{k,j} \quad , \quad i = 1,2,3 \quad , \text{ and } \quad q_4 = \frac{\rho}{V_p^2} f_{\ell,\ell} \quad .$$

The Green's function solution to the scalar wave equation is then obtained by exactly the same procedure as was used in sections I-2 and I-3. The generalized Green's theorem for the wave operator $\Box = \frac{1}{c^2} \frac{\partial}{\partial t^2} - \nabla^2$ can be written in a form parallel to (I-2-36)

$$(\Box \phi, \psi)_\Omega = (\phi, \Box \psi)_\Omega$$

$$+ \int_{t_1}^{t_2} dt \int_{S(t)+\Sigma(t)} \left[\!\!\left[\phi \left(\psi_{,i} + \frac{1}{c^2} \frac{\partial \psi}{\partial t} U_i \right) n_i \right.\right.$$

$$\left.\left. - \psi \left(\phi_{,i} + \frac{1}{c^2} \frac{\partial \phi}{\partial t} U_i \right) n_i \right]\!\!\right] da$$

$$+ \frac{1}{c^2} \int_{t_1}^{t_2} \frac{d}{dt} \int_{V(t)} \left(\psi \frac{\partial \phi}{\partial t} - \phi \frac{\partial \psi}{\partial t} \right) d^3x \, dt \qquad \text{(I-4-4)}$$

Further, the Green's function $G_\alpha(\mathbf{r},t;\mathbf{r}_o,t_o)$ satisfies the equation

$$\frac{1}{c_\alpha^2} \frac{\partial^2 G_\alpha}{\partial t^2} - \nabla^2 G_\alpha = 4\pi \, \delta(\mathbf{r} - \mathbf{r}_o) \, \delta(t - t_o) \quad . \qquad \text{(I-4-5)}$$

By combination of (I-4-4) and (I-4-5) and noting that the wave

operator is formally self-adjoint, we obtain the formal Green's function solution in a form analogous to (I-3-26)

$$4\pi\,\chi_\alpha(\mathbf{r},t) = \int_o^{t^+} dt_o \int_{V(t_o)} q_\alpha(\mathbf{r}_o,t_o)\, G_\alpha(\mathbf{r},t;\,\mathbf{r}_o,t_o)\, d^3x^{(o)}$$

$$+ \int_o^{t^+} dt_o \int_{S(t_o)+\Sigma(t_o)} \left[\!\!\left[G_\alpha \left(\nabla_o \chi_\alpha + \frac{1}{c_\alpha^2} \frac{\partial \chi_\alpha}{\partial t_o} \mathbf{U} \right) \right.\right.$$

$$\left.\left. - \chi_\alpha \left(\nabla_o G_\alpha + \frac{1}{c_\alpha^2} \frac{\partial G_\alpha}{\partial t_o} \mathbf{U} \right) \right]\!\!\right] \cdot \hat{n}\, da^{(o)}$$

$$+ \frac{1}{c_\alpha^2} \int_o^{t^+} \frac{d}{dt_o} \int_{V(t_o)} \left(\chi_\alpha \frac{\partial G_\alpha}{\partial t_o} - G_\alpha \frac{\partial \chi_\alpha}{\partial t_o} \right) d^3x^{(o)}\, dt_o$$

(I-4-6)

In the case of stationary boundaries this result reduces to the usual form of the formal Green's function solution (e.g., Morse and Feshbach, 1953). The discussion of the effects of boundary values and initial values is completely parallel to the discussion presented in section I-3 and will not be repeated here.

Just as in the case of the vector wave equation, the last term in (I-4-6) is to be understood in the sense of a Stieltjes integral. Its evaluation in specific cases will be presented in Chapter II.

Conclusions

We have shown in this chapter how the generalized transport theorem leads to both the usual conservation equations in continuum mechanics, and to the various "jump" conditions to be satisfied at flow discontinuities. The same theorem was applied again to derive the final form of Green's theorem in linear elasticity; thus it was used specifically in the formulation of the formal Green's tensor solution in elastodynamics. We now have a powerful tool to solve a wide variety of elastodynamic problems. The specific solution will be obtained if the Green's tensor can be found. When this is not the case, the nature and the properties of the solution may still be investigated in many instances, by use of this formalism. Specific applications will be found in the subsequent chapters.

However, we must point out a limitation of the present theory: the velocity $\mathbf{U}$ of the boundary Σ, appearing in (I-3-26) and (I-4-6) has been supposed known, and is treated as a parameter of the problem (instead of an unknown). As was pointed out in section I-1 when we discussed the conservation of energy, the problem of solving for $\mathbf{U}$ is fundamentally an energy problem, and can be described as the generalized problem of Stephan. Caslaw and Jaeger (1959) point out that it is a nonlinear problem even in the simplest case of one-dimensional heat conduction. This means that it does not afford a Green's function solution. In fact, only the linearized heat conduction equation, in a medium with stationary boundaries, can be solved using a Green's function. This is done in various textbooks (e.g., Stakgold, 1968).

We shall therefore be obliged either to assume the evolution of the boundaries to be known, or to determine this evolution on the basis of another criterion, independent of the Green's function formalism. A more complete discussion of this question will be given in Chapter III.

Chapter II

FAILURE AS AN INITIAL AND BOUNDARY VALUE PROBLEM

Introduction

The purpose of this chapter is to link some of the physical characteristics of a failure process in a prestressed medium with appropriate mathematical formulations of the problem. In particular, we shall emphasize the fundamental similarities as well as differences between initial value and boundary value problems. An apparently rather trivial result is that, for a problem with a unique solution, two different mathematical formulations are totally equivalent. However, for reasons of simplicity or convenience, one is often led to make some approximations in computing the solutions. Obviously, it is desirable to make those approximations which afford some physical justification, rather than arbitrary ones. Thus, by choosing the adequate mathematical formulation and by making well founded approximations, it is possible to emphasize a particular physical characteristic of the phenomenon at the expense of another one. For example, we shall be able to exhibit in a simple fashion the effect of a bounded prestressed zone, but in order to achieve simplicity we shall neglect the scattered fields generated by the rupture zone itself: we shall make the source "transparent."

The spontaneous (or induced) failure of an elastic material can be basically modelled by the creation of a new (internal) boundary within the medium. Appropriate boundary conditions are then required

along this boundary. For this reason one is easily led to treat the elastic radiation problem as a boundary value problem. The simplest kinematical representation of the radiation field is then obtained by specifying the displacement time function on the rupture boundary. This method leads to the dislocation representation widely used in the seismological literature (e.g., Haskell, 1964; Aki, 1967; Savage, 1966). A dynamical approach consists of specifying traction conditions on the rupture boundary. For example, if the shear tractions are to vanish, one can apply on the boundary a set of tractions cancelling exactly those generated by the prestress (e.g., Burridge and Alterman, 1972). This method is particularly appropriate to the modelling of an underground explosion by creation of a pressurized cavity (e.g., Haskell, 1967).

But a third approach--also a dynamical one--is to recognize that the introduction of the rupture changes the equilibrium configuration of the medium so that, upon creation of the rupture zone, the medium finds itself away from equilibrium. This approach clearly leads to an initial value formulation of the radiation problem, where the medium evolves dynamically towards its new equilibrium configuration according to the elastic equations of motion (e.g., Archambeau, 1964; Randall, 1966).

We shall see in this chapter how and under what conditions the three approaches described are equivalent. We shall also point out their respective merits and drawbacks. For these purposes the Green's tensor formalism developed in the preceeding chapter will prove particularly convenient.

Our approach will be to consider first the elementary mass-spring system in order to clarify the ideas proposed above. The next step will be to generalize the results to the case of instantaneous failure in a three-dimensional elastic medium; at that point we shall discuss the possible approximations and simplifications. The extension of the theory to the case of a growing rupture zone will be made by use of scalar potentials. Finally, we shall investigate in greater detail the static limit of the problem.

II-1 Mechanics of the spring-mass system

Figure II-1-1 describes the elementary mechanical system constituted by a mass m suspended to a massless spring of constant k. We denote by x_f the equilibrium position of the mass under its own weight and by x_i the new equilibrium position it takes when force $F = k(x_i - x_f) = kL$ is applied.

Let us consider the elementary dynamical problem of the evolution of the system for positive time t, if the force F is suppressed instantaneously at time $t = 0$. The origin of the x-axis is understood to be chosen at the extremity of the unloaded spring, but the problem is evidently independent of this origin so that we can define the following relative displacements: y is measured with respect to x_f, and z is measured with respect to x_i. Clearly the problem can be expressed in terms of y only or in terms of z only. The geometry is described on figure II-1-1. The mass m, starting from the position x_i at $t = 0$ would end up at position

x_f if there was any dissipation in the system; however, we shall ignore dissipative phenomena here.

i) Solution for the displacement y

Consider the relative displacement y. For $t \leq 0$, it is constantly equal to L, and in the presence of any dissipation y would vanish after a long time. We are thus led to solve the initial value problem

$$\begin{cases} m\ddot{y} = -ky \\ y(0) = L \end{cases} \qquad \text{(II-1-1)}$$

which is the natural formulation of the plucked spring problem. Taking the Laplace transform of the equation we have

$$p^2\tilde{y} - pL = -\left(\frac{k}{m}\right)\tilde{y} \quad , \qquad \text{(II-1-2)}$$

where the initial value appears explicitly as a forcing term. From (II-1-2) we have

$$\tilde{y} = \frac{pL}{p^2 + k/m} \quad ,$$

and taking the inverse transform we obtain the solution

$$y(t) = L \cos\left(\sqrt{\frac{k}{m}}\, t\right) \quad . \qquad \text{(II-1-3)}$$

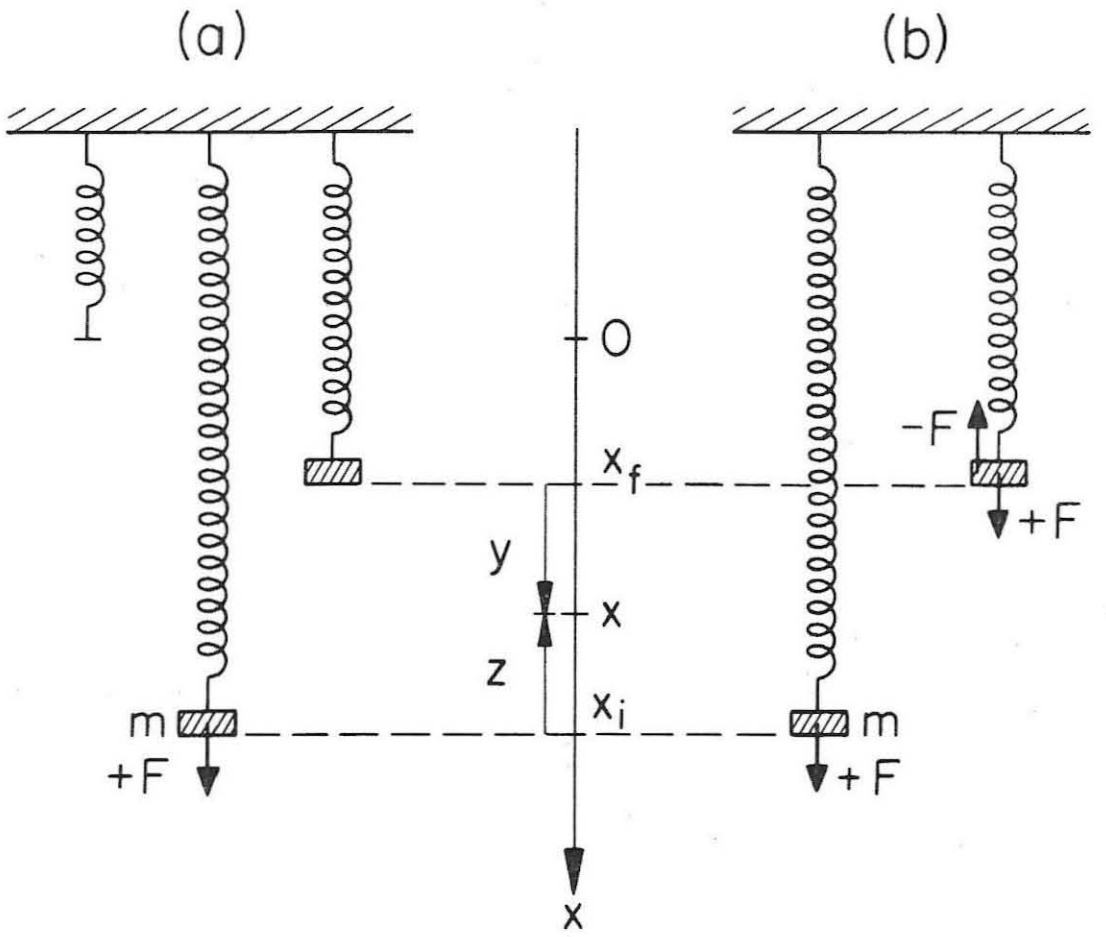

Figure II-1-1. The mass-spring system. a) initial value formulation, b) boundary value formulation. x is the displacement with initial value x_i and final value x_f . y and z are relative displacements, measured from x_f and x_i respectively.

ii) Solution for the displacement z

The relative displacement z vanishes identically for $t \leq 0$, and would converge to $-L$ after a long time in the presence of any amount of dissipation. For positive time z satisfies the equation

$$m\ddot{z} = -kz - kL\,H(t) \quad , \tag{II-1-4}$$

where $H(t)$ is a step function. In other words, the problem can be solved equally well by applying instantaneously, at time $t = 0$, a force $-F$ which cancels the force F. From this point of view we have a boundary value problem wherein a force is applied at the boundary $z = 0$. Taking the Laplace transform of (II-1-4) we get

$$p^2\tilde{z} = -\frac{k}{m}\tilde{z} - \frac{kL}{mp}$$

or

$$z = \frac{-kL/m}{p(p^2 + k/m)} \quad , \tag{II-1-5}$$

and, taking the inverse transform

$$z(t) = L\sqrt{\frac{k}{m}}\int_0^t \sin\left(\sqrt{\frac{k}{m}}\,\tau\right)d\tau$$

$$= L\left[1 - \cos\left(\sqrt{\frac{k}{m}}\,t\right)\right] \quad . \tag{II-1-6}$$

If we note that $y(t) - z(t) = L$ at all times, we see that (II-1-3) and (II-1-6) represent the same motion of the mass as a function of time and the two solutions are identical.

This elementary example shows the duality of the two points of view. If we choose the final equilibrium displacement x_f as the reference state for the problem, then the natural formulation to use is that of an initial value problem; on the other hand, if the chosen reference is the initial displacement x_i, then the natural formulation is that of a boundary value problem. One could also suggest a trivial third point of view, where the experimenter would guess the proper motion of the mass m, and impose it artifically, but this kinematical guess is of no physical interest.

We shall now generalize these simple ideas to the three-dimensional elastic problem. The problem treated above is really an elementary one, and its understanding poses no great challenge. On the other hand, a three-dimensional problem is not as easy to conceive and to comprehend. However, there is no fundamental difference between the concept of a one-dimensional elastic problem, and that of a three-dimensional problem. The main difficulty arises from the complexity of the analysis involved due, in part, to the fact that a three-dimensional problem depends on a greater number of parameters. But the basic attacks available are identical in nature to those described in this section. One of them will give rise to an initial value problem and will correspond to a stress relaxation phenomenon, another one will give rise to a boundary value problem, where forces are being applied on the rupture boundary.

II-2 Instantaneous failure in a prestressed elastic medium

We now turn to the description of a rupture phenomenon occurring in an elastic medium. A more complete discussion of the failure mechanism itself will be found in Chapter III. For our present purposes it is sufficient to assume that the material lying inside a closed surface Σ within the medium undergoes some transformation through which its physical properties are abruptly changed. To fix the ideas we may assume that within the rupture zone the material becomes unable to sustain shear stress. Other assumptions could be made which depend on the particular physical mechanism one wishes to model. The treatment given in this section is quite general and may be easily adapted to a wide variety of cases. We can thus formulate the problem as follows.

Consider a body made of an elastic homogeneous isotropic medium, bounded by a surface S (for the case of an unbounded medium, S recedes to infinity). We assume that this body is in a state of stress. The prestress $\sigma_{ij}^{(o)}$ is not assumed to have been generated by elastic loading of the body from some unstressed state, but is only required to satisfy, at all points, the static equations of equilibrium with some body force density f_i

$$\sigma_{ij,j}^{(o)} + \rho f_i = 0 \quad , \tag{II-2-1}$$

as well as some suitable boundary conditions on S . If S is a free surface, then on S

$$\sigma_{ij}^{(o)} \, n_j = 0 \qquad . \qquad \text{(II-2-2)}$$

We can further describe the configuration of the body by a displacement field $u_i^{(o)}$ (which could be arbitrarily defined to be zero everywhere). The virtual closed surface Σ shown on figure II-2-1 represents the boundary of the rupture zone before failure.

Let us now assume that failure occurs instantaneously within Σ at some instant of time which we may choose as $t = 0$ without loss of generality. To fix the ideas we shall consider the case where a cavity is created with boundary Σ . More complex cases with various rheologies of the material inside Σ may be handled in a similar fashion. After an infinite time, the body will reach a new state of equilibrium characterized by the fields $\sigma_{ij}^{(1)}$ and $u_i^{(1)}$. If we assume that, to first order, the density of externally applied body forces is left unchanged in the process (this is true to first order, for infinitesimal strains), then we have

$$\begin{cases} \sigma_{ij,j}^{(1)} + \rho f_i = 0 \\ \sigma_{ij}^{(1)} \, n_j = 0 \qquad \text{on } S \text{ and } \Sigma. \end{cases} \qquad \text{(II-2-3)}$$

The final field $\sigma_{ij}^{(1)}$ must satisfy new boundary conditions on Σ , whereas $\sigma_{ij}^{(o)}$ was only required to satisfy the equilibrium conditions there, since Σ was not a physical boundary.

We now make the important assumption that the material outside Σ

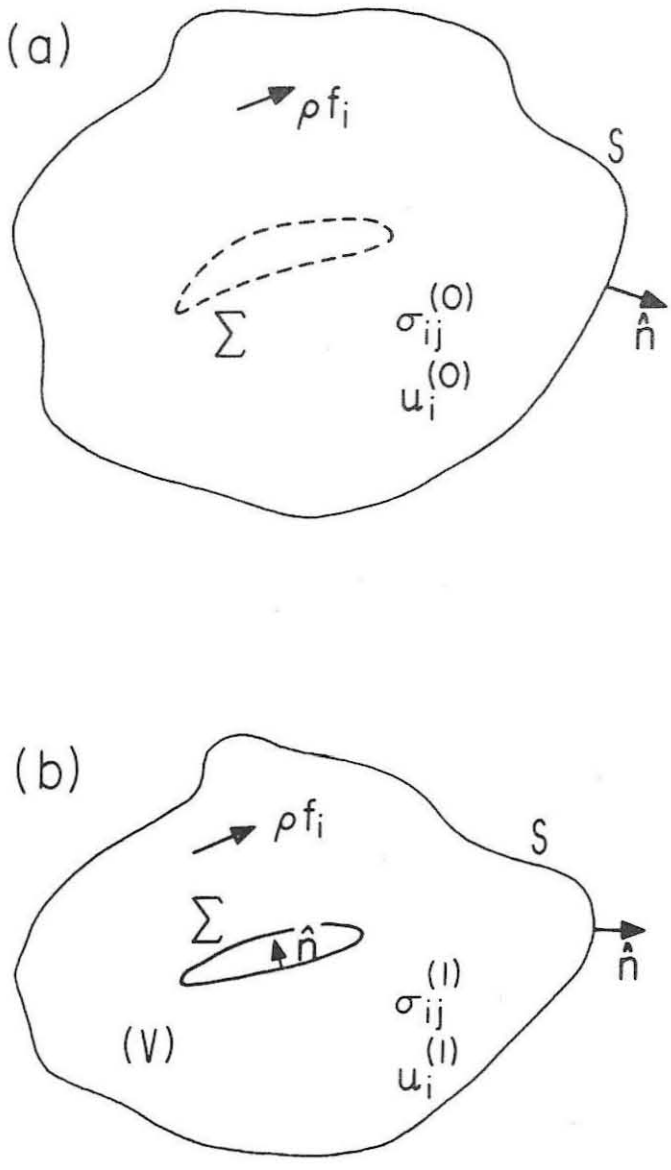

Figure II-2-1. Geometry of failure inside a body of volume V and surface S . a) before failure, b) after failure.
Σ is the failure surface.

goes from its initial equilibrium state to its final equilibrium state elastically. This implies that the relative static fields

$$\begin{cases} \sigma^{*}_{ij} = \sigma^{(o)}_{ij} - \sigma^{(1)}_{ij} \\ u^{*}_{i} = u^{(o)}_{i} - u^{(1)}_{i} \end{cases} \qquad \text{(II-2-4)}$$

are now related by the constitutive equation of linearized elasticity--Hooke's law. By subtraction of (II-2-1) and (II-2-3) we see that

$$\begin{cases} \sigma^{*}_{ij,j} = 0 \\ \sigma^{*}_{ij}\, n_j = 0 \qquad \text{on } S\,, \\ \sigma^{*}_{ij}\, n_j = \sigma^{(o)}_{ij}\, n_j \qquad \text{on } \Sigma\,. \end{cases} \qquad \text{(II-2-5)}$$

The evolution of the dynamic fields $u_i(\mathbf{r},t)$ and $\sigma_{ij}(\mathbf{r},t)$ will be governed by the equations of motion for the medium. However, in order to apply the linearized elastic equations of motion, one must use fields for which Hooke's law is valid. By comparison with the spring-mass problem discussed in the previous section, we are led to define the dynamic relative fields

$$\begin{cases} y_i = u_i - u^{(1)}_i \\ \tau_{ij} = \sigma_{ij} - \sigma^{(1)}_{ij}\,, \end{cases} \qquad \text{(II-2-6)}$$

and

$$\begin{cases} z_i = u_i - u_i^{(o)} \\ t_{ij} = \sigma_{ij} - \sigma_{ij}^{(o)} \end{cases} \quad . \tag{II-2-7}$$

The evolution of the medium for $t \geq 0$ can then be described by either one of the two systems:

$$\begin{cases} \dfrac{\partial^2 y_i}{\partial t^2} = \tau_{ij,j} \\ \tau_{ij}\, n_j = 0 \qquad \text{on } S\,, \\ \tau_{ij}\, n_j = 0 \qquad \text{on } \Sigma\,, \\ y_i(r,0) = u_i^*(r)\,;\ y_i(r,\infty) = 0 \end{cases} \quad . \tag{II-2-8}$$

or

$$\begin{cases} \dfrac{\partial^2 z_i}{\partial t^2} = t_{ij,j} \\ t_{ij}\, n_j = 0 \qquad \text{on } S\,, \\ t_{ij}\, n_j = -\sigma_{ij}^{(o)}\, n_j \qquad \text{on } \Sigma\,, \\ z_i(r,0) = 0 \quad ; \quad z_i(r,\infty) = -u_i^*(r) \end{cases} \quad . \tag{II-2-9}$$

The displacements y_i and z_i behave quite analogously to the displacements y and z encountered in the mass-spring problem of section II-1. From (II-2-8) the displacement y_i is clearly the solution of an

initial value problem. From (II-2-9) we see that z_i has an initial value of zero, but is caused by the application of tractions $-\sigma_{ij}^{(o)} n_j$ on the boundary Σ. As in the mass-spring problem, y_i and z_i differ only by a constant since $y_i - z_i = u_i^*$ so that the analogy is complete.

To investigate the differences between the two formulations in a more precise manner, we use the formal Green's function solution (I-3-26), specialized to the case of an instantaneous rupture with no initial particle velocity. Making use of the boundary and initial conditions in (II-2-8) and (II-2-9), and noting that the volume V is independent of time for $t > 0$ (see figure II-2-1), we get

$$4\pi y_m(r,t) = -\int_0^{t^+} dt_o \int_{S+\Sigma} G_{ijm}\, y_i\, n_j\, da^{(o)}$$

$$+ \int_V \rho\, u_i^* \left.\frac{\partial G_{im}}{\partial t_o}\right|_{t_o=0} d^3x^{(o)}$$

$$= 4\pi y_m^{(S)} + 4\pi y_m^{(\Sigma)} + 4\pi y_m^{(i)} \quad , \qquad \text{(II-2-10)}$$

and similarly

$$4\pi z_m(r,t) = -\int_0^{t^+} dt_o \int_S G_{ijm}\, z_i\, n_j\, da^{(o)}$$

$$-\int_0^{t^+} dt_o \int_\Sigma \left(G_{im}\, \sigma_{ij}^{(o)} - G_{ijm}\, z_i\right) n_j\, da^{(o)}$$

or

$$4\pi z_m = 4\pi z_m^{(S)} + 4\pi z_m^{(\Sigma)} \quad . \qquad \text{(II-2-11)}$$

So far $G_{im}(\mathbf{r},t;\mathbf{r}_o,t_o)$ may be any fundamental solution of the equations of motion and (II-2-10) and (II-2-11) can be considered to be integral equations in y and z respectively. However, for G_{im} to be the Green's tensor for the problem, it has to satisfy the following adjoint boundary conditions

$$G_{ijm}\, n_j = 0 \qquad \text{on } S \text{ and } \Sigma \; . \qquad \text{(II-2-12)}$$

In that case we obtain immediately the following solutions

$$4\pi y_m = 4\pi y_m^{(i)} = \int_V \rho\, u_i^* \left.\frac{\partial G_{im}}{\partial t_o}\right|_{t_o=0} d^3x^{(o)} \qquad \text{(II-2-13)}$$

and

$$4\pi z_m = 4\pi z_m^{(\Sigma)} = -\int_0^{t^+} dt_o \int_\Sigma G_{im}\sigma_{ij}^{(o)}\, n_j\, da^{(o)} \quad . \qquad \text{(II-2-14)}$$

These two equations corroborate precisely the claims made earlier about the respective properties of the solutions. In particular, y_m depends exclusively upon its initial value: at time $t = 0$ the medium finds itself away from equilibrium and starts evolving towards its equilibrium configuration. Following Archambeau (1964, 1968) we say that y_m is

the solution to a stress relaxation problem, and we shall call y_i and τ_{ij} the "relaxation fields." On the other hand, z_m represents the response of the medium to a set of tractions $-\sigma^{(o)}_{ij}\, n_j$ suddenly applied at $t = 0$ along the surface Σ. For this reason, we shall refer to it as the "stress-pulse" solution.

Finally, when the surface Σ is taken to the limit in which it envelopes zero volume, so that it is in fact made up of two sides Σ_+ and Σ_-, then we can treat Σ as a surface of discontinuity in displacement. In that case, from the formal Green's tensor solution (I-3-26) we see that (II-2-14) becomes

$$4\pi z_m = -\int_0^{t^+} dt_o \int_\Sigma \left[\!\left[G_{im} \right]\!\right]_\Sigma \sigma^{(o)}_{ij}\, n_j\, da^{(o)} \quad , \qquad \text{(II-2-15)}$$

where the jump figuring in the integrand could be obtained from knowledge of the Green's tensor. However, with this particular geometry, the natural boundary condition for the solution is expressed by the continuity of tractions $\left[\!\left[t_{ij}\, n_j \right]\!\right]_\Sigma = 0$. If one uses then a Green's tensor H_{im} satisfying the adjoint condition $\left[\!\left[H_{ijm}\, n_j \right]\!\right]_\Sigma = 0$, then the formal Green's tensor solution yields the integral equation in z_m

$$z_m = -\int_0^{t^+} dt_o \int_\Sigma \left[\!\left[z_i \right]\!\right]_\Sigma H_{ijm}\, n_j\, da^{(o)} \quad . \qquad \text{(II-2-16)}$$

We recognize in (II-2-16) the usual formula yielding the displacement field due to a Somigliana dislocation. This last equation is only

useful if the displacement jump $[\![z_i]\!]_\Sigma$ can be guessed, or observed. The use of dislocation theory has been widely used in seismology (e.g., Maruyama, 1963), but analytical computations are simple only in the case of a Volterra dislocation, where the displacement jump is constant over Σ . For more complex problems, one usually resorts to numerical techniques, where a relatively complex dislocation is modelled by juxtaposition of several "elementary" Volterra dislocations (e.g., Trifunac, 1973; Alewine and Jungels, 1973). This amounts to a discretization of the source, and can also be achieved by use of a finite element method for example (e.g., Jungels, 1973).

The solutions (II-2-13) , (II-2-14) and (II-2-16) are exact, provided that the Green's tensor can be found. But, as we pointed out in section I-3, such cases are rare, and therefore one resorts to approximations. These approximations are discussed in the next section.

II-3 Discussion of the solutions, and approximations

In order to evaluate the possible approximations to the solutions given in the preceding sections, we first write the Green's tensor as

$$G_{im} = \Gamma_{im} + g^{(S)}_{im} + g^{(\Sigma)}_{im} \quad , \tag{II-3-1}$$

in accordance with the discussion of section I-3. Here Γ_{im} is again the Green's function for the infinite domain, and the two other terms are regular solutions of the homogeneous equations of motion which satisfy certain boundary conditions. We required in equations (II-2-12) that the Green's tensor satisfy the following condition

$$G_{ijm}\, n_j = 0 \qquad \text{on } S \text{ and } \Sigma \ .$$

We therefore see that sufficient conditions for this to be satisfied are

$$\begin{cases} \dfrac{\partial^2 g^{(S)}_{im}}{\partial t^2} = g^{(S)}_{ijm,j} \\ \\ g^{(S)}_{ijm}\, n_j = \begin{cases} -\gamma_{ijm}\, n_j & \text{on } S \ , \\ 0 & \text{on } \Sigma \ , \end{cases} \end{cases} \tag{II-3-2}$$

and, similarly

$$\begin{cases} \dfrac{\partial^2 g_{im}^{(\Sigma)}}{\partial t^2} = g_{ijm,j}^{(\Sigma)} \\ \\ g_{ijm}^{(\Sigma)} n_j = \begin{cases} 0 & \text{on } S \ , \\ -\gamma_{ijm} n_j & \text{on } \Sigma \ . \end{cases} \end{cases} \qquad \text{(II-3-3)}$$

Here again, $g_{im}^{(S)}$ and $g_{im}^{(\Sigma)}$ are regular everywhere in V . Following the same argument, in the case where Σ envelopes no volume, since the tractions $\gamma_{ijm} n_j$ are continuous, we may write the Green's tensor appearing in (II-2-16) as

$$H_{im} = \Gamma_{im} + g_{im}^{(S)} \ . \qquad \text{(II-3-4)}$$

We now seek to answer the following question: Is it a reasonable approximation to use directly Γ_{im} --which is known--in the solutions (II-2-13) , (II-2-14) and (II-2-16) , instead of G_{im} or H_{im} which are considerably more difficult to get? In other words, when can we ignore the effects of $g_{im}^{(\Sigma)}$ and $g_{im}^{(S)}$, and what is the approximation involved?

The effect of $g_{im}^{(S)}$ is simpler to discuss. This term represents the effects of the external boundary of V . Thus, if we ignore it, the solution obtained will not contain the waves reflected from S , the surface waves along S , and the free oscillations of the body within S . In fact, when the radiation emanating from the source region is known, such contributions to the displacement field may be

evaluated separately by a number of well developed techniques (e.g., ray theory, mode theory). Further, for theoretical source investigations the body is generally taken to be unbounded and S recedes to infinity; in that case $g_{im}^{(S)}$ does not have to be introduced. In that case also the boundary condition at infinity must be a Sommerfeld radiation condition, with no incoming waves from infinity; this condition will be satisfied if we use Γ_{im} for the Green's function. From now on we shall choose this to be the case.

Discussion of $g_{im}^{(\Sigma)}$ is somewhat more subtle. We shall treat separately the three different approaches--dislocation, stress-pulse, and relaxation sources--by order of increasing complexity.

i) Dislocation sources

From equation (II-3-1) , we see immediately that there is no approximation involved in using Γ_{im} for the Green's tensor in the dislocation solution (II-2-16) , provided that the volume V is unbounded. This is a known result (e.g., Maruyama, 1963). Thus the dislocation solution provides an exact and accurate representation of the radiation field generated by a known history of displacement along an internal surface. The obvious drawback is that the history of slip is not known. It will depend on a large number of physical parameters upon which we have little or no control.

The multitude of published investigations which use dislocation theory in earthquake modeling makes it superfluous for us to discuss in detail the variety of possible dislocation models and their properties. The most popular model is that of a Volterra dislocation where a

displacement jump, constant over the whole surface of the dislocation, is created with a given time history. This time history is usually chosen to be a variation of a ramp function. A step function in time will intuitively yield an asymptotically correct solution at very low frequencies for most physical problems.

A relatively complete account of the results obtained from such models may be obtained from Maruyama (1963), Haskell (1964), and Savage (1966). Richards (1973) studies a more complex problem with a dislocation along an elliptic plane crack with friction. In this case, the displacement jump is a function of both the position on the crack surface, and of time. It is therefore a dynamical Somigliana dislocation (e.g., Maruyama, 1963). Alewine and Jordan (1973) show how the static dislocation theory can be coupled with numerical inversion techniques to explain the observations of "zero-frequency seismology." Finally, Jungels (1973) and Jungels and Frazier (1973) present a completely numerical approach to the problem, using a finite element method.

The principal success of dislocation theory in seismology is that its results may be put in a simple form. Also, dislocation sources can be easily investigated by use of point force equivalents, as discussed by Maruyama (1963) and Burridge and Knopoff (1964). This method furnishes a powerful method to model, to a first order approximation, gross properties of the radiation fields.

We shall see below the implications involved in using a Somigliana dislocation, where the (variable) jump in displacement is created instantaneously. We shall further show that this is equivalent to solving approximately an initial value problem (relaxation source).

ii) Stress-pulse sources

First of all, in the case of an infinite domain, the solution to the stress-pulse problem given in (II-2-11) reduces to the term $z_m^{(\Sigma)}$. Denoting by G_{im} the Green's function to the problem, we have

$$4\pi z_m = -\int_0^{t^+} dt_o \int_\Sigma G_{im}\sigma_{ij}^{(o)}\, n_j\, da^{(o)}$$

$$= -\int_0^{t^+} dt_o \int_\Sigma \left(\Gamma_{im}\sigma_{ij}^{(o)} - \gamma_{ijm}z_i\right) n_j\, da^{(o)} \quad , \tag{II-3-5}$$

where the second equality is obtained by use of (II-2-11).

As was pointed out earlier the second equality in (II-3-5) defines an integral equation, since the displacement z_m figures both on the left-hand side and in the integrand. The extra term appearing in the integrand when one uses Γ_{im} comes from the fact that this tensor does not satisfy the proper boundary conditions (II-2-12) on Σ. It is easy to see that one cannot, in general, neglect this extra term since in the limit where Σ encloses zero volume, this term gives the solution, in the form of a dislocation solution. The first term $\Gamma_{im}\sigma_{ij}^{(o)}$ does not give any contribution to the integral over $\Sigma_+ + \Sigma_-$ because it is continuous across the crack. One also sees that the Green's tensor G_{im} must have a non-vanishing jump across Σ for the first integral to take non-zero value in that case. But since Γ_{im} is continuous, this jump must come from the contribution $g_{im}^{(\Sigma)}$, according to (II-3-1). It is thus clear that $g_{im}^{(\Sigma)}$ cannot be

ignored and one may not use Γ_{im} , but rather one must determine the exact Green's tensor for the problem to use in the stress-pulse solution (II-2-14) .

The stress-pulse approach has been adopted by several authors because of its intuitive simplicity. However, these authors did not, in general, use directly the Green's tensor formalism.

The problem of a stress-pulse applied on the surface of a spherical cavity was treated by Jeffreys (1931) and his results are given also in Bullen (1963). For the case of a zero-volume rupture, Burridge and Halliday (1971) use a method derived from the Cagniard-de Hoop technique. The stress-pulse approach allows them to introduce dry friction on the fault surface in a relatively straightforward manner. However, they restrict their investigation to a two-dimensional situation. Richards (1973) extended such results to the case of a growing elliptic crack. Burridge and Alterman (1972) solved the problem of the self-similar growing spherical cavity by expanding the solution in a complete set of tensor spherical functions. These techniques yield solutions which are exact--or asymptotically exact in the high frequency limit--and they could, in fact, be used to generate the Green's tensor for the problem at hand.

Perhaps the most popular version of the stress-pulse approach is that of Brune (1970). This author constructed a simple two-dimensional model to study the generation of shear wave radiation by strike-slip motion. In that case the equations of motion take a very simple form very close to the rupture surface and can be integrated to compute the displacement in a vanishingly thin layer along that surface. The model

then reduces to a dislocation model and can be treated as such.

iii) Relaxation sources

If we use Γ_{im} in the relaxation solution (II-2-10), we get, for $t > 0$,

$$4\pi y_m = 4\pi y_m^{(\Sigma)} + 4\pi y_m^{(i)} = -\int_0^{t^+} dt_o \int_\Sigma \gamma_{ijm} y_i \, n_j \, da^{(o)}$$

$$+ \int_V \rho \, u_i^* \left. \frac{\partial \Gamma_{im}}{\partial t_o} \right|_{t_o=0} dv^{(o)} \qquad \text{(II-3-6)}$$

This is an integral equation in y_m. But we know that if G_{im} is the Green's tensor, so that $G_{ijm} \, n_j = 0$ on Σ, then

$$4\pi y_m = \int_V \rho \, u_i^* \left. \frac{\partial G_{im}}{\partial t_o} \right|_{t_o=0} dv^{(o)} \quad . \qquad \text{(II-3-7)}$$

Thus, the use of the infinite domain Green's tensor in (II-3-7) is equivalent to approximating y_m by $y_m^{(i)}$ in (II-3-6). We therefore seek to understand the nature of the terms $y_m^{(i)}$ and $y_m^{(\Sigma)}$ in order to evaluate the approximation. We know that $y_i = z_i + u_i^*$, which permits us to write

$$4\pi y_m^{(\Sigma)} = -\int_0^{t^+} dt_o \int_\Sigma \gamma_{ijm} \left(u_i^* + z_i \right) n_j \, da^{(o)} \quad . \qquad \text{(II-3-8)}$$

$y_m^{(i)}$ may be obtained by using (II-2-11) in this equation, we have

$$4\pi y_m^{(\Sigma)} = -4\pi z_m - \int_0^{t^+} dt_o \int_\Sigma \Gamma_{im} \sigma_{ij}^{(o)} n_j \, da^{(o)}$$

$$- \int_0^{t^+} dt_o \int_\Sigma \gamma_{ijm} u_i^* n_j \, da^{(o)} \quad ,$$

and now replacing z_m by $y_m - u_m^*$ we get

$$4\pi y_m^{(i)} = 4\pi u_m^* - \int_0^{t^+} dt_o \int_\Sigma \Gamma_{im} \sigma_{ij}^{(o)} n_j \, da^{(o)}$$

$$- \int_0^{t^+} dt_o \int_\Sigma \gamma_{ijm} u_i^* n_j \, da^{(o)} \quad . \qquad \text{(II-3-9)}$$

Since u_m^* does not depend on time, we see that the approximate solution $y_m^{(i)}$ is totally equivalent to a superposition of a "stress-pulse" field and a dislocation field. When Σ envelopes zero volume, only the dislocation field survives. Further, since u_i^* is time independent, in that case, $y_m^{(i)}$ is the field generated by the instantaneous creation at time $t = 0$ of a Somigliana dislocation along Σ. In addition, (II-3-8) shows that, in that case, $y_m^{(\Sigma)}$ represents that component of the radiation field which is specifically due to the departure from instantaneity in the creation of the dislocation.

We have thus proved that in the case of a very thin rupture zone,

the field y_m is the superposition of 1) the radiation field caused by the instantaneous creation of a Somigliana dislocation, and 2) a term which represents the additional radiation due to departures from instantaneity in the creation of the final displacement jump $[\![u_i^{(1)}]\!]$. This result holds for an instantaneous rupture occurring in an infinite domain. If Σ envelopes a non-zero volume, then the field $y_m^{(i)}$ contains, in addition, the radiation field caused by a stress-pulse applied instantaneously on Σ . These observations permit us to see in even greater detail the relationships between the three approaches considered in this section, and also to push the argument further, albeit in a somewhat more heuristic fashion.

From the definition (II-3-6) , the presence of the surface Σ manifests itself in the field $y_m^{(i)}$ only through the initial displacement u_i^* . $y_m^{(i)}$ is thus the radiation field that would be observed if the medium were given an initial displacement u_i^* , in the absence of Σ . The reason why the additional field $y_m^{(\Sigma)}$ must be introduced is precisely the continuous presence of Σ during the relaxation process. Thus, $y_m^{(i)}$ is the direct field generated by stress relaxation, and $y_m^{(\Sigma)}$ can be thought of as the field due to the interaction of $y_m^{(i)}$ and Σ : it is the scattered field that contains all the waves that are reflected, trapped, etc..., by Σ .

We shall define as a transparent source one which does not interact with the dynamic fields in its vicinity. In other words, when ignoring $y_m^{(\Sigma)}$ and thus approximating y_m by $y_m^{(i)}$, we are in effect making the rupture zone transparent. With reference to scattering theory, this is justified for waves with a wavelength greater than the source width,

and in particular in the long period limit.

The stress relaxation phenomenon may thus be described heuristically as follows. Consider an instantaneous rupture occurring at $t = 0$ in a stressed medium. A particle in this medium, located at some distance from the source, will not "know" about the rupture until a time such that elastic waves have reached it (whence the necessity of using a causal Green's tensor). At that time, the material point will "learn" that rupture has occurred, and therefore that it is away from its equilibrium position, and proceed to evolve towards it. In that process it will interact with the neighboring points and radiate elastic energy. The superposition of all the elementary fields thus generated will constitute the total radiation field due to the rupture, in a manner similar to that implied by Huyghens' principle. Part of the radiation will be directed towards the rupture surface and interact with it, thus creating a feedback to the rupture process: it is this interaction which is ignored when one makes the source transparent. We understand from this heuristic concept the reason why $y_m^{(i)}$ is expressed as a volume integral. In this approach, the seismic radiation has its source in the prestressed volume surrounding the rupture zone, not on the rupture surface.

This is not to say that this model does not involve a fault (Randall, 1966): the rupture zone and the physical processes involved in the rupture manifest themselves in a very precise and clear fashion through the initial value u_i^* . This initial field will depend both on the nature of the rupture mechanism, and also on the initial state of stress of the medium before rupture.

This last observation leads to the concept of a localized source region. The Earth is a finite body and is certainly not stressed uniformly. Even if we ignore the interaction of the radiation fields with the free surface (reflections, etc...), it is not necessary to model the Earth by an unbounded prestressed body. The calculation of the initial value u_i^* in a finite body is possible but is often a cumbersome one; such a calculation is hardly warranted in view of the many other approximations involved. In this work we shall resort to the following very crude approximation: u_i^* is computed for an infinite body, and then the volume integration is simply truncated at some distance from the rupture zone. This method is obviously not accurate, but will give us a qualitative idea of what to expect if the prestress zone is limited in size. A more complete discussion will be given in Chapter IV.

We have described three approaches to the instantaneous problem and have shown how they are really equivalent. Two of them--dislocation and stress-pulse--correspond to a boundary source on the rupture surface. The third one--relaxation--treats the source as a volume source, in which the radiated energy comes specifically from the region where it was stored before rupture, i.e., from the medium surrounding the failure zone.

Boundary sources are often advantageous because of their relative simplicity. However, we shall adopt in this study the relaxation model, in spite of its greater analytical complications, because it is related more directly to the physical phenomena associated with failure, and because the initial state of the medium is explicitly present in the

solution.

The relaxation model was adopted by Archambeau (1964, 1968) to model the seismic radiation caused by a sudden phase change within a prestressed medium. Randall (1966) attacks this problem from a somewhat more geometrical point of view. For the simple spherical geometry these authors get similar results (Randall, 1973). Both authors make use of the Green's function for the infinite domain, and thus assume the source to be transparent. Archambeau (1964) generalized the theory to include growing and propagating ruptures, and specialized the results to model the tectonic release associated with underground explosions in tectonically stressed regions (Archambeau, 1964, 1971; Archambeau and Sammis, 1970). However, for ruptures which do not grow self-similarly, Archambeau's attack leads to rather cumbersome algebra. Some of the work presented in the following chapters will yield results similar to his, but in a simpler analytical form. We shall also present in Chapter IV a new attack on the problem of a propagating rupture, which yields more complete results.

II-4) The case of a time-dependent boundary

We now turn our attention to a phenomenon of slightly greater complexity. Instead of assuming that the cavity considered in the previous section is created instantaneously at $t = 0$, we shall let it grow at a finite rate.

Following Archambeau (1964, 1968, 1971), we shall make use of the potentials defined in section I-4; these are the cartesian components of rotation and the dilatation. We shall compute them from the relaxation field y_m discussed in the previous sections. We denote by χ any one of these potentials, by c the wave velocity associated with it, then, by the formal Green's function solution (I-4-6) and by virtue of the discussion in the previous section, the relaxation field is given by

$$4\pi\chi(\mathbf{r},t) = \frac{1}{c^2}\int_o^{t^+} \frac{d}{dt_o} \int_{V(t_o)} \left[\chi \frac{\partial \Gamma}{\partial t_o} - \Gamma \frac{\partial \chi}{\partial t_o} \right] dv^{(o)}\, dt_o \quad . \tag{II-4-1}$$

Here Γ is the scalar Green's function for the wave equation in an infinite domain.

As pointed out earlier, the right-hand side of (II-4-1) is to be understood as a Stieltjes integral. Our present purpose is to evaluate this integral.

In the case of an instantaneous rupture, the result is immediate: χ is a potential of the field y_m, and if χ^* is the corresponding potential of the field u_m^*, then

$$4\pi\chi = \frac{1}{c^2} \int_V \chi^* \left. \frac{\partial \Gamma}{\partial t_o} \right|_{t_o=0} dv^{(o)} \quad . \qquad \text{(II-4-2)}$$

But the difference field u_m^* is defined as $u_m^{(o)} - u_m^{(1)}$, where $u_m^{(1)}$ is the final equilibrium field. The relaxation field y_m is measured relative to $u_m^{(1)}$. For a growing rupture zone $u_m^{(1)}$ is a function of the source time during the rupture process, and a constant afterwards. Thus for all source times t_o earlier than τ_o, the duration of the rupture process, u_m^* is a function of t_o, and so is χ^*.

Archambeau (1968, 1971) suggested that a continuously growing rupture zone may be construed as the limiting case of a succession of elementary instantaneous ruptures. We shall make use of a similar idea here by studying the effect of an infinitesimal rupture increment when it is added to a finite rupture.

Let us suppose that we know how to compute the solution up to some time $t_1 < \tau_o$. At that time the potential has the value $\chi(\mathbf{r},t_1)$. If the rupture would stop at t_1, then χ would be measured, for $t > t_1$, relative to the equilibrium configuration associated with $V(t_1)$, and would be given at all times $t > t_1$ by

$$4\pi\chi(\mathbf{r},t;t_1) = \frac{1}{c^2} \int_{V(t_1)} \left[\chi \frac{\partial \Gamma}{\partial t_o} - \Gamma \frac{\partial \chi}{\partial t_o} \right]_{t_o=t_1} dv^{(o)} \qquad \text{(II-4-3)}$$

In other words, we would have the solution of an initial value problem,

the initial values $\chi(t_1)$ and $\frac{\partial \chi}{\partial t}(t_1)$ being created at t_1 . However, we know that in a short interval δt_1 , the rupture would grow and the volume would become $V(t_1 + \delta t_1)$. Let us approximate this growth to first order by an instantaneous elementary additional rupture occurring at t_1 . Then the left-hand side of (II-4-3) would change for two reasons. First the state with respect to which the relative field χ is measured has to be changed to the equilibrium field associated with $V(t + \delta t_1)$. But this is a simple change of origin (c.f. the mass-spring system) and does not represent a radiated field, but rather a static field. We need not concern ourselves with this at the moment. Second, the initial value $\chi(t_1)$, appearing in the integrand on the right-hand side, has to be increased by $\left.\frac{\partial \chi^*}{\partial t_o}\right|_{t_o=t_1} \delta t_1$ while the initial velocity $\left.\frac{\partial \chi}{\partial t_o}\right|_{t_o=t_1}$ is <u>unchanged</u>, since it does not depend on the reference state. The fact that the initial velocity does not undergo a sudden change is important because it means that the rupture phenomenon is spontaneous and that no impulse is imparted to the medium during the elementary rupture. We thus see that, to first order in δt ,

$$\chi(\mathbf{r},t;t_1 + \delta t_1) = \chi(\mathbf{r},t;t_1) + \left.\frac{\partial \chi^*}{\partial t_o}\right|_{t_o=t_1} \delta t_1$$

$$+ \frac{\delta t_1}{4\pi c^2} \int_{V(t_1+\delta t_1)} \left[\frac{\partial \chi^*}{\partial t_o} \frac{\partial \Gamma}{\partial t_o}\right]_{t_o=t_1} dv^{(o)} + O\left(\delta t_1^2\right) . \qquad \text{(II-4-4)}$$

The second term on the right-hand side corresponds to the (static) change in equilibrium values mentioned above, so that the sum of the two first terms represents the dynamic fields existing at t_1^- , measured relative to the equilibrium state valid at t_1^+ . The third term is the additional contribution to the radiation field due to the incremental rupture, expressed relative to the same equilibrium state. Thus, (II-4-4) may be rewritten

$$\frac{1}{\delta t_1}\left[\chi(\mathbf{r},t;t_1+\delta t_1)-\chi(\mathbf{r},t;t_1)\right]=$$

$$\frac{1}{4\pi c^2}\int_{V(t_1+\delta t_1)}\left[\frac{\partial\chi^*}{\partial t_o}\frac{\partial\Gamma}{\partial t_o}\right]_{t_o=t_1} dv^{(o)}+O(\delta t_1) \quad , \text{(II-4-5)}$$

which is valid for $t > t_1 + \delta t_1$ and for observer's points $\mathbf{r}$ exterior to $V(t_1 + \delta t_1)$, and where the fields are reckoned with respect to the equilibrium state associated with $V(t_1 + \delta t_1)$. But the right-hand side does not depend on the reference state since only the derivative $\frac{\partial\chi^*}{\partial t_o}$ appears; similarly, the left-hand side does not depend on the reference state either, since it is unchanged when one adds a constant to χ . Therefore, taking the limit $\delta t_1 \to 0$, and using the definition of a derivative we get

$$\frac{d}{dt_1}\chi(\mathbf{r},t;t_1)=\frac{1}{4\pi c^2}\int_{V(t_1)}\left[\frac{\partial\chi^*}{\partial t_o}\frac{\partial\Gamma}{\partial t_o}\right]_{t_o=t_1} dv^{(o)} \quad , \quad \text{(II-4-6)}$$

which is independent of the reference state. This equation is valid for fixed t, for fixed $\mathbf{r} \in V(t_1)$, and for any t_1 such that $0 \leq t_1 < \min(t,\tau_o)$.

The meaning of (II-4-6) is somewhat subtle and deserves comment: this equation gives the parametric dependence of the dynamic field $\chi(\mathbf{r},t)$ upon the elapsed rupture duration t_1. For a rupture occurring at a finite rate, and of total duration τ_o, the derivative on the left-hand side vanishes identically for $t_1 > \tau_o$. Thus by integration with respect to t_1 of (II-4-6) we get

$$\chi(\mathbf{r},t) = C + \frac{1}{4\pi c^2}\int_o^{\min(t,\tau_o)} dt_1 \int_{V(t_1)} \left[\frac{\partial \chi^*}{\partial t_o}\frac{\partial \Gamma}{\partial t_o}\right]_{t_o=t_1} dv^{(o)} \qquad \text{(II-4-7)}$$

where C is an integration constant to be determined. The second term on the right-hand side is the dynamic field referred to the equilibrium field which the medium would reach if the rupture were stopped in its configuration at time t. But the logical reference state is that which is associated with the final rupture configuration (at $t_1 = \tau_o$). This allows us to determine the constant C, which is

$$C = \chi^*(\mathbf{r},\tau_o) - \chi^*(\mathbf{r},t) \quad .$$

Note that C vanishes for $t \geq \tau_o$. Note also that t_1 is just a dummy variable in (II-4-7), so that the final result is

$$\chi(\mathbf{r},t) = \chi^*(\mathbf{r},\tau_o) - \chi^*(\mathbf{r},t)$$

$$+ \frac{1}{4\pi c^2} \int_o^t H(\tau_o - t_o)\, dt_o \int_{V(t_o)} \frac{\partial \chi^*}{\partial t_o} \frac{\partial \Gamma}{\partial t_o}\, dv^{(o)} \quad . \quad \text{(II-4-8)}$$

This reduces, for $t \geq \tau_o$, to the result of Archambeau (1972).

One sees immediately that (II-4-8) reduces to (II-4-2) in the case of an instantaneous rupture at $t = 0$. Indeed, in that case, we have $\chi^*(\mathbf{r},t) = \chi^*(\mathbf{r})H(t)$ and thus $\frac{\partial \chi^*}{\partial t} = \chi^*(\mathbf{r})\delta(t)$, so that the integrand in (II-4-8) is a delta distribution in time, at $t_o = 0$. This remark leads to the following interesting interpretation of (II-4-8) : If (II-4-2) is construed as an "impulse rupture" solution, then the solution (II-4-8) can be thought of as the convolution of this elementary solution with the "growth function" of the rupture zone.

The solution (II-4-8) is the one which we shall evaluate in Chapter IV in a case of a growing and propagating spherical rupture.

II-5 An equivalence theorem in the static case

We have shown so far the equivalence of three basic approaches to the dynamical source problem. This equivalence holds under fairly general circumstances. In this section we shall examine in greater detail, in the static limit and under more restrictive circumstances, the equivalence between relaxation and dislocation models. Here again we shall use the Green's tensor formalism, but we shall use specifically the static Green's tensor, so that both source time and receiver time disappear from the formal Green's tensor solution (I-3-36).

Consider an infinite domain filled with a homogeneous isotropic material (1) , except for an inhomogeneity bounded by a closed surface Σ , filled with an homogeneous isotropic elastic material (2) . We assume the inhomogeneity to be bonded to the matrix, and for simplicity we assume also that any intrinsic elastic field associated with this inhomogeneity can be linearly superposed to the solution of an elastic problem in this composite medium. This is a good assumption in the limit of infinitesimal strain theory. The intrinsic fields would be those directly associated with the inhomogeneity, and thus those present in the composite in the absence of any external loading.

Our present purpose is to investigate the effect of the inhomogeneity on the fields generated by external loading of the composite. Clearly, if the superposition principle described above holds, then we need only consider the case where a state of no strain and no stress throughout the composite material exists. We shall use such a state as a natural reference state.

Eshelby (1957) presented a solution for the elastic fields inside,

and immediately outside an inhomogeneity, as well as the fields at large distances. Kupradze (1963) attacked the problem by using Green's tensors and the theory of multidimensional integral equations. We shall combine the relatively simple approach of Eshelby with the Green's tensor formalism developed in Chapter I.

Let us load the composite by, say, a set of body forces applied outside the inhomogeneity, and let $\sigma_{ij}^{(1)}$ and $u_i^{(1)}$ be the elastic fields generated within the material (1) --outside the inhomogeneity-- and $\sigma_{ij}^{(2)}$ and $u_i^{(2)}$ the fields generated in the material (2) -- inside the inhomogeneity. Because the inhomogeneity is bonded to the matrix, then if $\hat{n}$ is the outer normal to Σ, we must have

$$\begin{cases} \sigma_{ij}^{(1)} n_j = \sigma_{ij}^{(2)} n_j \\ \\ u_i^{(1)} = u_i^{(2)} \qquad \text{on } \Sigma , \end{cases} \tag{II-5-1}$$

which expresses continuity of tractions and displacements across Σ (if the material (2) is a liquid, then only the normal component of displacement should be considered). Let $\sigma_{ij}^{(o)}$ and $u_i^{(o)}$ be the fields that would be generated throughout the space in the absence of the inhomogeneity. Here if we wish to think of $\sigma_{ij}^{(o)}$ as the prestress considered in the former sections, we must point out that the problem has been specialized to the case where the prestress is created purely elastically, so that $\sigma_{ij}^{(o)}$ and $u_i^{(o)}$ are related via Hooke's law. The fields $\sigma_{ij}^{(o)}$ and $u_i^{(o)}$ are continuous everywhere.

Let $\overset{\circ}{\Gamma}{}^{(1)}_{im}$ and $\overset{\circ}{\Gamma}{}^{(2)}_{im}$ be the static Green's tensors for the infinite domain valid for materials (1) and (2) respectively. Then

$$4\pi u_m^{(o)} = \int_V \rho f_i \, \overset{\circ}{\Gamma}{}^{(1)}_{im} dv^{(o)} \quad , \tag{II-5-2}$$

where V is the whole domain. Similarly, if $V^{(1)}$ is the domain external to the inhomogeneity, and $V^{(2)}$ the domain filled by it, then

$$4\pi u_m^{(1)} = \int_{V^{(1)}} \rho f_i \, \overset{\circ}{\Gamma}{}^{(1)}_{im} dv^{(o)} - \int_\Sigma \left(\overset{\circ}{\Gamma}{}^{(1)}_{im} \, \sigma_{ij}^{(1)} - \overset{\circ}{\gamma}{}^{(1)}_{ijm} \, u_i^{(1)} \right) n_j \, da^{(o)} \tag{II-5-3}$$

and

$$4\pi u_m^{(2)} = \int_\Sigma \left(\overset{\circ}{\Gamma}{}^{(2)}_{im} \, \sigma_{ij}^{(2)} - \overset{\circ}{\gamma}{}^{(2)}_{ijm} \, u_i^{(2)} \right) n_j \, da^{(o)} \quad . \tag{II-5-4}$$

These last two equations, when coupled with the boundary conditions (II-5-1) form a system of coupled integral equations to be solved for $u_m^{(1)}$ and $u_m^{(2)}$.

Let us perform the following fictional operations (cf. Eshelby, 1957).

1) Remove the inhomogeneity--material (2) --from its site in the composite, while applying tractions $\sigma_{ij}^{(1)} n_j$ on the wall of the cavity thus created, so that the material outside stays in equilibrium.

2) Cut a piece of material (1) such that, when tractions $\sigma_{ij}^{(1)} n_j$ are applied on its boundary, it takes exactly the shape of the cavity.

3) Insert this piece of material (1) into the cavity; tractions are now continuous again across Σ, so that we have equilibrium. We have thus transformed the inhomogeneity into an inclusion. The space is now filled with material (1) everywhere.

Let $v_m^{(1)}$ be the displacement field inside the inclusion, it is given by

$$4\pi v_m^{(1)} = \int_\Sigma \left(\overset{\circ}{\Gamma}{}_{im}^{(1)} \sigma_{ij}^{(1)} - \overset{\circ}{\gamma}{}_{ijm}^{(1)} v_i^{(1)} \right) n_j \, da^{(o)} \quad . \qquad \text{(II-5-5)}$$

The displacement outside the inclusion is still $u_m^{(1)}$. The tractions are continuous everywhere, but the displacements cannot be continuous, since the continuous solution of the equations of equilibrium in an infinite domain, filled with material (1), under the load ρf_i, is given by $u_m^{(o)}$, which is different from $u_m^{(1)}$. We thus expect that $u_m^{(1)}$ and $v_m^{(1)}$ do not take the same value on Σ, and thus Σ is a surface of discontinuity for the displacement: a dislocation surface.

Before we can state the complete equivalence theorem, we still have to prove that the difference field $u_m^* = u_m^{(o)} - u_m^{(1)}$ outside the inclusion can be expressed as a static dislocation solution. Henceforth, we shall denote by Σ_+ the internal side of Σ and by Σ_-

its external side, since $\hat{n}$ is the outward normal (see figure II-5-1).

The displacement jump is given by

$$\left[\!\left[u_m \right]\!\right]_\Sigma = \lim_{r \to \Sigma_+} v_m^{(1)} - \lim_{r \to \Sigma_-} u_m^{(1)} \quad . \tag{II-5-6}$$

Further, since the displacement $u_m^{(2)}$ matches $u_m^{(1)}$ on Σ, we also have

$$\left[\!\left[u_m \right]\!\right]_\Sigma = \lim_{r \to \Sigma_+} \left(v_m^{(1)} - u_m^{(2)} \right) \quad , \tag{II-5-7}$$

which permits to evaluate the jump from the knowledge of two interior solutions.

Let us evaluate the dislocation field

$$4\pi u_m^{(d)} = - \int_\Sigma \mathring{\gamma}_{ijm}^{(1)} \left[\!\left[u_i \right]\!\right] n_j \, da^{(o)} \tag{II-5-8}$$

for points lying outside the inclusion. From (II-5-6) we have

$$4\pi u_m^{(d)} = - \int_\Sigma \mathring{\gamma}_{ijm}^{(1)} v_i^{(1)} n_j \, da^{(o)} + \int_\Sigma \mathring{\gamma}_{ijm}^{(1)} u_i^{(1)} n_j \, da^{(o)} \quad . \tag{II-5-9}$$

We can apply Gauss' theorem to the first integral which we denote by I ; we get

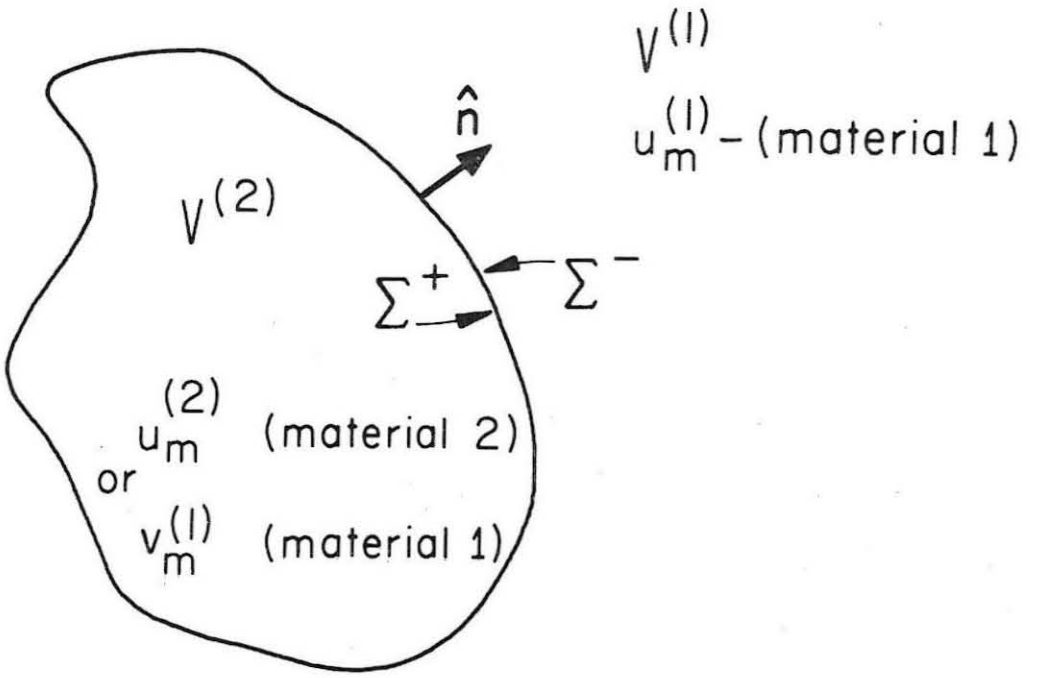

Figure II-5-1. Static fields associated with failure within a closed surface Σ . $V^{(1)}$ is the volume occupied by a matrix of material (1). $V^{(2)}$ is the volume of the failure filled with material (2) . $u_m^{(1)}$ and $u_m^{(2)}$ are the static displacement fields in the matrix and inclusion respectively. When the inclusion is replaced by a suitable body of material (1) the static displacement field inside Σ becomes $v_m^{(1)}$.

$$I = \int_{V^{(2)}} \left(\mathring{\gamma}^{(1)}_{ijm} \, v^{(1)}_i \right)_{,j} \, da^{(o)} \quad .$$

But we know that

$$\left(\mathring{\gamma}^{(1)}_{ijm} \, v^{(1)}_i \right)_{,j} = \mathring{\gamma}^{(1)}_{ijm,j} \, v^{(1)}_i + \mathring{\gamma}^{(1)}_{ijm} \, v^{(1)}_{i,j} \quad ,$$

and also, in the static case

$$\mathring{\gamma}^{(1)}_{ijm,j} = -4\pi\delta_{im} \, \delta(\mathbf{r} - \mathbf{r}_o) \quad ,$$

so that

$$I = \int_{V^{(2)}} \left[-4\pi\delta_{im} \, \delta(\mathbf{r} - \mathbf{r}_o) \, v^{(1)}_i + \mathring{\gamma}^{(1)}_{ijm} \, v^{(1)}_{i,j} \right] dv^{(o)} \quad .$$

For $\mathbf{r}$ outside $V^{(2)}$, the first term in the integrand does not bring any contribution to the integral. Furthermore, from Hooke's law (or equivalently by the Rayleigh-Betti theorem), we have

$$I = \int_{V^{(2)}} \mathring{\gamma}^{(1)}_{ijm} \, v^{(1)}_{i,j} \, dv^{(o)} = \int_{V^{(2)}} \mathring{\Gamma}^{(1)}_{im,j} \, t^{(1)}_{ij} \, dv^{(o)}$$

where $t^{(1)}_{ij}$ is the stress tensor associated with $v^{(1)}_i$. Since there

are no body forces within $V^{(2)}$ we have $t^{(1)}_{ij,j} = 0$ and thus

$$I = \int_{V^{(2)}} \left(\overset{\circ}{\Gamma}{}^{(1)}_{im} t^{(1)}_{ij} \right)_{,j} dv^{(o)} \quad .$$

We can now use Gauss' theorem, and recalling that, on Σ , $t^{(1)}_{ij} n_j = \sigma^{(1)}_{ij} n_j$ we have

$$I = \int_{\Sigma} \overset{\circ}{\Gamma}{}^{(1)}_{im} \sigma^{(1)}_{ij} n_j \, da^{(o)} \quad . \qquad \text{(II-5-10)}$$

Substituting (II-5-10) into (II-5-9) yields

$$4\pi u^{(d)}_m = - \int_{\Sigma} \left(\overset{\circ}{\Gamma}{}^{(1)}_{im} \sigma^{(1)}_{ij} - \overset{\circ}{\gamma}{}^{(1)}_{ijm} u^{(1)}_i \right) n_j \, da^{(o)} \qquad \text{(II-5-11)}$$

Now if we note that the volume integral in (II-5-2) needs only to be computed over $V^{(1)}$ since there are no body forces within $V^{(2)}$, then by subtraction of (II-5-3) and (II-5-2) and comparison with (II-5-11) we see that

$$u^{(1)}_m - u^{(o)}_m = u^{*}_m = u^{(d)}_m \quad , \qquad \text{(II-5-12)}$$

which completes the proof. We thus have the following theorem:

The perturbation to the elastic fields in a stressed

medium, due to the presence of an elastic inhomogeneity, can be represented as the field of a Somigliana dislocation, the dislocation surface being the boundary of this inhomogeneity.

In the limiting case where Σ envelopes a vanishingly small volume, Σ consists of two sides Σ_1 and Σ_2. Since $v_m^{(1)}$ is continuous inside $V^{(2)}$, the integral in (II-5-8) reduces to

$$4\pi u_m^{(d)} = - \int_{\Sigma_1} \overset{\circ}{\gamma}{}_{ijm}^{(1)} \left[\!\left[u_i^{(1)} \right]\!\right] n_j^{(1)} \, da^{(o)} \quad , \qquad \text{(II-5-13)}$$

which is the classical dislocation field (see e.g., McGinley, 1969). Here the jump is taken as the difference between the limiting values of $u_m^{(1)}$ on Σ_1 and Σ_2, and $\hat{n}^{(1)}$ is the positive normal to Σ_1.

Conclusion

We have used in this chapter the theory of Green's tensor solutions developed in Chapter I, to investigate the fundamental properties of three approaches to the seismic source problem. At no point did we need to know the Green's tensor itself. In fact, in section II-3, we were able to discuss the approximations involved in using an approximate Green's tensor: that for the infinite domain.

The relaxation model, corresponding to the solution of an initial value problem, is the one we shall use in Chapters IV and VI for particular rupture geometries. We have shown how to compute the solution in the case of a growing and propagating rupture. This choice of approach is based on the fact that the relaxation model depends explicitly on physical parameters of interest, for example, the rheology of the material in the failure zone, the prestress existing before rupture, etc... We shall see later in specific cases how rupture length, rupture velocity, size of the prestressed region (i.e., "relaxation radius"), and other similar physical parameters affect the radiation fields.

As was pointed out in the introduction to this chapter, the equivalence of the various attacks may seem to be a rather trivial concept. However, our analysis showed that some of the detailed aspects of this equivalence are rather subtle. In particular, the equivalence of a boundary source and of a volume source is somewhat difficult to grasp intuitively. From this point of view, when modeling an earthquake, the choice of approach should be made according to which approximations one wishes to make.

Chapter III

THE ENERGY OF A STRESS RELAXATION SOURCE

Introduction

Before going to the evaluation of specific source models, which will be done in Chapters IV and VI, we still have to discuss another general aspect of the rupture phenomenon: its energetics. We saw in Chapter I that the equations governing the flow of energy in a continuum are nonlinear and thus cannot be solved by a Green's function technique. This is one of the main difficulties encountered in energy problems. Another difficulty stems from the fact that the basic failure mechanisms for geologic materials are not very well known.

Most of the work in that domain has been concentrated around the determination of static or quasi-static rupture conditions at the time of incipient rupture. Failure criteria such as a Von Mises criterion, involving a comparison of the state of stress of the material and of its "strength," have been developed mainly in view of metallurgical studies. These criteria can be extended to Earth materials and meet with reasonable success in explaining experimental data (e.g., Mogi, 1971). If such a criterion is adopted and generalized to the dynamic case, then one only needs to know the dynamic state of stress of the material at every point in order to predict where it fails. This is the basis for Griffith's (1921) early work on crack propagation, and for much of the later work. The rupture is then statically controlled by the stress concentration factors prevailing in the vicinity of crack tips, and

dynamically the energy balance is obtained by equating the energy flux into the crack tip to the rate of absorption of energy in the form of surface energy (see e.g., Freund, 1972). Since for a frictionless crack, the stress has a singularity at the tip (e.g., Ida, 1972), and since no material has infinite strength, such a crack must grow under any load. Ida (1973) shows how this problem can be circumvented by appropriate choices of boundary conditions and fracture criterion. In particular, there must be friction between the faces of the crack. For example, Ida and Aki (1972) obtain the seismic source time function for a propagating longitudinal shear crack under these conditions. (See Ida, 1973, for an exposition of the theory and a bibliography.)

Experimental considerations have led many authors to suggest that stick-slip rupture is an adequate model for earthquakes. This is supported by laboratory experiments (e.g., Brace and Byerlee, 1966; Byerlee and Brace, 1968; Scholz, et al., 1972). The stick slip model calls, in general, for both a static friction and a lower dynamic one, but experiments show that friction is time dependent for most materials (e.g., Scholz, et al., 1972). This suggests that nonlinear phenomena such as creep may be of importance, in particular ahead of the rupture front. Ida (1973) proposes a theoretical model in which such phenomena can be taken into account. This points out the need for a yield criterion as well as a fracture criterion. Mogi (1971) proposes such criteria. Thus by allowing for anelastic flow of the material under certain stress conditions, the range of possible failure modes can be enlarged to contain brittle fracture, ductile fracture, or only

creep-like flow (see Malvern, 1969, for a discussion).

We do not intend to provide a comprehensive discussion of all the work done in this area; the bibliographies of the various publications mentioned above should, hopefully, enable the reader to trace the major part of the geophysical research in this field.

Because the occurrence of material failure depends on the notion of material strength in the models mentioned above, it essentially depends exclusively on the state of stress of the material. Therefore, rupture propagation in these models will be controlled by the propagation of stress waves, that is, by the equations of motion for the material. Thus for longitudinal shear cracks, in simple cases, the rupture velocity equals the shear velocity of the material (e.g., Burridge and Halliday, 1971). By generalizing the crack-tip model with cohesive forces introduced by Barenblatt (1958), Kostrov (1966) and Ida (1972, 1973) found that rupture propagation can occur either in a smooth or in a "bumpy" mode, depending on the boundary conditions on the crack and on the amount of creep taking place ahead of the tip.

But all the considerations mentioned so far point to the fact that rupture initiation and rupture propagation are fundamentally energy problems. Therefore, the energy equation should really be considered in solving such problems. This would also be more appropriate for the relaxation model that we have adopted. Then, instead of defining a kinematical coefficient of friction on a crack boundary, one would have to specify the rheology of the material within the failure zone, and study the dynamic flow of energy in the vicinity of the rupture

boundary. The methods and equations of Chapter I are then the appropriate ones to use.

In such an approach, the rupture boundary is to be treated as a propagating phase boundary. The rupture process is thus an activated process, where the energy density at which transformation can occur plays the role of the material strength, and the energy absorbed in the transformation ("latent heat") plays a role analogous to the surface energy usually considered. Further, any anelastic work done inside the rupture zone or immediately outside will play the role of frictional work on the surface of a crack or the work done against internal friction ahead of the crack tip. Because of the complexity of the problem and the nonlinearity of the equations, we shall not be able to find analytical solutions, and the theory will have to be applied through numerical approaches; but this is the case anyway for the usual crack propagation problems (e.g., Ida, 1973).

In this chapter we shall propose such a line of attack; but we shall first examine the global energy balance in the relaxation source model, and discuss the source of the energy available for both failure and radiation phenomena. The concept of seismic efficiency will be introduced in the usual fashion (e.g., Wyss, 1970; Scholz, et al., 1972).

III-1 Global energy balance for a relaxation source

Throughout this section, we shall assume that 1) the stress fields are related to the displacement by Hooke's law, and 2) that there exists a positive quadratic form of the strains W, the elastic energy density, which may be written

$$W = \frac{1}{2} \sigma_{ij} e_{ij} \quad . \qquad \text{(III-1-1)}$$

Here σ_{ij} is the elastic stress tensor associated with the strain e_{ij}. We shall adopt the same notation as in section II-5.

Consider a finite elastic body made up of material (1), of elastic constants $C^{(1)}_{ijk\ell}$, bounded by a surface S and occupying a volume V. This body may be stressed by one or several of the following mechanisms.

1) Applying given surface tractions on all or part of S.
2) Applying body forces to the material within V.
3) Specifying surface displacements on all or part of S and maintaining these displacements by rigid grips.
4) Existence of internal stresses.

It is not necessary for our present purposes to develop the theory of internal stresses. We shall refer the reader to Eshelby (1956) for a clear and simple explanation. It suffices here to state that these stresses are the Hookean stresses associated with that part of the strain which does not satisfy the compatibility equations. Such internal stresses can be created by the presence of dislocations or similar

defects in the material.

We stated in Chapter II that material failure in a continuum can be thought of as a sudden phase change of the medium, occurring in a limited region. This can mean a phase change in the usual sense if, for instance, shear melting occurs (e.g., Griggs and Handin, 1960). For deep earthquakes, rapid phase transformation of a medium initially in a metastable thermodynamical state has been suggested as a possible earthquake mechanism (e.g., Archambeau, 1968). But we can extend this idea to the case where the material is finely broken into a "fault gouge." A continuum representation of such granular or powdery material can be obtained from standard observations in soil mechanics.

The macroscopic properties of a medium with a high density of microscopic cracks are different from those of the uncracked medium. When failure occurs on a scale sufficiently large so as to generate an earthquake, the material does not fail along a simple crack. Instead, a zone is created where grains are disjointed along their boundaries, and where a high density of cracks is generated on a microscopic scale. Thus, within the rupture zone, the macroscopic behavior of the medium is changed. In other words, even upon failure of virgin material, the phenomenon may be represented by a generalized change of phase of the medium. In come cases, for example, the material can be taken to go upon failure to some elastoplastic phase.

In this section we are concerned with the global energy balance of the phenomenon, and this will be controlled by the long-term--i.e., static or quasi-static--mechanical properties of the material, both within and without the failure region. The dynamical behavior of the

phenomenon will depend on the thermomechanical and thermodynamical equations controlling the propagation of the phase boundary. These aspects of the question will be discussed in section III-3. If we assume the new phase to be purely elastic for the purposes of investigating the global energy balance of the phenomenon, then we shall obtain an upper bound to the energy released in the relaxation process since the anelastic effects and plastic work will be ignored. The greater energy change will be obtained when the material in the failure region loses all rigidity and thus becomes a liquid. In fact, if the material failure mode is that described above wherein grains are separated and disjointed by creation of a large number of microscopic cracks, then one does not expect this new phase to be capable of sustaining much shear stress: Granular material in the failure zone will set in a fashion similar to roller bearings, and then ease the relative displacement of the two sides of the rupture zone. Furthermore, if shear melting does occur, then it is certainly a good approximation to assume a drastic fall in rigidity of the material upon failure.

We shall therefore consider the following problem: Let $\sigma_{ij}^{(o)}$, $e_{ij}^{(o)}$, $u_i^{(o)}$ be the elastic fields generated within the volume V by any of the mechanisms (1-4) operating in a region $V^{(1)}$ of V. Suppose now that in a volume $V^{(2)}$ of this body, bounded by the closed surface Σ the medium is transformed into a material (2), with elastic constants $C_{ijk\ell}^{(2)}$ (see figure III-1-1).

Following the description given in Chapter II, the body, which is now a composite, goes to a new equilibrium field. We assume the inhomogeneity within $V^{(2)}$ to be bonded to the matrix occupying $V^{(1)}$. Let $\sigma_{ij}^{(1)}$, $e_{ij}^{(1)}$, $u_i^{(1)}$ be the new equilibrium fields in $V^{(1)}$,

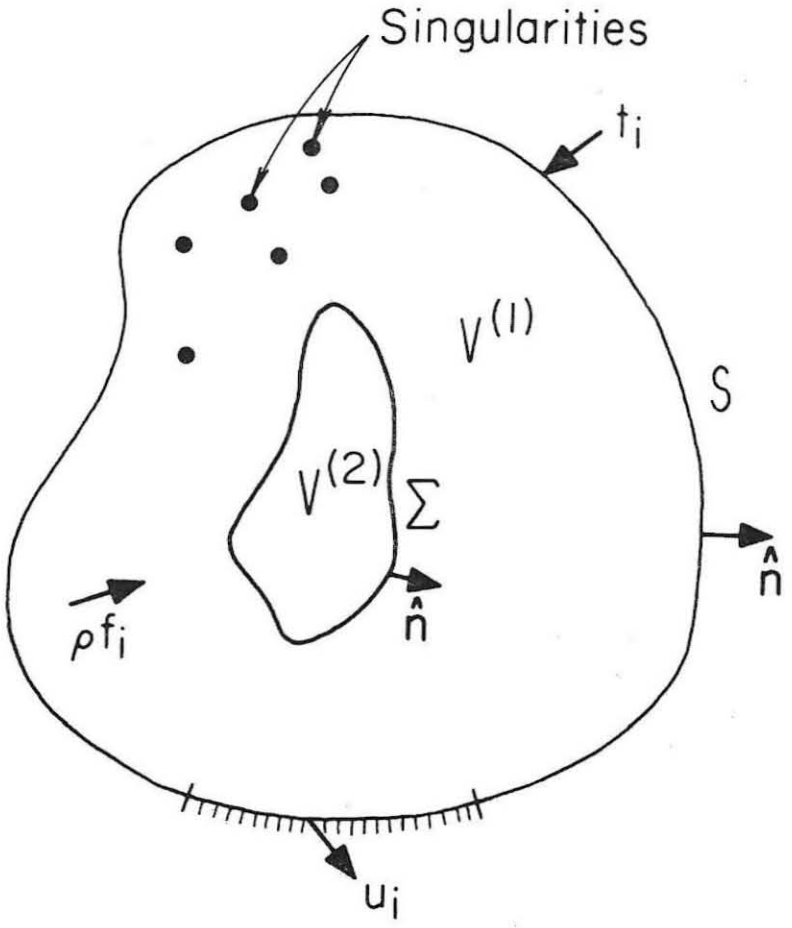

Figure III-1-1. Geometry of a body $V^{(1)}$, bounded by a surface S, and containing a failure zone $V^{(2)}$ bounded by Σ. The body may be stressed by specifying body forces ρf_i in $V^{(1)}$, surface tractions t_i on S, surface displacements u_i on S, or by singularities (e.g. dislocations) within $V^{(1)}$.

and $\sigma_{ij}^{(2)}$, $e_{ij}^{(2)}$, $u_i^{(2)}$ those present within $V^{(2)}$. Then, on the boundary Σ we have

$$\begin{cases} \sigma_{ij}^{(1)} \, n_j = \sigma_{ij}^{(2)} \, n_j \\ \\ u_i^{(1)} = u_i^{(2)} \end{cases} \qquad \text{(III-1-2)}$$

We can now evaluate the total change of energy of the body caused by the phase change. The change in elastic potential energy is

$$\Delta E_{el} = \frac{1}{2} \int_{V^{(2)}} \left[\sigma_{ij}^{(2)} \, e_{ij}^{(2)} - \sigma_{ij}^{(o)} \, e_{ij}^{(o)} \right] dv$$

$$+ \frac{1}{2} \int_{V^{(1)}} \left[\sigma_{ij}^{(1)} \, e_{ij}^{(1)} - \sigma_{ij}^{(o)} \, e_{ij}^{(o)} \right] dv \qquad \text{(III-1-3)}$$

In addition the work done by externally applied forces in the alteration process is ΔE_W if the phenomenon occurs at constant load, where

$$\Delta E_W = \int_{V^{(1)}} \rho f_i \left[u_i^{(o)} - u_i^{(1)} \right] dv + \int_S t_i \left[u_i^{(o)} - u_i^{(1)} \right] da \qquad \text{(III-1-4)}$$

so that the total change in energy is

$$\Delta E = \Delta E_{el} + \Delta E_W \qquad . \qquad \text{(III-1-5)}$$

Let us first derive a different expression for ΔE_{el} . Archambeau (1972) argues that the energy which would be released within $V^{(2)}$ is probably not really liberated, but absorbed in the rupture process. On these grounds, he ignores the first integral in (III-1-3) . Then, defining $\sigma^*_{ij} = \sigma^{(o)}_{ij} - \sigma^{(1)}_{ij}$ outside the rupture zone, and e^*_{ij} and u^*_i in a similar fashion, one gets

$$\Delta E_{el} \simeq \frac{1}{2} \int_{V^{(1)}} \left[\sigma^*_{ij}\, e^*_{ij} - \sigma^{(o)}_{ij}\, e^*_{ij} - \sigma^*_{ij}\, e^{(o)}_{ij} \right] dv \quad .$$

The two last terms in the integrand give identical contributions to the integral, a consequence of the Rayleigh-Betti theorem, so we may write

$$\Delta E_{el} \simeq \frac{1}{2} \int_{V^{(1)}} \left[\sigma^*_{ij} - 2\sigma^{(o)}_{ij} \right] e^*_{ij}\, dv$$

$$= -\frac{1}{2} \int_{V^{(1)}} \left[\sigma^{(o)}_{ij} + \sigma^{(1)}_{ij} \right] e^*_{ij}\, dv \quad . \qquad \text{(III-1-6)}$$

Recall that $e_{ij} = u_{(i,j)}$ so that

$$\sigma_{ij}\, e_{ij} = \sigma_{ij}\, u_{i,j} = (\sigma_{ij}\, u_i)_{,j} - \sigma_{ij,j}\, u_i \quad . \qquad \text{(III-1-7)}$$

Substituting (III-1-7) into (III-1-6) , we can apply Gauss' theorem,

and also make use of

$$\sigma^{(o)}_{ij,j} = \sigma^{(1)}_{ij,j} = \begin{cases} 0 \text{ in } V^{(2)} \\ -\rho f_i \text{ in } V^{(1)} \end{cases} . \qquad \text{(III-1-8)}$$

Then we have

$$\Delta E_{el} \simeq + \int_{\Sigma} \frac{\sigma^{(o)}_{ij}+\sigma^{(1)}_{ij}}{2} u^*_i n_j \, da - \int_{S} \frac{\sigma^{(o)}_{ij}+\sigma^{(1)}_{ij}}{2} u^*_i n_j \, da$$

$$- \int_{V^{(1)}} \rho f_i u^*_i \, dv \quad . \qquad \text{(III-1-9)}$$

However, if tractions are specified on S , then

$$\sigma^{(o)}_{ij} n_j = \sigma^{(1)}_{ij} n_j = t_i \quad ,$$

and if the displacement is specified, then $u^*_i = 0$, so that in all cases, we get, by combination of (III-1-9) and (III-1-4)

$$\Delta E = \Delta E_{el} + \Delta E_W \simeq \int_{\Sigma} \frac{\sigma^{(o)}_{ij}+\sigma^{(1)}_{ij}}{2} u^*_i n_j \, da \quad . \qquad \text{(III-1-10)}$$

This provides an estimate of the energy released by relaxation. This

result was obtained in a slightly different fashion by Archambeau (1972).

ΔE has the form of a dislocation energy (e.g., Steketee, 1958), which is not surprising in view of the equivalence theorem proved in section II-5. In fact, we see that ΔE is given by the work of the mean tractions between initial and final state, working through the change in displacement on Σ . We could have derived (III-1-10) directly from the results of section II-5, since the only difference occurs in the material within $V^{(2)}$, the elastic energy of which we ignored anyway.

Furthermore, in the case where Σ envelopes zero volume, then we can write approximately

$$\Delta E \simeq A < \sigma > < u > \quad ,$$

where A is the "fault" area, $< \sigma >$ the mean stress and $< u >$ the mean displacement jump across Σ . This approximate expression is the one used, for instance, by Wyss (1970) to estimate the energy released by faulting. We must point out, however, that this approximation can be made only if the rupture is a simple one, where the mean stress and the displacement jump are smooth functions over Σ and where the mean value theorem may be applied. Jungels (1973) showed that for a realistic fault model computed by a finite element method, this approximation is not, in general, a very good one.

Another interesting result is obtained if one does not ignore the first term on the right-hand side of (III-1-3) . Let us first

transform (III-1-3) by rewriting it as

$$\Delta E_{el} = \frac{1}{2} \int_{V^{(2)}} \left[\left(\sigma_{ij}^{(o)} \, e_{ij}^{(2)} - \sigma_{ij}^{(2)} \, e_{ij}^{(o)} \right) + \left(\sigma_{ij}^{(2)} - \sigma_{ij}^{(o)} \right) \left(e_{ij}^{(2)} + e_{ij}^{(o)} \right) \right] dv$$

$$+ \frac{1}{2} \int_{V^{(1)}} \left[\left(\sigma_{ij}^{(o)} \, e_{ij}^{(1)} - \sigma_{ij}^{(1)} \, e_{ij}^{(o)} \right) + \left(\sigma_{ij}^{(1)} - \sigma_{ij}^{(o)} \right) \left(e_{ij}^{(1)} + e_{ij}^{(o)} \right) \right] dv \quad .$$

By use of Hooke's law, and substituting (III-1-7) into this equation, we get, after applying Gauss' theorem

$$\Delta E_{el} = \frac{1}{2} \int_{V^{(2)}} \left(C_{ijk\ell}^{(1)} - C_{ijk\ell}^{(2)} \right) e_{ij}^{(2)} \, e_{k\ell}^{(o)} \, dv$$

$$+ \frac{1}{2} \int_{\Sigma} \left(\sigma_{ij}^{(2)} - \sigma_{ij}^{(o)} \right) \left(u_i^{(2)} + u_i^{(o)} \right) n_j \, da$$

$$- \frac{1}{2} \int_{\Sigma} \left(\sigma_{ij}^{(1)} - \sigma_{ij}^{(o)} \right) \left(u_i^{(1)} + u_i^{(o)} \right) n_j \, da$$

$$+ \frac{1}{2} \int_{S} \left(\sigma_{ij}^{(1)} - \sigma_{ij}^{(o)} \right) \left(u_i^{(1)} + u_i^{(o)} \right) n_j \, da \quad .$$

Because of the boundary conditions on Σ , the integrals over Σ cancel each other, and we have

$$\Delta E_{el} = \frac{1}{2} \int_{V^{(2)}} \left(C^{(1)}_{ijk\ell} - C^{(2)}_{ijk\ell} \right) e^{(2)}_{ij} \; e^{(o)}_{k\ell} \; dv$$

$$+ \frac{1}{2} \int_{S} \left(\sigma^{(1)}_{ij} - \sigma^{(o)}_{ij} \right) \left(u^{(1)}_{i} + u^{(o)}_{i} \right) n_j \; da \quad . \qquad \text{(III-1-11)}$$

An alternate form for ΔE_{el} may be obtained by applying directly (III-1-7) and Gauss' theorem to (III-1-3) . Then

$$\Delta E_{el} = + \frac{1}{2} \int_{V^{(1)}} \sigma^{(o)}_{ij,j} \; u^{*}_{i} \; dv$$

$$- \frac{1}{2} \int_{S} \left(\sigma^{(o)}_{ij} \; u^{(o)}_{i} - \sigma^{(1)}_{ij} \; u^{(1)}_{i} \right) n_j \; da \quad . \qquad \text{(III-1-12)}$$

Here we also used (III-1-8) in the first integral.

We can now discuss the effects of the various loading mechanisms mentioned at the beginning of this section. Following Eshelby (1957) we define the interaction energy between the inhomogeneity and the pre-stress as

$$E_{int} = - \frac{1}{2} \int_{V^{(2)}} \left(C^{(1)}_{ijk\ell} - C^{(2)}_{ijk\ell} \right) e^{(2)}_{ij} \; e^{(o)}_{k\ell} \; dv \quad .$$

a) If the body is stressed by means of a body force density within $V^{(1)}$ and/or known prescribed tractions on S, then, combining (III-1-12) and (III-1-4) and using the equilibrium equations (III-1-7), we have $\Delta E_{el} = -\frac{1}{2}\Delta E_W$ and thus

$$\Delta E = E_{el} + \Delta E_W = \frac{1}{2}\Delta E_W \quad .$$

Further, from (III-1-11)

$$\Delta E = E_{int} \quad .$$

Thus

$$\Delta E = E_{int} = -\Delta E_{el} \quad . \qquad \text{(III-1-13)}$$

We see that when the prestress is generated by externally applied forces, then during the relaxation process, work is done by these forces and half the work done goes to <u>increase</u> the internal energy of the body.

b) If the body is prestrained by imposing a known displacement u_i on the surface S, and by clamping S in rigid grips, then from (III-1-11) we get

$$\Delta E_{el} = -E_{int} + \int_S \left(\sigma_{ij}^{(1)} - \sigma_{ij}^{(o)}\right) u_i \, n_j \, da \quad . \qquad \text{(III-1-14)}$$

But, from (III-1-12) we also have

$$\Delta E_{el} = \frac{1}{2} \int_S \left(\sigma_{ij}^{(1)} - \sigma_{ij}^{(o)} \right) u_i \, n_j \, da \quad . \tag{III-1-15}$$

Further, ΔE_W vanishes in that case, thus, by combination of (III-1-14) and (III-1-15)

$$\Delta E = \Delta E_{el} = E_{int} \quad . \tag{III-1-16}$$

and the total change in internal energy is precisely the interaction energy in that case.

c) The case when the body is subject to internal stresses is a little more subtle. We assumed earlier that the sources of internal stresses are all within $V^{(1)}$. Let us consider a closed surface S' surrounding Σ , but such that the (singular) sources of internal stresses lie outside S' (figure III-1-2). Then the "body" can be taken to be the composite material within S' . The analysis proceeds as before and we can use (III-1-11) and (III-1-12) provided that we replace S by S' in these equations. This insures that the volume within S' is free of singularities, and the homogeneous equations of equilibrium are thus satisfied everywhere within S' . Then from (III-1-11)

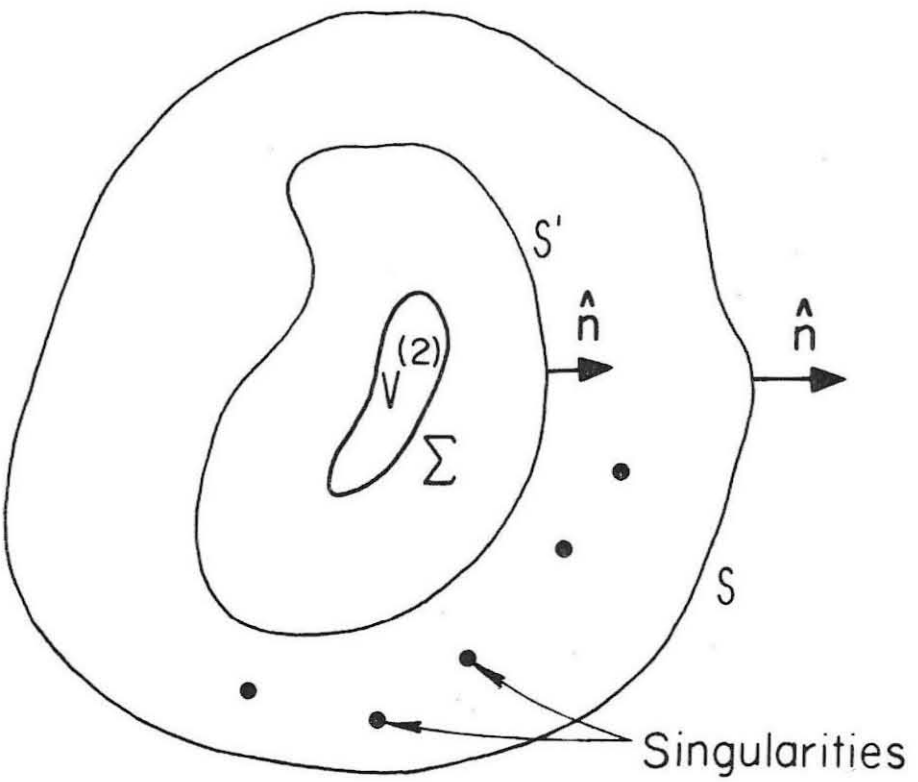

Figure III-1-2. Replacement of the surface S by a new surface S' such that no singularities are present within S' .

$$\Delta E_{el} = - E_{int} + \frac{1}{2} \int_{S'} \left(\sigma_{ij}^{(1)} - \sigma_{ij}^{(o)} \right) \left(u_i^{(1)} + u_i^{(o)} \right) n_j \, da \qquad \text{(III-1-17)}$$

and from (III-1-12)

$$\Delta E_{el} = \frac{1}{2} \int_{S'} \left(\sigma_{ij}^{(o)} \, u_i^{(o)} - \sigma_{ij}^{(1)} \, u_i^{(1)} \right) n_j \, da \quad . \qquad \text{(III-1-18)}$$

Expanding the integrand in (III-1-17) , and then using the Rayleigh-Betti theorem and comparing with (III-1-18) yields as in case b)

$$\Delta E = \Delta E_{el} = E_{int} \quad . \qquad \text{(III-1-19)}$$

Equations (III-1-13) , (III-1-16) , and (III-1-19) allow us to discuss which circumstances are favorable to the occurence of spontaneous rupture. This is done in the next section.

III-2 Discussion: The energy available for elastic radiation

We have studied in the last section the energy liberated by a relaxation source for four different loading mechanisms. Of course, in the Earth, several such competing mechanisms will, in general, be present simultaneously. If the stresses and strains generated by two such mechanisms are small enough so that they can be superposed linearly, then the total elastic energy is

$$E(1+2) = E(1) + E(2) + E_{int}(1,2) \quad , \qquad \text{(III-2-1)}$$

where $E(1)$ is the elastic energy present when only the first loading mechanism is present, $E(2)$ is associated with the second mechanism, and $E_{int}(1,2)$ is the interaction energy given by Eshelby (1956)

$$E_{int}(1,2) = \frac{1}{2} \int_V \left(\sigma_{ij}^{(1)} \, e_{ij}^{(2)} + \sigma_{ij}^{(2)} \, e_{ij}^{(1)} \right) dv \quad . \qquad \text{(III-2-2)}$$

When three mechanisms are present then

$$\begin{aligned} E(1+2+3) &= E(1+2) + E(3) + E_{int}(1+2,3) \\ &= E(1+3) + E(2) + E_{int}(1+3,2) \\ &= E(2+3) + E(1) + E_{int}(2+3,1) \quad . \end{aligned} \qquad \text{(III-2-3)}$$

By comparison of (III-2-3) and (III-2-1) one easily sees that, in the presence of N loading mechanisms

$$E(1+2+\ldots+N) = E(1) + E(2) +\ldots+ E(N) + E_{int}(1,2,\ldots,N) \qquad \text{(III-2-4)}$$

where the interaction energy may be written

$$E_{int}(1,2,\ldots,N) = E_{int}(1,2) + E_{int}(1+2,3) + \ldots$$

$$+ E_{int}[1+2+\ldots+(N-1),N] \quad . \qquad \text{(III-2-5)}$$

The order of application of the different loads does not matter in (III-2-5) --see equation (III-2-3) --, so that any permutation of this order may be chosen to compute the interaction energy. Thus we could easily generalize the analysis presented in the former section to the case of several competing mechanisms.

For the sake of simplicity, however, let us consider the various situations presented in section III-1 separately.

Two main results emerge from section III-1: 1) The amount of energy liberated in the relaxation process, if the prestress is given, is independent of the loading mechanism and is E_{int} , the interaction energy between the prestress and the inhomogeneity; but 2) the source of this energy is different for different loading mechanisms. More specifically two cases arise. If the prestress is generated by fixing

the displacement on the boundary of the body, or if it is due to a distribution of sources of internal stress, then the change of energy equals the change in elastic energy. In such a case one really has a relaxation phenomenon, where the total strain energy in the body decreases in the process, as a fraction of it is liberated. On the other hand, if the same prestress is generated by an adequate distribution of externally applied body forces or surface tractions, then the strain energy changes by the same amount, but increases rather than decreases. Then the work done by the external mechanism (change of its potential energy) is twice this amount, so that eventually the same total amount of energy is liberated. In this last instance, the liberated energy finds its source in the work done by the external loading mechanism.

This provides a ready explanation for the paradox raised by Steketee (1958). Using Connoletti's theorem, this author considered the energy balance in the creation of a dislocation in a prestressed medium. Using the fact that the dislocation energy is independent of the pre-existing stress state of the body, and arguing that the natural boundary condition to be applied at the surface of the Earth is that of a free surface, with constant and vanishing tractions, Steketee finds that the total internal energy of the Earth increases in all cases. This is a rather disquieting conclusion, but not a surprising one since it merely states that it takes energy to create a dislocation. The source of this energy is where the problem lies. If the loading mechanism is taken to be a body force density (such as gravitational

forces), then from our analysis, the internal energy of the material surrounding the rupture will indeed be increased. The total gravitational energy will then be decreased, half of this energy being used to increase the strain energy, the other half being "liberated." Part of the "liberated" energy is available for radiation, and part of it is dissipated in irreversible processes connected with failure and deformation.

On the other hand, internal deformation caused, for instance, by plate motion is more likely to be the source of the prestress. The highly stressed zones in the Earth that are associated with earthquakes appear to be confined to limited regions, as evidenced by the very distribution of earthquakes. Thus if the rupture occurs, say, within the thickness of a plate, or of a downgoing slab at a trench, then one can argue that the "body" to be considered for the analysis is that plate or slab, and not the Earth as a whole. If we envision the prestress to be due to a distribution of tractions acting on the boundary of this "body," then we cannot expect these tractions to be held constant during an earthquake. In fact, one rather expects the static displacements associated with the earthquake to vanish rather quickly with distance outside the slab. It appears then that a good approximation to the boundary conditions is to fix the displacements rather than the tractions on the boundary of a region surrounding the event. According to this argument, it is clear from our analysis that true stress relaxation must occur, and that the elastic energy of the slab decreases in the process.

Another point of view is to consider the state of prestress in the Earth to be due to internal causes. Then the slab considered above is

subject to internal stresses. If the sources of internal stress are thought to lie in the surrounding material, whatever they may be (e.g., convection), then the surface of the slab plays the role of the surface S' shown on figure III-1-2, and again our analysis predicts that elastic energy is liberated.

Another consideration yet may help clarify the situation: the phenomenon that we seek to describe is really a local one. Take the extreme case of a large body which would be prestressed by application of constant tractions t_i on all or part of its boundary. Let failure take place in a localized region within this body. Then we proved that the elastic energy of the body will increase because of the work done by the loading mechanism. But it is clear that the tractions t_i cannot start doing work until information has been propagated from the rupture zone to the boundary of the body. This information will be carried by elastic waves, which transport energy. Clearly the energy of these waves does not find its source in the work done by the tractions t_i, but in the strain energy released momentarily in the source region.

Thus because an earthquake is always a localized phenomenon in the Earth, it is always a good assumption to model it as a stress relaxation phenomenon. Except for the possible work done by body forces such as gravitational ones, the seismic energy emanating from the source region finds its origin in the release of strain energy. Of course, at any point the Earth will have to readjust its configuration, albeit infinitesimally, but information about the rupture is carried by the seismic radiation field, and this field has a localized source, of limited dimensions.

The effect of gravitational forces can be illustrated by the following trivial example. Suppose an object is dropped onto the surface of the Earth with no initial velocity, then, upon impact, the potential energy of this object has been transformed into kinetic energy. This energy is then partly transformed into strain energy stored in the ground supporting the object, and partly into radiation of elastic waves. Not until the elastic waves have reached it will a point in the Earth adjust to the new situation. This very simple example illustrated how locally, gravitational potential energy can be transformed into seismic energy. In the case of an earthquake, one can see intuitively how the work done by gravitational forces can contribute to the seismic radiation, particularly in the case of dip-slip faulting--of course, in pure strike-slip faulting, the particle motion occurs along equipotential surfaces, and no work is done by or against gravity.

Jungels (1973) used a numerical (finite element) method to construct a realistic model of the San Fernando earthquake of February 9, 1971. His findings corroborate the preceeding discussion, but also show that realistic situations can be quite complicated. The first important point to be realized is that the energy balance problem has to be solved by first isolating a region R surrounding the earthquake zone. The essential criterion for delineating the region R is to require that most of the energy liberated in the form of radiation find its source within R . The transfer of energy between R and the rest of the Earth will take place through the radiation field. We have just argued that this energy comes essentially from two possible sources in R : the release of strain energy and the possible work of gravitational

forces within R .

Observations of both static and dynamic fields suggest that most of the radiated energy comes from a limited region surrounding the rupture zone. This will be true, in particular, if the strain energy density released by the event outside R , and the work done by gravitational forces outside R , are small. Certainly the San Fernando earthquake did little to release the strain energy stored even 100 km away, let alone, say, in South America. Two criteria may be used to determine the dimension of the region R . If the prestress is thought to be a rather localized field around the event, the R should be essentially taken to englobe the prestressed zone; if the prestress is thought to be large on a much larger scale, then the characteristic dimension of R should be taken to be about the longest wave length under study.

Thus, Jungels, for example, proceeded to systematically investigate the various situations described above:

1) When the tractions were kept constant on the boundary of the region R , then the strain energy in R was increased.

2) When the displacements were held constant, then the elastic energy was decreased.

3) However, when gravitational forces were included in the model, Jungels found that the work done by them could be significant. In fact, for this particular earthquake, energy was expended in work done against gravity, so that the radiation field contained less energy than could have been expected from simple relaxation.

But more importantly, it was shown that the rupture geometry, the

failure process, the presence of a free surface, and the inhomogeneous nature of the crust could cause the faulting to be exceedingly complex. Strain energy could be increased locally, and decreased elsewhere, and similarly for gravitational energy. The energy underwent a complete redistribution in a very complicated fashion, and only the global balance appeared in the form of radiation leaving the region R .

One must therefore keep in mind that, not one, but several of the possible loading mechanisms enumerated in section III-1 can act in such an event, and there is no insurance that one of them might be more important than the others.

Another aspect of the question is worth mentioning at this point: we pointed out earlier that even if a body is prestressed by application of constant surface tractions on its boundary, then the radiation field associated with localized failure of the material within this body is generated by a dynamical stress relaxation mechanism. This is true if the points of application of the external loads are far enough from the rupture itself. Eventually the surface tractions will do some work and finally cause the strain energy to increase, but not until the radiated waves have reached their points of application. Now if the body is limited in size, so that surface tractions are applied at close proximity of the failure zone, then the loading device will start doing work during the relaxation process, and thus create a feedback to the rupture phenomenon. This can be the case in laboratory experiments (e.g., Scholz, et al., 1972) where a small sample is prestressed by applying a constant load on its boundary, and where the failure zone has dimensions comparable to those of the sample. In such cases, work will

be done by the loading apparatus during the failure process, and the elastic energy of the sample could increase as the rupture propagates. If this is the case, then energy is transferred continuously to the sample, and the rupture may be "driven" by the loading mechanism. As a consequence of this, one does not expect the rupture phenomenon to stop until the potential energy of the sample and that of the loading apparatus have been sufficiently decreased.

On the other hand, if the boundary of the sample is rigidly clamped so as to fix the displacements, then the only energy available for failure is that stored as strain energy in the sample itself. In such a case elastic energy is liberated, and one can see how, after sufficient stress relaxation, enough energy could have been released so that the rupture would not propagate further. Of course, the failure criterion must be applied point-wise, as we shall see, and stress concentrations in localized regions will be most important; but this observation must be kept in mind when designing an experimental device to study material failure, especially if one wishes to reach conclusions about the mechanism of earthquakes.

We have discussed so far the origin of "liberated" energy under various circumstances; we still have to discuss which form this energy takes. Clearly, some of this energy is to be radiated in the form of elastic waves; the question is: how much of it? Eshelby (1956) proposes that, in the quasi-static case, all the energy available appears in the form of surface energy, wherein the opening of a crack absorbs an energy proportional to the crack surface created. This is the basis for Griffith's (1921) solution to the crack propagation problem. Furthermore,

if friction is introduced between the two faces of a crack, energy will be dissipated (e.g., into heat), which equals the frictional work of the tractions across the crack. If creep occurs ahead of the crack tip before rupture (e.g., Ida, 1973), then some energy will be absorbed by this phenomenon in the form, say, of plastic work. Barenblatt (1958) considers the work which has to be done against intermolecular cohesive forces at the crack tip during crack formation. Cherry (1973) assumes a specific constitutive equation to evaluate the energy dissipated in plastic work numerically. Further, it is difficult to believe that an earthquake behaves as a single crack of enormous size. In fact, surface observations show a large number of secondary cracks of rather small size. The energy radiated by these small fractures will be carried by very high frequency waves which are likely to be very rapidly attenuated, and thus this energy will be dissipated very close to the failure zone or within the failure zone itself.

Then one realizes that, of all the "liberated" energy, much will be absorbed by the rupture phenomenon itself, and only a fraction of it will be radiated away and not all of it will be transmitted very far. The ratio $\eta = E_s/\Delta E$ of the seismic energy to the total energy available defines the seismic efficiency factor of the rupture. Further, the observed energy at teleseismic distances has been further affected by the travel path of the waves, and the ratio η should be defined as a function of frequency.

The seismic efficiency factor η plays therefore the role of a partition coefficient for the "liberated" energy. Hanks and Thatcher

(1972) show that it cannot be determined from the knowledge of the radiation field only, but that one needs either additional information or additional assumptions in order to evaluate it.

The foregoing discussion clearly ties material failure and rupture propagation problems to the energetics of the phenomenon. It is thus only natural to approach these problems from the point of view of energy considerations. We shall propose and outline such an approach in the next section.

III-3 Failure as an energy problem

Since the early work of Griffith (1921) and its generalization by Sack (1946), much attention has been devoted to crack problems, both static and dynamic. Most of this work was done in the context of metallurgical applications (e.g., Yokobori, 1965). The publications of Ida (1972, 1973) summarize well how the theory of crack propagation can be used in geophysics. The major problem associated with friction free longitudinal shear cracks stems from the stress singularity arising near the tip for the elastic solution. No material can sustain infinite stresses and the crack grows under any load. Kostrov (1966), and Ida (1972, 1973), show how crack propagation is governed both by the fracture criterion at the tip, and by the boundary conditions to be satisfied on the crack surface. Ida shows how stress singularities may be avoided, and how various conditions yield different regimes in the crack propagation. The propagation may be smooth or bumpy, and approaches the shear wave velocity after a long time. The bumpy propagation is observed in the case of a high frictional resistance to slippage along the crack; the propagation is smooth in the case of low friction, and also if a large amount of creep is allowed at the crack tip. The author identifies the two regimes with brittle and ductile behavior respectively.

Freund (1972) expresses the overall dynamic energy balance at the tip of a moving crack in the two dimensional case, and summarizes the results obtained by this approach. The main result consists of an expression of the energy release rate at the crack tip as a function of the elastic field of the moving crack. This is done by equating the

energy flux into the crack tip to some fracture energy.

The ideas that we outline below, albeit rather tersely, take the point of view that the energetics of the phenomenon constitute the critical aspect of the problem, and must yield a formulation that emphasizes the physical processes involved.

Since we are interested in a continuum representation of the failure phenomenon, and in view of the arguments made above that failure can be viewed as a generalized phase change of the material, the pertinent equations to be solved are those of section I-1. Recall that these equations include the conservation equations representing the conservation of mass, of linear and angular momentum, of energy, and also the Clausius-Duhem inequality, expressing the second law of thermodynamics. These are precisely the equations enumerated by Truesdell (1965).

Since we are in the presence of a material discontinuity Σ, we must also include as boundary conditions the jump conditions developed in section I-1. These are the conditions which control the evolution of Σ. As pointed out in section I-1, the critical equation needed in order to evaluate the velocity U of Σ (see Chapter I, or Appendix 1) is the energy jump condition

$$\left[\!\left[\rho E(V_i - U_i)\, n_i\right]\!\right]_\Sigma = \left[\!\left[(V_j\, T_{ij} - q_i)\, n_i\right]\!\right]_\Sigma \quad . \qquad \text{(III-3-1)}$$

Here V_i is the material velocity, q_i the heat flux vector, and E the total energy density. (It is the <u>total</u> energy which is conserved.)

(III-3-1) is a boundary condition to be met on Σ by the flow solutions on both sides of it. If the boundary velocity U is given as a parameter, then by solving the flow equations on both sides of Σ, one can determine from (III-3-1) the quantity of ρE which is absorbed (or liberated) as a unit mass of material traverses Σ (that is, undergoes the phase transition). For our present purpose, on the other hand, this equation must be solved for U. We must therefore state the problem as follows:

Having specified the state of the material on both sides of Σ, we first solve the flow equations (transport of mass and momentum) in the two regions separated by Σ, as a function of the parameter U. We then specify the amount of total energy density ρE which is absorbed or liberated upon crossing Σ. The problem is now to find a value of U such that the solutions of the energy equations on both sides of Σ be matched exactly on Σ by the boundary condition (III-3-1). In short, all the flow equations of section I-1 have to be solved simultaneously in the two regions bounded by Σ, and the boundary velocity U is then determined by requiring that the appropriate jump conditions be satisfied. This is obviously a complicated problem.

The simplest problem of this type is the problem of Stephan (Carslaw and Jaeger, 1959; O'Connell and Wasserburg, 1972) and, even in the simplest case, the problem is nonlinear --see section I-1. This means that analytical solutions may be found only in very particular situations, and also, that the problem does not afford a Green's function solution. Thus, the problem will have to be solved numerically,

in most cases (e.g., Cherry et al., 1973).

The material properties on both sides of Σ may be specified via suitable constitutive equations. There are no a priori restrictions imposed on these equations except for the following principles which hold for so-called simple materials (e.g., Truesdell, 1965):

1) The principle of determinism: causes operate only through their histories so that, in general, present effects are due to past and present causes.
2) Principle of equipresence: "a quantity present as an independent variable in one constitutive equation is so present in all."
3) Principle of local action: effects at a given point depend only on causes occurring in some neighborhood of this point.
4) Principle of material frame-indifference: the quantities present in the conservation equations have intrinsic meaning, independent of the observer, and two observers see the same material properties.
5) Principle of entropy growth: the Clausius-Duhem inequality must be satisfied in all cases.

A complete discussion of these principles lies outside the scope of this chapter and the reader is referred to Truesdell (1965), for example, for a remarkably clear and concise presentation.

We also need to know the quantity of E which is absorbed (or liberated) at the crossing of Σ. It includes several terms. The jump in kinetic energy will be obtained by solving the equations of

conservation of mass and momentum on both sides of Σ and satisfying the boundary conditions on Σ . Similarly, that part of the energy jump which is due to reversible processes, for example, the jump in elastic energy, does not pose any particular difficulty once constitutive equations have been chosen.

Much more delicate, on the other hand, is the estimation of irreversible phenomena. These include irreversible work done on the material, as well as thermal phenomena. We are talking here about irreversible processes involved in transporting a particle from one side of Σ to the other side, and not about dissipation and heat conduction leading to internal entropy production away from Σ (these can be estimated independently).

It is intuitively clear that there must be a complex interdependence between the physical nature of these irreversible processes and the boundary velocity. Several regimes may in fact occur: for example, for a slowly propagating failure, transfer of energy by diffusion mechanisms (e.g., heatflow, diffusion of point defects and crystal dislocations) can be critical, while kinetic energy terms may be neglected. On the other hand, Yokobori (1965) points out that little plastic work is done in the case of a rapid propagation of a brittle rupture. In that case, the propagation is more likely controlled by momentum transfer. Using the excitation of free oscillations of the Earth, Dziewonsky and Gilbert (1973) show evidence that two very different regimes of failure may take place successively during a seismic event; more particularly, two deep South American earthquakes were preceded by a slow compressive phase, with essentially no high frequency radiation. Possible creep

events taking place prior to earthquakes would fall in the same category of phenomena.

Since an elaborate discussion of such processes should be rather involved and quite lengthy, we shall simply write

$$\left[\!\left[\rho u\right]\!\right] = \left[\!\left[\rho W_{rev}\right]\!\right] + \left[\!\left[\rho Ts_{irr}\right]\!\right] \qquad \text{(III-3-2)}$$

where we have isolated the work done reversibly. The second term contains both reversible and irreversible thermal effects, as well as irreversible mechanical effects. It reduces to the latent heat of phase change in the simplest case (see Chapter I).

For shallow earthquakes, this term can be estimated approximately as follows: Suppose that the generalized phase present in the failure zone is formed of a highly cracked material, to the point where the medium is essentially granular. Then if δ is the new surface density (per unit mass) created upon failure, ε the surface energy per unit area, and ζ the surface plastic work per unit area (e.g., Yokobori, 1965), we have

$$\left[\!\left[\rho Ts_{irr}\right]\!\right]_{\Sigma} \simeq \rho\delta(\varepsilon+\zeta) \quad . \qquad \text{(III-3-3)}$$

Now, if we denote the grain size by ℓ, the surface created is proportional to ℓ^{-1}, so that the work done to finely grind the material becomes very large, and less energy is available for radiation. Of course the finest grain size is not expected to be reached immediately

upon failure, since further irreversible work of this type must occur inside the failure zone, which can be taken into account through the constitutive equations.

It should be noted in that respect that if gaseous or liquid material permeates the cracked medium, the surface tension is decreased (e.g., Yokobori, 1965). The work done in (III-3-3) is thereby lessened, increasing the chances of runaway rupture. This aspect is particularly interesting because of its obvious connection with the dilatancy-diffusion model of earthquake prediction (e.g., Whitcomb et al., 1973)

For deep earthquakes, the shear melting hypothesis proposed by Orowan (1960) and Griggs and Handin (1960) suggests that true phase change takes place, which can be treated by standard procedures (e.g., Ida, 1970). Using the "local equilibrium" theory, this author shows that a small pocket of molten material embedded in a non-hydrostatically stressed solid evolves into a thin sheet, and suggests that this could initiate the shear melting process.

As we saw in Chapter I, when no density jump occurs, and when the kinetic energy is continuous across Σ, then the jump in internal energy reduces to the latent heat of phase change. Thus the ideas developed above constitute in a formal sense a generalization of Stephan's problem, and one sees how the concept of latent heat has to be generalized to model the failure phenomenon as a generalized phase transformation.

The ideas which we have advanced so far allow for a solution to the failure propagation problem, once failure has been initiated;

nothing has been said, however, about the phenomenon of incipient rupture. This aspect of the question has been investigated in rather great detail from the microscopic point of view. Treatment of the nucleation problem, and its connection with the theory of crystal dislocations can be found, for example, in Yokobori (1965), along with an extensive bibliography. Clearly, because it takes into account the physical nature of crystalline materials, this treatment must be kept in mind when constructing a continuum mechanical failure criterion.

The stress-strain curve for many materials may often be separated into two parts. Figure III-3-1a shows an idealized curve where two regimes of material flow occur in succession as the load increases. The segment OA represents a perfectly elastic regime where the strain is fully recoverable, whereas the segment AR represents a purely plastic regime, in which the material is unable to sustain any further increment of stress, and flows in such a way so as to keep the stress level constant. The plastic strain thus generated is no longer recoverable, and the area of the rectangle ABCD is the plastic work done when the strain increases from B to C . Rupture occurs at the point R . Since plastic yield is primarily associated with deviatoric stresses, we may ignore, to first order, the hydrostatic stresses. A more complete description of the phenomenon and a comparison to experimental results can be found in any textbook on the subject.

On the basis of this idealized behavior, Cherry, et al. (1973) use the following rupture criterion in numerical calculations: the material is treated elastically up to the yield point A . This yield point is usually determined by a Von Mises criterion, or, equivalently, it is

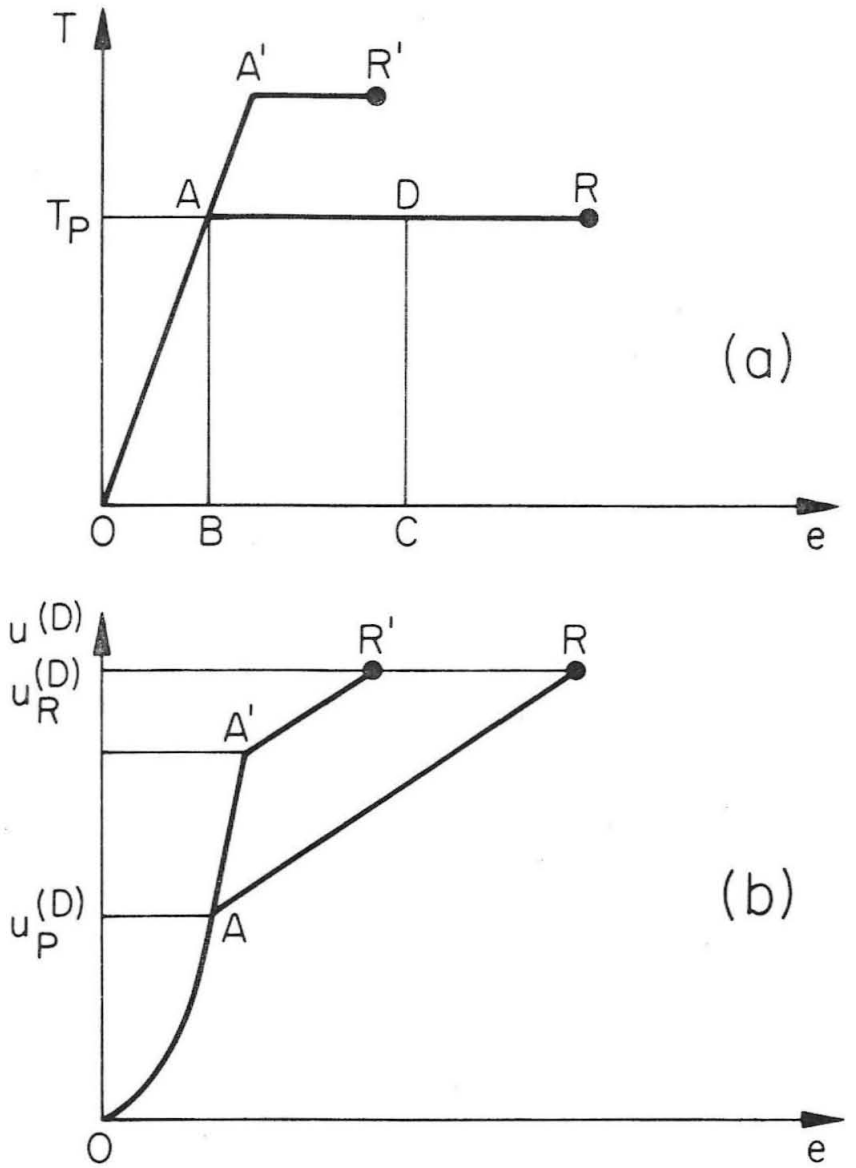

Figure III-3-1. a) Stress-strain curve for an elastoplastic material. OAR and O'A'R' are two possible regimes corresponding to different loading conditions. A and A' are yield points; R and R' are rupture points. b) Internal energy associated with 1) elastic deformations caused by the deviatoric stresses, and 2) plastic work, as a function of strain.

reached when a level $u_p^{(D)}$ of the internal elastic energy associated with the deviatoric stresses is attained (figure III-3-1b). The material is then treated plastically afterwards, and a specified amount of plastic work $u_R^{(D)} - u_p^{(D)}$ is required before rupture occurs.

The criterion can obviously be changed at will so as to use, say, the curves OA'R' . The geometry depicted in figure III-3-1 might correspond, for example, to two different strain rates. In that case OA'R' would correspond to a higher strain rate than OAR . This is not unreasonable since it is known experimentally that the yield stress T_p increases with the strain rate. The path OA'R' could also correspond to a lower temperature than OAR, since temperature effects can be traded off with strain rate effects (e.g., Yokobori, 1965). The additional assumption which we make in this figure is that the internal energy associated with 1) the deviatoric elastic strains and 2) the plastic work, reaches a specified value at rupture. This is also an acceptable simplification, since the more brittle the rupture (e.g., OA'R'), the less plastic deformation is observed before it (see e.g., Yokobori, 1965).

Such a rupture criterion based on energy, although it is very simplified, and would have to be checked against observations presents several advantages.

First of all, it can be applied point-wise, which is realistic, and rather convenient in numerical work. Furthermore, it would provide a natural tie with the dynamical concepts discussed earlier: $u_R^{(D)}$ is the energy level required before phase transformation can occur at all. Third, it can be generalized to include more sophisticated situations:

Coleman (1964) developed the theory of thermodynamics of simple materials with fading memory. This theory assumes very general constitutive relations for the material, which satisfy the principles mentioned earlier. More particularly, the stress, the internal energy, the entropy, and the heat flow are functionals of the deformation and temperature histories of the medium. The heat flux depends also on the present temperature gradient. The concept of fading memory is adopted as a principle which states that effects of the distant past are less important than those of the recent past. More specifically, the present state of the material depends strongly on recent deformations and temperature changes, but is practically independent of deformations and temperature changes which took place long ago. This results in a different material behavior under rapid deformations than under slow deformations. These circumstances have obvious applications in Earth sciences, where the long-term deformations associated with tectonics, or with isostatic rebound constitute one regime, while rapid deformations caused, for instance, by seismic events call for a different material behavior.

The problem obviously needs to be thought out very carefully; for example, if the material goes through a phase change, so that the new phase possesses a different memory function, then we are faced with the situation of a material having a memory, but no past. This idea is certainly worth further investigation, and could yield very useful results. Such work will be undertaken in the future.

Conclusion

The treatment of the energy balance for a seismic source model of the relaxation type, as given at the beginning of this chapter, clarifies the question of where the radiated energy finds its source. Particularly important is the realization that the radiation field serves to carry energy from the vicinity of the source to other points in the Earth. It serves, in particular, to redistribute the gravitational potential energy. Thus, while the seismic radiation comes essentially from the release of tectonic elastic energy, one is forced to take into account the work of gravitational body forces in the source region since it does contribute to the radiation field.

It is proposed that the detailed energetics of the phenomenon can be used to help model the dynamic failure process. Failure can be thought of as a generalized phase change of the material, and the evolution of the failure boundary is then controlled by the energy transport equations. In addition, an energy criterion can be devised to determine the occurrence of incipient failure.

This approach presents great potential, since it should lead to a more physical representation of earthquakes, in as far as it allows for the modeling of a completely spontaneous phenomenon, depending only on the thermodynamic state of the medium and its constitutive equations. Finally, the thermodynamic theory of simple materials with fading memory is particularly attractive in this context because of the broad range of time scales encountered in geophysics. Very long time scales apply to problems such as the recurrence of earthquakes, deformations of the crust by tectonic loading, isostatic rebound, etc., and, in that

case, viscous and plastic behavior of earth material cannot be ignored. On the contrary, wave propagation problems in the Earth can be treated by assuming a quasi-elastic behavior of the medium under rapid deformation.

Chapter IV

THE GROWING AND PROPAGATING SPHERICAL RUPTURE

Introduction

The representation theorems developed in Chapters I and II are quite general in nature since they only assume that the material retains its elastic properties up to the failure point. In particular, no assumption was made as to the rupture geometry, or as to the rupture propagation mode. It is clear, however, that these representation theorems will yield analytical solutions for the radiation field only in very special cases, and even then, under further simplifying assumptions. Any attempt to model accurately a realistic situation has to be handled via numerical techniques.

This is not to say that it is ludicrous to consider analytical solutions, even at the cost of oversimplifying the problem. On the contrary, we would like to emphasize their importance in terms of obtaining a basic understanding of the phenomenon. Whereas a numerical approach enables the investigator to handle simultaneously many parameters --including local heterogeneities in the material--it also prevents him from isolating the individual effects of these parameters; the more numerous the parameters are, the more difficult, the lengthier, and the costlier it is to conduct a parameter study. On the other hand, when constructing a model which can be investigated analytically, one often has to limit the free parameters to 1) those which lead to tractable analysis and 2) those which are deemed necessary for a reasonably complete representation of the phenomenon.

In modelling the relaxation source, one has to know the rupture geometry as a function of time, the rheology of the material within the failure zone, the intensity and orientation of the prestress, and a measure of the localization of the prestress.

The geometry that lends itself best to an analytical treatment is that of a spherical rupture zone. This is obviously an excellent configuration if one wishes to model the tectonic effects of an underground explosion (e.g., Archambeau, 1972), but it does not conform to one's intuitive idea of the geometry of a fault zone. However, if an underground nuclear explosion is detonated in a prestressed medium, then in addition to the direct field caused by the cavity overpressure, one observes an anomalous radiation field. Whereas the direct "explosion field" has a completely symmetric (monopole) radiation pattern, the anomalous field exhibits a quadrupolar radiation pattern (e.g., Lambert et al., 1972). A quadrupole is typically the radiation pattern of a double-couple, which is the widely accepted point force representation of an earthquake (e.g., Burridge and Knopoff, 1964). In fact, this anomalous radiation led Aki et al., (1969) to suggest that an earthquake was triggered by the BENHAM underground nuclear event. Archambeau and Sammis (1970) and Archambeau (1972) showed that the simple stress relaxation caused by the presence of the explosion generated cavity is sufficient to explain the anomalous part of the radiation (see also Lambert et al., 1972). One can thus say that the anomalous radiation of an undergound nuclear explosion is "earthquake like," justifying the suggestion that the radiation field generated by an earthquake can be adequately modelled even with a spherical geometry (e.g., Archambeau,

1964, 1968). In addition, several authors have presented arguments supporting the idea that deep earthquakes may be caused by a large scale rapid phase change of the material, which could be due to metastable thermodynamic initial conditions (see e.g., Archambeau, 1964 for a discussion). In that case the spherical geometry could very well be a good approximation to the real failure zone configuration. A much better approximation would be obtained by adopting an ellipsoidal rupture zone. Such a case will be considered in Chapter VI, but the analysis becomes very cumbersome and there is little reason to believe that the gross properties of the radiation field should be strongly dependent on the rupture geometry. In fact, physical experience, and field observations--which lead in particular to fault plane solutions--show that the basic radiation pattern of the radiation from an earthquake is a double couple. Thus any model should exhibit this feature, and this condition has to be satisfied independently of the choice of geometry. We shall see how it is so for the spherical rupture, and how rupture propagation effects alter this conclusion at high frequency.

The question of the rheology of the material within the rupture zone is to be considered next. If one wishes to model an underground nuclear explosion, then there is little argument that the material loses its rigidity inside a spherical region surrounding the detonation point: the shatter zone. Archambeau and Sammis (1970) and Archambeau (1972) present a detailed model of the radial variation of material behavior around the explosion cavity. We shall refer the reader to their work for a more complete discussion.

Earthquake modeling is somewhat more subtle. Many authors are in

favor of the stick slip model for shallow earthquakes, and thus friction could play a significant role. On the other hand, we argued in Chapter III that the cushion of granular material--the "fault gouge"--generated inside the rupture zone, probably has a very reduced resistance to shear motion, compared with the surrounding material, the grains composing this material acting in a way analogous to roller bearings. Further, if friction were high, and the confining pressure high also--as would be the case for a moderately deep earthquake--then one expects the energy dissipated by friction to generate a lot of heat in a localized zone, and possibly shear melting could occur (e.g., Griggs and Handin, 1960; Ida, 1970). Using arguments along those lines, and taking into account the possibility of fluid flow if the medium is porous, as well as the possibility of material dehydration under suitable thermodynamical conditions, Archambeau (1968) concludes that boundary conditions corresponding to vanishing shear strength in the rupture zone are appropriate. This may lead to some concern that oscillatory relative motions ("overshoot") between the two sides of the failure zone might occur under these circumstances (e.g., Molnar et al., 1973). However, under the definition of source transparency given in Chapter II, we have shown in section II-3 (equation II-3-9) that the instantaneous relaxation source model is equivalent, in an infinite space, to the instantaneous creation of a Somigliana dislocation with a step function time history, plus an instantaneous stress step pulse on the rupture boundary. There is, therefore, no overshoot in that case, and growth and propagation effects should not alter this conclusion. (The local nature of the prestressed zone, however, can lead to apparent

"overshooting," as will be shown in this chapter.)

Of course, the shear resistance of the material may not vanish completely in the rupture zone as non-elastic effects are likely to be important. In fact, a frequency dependent shear resistance could very well take place; these could be modelled as viscoplastic effects, but the only circumstance in which analytical solutions can easily be obtained is when the material inside the rupture zone is treated as elastic with small non-vanishing rigidity. Such an approximation is dynamically justified inasmuch as viscoelastic or viscoplastic materials, or for that matter any material with fading memory (e.g., Coleman, 1964), behave quasi-elastically when submitted to very rapid deformations, such as those encountered during the failure phenomenon. More complex models, including more general constitutive equations, would have to be treated numerically. In this chapter we shall assume that the shear strength of the medium vanishes upon rupture. As we pointed out in Chapter III, this assumption leads to the most efficient relaxation process, and thus since energy dissipation in non-elastic phenomena is ignored, we shall get an upper bound to the radiated energy. If the rheology of the material within the failure zone were viscoelastic, then one would have to introduce frequency dependent effective elastic moduli. The energy spectrum thus obtained would be somewhat different; more energy would be radiated at long periods, for which the effective rigidity would be small, and less energy at high frequencies for which the effective rigidity would be higher.

Growth and propagation of the failure region will be treated by use of the results given in section II-4. However, when these phenomena occur, one loses the spherical symmetry, inasmuch as the instantaneous

reference frame in which this symmetry is preserved moves with the failure zone. If the spherical rupture undergoes self-similar growth--a case appropriate to the modelling of an explosion--then a constant immovable reference frame can be used (e.g., Archambeau and Sammis, 1970). If there is propagation as well as growth, then a moving coordinate system with origin at the instantaneous center of symmetry has to be introduced, in which the initial value fields take a rather simple form. But the radiation field is best represented in a fixed coordinate system, with its origin chosen, say, at the point of initial rupture--the hypocenter. Two approaches are then available:

First, the dynamic part of the problem can be entirely handled in the fixed coordinate system. One must then express the initial value fields in that frame, and this can be done by use of the addition theorem for solid harmonics (see section IV-1). This is the attack chosen by Archambeau (1964, 1968). It calls for approximations made early in the solution of the problem, and leads to relatively simple results. The treatment given in section IV-2 is essentially similar to Archambeau's, but the results are cast in a much simpler form than his, and asymptotic behavior of the radiation spectrum can be studied quite easily.

The second attack consists of evaluating the dynamic field in the moving reference frame, and of finding its expression in the fixed reference frame by continuous, time-varying translation of the coordinates. This method calls for the addition theorem for spherical waves, proved in Appendix 9. With this method the approximations are not made until a fairly advanced stage of the analysis. The results are slightly more accurate when this approach is used, but take a somewhat

more complicated form. We shall show that the asymptotic behavior of the radiation spectra are the same whether one method is used or the other. This supports our contention that the gross features of these spectra are reasonably well predicted by our model.

One limitation to the propagation of the rupture zone is imposed by our ambition to treat the problem analytically. Healing phenomena are rather difficult to consider analytically other than by a pure kinematic representation, such as the one provided by a dislocation model. The stress concentration around a spherical failure zone is tractable only if the sphere is embedded in an homogeneous medium, which is not the case if this sphere is found at one extremity of a zone having failed and then healed. Indeed, there exists then a static deformation of the medium in that zone which will interact with the sphere and greatly complicate the analysis. Furthermore, there is not even any insurance that healing occurs when static equilibrium has already been reached. In fact the material can "freeze" in the rupture zone while relaxation is still in progress. In order to avoid such complications we shall assume that no healing occurs, and that, once a material point has failed, it stays within the rupture zone during the total duration of rupture.

Specification of the prestress is essential in the relaxation source model. Since we are mainly interested in failure mechanisms associated with the deviatoric stress tensor--in particular, failure under shear--we shall ignore here the effects of the lithostatic pressure. This is an approximation, especially in the case of an explosion, where a definite cavity is created, but then one can treat

this question in connection with the radiation field caused by the over-pressure in the cavity. In the case of an earthquake, the lithostatic pressure may have two effects: the first one is a direct effect associated with a possible change in specific volume of the material upon failure (see Randall, 1964). The second one is essentially a second order effect, taking place at very high pressures; then elastic waves must be treated as small deformations superposed on large deformations. Dahlen (1973) investigated the effect of pressure on a dislocation source.

We shall consider hereafter the case of a medium prestressed in pure shear only. In fact, for reasons of simplicity, we shall assume that only the off diagonal elements of the stress tensor σ_{ij} are non-zero, when expressed in a natural coordinate system of the source. Such a natural reference frame is one where the z-axis points in the direction of rupture propagation. This does not reduce the generality of the solution since the transformation of the radiation field under change of the reference frame can be found afterwards (this is done in Chapter V).

Much more important is the parameter specifying the site of the stressed zone. We have already argued several times (section II-3, section III-2) that the Earth is finite in size, and is certainly not adequately modeled by a uniformly stressed infinite space. Furthermore, earthquakes are confined to relatively narrow zones, and this suggests that the prestress is high enough only over limited regions. On intuitive grounds, one expects that the dimension of the prestressed regions might have a definite effect upon the shape of the radiation spectrum. In particular, one expects essentially two characteristic

wave lengths to appear in the spectrum, one of them related to the characteristic dimension of the rupture itself, and the other one related to the characteristic dimension of the prestressed zone. Following Archambeau (e.g., 1964), we shall designate the characteristic dimension of the prestress zone by R_s , and shall call it the relaxation radius. It is important to realize beforehand that R_s is a very physical parameter, even though we shall investigate its effects through a mathematical approximation. R_s is the radius beyond which the static stress change due to failure is negligible. In other words, we may assume that the initial value fields vanish very fast outside R_s .

The reasons why one should expect significant stress changes to occur only in a finite region have been enumerated before: the Earth is finite in size, and high stresses are apparently confined to limited regions; the proximity of the free surface, or of heterogeneities, are additional reasons; also measured static strain changes seem to be confined to the vicinity of the event (e.g., Jungels, 1973; Jungels and Frazier, 1973).

This concept is especially important for relaxation source models, because such models lead to volume sources (Chapter II). Stress pulse models or displacement dislocation models do not allow any convenient introduction of R_s . The effect of the relaxation radius is essentially to limit the volume of the source: All the radiated energy finds its source within R_s . An observer standing outside the relaxation zone is completely outside the source region, and can encapsulate it in a "black box" inside which all the radiation generating phenomena occur. An observer standing within the relaxation zone is inside the source

region, and we shall show that in that case, it is meaningless for him to speak of "far field" radiation, because stress relaxation takes place everywhere around him.

The mathematical approximation that we shall choose in order to introduce R_s is as follows: If the prestress is approximately uniform in the vicinity of the failure zone, then, in that vicinity the initial value can adequately be computed as if the medium filled the whole space, and were homogeneously stressed. This is a good static "near field" approximation. But we know that physically, because of inhomogeneities (or because of the proximity of a free surface), the prestress, and therefore the initial value, vanishes quickly outside the radius R_s. We shall approximate the initial value fields up to the distance R_s from the origin by those computed for the infinite space, and we shall truncate them at R_s. Archambeau and Sammis (1970) show that even in the case of an infinite space, most of the energy released comes from within a distance of less than five source dimensions from the rupture zone. Therefore we approximate a smooth decay of the initial value fields by an abrupt truncation. This will clearly lead to an overestimation of the radiation fields. The important aspect is that we have chosen here a mathematical approximation to a real physical situation.

Of course, a special case of interest is that where R_s is taken to be infinite. This was suggested by Randall (1973, a, b) to be the only correct choice for R_s, on the basis of the mathematical approach used above. But taking R_s infinite constitutes a very different kind of approximation: one then has an exact mathematical formulation of an

unphysical problem. The approximation of the Earth by an infinite homogeneously prestressed medium is of a physical nature, and although it leads to a convenient exact mathematical formulation of the problem, we consider that this is not desirable. Our philosophy is to choose an approximate mathematical solution in a likely physical situation over an exact mathematical solution to an unphysical problem.

We shall see in this chapter, and also in Chapter VII, that the size of the relaxation strongly affects the shape of the theoretical displacement spectrum: It is intuitively clear that the largest wave length efficiently radiated by the source will be connected with R_s. A source region of limited size will be a rather inefficient long-period radiator, and thus one expects the displacement spectral amplitude to decrease at long enough periods, except if R_s is taken to be infinite.

We shall show that the only case where R_s can usefully be taken to be infinite arises when the observer stands inside the relaxation zone. This can easily be explained by the fact that such an observer lies within the source region (as would any observer if R_s is infinite). Such an observer cannot speak in a meaningful way of long-period far-field radiation. Although it is possible to mathematically define such a concept, its physical significance is not clear: The fact is that an observer lying within the source region will always observe source near-field effects at long enough periods. The mathematically defined far-field radiation (that is, that part of the field which decays with distance as 1/r) can only be compared with the observations for wave lengths short compared to the distance between source and observer. If the far-field is to have meaning at longer periods, then the observer

must recede away from the rupture zone accordingly; however, since R_s must be finite for the reasons given above, the observer must eventually find himself beyond R_s, and the finiteness of the relaxation zone can no longer be neglected. A particularly interesting result is that this mathematically defined far-field radiation possesses a spectrum identical in shape with that predicted from the usual dislocation models for which the displacement jump history is a step function in time (e.g., Aki, 1967). This is not surprising in view of the equivalence that we proved in that case in section II-3. Further discussions of these aspects of the question will be found in this chapter, and also in Chapter VII.

The organization of this chapter will be as follows:

In the first section we shall formulate the problem and define the various variables to be considered. The potentials introduced in section I-4 will be used throughout, as well as the results of section II-4.

The two next sections will be devoted to solving the radiation problem by the two attacks described above respectively. In each case, asymptotic behavior of the spectra will be discussed, along with the effects of the various parameters. The multipolar representation of the radiation fields introduced by Archambeau (1964) will be used throughout.

Finally, a discussion of the displacement spectra and of other useful source characteristics will be given in a last section.

IV-1 Formulation of the problem

i) The potential solution in the frequency domain

Our ultimate goal is to obtain the displacement u_i at every point in the medium, as a function of time, or equivalently as a function of frequency. But rather than manipulating the complicated Green's tensor solution developed in Chapters I and II, we choose to consider the four scalar potentials χ_α , $\alpha = 1,\ldots,4$ defined in section I-4, namely

$$\begin{cases} \chi_i = \frac{1}{2}\,\varepsilon_{ijk\ell}\,u_{kij} & i = 1,2,3 \\ \\ \chi_4 = u_{\ell,\ell} \quad . \end{cases} \tag{IV-1-1}$$

The potentials χ_i , $i = 1,2,3$ are the cartesian components of the rotation vector potential, even though we shall use a spherical coordinate system; χ_4 is the dilatation. These scalar potentials satisfy wave equations.

The theory of stress relaxation sources was developed in Chapter II, and it was shown that, for a transparent source, the relative dynamic fields, measured with respect to the final equilibrium fields were given by

$$\chi_\alpha(\mathbf{r},t) = \chi^*_\alpha(\mathbf{r},\tau_o) - \chi^*_\alpha(\mathbf{r},t)$$

$$+ \frac{1}{4\pi c_\alpha^2}\int_o^t H(\tau_o - t_o)\,dt_o \int_{V(t_o)} \frac{\partial \chi^*_\alpha}{\partial t_o}\,\frac{\partial \Gamma_\alpha}{\partial t_o}\,dv^{(o)} \tag{IV-1-2}$$

Here χ^*_α is the initial value field, which is a function of the source time $t_o \leq \tau_o$ for a growing rupture zone. c_α is the wave velocity associated with the potential χ_α, and Γ_α is the infinite space Green's function for the wave equation satisfied by χ_α. We have

$$c_i = V_s \quad , \quad i = 1,2,3; \quad c_4 = V_p \quad , \tag{IV-1-3}$$

where V_s and V_p are the S-wave and the P-wave velocities, respectively. Also (Morse and Feshbach, chapter 7)

$$\Gamma_\alpha(r,t;r_o,t_o) = \frac{\delta(r^*/c_\alpha - t^*)}{r^*} \quad . \tag{IV-1-4}$$

Here $r^* = |r-r_o|$ is the distance between source point and observer's point, and $t^* = t-t_o$. It is clear, since $r^* \geq 0$, that Γ_α vanishes for t^* negative so that we have a causal Green's function (cf. section I-3).

In most cases, that is except for extreme near-field studies, the observer will be concerned about times greater than τ_o, the total rupture duration. In such a case (IV-1-2) takes a simpler form and, using (IV-1-4) we may write

$$\chi_\alpha(r,t) = \frac{1}{4\pi c_\alpha^2}\int_o^{\tau_o} dt_o \int_{V(t_o)} \frac{\partial \chi^*_\alpha}{\partial t_o} \frac{\partial}{\partial t_o}\left[\frac{\delta(r^*/c_\alpha - t^*)}{r^*}\right] dv^{(o)} \quad . \tag{IV-1-5}$$

This is the expression used by Archambeau (e.g., 1972). For time $t < \tau_o$, the analysis shown in this chapter can be duplicated by using (IV-1-2), and the results become more complicated.

It is convenient at this point to take the Fourier transform with respect to t of both sides of (IV-1-5) so as to work in the frequency domain. We define

$$\tilde{\chi}_\alpha(\mathbf{r},\omega) = \int_{-\infty}^{+\infty} \chi_\alpha(\mathbf{r},t)\ e^{-i\omega t}\ dt \qquad \text{(IV-1-6)}$$

so that

$$\chi_\alpha(\mathbf{r},t) = \frac{1}{2\pi}\int_{-\infty}^{+\infty} \tilde{\chi}_\alpha(\mathbf{r},\omega)\ e^{i\omega t}\ d\omega \quad . \qquad \text{(IV-1-7)}$$

We shall concern ourselves only with points $\mathbf{r}$ at large enough distances from the rupture zone so that $\chi_\alpha(\mathbf{r},t)$ vanishes for $t < \tau_o$, and that (IV-1-5) is then a valid representation at all times for such points.

Since t is only a parameter on the right-hand side of (IV-1-5), we can apply the transformation (IV-1-6) to both sides of this equation, and use the following relations

$$\frac{\partial}{\partial t_o}\left[\delta(r^*/c_\alpha - t^*)\right] = -\frac{\partial}{\partial t}\left[\delta(r^*/c_\alpha - t^*)\right]$$

and

$$-\int_{-\infty}^{+\infty} \frac{\partial}{\partial t}\left[\delta\left(r^*/c_\alpha - t^*\right)\right] e^{-i\omega t}\, dt = i\omega\, e^{-ik_\alpha r^*} e^{-i\omega t_o} \quad ,$$

where the wave number k_α is equal to ω/c_α .

The solution may therefore be written in the frequency domain as

$$\tilde{\chi}_\alpha(r,\omega) = \frac{i\omega}{4\pi c_\alpha^2}\int_o^{\tau_o} e^{-i\omega t_o}\, dt_o \int_{V(t_o)} \frac{\partial \chi_\alpha^*}{\partial t_o}\, \frac{e^{-ik_\alpha r^*}}{r^*}\, dv^{(o)} \qquad \text{(IV-1-8)}$$

Now the volume $V(t_o)$ is the volume lying outside the rupture zone itself, and within the relaxation radius R_s . We consider a spherical coordinate system with origin at the point of incipient rupture and polar axis along the direction of propagation of the rupture (see figure IV-1-1). Then (IV-1-8) becomes

$$\tilde{\chi}_\alpha(\ ,\omega) = \frac{i\omega}{4\pi c_\alpha^2}\int_o^{2\pi} d\phi_o \int_o^{\pi} \sin\theta_o\, d\theta_o$$

$$\cdot \int_o^{\tau_o} e^{-i\omega t_o}\, dt_o \int_{r(\theta_o,\phi_o,t_o)}^{R_s} \frac{\partial \chi_\alpha^*}{\partial t_o}\, \frac{e^{-ik_\alpha r^*}}{r^*}\, r_o^2\, dr_o \quad .$$

(IV-1-9)

This equation gives us the potential solution in the frequency domain, provided that we can perform the integrations.

ii) Geometry of the rupture

The geometry of the rupture is described in figure IV-1-1. The fundamental coordinate system, hereafter called the source coordinate system has its origin 0 at the point of incipient rupture. The source spherical coordinates are r_o , ϕ_o , θ_o . The failure zone is a sphere of variable radius $R(t_o)$ centered on the z axis at a distance $d(t_o)$. The constraint that no healing occurs can then be written

$$\left.\begin{aligned} d(t_o) &\leq R(t_o) \\ \frac{d}{dt_o}\left[d(t_o) + R(t_o)\right] &\geq 0 \end{aligned}\right\} \quad \text{for all } t_o \ . \qquad \text{(IV-1-10)}$$

Another coordinate system, hereafter called the moving system, is defined in order to take advantage of the spherical symmetry of the source. It has its origin at the center $0'$ of the rupture, and is obtained from the source system by a translation $d(t_o)$ along the z axis. The relaxation zone is taken to be the inside of a sphere with center at 0 and of radius R_s .

The point P is an arbitrary observer's point, with coordinates r , θ , ϕ in the source system; the point Q is an arbitrary source point.

If one wishes to model an explosion, then no propagation occurs and

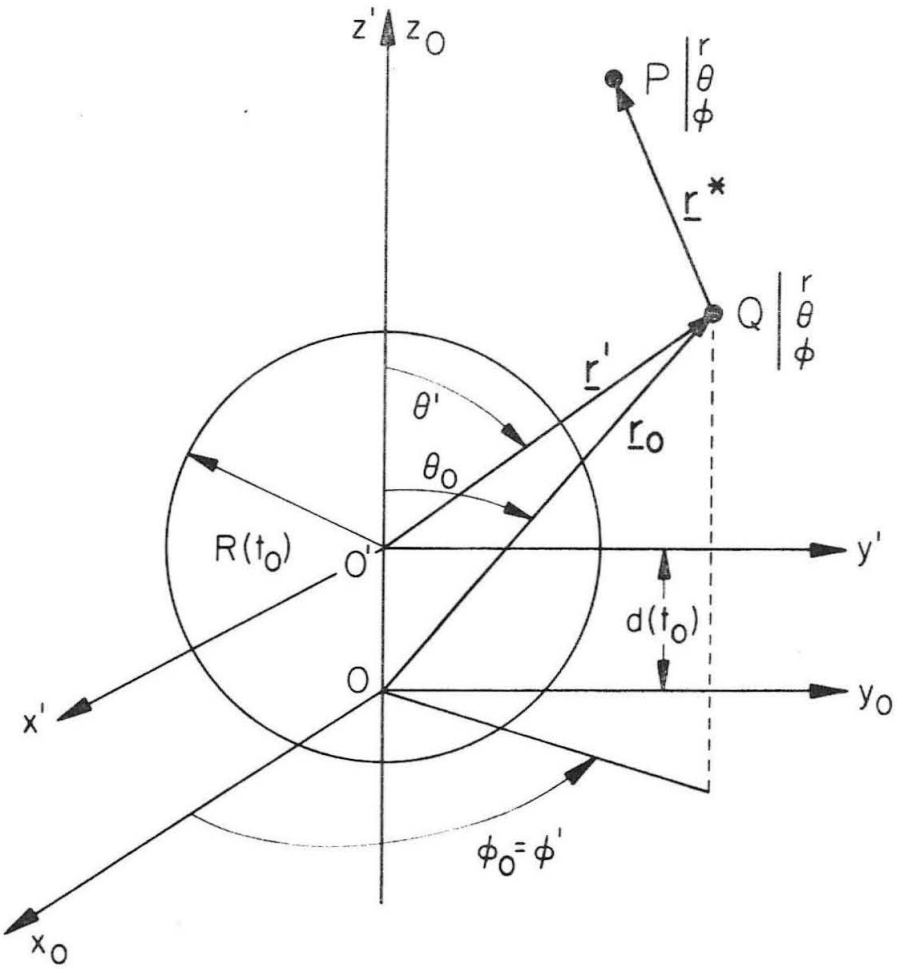

Figure IV-1-1. Geometry for a propagating spherical rupture of radius $R(t_o)$. O is the origin of the source system, O' the origin of the moving system. Q is a source point, and P the observer's point.

$d(t_o)$ is taken to vanish for all source times t_o . For an earthquake with unilateral rupture propagation one may choose $d(t_o) = R(t_o)$ at all times so that the rupture front propagates with the rupture velocity $V_R = 2 \frac{d}{dt_o} R(t_o)$, while no motion of the boundary occurs at the point of incipient rupture. It is intuitively clear that after a finite propagation most of the stress relaxation will occur ahead of the rupture front, while little energy will be radiated from the vicinity of the hypocenter. With this particular geometry the propagation effects will then be the strongest. We shall assume $V_R \leq V_s$.

If one is interested in studying the radiation field from a small rupture zone propagating rapidly, it is possible to consider the case where $d(t_o)$ grows faster than $R(t_o)$. One has to remember, however, that the permanent deformation present in the "healed" part of the rupture may have been ignored. Since this is essentially a static effect, such a model is not strictly appropriate for long periods; but since most of the relaxation occurs in the vicinity of the rupture front, this model yields approximately valid results at high frequency, provided that one removes from the solution the energy radiated from the "tail" of the rupture.

The geometry described on figure IV-1-1 is thus quite flexible and will permit us to model a reasonably wide variety of situations.

iii) Computation of the initial value

For each source time t_o , the potential χ^*_α is a harmonic function and may be expanded in solid harmonics (e.g., Archambeau, 1968), that is, in the moving system, at t_o ,

$$\chi_\alpha^*(r',t_o) = \sum_{n=0}^{\infty} \frac{1}{(r')^{n+1}} \sum_{m=0}^{n} \left[a_{nm}^{(\alpha)} \cos m\phi' + b_{nm}^{(\alpha)} \sin m\phi' \right] \cdot P_n^m(\cos\theta') \qquad \text{(IV-1-11)}$$

The perturbation to the elastic fields in an infinite medium under homogeneous stress at infinity caused by a liquid spherical inclusion can be calculated by a variety of methods. Archambeau (1964) used the solution given by Landau and Lifschitz (1951), who found the displacement solution as a combination of biharmonic functions. When the prestress is a pure shear at infinity, Archambeau was able to show that only the quadrupolar term (n=2) is in fact present in (IV-1-11), so that

$$\chi_\alpha^*(r',t_o) = \frac{1}{(r')^3} \sum_{m=0}^{2} \left[a_{2m}^{(\alpha)} \cos m\phi' + b_{2m}^{(\alpha)} \sin m\phi' \right] P_2^m(\cos\theta') \qquad \text{(IV-1-12)}$$

and the (static) coefficients $a_{2m}^{(\alpha)}$ and $b_{2m}^{(\alpha)}$ are given by †

---

† The coefficients given by Archambeau in his publications prior to 1973 have to be divided by -2 for $\alpha = 1,2,3$, they are correct for $\alpha = 4$.

$$a_{2m}^{(\alpha)}(t_o) = \frac{5[(1-\sigma)-\delta_{\alpha 4}\sigma]}{\mu(7-5\sigma)} R^3(t_o) \begin{bmatrix} -3\sigma_{23}^{(o)}/2 & -\sigma_{12}^{(o)}/2 & -\sigma_{23}^{(o)}/4 \\ 3\sigma_{13}^{(o)}/2 & 0 & \sigma_{13}^{(o)}/4 \\ 0 & \sigma_{23}^{(o)}/2 & \sigma_{12}^{(o)}/2 \\ 0 & \sigma_{13}^{(o)} & 0 \end{bmatrix}$$

(IV-1-13)

and

$$b_{2m}^{(\alpha)}(t_o) = \frac{5[(1-\sigma)-\delta_{\alpha 4}\sigma]}{\mu(7-5\sigma)} R^3(t_o) \begin{bmatrix} 0 & 0 & \sigma_{13}^{(o)}/4 \\ 0 & \sigma_{12}^{(o)}/2 & -\sigma_{23}^{(o)}/4 \\ 0 & -\sigma_{13}^{(o)}/2 & 0 \\ 0 & \sigma_{23}^{(o)} & \sigma_{12}^{(o)}/2 \end{bmatrix}$$

(IV-1-14)

Here the quantities $\sigma_{ij}^{(o)}$ are the components of the homogeneous prestress, chosen to be pure shear in this case.

In order to isolate the time dependence of these coefficients we write

$$\begin{cases} a_{2m}^{(\alpha)}(t_o) = a'^{(\alpha)}_{2m} R^3(t_o) \\ \\ b_{2m}^{(\alpha)}(t_o) = b'^{(\alpha)}_{2m} R^3(t_o) \quad . \end{cases}$$

(IV-1-15)

The expansion (IV-1-12) holds in the moving coordinate system. The azimuthal dependence exhibited by this expansion of the static fields must essentially be that of the very long period radiation, for which propagation effects are not expected to be very strong; we therefore see, since only the quadrupole term is excited, that the long period radiation pattern must be essentially quadrupole, which is in agreement with the observations.

Note that for geometries other than spherical, one does not expect only the harmonics of degree 2 to be excited, especially close to the rupture zone; but for r' sufficiently large, because of the radial dependence of the solid harmonics, one expects the quadrupole to dominate in all cases.

The solutions given in the next sections assume that the rupture velocity V_R is less than or equal to the wave velocity c_α. It is clear that for a supersonic rupture velocity, the rupture may be considered to be instantaneously created. In particular, if $V_s < V_R < V_p$ the problem is to be treated differently for the rotation potentials and for the dilatation. We shall not treat such cases explicitly; Archambeau (1972) presents a discussion of the subject, in the context of explosion modelling.

IV-2 Archambeau's method of solution

The first approach to the dynamical problem as described in the introduction to this chapter, consists of evaluating the dynamic solution (IV-1-9) in the source coordinate system. This is the attack adopted by Archambeau (1964). The results which we shall obtain in this section are of somewhat simpler appearance and of greater generality than Archambeau's results, and reduce to these results in specific circumstances.

i) Translation of the static fields

The first step we have to take is to find an expression for the initial value fields χ_α^* in the source coordinate system. We know that in the moving system we have

$$\chi_\alpha^*(r',t_o) = \sum_{n=0}^{\infty} \frac{\delta_{n2}}{(r')^{n+1}} \sum_{m=0}^{2} \left[a_{nm}^{(\alpha)} \cos m\phi' + b_{nm}^{(\alpha)} \sin m\phi' \right] \cdot P_n^m(\cos \theta') \qquad \text{(IV-2-1)}$$

where only the term for $n=2$ is present, and where the coefficients $a_{nm}^{(\alpha)}(t_o)$ and $b_{nm}^{(\alpha)}(t_o)$ are given by (IV-1-14) .

The coordinate transformation that we wish to perform is a simple translation, of amplitude $-d(t_o)$, along the polar axis. In that translation the azimuthal angle ϕ' does not change so that $\phi_o = \phi'$. Then from Hobson (1931, p. 140) we have the following addition theorem

$$\frac{P_n^m(\cos\theta')}{(r')^{n+1}} = \frac{1}{r_o^{n+1}} \sum_{s=0}^{\infty} \frac{(n-m+s)!}{(n-m)!\ s!} \left(\frac{d(t_o)}{r_o}\right)^s P_{n+s}^m(\cos\theta_o) \qquad \text{(IV-2-2)}$$

which converges uniformly with respect to r_o for $r_o > d(t_o)$.

Substituting (IV-2-2) into (IV-2-1) , where we need keep only the term $n=2$,

$$\chi_\alpha^*(r_o,t_o) = \sum_{s=0}^{\infty} \sum_{m=0}^{2} \frac{1}{r_o^3} \left[a_{2m}^{(\alpha)} \cos m\phi_o + b_{2m}^{(\alpha)} \sin m\phi_o \right]$$

$$\cdot \frac{(s+2-m)!}{(2-m)!\ s!} \left(\frac{d(t_o)}{r_o}\right)^s P_{2+s}^m(\cos\theta_o) \quad . \qquad \text{(IV-2-3)}$$

This equation may be transformed by defining $\ell = s+2$ and by using (IV-1-14) ; we get

$$\chi_\alpha^*(r_o,t_o) = \sum_{\ell=2}^{\infty} \sum_{m=0}^{2} \frac{R^3(t_o)\ d^{\ell-2}(t_o)}{r_o^{\ell+1}} \left[a'^{(\alpha)}_{2m} \cos m\phi_o + b'^{(\alpha)}_{2m} \sin m\phi_o \right]$$

$$\cdot \frac{(\ell-m)!}{(\ell-2)!\ (2-m)!} P_\ell^m(\cos\theta_o) \quad , \qquad \text{(IV-2-4)}$$

where the coefficients $a'^{(\alpha)}_{2m}$ and $b'^{(\alpha)}_{2m}$ are given by (IV-1-14) ,

and are time independent. Note that only the harmonics of degree ≥ 2 are present; in particular for $d(t_o) = 0$, one must keep only the term for $\ell=2$ in (IV-2-4) . This is the case for a purely expanding (non-propagating) spherical rupture, appropriate for the modeling of an underground explosion in a stressed medium.

The equation (IV-2-1) is merely a particular case of (IV-2-4) , where a sum over ℓ reduces to its first term. Recall that (IV-2-4) is only valid for $r_o > d(t_o)$. This means that the use of this expansion restricts the possible volume of integration in (IV-1-9) . However, as shown on figure IV-2-1 , the forbidden region, delineated by horizontal stripes is a region where the material is presumably already relaxed, so that one does not make a large error in ignoring the energy radiated from it. In fact, one would rather avoid including any part of the rupture zone itself from the volume of integration, and one is thus led to restrict the volume of integration to the exterior of the sphere of radius $d(t_o) + R(t_o)$ passing through the rupture front. One argument in favor of this choice is that most of energy radiated comes from the vicinity of the rupture front, while the energy ignored (that emanating from the vertically striped region) is likely to be absorbed by the inelastic, nonlinear processes of rupture.

Numerical calculations (Chapter VII) show that if the volume of integration is restricted to the exterior of a sphere centered at 0 , and of radius R_o such that $d(t_o) \leq R_o(t_o) \leq d(t_o) + R(t_o)$, then the rate of convergence of the solution improves notably when R_o is chosen close to the upper bound of this range. But we then found

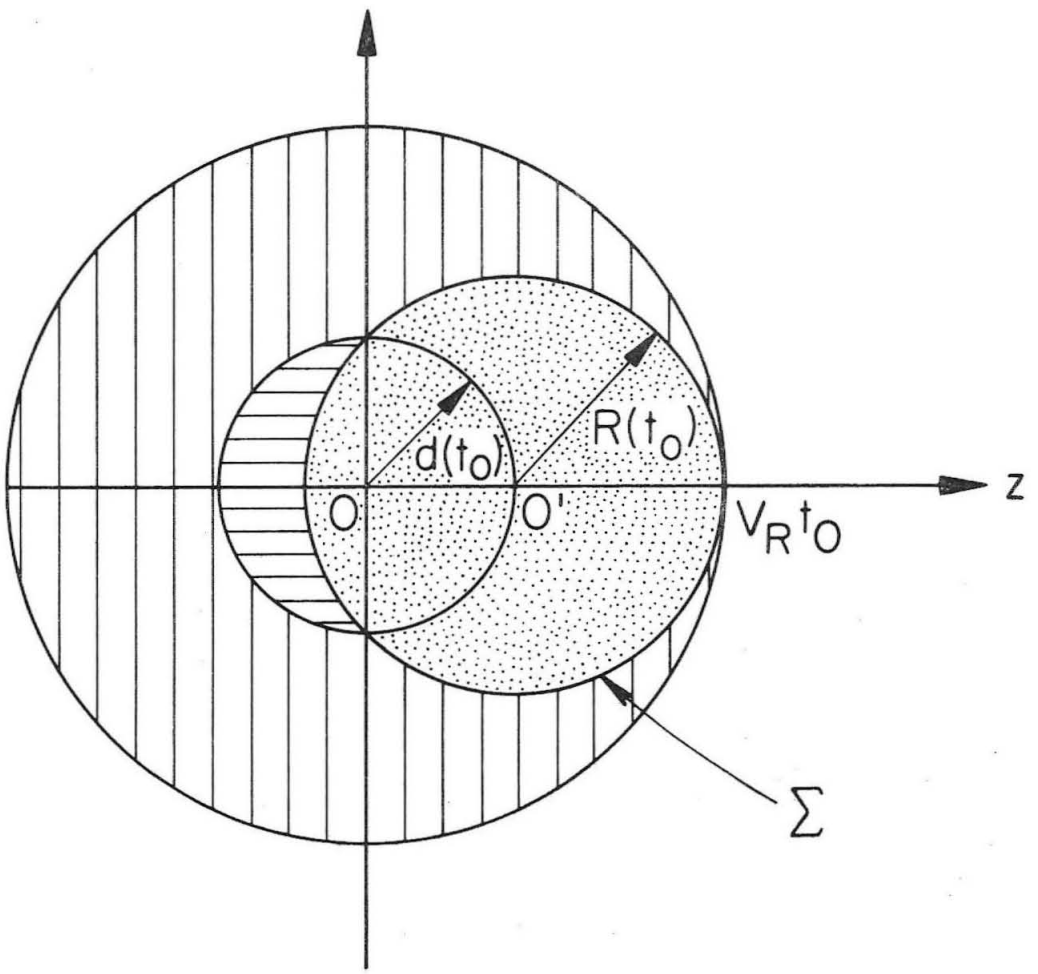

Figure IV-2-1. The sphere of center O' and radius $R(t_o)$ is the rupture zone. The rupture front propagates at the velocity V_R. The initial value volume integral can be taken external to the sphere of radius $V_R t_o$, or to the sphere of radius $d(t_o)$.

that the final result is rather insensitive to R_o . For our present purposes, we shall choose the upper bound of this inequality, and if V_R is the propagation velocity of the rupture front—hereafter called the rupture velocity—then the volume of integration is restricted to the exterior of the sphere of radius $V_R t_o$.

ii) Evaluation of the radiation fields

In view of the discussion presented above, the radiation field given by equation (IV-1-9) takes the form

$$\tilde{\chi}_\alpha(\mathbf{r},\omega) = \frac{i\omega}{4\pi c_\alpha^2}\int_o^{2\pi} d\phi_o \int_o^{\pi} \sin\theta_o \, d\theta_o$$

$$\cdot \int_o^{\tau_o} e^{-i\omega t_o} \, dt_o \int_{V_R t_o}^{R_s} \frac{\partial \chi_\alpha^*}{\partial t_o} \frac{e^{-ik_\alpha r^*}}{r^*} r_o^2 \, dr_o \qquad \text{(IV-2-5)}$$

We shall now evaluate the integrals appearing in (IV-2-5) . Two cases arise: either the observer's point lies within the relaxation zone, and $r < R_s$, or it lies beyond R_s . For convenience we shall consider the former instance first, then the results thus obtained may be easily adapted to the latter case.

Let us first replace the Green's function appearing in the integrand by its usual spherical wave expansion (e.g., Morse and Feshbach, 1953).

We have

$$\frac{e^{-ik_\alpha r^*}}{r^*} = -ik_\alpha \sum_{\lambda=0}^{\infty} (2\lambda+1)\, P_\lambda(\cos\gamma) \begin{cases} j_\lambda(k_\alpha r_o)\, h_\lambda^{(2)}(k_\alpha r) \ , \\ \\ j_\lambda(k_\alpha r)\, h_\lambda^{(2)}(k_\alpha r_o) \ , \end{cases}$$

(IV-2-6)

where the upper pair of Bessel functions are to be used when $r > r_o$, and the lower pair when $r < r_o$. Here the angle γ is the angle between the vectors $\mathbf{r}$ and $\mathbf{r}_o$ (e.g., Stratton, p. 407) and we have (Stratton, p. 408)

$$P_\lambda(\cos\gamma) = \sum_{k=0}^{\lambda} (2 - \delta_{ko}) \frac{(\lambda-k)!}{(\lambda+k)!} P_\lambda^k(\cos\theta)\, P_\lambda^k(\cos\theta_o) \cos k(\phi-\phi_o) \ .$$

(IV-2-7)

where δ_{ko} is the usual Kronecker delta. We also have the integral relation (Stratton, p. 407)

$$\int_o^{2\pi} \int_o^{\pi} P_\lambda(\cos\gamma)\, P_\nu^\mu(\cos\theta_o) \begin{pmatrix} \cos\mu\phi_o \\ \\ \sin\mu\phi_o \end{pmatrix} \sin\theta_o \, d\theta_o \, d\phi_o =$$

$$\frac{4\pi}{2\lambda+1} P_\lambda^\mu(\cos\theta) \begin{pmatrix} \cos\mu\phi \\ \\ \sin\mu\phi \end{pmatrix} \delta_{\lambda\nu} \ . \qquad \text{(IV-2-8)}$$

The radial integral in (IV-2-5) can be split in the form

$$\int_{V_R t_o}^{R_s} = \int_{V_R t_o}^{r} + \int_{r}^{R_s} \quad .$$

Then by substituting the appropriate expansion (IV-2-6) into each of these integrals, replacing the initial field χ_α^* by its expression given in (IV-2-4) , and making use of the orthogonality property (IV-2-8) , we obtain the radiation field in the form

$$\tilde{\chi}_\alpha(\mathbf{r},\omega) = \sum_{\ell=2}^{\infty} \sum_{m=0}^{2} P_\ell^m(\cos\theta)$$

$$\cdot \left[h_\ell^{(2)}(k_\alpha r) \left[{}_\ell A_{2m}^{(\alpha)} \cos m\phi + {}_\ell B_{2m}^{(\alpha)} \sin m\phi \right] \right.$$

$$\left. + j_\ell(k_\alpha r) \left[{}_\ell C_{2m}^{(\alpha)} \cos m\phi + {}_\ell D_{2m}^{(\alpha)} \sin m\phi \right] \right] \quad . \qquad \text{(IV-2-9)}$$

The coefficients ${}_\ell A_{2m}$, ${}_\ell B_{2m}$, ${}_\ell C_{2m}$, ${}_\ell D_{2m}$ are given by

$$\begin{pmatrix} {}_{\ell}A_{2m}^{(\alpha)}(r,\omega) \\ {}_{\ell}B_{2m}^{(\alpha)}(r,\omega) \end{pmatrix} = \begin{pmatrix} a'^{(\alpha)}_{2m} \\ b'^{(\alpha)}_{2m} \end{pmatrix} \frac{(\ell-m)!}{(\ell-2)!\ (2-m)!} \frac{k_\alpha^2}{c_\alpha}$$

$$\cdot \int_o^{\tau_o} e^{-i\omega t_o} \frac{d}{dt_o} [R^3(t_o)\ d^{\ell-2}(t_o)] \int_{V_R t_o}^{r} \left(\frac{1}{r_o}\right)^{\ell+1} j_\ell(k_\alpha r_o)\ r_o^2\ dr_o\ dt_o$$

(IV-2-10)

and

$$\begin{pmatrix} {}_{\ell}C_{2m}^{(\alpha)}(r,\omega) \\ {}_{\ell}D_{2m}^{(\alpha)}(r,\omega) \end{pmatrix} = \begin{pmatrix} a'^{(\alpha)}_{2m} \\ b'^{(\alpha)}_{2m} \end{pmatrix} \frac{(\ell-m)!}{(\ell-2)!\ (2-m)!} \frac{k_\alpha^2}{c_\alpha}$$

$$\cdot \int_o^{\tau_o} e^{-i\omega t_o} \frac{d}{dt_o} [R^3(t_o)\ d^{\ell-2}(t_o)] \int_{r}^{R_s} \left(\frac{1}{r_o}\right)^{\ell+1} h_\ell^{(2)}(k_\alpha r_o)\ r_o^2\ dr_o\ dt_o$$

(IV-2-11)

For the case of an expanding, non-propagating sphere ("explosion" model), the spherical symmetry is preserved, and thus only the term $\ell=2$ survives in (IV-2-9) , (IV-2-10) and (IV-2-11) .

If the observer's point lies outside the relaxation zone then we have $R_s < r$; in that case only the coefficients ${}_{\ell}A_{2m}^{(\alpha)}$ and ${}_{\ell}B_{2m}^{(\alpha)}$ are present, and the upper bound of the integral over r_o in (IV-2-10) must be changed to R_s .

In spite of its symmetrical appearance, the solution (IV-2-9) is not particularly convenient since the coefficients depend on r, the hypocentral distance of the observer. A more convenient form for computation can be obtained by evaluating the integrals in (IV-2-10) and (IV-2-11).

The following closed forms are evaluated in Appendix 2--equations (A-2-2) and (A-2-3) :

$$\int_a^b (r_o)^{-(\ell+1)}\, j_\ell(k_\alpha r_o)\, r_o^2\, dr_o = \frac{j_{\ell-1}(k_\alpha a)}{k_\alpha a^{\ell-1}} - \frac{j_{\ell-1}(k_\alpha b)}{k_\alpha b^{\ell-1}} \quad , \qquad \text{(IV-2-12)}$$

$$\int_a^b (r_o)^{-(\ell+1)}\, h_\ell^{(2)}(k_\alpha r_o)\, r_o^2\, dr_o = \frac{h_{\ell-1}^{(2)}(k_\alpha a)}{k_\alpha a^{\ell-1}} - \frac{h_{\ell-1}^{(2)}(k_\alpha b)}{k_\alpha b^{\ell-1}} \quad . \qquad \text{(IV-2-13)}$$

Inserting these formulae into (IV-2-10) and (IV-2-11) yields

$$\begin{pmatrix} {}_\ell A_{2m}^{(\alpha)}(r,\omega) \\ {}_\ell B_{2m}^{(\alpha)}(r,\omega) \end{pmatrix} = \begin{pmatrix} a'^{(\alpha)}_{2m} \\ b'^{(\alpha)}_{2m} \end{pmatrix} \frac{(\ell-m)!}{(\ell-2)!\ (2-m)!} \frac{k_\alpha^\ell}{c_\alpha}$$

$$\cdot \int_o^{\tau_o} e^{-i\omega t_o} \frac{d}{dt_o} [R^3(t_o)\ d^{\ell-2}(t_o)] \left[\frac{j_{\ell-1}(k_\alpha V_R t_o)}{(k_\alpha V_R t_o)^{\ell-1}} - \frac{j_{\ell-1}(k_\alpha r)}{(k_\alpha r)^{\ell-1}} \right] dt_o$$

(IV-2-14)

and

$$\begin{pmatrix} {}_{\ell}C_{2m}^{(\alpha)}(r,\omega) \\ \\ {}_{\ell}D_{2m}^{(\alpha)}(r,\omega) \end{pmatrix} = \begin{pmatrix} a_{2m}'^{(\alpha)} \\ \\ b_{2m}'^{(\alpha)} \end{pmatrix} \frac{(\ell-m)!}{(\ell-2)!\ (2-m)!} \frac{k_\alpha^\ell}{c_\alpha}$$

$$\cdot \int_o^{\tau_o} e^{-i\omega t_o} \frac{d}{dt_o} [R^3(t_o)\ d^{\ell-2}(t_o)] \left[\frac{h_{\ell-1}^{(2)}(k_\alpha r)}{(k_\alpha r)^{\ell-1}} - \frac{h_{\ell-1}^{(2)}(k_\alpha R_s)}{(k_\alpha R_s)^{\ell-1}} \right] dt_o \ . \qquad \text{(IV-2-15)}$$

In the case where $R_s < r$, the coefficients ${}_{\ell}C_{2m}^{(\alpha)}$ and ${}_{\ell}D_{2m}^{(\alpha)}$ vanish identically and r must be replaced by R_s in (IV-2-14) . One sees therefore that the only integrals left to evaluate are

$$I_\ell^{(1)}(\omega) = \int_o^{\tau_o} e^{-i\omega t_o} \frac{d}{dt_o} [R^3(t_o)\ d^{\ell-2}(t_o)]\ dt_o \quad , \qquad \text{(IV-2-16)}$$

$$I_\ell^{(2)}(\omega) = \int_o^{\tau_o} e^{-i\omega t_o} \frac{d}{dt_o} [R^3(t_o)\ d^{\ell-2}(t_o)] \frac{j_{\ell-1}(k_\alpha V_R t_o)}{(k_\alpha V_R t_o)^{\ell-1}}\ dt_o \quad , \qquad \text{(IV-2-17)}$$

and, in the case $R_s < r$,

$$I_\ell^{(3)}(\omega) = \int_o^{\tau_o} e^{-i\omega t_o} \frac{d}{dt_o} [R^3(t_o)\, d^{\ell-2}(t_o)]$$

$$\cdot \left[\frac{j_{\ell-1}(k_\alpha V_R t_o)}{(k_\alpha V_R t_o)^{\ell-1}} - \frac{j_{\ell-1}(k_\alpha R_s)}{(k_\alpha R_s)^{\ell-1}} \right] dt_o \quad . \qquad \text{(IV-2-18)}$$

The last integral $I_\ell^{(3)}$ is obviously a linear combination of $I_\ell^{(1)}$ and $I_\ell^{(2)}$. If $R(t_o)$ and $d(t_o)$ are taken to be polynomials of t_o , then these integrals are linear combinations of functions having the general form

$$G(a,\mu,\nu;\tau_o) = \int_o^{\tau_o} e^{-at}\, t^\mu\, J_\nu(t)\, dt \quad , \qquad \text{(IV-2-19)}$$

where ν and μ are half integers. Such functions are evaluated in closed form in Appendix 2, in the case where $\nu = n+1/2$ and where μ varies from $-n+1/2$ to $n+3/2$. This would limit the possible choice of growth and propagation functions for the source. In addition, the closed form derived in Appendix 2 was found to be poorly behaved for numerical computation. The integral (IV-2-19) can also be expanded in a series of generalized hypergeometric functions (Luke, 1969) but the algebra is extremely cumbersome and will be omitted here.

The integral $I_\ell^{(1)}(\omega)$ clearly has the form of a finite Fourier transform. $I_\ell^{(2)}$ is also of this form, except that $k_\alpha = \omega/c_\alpha$ appears

in the argument of the spherical Bessel function. Nevertheless, for a fixed value k_α , one can evaluate this integral as a finite Fourier transform, as a function of ω , and set $\omega = k_\alpha c_\alpha$ in the result. This approach was found to be, by far, the most efficient for numerical applications. Filon's method of numerical integration (e.g., Alexander, 1963) proved particularly appropriate to compute the Fourier transform numerically.

We can now combine the r-dependent terms in (IV-2-14) and (IV-2-15) , and make use in (IV-2-9) of the Wronskian relation (Abramovitz, 1964)

$$j_\ell(kr)\, h^{(2)}_{\ell-1}(kr) - h^{(2)}_\ell(kr)\, j_{\ell-1}(kr) = -\frac{i}{k^2 r^2} \quad . \qquad \text{(IV-2-20)}$$

This allows us to write the solution in the form

$$\tilde{\chi}_\alpha(r,\omega) = \sum_{\ell=2}^{\infty} \sum_{m=0}^{2} P^m_\ell(\cos\theta) \left\{ h^{(2)}_\ell(k_\alpha r) \left[A^{(\alpha)}_{\ell m} \cos m\phi + B^{(\alpha)}_{\ell m} \sin m\phi \right] \right.$$

$$+ j_\ell(k_\alpha r) \left[C^{(\alpha)}_{\ell m} \cos m\phi + D^{(\alpha)}_{\ell m} \sin m\phi \right]$$

$$\left. + \frac{i}{(k_\alpha r)^{\ell+1}} \left[E^{(\alpha)}_{\ell m} \cos m\phi + F^{(\alpha)}_{\ell m} \sin m\phi \right] \right\}$$

(IV-2-21)

where the various coefficients are now independent of r . We shall call them "multipole coefficients;" they are given by

$$\begin{pmatrix} A^{(\alpha)}_{\ell m}(\omega) \\ B^{(\alpha)}_{\ell m}(\omega) \end{pmatrix} = \begin{pmatrix} a'^{(\alpha)}_{2m} \\ b'^{(\alpha)}_{2m} \end{pmatrix} \frac{(\ell-m)!}{(\ell-2)!\ (2-m)!} \frac{k_\alpha^\ell}{c_\alpha} \begin{cases} I^{(2)}_\ell(\omega) & \text{if } r < R_s , \\ I^{(3)}_\ell(\omega) & \text{if } r > R_s , \end{cases} \tag{IV-2-22a}$$

and

$$\begin{pmatrix} C^{(\alpha)}_{\ell m}(\omega) \\ D^{(\alpha)}_{\ell m}(\omega) \end{pmatrix} = \frac{h^{(2)}_{\ell-1}(k_\alpha R_s)}{(k_\alpha R_s)^{\ell-1}} \begin{pmatrix} E^{(\alpha)}_{\ell m}(\omega) \\ F^{(\alpha)}_{\ell m}(\omega) \end{pmatrix} , \tag{IV-2-22b}$$

where

$$\begin{pmatrix} E^{(\alpha)}_{\ell m}(\omega) \\ F^{(\alpha)}_{\ell m}(\omega) \end{pmatrix} = - \begin{pmatrix} a'^{(\alpha)}_{2m} \\ b'^{(\alpha)}_{2m} \end{pmatrix} \frac{(\ell-m)!}{(\ell-2)!\ (2-m)!} \frac{k_\alpha^\ell}{c_\alpha} \begin{cases} I^{(1)}_\ell(\omega) & \text{if } r < R_s . \\ 0 & \text{if } r > R_s . \end{cases}$$

(IV-2-22c)

We notice, however, that the last term in (IV-2-21) does not represent a traveling wave. It emerges from the time dependence of the initial value field as it is created. To see this one just has to note that this term is merely the Fourier transform $\tilde{\chi}^*_\alpha(\mathbf{r},\omega)$ of the initial value field given by (IV-2-4) .

Because $\chi_\alpha(\mathbf{r},t)$ was defined originally as the relative field, measured from the final equilibrium state of the medium, by subtracting the initial value from it one gets the radiation field which is, in fact, observed and measured experimentally. This was discussed in Chapter II. Thus the final solution for the dynamic field above takes the form

$$\tilde{\chi}_\alpha(\mathbf{r},\omega) = \sum_{\ell=2}^{\infty} \sum_{m=0}^{2} P_\ell^m(\cos\theta) \left\{ h_\ell^{(2)}(k_\alpha r) \left[A_m^{(\alpha)} \cos m\phi + B_m^{(\alpha)} \sin m\phi \right] \right.$$

$$\left. + j_\ell(k_\alpha r) \left[C_{\ell m}^{(\alpha)} \cos m\phi + D_{\ell m}^{(\alpha)} \sin m\phi \right] \right\} , \qquad \text{(IV-2-23)}$$

where the multipole coefficients are given by (IV-2-22) .

iii) Discussion

The solution (IV-2-23) gives the scalar potentials $\tilde{\chi}_\alpha$ in the form of multipolar expansions. It is clear that the source model under consideration is not a separable source (Archambeau, 1968): one cannot in general separate the frequency dependence and the spatial dependence of the fields algebraically. Furthermore, if more than one multipole is present, the radial variation cannot be separated from the angular dependence by factorization. Archambeau (1968) pointed out that, in general, the multipole coefficients are linearly independent functions of frequency.

In the case of a non-propagating rupture, $d(t_o)$ vanishes

identically and only the term for $\ell=2$ is present in the expansion (IV-2-23) . The field is then pure quadrupole; this is the result obtained by Archambeau and Sammis (1970) and Archambeau (1964, 1972) for the tectonic release due to an explosion in a prestressed medium. Randall (1966) also found a pure quadrupole radiation in the case of the instantaneous creation of the rupture ($V_R = \infty$) . As shown by Archambeau (1972), this is a particular case of the general situation presented here, and one adequate to model a cavity growing faster than the P-wave velocity. Archambeau proposed a two-stage model for the purpose of modeling an underground nuclear explosion, where the velocity of expansion V_R is greater than the P-wave velocity in the first stage, and then drops to a subsonic velocity in the second stage. We refer the reader to his publications for a detailed description of the model.

The fact that the non-propagating spherical rupture generates a pure quadrupole radiation is in complete agreement with the observations of the anomalous radiation from underground nuclear explosions (e.g., Lambert, Flinn and Archambeau, 1972). The pure quadrupole radiation pattern corresponds to a double couple point source and is also found in association with simple Volterra dislocation models of earthquakes (e.g., Randall, 1971). The higher order multipoles appearing in (IV-2-23) are excited only if $d(t_o)$ is non-zero; in other words, the presence of multipoles of degree greater than 2 is intimately associated with rupture propagation phenomena, and the departure from self similar rupture growth.

For separable sources, rupture propagation effects can be

introduced by use of a propagation function (e.g., Ben Menahem, 1961; Haskell, 1964). These effects can be understood intuitively by analogy with the usual Doppler effects. One expects them to affect waves with a wave length comparable to, or smaller than, the total source dimension. In other words, propagation effects will be most evident in the high frequency part of the radiation spectrum. Archambeau (1964, 1968) showed how the multipoles of degree greater than 2 distort the radiation pattern at high frequency, while they have a negligible effect at long periods. The numerical results given in Chapter VII exhibit the same behavior: the radiation pattern is almost pure quadrupole at low frequencies, while more energy is radiated in the direction of rupture propagation than in the opposite direction at high frequencies.

The solution (IV-2-23) simplifies itself in two extreme cases of interest. Those are 1) $r > R_s$, and 2) $R_s = \infty$. In both cases the multipole coefficients $C_{\ell m}^{(\alpha)}$ and $D_{\ell m}^{(\alpha)}$ vanish identically and we have

$$\tilde{\chi}_\alpha(\mathbf{r},\omega) = \sum_{\ell=2}^{\infty} \sum_{m=0}^{2} P_\ell^m(\cos\theta)\, h_\ell^{(2)}(k_\alpha r) \left[A_{\ell m}^{(\alpha)} \cos m\phi + B_{\ell m}^{(\alpha)} \sin m\phi \right] . \qquad \text{(IV-2-24)}$$

The only difference comes in the computation of the multipole coefficients $A_{\ell m}^{(\alpha)}$ and $B_{\ell m}^{(\alpha)}$ by equation (IV-2-22a) . In the first instance the integral $I_\ell^{(3)}$ must be used, and in the second instance, $I_\ell^{(2)}$ is the proper choice.

We shall show below that these two cases lead to radically different behaviors of the radiation spectra at long-period, particularly

in the far-field approximations. As we pointed out in the introduction to this chapter, the two cases mentioned above correspond 1) to a mathematical approximation of the real physical situation, and 2) to an exact mathematical representation of an approximate physical situation. We feel that, although neither case may precisely model the real phenomenon, it is probable that the truth lies somewhere between the two extremes. Thus the two extreme spectral shapes obtained in this fashion ("peaked" spectrum, and "flat" spectrum, as we shall see) should bracket the range of possible observations. The first case corresponds to the model proposed and investigated by Archambeau (e.g., 1964), the second one was advocated by Randall (1973) and also by a number of other investigators using dislocation models. Unfortunately, to this date, field observations have not been obtained which would be of high enough quality to allow a clear choice between the two models (Molnar et al, 1973); however, it seems very likely, in view of our previous comments, that there is no clear-cut choice.

iv) Asymptotic behavior of the potential spectra.

The principal advantage of having an analytical solution for the radiation spectrum is that one can obtain the asymptotic behavior of this spectrum in a number of limiting cases. Such cases include the very high frequency limit, as well as the very low frequency limit of the spectrum. In addition, at low frequencies--that is, at long periods--we shall distinguish between near-field and far-field approximations. These approximations take into account the decay with distance of the spectral amplitude.

In this section we shall only consider the spectra of the various potentials $\tilde{\chi}_\alpha$; the extension of these results to the displacement spectra will be made in section IV-4.

a) High frequency behavior

This case is the simplest to investigate. It is shown in Appendix 4 that, if $R(t_o)$ and $d(t_o)$ both are linear in t_o , which is the case for the model considered here, then the following results hold in the case $R_s >> V_R \tau_o$

$$\text{for } \omega >> 1 \begin{cases} I_\ell^{(1)} = 0(1/\omega) \\ I_\ell^{(2)} = 0(1/\omega^{\ell+1}) \\ I_\ell^{(3)} = 0(1/\omega^{\ell+1}) \ . \end{cases} \qquad \text{(IV-2-25)}$$

Further, in that case, for any finite value of r , we have $k_\alpha r >> 1$ and $k_\alpha R_s >> 1$. Thus the following asymptotic relations hold

$$j_\ell(k_\alpha r) \sim \text{Re}\left(i^{\ell+1} \frac{e^{-ik_\alpha r}}{k_\alpha r} \right) \ , \qquad \text{(IV-2-26a)}$$

$$h_\ell^{(2)}(k_\alpha r) \sim i^{\ell+1} \frac{e^{-ik_\alpha r}}{k_\alpha r} \ , \qquad \text{(IV-2-26b)}$$

$$\frac{h^{(2)}_{\ell-1}(k_\alpha R_s)}{(k_\alpha R_s)^{\ell-1}} \sim i^{\ell} \frac{e^{-ik_\alpha R_s}}{(k_\alpha R_s)^{\ell}} \quad . \qquad \text{(IV-2-26c)}$$

By comparison of (IV-2-22a) and (IV-2-22b) and by use of (IV-2-25) and (IV-2-26) , we see that the only term in (IV-2-23) which is important at high frequencies is the first one, if R_s is large enough with respect to the rupture dimensions. We have then

$$\begin{pmatrix} A^{(\alpha)}_{\ell m}(\omega) \\ \\ B^{(\alpha)}_{\ell m}(\omega) \end{pmatrix} = 0(1/\omega) \quad , \qquad \text{(IV-2-27)}$$

and thus by use of (IV-2-26b) the spectral amplitude for the potentials has the following high frequency asymptotic behavior:

$$|\tilde{\chi}_\alpha(r,\omega)| = 0(1/\omega^2) \qquad \text{for} \quad \omega >> 1 \; . \qquad \text{(IV-2-28)}$$

It is interesting that this result is independent of the relaxation radius R_s . This corresponds physically to the fact that, at high frequency, most of the energy is radiated from a small region surrounding the rupture zone, of characteristic dimension comparable to the wave length under consideration. Thus one does not expect the high frequency side of the radiation spectrum to be sensitive to R_s .

Another important aspect is that the results shown in (IV-2-25) assume specifically that both $R(t_o)$ and $d(t_o)$ are linear in t_o .

For more complex ruptures, an "acceleration" phase could occur at the beginning of the rupture, and thus $R(t_o)$ and $d(t_o)$ could be more complicated functions of the source time t_o. However the analysis becomes rather complicated in such cases, so that numerical methods have to be used. Multipole fields of all degrees are contributing to the high frequency radiation, and their relative excitations could well depend on the detailed character of the rupture propagation. For the model investigated here, the convergence of the multipolar expansion is controlled by that of the addition theorem (IV-2-2), which is not particularly rapid. However, it can be noted that, because of our choice of volume of integration a factor of $1/2^{\ell+1}$ appears in the integral $I_\ell^{(2)}$ (see Appendix 4). This means that the multipole coefficients become eventually exponentially small with increasing ℓ. It was found from numerical calculations that convergence is very rapid for $\ell > 10$. However, even if the series is truncated at a lower degree, most of the characteristics of the radiation fields can be obtained with sufficient accuracy, as long as one does not try to compute these fields at too high frequencies (see Chapter VII).

Of course, as one can expect on simple intuitive grounds, the term "high frequency" must be defined in relation to the rupture dimension. We shall see that a convenient convention is to consider as high frequencies those for which the wave length is comparable to or smaller than the characteristic dimension of the rupture.

The last observation which we may make about the high frequency radiation is that it exhibits an amplitude decay with distance proportional to $1/r$ --see equation (IV-2-26b). This corresponds to

our definition of the far-field radiation, given below. It is not surprising that there should not be any significant near-field high frequency radiation since practically any observer will be several wave lengths away from the source at such frequencies. High frequency near-field effects can only be observed extremely close to the source.

b) Long-period behavior

The long-period limit corresponds to $\omega << 1$, but since the Hankel functions and the Bessel functions in (IV-2-25) have $k_\alpha r = \omega r/c_\alpha$ for argument, one must take into account hypocentral distance r of the observer. We shall thus make the following definitions:

1) The (unqualified) long-period limit corresponds to $\omega << 1$

2) The long-period limit in the far-field approximation is defined by

$$\omega << 1 \quad \underline{\text{and}} \quad k_\alpha r >> 1 \ .$$

3) The long-period limit in the near-field approximation is defined by

$$\omega << 1 \quad \underline{\text{and}} \quad k_\alpha r << 1 \ .$$

These definitions correspond to the usual ones in use in electromagnetic theory (e.g., Stratton, 1941) and in seismology (e.g., Haskell, 1964). One sees immediately that the very long period far-field radiation can only have physical meaning for extremely large distances. However, because of the following asymptotic forms for $k_\alpha r >> 1$

$$\begin{cases} h_\ell^{(2)}(k_\alpha r) \sim i^{\ell+1} \dfrac{e^{-ik_\alpha r}}{k_\alpha r} \\ \\ j_\ell(k_\alpha r) \sim \mathrm{Re}\left(i^{\ell+1} \dfrac{e^{-ik_\alpha r}}{k_\alpha r} \right) \end{cases} , \qquad \text{(IV-2-30)}$$

one may wish to choose another definition for the far-field radiation: it is that part of the field which shows an amplitude decay with distance as $1/r$. This second definition allows us to define the "far-field" radiation at any frequency and any distance, but it is a purely mathematical definition, which ignores the physical concept of "far-field."

The "near-field" asymptotic behavior, on the other hand, should be observed at any finite distance r , provided that one considers long enough periods.

We shall consider successively the case of an observer lying outside the relaxation zone and then that of an observer lying within R_s , and in each case we shall separate near-field and far-field behavior.

α) $r > R_s$, near-field approximation

In that case, from Appendix 4, equation (A-4-10) , we have for $\omega << 1$

$$I_\ell^3(\omega) \sim \frac{k_\alpha^2/2}{1\cdot3\cdot5\ldots\cdot(2\ell-1)} \int_o^{\tau_o} \left[R_s^2 - V_R^2 t_o^2 \right] \frac{d}{dt_o} \left[R^3(t_o)\, d^{\ell-2}(t_o) \right] dt_o \, . \qquad \text{(IV-2-31)}$$

Thus, from the expression for the multipole coefficients (IV-2-22)

$$\begin{pmatrix} A^{(\alpha)}_{\ell m}(\omega) \\ B^{(\alpha)}_{\ell m}(\omega) \end{pmatrix} \sim \begin{pmatrix} a'^{(\alpha)}_{2m} \\ b'^{(\alpha)}_{2m} \end{pmatrix} \frac{(\ell-m)!}{(\ell-2)!\ (2-m)!} \frac{k_\alpha^{\ell+2}}{2c_\alpha} \frac{2^\ell \ell!}{(2\ell)!} \int_o^{\tau_o} [\quad] \, dt_o$$

$$= O(\omega^{\ell+2}) \ . \qquad \text{(IV-2-32)}$$

Further, in the near-field, $k_\alpha r << 1$ and the dominant term in the Hankel function is

$$h^{(2)}_\ell(k_\alpha r) \sim \frac{i(2\ell)!}{2^\ell \ell!\ k_\alpha^{\ell+1}\ r^{\ell+1}} \ . \qquad \text{(IV-2-33)}$$

Using the results (IV-2-32) and (IV-2-33) in the potential solution (IV-2-24) , we get the following asymptotic behavior

$$|\tilde{\chi}_\alpha(r,\omega)| = O(\omega) \quad \text{for} \quad \omega << 1 \quad \text{and} \quad k_\alpha r << 1 \ . \qquad \text{(IV-2-34)}$$

The spectral density for the potentials vanishes in the (static) limit of zero frequency. A static offset would yield an asymptotic behavior as $(1/\omega)$. There is, therefore, no permanent change in the dilatation and rotation outside R_s , which is the correct result since this argument was used to introduce R_s in the first place: the stress relaxation taking place outside the relaxation zone was assumed to be

negligible.

Further, the multipolar field of degree ℓ is proportional to $\omega/r^{\ell+1}$, and r must be reasonably large $(r > R_s)$, thus we see that the radiation field is dominated by the lowest degree multipoles, in particular by the quadrupole. In other words, the long-period radiation is essentially that of a double couple.

β) $r > R_s$, far-field approximation

Equations (IV-2-31) and (IV-2-32) still hold in that case, but we have now $k_\alpha r \gg 1$ so that

$$h_\ell^{(2)}(k_\alpha r) \sim i^{\ell+1} \frac{e^{-ik_\alpha r}}{k_\alpha r} .$$

We see, then, that the partial field associated with the multipole of degree ℓ will have an asymptotic behavior as $\omega^{\ell+1}$ as $\omega \to 0$. Clearly, only the lowest degree multipole, the quadrupole, dominates at long periods and we have

$$|\tilde{\chi}_\alpha(r,\omega)| = 0(\omega^3) \quad \text{for} \quad \omega \ll 1 \quad \text{and} \quad k_\alpha r \gg 1 . \tag{IV-2-35}$$

As we pointed out, this "far-field" term may be isolated mathematically even for values of r and ω where it is not dominant. One must then keep in mind that it does not bear any relation to the observations.

Of course, in that case again, no static offset is observed.

γ) $r < R_s$, near-field approximation

This case is slightly more complicated. We have $\omega << 1$, and $k_\alpha r << 1$, so that from Appendix 4—equations (A-4-8) and (A-4-9) —

$$I_\ell^{(1)}(\omega) \sim R^3(\tau_o)\, d^{\ell-2}(\tau_o) \ , \tag{IV-2-36}$$

$$I_\ell^{(2)}(\omega) \sim \frac{1}{1\cdot 3\cdot 5\ldots\cdot(2\ell-1)}\, R^3(\tau_o)\, d^{\ell-2}(\tau_o) \ , \tag{IV-2-37}$$

and also

$$h_\ell^{(2)}(k_\alpha r) \sim \frac{i(2\ell)!}{\ell!(2k_\alpha r)^\ell}\ \frac{1}{k_\alpha r} \ , \tag{IV-2-38}$$

$$j_\ell(k_\alpha r) \sim \frac{k_\alpha^\ell r^\ell}{1\cdot 3\cdot 5\ldots\cdot(2\ell-1)} \ . \tag{IV-2-39}$$

Then, from (IV-2-22) we have

$$\begin{pmatrix} A_{\ell m}^{(\alpha)}(\omega) \\ B_{\ell m}^{(\alpha)}(\omega) \end{pmatrix} = \begin{pmatrix} a'^{(\alpha)}_{2m} \\ b'^{(\alpha)}_{2m} \end{pmatrix} \frac{(\ell-m)!}{(\ell-2)!\ (2-m)!}\, \frac{R^3(\tau_o)\, d^{\ell-2}(\tau_o)}{1\cdot 3\cdot 5\ldots\cdot(2\ell-1)}\, \frac{k_\alpha^\ell}{c_\alpha} + O(\omega^{\ell+1}) \ , \tag{IV-2-40}$$

so that, with reference to the general solution (IV-2-23) , we have, for $\omega << 1$

$$h_\ell^{(2)}(k_\alpha r)\left[A_{\ell m}^{(\alpha)}\cos m\phi + B_{\ell m}^{(\alpha)}\sin m\phi\right] = 0(\omega^{-1}) \ . \qquad \text{(IV-2-41)}$$

From the definition (IV-2-22) we also have

$$\begin{pmatrix} C_{\ell m}^{(\alpha)}(\omega) \\ D_{\ell m}^{(\alpha)}(\omega) \end{pmatrix} \sim \begin{pmatrix} a_{2m}^{\prime(\alpha)} \\ b_{2m}^{\prime(\alpha)} \end{pmatrix} \frac{(\ell-m)!}{(\ell-2)!\ (2-m)!} R^3(\tau_o)\ d^{\ell-2}(\tau_o)$$

$$\cdot \frac{-h_{\ell-1}^{(2)}(k_\alpha R_s)}{(k_\alpha R_s)^{\ell-1}} \frac{k_\alpha^\ell}{c_\alpha} \ . \qquad \text{(IV-2-42)}$$

This last equation deserves further discussion.

If R_s is small enough (or if k_α is small enough, for any finite value of R_s) then we have $k_\alpha R_s \ll 1$ and the Hankel function in (IV-2-41) must be approximated using the asymptotic form (IV-2-38). In that case

$$\begin{pmatrix} C_{\ell m}^{(\alpha)}(\omega) \\ D_{\ell m}^{(\alpha)}(\omega) \end{pmatrix} \sim - \begin{pmatrix} a_{2m}^{\prime(\alpha)} \\ b_{2m}^{\prime(\alpha)} \end{pmatrix} \frac{i(\ell-m)!\ (2\ell-2)!}{(\ell-2)!\ (2-m)!\ (\ell-1)!\ 2^{\ell-1}} R^3(\tau_o)\ d^{\ell-2}(\tau_o)$$

$$\cdot \frac{1}{(k_\alpha R_s)^{2\ell-1}} \frac{k_\alpha^\ell}{c_\alpha} \ . \qquad \text{(IV-2-43)}$$

Then, with reference to the solution (IV-2-23) we have

$$j_\ell(k_\alpha r)\left[C_{\ell m}^{(\alpha)} \cos m\phi + \mathcal{D}_{\ell m}^{(\alpha)} \sin m\phi\right] = O(\omega) \quad . \qquad \text{(IV-2-44)}$$

This term may be thus ignored compared to the one given by (IV-2-41) . We noted earlier that this is equivalent to taking $R_s = \infty$, as can be seen directly from (IV-2-43) .

On the other hand, if R_s is large enough so that $k_\alpha R_s >> 1$, then we must use

$$h_{\ell-1}^{(2)}(k_\alpha R_s) \sim i^\ell \frac{e^{-ik_\alpha R_s}}{k_\alpha R_s}$$

in (IV-2-42) . We find in that case that

$$j_\ell(k_\alpha r)\left[C_{\ell m}^{(\alpha)} \cos m\phi + \mathcal{D}_{\ell m}^{(\alpha)} \sin m\phi\right] = O(\omega^\ell) \quad . \qquad \text{(IV-2-45)}$$

Again this term may be ignored, when compared to (IV-2-41) .

Thus if the observer finds himself inside the relaxation zone, the near-field spectrum of the observed radiation is insensitive to R_s at very long periods and the spectrum behaves as if R_s were infinite. In that case we have

$$|\tilde{\chi}_\alpha(r,\omega)| = O(\omega^{-1}) \qquad \text{for} \quad \omega << 1 \quad \text{and} \quad k_\alpha r << 1 \quad . \qquad \text{(IV-2-46)}$$

This long-period spectral behavior corresponds in the time domain to a non-vanishing static offset (compare with the Fourier transform of a step function in time, which is $-i\omega^{-1}$). In fact, noting that

$$1\cdot 3\cdot 5\ldots\cdot(2\ell-1) = \frac{(2\ell)!}{2^{\ell}\ell!} \quad ,$$

we find that the coefficient of the term in $-i\omega^{-1}$ for the asymptotic form of the potential spectrum $\tilde{\chi}_{\alpha}(\mathbf{r},\omega)$ is

$$-\sum_{\ell=2}^{\infty}\sum_{m=0}^{2}\frac{(\ell-m)!}{(\ell-2)!\,(2-m)!}\frac{R^3(\tau_o)\,d^{\ell-2}(\tau_o)}{r^{\ell+1}}\left[a'^{(\alpha)}_{2m}\cos m\phi + b'^{(\alpha)}_{2m}\sin m\phi\right]$$

$$\cdot P^m_{\ell}(\cos\theta) \quad ,$$

which we immediately identify with $-\chi^{*}_{\alpha}(\mathbf{r},\tau_o)$ as given in (IV-2-4).

Again this result was to be expected, since the initial value fields χ^{*}_{α} were computed for an infinite domain ($R_s = \infty$) and have then been truncated at R_s. We have therefore obtained a consistency check for our calculations.

One must remember at this point that the solution for $\tilde{\chi}(\mathbf{r},\omega)$ that we obtained in (IV-2-23) is only valid 1) for $r > d(\tau_o)$ and 2) for points such that no information has propagated to them at τ_o, that is, grossly for $r > V_p\tau_o$. This constrains r to be relatively large in the static limit shown above, so that the term of lowest degree--the quadrupole term--will again be the dominant one. Furthermore, in the

static limit, higher degree multipoles are present only because the final rupture zone is not centered at the hypocenter, but at a distance $d(\tau_o)$ along the z-axis of the source system. In the moving system (figure III-1-1), in the final position at τ_o the static field is pure quadrupole. The offset position of the rupture zone in its final configuration is thus the reason for the presence of higher degree multipoles, and this effect dies rapidly with distance.

δ) $r < R_s$, far-field approximation

This limit is obtained when $\omega << 1$ and $k_\alpha r >> 1$; since we have $r < R_s$, this also means $k_\alpha R_s >> 1$. We can therefore use the approximations

$$h^{(2)}_{\ell-1}(k_\alpha R_s) \sim i^{\ell} \frac{e^{-ik_\alpha R_s}}{k_\alpha R_s} ,$$

$$h^{(2)}_{\ell}(k_\alpha r) \sim i^{\ell+1} \frac{e^{-ik_\alpha r}}{k_\alpha r} ,$$

$$j_\ell(k_\alpha r) \sim \mathrm{Re}\left[i^{\ell+1} \frac{e^{-ik_\alpha r}}{k_\alpha r} \right] .$$

The asymptotic behavior of the multipole coefficients are still given by (IV-2-40) and (IV-2-42) , and we may write, for $k_\alpha R_s >> 1$,

$$\begin{pmatrix} C_{\ell m}^{(\alpha)}(\omega) \\ D_{\ell m}^{(\alpha)}(\omega) \end{pmatrix} \sim \begin{pmatrix} A_{\ell m}^{(\alpha)}(\omega) \\ B_{\ell m}^{(\alpha)}(\omega) \end{pmatrix} \frac{-i^{\ell}(2\ell)!}{2^{\ell}\ell!(k_\alpha R_s)^{\ell}} e^{-ik_\alpha R_s} \quad . \qquad \text{(IV-2-47)}$$

Because the multipole coefficients $A_{\ell m}^{(\alpha)}$ and $B_{\ell m}^{(\alpha)}$ are proportional to ω^{ℓ}, we need only consider the lower values of ℓ, in particular, the quadrupole term $\ell=2$. Then the proportionality factor in (IV-2-47) is $3/(k_\alpha R_s)^2$, which is very small.

Therefore, here again, we can ignore the term in $j_\ell(k_\alpha r)$ in the general solution (IV-2-23), provided that indeed

$$k_\alpha R_s > k_\alpha r >> 1 \quad .$$

In other words, the "far-field" approximation can only have physical meaning within the relaxation zone if one considers frequencies such that simultaneously

$$\omega << 1 \quad \underline{\text{and}} \quad k_\alpha R_s > k_\alpha r >> 1 \quad .$$

In that case, just as in the near-field approximation, the spectral behavior is insensitive to R_s and one may take R_s to be infinite. Furthermore, by use of (IV-2-40) and of the asymptotic behavior for the Hankel function given above, we find that the multipole of degree ℓ yields a partial field which behaves as $\omega^{\ell-1}$ at low frequencies. Thus

only the lowest degree multipole (the quadrupole) is important and

$$|\tilde{\chi}_\alpha(r,\omega)| = 0(\omega) \quad \text{for} \quad \omega << 1 \quad \text{and} \quad k_\alpha r >> 1 \ . \qquad \text{(IV-2-48)}$$

If R_s is kept finite and if one tries to isolate mathematically the part of the radiation field which decays as $1/r$, the results do not present, in general, any simple asymptotic behavior as ω tends towards zero. This is not a disturbing fact since we just argued that such results do not have any relation to the physics of the phenomenon. On the other hand, if R_s is taken to be infinite in the first place--although this is not desirable, as we pointed out earlier--then any observer point is within the relaxation zone, and a mathematical "far-field" term may be defined everywhere, which decays with distance as $1/r$. Its asymptotic behavior is then given again by (IV-2-48). Again, this term may be usefully compared with the observations only if $k_\alpha r >> 1$, that is, at large distances from the rupture.

We may thus summarize the long-period behavior of the potential spectra in the following table for $|\tilde{\chi}_\alpha(r,\omega)|$:

	$r < R_s$	$r > R_s$
$k_\alpha r << 1$, "near-field"	$0(\omega^{-1})$	$0(\omega)$
$k_\alpha r >> 1$, "far-field"	$0(\omega)$	$0(\omega^3)$

(IV-2-49)

In all cases the field is dominantly quadrupole at long periods. Further, we have shown that when the observer is within the relaxation zone, the spectrum is insensitive to R_s . This was true at high frequencies also, so that, when $r < R_s$, the phenomenon is adequately modeled mathematically by taking the results valid for R_s infinite. Clearly this is not true for $r > R_s$.

Thus, two cases arise from our model, either the observer is clearly outside the source region, and R_s is to be chosen finite, or the observer is inside the source region and R_s may be taken to be infinite. From (IV-2-49) one sees that these two cases give rise to drastically different spectral behavior for the potentials. The corresponding behavior of the displacement spectra will be considered in section IV-4.

The method described in this section was used by Archambeau in several publications (e.g., Archambeau, 1964, 1968, 1972). However, Archambeau considered only the case where the relaxation zone is kept finite and the observer is outside of it. We see now that this case represents only part of the solution, and that the position of the observer with respect to the relaxation zone has a rather drastic effect on the predicted radiation field.

It still remains to be seen whether any of the global characteristics discussed above, in particular, the asymptotic behavior of the potential spectra--and, by inference--of the displacement spectra (see section IV-5) depend on the approximations made in computing the solution. More specifically, we should make sure that the approximations shown on figure IV-2-1 are not critical. For this purpose,

we develop in the next section a more complicated solution, which does not require these approximations.

The results presented above are those that we shall use in Chapter VII for numerical applications. We shall see that even this very simple model depends on enough parameters so that the predicted radiation field is, in fact, quite complex.

IV-3 A general method of solution for propagating ruptures

The method of solution presented in the last section required that we express the initial value fields χ^*_α in the source coordinate system. For that reason, we had to approximate the volume $V(t_o)$, and ignored a portion of the source volume in the vicinity of the hypocenter 0 (see figure IV-2-1).

There are several reasons in favor of performing the analysis in the moving coordinate system of figure IV-1-1 rather than in the source system. The first one is that the rupture zone exhibits the greatest symmetry in the moving system, of origin 0' , the center of the spherical rupture. As a corollary, the initial value fields χ^*_α have a much simpler analytical expression in that frame than in the source system. Second, the source volume $V(t_o)$ is defined to be external to the rupture zone itself, and, in the moving system, can easily be defined by $r' > R(t_o)$. The volume integration can then be performed easily, and without approximation. Third, this method will enable us to compute the radiation fields even very close to the source, provided that we use the correct Green's function solution.

We shall present in this section the solution for the case of a growing and propagating spherical rupture. The solution, eventually expressed in the source system, is obtained by continuous translation of the reference frame along the z-axis, just as before, but the operation is performed on the dynamic fields rather than on the initial value (static) fields. We shall use the addition theorem for spherical wave functions proved in Appendix 9, and specialized in section V-3 to multipolar expansions.

i) Formulation of the problem

As we showed in section IV-1, for times t greater than τ_o, the total rupture duration, the dynamic potential solution is given by

$$\tilde{\chi}_\alpha(\mathbf{r},\omega) = \frac{i\omega}{4\pi c_\alpha^2} \int_o^{\tau_o} e^{-i\omega t_o} dt_o \int_{V(t_o)} \frac{\partial \chi_\alpha^*}{\partial t_o} \frac{e^{-ik_\alpha r^*}}{r^*} dv^{(o)} . \qquad \text{(IV-3-1)}$$

The source volume $V(t_o)$ is that volume lying outside the rupture zone at t_o, and within the relaxation radius R_s. Our purpose is now to evaluate the volume integral in (IV-3-1) in the moving coordinate system. The geometry is described on figure IV-3-1. For simplicity we shall choose the relaxation zone to be the interior of a sphere of radius R_s, entered at $0'$, the center of the rupture. This means that the relaxation zone propagates along with the rupture. If R_s is large enough compared to $d(\tau_o)$, one does not expect this to have any strong effect on the solution. Furthermore, it is rather desirable to take the relaxation zone to propagate along with the rupture, especially if the prestress is inhomogeneous. In such a situation one expects that the efficiency of the stress relaxation phenomenon will be a function of the source time t_o. Further, since the size of the rupture itself varies with time, the region in which significant stress relaxation takes place can be expected to vary in size with t_o. We shall therefore take R_s to be a function of t_o in this section.

This seems to complicate the situation a little. We saw in the

preceding section that the results are different for an observer point lying within the relaxation zone, and one lying outside of it. We are now faced with the possibility of having an observer lying inside R_s during part of the total rupture duration, and outside R_s the rest of the time. This complication can theoretically be handled by separating the interval $[0,\tau_o]$ into several subintervals during which the observer point is inside (or outside) R_s and by superposing the solutions for these subintervals.

For simplicity we shall consider in this section only the two fundamental cases where the observer point is 1) inside $R_s(t_o)$ for all $0 < t_o < \tau_o$ or 2) outside $R_s(t_o)$ for all $0 < t_o < \tau_o$. The adaptation of the results so obtained to more general cases may lead to rather complicated algebra, but does not present any theoretical difficulty.

The initial fields may be expressed very simply in the moving system and were found to be given by (e.g., equation IV-1-12)

$$\chi^*_\alpha(r'_o,t_o) = \frac{R^3(t_o)}{r'^3_o} \sum_{m=0}^{2} \left[a'^{(\alpha)}_{2m} \cos m\phi'_o + b'^{(\alpha)}_{2m} \sin m\phi'_o \right] P^m_2(\cos\theta'_o) \qquad \text{(IV-3-2)}$$

The static coefficients $a'^{(\alpha)}_{2m}$ and $b'^{(\alpha)}_{2m}$ are given by (IV-1-13) through (IV-1-15). Here r'_o, θ'_o, and ϕ'_o are the spherical coordinates of a source point Q in the moving system (see figure IV-3-1).

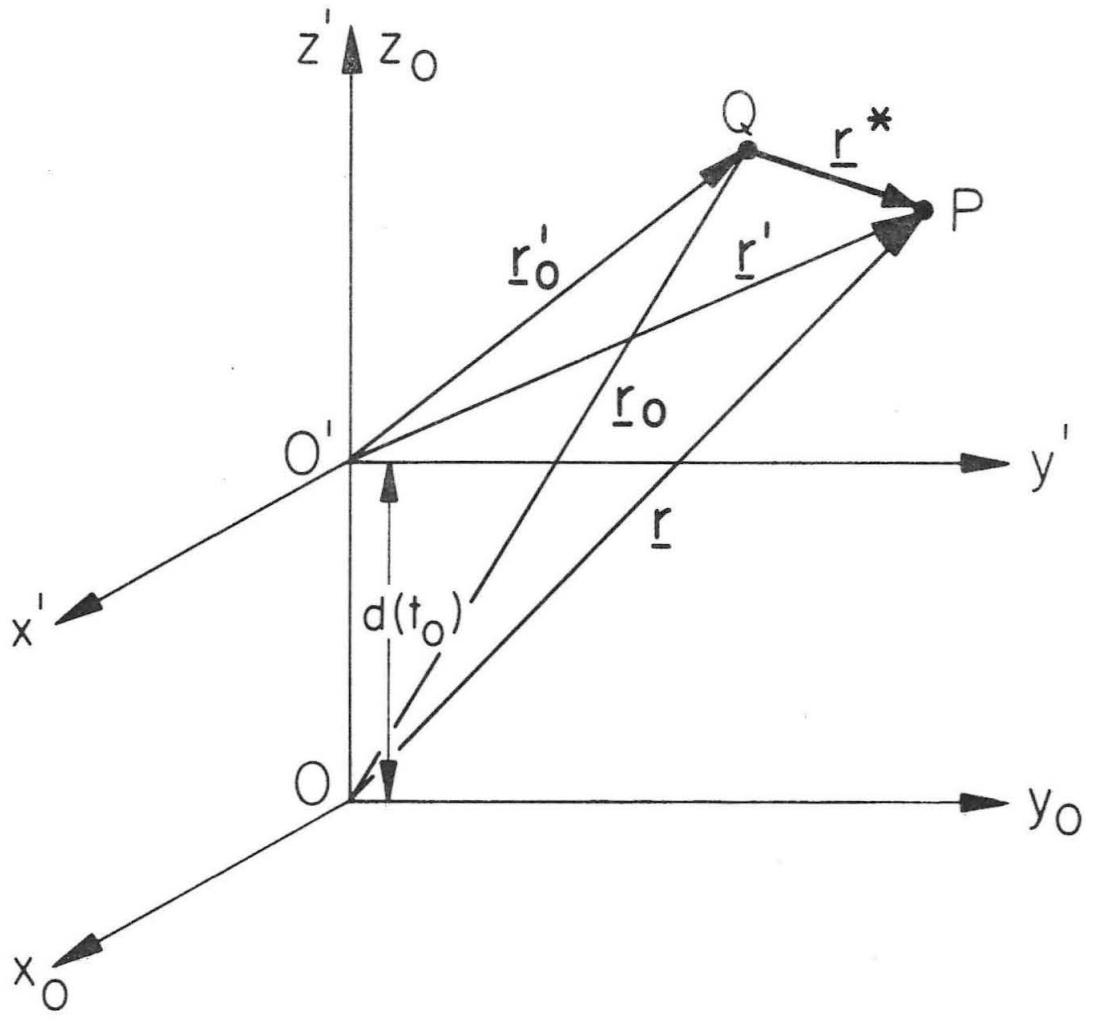

Figure IV-3-1. Coordinate systems used for the propagating rupture. O is the origin of the source system, O' the origin of the moving system. Q is an arbitrary source point, P the observer's point.

Further, the spherical wave expansion of the Green's function in (IV-3-1) is

$$\frac{e^{-ik_\alpha r^*}}{r^*} = -ik_\alpha \sum_{\lambda=0}^{\infty} (2\lambda+1)\, P_\lambda(\cos\gamma') \begin{cases} j_\lambda(k_\alpha r_o')\, h_\lambda^{(2)}(k_\alpha r') \\ \\ j_\lambda(k_\alpha r')\, h_\lambda^{(2)}(k_\alpha r_o') \end{cases} ,$$

(IV-3-3)

where the upper pair of Bessel functions is to be used if $r' > r_o'$, and the lower pair if $r' < r_o'$. The angle γ' is measured between the vectors $\mathbf{r}'$ and $\mathbf{r}_o'$, and we have

$$P_\lambda(\cos\gamma) = \sum_{k=0}^{\lambda} (2-\delta_{ko}) \frac{(\lambda-k)!}{(\lambda+k)!} P_\lambda^k(\cos\theta')\, P_\lambda^k(\cos\theta_o')\, \cos k(\phi' - \phi_o') .$$

(IV-3-4)

Thus, in the moving system, the problem may be formulated instantaneously at time t_o exactly as in section IV-2 for the case of a non-propagating rupture ("explosion" model).

By simple adaptation of the methods of section IV-2, we obtain in the case where $r' < R_s(t_o)$ for all t_o

$$\int_{V(t_o)} \frac{\partial \chi_\alpha^*}{\partial t_o} \frac{e^{-ik_\alpha r^*}}{r^*} dv^{(o)} = \frac{dR^3(t_o)}{dt_o} \sum_{\ell=o}^{\infty} \sum_{m=0}^{2} (-ik_\alpha)\ (2\ell+1)$$

$$\cdot \int_o^{\pi} \int_o^{2\pi} \left[a'^{(\alpha)}_{2m} \cos m\phi'_o + b'^{(\alpha)}_{2m} \sin m\phi'_o \right] P_2^m(\cos \theta'_o)\ P_\ell(\cos \gamma)$$

$$\cdot \sin \theta'_o\ d\theta'_o\ d\phi'_o$$

$$\cdot \left\{ h_\ell^{(2)}(k_\alpha r') \int_{R(t_o)}^{r'} \frac{j_\ell(k_\alpha r'_o)}{r'_o} dr'_o \right.$$

$$\left. + j_\ell(k_\alpha r') \int_{r'}^{R_s(t_o)} \frac{h_\ell^{(2)}(k_\alpha r'_o)}{r'_o} dr'_o \right\} . \qquad \text{(IV-3-5)}$$

We can now apply the orthogonality property (IV-2-8) and use the closed form integrals given in Appendix 2--equations (A-2-2) and (A-2-3) . We have

$$\int_o^{2\pi} \int_o^{\pi} P_\ell(\cos \gamma)\ P_2^m(\cos \theta'_o) \begin{pmatrix} \cos m\phi'_o \\ \\ \sin m\phi'_o \end{pmatrix} \sin \theta'_o\ d\theta'_o\ d\phi'_o =$$

$$\frac{4\pi}{2\ell+1} P_\ell^m(\cos \theta') \begin{pmatrix} \cos m\phi' \\ \\ \sin m\phi' \end{pmatrix} \delta_{\ell 2} .$$

which may be substituted into (IV-3-5) . We get

$$\int_{V(t_o)} \frac{\partial \chi_\alpha^*}{\partial t_o} \frac{e^{-ik_\alpha r^*}}{r^*} dv^{(o)} = \sum_{m=0}^{2} (-4\pi i k_\alpha) \left[a_{2m}'^{(\alpha)} \cos m\phi' + b_{2m}'^{(\alpha)} \sin m\phi' \right]$$

$$\cdot P_2^m(\cos\theta') \frac{dR^3(t_o)}{dt_o} \left\{ h_2^{(2)}(k_\alpha r') \frac{j_1(k_\alpha R(t_o))}{k_\alpha R(t_o)} \right.$$

$$\left. - j_2(k_\alpha r') \frac{h_1^{(2)}(k_\alpha R_s(t_o))}{k_\alpha R_s(t_o)} \right\} . \qquad \text{(IV-3-6)}$$

Here we have left out the wronskian term in $-i/(k_\alpha r')^3$, for the same reasons as given before--e.g., equation (IV-2-21): This term does not represent a travelling wave, but is the Fourier transform of the initial value fields.

If the observer's point is outside the relaxation zone, then the last bracket in (IV-3-6) must be replaced by

$$\left\{ h_2^{(2)}(k_\alpha r') \left[\frac{j_1(k_\alpha R(t_o))}{k_\alpha R(t_o)} - \frac{j_1(k_\alpha R_s(t_o))}{k_\alpha R_s(t_o)} \right] \right\} . \qquad \text{(IV-3-7)}$$

From (IV-3-6) we recognize one of the results obtained in the previous section—in the coordinate system with origin at the center of the rupture zone, the radiation field is instantaneously pure quadrupole. We now have to substitute (IV-3-6) into (IV-3-1) by first expressing

the volume integral (IV-3-6) in terms of the source coordinates r, θ, ϕ.

The transformation that we wish to perform is a translation of magnitude $-d(t_o)$ along the z-axis. Let us denote this transformation by $\mathscr{T}(t_o)$. In such a translation, the azimuthal angle ϕ is left unchanged, so that we may write

$$\tilde{\chi}_\alpha(r,\omega) = \frac{k_\alpha^2}{c_\alpha} \sum_{m=0}^{2} \left[a'^{(\alpha)}_{2m} \cos m\phi + b'^{(\alpha)}_{2m} \sin m\phi \right]$$

$$\cdot \int_o^{t_o} e^{-i\omega t_o} \frac{dR^3(t_o)}{dt_o} \left\{ \frac{j_1(k_\alpha R(t_o))}{k_\alpha R(t_o)} \mathscr{T}(t_o) \left[h_2^{(2)}(k_\alpha r') P_2^m(\cos\theta') \right] \right.$$

$$\left. - \frac{h_1^{(2)}(k_\alpha R_s(t_o))}{k_\alpha R_s(t_o)} \mathscr{T}(t_o) \left[j_2(k_\alpha r') P_2^m(\cos\theta') \right] \right\} dt_o$$

(IV-3-8)

Here the quantity $\mathscr{T}(t_o)[f(r')]$ is a function of r.

(IV-3-8) is the solution that we must now evaluate, and recast in the form of a multipolar expansion. For an observer external to the relaxation zone, the bracket in the integrand of (IV-3-8) must be replaced by

$$\left\{ \left[\frac{j_1(k_\alpha R(t_o))}{k_\alpha R(t_o)} - \frac{j_1(k_\alpha R_s(t_o))}{k_\alpha R_s(t_o)} \right] \mathcal{T}(t_o) \left[h_2^{(2)}(k_\alpha r') \; P_2^m(\cos\theta') \right] \right\} .$$

(IV-3-9)

ii) Evaluation of the solution

The quantities which we must operate on with the transformation $\mathcal{T}(t_o)$ are of the form

$$Z_2(k_\alpha r') \; P_2^m(\cos\theta') = (-1)^m \sqrt{\frac{4\pi(2+m)!}{5(2-m)!}} \, e^{-im\phi} \, Z_2(k_\alpha r') \; Y_2^m(\theta',\phi') \; ,$$

(IV-3-10)

with Z_2 representing either j_2 or $h_2^{(2)}$.

We prove in Appendix 9 a general addition theorem for spherical wave functions, and specialize it to the case of a simple translation along the z-axis. These results are then used in section V-3 to investigate the transformation of a multipolar expansion under such a translation. The result which we want to use here will thus be proved in Chapter V--equation (V-3-4) . For $r > d(t_o)$ and for a translation of amplitude $-d(t_o)$, we have

$$Z_n(k_\alpha r') \; Y_n^m(\theta',\phi') = \sum_{\ell=0}^{\infty} \sum_{\nu=|\ell-n|}^{|\ell+n|} C_1(\nu,\ell|n,m)$$

$$\cdot \; j_\nu(k_\alpha d(t_o)) \, Z_\ell(k_\alpha r) \; Y_\ell^m(\theta,\phi) \quad , \qquad \text{(IV-3-11)}$$

where

$$C_1(\nu,\ell|n,m) = (-1)^{\nu} i^{\nu+\ell-n}(2\nu+1)(2\ell+1)^{\frac{1}{2}}(2n+1)^{-\frac{1}{2}}$$

$$\cdot (\ell\ \nu\ m\ 0 \mid n\ m)(\ell\ \nu\ 0\ 0 \mid n\ 0)\ . \qquad \text{(IV-2-12)}$$

The coefficients appearing on the right-hand side of (IV-3-12) are Clebsch-Gordan coefficients.

A similar formula may be derived for the case $r < d(t_o)$; we shall not investigate this case here since it corresponds to an extreme near-field situation, and shall refer the reader to Appendix 9 and section V-3 for the derivation of the corresponding results.

Using (IV-2-10) and (IV-2-11) we get

$$Z_2(k_\alpha r')\ P_2^m(\cos\theta') = (-1)^m \sqrt{\frac{4\pi(2+m)!}{5(2-m)!}} \sum_{\ell=0}^{\infty} \sum_{\nu=|\ell-2|}^{\ell+2} C_1(\nu,\ell|2,m)$$

$$\cdot\ j_\nu(k_\alpha d(t_o))\,(-1)^m \sqrt{\frac{(2\ell+1)(\ell-m)!}{4\pi(\ell+m)!}}\ Z_\ell(k_\alpha r)\ P_\ell^m(\cos\theta)\ . \qquad \text{(IV-3-13)}$$

This last equation gives us the result of the operation $\mathscr{T}(t_o)$ on $Z_2(k_\alpha r')\ P_2^m(\cos\theta')$. We can now substitute (IV-3-13) into (IV-3-9), and write the solution in the form of a multipolar expansion:

$$\tilde{\chi}_\alpha(r,\omega) = \sum_{\ell=0}^{\infty} \sum_{m=0}^{\min(2,\ell)} P_\ell^m(\cos\theta)$$

$$\cdot \left\{ h_\ell^{(2)}(k_\alpha r) \left[A_{\ell m}^{(\alpha)} \cos m\phi + B_{\ell m}^{(\alpha)} \sin m\phi \right] \right.$$

$$\left. + j_\ell(k_\alpha r) \left[C_{\ell m}^{(\alpha)} \cos m\phi + D_{\ell m}^{(\alpha)} \sin m\phi \right] \right\} . \qquad \text{(IV-3-14)}$$

Here the multipole coefficients are given by

$$\begin{pmatrix} A_{\ell m}^{(\alpha)}(\omega) \\ B_{\ell m}^{(\alpha)}(\omega) \end{pmatrix} = \begin{pmatrix} a'^{(\alpha)}_{2m} \\ b'^{(\alpha)}_{2m} \end{pmatrix} \frac{k_\alpha^2}{c_\alpha} \sum_{\nu=|\ell-2|}^{\ell+2} (-1)^{\nu+1} i^{\nu+\ell} \frac{(2\nu+1)(2\ell+1)}{5}$$

$$\cdot \sqrt{\frac{(\ell-m)!(2+m)!}{(\ell+m)!(2-m)!}} (\ell\ \nu\ m\ 0 \mid 2\ m)(\ell\ \nu\ 0\ 0 \mid 2\ 0) \cdot \begin{cases} J_\nu^{(2)}(\omega) \\ J_\nu^{(3)}(\omega) \end{cases} ,$$

$$\text{(IV-3-15)}$$

where $J_\nu^{(2)}(\omega)$ is to be used if the observer's point is inside the relaxation zone for all times $0 \leq t_o \leq \tau_o$, and $J_\nu^{(3)}(\omega)$ is to be used if $r > R_s(t_o)$ for all t_o such that $0 \leq t_o \leq \tau_o$. Similarly the coefficients $C_{\ell m}^{(\alpha)}$ and $D_{\ell m}^{(\alpha)}$ are given by

$$\begin{pmatrix} C_{\ell m}^{(\alpha)}(\omega) \\ D_{\ell m}^{(\alpha)}(\omega) \end{pmatrix} = - \begin{pmatrix} a'^{(\alpha)}_{2m} \\ b'^{(\alpha)}_{2m} \end{pmatrix} \frac{k_\alpha^2}{c_\alpha} \sum_{\nu=|\ell-2|}^{\ell+2} (-1)^{\nu+1} i^{\nu+\ell} \frac{(2\nu+1)(2\ell+1)}{5}$$

$$\cdot \sqrt{\frac{(\ell-m)!(2+m)!}{(\ell+m)!(2-m)!}} (\ell\ \nu\ m\ 0 \mid 2\ m)(\ell\ \nu\ 0\ 0 \mid 2\ 0) \cdot \begin{cases} J_\nu^{(4)}(\omega) & \text{if } r < R_s(t_o). \\ 0 & \text{if } r > R_s(t_o). \end{cases}$$

(IV-3-16)

The functions $J_\nu^{(2)}(\omega)$, $J_\nu^{(3)}(\omega)$ and $J_\nu^{(4)}(\omega)$ are integrals which are given by

$$J_\nu^{(2)}(\omega) = \int_o^{\tau_o} e^{-i\omega t_o} \frac{dR^3}{dt_o} \frac{j_1(k_\alpha R)}{k_\alpha R} j_\nu(k_\alpha d)\, dt_o \ , \qquad \text{(IV-3-17)}$$

$$J_\nu^{(3)}(\omega) = \int_o^{\tau_o} e^{-i\omega t_o} \frac{dR^3}{dt_o} \left[\frac{j_1(k_\alpha R)}{k_\alpha R} - \frac{j_1(k_\alpha R_s)}{k_\alpha R_s} \right] j_\nu(k_\alpha d)\, dt_o \ ,$$

(IV-3-18)

and

$$J_\nu^{(4)}(\omega) = \int_o^{\tau_o} e^{-i\omega t_o} \frac{dR^3}{dt_o} \frac{h_1^{(2)}(k_\alpha R_s)}{k_\alpha R_s} j_\nu(k_\alpha d)\, dt_o \ . \qquad \text{(IV-3-19)}$$

In the above expressions, R , d , and R_s are all functions of t_o . If R_s is a constant (independent of t_o) , then the

integral $J_\nu^{(4)}$ is simplified by bringing the Hankel function outside the integral. We write

$$J_\nu^{(4)}(\omega) = \frac{h_1^{(2)}(k_\alpha R_s)}{k_\alpha R_s} J_\nu^{(1)}(\omega) ,$$

with

$$J_\nu^{(1)}(\omega) = \int_o^{\tau_o} e^{-i\omega t_o} \frac{dR^3}{dt_o} j_\nu(k_\alpha d)\, dt_o . \qquad \text{(IV-3-20)}$$

In that case also, $J_\nu^{(3)}(\omega)$ is a linear combination of $J_\nu^{(1)}$ and $J_\nu^{(2)}$. For reasons of simplicity we shall take R_s to be constant throughout the remainder of this section.

iii) Discussion

The solution (IV-3-14) is of the same form as that obtained in section IV-2, except for the fact that the terms $\ell=0$ and $\ell=1$ are now present. These terms correspond to a monopole and a dipole field respectively. In terms of point force equivalents they correspond respectively to an isotropic dilatational (or compressional) nucleus of strain, and to a single couple.

This is a somewhat startling result since 1) a monopole radiator corresponds to an "explosion-like" component of radiation (e.g., Archambeau, 1972) and the reason for its appearance here is not intuitively obvious since we assumed the prestress to be pure shear,

and since we did not take into account a possible density change in the rupture zone; and 2) a single couple point force does not lead to the conservation of angular momentum (e.g., Burridge and Knopoff, 1964).

Let us first note that the appearance of all multipoles different from the quadrupole ($\ell=2$) occurred when we applied the addition theorem (IV-3-11) . In other words, for an expanding, non-propagating sphere we obtain here again a pure quadrupole radiation. In fact, we can easily satisfy ourselves that, in that case, the results obtained are identical with those obtained in section IV-2.

The excitation of the monopole and dipole terms, as well as the multipoles of degree greater than two is thus intimately associated with the propagation of the rupture. But since observations support the fact that the radiation field should be dominantly quadrupole in nature, at low frequencies, an important check of the validity of our model is then to show that it possesses this property. This is done below from long-period asymptotic expressions. Further, since conservation of angular momentum was inherently assumed in the basic formulation of the problem, the net angular momentum carried by the dipole term must be counterbalanced by the angular momentum carried by all other multipoles of odd degree. Unfortunately, this is quite difficult to show analytically, and cumbersome to show numerically.

The solution (IV-3-14) is suitable for numerical computations, although it is more complicated than the solution obtained in section IV-2. Here again the integrals $J_{\nu}^{(1),(2),(3)}(\omega)$ may be evaluated numerically as finite Fourier transforms, by use of Filon's method of integration .

The Clebsch-Gordan coefficients appearing in (IV-3-15) and (IV-3-16) may be evaluated by a number of well-known techniques found in textbooks on quantum mechanics (e.g., Edmonds, 1957), in particular through recursion relations. However, we note that the second of these coefficients vanishes identically unless $\ell+\nu+2$ is even. This means that the sum over ν in (IV-3-15) or (IV-3-16) reduces to the three terms

$$\nu = |\ell-2| \quad ; \quad \nu = \ell \; ; \quad \nu = \ell+2 \quad .$$

We can then transform these coefficients into 3-j coefficients by the relation (Edmonds, 1957)

$$\begin{pmatrix} j_1 & j_2 & j_3 \\ m_1 & m_2 & m_3 \end{pmatrix} = (-1)^{j_1-j_2-m_3} (2j_3+1)^{-\frac{1}{2}} (j_1\, j_2\, m_1\, m_2 | j_3\, m_3) \; , \tag{IV-3-21}$$

so that the only coefficients which we need compute are of the form

$$\begin{pmatrix} \ell & \nu & 2 \\ m & 0 & -m \end{pmatrix} \text{ , with } \begin{cases} \nu = |\ell-2| \; , \; \ell \; , \; \ell+2 \\ m = 0,1,2 \; . \end{cases} \tag{IV-3-22}$$

A table of closed forms for these nine coefficients is given in

Appendix 10.

iv) Asymptotic behavior of the potential spectra

The various asymptotic cases that we shall investigate now are identical to those discussed in the previous section. Therefore, we shall not describe in detail their meaning, and range of validity, but shall refer the reader back to section IV-2 for a discussion. Asymptotic forms for the integrals $J_\nu^{(1)}$, $J_\nu^{(2)}$ and $J_\nu^{(3)}$ are discussed in Appendix 4, both in the high frequency and low frequency limits. We assume R_s to be independent of t_o .

a) High frequency behavior

In that case, from Appendix 4 we have, for $\omega >> 1$, and assuming that $R(t_o)$ and $d(t_o)$ are linear in t_o ,

$$\left.\begin{matrix} J_\nu^{(1)}(\omega) \\ J_\nu^{(2)}(\omega) \\ J_\nu^{(3)}(\omega) \end{matrix}\right\} = 0(1/\omega^3) , \qquad \text{(IV-3-23)}$$

and thus, from (IV-3-20)

$$J_\nu^{(4)}(\omega) = 0(1/\omega^5) . \qquad \text{(IV-3-24)}$$

Therefore the multipole coefficients $C_{\ell m}^{(\alpha)}$ and $D_{\ell m}^{(\alpha)}$ are negligible with respect to $A_{\ell m}^{(\alpha)}$ and $B_{\ell m}^{(\alpha)}$ and the high frequency spectral content of the radiation field is insensitive to R_s . From (IV-3-15) and (IV-3-23) we see that the multipole coefficients behave as ω^{-1} for large values of ω , and since

$$h_\ell^{(2)}(k_\alpha r) \sim i^{\ell+1} \frac{e^{-ik_\alpha r}}{k_\alpha r} \qquad \text{for} \quad \omega >> 1 \ ,$$

we have

$$|\tilde{\chi}_\alpha(r,\omega)| = O(\omega^{-2}) \qquad \text{for} \quad \omega >> 1 \ . \qquad \text{(IV-3-25)}$$

This result is identical to the one obtained in section IV-2, equation (IV-2-28) . We shall not repeat the discussion presented at that time.

The relative importance of the monopole and dipole terms to the other multipoles is rather difficult to evaluate analytically. We shall comment on this on the basis of numerical results in Chapter VII.

Because the addition theorem (IV-3-11) holds for $r > d(t_o)$, we can expect the solution to converge rather well at large distances from the source. However, a detailed discussion of the convergence rate will not be attempted here: it depends on the size of the multipole coefficients (IV-3-15) , which is quite difficult to investigate.

b) Long-period behavior

We shall consider here the same cases as in section IV-2.

α) $r > R_s$, near-field approximation

This case corresponds to $\omega << 1$ and $k_\alpha r << 1$. Then from Appendix 4 we have

$$J_\nu^{(3)}(\omega) \sim \frac{k_\alpha^{\nu+2}/30}{1\cdot3\cdot5\ldots\cdot(2\nu+1)} \int_o^{\tau_o} d^\nu(t_o)\left[R_s^2 - R^2(t_o)\right] \frac{dR^3(t_o)}{dt_o}\, dt_o \qquad \text{(IV-3-26)}$$

Thus from (IV-3-15) , for $\ell \geq 2$ the multipole coefficients will be controlled by the term $\nu = \ell-2$, and

$$\begin{pmatrix} A_{\ell m}^{(\alpha)} \\ \\ B_{\ell m}^{(\alpha)} \end{pmatrix} = O(\omega^{\ell+2}) \ . \qquad \text{(IV-3-27)}$$

For the dipole $\ell = 1$, and the dominant behavior is obtained for $\nu = 1$, thus

$$\begin{pmatrix} A_{1m}^{(\alpha)} \\ \\ B_{1m}^{(\alpha)} \end{pmatrix} = O(\omega^5) \ . \qquad \text{(IV-3-28)}$$

For the monopole $\ell = 0$, and the only value taken by ν is $\nu = 2$, so that

$$\begin{pmatrix} A_{oo}^{(\alpha)} \\ \\ B_{oo}^{(\alpha)} \end{pmatrix} = 0(\omega^6) \quad . \tag{IV-3-29}$$

Furthermore, in the near field

$$h_\ell^{(2)}(k_\alpha r) \sim \frac{i(2\ell)!}{2^\ell \ell!\, k_\alpha^{\ell+1}\, r^{\ell+1}} \quad . \tag{IV-3-30}$$

Thus in the multipolar expansion (IV-3-14) the monopole field behaves asymptotically as ω^5 , the dipole field behaves as ω^3 , and the multipole fields of higher degree behave as ω . Therefore

$$|\tilde{\chi}_\alpha(r,\omega)| = 0(\omega) \qquad \text{for } \omega << 1 \text{ and } k_\alpha r << 1 \, . \tag{IV-3-31}$$

In addition, because of the radial dependence of the multipole fields shown in (IV-3-30) , and because $r > R_s$, we expect the quadrupole term to dominate here again.

β) $r > R_s$, far-field approximation

This case is identical with α) , except that we have $k_\alpha r >> 1$ so that

$$h_\ell^{(2)}(k_\alpha r) \sim i^{\ell+1} \frac{e^{-ik_\alpha r}}{k_\alpha r} \quad . \qquad \text{(IV-3-32)}$$

By comparison of (IV-3-32) and (IV-3-27) through (IV-3-29), we see immediately that the asymptotic behavior is obtained for $\ell = 2$, and

$$|\tilde{\chi}_\alpha(r,\omega)| = 0(\omega^3) \qquad \text{for} \quad \omega << 1 \quad \text{and} \quad k_\alpha r >> 1 \; . \qquad \text{(IV-2-33)}$$

The far-field radiation is controlled by the quadrupole at long periods.

γ) $r < R_s$, near-field approximation

This approximation corresponds to the limits $\omega << 1$ and $k_\alpha r << 1$. From Appendix 4 we have in that case

$$J_\nu^{(1)}(\omega) \sim 3J_\nu^{(2)}(\omega) \sim \frac{k_\alpha^\nu}{1\cdot3\cdot5\ldots\cdot(2\nu+1)} \int_o^{\tau_o} d^\nu(t_o) \frac{dR^3(t_o)}{dt_o} dt_o \quad .$$

Then, following the same reasoning as in the case α), we obtain

$$\begin{pmatrix} A_{oo}^{(\alpha)} \\ B_{oo}^{(\alpha)} \end{pmatrix} = 0(\omega^4) \; ; \quad \begin{pmatrix} A_{1m}^{(\alpha)} \\ B_{1m}^{(\alpha)} \end{pmatrix} = 0(\omega^3) \; ; \qquad \text{(IV-3-34)}$$

and

$$\begin{pmatrix} A_{\ell m}^{(\alpha)} \\ \\ B_{\ell m}^{(\alpha)} \end{pmatrix} = 0(\omega^{\ell}) \qquad \text{for} \quad \ell \geq 2 \quad . \qquad \text{(IV-3-35)}$$

The asymptotic behavior for the coefficients $C_{\ell m}^{(\alpha)}$ and $D_{\ell m}^{(\alpha)}$ is easily obtained by multiplication of (IV-3-34) and (IV-3-35) by the factor $h_1^{(2)}(k_\alpha R_s)/k_\alpha R_s$. Their contribution will be the largest in the case where $k_\alpha R_s << 1$ since then

$$\frac{h_1^{(2)}(k_\alpha R_s)}{k_\alpha R_s} \sim \frac{i}{k_\alpha{}^3 R_s{}^3} \quad ,$$

so that

$$\begin{pmatrix} C_{oo}^{(\alpha)} \\ \\ D_{oo}^{(\alpha)} \end{pmatrix} = 0(\omega) \quad ; \quad \begin{pmatrix} C_{1m}^{(\alpha)} \\ \\ D_{1m}^{(\alpha)} \end{pmatrix} = 0(1) \quad ; \qquad \text{(IV-3-36)}$$

and

$$\begin{pmatrix} C_{\ell m}^{(\alpha)} \\ \\ D_{\ell m}^{(\alpha)} \end{pmatrix} = O(\omega^{\ell-3}) \qquad \text{for} \quad \ell \geq 2 \ . \tag{IV-3-37}$$

Now the coefficients $A_{\ell m}^{(\alpha)}$ and $B_{\ell m}^{(\alpha)}$ are associated with the Hankel function

$$h_{\ell}^{(2)}(k_{\alpha}r) \sim \frac{i(2\ell)!}{2^{\ell}\ \ell!(k_{\alpha}r)^{\ell+1}} \ , \tag{IV-3-38}$$

and the coefficients $C_{\ell m}^{(\alpha)}$ and $D_{\ell m}^{(\alpha)}$ are associated with the Bessel function

$$j_{\ell}(k_{\alpha}r) \sim \frac{(k_{\alpha}r)^{\ell}\ 2^{\ell}\ \ell!}{(2\ell)!} \ . \tag{IV-3-39}$$

By comparison of the results (IV-3-34) through (IV-3-39) we see that 1) the terms associated with the Bessel function $j_{\ell}(k_{\alpha}r)$ are negligible at long periods for all degrees ℓ ; 2) the monopole and dipole terms associated with the Hankel function $h_{\ell}^{(2)}(k_{\alpha}r)$ vanish as $\omega \to 0$; and 3) the terms proportional to $h_{\ell}^{(2)}(k_{\alpha}r)$ for $\ell \geq 2$ behave asymptotically as ω^{-1} for $\omega << 1$. Thus

$$|\tilde{\chi}_{\alpha}(r,\omega)| = O(\omega^{-1}) \quad \text{for} \quad \omega << 1 \quad \text{and} \quad k_{\alpha}r << 1 \ . \tag{IV-3-40}$$

and this result is insensitive to R_s .

Furthermore, let us recall that the fundamental Green's function solution (IV-3-1) , which we started from, is only valid for $t > \tau_o$; it will thus yield correct results only for (roughly) $r > V_p \tau_o$. Also the addition theorem for spherical wave functions (IV-3-11) requires $r > d(\tau_o)$. Thus the particular results derived here hold only for r relatively large, and from the radial dependence present in (IV-3-38) , one sees that the quadrupole term becomes more and more predominant as r increases.

At very short distances, the quadrupole will not be predominant any more; but in such cases our analysis is no longer valid and the correct Green's function solution for $t < \tau_o$ should be used (see section IV-1) .

δ) $r < R_s$, far-field approximation

The only difference with the case γ) is that now we assume $k_\alpha R_s > k_\alpha r >> 1$. The results (IV-3-34) and (IV-3-35) still hold, but we now have

$$\begin{pmatrix} C_{\ell m}^{(\alpha)} \\ D_{\ell m}^{(\alpha)} \end{pmatrix} \sim \begin{pmatrix} A_{\ell m}^{(\alpha)} \\ B_{\ell m}^{(\alpha)} \end{pmatrix} \frac{-e^{-ik_\alpha R_s}}{(k_\alpha R_s)^2} \quad , \qquad \text{(IV-3-41)}$$

and

$$h_\ell^{(2)}(k_\alpha r) \sim i^{\ell+1} \frac{e^{-ik_\alpha r}}{k_\alpha r} \quad ,$$

$$j_\ell(k_\alpha r) \sim \mathrm{Re}\left[i^{\ell+1} \frac{e^{-ik_\alpha r}}{k_\alpha r} \right] .$$

Clearly the Bessel function terms may be neglected. Furthermore the behavior of the spectrum is controlled again by the quadrupole term and we have

$$|\tilde{\chi}_\alpha(r,\omega)| = O(\omega) \quad \text{for} \quad \omega << 1 \quad \text{and} \quad k_\alpha r >> 1 . \qquad \text{(IV-3-42)}$$

We have therefore proved that in all cases, the solution obtained in this section has the same asymptotic behavior as the solution obtained in section IV-2. This provides at least a partial check on the correctness of our approach and of our results. Further, we have shown that except possibly in the close vicinity of the rupture zone, the radiation field is dominantly quadrupole at long periods. In particular, the monopole and dipole fields are negligible at low frequencies. The same holds at very high frequencies, as we saw earlier. Also, just as in section IV-2, none of the limiting cases we just discussed is sensitive to R_s , so that when the observer's point lies within the relaxation zone, we can again take $R_s = \infty$.

It is very difficult to characterize the spectra at intermediate frequencies other than by numerical calculations. Such calculations

will be undertaken in Chapter VII . However, since most of the observational work concerns displacement spectra, we still have to show how to obtain the displacements from the potentials. This is done in the next section.

IV-4) The displacement spectra

The dynamic solutions which we obtained in the previous sections were given in terms of potentials. However, seismological observations do not yield the dilatation or rotation potentials as a function of time. The measured quantities are the displacement, velocity or acceleration fields, depending on the instrument used. Mainly for that reason most of the observational work in seismology or in earthquake engineering has been concerned 1) with displacement spectra (e.g., Ben-Menahem et al, 1965; Molnar, 1971; Wyss, 1970; Linde and Sacks, 1972; Hanks and Thatcher, 1972; Hanks and Wyss, 1972; Tucker and Brune, 1973; Niazi, 1973; etc.); or 2) with displacement as a function of time (e.g., Berckhemer and Jacob, 1968; Helmberger and Wiggins, 1971; Mitchell and Helmberger, 1973; Burdick and Helmberger, 1973; Usami et al, 1970, etc.); or 3) with the velocity and acceleration fields, both in the time domain and in the spectral domain (e.g., Trifunac and Hudson, 1971; Hanks, 1972; Trifunac, 1973; etc.).

Similarly, and for the same reasons, theoretical investigations have been oriented towards the interpretation and the prediction of these fields (e.g., Archambeau, 1964, 1968; Haskell, 1966; Randall, 1966; Savage, 1966; Aki, 1967; Brune, 1970; Burridge and Halliday, 1971; Ida and Aki, 1972; Cherry et al., 1973; Dahlen, 1973).

We shall, therefore, devote this section to the derivation of the displacement spectra from the potential spectra obtained in the previous sections. Velocity and acceleration spectra may be readily obtained from the displacement by simple differentiation with respect to time. Asymptotic limits will be discussed much along the same pattern as we

followed for the potential spectra. This will allow us to discuss the range of possible spectral shapes allowed by our model, and thus to complete the discussion of source representations initiated in Chapter II. In particular, we shall emphasize the long-period asymptotic behavior of the displacement spectra, and clarify one of the controversial topics of seismology: is the displacement spectrum "flat" at long periods (e.g., Aki, 1967; Brune, 1970) or is it peaked (e.g., Archambeau, 1968, 1972)? In addition we shall present a short discussion of the phase spectra, scaling laws and seismic moments associated with our source model.

i) Evaluation of the displacement spectra

The potentials χ_α that we used in the former sections were the cartesian components of the rotation vector potential

$$\Omega_i = \chi_i \qquad i = 1,2,3,$$

and the dilatation

$$\Theta = \chi_4 \ .$$

We showed in section I-4 how the wave equations satisfied by these potentials were derived by taking the curl and divergence of the equations of motion in an elastic medium. It is easy to show that the displacement spectrum is then given by (e.g., Archambeau, 1968)

$$\tilde{\mathbf{u}}(\mathbf{r},\omega) = -\frac{1}{k_p^2}\nabla\tilde{\Theta}(\mathbf{r},\omega) + \frac{2}{k_s^2}\nabla\times\tilde{\boldsymbol{\Omega}}(\mathbf{r},\omega) \quad . \qquad \text{(IV-4-1)}$$

Here, the wave numbers k_p and k_s are

$$k_p = \omega/V_p \quad ; \quad k_s = \omega/V_s \quad , \qquad \text{(IV-4-2)}$$

where V_p and V_s are respectively the P-wave and S-wave velocities of the medium.

Archambeau (1964) derived the analytical expressions for the components of the vector $\tilde{\mathbf{u}}$ in orthogonal curvilinear coordinates with arbitrary metric coefficients. We must here again emphasize that Ω_i , $i = 1,2,3$ represent the cartesian components of $\boldsymbol{\Omega}$ in a chosen reference frame.

Since the potential solutions derived in sections IV-2 and IV-3 were obtained by use of spherical coordinates, and since these spherical coordinates appear explicitly as independent variables in the multipolar expansions, it is logical and convenient to use the spherical components of $\tilde{\mathbf{u}}$. Furthermore, longitudinal and transverse waves separate naturally in spherical coordinates. The first term in (IV-4-1) represents the P-wave radiation and the second term represents the S-wave radiation. But we shall see that while this separation is a valid one in the far-field, it is purely mathematical in the near-field, and is not very convenient in that case. The analytical expressions for the spherical components $\tilde{u}_r$, $\tilde{u}_\theta$, $\tilde{u}_\phi$ of the displacement

vector $\tilde{u}$ are rather complicated and are given in Appendix 5. We shall not reproduce them here in their totality, but the far-field components will be useful to us in this section. They are obtained in the limit $k_s r > k_p r >> 1$

$$\left[\tilde{u}_r\right]_F = -\frac{1}{k_p^2}\frac{\partial\tilde{\Theta}}{\partial r} \qquad \text{(IV-4-3)}$$

$$\left[\tilde{u}_\theta\right]_F = \frac{2}{k_s^2}\left[\sin\phi\,\frac{\partial\tilde{\Omega}_1}{\partial r} - \cos\phi\,\frac{\partial\tilde{\Omega}_2}{\partial r}\right] \qquad \text{(IV-4-4)}$$

$$\left[\tilde{u}_\phi\right]_F = \frac{2}{k_s^2}\left[\cos\theta\cos\phi\,\frac{\partial\tilde{\Omega}_1}{\partial r} + \cos\theta\sin\phi\,\frac{\partial\tilde{\Omega}_2}{\partial r} - \sin\phi\,\frac{\partial\tilde{\Omega}_3}{\partial r}\right] . \qquad \text{(IV-4-5)}$$

Indeed, one can see from Appendix 5, equations (A-5-2a,b,c), that all the other terms appearing in those equations have an additional factor of 1/r attached to them, and thus are negligible in the far-field. We note that only the radial derivatives of the various potentials (in fact, their far-field approximations) survive in the far-field. This is a useful observation: since all potentials have similar multipolar expansions, we can see immediately that all components of displacement will have roughly similar spectral shapes in the far-field. We need, therefore, only study one of them.

Also, the P-wave displacement is purely radial in that case and the S-wave displacement is purely transverse. This corresponds to the

usual notions of longitudinal and transverse waves. The θ component of displacement may also be called the SV-wave and the ϕ component the SH-wave, but these definitions are purely arbitrary in an homogeneous space, and are only useful when the waves encounter an interface between two different materials.

The displacement components in other coordinate systems, such as cartesian or cylindrical coordinates may be obtained directly from general formulae given by Archambeau (1964). However, it is considerably more convenient to operate on the vector $\tilde{\mathbf{u}}$, as shown in Appendix 5. Its spherical components are the easiest to obtain, and components in other coordinate systems can then be obtained by the standard methods of vectorial analysis.

For obvious reasons of simplicity we shall consider only one component of motion to discuss the character of the displacement spectra. The simplest case is the radial component of the P-wave. As pointed out above, the other components will exhibit similar properties. We have

$$\tilde{u}_r^{(p)} = -\frac{1}{k_p^2}\frac{\partial\tilde{\Theta}}{\partial r} \quad , \qquad \text{(IV-4-6)}$$

where the radial derivative of the dilatation is taken without approximation in this case. From the results of Appendix 5, combined with those of sections IV-2 and IV-3, we can write

$$\tilde{u}_r^{(p)}(r,\omega) = \sum_{\ell=0}^{\infty} \sum_{m=0}^{2} - \frac{1}{(2\ell+1)\ k_p} P_\ell^m(\cos\theta)$$

$$\cdot \left\{ \left[\ell h_{\ell-1}^{(2)}(k_p r) - (\ell+1)\ h_{\ell+1}^{(2)}(k_p r) \right] \left[A_{\ell m}^{(4)} \cos m\phi + B_{\ell m}^{(4)} \sin m\phi \right] \right.$$

$$\left. + \left[\ell j_{\ell-1}(k_p r) - (\ell+1)\ j_{\ell+1}^{(2)}(k_p r) \right] \left[C_{\ell m}^{(4)} \cos m\phi + D_{\ell m}^{(4)} \sin m\phi \right] \right\} . \qquad \text{(IV-4-7)}$$

It is immediately obvious from Appendix 5 that the other components of displacement, particularly for the S-waves, will have even more complicated expressions.

The velocity and acceleration spectra can immediately be obtained by differentiation with respect to time. With reference to our choice of Fourier transforms as shown in equations (IV-1-6) and (IV-1-7) we have for the velocity

$$\tilde{v}(r,\omega) = -i\omega\tilde{u}(r,\omega) \quad , \qquad \text{(IV-4-8)}$$

and, similarly, for the acceleration

$$\tilde{a}(r,\omega) = -\omega^2\tilde{u}(r,\omega) \quad . \qquad \text{(IV-4-9)}$$

Thus the kinetic energy spectrum is

$$\kappa(\mathbf{r},\omega) = \frac{1}{2}\,\tilde{\mathbf{v}}\cdot\tilde{\mathbf{v}} \quad . \qquad \text{(IV-4-10)}$$

This represents the energy flux at $\mathbf{r}$ as a function of frequency. The total energy radiated through a sphere of radius r is

$$E = \int_0^{2\pi}\int_0^{\pi}\int_0^{\infty} \kappa(\mathbf{r},\omega)\; d\omega\; r^2 \sin\theta\; d\theta\; d\phi \quad . \qquad \text{(IV-4-11)}$$

The total energy flux at any given point is given by

$$K(\mathbf{r}) = \int_0^{\infty} \kappa(\mathbf{r},\omega)\; d\omega \quad . \qquad \text{(IV-4-12)}$$

We require it to be finite everywhere: This constraint will be used to place an upper bound on the displacement amplitude spectral density in the various limits considered below. These limits will be the same as those considered for the potential spectra in sections IV-2 and IV-3. In all these limiting cases we found that the asymptotic behavior was insensitive to R_s . This means that only the terms involving $A^{(4)}_{\ell m}$ and $B^{(4)}_{\ell m}$ need be considered both at high frequency and at low frequencies.

ii) <u>High frequency asymptotic behavior</u>

We just pointed out that the total energy flux must be finite at

every point. From (IV-4-12) this requires that

$$\begin{cases} \kappa(\mathbf{r},\omega) = 0(\omega^{\alpha}) \quad \text{as} \quad \omega \to \infty \ , \\ \\ \alpha < -1 \ . \end{cases} \tag{IV-4-13}$$

This in turn generates the constraint

$$\begin{cases} |\tilde{\mathbf{v}}(\mathbf{r},\omega)| = 0(\omega^{\beta}) \quad \text{as} \quad \omega \to \infty \ , \\ \\ \beta < -0.5 \ . \end{cases} \tag{IV-4-14}$$

Or, from (IV-4-8)

$$\begin{cases} |\tilde{\mathbf{u}}(\mathbf{r},\omega)| = 0(\omega^{\gamma}) \quad \text{as} \quad \omega \to \infty \ , \\ \\ \gamma < -1.5 \ . \end{cases} \tag{IV-4-15}$$

As an example, let us consider the radial component $\tilde{u}_r^{(p)}$ given by (IV-4-7) . We have

$$\frac{1}{k_p}\left[\ell k_{\ell-1}^{(2)}(k_p r) - (\ell+1)\, h_{\ell+1}^{(2)}(k_p r)\right] = 0(\omega^{-2}) \quad \text{for} \quad \omega >> 1 \ .$$

And we saw in sections IV-2 and IV-3 that the dominant multipole coefficients at high frequencies were $A_{\ell m}^{(\alpha)}$ and $B_{\ell m}^{(\alpha)}$, and that

they behaved asymptotically as ω^{-1} . Thus

$$|\tilde{u}_p(r,\omega)| = 0(\omega^{-3}) \quad \text{for} \quad \omega >> 1 \quad , \tag{IV-4-16}$$

The same behavior should hold for the other components of displacement. However, as pointed out in Appendix 4 this asymptotic result holds as long as $V_R < V_s < V_p$, and we also know (e.g., Archambeau, 1972) that sonic or supersonic rupture velocities yield a spectral behavior of ω^{-2} at high frequency. Thus if the rupture velocity V_R approaches the shear wave velocity V_s , we expect the spectrum to decrease as ω^{-3} only for very high frequencies. Numerical calculations show that when V_R approaches V_s , the S-wave spectrum decreases as ω^{-2} over a rather large frequency band before it eventually steepens to ω^{-3} .

Also the multipole fields of higher degree are important at high frequencies, and affect the spectral shape differently at different azimuths, because of interferences between the various fields. The net result is that the observed high frequency behavior of the amplitude spectrum may be given by

$$\begin{cases} |\tilde{\mathbf{u}}(\mathbf{r},\omega)| = 0(\omega^{\alpha}) \quad \text{for} \quad \omega >> 1 \ . \\ \\ \alpha \leq -2 \ . \end{cases} \tag{IV-4-17}$$

and the value $\alpha = -3$ given by (IV-4-16) is to be understood in a gross average sense.

iii) Long-period asymptotic behavior

In order for the total energy flux to be finite at every point, we

need

$$\begin{cases} \kappa(\mathbf{r},\omega) = 0(\omega^{\alpha}) \quad \text{as} \quad \omega \to 0 \ , \\ \\ -1 < \alpha \ . \end{cases} \tag{IV-4-18}$$

This means that we require

$$\begin{cases} |\tilde{\mathbf{u}}(\mathbf{r},\omega)| = 0(\omega^{\beta}) \quad \text{as} \quad \omega \to 0 \ , \\ \\ -1.5 < \beta \ . \end{cases} \tag{IV-4-19}$$

Further, we note that β takes the value -1 if the displacement presents a net (static) change as a function of time (cf. the Fourier transform of a step function $H(t)$, which is $-i\omega^{-1}$).

We shall adopt the same pattern of discussion as we did in the previous sections. But we already know from our study of the potential spectra that we need only consider the quadrupole term, and also that the results are insensitive to R_s. The analysis will be performed on the component $\tilde{u}_r^{(p)}$, in which we only keep the Hankel function term for $\ell = 2$. From the results of the previous sections we can summarize the behavior of the multipole coefficients $A_{2m}^{(4)}$ and $B_{2m}^{(4)}$ in the following table

	$r < R_s$	$r > R_s$
$k_p r << 1$	$0(\omega^2)$	$0(\omega^4)$
$k_p r >> 1$	$0(\omega^2)$	$0(\omega^4)$

(IV-4-20)

The corresponding table for the factor

$$\frac{1}{k_p}\left[\ell h^{(2)}_{\ell-1}(k_p r) - (\ell+1)\, h^{(2)}_{\ell+1}(k_p r)\right]$$

may be written as follows

	$r < R_s$	$r > R_s$
$k_p r << 1$	$0(\omega^{-5})$	$0(\omega^{-5})$
$k_p r >> 1$	$0(\omega^{-2})$	$0(\omega^{-2})$

(IV-4-21)

By combination of (IV-4-20) and (IV-4-21) and by comparison with (IV-4-7) we obtain the following table of asymptotic behavior for $|\tilde{u}^{(p)}_r(r,\omega)|$

	$r < R_s$	$r > R_s$
$k_p r << 1$, "near-field"	$0(\omega^{-3})$	$0(\omega^{-1})$
$k_p r >> 1$, "far-field"	$0(1)$	$0(\omega^{2})$

(IV-4-22)

Identical results hold for the other components of displacement, as can be shown numerically (see Chapter VII).

A puzzling result, at first sight, is the near-field behavior for $r < R_s$. Clearly the restriction (IV-4-19) is violated, and it seems that the energy flux is unbounded in that case. This is also the result obtained by Randall (1972) for the case of a stationary rupture and with $R_s = \infty$. (On that basis, Randall attempts to define a "long-period corner frequency.") A similar result would be obtained by expressing the Green's tensor $\Gamma_{mk}(r^*,t^*)$ given in Chapter I--equation (I-3-35)--in the frequency domain.

The answer to this puzzle is that one cannot physically separate a P-wave and an S-wave in the near-field: the two waves merge in that case into one single pulse, especially at long periods. The separation which we suggested in equation (IV-4-1) is purely mathematical and does not bear any relation to the physical situation and to the observations.

The correct quantity that we should consider in that case is $|\tilde{u}_r^{(p)} + \tilde{u}_r^{(s)}|$. It may be shown analytically, although with great difficulty, that the mathematically defined "P-wave" and "S-wave" cancel each other exactly at long periods and that in such a case

$$\left|\tilde{u}_r^{(p)} + \tilde{u}_r^{(s)}\right| = O(\omega^{-1}) \quad \text{for} \quad \omega << 1 \ . \qquad \text{(IV-4-23)}$$

and similarly for the θ and ϕ components.

We shall omit the proof here; more importantly, however, this cancellation should and will be obtained numerically as well. This will obviously provide an exceedingly useful check on the correctness and accuracy of our numerical calculations.

iv) Discussion: "peaked" and "flat" spectra

As we said earlier, one of the main interests of analytically evaluating asymptotic forms for the various spectra considered in this chapter is that they will provide a check on eventual numerical calculations. But they also give us preliminary information on the general shape of the amplitude spectra predicted by the model. For instance, we see that while the high frequency side of the displacement spectrum is quite the same in most cases considered above, the spectral shape at long periods may be very different under different circumstances as shown in (IV-4-22) .

It is usual in seismology to plot the logarithm of the amplitude spectral density against the logarithm of frequency. For that reason the asymptotic behavior $O(\omega^{\alpha})$ is said to have a "slope" of α . This is a convenient phraseology and we shall use it here.

For example, we found that the amplitude spectrum has a slope of -3 at very high frequencies. This is an asymptotic limit and our

analysis did not predict when it should be reached. As we pointed out, the average slope is controlled by the rupture velocity for the S-wave spectrum, and is also azimuthally dependent because of interferences between the multipole fields of various degrees; in particular, it could be steeper at certain azimuths, and less steep in other directions. Furthermore, Archambeau (1972) shows that this slope becomes -2 for a supersonic rupture velocity, such as might occur in the case of an underground explosion.

These results may be compared with the slope of -2 obtained from simple dislocation models (e.g., Aki, 1967). Brune (1970) also obtained a slope of -2 for his model.

Observations yield a rather wide range of high frequency slopes, although the value -2 appears to be roughly adequate in many cases (e.g., Hanks and Thatcher, 1972; Hanks and Wyss, 1972). There is no real discrepancy here since the term "high frequency" should be defined as that frequency range for which the wave length is very much smaller than the source dimensions so that the predicted asymptotic behavior may not be observable in most cases. Further, at such high frequencies the observed spectrum must be corrected for instrument response, the effects of attenuation must be taken into account, and the spectral amplitude becomes comparable to that of the seismic noise (e.g., Tucker et al., 1973). These effects all add up to rather uncertain spectral amplitudes. Of course, the critical test will be to try and match the model against the observations, and this requires computing a complete spectrum, so that we shall defer a more complete discussion until later.

However, we may already point out that a rupture velocity

$V_R \simeq 0.9\ V_s$ is high enough to yield a slope of -2 for the S-spectrum over much of the observable frequency range. On the other hand, we shall also show that our model-predicted slope of -3 would provide a ready interpretation of a large body of data obtained by plotting the body wave magnitude m_b against the surface wave magnitude M_s for many events.

The long-period near-field behavior does not generate a lot of argument, mostly because of observational difficulties, and also because a slope of -1 is readily explainable in terms of a net static offset in displacement. Static and quasi-static displacement studies fall outside the scope of this discussion, and are generally treated by a variety of numerical methods (e.g., Alewine and Jungels, 1973; Alewine, 1973). In addition, most of the available near-field strong motion data were gathered for engineering purposes and were high-pass filtered with a cut-off frequency of about 0.1 hz (e.g., Trifunac and Hudson, 1971; Trifunac, 1973).

Much more controversial is the long-period spectral behavior in the far-field. The results in (IV-4-22) show that if the observer is inside the relaxation zone, the long-period spectral amplitude has a slope of 0 , and similarly, if the observer is outside the relaxation zone, the slope is 2 . The former case yields a spectral shape which is flat at long periods; in the latter case, however, the spectrum must clearly exhibit at least one maximum and is therefore peaked. We saw earlier that the first behavior is insensitive to R_s and that, for practical purposes, R_s may be taken to be infinite in that case. In the second case, however, the size of the relaxation zone has a definite

effect on the shape of the spectrum. Quantitative results will have to be obtained numerically, but it is clear on intuitive grounds that the finiteness of the relaxation zone will only be felt at periods long enough so that the wave length is comparable to R_s , so that the predicted slope of 2 will only be observed at such periods. (See also the next section for the analytical treatment in a particular case.)

"Flat" spectra are typically obtained on the basis of dislocation models in which the time dependence of the displacement jump is chosen to be a step function or some variation of it (e.g., Aki, 1967; Savage, 1966). Such is also the case for Brune's (1970) model. This is consistent with the equivalence theorem proved in Chapter IV, between such models and a relaxation source in an unbounded medium.

In contrast, Archambeau (1964, 1968) proposed a relaxation source model in which R_s was kept finite and the observer was outside R_s : he predicted on that basis a marked peak in the far-field displacement spectrum. In an effort to reconcile the various models, Randall (1973) suggested that it is erroneous to keep R_s finite, and by making the relaxation zone extend to infinity, obtained the same behavior as we do for $r < R_s$.

It would be superfluous for us to repeat here the arguments concerning the introduction of a finite relaxation zone. This was done in the introduction to this chapter. It is essential, however, to comment on the interpretation of body wave spectra.

Much of the interpretation of such spectra in terms of various source parameters is based on their low frequency end, and more

specifically on the fact that the spectrum is flat at long periods and exhibits a "corner" at some intermediate frequency. The spectral level in the flat portion is thus assumed to be about the same as it is at the corner frequency (e.g., Brune, 1970; Hanks and Wyss, 1972; Wyss and Molnar, 1972). We just saw that this holds when $r < R_s$. For the case $r > R_s$, the spectrum presents a peak instead of a corner; but the peak level is identical to the corner level provided that R_s is large enough (i.e., a few rupture lengths). In other words, if R_s is large enough, the finiteness of the relaxation zone will affect the spectrum only at frequencies lower than the corner or peak frequency. Thus the interpretations based on this spectral level should be correct whether the spectrum is indeed flat or not. This will be discussed in greater detail in Chapter VII.

But this leaves a fundamental question unanswered: is R_s to be chosen finite or infinite? And, if R_s is finite, what is its size in relation to the size of the rupture?

The answer may only be obtained on the basis of reliable long-period data. As pointed out by Linde (1971), such data are rather difficult to obtain. In fact, Linde argues that most problems associated with their obtainment, such as correction for instrument response, and limitations in the time series analysis--truncation, detrending, noise contamination--all contribute to an overestimate of the long-period spectral level. Therefore a seemingly flat spectrum might really be peaked.

Linde and Sacks (1972) found indications of a spectral peak in their analysis of South American deep earthquakes. This suggests a

finite relaxation zone. On the other hand, the excellent study of S-wave spectra by Tucker and Brune (1973) for aftershocks of the San Fernando earthquake shows that the spectra for these events may be quite flat over a relatively broad frequency range. Their observations were gathered at close range, and one may speculate that the assumption $r < R_s$ might apply in that case.

Hanks and Wyss (1972) showed that the body-wave spectra of three shallow earthquakes could be interpreted in terms of flat spectra, and showed how such an interpretation can be used to estimate source parameters. However, in most cases, their data could also be interpreted in terms of peaked spectra. This is also true of many of the body-wave spectra of the San Fernando earthquake computed by Wyss and Hanks (1972). On the other hand, some of the averaged spectra for deep earthquakes gathered by Wyss and Molnar (1972) require a relatively wide spectral peak--a decade in frequency--if one wishes to interpret them in terms of peaked spectra.

In the absence of a large body of data pertaining to a wide class of different events, which would prohibit a dual interpretation, we shall take the position that there is no clear cut choice for R_s. The two cases $r < R_s$ (or $R_s = \infty$) and $r > R_s$ which we investigated in this chapter represent two possible extreme situations, and the truth probably lies between these two extremes. In other words, we feel that the two extreme spectral shapes--flat spectrum and peaked spectrum--bracket the range of possible observations. The figures of Chapter VII give a more quantitative description of this range.

Molnar et al. (1973) show that a flat spectrum corresponds to a

unipolar far-field displacement pulse in the time domain (one for which the displacement in any direction does not change sign as a function of time). A peaked spectrum corresponds in turn to a pulse which is not unipolar. In terms of a dislocation model, a unipolar pulse can only be generated if the time derivative of the displacement dislocation jump does not change sign (i.e., in the absence of "overshoot"). This fact is entirely consistent with the equivalence theorem between relaxation sources and dislocation sources shown in Chapter II in the case $R_s = \infty$, since we predict a flat spectrum in that case. We argued then that no overshoot occurs for transparent sources. The spectrum is peaked in the case $r > R_s$, but the fact that the far-field displacement pulse is therefore not unipolar does not mean that "overshooting" takes place in that case. Rather, it means that the equivalence theorem does not hold any more; one can still find (probably with great difficulty) an <u>equivalent</u> dislocation source generating the same radiation field in that case, but the displacement jump of this equivalent dislocation will no longer represent the true displacement on the rupture boundary. As proven by Molnar <u>et al.</u>, this equivalent dynamic dislocation will exhibit an overshoot, but we cannot conclude that there is physical overshoot.

We see, therefore, that the model that we propose in this chapter is very flexible, and that a broad range of possible spectral shapes may be interpreted in terms of it. For completeness, we shall discuss next some other aspects of the solution which require a more quantitative knowledge of the spectral amplitude.

IV-5) Phase spectra, scaling laws, moments

We shall discuss in this section a number of miscellaneous topics concerning the radiation fields obtained earlier in this chapter. Since the discussion necessitates that we compute more complete expressions for the displacement spectrum, we shall center it around a very particular example.

We shall assume a symmetrically expanding rupture ("explosion-like"); we also assume that only the component $\sigma_{13}^{(o)}$ of the prestress is present. Thus, from (IV-1-13) the only non-zero static coefficient for the dilatation is

$$a'_{21} = \frac{5(1-2\sigma)\ \sigma_{13}^{(o)}}{\mu(7-5\sigma)} \quad . \qquad \text{(IV-5-1)}$$

Furthermore, we have a pure quadrupole field in that case. Taking the results of section IV-2 we have

$$A_{21}^{(4)}(\omega) = a'_{21}\ \frac{\omega^2}{V_p^3} \begin{cases} I_2^{(2)}(\omega) & \text{for } r < R_s \ . \\ I_2^{(3)}(\omega) & \text{for } r > R_s \ . \end{cases} \qquad \text{(IV-5-2)}$$

We shall take $R(t_o) = V_R t_o$, and define $L = R(\tau_o)$ as the characteristic dimension of the rupture (its final radius). Then, from Appendix 4, we have

$$I_2^{(2)}(\omega) \sim L^3/3 \quad \text{for} \quad \omega \to 0 \quad , \tag{IV-5-3}$$

and

$$I_2^{(3)}(\omega) \sim \frac{\omega^2}{10V_p^2}\left[\frac{R_s^2 L^3}{3} - \frac{L^5}{5}\right] \quad \text{for} \quad \omega \to 0 \quad . \tag{IV-5-4}$$

Then by using the various results of section IV-4 and the expression (IV-4-7) for the radial component of the P-wave, we obtain the following low frequency limits

a) $r > R_s$, far-field

$$\tilde{u}_r^{(p)} \sim \frac{a'_{21}}{20}\left[R_s^2 - \frac{3L^2}{5}\right]\frac{L^3\omega^2 e^{-ik_p r}}{V_p^3 r}\sin 2\theta \cos\phi \quad . \tag{IV-5-5}$$

b) $r > R_s$, near-field

$$\tilde{u}_r^{(p)} \sim \frac{27i\, a'_{21}}{20}\left[\frac{R_s^2}{3} - \frac{L^2}{5}\right]\frac{L^3}{\omega r^4}\sin 2\theta \cos\phi \quad . \tag{IV-5-6}$$

c) $r < R_s$, far-field

$$\tilde{u}_r^{(p)} \sim \frac{a'_{21}}{2}\frac{L^3}{V_p r} e^{-ik_p r} \sin 2\theta \cos\phi \quad . \tag{IV-5-7}$$

d) $r < R_s$, near-field

$$\tilde{u}_r^{(p)} \sim \frac{9i\, a'_{21}}{2} \frac{V_p^2\, L^3}{\omega^3 r^4} \quad . \qquad \text{(IV-5-8)}$$

This last equation yields the mathematically defined P-wave in the near-field, and should really be combined with the corresponding S-wave component as we showed earlier. But we shall only use it to define a frequency range where the near-field effects become important.

As shown in Appendix 4, the high frequency spectrum is more complicated and the solution does not lend itself to convenient asymptotic expansion. According to equation (A-4-8) we may write

$$I_2^{(2)}(\omega) = \frac{3V_p^3}{8\omega^3} \int_o^{\omega L/V_p} e^{-i\zeta t}\, t\, j_1(t)\, dt \quad , \qquad \text{(IV-5-9)}$$

or

$$I_2^{(2)}(\omega) = \frac{3V_p^3}{8\omega^3} \int_o^{\omega L/V_p} e^{-i\zeta t} \left[\frac{\sin t}{t} - \cos t\right] dt, \qquad \text{(IV-5-10)}$$

where $\zeta = V_p/V_R$ is greater than one.

It is pointed out in Appendix 4 that the integral in (IV-5-10) has no limit, but stays finite as $\omega \to \infty$. Archambeau (1972, equation 5-8) investigates precisely this integral, but did not find any convenient analytic form for it either. His series expansion in terms

of hypergeometric functions is only convenient for low frequencies. Just as in Appendix 4, we write

$$\int_o^{\omega L/V_p} = \int_o^{X} + \int_X^{\omega L/V_p} ,$$

where X is a fixed number, chosen large enough so that $t\, j_1(t)$ may be approximated by $-\cos t$ in the second of these integrals. Then

$$I_2^{(2)}(\omega) \sim \frac{3V_p^3}{8\omega^3} \left[\int_o^X e^{-i\zeta t}\, t\, j_1(t)\, dt \right.$$

$$+ \frac{i}{2} \frac{e^{i(1-\zeta)\, \omega L/V_p} - e^{i(1-\zeta)\, X}}{1-\zeta}$$

$$\left. - \frac{i}{2} \frac{e^{-i(1+\zeta)\, \omega L/V_p} - e^{-i(1+\zeta)\, X}}{1+\zeta} \right] . \qquad \text{(IV-5-11)}$$

Now the first term in the bracket is a number that depends only on ζ and thus on the rupture velocity V_R ; in particular, it does not depend on the frequency ω . However, on account of the parity of the function to be integrated in (IV-5-10) , we can investigate this integral further. Let us designate by K the integral on the right-hand side of (IV-5-10) . We have

$$2Re(K) = \int_{-\omega L/V_p}^{\omega L/V_p} e^{-i\zeta t} \left[\frac{\sin t}{t} - \cos t\right] dt \quad .$$

As ω goes to infinity, we recognize that this integral converges to the sum of distributions

$$2Re(K) \xrightarrow[\omega \to \infty]{} H(\zeta+1) - H(\zeta-1) - \delta(\zeta+1) - \delta(\zeta-1) \qquad \text{(IV-5-11)}$$

so that, for $\zeta > 1$, the real part of K tends to zero. On the other hand, we have

$$Im(K) = -\int_{o}^{\omega L/V_p} \sin \zeta t \left[\frac{\sin t}{t} - \cos t\right] dt \quad .$$

As ω tends to infinity, the first term tends to the sine transform of of $\frac{\sin t}{t}$, and the second term can be evaluated by two successive integrations by parts. We get

$$Im(K) \xrightarrow[\omega \to \infty]{} -\frac{1}{2} \operatorname{Ln} \left|\frac{\zeta+1}{\zeta-1}\right| - \frac{1}{\zeta^2-1}\left[\sin \frac{\omega L}{V_p} \sin \frac{\omega L}{V_R} + \zeta\left(\cos \frac{\omega L}{V_p} \cos \frac{\omega L}{V_R} - 1\right)\right] .$$

(IV-5-12)

It is not our purpose to discuss here the nature of the convergence in those various cases. It is sufficient to point out that we have a singularity for $\zeta = 1$, which is consistent with the fact that our solution is no longer valid when the rupture propagates at sonic velocity. For that reason, the above proof does not achieve complete rigor. Nevertheless, we can see that the dependence of the high frequency spectral level on the rupture length is weak: both in (IV-5-11) and (IV-5-12) L appears only in the argument of trigonometric functions, and thus does not affect the average amplitude of $I_2^{(2)}(\omega)$. On the other hand, we note that rupture velocity is an important parameter at high frequency, and that it affects the spectral amplitude in a very complex fashion.

i) The phase spectrum

Niazi (1973) computed the phase spectrum as well as the amplitude spectrum for the body waves of a number of earthquakes. Little work has been done on this aspect of the problem, in particular for relaxation source models. Ben-Menahem (1962) shows that the phase spectrum should be a decreasing function of frequency for a moving source.

From (IV-5-7) and (IV-5-9) we see immediately that, in the near-field, the phase is $\pm \pi/2$, depending on the sign of the radiation pattern coefficient. This agrees with the fact that the Fourier transform of a step function is imaginary.

The far-field phase spectrum is more interesting, since it corresponds to teleseismic observations, as well as high frequency observations. Of course, the dominant term will be $-\omega r/V_p$, as we can

see from (IV-5-6) and (IV-5-8) . This term is easily recognized as the phase of a wave travelling over the distance r , and can be deleted from the solution.

It is more difficult to evaluate analytically the initial phase at the source, and more particularly its frequency dependence. This initial phase is controlled by the multipole coefficients $A_{\ell m}(\omega)$ and $B_{\ell m}(\omega)$, and thus by $I_{\ell}^{(2)}(\omega)$ and $I_{\ell}^{(3)}(\omega)$. In the long-period limit, we can expand these integrals for small ω and find, for the quadrupole term

$$I_2^{(2)}(\omega) = \frac{L^3}{3}\left(1 - i\,\frac{3\tau_o}{4}\,\omega\right) + O(\omega^2) \quad , \qquad \text{(IV-5-13)}$$

and

$$I_2^{(3)}(\omega) = \frac{\omega^2 L^3}{10 V_p^2}\left[\left(\frac{R_s^2}{3} - \frac{L^2}{5}\right) - i\,\tau_o\omega\left(\frac{R_s^2}{4} - \frac{L^2}{6}\right)\right] + O(\omega^4) . \qquad \text{(IV-5-14)}$$

Thus we find that, in the far-field, the long-period phase is 0 or π --depending on the sign of the radiation pattern coefficient--and that it decreases with increasing frequency. The derivative of the phase with respect to ω, at the source, has dimension of time and is called the group delay at the source (e.g., Archambeau et al., 1965; Alexander, 1965). We shall denote it by $t_g(\omega)$. This group delay comes in explicitly in the theory of mode separation for surface waves (Alexander, 1963). If it is large, it should be noticeable in body wave observations as well. From (IV-5-13) and (IV-5-14) we see that, if R_s is large with respect to L , then in both cases

$$t_g(\omega) \simeq \frac{3}{4}\tau_o \qquad \text{for} \quad \omega << 1 \quad . \tag{IV-5-15}$$

We take the convention that t_g is positive if it is indeed a delay, as is the case here. The numerical factor in (IV-5-15) is dependent on the specific history of growth chosen for the source; that is, on the functional form of $R(t_o)$ in particular.

At high frequencies, we showed that $I_\ell^{(2)}$ becomes pure imaginary, and thus its phase does not depend on frequency any more, so that

$$t_g(\omega) \to 0 \quad \text{as} \quad \omega \to \infty \quad . \tag{IV-5-16}$$

The group delay at the source is therefore not a constant function of ω . The immediate conclusion is that our source model is a dispersive radiator. More specifically, the radiation is inversely dispersed, according to the seismological terminology: the high frequency part of the wave train travels ahead of the long-period part.

This requires a physical interpretation or, at least, a heuristic explanation. For a growing rupture, the major part of the long-period energy will be radiated during the last stages of the phenomenon, that is, when the rupture has reached its maximum size. On the other hand, the high frequency radiation emanates essentially from the vicinity of the rupture front and the source is an efficient high frequency radiator even during the early stages of the phenomenon. One therefore expects intuitively the long-period radiation to be delayed with respect

to the high frequency radiation, and the delay should be of the order of the total rupture duration, as shown in (IV-5-15) .

The long-period group delay can be quite large: for a 20 km rupture and a rupture velocity of 2 km/s., it approaches 10 seconds. This is consistent with the data obtained by Niazi (1973). Burdick (personal communication, 1973) also finds delays of this order. If this phenomenon yields different delays for P-waves and S-waves over significant frequency bands, then this could be a source of complications in the interpretation of seismic data, in particular, travel time data which might have to undergo a sizeable "base-line correction." However, further investigations of this particular aspect of the problem will have to be undertaken before any significant conclusion can be reached: for instance, alteration of the phase spectrum by attenuation effects could be important.

Similar results hold for the S-waves; the radiation pattern and static coefficients are then different, but, for reasons of homogeneity, V_p must clearly be replaced by V_s .

This elementary treatment does not cover all the characteristics of the phase spectrum. Niazi (1973) notes that bilateral ruptures have a phase spectrum different from that of unilateral ruptures. Savage (1966) points out that the source geometry (i.e., very long faults versus nearly circular faults) may also be a significant parameter. Introduction of multipole fields of higher degrees will complicate the global phase spectrum. In particular, there may be some fine structure of the spectrum, as suggested by Niazi's (1973) data, and azimuthal effects will then be taken into account. A numerical investigation will

be undertaken in Chapter VII.

ii) Scaling laws

Aki (1967) attempted to define scaling laws for the seismic spectrum in order to facilitate the interpretation of seismological data.

The asymptotic forms (IV-5-5) through (IV-5-8) permit us to derive also a number of such scaling laws which will be found useful. Figure IV-5-1 shows a sketch of the various asymptotes given by these equations, and thus gives us a rough idea of the global shape for the amplitude spectrum.

The most trivial of the scaling laws is given by the fact a'_{21} which is proportional to the prestress. This is a very general result: the spectral amplitude is directly proportional to the prestress.

We have seen in the former section that, provided R_s is large enough, the displacement spectrum is "flat" at long periods, at least in some frequency band. For this reason, it has become customary in seismology to talk about a corner frequency ω_o, which is a frequency separating the high frequency side from the low frequency side of the spectrum in a gross sense (see figure IV-5-1). However, we have been unable to obtain a simple asymptotic expression for the spectral density at high frequency. Furthermore, there is no insurance that an approximation which holds at very high frequency is still adequate at intermediate frequency. We shall therefore obtain an approximation to $I_\ell^{(2)}$ in the following fashion:

The ascending series for spherical Bessel functions converge very well even for arguments of moderate size. We therefore replace $j_1(t)$

by its ascending power series in (IV-5-9) , integrate term by term, and use the following high frequency result

$$\int_o^z e^{-i\omega t}\, t^n\, dt = \frac{i\, z^n\, e^{-i\omega z}}{\omega} + O(\omega^{-2}) \quad .$$

Then by regrouping terms we obtain

$$I_2^{(2)}(\omega) \sim \frac{3iV_R V_p L}{\omega^2}\, e^{-i\omega\tau_o}\, j_1(\omega L/V_p) \quad .$$

Replacing the spherical Bessel function by its asymptotic term we eventually get

$$\left| I_2^{(2)}(\omega) \right| \sim \frac{3V_R V_p^2}{\omega^3} \qquad \text{for} \quad \omega >> 1 \quad . \tag{IV-5-17}$$

There is no analytical proof that the procedure truly yields an asymptotic series, but this result is in remarkable agreement with numerical calculations. Equating (IV-5-17) with the long-period asymptotic value (IV-5-3) , we find that the corner frequency is then given by

$$\omega_o^3 = \frac{3V_R V_p^2}{L^3} \quad . \tag{IV-5-18}$$

Comparison of (IV-5-18) with numerically calculated spectra showed

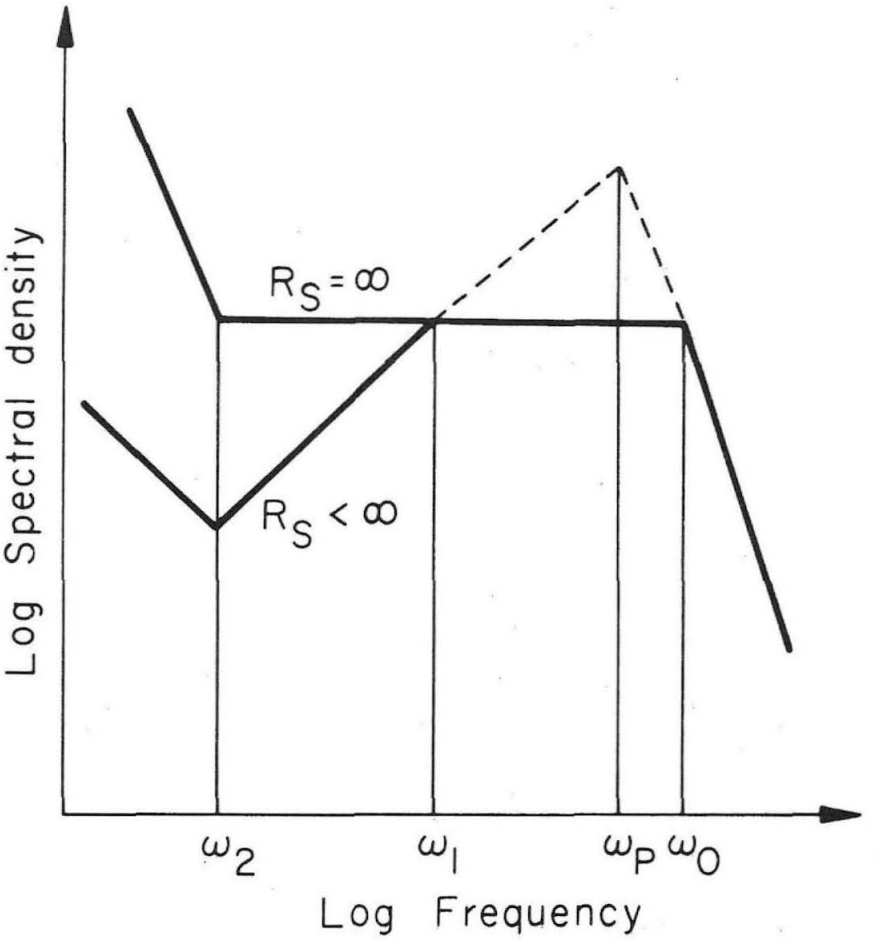

Figure IV-5-1. Schematic representation of the displacement amplitude spectrum based on asymptotic forms. When R_s is finite and the observer is outside R_s, a peaked spectrum is predicted.

that it gives an excellent measure of the corner frequency for P-wave spectra. The same formula was found to hold for S-spectra if one replaces V_p by V_s . The formula was also found to give good results in the case of a unilateral rupture, even in the presence of higher degree multipoles. In such a case L represents the rupture length, and not the final radius (recall that $L = V_R \tau_o$). We note that (IV-5-18) predicts a corner frequency occurring at a lower frequency for the S-spectrum. This is consistent with the observations (e.g., Hanks, 1972).

Similarly, by taking the intersection of (IV-5-18) and (IV-5-4) we can get a "peak frequency" which is given by

$$\omega_p^5 = \frac{10 V_R V_p^4}{L^3 \left[R_s^2 - \frac{3}{5} L^2 \right]} \quad . \qquad \text{(IV-5-19)}$$

This formula is to be used when the spectrum is truly peaked, in particular, when R_s is small. The difference between P and S peak frequencies is slightly more pronounced in that case. In the case where R_s is relatively large one can define a new characteristic frequency ω_1 (see figure IV-5-1), associated with the size of the relaxation zone. By comparison of (IV-5-3) and (IV-5-4) we find

$$\omega_1^2 \simeq \frac{10 V_p^2}{R_s^2 - \frac{3L^2}{5}} \quad . \qquad \text{(IV-5-20)}$$

The relative size of ω_o and ω_1 is a measure of the peak width. The peak width is a decade in frequency if $\omega_o = 10\omega_1$. In the case where $V_R = V_p/2$, we get by comparing (IV-5-18) and (IV-5-20)

$$R_s \simeq 20L \quad .$$

Of course, this does not mean that the spectrum will be exactly flat over a decade, since we extrapolated the asymptotes to arrive at this result. But it is clear that if R_s is about ten rupture dimensions, the peak amplitude is a good approximation of the "flat level" amplitude.

It is worth noting at this point that R_s can easily be much greater than L for small events, but that this cannot be the case for large earthquakes, so that the spectra for small events can be quite flat in the far-field while those for large events must be peaked. However, the free surface of the Earth is usually not further than one rupture length or less away from the failure zone of great earthquakes, and such earthquakes are often multiple events (e.g., Wyss and Brune, 1967), and the problem is more complicated in such cases.

Finally, the intersection of the far-field and near-field asymptotes at long periods yields a frequency ω_2 at which near-field effects become important:

$$\omega_2 \simeq 2.1 \frac{V_p}{r} \quad . \qquad \text{(IV-5-21)}$$

The range $[\omega_2,\omega_o]$ will be an order of magnitude in frequency if

$$r \simeq 20L \quad .$$

The geometrical relationships between these various quantities is shown on figure IV-5-1. Thus the corner frequency ω_o given by (IV-5-10) leads to a tradeoff between V_R and L for purposes of interpretation if the wave velocity is known. This was pointed out by Berckhemer and Jacob (1968). Similarly, from (IV-5-18) and (IV-5-20) the measure of the peak width yields a tradeoff between R_s, L, and V_R.

If A_p is the peak amplitude (or flat level), we see from (IV-5-8) that it does not depend on the rupture velocity. Thus, at constant prestress, the long-period level is proportional to L^3, and for events smaller than a certain size, the surface wave magnitude is a measure of the rupture dimensions.

On the other hand, we pointed out earlier that the high frequency asymptote is independent of L but is strongly dependent on V_R; thus for events larger than a certain size, the spectral amplitude at 1 hertz will be independent of L. Within these restrictions, the body wave magnitude of such events is a measure of the rupture velocity.

It is easy to see from their definition that the ratio of the coefficients a'_{21}/b'_{21} is proportional to V_s^2/V_p^2. Therefore, the ration S/P of the long-period spectral amplitudes given by (IV-5-7) is proportional to V_p^3/V_s^3. This is confirmed by the observations (e.g., Hanks, 1972).

All the scaling laws described here were obtained from the asymptotes in a very particular situation. Of course, because of higher degree multipoles, and because of the radiation pattern modulation, they will only hold in an average sense. However, we shall see that they are upheld by numerical calculations.

iii) Moments

Archambeau (1964, 1968) shows that the general theory of tensorial moments used in electromagnetic theory (e.g., Jackson, 1962) may be adapted to elastodynamic theory as well. However the expressions that he gives are rather complicated and cumbersome to use, so that we shall not duplicate them here.

The notion of multipole moments is essentially a long wave length concept (e.g., Stratton, 1941). For our model, however, a seismic moment can be usefully defined only where the (static) initial value fields do not vanish, that is, inside the relaxation zone. Then by using (IV-5-8) and the usual expression for the seismic moment, we get, for a Poisson solid

$$M = \frac{60\pi}{23} L^3 \sigma_{13}^{(o)} \quad . \qquad \text{(IV-5-22)}$$

This is the expression given by Aki and Tsai (1972) and obtained by Randall (1973) for the case $R_s = \infty$. Now, because we have shown that "flat-level" and "peak-level" are the same for our model, provided that R_s is not too small, it is clear that the seismic moment can be

obtained from the peak level as well. Thus our model does not require a reinterpretation of published data: Inside the relaxation zone, the long-period level is used much in the same way as it is for dislocation sources, and outside the relaxation zone, the peak level must be used to get the same result.

Conclusion

The elastodynamic relaxation source model presented in this chapter is a specialized case of the very general class of models presented in Chapter II. It is a volume source as opposed to the usual boundary source models such as dislocation and stress pulse models. The radiation field is obtained as the solution to an initial value problem as opposed to a boundary value problem. The very concepts behind this model and the more classical models are thus different. The equivalence of the various source models was shown in Chapter II, and confirmed in this chapter on the basis of a particular example. However, whereas boundary source models implicitly assume the rupture phenomenon to take place in an infinite homogeneous space, our model permits us to introduce explicitly an additional parameter of the source: the size of the prestressed region in which rupture takes place. This parameter was first introduced by Archambeau (1964, 1968). Because Archambeau considered only the case of an observer external to the relaxation zone, he predicted a peaked displacement spectrum in the far-field. This contrasted with the flat spectrum predicted, in particular, by dislocation models. The results of this chapter permit us to pinpoint the fundamental similarities and differences between the two model types, and to determine exactly the cause of this discrepancy. In fact, we confirmed this discrepancy while at the same time reconciling the various models.

This chapter contains a detailed study of a growing and propagating spherical rupture model; we can summarize the conclusions as follows:

The critical parameter controlling the shape of the displacement amplitude spectrum is the position of the observer with respect to the relaxation zone. If the observer is inside the relaxation zone, the far-field displacement spectrum is flat at long periods, and the relaxation radius may be chosen to be infinite for practical purposes. If the observer is outside the relaxation zone, a spectral peak will be observed in the far-field. The argument as to whether the far-field spectrum is flat or peaked is thus now shifted to a physical argument: For any particular event, what is the size of the relaxation zone in relation to that of the rupture zone and to the hypocentral distance of the observer? This is a much more satisfying question because it bears directly on the physical conditions in the vicinity of the event.

The near-field is only important at long periods and causes the spectrum to have a slope of -1 at such periods. On the other hand, the high frequency slope is independent of R_s and of other source parameters, and is equal to -3 . Multipole fields of higher degree become important at intermediate to high frequencies, but their effects must be evaluated numerically. The phase spectrum is asymptotically constant at high frequency and a quasi-linearly decreasing function of frequency at long periods.

A most important aspect of this study is that the interpretation of observations based on the spectral levels in the vicinity of the peak frequency (peaked spectrum) or of the corner frequency (flat spectrum) is relatively model independent. Thus many of the concepts developed on the basis of dislocation models, for example, and most of the observational work found in the seismological literature retain

their value, in the light of our model. In fact, we have shown how the various source models proposed earlier may be reconciled.

The theory presented in this chapter may be adapted to include more complex as well as more realistic situations. We shall show in Chapter VI how to treat analytically the case of a fairly general ellipsoidal rupture. But in as far as analytical models can hardly take into account the complexities of a real phenomenon, one can also use this theory in connection with finite difference or finite element numerical techniques. The multipole coefficients can then be computed numerically for very complicated rupture geometries, and also for very general rheological properties of the material within the failure zone. Further investigations along these lines will be undertaken in the future.

Some numerical applications of the spherical rupture model will be presented in Chapter VII. We shall then discuss the spectral characteristics of the displacement field in more detail, especially at intermediate frequencies.

Chapter V

USE OF MULTIPOLAR RADIATION FIELDS IN SEISMOLOGY

Introduction

We have used in the previous chapter the theory of multipolar representations of an elastodynamic radiation field. This provides, in fact, an equivalent point source representation of the source (e.g., Archambeau, 1968, 1972), especially in view of the fact that multipole fields can be generated by various nuclei of strains and their derivatives (e.g., Randall, 1971; Turnbull, 1973). Further, inasmuch as spherical wave functions form a complete set (e.g., Morse and Feshbach, 1953), any radiation field which is not pathological affords a multipolar expansion. In addition, if the source of radiation is bounded in extent, the fields outside a closed surface surrounding the source region will afford an expansion in outgoing waves only (incoming waves will be required if a scatterer is found at some distance from the source).

These properties of multipolar expansions, along with uniqueness theorems, have been used extensively in electromagnetic radiation theory (e.g., Stratton, 1941). The elastodynamic problem, as treated on the basis of a fairly simple model in Chapter IV, is complicated by the fact that the source is a volume source, the extent of which is not necessarily well known. An electromagnetic antenna is a well defined source; the relaxation zone defined in Chapter IV will not, in general, have a sharply defined boundary, and any attempt to model it will necessarily involve some approximations.

Nevertheless, the use of multipolar expansions permits us to extend the notion of equivalent seismic sources mentioned in Chapter II in a somewhat more axiomatic fashion. Given two sources of limited spatial extent, we can always enclose them in a "black box," and worry only about the radiation field emerging from this "black box." We shall say that the two sources are equivalent if the two observed radiation fields have the same multipolar expansion with respect to the same origin. Now two multipolar expansions with respect to two distinct origins and related by the addition theorem of Appendix 9 are obviously equivalent, so that one cannot, in general, obtain a unique physical interpretation of the phenomena occurring inside the "black box." Further interpretation requires, therefore, that one use other information. This information can be extraneous, such as field observations of a fault, or it can be present in the multipolar expansion, but hidden in such a way that it is difficult to extract: The hypocenter of the earthquake can be located from time domain information such as first arrival times at an array of stations. If the hypocenter is used as origin to compute a multipolar expansion, there is a good chance that the expansion will be simpler (as it is for the model of the previous chapter). If any other origin is used, the multipolar expansion so obtained will contain the necessary information to locate the hypocenter but the location will be rather difficult to perform.

This chapter will be concerned with the manipulation and use of multipolar radiation fields for seismological purposes. We shall not make any assumption about the physical nature of the source, nor shall we assume any particular source model. We shall only assume that the

radiation field is known in the form of a multipolar expansion in a given coordinate system. Without loss of generality we can take this coordinate system to be a natural reference frame of the rupture, labelled "source system" in Chapter IV. The z-axis is oriented along the direction of propagation, and the y-axis may then be chosen to lie in the fault plane.

On the other hand, wave propagation problems can be best treated in a coordinate system where the z-axis is along the local vertical. This reference frame may also be a cartesian system, or a cylindrical one, or yet a spherical one. We shall define in this chapter a "geographical" reference frame, where the z-axis is along the upward vertical, the x-axis is arbitrarily chosen in a northerly direction, and the y-axis points therefore to the west. Such a frame is reasonably convenient for wave propagation problems. These problems include the propagation of body waves in the Earth, according to ray theory (e.g., Julian and Anderson, 1968), or generalized ray theory (e.g., Gilbert and Helmberger, 1972). They also include the propagation of surface waves in a layered Earth model (e.g., Harkrider, 1963). The excitation of free oscillations of the Earth can also be treated by use of such a frame.

We shall address ourselves essentially to the problem of representing the radiation fields in a new coordinate system when they are known in the source system. In the first section the operation will be performed on the displacement vector fields, and is rather simple. The next two sections will be concerned with the transformation of a multipolar expansion under rotation and translation of the reference

frame. Finally, we shall present a very succinct discussion concerning the use of potentials other than the dilatation and rotation.

Because no use is made in seismology of left-handed systems, we shall confine ourselves to proper transformations.

V-1 Elementary transformations of the displacement fields

We saw in Chapter IV how to obtain displacement spectra from potential spectra, and this operation may be performed in the source system S. As shown in figure V-1-1, a ray can be defined in the geographical frame G by its azimuth $\phi_A^{(G)}$ and its take-off angle τ_A. The take-off angle is usually measured from the downward vertical direction so that $\tau_A = \pi - \theta_A^{(G)}$. The point A is taken to be on the focal sphere of unit radius so that the vector $\overrightarrow{OA}$ has geographical components

$$\begin{cases} x_A^{(G)} = \sin \tau_A \cos \phi_A^{(G)} , \\ y_A^{(G)} = \sin \tau_A \sin \phi_A^{(G)} , \\ z_A^{(G)} = - \cos \tau_A . \end{cases} \qquad \text{(V-1-1)}$$

The first problem is now to find the spherical coordinates of A in the source system. This is easily done if one knows the orthogonal transformation matrix $\mathbf{T}$ transforming the system G into the system S. This matrix is given in Appendix 7, both in terms of "fault orientation parameters"--strike, dip, and plunge angles--and in terms of Euler angles. Then the cartesian coordinates of A in the source system are given by

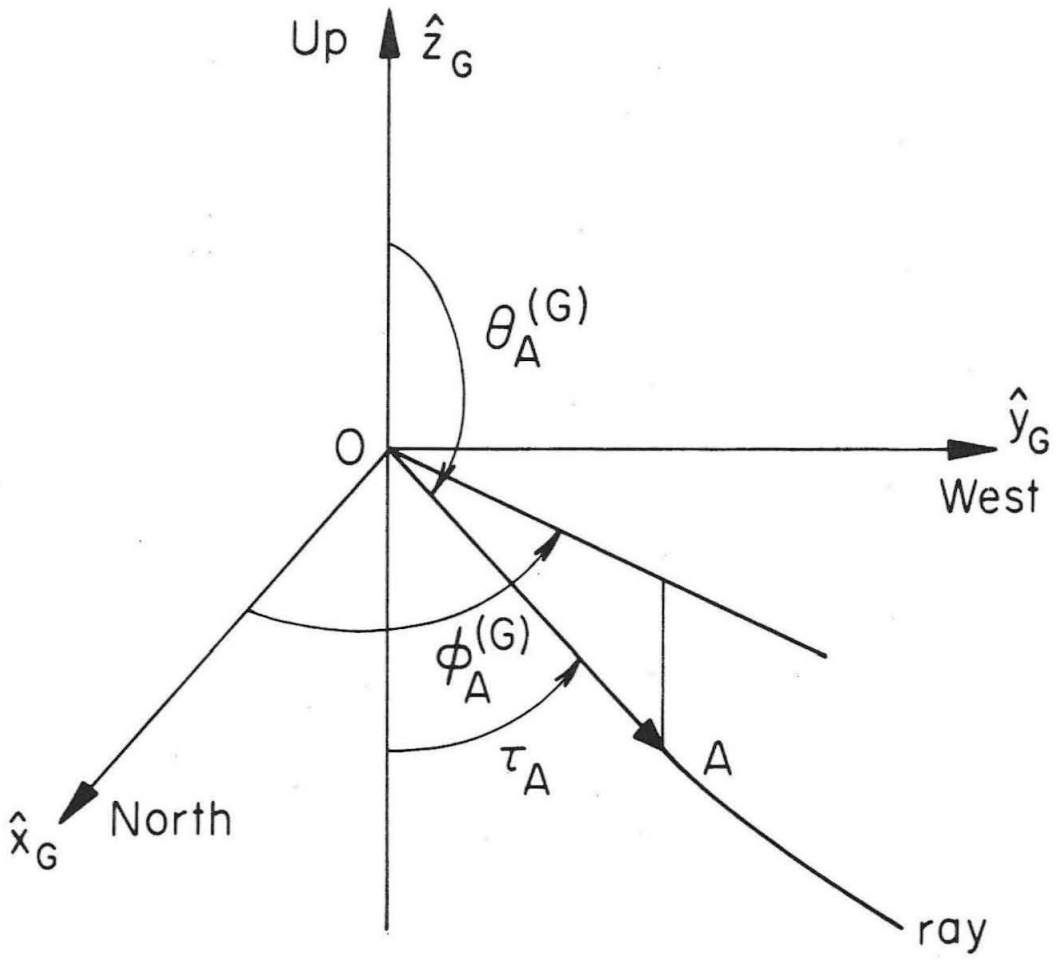

Figure V-1-1. Specification of a ray by its azimuth $\phi_A^{(G)}$ and take-off angle τ_A in the geographical coordinate system.

$$\begin{bmatrix} x_A^{(S)} \\ y_A^{(S)} \\ z_A^{(S)} \end{bmatrix} = \mathbf{T}^* \begin{bmatrix} x_A^{(G)} \\ y_A^{(G)} \\ z_A^{(G)} \end{bmatrix} \qquad \text{(V-1-2)}$$

where $\mathbf{T}^*$ denotes the transposed (and therefore the inverse) of $\mathbf{T}$. The spherical coordinates of A in the source system are then trivially obtained as

$$\begin{cases} \theta_A^{(S)} = \cos^{-1} z_A^{(S)} \\ \phi_A^{(S)} = \begin{cases} \cos^{-1}\left(x_A^{(S)}\ \rho^{-1}\right) & \text{if } y_A^{(S)} > 0\ , \\ 2\pi - \cos^{-1}\left(x_A^{(s)}\ \rho^{-1}\right) & \text{if } y_A^{(S)} < 0\ , \end{cases} \end{cases} \qquad \text{(V-1-3)}$$

where

$$\rho = \left[\left(x_A^{(S)}\right)^2 + \left(y_A^{(S)}\right)^2\right]^{1/2}.$$

Knowing the spherical coordinates of A in the source system, we can easily get the spherical components of the displacement fields at A, in the source system, where the fields are given by multipolar expansions. These components are $u_r^{(S)}$, $u_\theta^{(S)}$, and $u_\phi^{(S)}$, and are computed in Appendix 5.

The spherical components of displacement at A in the geographical frame are then obtained by a sequence of three rotations: $u_r^{(S)}$, $u_\theta^{(S)}$ and $u_\phi^{(S)}$ are transformed successively into the cartesian components of displacement in the source system by a rotation of matrix $\mathbf{M}_1$; these are in turn transformed into the cartesian components in the geographical frame by the rotation of matrix $\mathbf{T}$; finally the components $u_r^{(G)}$, $u_\theta^{(G)}$ and $u_\phi^{(G)}$ are obtained through a rotation of matrix $\mathbf{M}_2$. Thus we have

$$\begin{bmatrix} u_r^{(G)} \\ u_\theta^{(G)} \\ u_\phi^{(G)} \end{bmatrix} = \mathbf{M}_2 \, \mathbf{T} \, \mathbf{M}_1 \begin{bmatrix} u_r^{(S)} \\ u_\theta^{(S)} \\ u_\phi^{(S)} \end{bmatrix} \qquad \text{(V-1-4)}$$

If we define

$$\mathbf{M}(\theta,\phi) = \begin{bmatrix} \sin\theta\cos\phi & \cos\theta\cos\phi & -\sin\phi \\ \sin\theta\sin\phi & \cos\theta\sin\phi & \cos\phi \\ \cos\theta & -\sin\theta & 0 \end{bmatrix} \qquad \text{(V-1-5)}$$

then we have

$$\begin{cases} \mathbf{M}_1 = \mathbf{M}\left(\theta_A^{(S)}, \phi_A^{(S)}\right) \quad , \\ \\ \mathbf{M}_2 = \mathbf{M}^*\left(\theta_A^{(G)}, \phi_A^{(G)}\right) \quad . \end{cases} \tag{V-1-6}$$

Clearly the second one of these matrices can equally well be expressed in terms of the take-off angle τ_A . It is also evident that the radial component of displacement is left unchanged under the rotation of reference frame, so that (V-1-4) yields $u_r^{(G)} = u_r^{(S)}$.

In the far-field approximation, $u_r^{(G)}$ is the P-wave displacement, and is measured along the ray. Similarly $u_\theta^{(G)}$ is the SV displacement and $u_\phi^{(G)}$ the SH displacement, and these components are measured perpendicular to the ray, in two orthogonal directions. All the operations described above can be performed in the frequency domain on the various spectral components, which must obviously contain both amplitude and phase information.

Given the displacement on the focal sphere in the frequency domain, and given a layered Earth model for which the ray path can be calculated as a function of take-off angle, then the displacement spectrum at the emergence point B of the ray can be written as

$$\tilde{u}(B,\omega) = \mathscr{R}_{AB}(\omega) \bullet \tilde{u}(A,\omega) \quad . \tag{V-1-7}$$

Here $\mathscr{R}_{AB}(\omega)$ is the transfer function of the ray. It contains the integrated effects of both geometrical spreading and attenuation in each

layer (e.g., Julian and Anderson, 1968). Note that for the same take-off vector $\overrightarrow{OA}$ the rays are different for P and S waves, and also that longitudinal and shear waves undergo different attenuation, so that the transfer function must be defined for each ray and each component of displacement. Conversely, at fixed emergence point B , the record is composed of a number of body phases having each a different path in the Earth and a different take-off angle at the source. It must also be emphasized here that the transfer function is complex and that its phase contains both the phase shift as a function of distance for a travelling wave, and the phase shift due to attenuation (e.g., Futterman, 1962). Failure to take into account the phase shift due to attenuation in (V-1-7) would yield a non-causal signal at the receiver point B in the time domain.

Through equation (V-1-7) , one obtains the radial and/or transverse components of displacement along the ray at B . The spectra for the actual components of ground motion can be derived by the reflection and refraction coefficients at the free surface. They are obtained as solutions to the Zöppritz equations (e.g., Richter, 1958), and are given in Appendix 6. Further multiplication of the spectra by the transfer function of a chosen instrument and Fourier transformation into the time domain yields a theoretical seismogram. Each body phase can be treated separately in the same fashion, provided that the proper take-off angle and ray transfer function are used in each case.

Generalized ray theory may be applied in a similar fashion. In such a treatment, the source is handled via a "source-function," suitable for far-field representations (e.g., Burdick and Helmberger,

1973). Because a multipolar expansion does not represent in general a separable source, the source function is different for each generalized ray; and the radiation pattern effects cannot be represented by a simple multiplication factor. The simplest way to get the source function for a particular generalized ray is to compute the far-field approximation of the displacement (or of a potential) at some distance r_o from the source in the direction of the ray, and then divide it by $e^{-ik_\alpha r_o}/k_\alpha r_o$. The procedure is quite lengthy, however, and some attempts should be made to incorporate multipolar sources in the analytical theory of generalized rays.

An interesting aspect of the source problem which may be discussed in the frame of ray theory arises for shallow events (and, in particular, for underground explosions). As shown on figure V-1-2, the wave train observed at teleseismic distances will then be quite complicated as it will contain waves reflected from the free surface. Let us consider more particularly the P-wave train. For such a shallow source, it contains the direct P-wave, the reflected wave pP , and the converted wave sP . The time delays between these different phases may be derived from elementary geometrical arguments.

At high frequencies, for which the wave length is small compared to the depth h , three separate arrivals will be observed; in fact, the difference in arrival times provides a convenient measure of the focal depth (e.g., Richter, 1958). On the other hand, for long enough periods, the three waves will be essentially blended into one. Now, the incidence of pP upon the free surface is very nearly normal for

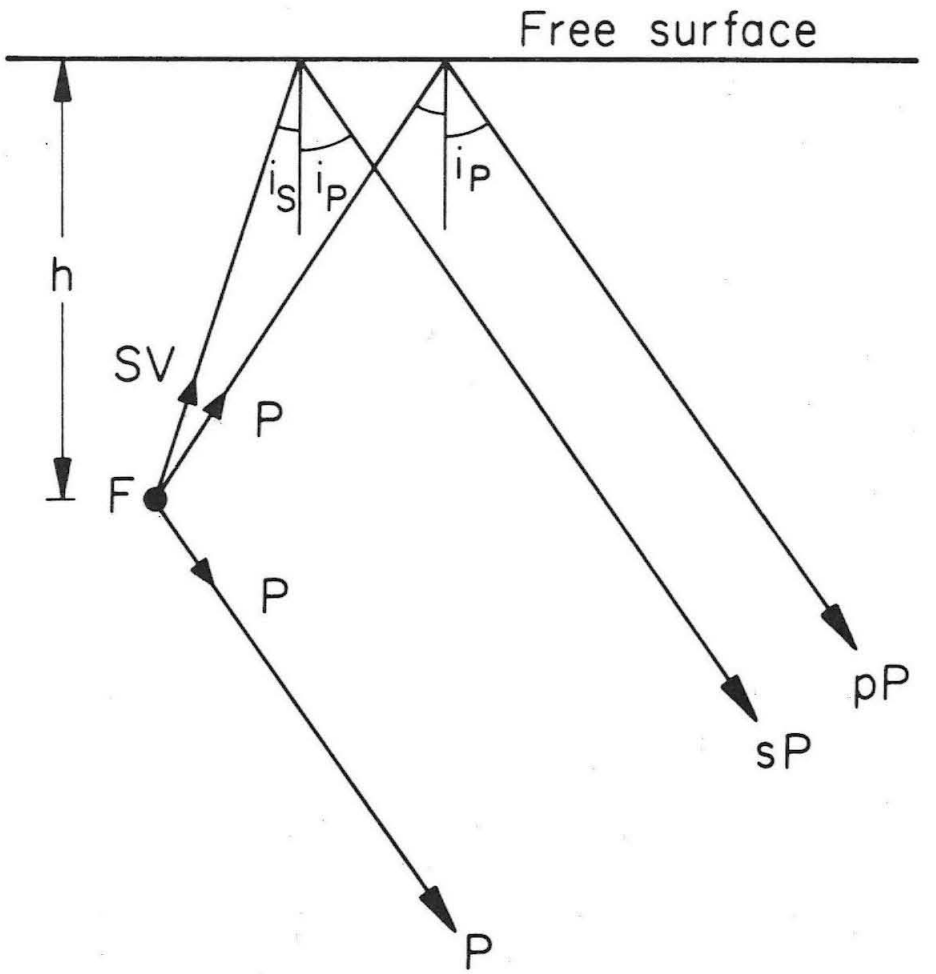

Figure V-1-2. Generation of pP and sP rays by interaction with a free surface. F is the focus, located at depth h .

teleseismic distances so that the reflection coefficient approaches -1 . If the radiation in the direction FP is comparable in amplitude and phase to the direct P radiation, then pP will nearly annihilate P at long periods. The long period spectral content of the first arrival train at teleseismic distances may then be controlled by sP , especially since the long-period amplitude is grossly an order of magnitude larger for the S-wave than for the P-wave.

We already know that the long-period radiation patterns for the various fields are quadrupole in nature. It is thus not difficult to see that the efficiency of the phenomenon will depend on the orientation of the quadrupole with respect to the free surface. In particular, the ray FQ to be considered on figure V-1-2 is an SV ray in the geographical frame and its radiation pattern is to be determined by taking into account the orientation of the rupture and that of the prestress through the methods described above. Thus for an underground nuclear explosion detonated in a highly sheared material, with a shear plane normal to the surface, the phenomenon can be very efficient (Archambeau, 1973, personal communication). On the other hand, the orientation of the focal mechanism for the San Fernando earthquake of 1971 is such that this phenomenon is unlikely to occur in that case (Hanks, 1973, personal communication). In fact, for this particular case, the ray FQ corresponds to a node of the SV radiation pattern.

Finally, let us recall that one can easily obtain the cartesian and cylindrical components of displacement from the spherical components. This is done in Appendix 7, and will not be repeated here.

The cylindrical components of displacement will also be given in section V-4, in the case where the potentials are given by cylindrical multipolar expansions.

The discussion presented in this section assumes essentially that ray theory is applicable; in other words, it breaks down in the vicinity of caustics and also at very long periods. Where ray theory is not valid, one must resort to other methods of solution of wave propagation problems (e.g., asymptotic ray theory, mode theory). Discussion of such questions lies beyond the scope of the present treatment.

V-2 Transformation of multipolar expansions under rotation of the coordinate system

As was pointed out in the introduction to this chapter, it is sometimes more convenient to manipulate the radiation fields described in Chapter IV in their multipolar form. This is true in particular when solving a wave propagation problem by use of the mode theoretic representation. For a propagating source (see Chapter IV) the natural spherical coordinate system to be used has a polar axis oriented along the direction of rupture propagation. But many wave propagation problems will be most easily solved in a spherical coordinate system with polar axis along the local vertical (e.g., Gilbert and Helmberger, 1972), or in a cylindrical coordinate system when use is made of a flat Earth approximation (e.g., Harkrider, 1970).

These circumstances raise the following question: knowing the multipolar representation of the radiation fields in a particular coordinate system, what is the equivalent representation in a new coordinate system, obtained by rotation of the first one? A solution to this problem was obtained by Y. Satô (1950). Unfortunately, Satô's solution is somewhat bulky and certainly cumbersome for use in numerical applications. In addition, the published solution suffers from numerous misprints and possibly some confusion in the definition of the Legendre associated functions (Hobson, 1931; Ferrers, 1877). Indeed, the product of two rotations inverse to each other will generally not yield the original multipolar expansion if Satô's results are used in their published form.

In this section we shall obtain a very simple solution as a direct

application of group theory. We shall use representations of the rotation group described by Gel'fand et al.(1963), and used by Burridge (1969) and Phinney and Burridge (1973). The notation used for ultraspherical functions is that of Gel'fand, and Jacobi polynomials will be introduced in the notation of Erdelyi (1953). Edmonds (1957) uses a similar approach to describe the transformation of angular momentum under finite rotations.

An arbitrary rotation of the coordinate system can be represented by three Euler angles $0 \leq \Phi_1 \leq 2\pi$, $0 \leq \Theta \leq \pi$, and $0 \leq \Phi_2 \leq 2\pi$. These angles are described on figure V-2-1 . We have used here Gel'fand's choice for the line of nodes (L) , that is, the new x-axis after the vertical rotation of angle Φ_1 . Edmonds uses the new y-axis . The expression of these Euler angles in terms of the usual "geological" fault orientation parameters--strike, dip, plunge--is derived in Appendix 7, and will not be reproduced here.

We call the original (source) system S , and the rotated (geographical) system G . Let r_s , ϕ_s , θ_s be the usual spherical coordinates in the system S , then from the results of Chapter IV, the multipolar expansion of a scalar potential of the radiation field is

$$\tilde{\chi}(r_s,\omega) = \sum_{n=0}^{\infty} h_n^{(2)}(kr_s) \sum_{m=0}^{n} \left[A_{nm}(\omega) \cos m\phi_s + B_{nm}(\omega) \sin m\phi_s \right] \cdot P_n^m(\cos \theta_s) \quad . \qquad (V\text{-}2\text{-}1)$$

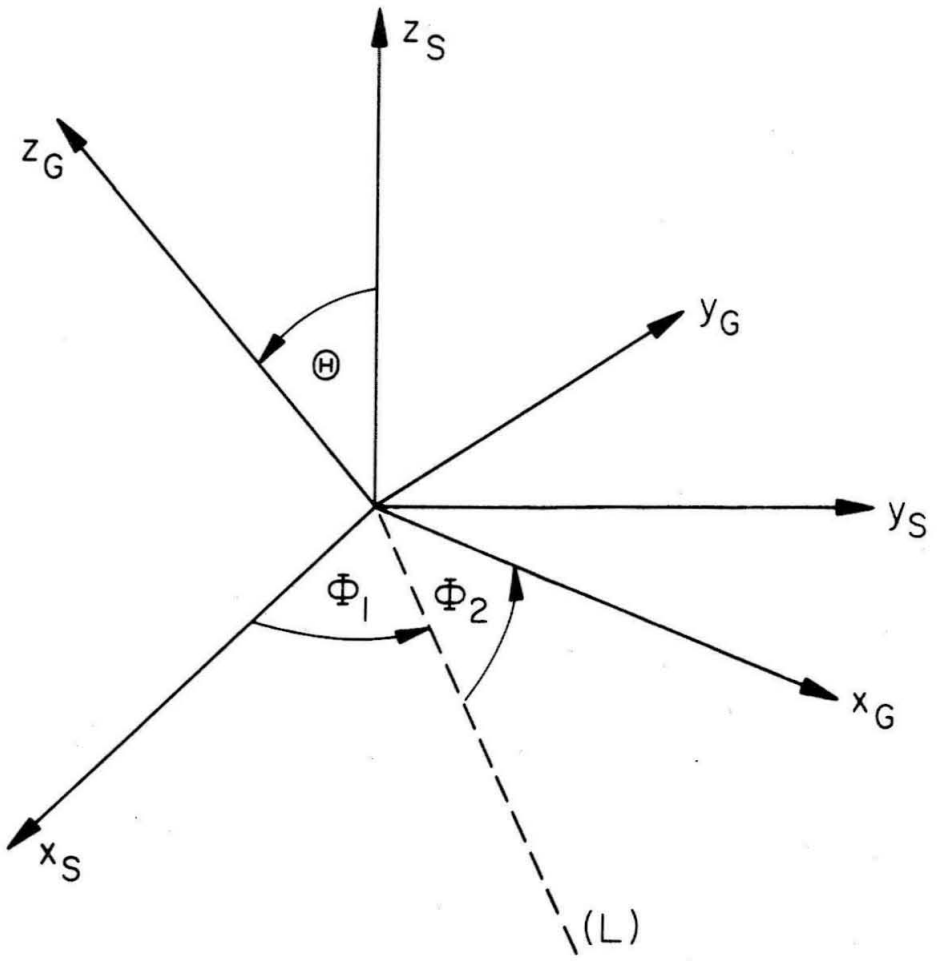

Figure V-2-1. Definition of Euler angles. The rotations of angles Φ_1 , Θ , Φ_2 , are performed successively. (L) is the line of nodes, axis of the rotation Θ .

Here $A_{nm}(\omega)$ and $B_{nm}(\omega)$ are the multipole coefficients. We can rewrite this expansion in the more convenient form

$$\tilde{\chi}(r_s,\omega) = \sum_{n=0}^{\infty} h_n^{(2)}(kr_s) \sum_{m=-n}^{n} A_m^n(\omega)\, Y_n^m(\theta_s,\phi_s) \quad , \tag{V-2-2}$$

where $Y_n^m(\theta_s,\phi_s)$ is the normalized spherical function given by

$$Y_n^m(\theta_s,\phi_s) = (-1)^m \sqrt{\frac{(n-m)!}{(n+m)!}}\ \sqrt{\frac{2n+1}{2}}\ \frac{1}{\sqrt{2\pi}}\, e^{im\phi_s}\, P_n^m(\cos\theta_s)$$

$$= \frac{(-1)^m}{\sqrt{2\pi}} e^{im\phi_s}\, \bar{P}_n^{\,m}(\cos\theta_s) \quad . \tag{V-2-3}$$

Here $\bar{P}_n^{\,m}(\mu)$ is the normalized associated Legendre function (e.g., Jahnke and Emde,[†] 1945), satisfying $\bar{P}_n^{\,-m}(\mu) = (-1)^m\, \bar{P}_n^{\,m}(\mu)$. Then the coefficients $A_m^n(\omega)$ are obtained by identification of (V-2-1) and (V-2-2) ; we get

---

[†] The definition of $P_n^{-m}(\mu)$ given by Jahnke and Emde (p. 114) can hardly be correct since it is in conflict, for $m = 0$, with the recursion relation given just below (cf. Appendix 5).

$$A_m^n(\omega) = \begin{cases} (-1)^m \sqrt{\frac{(n+m)!}{(n-m)!}} \sqrt{\frac{\pi}{2n+1}} (A_{nm} - iB_{nm}) & \text{for } m > 0 . \\ 2 \sqrt{\frac{\pi}{2n+1}} A_{no} & \text{for } m = 0 . \\ \sqrt{\frac{(n+|m|)!}{(n-|m|)!}} \sqrt{\frac{\pi}{2n+1}} (A_{n|m|} + iB_{n|m|}) & \text{for } m < 0 . \end{cases}$$

(V-2-4)

Let us now denote by $\mathbf{R}$ both the rotation transforming the system S into the system G, and the matrix representing this rotation in S. That is, the components in G of a vector $\mathbf{v}$ known in S are given by

$$v_i^{(G)} = R_{ik} v_k^{(S)} .$$

In particular, if $\hat{e}_i^{(S)}$, $\hat{e}_i^{(G)}$ are the basis vectors of S and G, then R_{ik} is the i^{th} component of $\hat{e}_k^{(S)}$ in the G system. By definition the functions $Y_n^m(\theta,\phi)$ form the canonical basis in the space of spherical functions of the n^{th} degree. In this space the rotation $\mathbf{R}$ is represented by an operator $\mathbf{T}_R$. In the canonical basis this operator is represented by an $n \times n$ matrix; we denote the (m,k) element of this matrix by T_n^{mk}, adopting the notation in use in the geophysical literature (Phinney and Burridge, 1973).

The inner product of two spherical functions, f and h, of

degree n , is defined by

$$< f,h > = \int_o^{2\pi} \int_o^{\pi} f(\theta,\phi)\ \overline{h}(\theta,\phi)\ \sin\theta\ d\theta\ d\phi \quad , \qquad \text{(V-2-5)}$$

where $\overline{h}(\theta,\phi)$ is the complex conjugate of $h(\theta,\phi)$. With respect to the inner product the transformation $\mathbf{T}_R$ is then unitary, that is

$$< \mathbf{T}_R f, \mathbf{T}_R h > = < f,h > \quad .$$

The analytical form of T_n^{mk} is derived by Gel'fand (1963); changing his notation slightly, we have

$$T_n^{mk} = e^{-im\Phi_2}\ \mathbf{P}_n^{mk}(\cos\ \Theta)\ e^{-ik\Phi_1} \quad , \qquad \text{(V-2-6)}$$

where the functions $\mathbf{P}_n^{mk}(\mu)$ are called generalized spherical functions by Gel'fand, and are related very closely to ultraspherical functions (Erdelyi, 1953); they are computed in Appendix 8 and are given below. Burridge (1969) and Phinney and Burridge (1973) make use of such functions to define generalized spherical harmonics. Since $\mathbf{T}_R$ is unitary, then $\sum_{m=-n}^{n} |\mathbf{P}_n^{mk}(\cos\ \Theta)|^2 = 1$ (Gel'fand, 1963).

Since (V-2-6) is the expression of T_n^{mk} in the canonical basis $Y_n^m(\theta,\phi)$, we can now operate with $\mathbf{T}_R$ on the expansion (V-2-2) to get

$$\tilde{\chi}(r_G,\omega) = \sum_{n+0}^{\infty} h_n^{(2)}(kr_G) \sum_{m=-n}^{n} G_m^n(\omega)\ Y_n^m(\theta_G,\phi_G) \quad , \qquad \text{(V-2-7)}$$

where

$$G_m^n(\omega) = \sum_{k=-n}^{n} \overline{T_n^{km}(\Phi_1,\Theta,\Phi_2)}\ A_k^n(\omega) \quad . \qquad \text{(V-2-8)}$$

To complete the transformation we rewrite (V-2-8) as

$$\tilde{\chi}(r_G,\omega) = \sum_{n=0}^{\infty} h_n^{(2)}(kr_G) \sum_{m=0}^{n} \left[C_{nm}(\omega) \cos m\phi_G + D_{nm}(\omega) \sin m\phi_G \right] \cdot P_n^m(\cos\theta_G) \quad . \qquad \text{(V-2-9)}$$

The new multipole coefficients are then given by

$$\begin{cases} C_{nm}(\omega) = \dfrac{(-1)^m}{2} \sqrt{\dfrac{(n-|m|)!}{(n+|m|)!}}\ \sqrt{\dfrac{2n+1}{\pi}} \left[G_m^n(\omega) + (-1)^m\, G_{-m}^n(\omega) \right] & \text{for } m > 0. \\ C_{no}(\omega) = \dfrac{1}{2}\ \sqrt{\dfrac{2n+1}{\pi}}\, G_o^n(\omega); \quad D_{no}(\omega) = 0 & \text{for } m = 0. \\ D_{nm}(\omega) = \dfrac{i(-1)^m}{2}\ \sqrt{\dfrac{(n-|m|)!}{(n+|m|)!}}\ \sqrt{\dfrac{2n+1}{\pi}} \left[G_m^n(\omega) - (-1)^m\, G_{-m}^n(\omega) \right] & \text{for } m > 0. \end{cases}$$

(V-2-10)

These coefficients are those of the multipolar expansion in the new coordinate system.

We still have to express the ultraspherical functions in closed form, in order to apply (V-2-6) . The derivation is made in Appendix 8, and the result is

$$P_n^{mk}(\mu) = (-i)^{\alpha}\, 2^{-n} \sqrt{\frac{s_+!\,s_-!}{t_+!\,t_-!}}(1-\mu)^{\alpha/2}(1+\mu)^{\beta/2}$$

$$\cdot \sum_{j=0}^{s_-} \binom{s_- + \alpha}{j} \binom{s_- + \beta}{s_- - j} (\mu-1)^{s_- - j} (\mu+1)^{j} \,, \qquad \text{(V-2-11)}$$

where the following definitions hold

$$\alpha = |m-k| \quad , \quad \beta = |m+k| \quad , \quad s_- = n - \tfrac{1}{2}(\alpha+\beta) \quad , \quad s_+ = n + \tfrac{1}{2}(\alpha+\beta)$$

$$t_- = n - \tfrac{1}{2}(\alpha-\beta) \quad , \quad t_+ = n + \tfrac{1}{2}(\alpha-\beta) \,.$$

All these quantities are integers. The formula (V-2-11) is then particularly easy to use since it is merely a polynomial. It yields good results, especially for low n . From the discussion in Chapter IV, we are rarely interested in computing more than a few multipoles, and (V-2-11) is more than adequate. For larger degrees and orders, Edmonds (1957) gives recursion relations which are easy to use. The reader should be cautioned, however, that Edmonds' choice of Euler angles is slightly different from ours .

The adaptation of Edmonds' results does not pose any major theoretical problem.

Because of the unitarity of the operator $\mathbf{T}_R$, the coefficients appearing in (V-2-8) correspond to the inverse rotation of Euler angles $\pi - \Phi_2$, Θ , and $\pi - \Phi_1$. In other words, we can write

$$\overline{T_n^{km}(\Phi_1,\Theta,\Phi_2)} = T_n^{mk}(\pi-\Phi_2,\Theta,\pi-\Phi_1) \quad . \tag{V-2-12}$$

That this property should be satisfied constitutes a useful check on numerical calculations. Another important check is that, for each n , the power should be conserved under rotation, that is

$$\sum_{m=-n}^{n} |A_m^n|^2 = \sum_{m=-n}^{n} |G_m^n|^2 \quad . \tag{V-2-13}$$

This result expresses the intuitive fact that the relative excitation of the various multipoles is unchanged by rotation of the coordinate system. This is not the case for a translation as we shall see in the next section.

V-3 Transformation of multipolar expansions under translation of the coordinate system

The necessity to be able to express a multipolar expansion in a new coordinate system obtained from the original one by pure translation arose in Chapter IV. This is particularly useful to study propagating ruptures, where the most convenient coordinate system is chosen according to the symmetry of the rupture zone, and moves along with the rupture. Then a fixed reference frame is needed to solve wave propagation problems.

The theorem needed for this purpose is an addition theorem for spherical waves. Satô (1950) proved such a theorem in the case of a translation along the polar axis. His results are given in the form of recursion relations which can be easily coded on a high speed numerical machine. A more general theorem was derived by Friedman and Russek (1954) for an arbitrary translation. Ben-Menahem (1962) used their results to obtain an elegant operational form for the theorem. Unfortunately, there is an error in Friedman and Russek's results, which is pointed out in Appendix 9. In this appendix, we derive the theorem in a general form, and show how it reduces to Miller's (1964) results for the case of standing waves. Miller attacked the problem from the point of view of group theory; we adapted the method of Friedman and Russek, and used some classical results of quantum mechanics given by Edmonds (1957).

Let S be the original system, and T the new system obtained by translation of vector $\mathbf{d} = (d,\theta_d,\phi_d)$. Then as in section V-2 we write

$$\tilde{\chi}(r_s,\omega) = \sum_{n=o}^{\infty} \sum_{m=-n}^{n} A_m^n(\omega)\, h_n^{(2)}(kr_s)\, Y_n^m(\theta_s,\phi_s) \quad , \qquad \text{(V-3-1)}$$

where the coefficients $A_m^n(\omega)$ are given by (V-2-4) . Because the general addition theorem is quite complicated and would lead to rather cumbersome algebra, and because we have seen in section V-2 how to operate a rotation of the coordinate system, we need only consider here a translation along the polar axis of S . In that case ϕ_d can be taken to be zero, and θ_d is 0 or π .

Then according to the results of Appendix 9, we have for $r_T > d$,

$$h_n^{(2)}(kr_s)\, Y_n^m(\theta_s,\phi_s) = \sum_{\nu=o}^{\infty} \sum_{\ell=|n-\nu|}^{n+\nu} C_1(\nu,\ell|n,m)$$

$$\cdot\, j_\nu(kd)\, h_\ell^{(2)}(kr_T)\, Y_\ell^m(\theta_T,\phi_s) \quad , \qquad \text{(V-3-2)}$$

with

$$C_1(\nu,\ell|n,m) = \varepsilon^\nu\, i^{\nu+\ell-n}(2\nu+1)(2\ell+1)^{1/2}(2n+1)^{-1/2}$$

$$\cdot\, (\ell\ \nu\ m\ 0 \mid n\ m)\ (\ell\ \nu\ 0\ 0 \mid n\ 0) \quad , \qquad \text{(V-3-3)}$$

where $\varepsilon = \cos\theta_d$ and we have used the fact that $\phi_T = \phi_s$. The coefficients appearing on the right-hand side of (V-3-3) are

Clebsch-Gordan coefficients. The coefficient C_1 vanishes unless $\ell+n+\nu$ is even, $m \leq \ell$, and $|\ell-n| \leq \nu \leq \ell+n$. Thus the inner sum is a finite one, and it is possible to interchange the order of summation and to reorder the terms so that

$$h_n^{(2)}(kr_s)\, Y_n^m(\theta_s,\phi_s) = \sum_{\ell=o}^{\infty} \sum_{\nu=|\ell-n|}^{\ell+n} C_1(\nu,\ell|n,m) \cdot j_\nu(kd)\, h_\ell^{(2)}(kr_T)\, Y_\ell^m(\theta_T,\phi_s) \ . \qquad \text{(V-3-4)}$$

We observe that the order m is left unchanged in such a translation. This makes the analysis much more tractable. The series (V-3-4) converges uniformly with respect to r_T provided that $r_T > d$. If we suppose that the series in (V-3-1) converges uniformly with respect to r_s in the same region, then by combining these two equations we can write

$$\tilde{\chi}(r_T,\omega) = \sum_{\ell=o}^{\infty} \sum_{m=-n}^{n} T_m^\ell(\omega)\, h_\ell^{(2)}(kr_T)\, Y_\ell^m(\theta_T,\phi_T) \ , \qquad \text{(V-3-5)}$$

and the new multipole coefficients are given by

$$T_m^\ell(\omega) = \sum_{n=o}^{\infty} \sum_{\nu=|\ell-n|}^{\ell+n} A_m^n(\omega)\, C_1(\nu,\ell|n,m)\, j_\nu(kd) \ . \qquad \text{(V-3-6)}$$

In Chapter IV, we encountered the case where only one value of n,

(n=2) , was present in the initial expansion (V-3-1) . In that case, there is no convergence problem since we have only a finite sum in (V-3-6) . For the case where $r_T < d$, the same analysis can be easily duplicated by interchanging the roles of $\mathbf{r}_T$ and $\mathbf{d}$ from the beginning (see Appendix 9).

It is clear that a translation does not preserve the power contained in a multipole of a given degree. This is intuitively understandable since a translation does not preserve spherical symmetry. In fact, if a pure double-couple source is expanded in the coordinate system satisfying its symmetry, the expansion will be a pure quadrupole. But if it is a shallow source and we want to expand it in a geocentric system, it is obvious that a large number of very high order multipoles will be necessary to represent it: When seen from the center of the Earth this source is very localized, and seems like a singularity at the surface.

V-4 Use of displacement potentials

The introduction of the dilatation $\Theta = \chi_4$, and of the rotation vector potential $\Omega = (\chi_1, \chi_2, \chi_3)$ was made essentially to reduce the elastodynamic problem to the solution of wave equations. We saw that these potentials may be given in terms of multipolar expansions such as

$$\tilde{\chi}_\alpha(r,\omega) = \sum_{n=0}^{\infty} \sum_{m=0}^{n} h_n^{(2)}(k_\alpha r) \left[A_{nm}^{(\alpha)} \cos m\phi + B_{nm}^{(\alpha)} \sin m\phi \right] P_n^m(\cos\theta). \qquad \text{(V-4-1)}$$

However, for wave propagating problems in plane stratified media (e.g., Ewing, Jardetsky and Press, 1957), one uses, in general, a cylindrical coordinate system with polar axis normal to the stratification. Let ρ , ϕ , z be the cylindrical coordinates, then, by using the results of Satô (1950), Archambeau (1964) and Harkrider and Archambeau (1973) show that the cylindrical multipolar expansion corresponding to (V-4-1) is

$$\tilde{\chi}_\alpha(\rho,\phi,z;\omega) = \sum_{n=0}^{\infty} \sum_{m=0}^{n} \left[A_{nm}^{(\alpha)'} \cos m\phi + B_{nm}^{(\alpha)'} \sin m\phi \right]$$

$$\cdot \int_0^{\infty} J_m(k\rho)\, \bar{P}_n^m(\nu_\alpha/k_\alpha)\, \frac{e^{-i\nu_\alpha |z|}}{\nu_\alpha}\, k\, dk \quad , \qquad \text{(V-4-2)}$$

where k is a wave number and where

$$\nu_\alpha = \begin{cases} \left(k_\alpha^2 - k^2\right)^{1/2} & \text{if } k < k_\alpha \ . \\ -i\left(k^2 - k_\alpha^2\right)^{1/2} & \text{if } k > k_\alpha \ . \end{cases} \qquad \text{(V-4-3)}$$

Here $\overline{P}_n^m$ denotes Hobson's definition of the associated Legendre functions and we have

$$P_n^m(\xi) = (1-\xi^2)^{m/2} \frac{d^m}{d\xi^m} P_n(\xi) \ ,$$

$$\overline{P}_n^m(\xi) = (\xi^2-1)^{m/2} \frac{d^m}{d\xi^m} P_n(\xi) \ .$$

Then the multipole coefficients appearing in (V-4-2) are given by

$$\begin{pmatrix} A_{nm}^{(\alpha)'} \\ B_{nm}^{(\alpha)'} \end{pmatrix} = \frac{(-1)^{2n+m} \, i^n}{k_\alpha} \left(\frac{z}{|z|}\right)^{m+n} \begin{pmatrix} A_{nm}^{(\alpha)} \\ B_{nm}^{(\alpha)} \end{pmatrix} \ . \qquad \text{(V-4-4)}$$

The displacement components in cylindrical coordinates are then derived by Archambeau (1964) and found to be

$$\tilde{u}_\rho = -\frac{1}{k_p^2}\frac{\partial\tilde{\chi}_4}{\partial\rho} + \frac{2}{\rho k_s^2}\left[\rho\sin\phi\,\frac{\partial\tilde{\chi}_1}{\partial z} - \rho\cos\phi\,\frac{\partial\tilde{\chi}_2}{\partial z} + \frac{\partial\tilde{\chi}_3}{\partial\phi}\right],$$

$$\tilde{u}_\phi = -\frac{1}{\rho k_p^2}\frac{\partial\tilde{\chi}_4}{\partial\phi} + \frac{2}{k_s^2}\left[\cos\phi\,\frac{\partial\tilde{\chi}_1}{\partial z} + \sin\phi\,\frac{\partial\tilde{\chi}_2}{\partial z} - \frac{\partial\tilde{\chi}_3}{\partial\rho}\right],$$

$$\tilde{u}_z = -\frac{1}{k_p^2}\frac{\partial\tilde{\chi}_4}{\partial z} + \frac{2}{\rho k_s^2}\left\{\left[\rho\sin\phi\,\frac{\partial}{\partial\rho} + \cos\phi\,\frac{\partial}{\partial\phi}\right]\tilde{\chi}_1 + \left[\rho\cos\phi\,\frac{\partial}{\partial\rho} + \sin\phi\,\frac{\partial}{\partial\phi}\right]\tilde{\chi}_2\right\}. \qquad \text{(V-4-5)}$$

On the other hand, wave propagation problems in layered media are best handled via the following implicitly defined displacement potentials (e.g., Harkrider, 1964)

$$\tilde{u}_\rho = \frac{\partial\tilde{\psi}_1}{\partial\rho} + \frac{\partial^2\tilde{\psi}_2}{\partial\rho\,\partial z} + \frac{1}{\rho}\frac{\partial\tilde{\psi}_3}{\partial\phi},$$

$$\tilde{u}_\phi = \frac{1}{\rho}\frac{\partial\tilde{\psi}_1}{\partial\phi} + \frac{1}{\rho}\frac{\partial^2\tilde{\psi}_2}{\partial z\,\partial\phi} - \frac{\partial\tilde{\psi}_3}{\partial\rho}, \qquad \text{(V-4-6)}$$

$$\tilde{u}_z = \frac{\partial\tilde{\psi}_1}{\partial z} + \frac{\partial^2\tilde{\psi}_2}{\partial z^2} + k_s^2\,\tilde{\psi}_2 = \frac{\partial\tilde{\psi}_1}{\partial z} + k^2\,\tilde{\psi}_2 .$$

Here (V-4-2) was used in the last equation. By simple identification of (V-4-5) and (V-4-6) one sees immediately that

$$\begin{cases} \tilde{\psi}_1 = -\dfrac{1}{k_p^2}\,\tilde{\chi}_4 \\ \\ \tilde{\psi}_3 = \dfrac{2}{k_s^2}\,\tilde{\chi}_3 \quad . \end{cases} \tag{V-4-7}$$

These potentials are called the dilatational and SH potentials respectively, and their multipolar expansions may be found trivially from (V-4-7). The SV potential $\tilde{\psi}_2$ may then be found by comparing the last equation in (V-4-6) and the last equation in (V-4-5); this yields

$$k^2\,\tilde{\psi}_2 = \frac{2}{k_s^2}\left[\frac{\partial\tilde{\chi}_2}{\partial x} - \frac{\partial\tilde{\chi}_1}{\partial y}\right] \quad . \tag{V-4-8}$$

Thus the SV displacement potential is, in fact--up to a multiplicative factor--the z component of the curl of the rotation vector potential $\boldsymbol{\Omega}$. This last relation will yield the multipolar expansion for $\tilde{\psi}_2$. The algebra may be found in Harkrider and Archambeau (1973), in the context of the generation of Rayleigh waves by a buried multipolar source in a layered medium.

It is clearly possible to develop a large number of possible applications for multipolar sources, but each application is best handled in the context of a specific problem and we shall limit our discussion to the brief description given above.

Conclusion

Each one of the four sections of this chapter has been concerned with a specific application of multipolar sources. Although the discussion was rather confined to specific operations, suitable combinations of these various operations provide us with a very flexible tool which should find numerous applications in seismology.

We want to emphasize again the generality of the types of sources considered here. Since no mention is made in this chapter of the specific physical nature of the source mechanism, it is clear that the methods presented above may be used to handle a broad range of different source models. These include separable and non-separable sources, explosions, earthquakes, any of the models discussed in Chapter II, as well as numerically modeled sources. The only constraint is that one should be able to find a multipolar expansion for the radiation field. This constraint may be a very stringent one for analytical models, but is not very severe for numerical models. Numerical models using finite difference or finite element techniques are mostly useful to perform the complex near-source calculations. The dynamic fields may then be computed at an array of points, and then expanded in multipoles by numerical integration and by use of the orthogonality properties of the various multipoles. Once the multipolar expansion is known, the methods described in this chapter can be used to study the propagation of the dynamic fields away from the source region.

Chapter VI

THE ELLIPSOIDAL RUPTURE

Introduction

The major properties of elastodynamic sources were described in Chapter IV on the basis of a rather simple geometry: that of a spherical rupture. We argued then that this model should be excellent for the case of underground explosions, and should exhibit most of the desired features to model adequately spontaneous phenomena such as earthquakes. Nevertheless, there is no question that a spherical geometry does not even approximate the geometry of the failure zone for shallow earthquakes; and, even for deep earthquakes, the idea of a spherical failure zone with a radius of several kilometers is somewhat disquieting. For that reason we shall attempt to investigate in this chapter the case of an ellipsoidal rupture zone. This does not invalidate the arguments and conclusions presented in Chapter IV. Instead, the results obtained for the spherical case will play a fundamental role insofar as they give us some insight into the problem, and therefore give us an idea of what results we should expect from the ellipsoidal model. This insight should in turn be of great help when we seek a convenient mathematical formulation of the results.

Archambeau (1964) made some attempts to solve the problem of an ellipsoidal elastodynamic source. However, his attack leads to rather inconvenient algebraic expressions, which lack symmetry. The main difficulty encountered is not theoretical since the theory presented in Chapter II does not require any assumptions about the geometry of the

problem. Rather, one is faced with the difficulty of having to manipulate extremely large algebraic equations. Another difficulty arises from the fact that the problem is to be solved by use of ellipsoidal coordinates, and that harmonic functions must therefore be expanded in terms of Lamé products. The literature is somewhat confusing on the subject of Lamé's equation. As pointed out by Arscott (1964), there are five different forms used for the equation itself, and there is no standard notation. We shall use the Jacobian form of the equation (e.g., Erdelyi, 1953). Most of the standard results concerning Lamé's equation and its solutions, as well as the Jacobi elliptic functions can be found in Erdelyi (1953), Whittaker and Watson (4th Edition, 1969), Arscott (1964). Additional references are Hobson (1931) and Jahnke and Emde (1945). The reader will find in the above references extensive bibliographies about the original research papers on the subject.

The problem of the static ellipsoidal inclusion in a stressed matrix was investigated by Eshelby (1957), who gives solutions valid immediately outside the ellipsoid, and also asymptotic solutions at large distances. Sadowsky and Sternberg (1949) determined the stress concentration around an arbitrary ellipsoidal cavity in the case where the principal stress directions at infinity coincide with the principal axes of the ellipsoid. Robinson (1951) extended their results to include the case of an elastic inhomogeneity under thermal stresses. These cases are not appropriate for our purposes, however, since one expects the material to fail under shear during an earthquake, so that the principal axes of the ellipsoid do not coincide with the principal

stress directions. Turnbull (1973) adapted Archambeau's (1964) method of solution to the case of an ellipsoidal cavity under shear. However, he does not use uniformized ellipsoidal coordinates, so that his solution holds only for problems with a large degree of symmetry. We shall give the solution for the case of an arbitrary, triaxial ellipsoidal elastic inclusion embedded in an infinite space, under a stress homogeneous at infinity, but with arbitrary relative orientation of the principal stress directions and the principal axes of the inclusion.

This represents a formidable algebraic problem and we shall not give all the details of the solution. However, a large number of useful relations between Jacobi elliptic functions will be given in Appendices. We shall also give a flow chart of the solution algorithm which will hopefully permit the interested reader to reconstruct the line of reasoning. The method is essentially the same as the one adopted by Sadowsky and Sternberg (1949) and the reader may find it helpful to read their publication beforehand, since they treat a simpler problem.

The dynamic problem is even more complicated. First of all, since we are in the presence of a volume source (see Chapter II) we should know the initial value fields at every point around the failure zone and we should also be able to perform a volume integration over the relaxation volume, just as in Chapter IV. In addition, in order to find a multipolar expansion of the source, one needs to expand the Green's function to the Helmholtz equation in wave functions. Very little is known about ellipsoidal wave functions (Arscott, 1964), so that the

most promising approach is to try and express both the static and dynamic solution in a spherical coordinate system. We have made little progress in that direction at this point, so that we shall confine ourselves to a description of possible methods of solution and to a discussion of the problems which are likely to arise.

In an effort to strike a reasonable middle ground between terseness and completeness, we shall confine the discussion to the minimum necessary for the solution of the problem at hand, but at the same time shall attempt to define each new quantity or symbol as it appears, without relying too heavily on the literature.

VI-1 Elastic fields associated with an elastic triaxial ellipsoidal inclusion

We consider in this section an arbitrary triaxial ellipsoidal inclusion, filled with elastic material, and embedded in an infinite homogeneous elastic matrix. The problem is to find the (static) elastic fields everywhere when an homogeneous stress field is applied at infinity, with arbitrary orientation relative to the inclusion.

Such a boundary value problem is much easier to solve if the boundary of the inclusion is a coordinate surface. Therefore, we shall use ellipsoidal coordinates (e.g., Sadowsky and Sternberg, 1949).

i) Ellipsoidal coordinates

Consider a cartesian system with axes along the principal axes of the ellipsoidal inclusion. In that frame the surface of the inclusion can be represented by the equation

$$\frac{x^2}{a^2} + \frac{y^2}{b^2} + \frac{z^2}{c^2} = 1 \quad , \tag{VI-1-1}$$

where a , b , c are the principal axes of the ellipsoid and we can assume, without loss of generality,

$$a > b > c > 0 \quad . \tag{VI-1-2}$$

Then the equation

$$\frac{x^2}{a^2+\theta} + \frac{y^2}{b^2+\theta} + \frac{z^2}{c^2+\theta} = 1 \qquad \text{(VI-1-3)}$$

represents a triply orthogonal family of confocal quadrics parameterized by θ . Thus the equation $\theta = \theta_o$ represents one of the following quadrics

if $-c^2 < \theta$	Ellipsoid ,
if $-b^2 < \theta < -c^2$	Hyperboloid of one sheet ,
if $-a^2 < \theta < -b^2$	Hyperboloid of two sheets,
if $\theta < -a^2$	Imaginary quadric .

The values $\theta = -a^2, -b^2, -c^2$ correspond to degenerate quadrics (e.g., cones, focal ellipse). If we solve (VI-1-3) for θ , we obtain a cubic equation, and for each point (x,y,z) <u>not belonging</u> to any of the degenerate quadrics , this equation always has three roots, one in each of the intervals described above (e.g., Hobson, 1931). Thus, through each point pass three mutually orthogonal quadrics, corresponding to $\theta = \theta_1, \theta_2, \theta_3$. The three roots in θ may be used as curvilinear coordinates. However, these roots can only be expressed in terms of x^2, y^2, z^2 , so that the eight apices of a cube centered at the origin and with edges parallel to the axes have the same curvilinear coordinates. In order to generate uniformized coordinates (e.g., Erdelyi, 1953) we define the following moduli

$$k^2 = \frac{a^2-b^2}{a^2-c^2} \quad , \quad k'^2 = \frac{b^2-c^2}{a^2-c^2} = 1 - k^2 \ ,$$

(VI-1-4)

$$0 < k,\ k' < 1 \ .$$

The quantities k and k' will be the modulus and complementary modulus of Jacobi elliptic functions and will be referred to in those terms hereafter.

Let us introduce the following shorthand notation for the Jacobi elliptic function of modulus k and argument ζ :

$$s_\zeta = sn(k,\zeta) \quad , \quad c_\zeta = sn(k,\zeta) \quad , \quad d_\zeta = dn(k,\zeta) \ .$$

(VI-1-5)

The properties of Jacobi elliptic functions are extensively discussed by Whittaker and Watson (1927) , the most important one being their periodicity. If we define

$$K = \int_0^1 (1-t^2)^{-1/2} \ (1-k^2t^2)^{-1/2} \ dt \qquad \text{(VI-1-6)}$$

and K' in a similar fashion, then

s_ζ	has periods	$4K$	,	$2iK'$	,	$4K+4iK'$.
c_ζ	has periods	$4K$	,	$4iK'$	,	$2K+2iK'$.
d_ζ	has periods	$2K$	,	$4iK'$	,	$4K+4iK'$.

We can now define the three coordinates α, β, γ implicitly by (e.g., Erdelyi, 1953).

$$\begin{cases} \theta_1 = -(ac_\alpha)^2 - (bs_\alpha)^2, \\ \theta_2 = -(ac_\beta)^2 - (bs_\beta)^2, \\ \theta_3 = -(ac_\gamma)^2 - (bs_\gamma)^2 . \end{cases}$$

These relations are invertible, and one can in fact establish the following correspondence (e.g., Sadowsky and Sternberg, 1949)

$$\begin{cases} x = km\, s_\alpha s_\beta s_\gamma , \\ y = -\frac{km}{k'}\, c_\alpha c_\beta c_\gamma , \\ z = \frac{im}{kk'}\, d_\alpha d_\beta d_\gamma . \end{cases} \qquad \text{(VI-1-7)}$$

where $m = (a^2-b^2)^{1/2}$.

These equations establish a one-to-one mapping between the triplets (x,y,z) and (α,β,γ) . α,β,γ are the uniformized ellipsoidal curvilinear coordinates that we shall use throughout this chapter. Because of the periodicity of the Jacobi elliptic functions we can restrict their range to

$$\begin{cases} iK' < \alpha < K+iK' , \\ K < \beta < K+2iK' , \\ 0 < \gamma < 4K . \end{cases}$$

Furthermore the first octant corresponds to the range

$$\begin{cases} iK' < \alpha < K+iK' , \\ K < \beta < K+iK' , \\ 0 < \gamma < K . \end{cases}$$

The quadrics at constant α are confocal ellipsoids. We shall define the boundary of the inclusion by $\alpha = \alpha_o$. Note that the value $\alpha = K+iK'$ represents the focal ellipse. Similarly the limiting values for β and γ represent degenerate quadrics. By analogy with spherical coordinates α represents the radial coordinate, β the latitudinal one, and γ the longitudinal one.

If we define the square of the differential arc length by

$$ds^2 = \left(\frac{d\alpha}{h_\alpha}\right)^2 + \left(\frac{d\beta}{h_\beta}\right)^2 + \left(\frac{d\gamma}{h_\gamma}\right)^2 , \qquad \text{(VI-1-8)}$$

then the metric coefficients are given by

$$h_\alpha = \frac{1}{km\ q_\beta q_\gamma} \quad ; \quad h_\beta = \frac{i}{km\ q_\alpha q_\gamma} \quad ; \quad h_\gamma = \frac{-1}{km\ q_\alpha q_\beta} , \qquad \text{(VI-1-9)}$$

where

$$q_\alpha = \left(s_\beta^2 - s_\gamma^2\right)^{1/2} \quad ; \quad q_\beta = \left(s_\alpha^2 - s_\gamma^2\right)^{1/2} \quad ; \quad q_\gamma = \left(s_\alpha^2 - s_\beta^2\right)^{1/2} . \qquad \text{(VI-1-10)}$$

The angle between the unit vectors $\hat{\alpha}$ and $\hat{x}$ is given by

$$\cos(\alpha,x) = h_\alpha \frac{\partial x}{\partial \alpha} = \frac{1}{h_\alpha} \frac{\partial \alpha}{\partial x} \quad . \tag{VI-1-11}$$

Similarly the gradient operator is given by

$$\nabla = \left[h_\alpha \frac{\partial}{\partial \alpha} \, , \, h_\beta \frac{\partial}{\partial \beta} \, , \, h_\gamma \frac{\partial}{\partial \gamma} \right] \, . \tag{VI-1-12}$$

We shall also make use of similar formulae valid for orthogonal curvilinear coordinates. Such formulae are given, for example, by Morse and Feshbach (1953).

ii) Potential solutions to the equation of equilibrium

We are seeking solutions of the elastic equations of equilibrium

$$\nabla^2 \mathbf{u} + \frac{1}{1-2\sigma} \nabla(\nabla \cdot \mathbf{u}) = 0 \quad , \tag{VI-1-13}$$

such that $|\mathbf{u}| = 0(r^\alpha)$ at large distances, with $\alpha \leq -2$ (e.g., Archambeau, 1964). Here σ represents the Poisson ratio of the elastic medium. We shall use the general solution of Boussinesq

$$2\mu \, \mathbf{u} = \nabla(\phi + \mathbf{r} \cdot \boldsymbol{\omega}) - 4(1-\sigma)\boldsymbol{\omega} \quad , \tag{VI-1-14a}$$

where the scalar potential ϕ , and the cartesian components

ω_x ,ω_y and ω_z of the vector potential $\boldsymbol{\omega}$ are all harmonic functions. Following Sadowsky and Sternberg, we seek the solution as a superposition of elementary solutions of the four types

	ϕ	ω_x	ω_y	ω_z
1)	W	0	0	0
2)	0	X	0	0
3)	0	0	Y	0
4)	0	0	0	Z

(VI-1-14b)

If we write Laplace's equation in the form

$$\frac{\Delta U}{kmh_\alpha h_\beta h_\gamma} = \left[q_\alpha^2 \frac{\partial^2}{\partial \alpha^2} + q_\beta^2 \frac{\partial^2}{\partial \beta^2} + q_\gamma^2 \frac{\partial^2}{\partial \gamma^2} \right] U = 0 \quad ,$$

and look for normal solutions of the form

$$U(\alpha,\beta,\gamma) = A(\alpha)\ B(\beta)\ C(\gamma) \quad , \qquad \text{(VI-1-15)}$$

then, by the usual method of separation of variables, we find that A, B, and C all satisfy Lamé's equation. In Jacobian form, this equation reads

$$\frac{d^2\Lambda(z)}{dz^2} - \left[n(n+1)\ k^2 s_z^2 - h \right] \Lambda(z) = 0 \quad , \qquad \text{(VI-1-16)}$$

where n and h are separation constants. Discussion of the properties and periodicities of the solutions of this equation can be found, for example, in Arscott (1964). Without entering into the details, let us note that if n is a non-negative integer, there are $2n+1$ values of h for which (VI-1-16) admits solutions with periods $4K$ and $4iK'$. We shall also call them Lamé functions of the first kind, and of degree n. Let $\lambda(z)$ be such a function. If $B(\beta)$ and $C(\gamma)$ both are Lamé functions of the first kind, their product will be called an ellipsoidal surface harmonic.

If $A(\alpha)$ is also a Lamé function of the first kind, then the Lamé product (VI-1-15) is regular inside any ellipsoid $\alpha = \alpha_o$, and is called an ellipsoidal internal harmonic. Lamé products which are regular outside $\alpha = \alpha_o$ are called ellipsoidal external harmonics. In such a case $A(\alpha)$ must be a Lamé function of the second kind, defined by the integral relation

$$\Lambda_n(z) = W_\lambda \, \lambda_n(z) \int_{iK'}^{z} \frac{du}{\left(\lambda_n(z)\right)^2} \quad , \qquad \text{(VI-1-17)}$$

so that it vanishes at infinity.

In the future we shall denote the Lamé functions of the first kind by lower case symbols, and the Lamé functions of the second kind by capital letters. Note that if we choose the normalization factor W_λ to be

$$W_\lambda = \left[\int_{iK'}^{\alpha_o} \frac{du}{\left(\lambda_n(z)\right)^2} \right]^{-1} \quad , \qquad \text{(VI-1-18)}$$

then we have

$$\Lambda_n(\alpha_o) = \lambda_n(\alpha_o) \quad . \tag{VI-1-19}$$

Furthermore, it is easy to show that, in that case

$$W_\lambda = \Lambda_n'(\alpha_o)\ \lambda_n(\alpha_o) - \Lambda_n(\alpha_o)\ \lambda_n'(\alpha_o) \quad , \tag{VI-1-20}$$

so that, for this particular normalization, W_λ is the wronskian of Λ_n and λ_n, computed at α_o. We shall always assume this to be the case in the future.

The ellipsoidal harmonics possess completeness and orthogonality properties similar to those of the spherical harmonics. In particular, functions defined on the surface of an ellipsoid may be expanded in ellipsoidal surface harmonics; functions defined and regular inside the ellipsoid may be expanded in ellipsoidal internal harmonics; and functions defined and regular outside may be expanded in ellipsoidal external harmonics.

iii) Displacements and stresses in ellipsoidal coordinates

The elastic fields inside the ellipsoidal inclusion will be sought in the form of a superposition of elementary solutions of the type (VI-1-14), and the harmonic potentials will then be expanded in ellipsoidal internal harmonics. Similarly, following Sadowsky and Sternberg (1949) we shall obtain the fields outside the inclusion by

extending the fields at infinity everywhere, and then superposing elementary solutions (VI-1-14) where external harmonics are then used.

The boundary conditions to be met are as follows: The external fields should match the applied fields at infinity, and there should be continuity of the displacements and the tractions on the surface of the inclusion $\alpha = \alpha_o$. This assumes that the inclusion does not generate any intrinsic fields and is consistent with the discussion of Chapter II.

Let $\tau^{(o)}_{xx}$,..., $\tau^{(o)}_{zx}$ be the cartesian components of the homogeneous stress applied at infinity. Then the ellipsoidal components of the stress field--which we shall call the "prestress"--are given by (Love, 1927)

$$\tau^{(o)}_{\alpha\alpha} = \ell_\alpha^2 \tau^{(o)}_{xx} + m_\alpha^2 \tau^{(o)}_{yy} + n_\alpha^2 \tau^{(o)}_{zz} + 2m_\alpha n_\alpha \tau^{(o)}_{yz} +$$

$$2n_\alpha \ell_\alpha \tau^{(o)}_{zx} + 2\ell_\alpha m_\alpha \tau^{(o)}_{xy} \quad ,$$

$$\tau^{(o)}_{\alpha\beta} = \ell_\alpha \ell_\beta \tau^{(o)}_{xx} + m_\alpha m_\beta \tau^{(o)}_{yy} + n_\alpha n_\beta \tau^{(o)}_{zz}$$

$$+ (m_\alpha n_\beta + n_\alpha m_\beta) \tau^{(o)}_{zy} + (n_\alpha \ell_\beta + \ell_\alpha n_\beta) \tau^{(o)}_{zx}$$

$$+ (m_\alpha \ell_\beta + m_\beta \ell_\alpha) \tau^{(o)}_{xy} \quad , \qquad \text{(VI-1-21)}$$

and the other components are obtained by circular permutation of the indices $\alpha\ \beta\ \gamma$. The direction cosines ℓ_α , ℓ_β ,...etc., are given by

$$\ell_\alpha = \frac{c_\alpha d_\alpha s_\beta s_\gamma}{q_\beta q_\gamma} \quad ; \quad \ell_\beta = \frac{i s_\alpha c_\beta d_\beta s_\gamma}{q_\gamma q_\alpha} \quad ; \quad \ell_\gamma = \frac{-s_\alpha s_\beta c_\gamma d_\gamma}{q_\alpha q_\beta}$$

$$m_\alpha = \frac{s_\alpha d_\alpha c_\beta c_\gamma}{k' q_\beta q_\gamma} \quad ; \quad m_\beta = \frac{i c_\alpha s_\beta d_\beta c_\gamma}{k' q_\gamma q_\alpha} \quad ; \quad m_\gamma = \frac{-c_\alpha c_\beta s_\gamma d_\gamma}{k' q_\alpha q_\beta}$$

$$n_\alpha = \frac{-i s_\alpha c_\alpha d_\beta d_\gamma}{k' q_\beta q_\gamma} \quad ; \quad n_\beta = \frac{d_\alpha s_\beta c_\beta d_\gamma}{k' q_\gamma q_\alpha} \quad ; \quad n_\gamma = \frac{i d_\alpha d_\beta s_\gamma c_\gamma}{k' q_\alpha q_\beta} \quad .$$

(VI-1-22)

Similarly, by simple integration, the displacement associated with the prestress is, up to a rigid body displacement

$$u_x^{(o)} = \left[\frac{\tau_{xx}^{(o)}}{2\mu} - \frac{\sigma\left(\tau_{xx}^{(o)} + \tau_{yy}^{(o)} + \tau_{zz}^{(o)}\right)}{2\mu(1+\sigma)} \right] x + \frac{\tau_{xy}^{(o)}}{2\mu} y + \frac{\tau_{xz}^{(o)}}{2\mu} z \qquad \text{(VI-1-23)}$$

and similar expressions hold for $u_y^{(o)}$ and $u_z^{(o)}$. The ellipsoidal components are then

$$\begin{cases} u_\alpha^{(o)} = \ell_\alpha u_x^{(o)} + m_\alpha u_y^{(o)} + n_\alpha u_z^{(o)} \\ u_\beta^{(o)} = \ell_\beta u_x^{(o)} + m_\beta u_y^{(o)} + n_\beta u_z^{(o)} \\ u_\gamma^{(o)} = \ell_\gamma u_x^{(o)} + m_\gamma u_y^{(o)} + n_\gamma u_z^{(o)} \quad . \end{cases} \qquad \text{(VI-1-24)}$$

Equations (VI-1-21) and (VI-1-24) allows us to express the fields that would be present in the absence of any inclusion, in terms of ellipsoidal coordinates.

We also need to be able to compute the various fields associated with the four types of elementary solutions (VI-1-14b) .

a) Solutions of the first kind

Then, with reference to (VI-1-14) we have $\phi = W$, $\omega = 0$ and

$$2\mu\, u_\alpha = h_\alpha \frac{\partial W}{\partial \alpha} \quad . \tag{VI-1-25}$$

u_β and u_γ are obtained by cyclic permutation of the indices. The stress is obtained by use of the general expressions valid in arbitrary curvilinear coordinates (Love, 1927). Sadowsky and Sternberg (1949) give the following expressions

$$\left\{ \begin{array}{l} \tau_{\alpha\alpha} = h_\alpha^2 \dfrac{\partial^2 W}{\partial \alpha^2} + h_\alpha \dfrac{\partial h_\alpha}{\partial \alpha} \dfrac{\partial W}{\partial \alpha} - \dfrac{h_\beta^2}{h_\alpha} \dfrac{\partial h_\alpha}{\partial \beta} \dfrac{\partial W}{\partial \beta} - \dfrac{h_\gamma^2}{h_\alpha} \dfrac{\partial h_\alpha}{\partial \gamma} \dfrac{\partial W}{\partial \gamma} \quad , \\ \\ \tau_{\beta\alpha} = h_\beta h_\gamma \dfrac{\partial^2 W}{\partial \gamma \partial \beta} + h_\gamma \dfrac{\partial h_\beta}{\partial \gamma} \dfrac{\partial W}{\partial \beta} + h_\beta \dfrac{\partial h_\gamma}{\partial \beta} \dfrac{\partial W}{\partial \gamma} \quad . \end{array} \right. \tag{VI-1-26}$$

and the other components are obtained by cyclic permutations of α, β, γ .

b) Solution of the second, third and fourth kind

In that case $\phi = 0$, and $\boldsymbol{\omega} = X\hat{\mathbf{x}}$, for example, then we have

$$2\mu\, u_\alpha = h_\alpha \left[x \frac{\partial X}{\partial \alpha} - (3-4\nu) \frac{\partial x}{\partial \alpha} X \right] . \qquad \text{(VI-1-27)}$$

The other components are obtained by replacing α by β or γ ; the components for solutions of the third and fourth kind are obtained in a similar fashion, by replacing the couple (x,X) by (y,Y) or (z,Z) respectively (note that x, y, z, are given by (VI-1-7)). The stress components have been computed by Sadowsky and Sternberg (1949) and are

$$\tau_{\alpha\alpha} = h_\alpha^2 \, x \frac{\partial^2 X}{\partial \alpha^2} + \left[h_\alpha \frac{\partial h_\alpha}{\partial \alpha} x - 2h_\alpha^2 \frac{\partial x}{\partial \alpha} \right] \frac{\partial X}{\partial \alpha}$$

$$- \frac{h_\beta^2}{h_\alpha} \frac{\partial h_\alpha}{\partial \beta} x \frac{\partial X}{\partial \beta} - \frac{h_\gamma^2}{h_\alpha} \frac{\partial h_\alpha}{\partial \gamma} x \frac{\partial X}{\partial \gamma}$$

$$+ 2\nu \left[h_\alpha^2 \frac{\partial x}{\partial \alpha} \frac{\partial X}{\partial \alpha} - h_\beta^2 \frac{\partial x}{\partial \beta} \frac{\partial X}{\partial \beta} - h_\gamma^2 \frac{\partial x}{\partial \gamma} \frac{\partial X}{\partial \gamma} \right] .$$

$$\tau_{\beta\gamma} = h_\beta h_\gamma \frac{\partial^2 X}{\partial \beta \partial \gamma} + \left[h_\beta \frac{\partial h_\alpha}{\partial \beta} \frac{\partial X}{\partial \gamma} + h_\gamma \frac{\partial h_\beta}{\partial \gamma} \frac{\partial X}{\partial \beta} \right] x$$

$$- (1-2\nu)\, h_\beta h_\gamma \left[\frac{\partial x}{\partial \gamma} \frac{\partial X}{\partial \beta} + \frac{\partial x}{\partial \beta} \frac{\partial X}{\partial \gamma} \right] .$$

(VI-1-28)

Again, the other stress components, and those for solutions of the third and fourth kind are obtained through suitable cyclic permutations of (α,β,γ) , (x,y,z) and (X,Y,Z) .

iv) Formulation of the problem

We are now in a position to replace the potentials W, X, Y, Z by suitable Lamé products. First of all, by careful comparison of the prestress field (VI-1-21) and the solutions (VI-1-26) and (VI-1-28) as well as the associated displacements, it can be shown that only Lamé functions of degree 0, 1, 2 are to be used. This is consistent with the results obtained in the spherical case (see section IV-1). These Lamé functions are, in the notation of Erdelyi (1953)

$$Ec_0^0 = 1 \quad ; \quad Ec_1^0 = d_z \quad ; \quad Ec_1^1 = s_z \quad ; \quad Es_1^1 = c_z$$

$$Ec_2^0 = s_z^2 - P_1 = \ell_z \quad ; \quad Ec_2^1 = s_z d_z = m_z \quad ; \quad Ec_2^2 = s_z^2 - P_2 = n_z$$

$$Es_2^1 = c_z d_z = o_z \quad ; \quad Es_2^2 = s_z c_z = p_z \quad . \qquad \text{(VI-1-29)}$$

where we define our own simplifying notation. Here P_1 and P_2 are constants given by

$$P_1 = \frac{1}{1+k^2-\sqrt{1-k^2k'^2}} \quad ; \quad P_2 = \frac{1}{1+k^2+\sqrt{1-k^2k'^2}} \quad . \qquad \text{(VI-1-30)}$$

Functions of the type Ec_n^m are even functions of $z - K$, and functions of the type Es_n^m are odd functions of $z - K$, where K is given by (VI-1-6) . Further properties of these functions can be found in Arscott (1964) or Erdelyi (1953) . We shall use below the notation defined in (VI-1-29) which will considerably simplify the algebra. Note that the symbols ℓ_z, m_z, n_z have been redefined in (VI-1-29). There is little danger of confusion with the direction cosines (VI-1-22) since these direction cosines will not be used again.

The solutions (VI-1-26) and (VI-1-28) should also exhibit the same periodicities and symmetries as the prestress (VI-1-21) (e.g., Sadowsky and Sternberg, 1949). A systematic, but lengthy survey of all symmetries of the Lamé functions reveals that because of the arbitrary relative orientation of the prestress and the inclusion, the only helpful symmetry is the following

$$(x,y,z) \longrightarrow (-x,-y,-z)$$

$$\gamma \to \gamma + 2K \quad ; \quad \beta \to 2K + 2iK' - \beta \quad ,$$

and then

$$\tau_{\alpha\alpha} \to \tau_{\alpha\alpha} \quad ; \quad \tau_{\beta\beta} \to \tau_{\beta\beta} \quad ; \quad \tau_{\gamma\gamma} \to \tau_{\gamma\gamma}$$

$$\tau_{\alpha\beta} \to - \tau_{\alpha\beta} \quad ; \quad \tau_{\alpha\gamma} \to \tau_{\alpha\gamma} \quad ; \quad \tau_{\beta\gamma} \to - \tau_{\beta\gamma} \ .$$

Using this symmetry, we find that the only Lamé products which are acceptable for the various potentials are the following:

a) For W , (m^2 is a convenient homogeneity factor)

Internal harmonics	External harmonics	Solution number
m^2	$m^2\alpha$	1
$m^2\ell_\alpha\ell_\beta\ell_\gamma$	$m^2L_\alpha\ell_\beta\ell_\gamma$	11
$m^2m_\alpha m_\beta m_\gamma$	$m^2M_\alpha m_\beta m_\gamma$	12
$m^2n_\alpha n_\beta n_\gamma$	$m^2N_\alpha n_\beta n_\gamma$	13
$m^2o_\alpha o_\beta o_\gamma$	$m^2O_\alpha o_\beta o_\gamma$	14
$m^2p_\alpha p_\beta p_\gamma$	$m^2P_\gamma p_\beta p_\gamma$	15

b) For X, Y, Z , (m is a convenient homogeneity factor)

Internal harmonics	External harmonics	Solution number		
		X	Y	Z
$md_\alpha d_\beta d_\gamma$	$mD_\alpha d_\beta d_\gamma$	2	5	8
$ms_\alpha s_\beta s_\gamma$	$mS_\alpha s_\beta s_\gamma$	3	6	9
$mc_\alpha c_\beta c_\gamma$	$mC_\alpha c_\beta c_\gamma$	4	7	10

We are therefore in the presence of 30 elementary solutions (15 external solutions and 15 internal solutions). If $\tau^{(N)}$ and $u^{(N)}$, N = 1,...,15 indicate the 15 external stress and displacement solutions, and $\sigma^{(N)}$

and $v^{(N)}$, N = 1,...,15 , indicate the 15 internal solutions, then the boundary conditions--continuity of tractions and displacements--on the boundary $\alpha = \alpha_o$ may be written as

$$\left\{\begin{array}{l}
\tau_{\alpha\alpha}^{(o)} + \sum_{N=1}^{15} A_N \tau_{\alpha\alpha}^{(N)} = \sum_{N=1}^{15} B_N \sigma_{\alpha\alpha}^{(N)} \quad , \\
\tau_{\alpha\beta}^{(o)} + \sum_{N=1}^{15} A_N \tau_{\alpha\beta}^{(N)} = \sum_{N=1}^{15} B_N \sigma_{\alpha\beta}^{(N)} \quad , \\
\tau_{\alpha\gamma}^{(o)} + \sum_{N=1}^{15} A_N \tau_{\alpha\gamma}^{(N)} = \sum_{N=1}^{15} B_N \sigma_{\alpha\gamma}^{(N)} \quad , \\
u_{\alpha}^{(o)} + \sum_{N=1}^{15} A_N u_{\alpha}^{(N)} = \sum_{N=1}^{15} B_N v_{\alpha}^{(N)} \quad , \\
u_{\beta}^{(o)} + \sum_{N=1}^{15} A_N u_{\beta}^{(N)} = \sum_{N=1}^{15} B_N v_{\beta}^{(N)} \quad , \\
u_{\gamma}^{(o)} + \sum_{N=1}^{15} A_N u_{\gamma}^{(N)} = \sum_{N=1}^{15} B_N v_{\gamma}^{(N)} \quad .
\end{array}\right. \qquad \text{(VI-1-31)}$$

These equations must be identically satisfied in β and γ for $\alpha = \alpha_o$.

v) Reduction of the system

The system (VI-1-31) possesses 30 unknowns. This number is immediately reduced to 29 if one notices that the internal elementary solution associated with the coefficient B_1 is identically zero. Thus $B_1 = 0$. The system (VI-1-31) must be satisfied identically in β and γ for $\alpha = \alpha_o$. This means that each independent function of β and γ appearing on both sides of each boundary condition equation gives rise to a separate equation, obtained by equating its coefficient on the left-hand side with its coefficient on the right-hand side.

The developed forms of these equations are given in Appendix 11. The necessary identities to reduce these equations and the list of independent functional dependences on β and γ emerging in (VI-1-31) are given in Appendix 12. One obtains a redundant system of 39 equations for 29 unknowns, which is extremely lengthy to write, but does not present any fundamental difficulty. This system is compatible and separates very conveniently into four subsystems, as described in Appendix 12. Some of the elementary solutions proposed above are found to be linearly dependent on the others. Thus coefficients B_{11} , B_{12} , B_{13} , B_{14} , B_{15} are found to vanish. We get three systems of five equations and five unknowns, corresponding each to a pure shear loading at infinity. There is a separate system for each of the components $\tau_{zx}^{(o)}$, $\tau_{xy}^{(o)}$, $\tau_{yz}^{(o)}$. In addition, we obtain a system of nine equations and nine unknowns, where the only prestress components appearing are the diagonal components. These systems are given below in matrix form. The constants σ and μ are the Poisson ratio and the

rigidity of the matrix, respectively, σ' and μ' are those of the inclusion. All the functions of α appearing in these equations, including the wronskians such as W_s, are to be evaluated at $\alpha = \alpha_o$. For simplicity, we have defined the function $\Pi_\alpha = s_\alpha c_\alpha d_\alpha$ in these systems. In the case where the inclusion should be filled with a liquid, the systems are greatly simplified. For a pure shear prestress, a liquid inclusion behaves to first order as a cavity, since we did not take into account the perturbation of the boundary. For the diagonal stress components, the fluid pressure can be taken into account very easily by introducing it on the right-hand side of (VI-1-35) below. In the case where the inclusion is in fact a cavity, no internal solution should be present and the coefficients B_i, $i=1,\ldots,15$ all vanish. However, when we have a liquid inclusion, the system is reduced by application of the following rules:

a) Expressions of the form $(1-\sigma')/\mu'$ are unbounded and the corresponding coefficient must accordingly be set to zero.

b) Expressions of the form $(1-2\sigma')/\mu'$ must simply be replaced by their limiting value as $\mu' \to 0$ and $\sigma' \to 1/2$, which is $1/\lambda'$ where λ' is the bulk modulus of the liquid.

These rules are easily applied below.

$$
\begin{bmatrix}
W_d & k^2 W_s & 0 & 0 & 0 \\
s_\alpha^2 W_d & d_\alpha^2 W_s & W_m & 0 & 0 \\
(1-\sigma)W_d & -k^2(1-\sigma)W_s & k^2\Pi_\alpha & k^2(1-2\sigma')\Pi_\alpha & k^2(1-2\sigma')\Pi_\alpha \\
-k^2(1-2\sigma)\Pi_\alpha & -k^2(1-2\sigma)\Pi_\alpha & & & \\
1-\sigma & -1+\sigma & 0 & -\frac{\mu}{\mu'}(1-\sigma') & \frac{\mu}{\mu'}(1-\sigma') \\
1-2\sigma & 1-2\sigma & -1 & -\frac{\mu}{\mu'}(1-2\sigma') & -\frac{\mu}{\mu'}(1-2\sigma')
\end{bmatrix}
\begin{bmatrix}
k\,A_2 \\ \frac{i\,A_9}{kk'} \\ A_{12} \\ k\,B_2 \\ \frac{i\,B_9}{kk'}
\end{bmatrix}
=
\begin{bmatrix}
0 \\ 0 \\ -\frac{ik^2}{k'}\Pi_\alpha \tau_{xz}^{(o)} \\ 0 \\ \frac{i}{k'}\tau_{xz}^{(o)}
\end{bmatrix}
$$

Equation (VI-1-32). Case when the prestress component $\tau_{xz}^{(o)}$ is nonzero.

When the inclusion is filled with a liquid, the system reduces then to the upper left 3×3 subsystem, and the coefficients B_2 and B_9 vanish.

$$
\begin{bmatrix}
W_c & W_s & 0 & 0 & 0 \\
s_\alpha^2 W_c & c_\alpha^2 W_s & W_p & 0 & 0 \\
(1-\sigma)W_c \\ -(1-2\sigma)\Pi_\alpha & -(1-\sigma)W_s \\ -(1-2\sigma)\Pi_\alpha & \Pi_\alpha & (1-2\sigma')\Pi_\alpha & (1-2\sigma')\Pi_\alpha \\
1-\sigma & -1+\sigma & 0 & -\frac{\mu}{\mu'}(1-\sigma') & \frac{\mu}{\mu'}(1-\sigma') \\
1-2\sigma & 1-2\sigma & -1 & -\frac{\mu}{\mu'}(1-2\sigma') & -\frac{\mu}{\mu'}(1-2\sigma')
\end{bmatrix}
\begin{bmatrix}
k\,A_4 \\ -\frac{k}{k'}A_6 \\ A_{15} \\ k\,B_4 \\ -\frac{k}{k'}B_6
\end{bmatrix}
=
\begin{bmatrix}
0 \\ 0 \\ \frac{k^2}{k'}\Pi_\alpha \tau_{xy}^{(o)} \\ 0 \\ -\frac{k^2}{k'}\tau_{xy}^{(o)}
\end{bmatrix}
$$

Equation (VI-1-33). Case when the prestress component $\tau_{xy}^{(o)}$ is nonzero.

When the inclusion is liquid, the system reduces to the upper left 3×3 subsystem and, in that case, the coefficients B_4 and B_6 vanish.

$$
\begin{bmatrix}
W_d & -k^2 W_c & 0 & 0 & 0 \\
c_\alpha^2 W_d & d_\alpha^2 W_c & W_o & 0 & 0 \\
(1-\sigma)W_d \quad -k^2(1-2\sigma)\Pi_\alpha & k^2(1-\sigma)W_c \quad -k^2(1-2\sigma)\Pi_\alpha & k^2\Pi_\alpha & k^2(1-2\sigma')\Pi_\alpha & k^2(1-2\sigma')\Pi_\alpha \\
1-\sigma & -1+\sigma & 0 & -\frac{\mu}{\mu'}(1-\sigma') & \frac{\mu}{\mu'}(1-\sigma') \\
1-2\sigma & 1-2\sigma & -1 & -\frac{\mu}{\mu'}(1-2\sigma') & -\frac{\mu}{\mu'}(1-2\sigma')
\end{bmatrix}
\begin{bmatrix}
-\frac{k}{k'} A_5 \\
\frac{i}{kk'} A_{10} \\
A_{14} \\
-\frac{k}{k'} B_5 \\
\frac{i}{kk'} B_{10}
\end{bmatrix}
=
\begin{bmatrix}
0 \\
0 \\
\frac{ik^2}{k'^2} \Pi_\alpha \tau_{yz}^{(o)} \\
0 \\
-\frac{i}{k'^2} \tau_{yz}^{(o)}
\end{bmatrix}
$$

Equation (VI-1-34) . Case when the prestress component $\tau_{yz}^{(o)}$ is nonzero.

When the inclusion is liquid, the system reduces to the upper left 3×3 subsystem, and the coefficients B_5 and B_{10} vanish.

The system to be solved for the case of diagonal stress component is much more complicated. We write it in matrix form as

$$\mathbf{M}\,\mathbf{c} = \mathbf{d} \qquad \text{(VI-1-35)}$$

Here $\mathbf{c}$ represents the vector of 9 unknown coefficients

$$\mathbf{c} = \left[A_1, k\,A_3, -\frac{k}{k'}A_7, \frac{i}{kk'}, A_8, A_{11}, A_{13}, k\,B_3, -\frac{k}{k'}B_7, \frac{i}{kk'}, B_8 \right]$$

The vector $\mathbf{d}$ appearing on the right-hand side has the following components

$$d_1 = -\frac{k^2}{2}\Pi_\alpha\,\tau_{xx}^{(o)} \quad ; \quad d_2 = -\frac{k^2}{2}\Pi_\alpha\,\tau_{yy}^{(o)} \quad ; \quad d_3 = \frac{k^2}{2}\Pi_\alpha\,\tau_{zz}^{(o)}$$

$$d_4 = 0 \quad ; \quad d_5 = 0 \quad ; \quad d_6 = 0 \quad ; \quad d_7 = 0 \quad ; \quad d_8 = 0$$

and $$d_9 = \frac{k^2}{2k'^2}\left[\tau_{yy}^{(o)} - \frac{1}{k^2}\tau_{zz}^{(o)}\right] + \frac{\Delta}{2(1+\sigma)}$$

The matrix $\mathbf{M}$ is given here by rows:

First row

$$M_{11} = 0 \quad ; \quad M_{12} = -(1-\sigma)(W_s+\Pi_\alpha) \quad ; \quad M_{13} = -k'^2\sigma\Pi_\alpha \quad ;$$

$$M_{14} = k^4k'^2\sigma\Pi_\alpha \quad ;$$

$$M_{15} = \frac{s_\alpha \ell_\alpha}{c_\alpha d_\alpha}\left[\left(1-P_1\right)\left(1-k^2P_1\right)\left(3k^2s_\alpha^2 - \frac{1}{P_1}\right) + \left(d_\alpha^2+k^2c_\alpha^2\right)\left(1-P_1k^2s_\alpha^2\right)\right]$$

M_{16} is obtained from M_{15} by changing P_1 into P_2 and ℓ_α into n_α.

$$M_{17} = (1-\sigma')\,\Pi_\alpha \quad ; \quad M_{18} = k'^2\sigma'\Pi_\alpha \quad ; \quad M_{19} = -k^4k'^2\sigma'\Pi_\alpha$$

Second row

$$M_{21} = 0 \quad ; \quad M_{22} = -\sigma\Pi_\alpha \quad ; \quad M_{23} = k'^2(1-\sigma)(W_c-\Pi_\alpha) \quad ;$$

$$M_{24} = k^4k'^2\sigma\Pi_\alpha$$

$$M_{25} = \frac{c_\alpha \ell_\alpha}{s_\alpha d_\alpha}\left[P_1\left(1-k^2P_1\right)\left(3k^2s_\alpha^2 - \frac{1}{P_1}\right) - P_1k^2c_\alpha^2\left(d_\alpha^2-k^2s_\alpha^2\right)\right]$$

M_{26} is obtained from M_{25}

$$M_{27} = \sigma'\Pi_\alpha \quad ; \quad M_{28} = k'^2(1-\sigma')\,\Pi_\alpha \quad ; \quad M_{29} = -k^4k'^2\sigma'\Pi_\alpha$$

Third row

$$M_{31} = 0 \quad ; \quad M_{32} = \sigma\Pi_\alpha \quad ; \quad M_{33} = k'^2\sigma\Pi_\alpha \quad ; \quad M_{34} = k^2k'^2(1-\sigma)(W_d-k^2\Pi_\alpha)$$

$$M_{35} = \frac{d_\alpha \ell_\alpha}{s_\alpha c_\alpha}\left[P_1(P_1-1)\left(3k^2 s_\alpha^2 - \frac{1}{P_1}\right) + P_1 d_\alpha^2 \left(c_\alpha^2 - s_\alpha^2\right)\right]$$

M_{36} can be obtained from M_{35}

$$M_{37} = -\sigma' \Pi_\alpha \quad ; \quad M_{38} = -k'^2 \sigma' \Pi_\alpha \quad ; \quad M_{39} = k^4 k'^2 (1-\sigma')\ \Pi_\alpha \quad .$$

Fourth row

$$M_{41} = W_\alpha \quad ; \quad M_{42} = 0 \quad ; \quad M_{43} = W_c \quad ; \quad M_{44} = W_d$$

$$M_{45} = P_1^2 \frac{W_\ell}{\ell_\alpha} + 2P_1 s_\alpha^2 \Pi_\alpha \quad ; \quad M_{46} = P_2^2 \frac{W_n}{n_\alpha} + 2P_2 s_\alpha^2 \Pi_\alpha$$

$$M_{47} = 0 \quad ; \quad M_{48} = 0 \quad ; \quad M_{49} = 0 \quad .$$

Fifth row

$$M_{51} = 0 \quad ; \quad M_{52} = 0 \quad ; \quad M_{53} = W_c \quad ; \quad M_{54} = k^2 W_d \quad ;$$

$$M_{55} = P_1 \frac{W_\ell}{\ell_\alpha} + 2P_1 \Pi_\alpha \quad ; \quad M_{56} = P_2 \frac{W_n}{n_\alpha} + 2P_2 \Pi_\alpha \quad ;$$

$$M_{57} = 0 \quad ; \quad M_{58} = 0 \quad ; \quad M_{59} = 0 \quad .$$

Sixth row

$$M_{61} = 0 \quad ; \quad M_{62} = W_s \quad ; \quad M_{63} = W_c \quad ; \quad M_{64} = k^4 W_d \quad ;$$

$$M_{65} = \frac{W_\ell}{\ell_\alpha} + 2P_1 \frac{c_\alpha d_\alpha}{s_\alpha} \quad ; \quad M_{66} = \frac{W_n}{n_\alpha} + 2P_2 \frac{c_\alpha d_\alpha}{s_\alpha}$$

$$M_{67} = 0 \quad ; \quad M_{68} = 0 \quad ; \quad M_{69} = 0 \quad .$$

Seventh row

$$M_{71} = 0 \quad ; \quad M_{72} = (1-\sigma)\, W_s \quad ; \quad M_{73} = (1-\sigma)\, W_c \quad ; \quad M_{74} = k^4(1-\sigma)\, W_d$$

$$M_{75} = 0 \quad ; \quad M_{76} = 0 \quad ;$$

$$M_{77} = \frac{\mu-\mu'}{\mu'}(1-2\sigma') \quad ; \quad M_{78} = -\frac{\mu-\mu'}{\mu'}(1-2\sigma') \quad ; \quad M_{79} = -k^6 \frac{\mu-\mu'}{\mu'}(1-2\sigma')$$

Eighth row

$$M_{81} = 0 \quad ; \quad M_{82} = 0 \quad ; \quad M_{83} = -(1-\sigma)\, W_c \quad ; \quad M_{84} = -k^2(1-\sigma)\, W_d$$

$$M_{85} = 0 \quad ; \quad M_{86} = 0 \quad ;$$

$$M_{87} = 0 \quad ; \quad M_{88} = \frac{\mu-\mu'}{\mu'}(1-2\sigma') \quad ; \quad M_{89} = k^4 \frac{\mu-\mu'}{\mu'}(1-2\sigma')$$

Ninth row

$$M_{91} = 0 \quad ; \quad M_{92} = 0 \quad ; \quad M_{93} = 1-2\sigma \quad ; \quad M_{94} = k^2(1-2\sigma)$$

$$M_{95} = -P_1 \ell_\alpha \quad ; \quad M_{96} = -P_2 n_\alpha$$

$$M_{97} = 0 \quad ; \quad M_{98} = -\frac{\mu}{\mu'}(1-2\sigma') \quad ; \quad M_{99} = -k^2 \frac{\mu}{\mu'}(1-2\sigma') \quad .$$

In the case where we have a cavity, then the system reduces to the upper left 6×6 subsystem, and the coefficients B_3 , B_7 , B_8 vanish.

In order to be able to compute all the terms in the above systems, we still need expressions for the various wronskians appearing in the matrix elements. These wronskians are given in Appendix 13. The results of Appendix 13, together with the expression $\text{sn}\, \alpha_o = a/m$ (cf. Sadowsky and Sternberg, 1949), are sufficient to compute all of the terms in these systems. Clearly, the analytical solution of the systems given above is not convenient, and one must resort to a numerical solution for the coefficients A_i and B_i . However, a few aspects of the problem can be discussed at this point.

vi) Discussion

The systems (VI-1-32) through (VI-1-35) permit us to compute the elastic fields at every point in the medium. The first remark we wish to make about these systems concerns the fields inside the inclusion.

Since the coefficients B_1 , B_4 , B_{12} , B_{13} , B_{14} , and B_{15} do not appear in the solution, then the only Lamé products contributing to the fields inside the ellipsoid are those appearing in the expression for the prestress (VI-1-21) . Recalling that we assumed the prestress to be uniform, we see that the stress is uniform inside the inclusion. This is in agreement with the results of Eshelby (1957). The fact that we did not assume this to hold from the beginning, but instead proved it independently as a result of our analysis, constitutes a favorable check of our solution. Furthermore, if the material inside the inclusion is chosen to be identical to the material constituting the matrix, it can easily be shown that 1) all the coefficients A_i , i=1,...,15 , vanish, and 2) the coefficients B_i that do not vanish are identical to the coefficients of the Lamé products appearing in (VI-1-21) . In other words, there is no perturbation to the prestress field outside the inclusion, and the field inside the inclusion is found to be identical to the prestress, as should indeed be expected.

We can see from (VI-1-32) through (VI-1-35) that the solution for the coefficients A_i and B_i depend on the prestress, the elastic properties of the matrix and the inclusion, and the moduli k and k' . These moduli may in turn be written in terms of the aspect ratios $\rho_1 = b/a$ and $\rho_2 = c/b$ of the ellipsoid. By comparison with equations (VI-1-25) through (VI-1-28) , and with the definition of the Lamé products used here, we note that 1) the stress concentrations in the vicinity of the inclusion do not depend on its absolute size, but only on its shape, but 2) the displacement field depends on the parameter m , which is a measure of the size of the inclusion. As pointed out

by Sadowsky and Sternberg (1949), the first of these conclusions is characteristic of all problems of this type. The second conclusion is intuitively correct.

In the case of a liquid inclusion, we pointed out earlier that expressions of the form $(1-\sigma')/\mu'$ are unbounded, so that the corresponding coefficient must be set to zero in the above systems. Applying this rule to systems (VI-1-32) through (VI-1-34), we see that no fields are generated inside the inclusion (in particular, no pressure is generated in the fluid) when the prestress is pure shear at infinity. Thus a liquid inclusion behaves as a cavity under pure shear. This result stems from the fact that we ignored perturbations to the boundary of the inclusion, and applied the boundary conditions (VI-1-31) on the boundary $\alpha = \alpha_o$ of the unstressed inclusion. This is correct to first order and is in agreement with the results of Eshelby (1957). This author shows how to calculate the average elastic properties of a material containing a dilute distribution of ellipsoidal inclusions. Using Eshelby's results, Anderson, Minster and Cole (1973) showed that for liquid inclusions, the shear properties of the composite material do not depend, to first order, on the bulk modulus of the liquid.

Examination of (VI-1-35), on the other hand, shows that the quantity $(1-2\sigma')/\mu'$ appears in this system. This quantity must be replaced by $1/\lambda'$ in the case of a liquid inclusion, where λ' is the bulk modulus of the liquid. Therefore, the system (VI-1-35) does not simplify appreciably in that case, and the solution depends on λ'. This is consistent with the results of Anderson, Minster and Cole (1973). Robinson (1951) investigated the deformation of the inclusion when the

prestress tensor is diagonal, and found that the ellipsoid is deformed into a new ellipsoid in that case. This holds also when thermoelastic effects are taken into account.

One last special case is easily discussed: in the case of an ellipsoidal cavity, the system (VI-1-35) reduces to its upper left 6×6 subsystem. There is here a discrepancy, since Sadowsky and Sternberg (1949) found a system of 5 equations and 5 unknowns in that case. Specifically, these authors claim that the elementary solution with coefficient A_{13} is not linearly independent from the others. We should, therefore, be able to reduce our 6×6 subsystem further. Now the first three equations of (VI-1-35) must be independent since their right-hand sides contain $\tau_{xx}^{(o)}$, $\tau_{yy}^{(o)}$ and $\tau_{zz}^{(o)}$ respectively. Thus the fourth, fifth and sixth equations must be those which are linearly dependent. However, we have been unable so far to find any vanishing linear combination of these equations. Similarly, repeated efforts to show any linear dependence between the elementary displacement solutions with coefficients A_1, A_3, A_7, A_8, A_{11}, and A_{13} have also failed. Sadowsky and Sternberg have shown their solution to reduce to the correct results in the limiting cases of spheroidal and spherical cavities; although this does not constitute absolute proof of the correctness of their results, there is here a suggestion that the system (VI-1-35) is incompletely reduced and could be further reduced to an 8×8 system. The discrepancy between Sadowsky and Sternberg's results and ours may be related to another discrepancy pointed out in Appendix 13. Our expressions for the wronskians W_ℓ and W_n (associated with the

coefficients A_{11} and A_{13}) are not reconcilable with their expression for the Lamé function of the second kind L_{α} . After careful checking of our analysis, we feel that our results are error free, but, of course, we shall need further verifications before we can reach a definitive conclusion.

Further verifications of the solution presented in this section should include a thorough study of various limiting geometries, such as spheroidal and spherical geometries. However, this is not an easy task to perform analytically, and it is best to compare numerical results for this purpose. We shall attempt to do so in future work.

We need not point out here the many possible uses of the solution presented in this section. We refer the reader to the Engineering literature for this purpose. In the context of the present study, the static solution given above yields the initial value fields needed to investigate a relaxation source with ellipsoidal rupture geometry. This is the first step towards a dynamical solution, discussed in the next section.

VI-2 The dynamic ellipsoidal rupture

As we pointed out in the introduction to this chapter, we shall not give here the complete dynamical solution to the elastodynamic source with ellipsoidal geometry. We shall confine ourselves in this section to a discussion of possible ways of attacking the problem.

First of all, it is clear that the results of Chapter II are applicable here as well. Much of the discussion of Chapter IV also retains its validity. For example, since we wish to make the rupture zone transparent, we only need to know the initial value fields outside the rupture zone. Thus we need only consider the elementary solutions with coefficients A_i , i=1,...,15 , obtained in the previous section. Similarly the question of whether the material inside the rupture retains any rigidity can be discussed just as it was in Chapter IV. We recall that a finite rigidity may be used to model approximately the high frequency behavior of the material. We also recall that the energy release process is most efficient when the rupture zone is a zone of vanishing rigidity. The discussion concerning the size of the relaxation zone also retains its validity and will not be repeated here.

As shown in Chapters II and IV, the only problem that needs to be solved is the case of the instantaneous rupture. Growing and propagating ruptures can then be treated, for example, just as in section IV-3. The major difficulty which we are now confronted with is a mathematical one. Let us separate the problem into two major steps.

i) Dilatation and rotation potentials

We saw in Chapter IV that there are considerable advantages in

reducing the elastodynamic problems to the solution of scalar wave equations by means of potentials. These potentials were the cartesian components χ_1 , χ_2 , χ_3 of the rotation vector potential, and the dilatation χ_4 .

By taking successively the curl and divergence of the static initial displacement fields given in the form

$$2\mu\, \mathbf{u}^* = \nabla(\phi + \mathbf{r}\cdot\boldsymbol{\omega}) - 4(1-\sigma)\,\boldsymbol{\omega} \quad , \qquad \text{(VI-2-1)}$$

Archambeau (1964) showed that the initial values for rotation and dilatation potentials are

$$\theta^* = \chi_4^* = -2(1-2\sigma)\ \nabla\cdot\boldsymbol{\omega} \quad , \qquad \text{(VI-2-2)}$$

$$\boldsymbol{\Omega}^* = \left[\chi_1^*, \chi_2^*, \chi_3^*\right] = -2(1-\sigma)\ \nabla\times\boldsymbol{\omega} \quad . \qquad \text{(VI-2-3)}$$

We note that only the Boussinesq potential $\boldsymbol{\omega}$ is involved. From the previous section, we know its cartesian components as combinations of Lamé products. In fact, only ellipsoidal harmonics of degree one are present in $\boldsymbol{\omega}$. We have

$$\begin{cases} \omega_x = m[A_2 D_\alpha d_\beta d_\gamma + A_3 S_\alpha s_\beta s_\gamma + A_4 C_\alpha c_\beta c_\gamma] \\ \omega_y = m[A_5 D_\alpha d_\beta d_\gamma + A_6 S_\alpha s_\beta s_\gamma + A_7 C_\alpha c_\beta c_\gamma] \\ \omega_z = m[A_8 D_\alpha d_\beta d_\gamma + A_9 S_\alpha s_\beta s_\gamma + A_{10} C_\alpha c_\beta c_\gamma] \end{cases} . \qquad \text{(VI-2-4)}$$

In order to perform the differentiations in (VI-2-2) and (VI-2-3) we can either find the ellipsoidal components of ω by means of a relation similar to (VI-1-24) and then apply the operator ∇ in the form (VI-1-12); or we may differentiate the Lamé products of (VI-2-4) with respect to the cartesian coordinates by use of the chain rule. The algebra is rather complicated and will be omitted here. The necessary formulae to carry out the differentiations may be found in Appendix 12. (Recall that we need to compute the cartesian components of Ω .)

ii) Solution of the initial value problem

The most difficult part of the solution lies in computing the Green's function solution presented in Chapters II and IV. Let us suppose that we know the initial values χ_α^* , $\alpha=1,\ldots,4$ in the form of (finite) series of ellipsoidal harmonics. Then in order to follow the method used in Chapter IV one needs to expand the Green's function to Helmholtz' equation in a series of ellipsoidal wave functions. To our knowledge, such a result is not known. In fact, Arscott (1964) points out how little is known about ellipsoidal wave functions, so that this approach, although the most natural one, does not look very promising.

Since we know how to solve the problem in spherical coordinates, it is reasonable to try and express the initial value fields in terms of spherical harmonics. The easiest method, proposed by Archambeau (1964) is to expand each ellipsoidal harmonic in spherical harmonics by Niven's theorem (e.g., Hobson, 1931). However, we are in the presence of external harmonics and, in that case, Niven's theorem has only been

proved to converge outside a sphere of radius $a(\sqrt{2}+1)$, where a is the major semi-axis of the ellipsoid. This is not sufficient for our problem since we want to compute the initial value integral over the volume lying immediately outside the rupture zone; in particular, we do not wish to ignore contributions coming from the vicinity of the tip of the ellipsoid since much of the radiated energy comes from that region.

Thus it seems that such conventional methods are apparently doomed to failure. On the other hand, we know that such a physical problem must have a well behaved solution. It is this author's feeling that, unless a more sophisticated mathematical apparatus is used, the analytical solution will be most likely obtained through some mathematical trick--possibly by inspection! It should be noted in that respect that, if it were not for the presence of Lamé functions of second kind, the Lamé products in (VI-2-4) would simply be the cartesian coordinates x , y, z .

Faced with the obvious impracticality of purely analytical attacks, we now turn to numerical solutions. Let us note first that, although the initial values θ^* and Ω^* can be found analytically, the solution to the static problem of section VI-1 is most conveniently obtained by numerical inversion of the systems (VI-1-32) through (VI-1-35) . Thus the potentials χ_α^* , $\alpha=1,\ldots,4$ can be computed numerically at any point in the medium. Being harmonic functions, they afford an expansion in solid harmonics. We write

$$\chi_\alpha^* = \sum_{n=0}^{\infty} \sum_{m=0}^{n} \frac{1}{r^{n+1}} \left[a_{nm}^{(\alpha)} \cos m\phi + b_{nm}^{(\alpha)} \sin m\phi \right] P_n^m(\cos\theta) \quad . \tag{VI-2-5}$$

Thus, if χ_α^* is known on the surface of a sphere of radius R_o, the static coefficients $a_{nm}^{(\alpha)}$ and $b_{nm}^{(\alpha)}$ can be evaluated as integrals over the surface of this sphere and by use of the usual orthogonality relations. This is a classical problem of potential theory (e.g., Hobson, 1931). These integrals may be evaluated numerically on a high speed computer by a number of well known techniques. Then (VI-2-5) provides a representation of χ_α^* valid for $r > R_o$.

Since this method is tantamount to expanding ellipsoidal harmonics in spherical harmonics numerically, there is no insurance that the method should yield a convergent series for $R_o < a(\sqrt{2}+1)$. However, it is intuitively clear that the complications arise mainly from the complicated azimuthal dependence of the fields caused by the ellipsoidal geometry, which is more pronounced in the close vicinity of the ellipsoid itself. When χ_α^* is known only at discrete points over the sphere of radius R_o, much of its "high frequency" azimuthal dependence is filtered out by the discretization, and we can expect (VI-2-5) to converge relatively fast, even if R_o is chosen as $R_o = a$. Of course, in that case, (VI-2-5) yields a "smoothed" potential χ_α^*. But the error made will involve only the harmonics of high degree, and should be felt only in extreme near-field studies.

Once we know (VI-2-5), the entire mathematical apparatus of Chapter IV is at our disposal to complete the dynamical solution. The radius R_o is used in exactly the same fashion as it was in section IV-2. Here also, any contribution to the radiation fields coming from inside the sphere of radius R_o is ignored. However, this omission can be justified by exactly the same arguments as in section IV-2:

The essential contribution to the radiation field comes from the vicinity of the rupture front, and the energy which is ignored is assumed to be absorbed in the non-elastic processes of the failure.

We saw in section VI-1 that the elastic fields associated with the ellipsoidal inclusion scale in a very simple fashion with its size, provided that the aspect ratios $\rho_1 = a/b$ and $\rho_2 = b/c$ are kept constant. Thus the problem of an ellipsoidal rupture undergoing self-similar growth does not pose any major difficulty. In addition, the results of Chapter IV concerning the propagation of the failure zone can be applied without modification.

This approach presents the enormous advantage that χ_α^* could have been obtained by an entirely numerical method such as a finite element technique. Thus very complex geometries can be handled in that way. However, we should note that growing sources for which the initial field does not scale simply with rupture size must be handled through a succession of static computations at a discrete sequence of source times $t_o^{(n)}$, n=1,...,N . This may be time consuming, but does not add to the difficulty of the problem since the integrals over the source time t_o (Chapter IV, Appendix 4) are evaluated numerically anyway.

As a final remark, let us also point out that the dynamical near-source calculation can also be performed through a numerical scheme. If this is the case, the connection with the results of Chapter IV must be done via the dynamic multipole coefficients, which are then to be calculated numerically, either as functions of time or as functions of frequency. This scheme is rather more complicated, but perfectly feasible.

Conclusion

The major result of this chapter is the derivation of the elastic fields associated with an arbitrary ellipsoidal inclusion. In spite of considerable work needed to solve the problem, it should be noted that the final systems are remarkably simple and exhibit a fairly high degree of symmetry.

As pointed out earlier the correctness of the final solution has not yet been checked completely. One particularly useful check would be to compare the results given here with numerical calculations based, for example, on a finite element technique.

The method of solution, which we propose for the dynamical problem, is of great importance because of its great potentiality. Purely numerical solutions to elastodynamic problems are notoriously limited, given the present state of the art. In particular, far-field calculations are next to impossible to perform, especially at high frequency, because of physical limitations placed on the grid size, the coarseness of the mesh, and the allowable computing time. On the other hand, finite element techniques have proved to be excellent for static near-field calculations (e.g., Alewine and Jungels, 1973). The method that we describe above provides a very convenient tie between such techniques, and our elastodynamic solutions. This opens the possibility of constructing realistic models for seismic sources, and of predicting their theoretical radiation by use of the methods described in Chapter V.

Chapter VII

NUMERICAL APPLICATIONS

Introduction

Theoretical work in an applied field such as geophysics is of limited help if one does not develop simultaneously a capability to translate mathematical expressions into numbers. We shall now present the computed radiation field for the spherical rupture model described in section IV-2.

The most important lesson which one can draw from these numerical applications is that even such a simple model depends on enough parameters so as to be, in fact, quite complex. A complete discussion of all of its aspects is thus a major undertaking in itself. We shall focus in this chapter on the major features of the radiation field, which we shall discuss on the basis of selected examples.

The far-field radiation will be analyzed first, and then some of near-field effects. Starting from the simplest model of a symmetrically expanding sphere, we shall continue with a discussion of the effects of unilateral rupture propagation. The azimuthal dependence of the radiation fields will be discussed as a function of frequency, both on the basis of selected amplitude spectra and of selected radiation patterns. Phase spectra will be shown which further illustrate the complexity of the radiated fields and may revive the concept of the Z phenomenon. Finally, for the sake of completeness, a brief comparison with the observations will be given.

We wish to emphasize in this chapter the fact that there is a

de facto trade-off between model flexibility and convenience. Of course, the dilemma must be solved according to the quality of the data to be interpreted. But in view of the complexity of this simple model, there can be no doubt that an earthquake is a very complicated phenomenon indeed, and we are probably still a long way from understanding it well.

In order to fix the ideas we shall assume throughout this chapter that the stress field is pure shear, and such that it should generate a north-south vertical strike slip fault. In the source coordinate system (see Chapter V) this corresponds to the condition $\sigma_{12}^{(o)} = \sigma_{23}^{(o)} = 0$, $\sigma_{13}^{(o)} \neq 0$. We shall in fact specify the prestrain $e = e_{13}^{(o)}$ rather than the prestress. Furthermore, whenever the rupture propagates it is assumed to propagate towards the north. Azimuths are then measured from the northern direction, and take-off angles from the downward vertical (e.g., Chapter V). The free-space radiation is computed in all cases, so that we are discussing source effects only.

VII-1 The far-field amplitude spectra

We already know from the discussion of Chapter IV that, at fixed rupture dimension, two essential parameters affect the shape of the far-field amplitude spectrum: the rupture velocity V_R controls the high frequency spectral shape, while the relaxation radius R_s determines the long-period behavior. Let us start with the simplest case of a non-propagating, expanding spherical rupture of final radius R_o .

i) Stationary rupture with equilateral growth

In that case we know from the analytical solution that the radiation field is pure quadrupole at all frequencies. Figure VII-1-1 shows the high frequency part of the displacement amplitude spectrum computed for a sequence of several rupture velocities. The lowest rupture velocity is .3 km/sec, which is very low, and the highest one is 3.45 km/sec, which approaches the shear wave velocity, chosen at 3.5 km/sec. The figure exhibits several noteworthy features.

First of all, we note that the average slope of the spectra always tends to -3 at high frequencies. However, this asymptotic behavior is only reached at very high frequency for the S-spectra when the rupture velocity approaches V_s . This confirms the analytical results of Chapter IV, and one can see quite clearly that the S-spectrum will have a slope of -2 when $V_R = V_s$. We should note that this effect becomes strong only when V_R is greater than, say, 0.9 V_s . No such effect is observed for the P-spectrum, since V_R never approaches V_p .

On the other hand, for low rupture velocities P- and S-spectra are affected in a similar fashion. In fact, it is clear from the figure

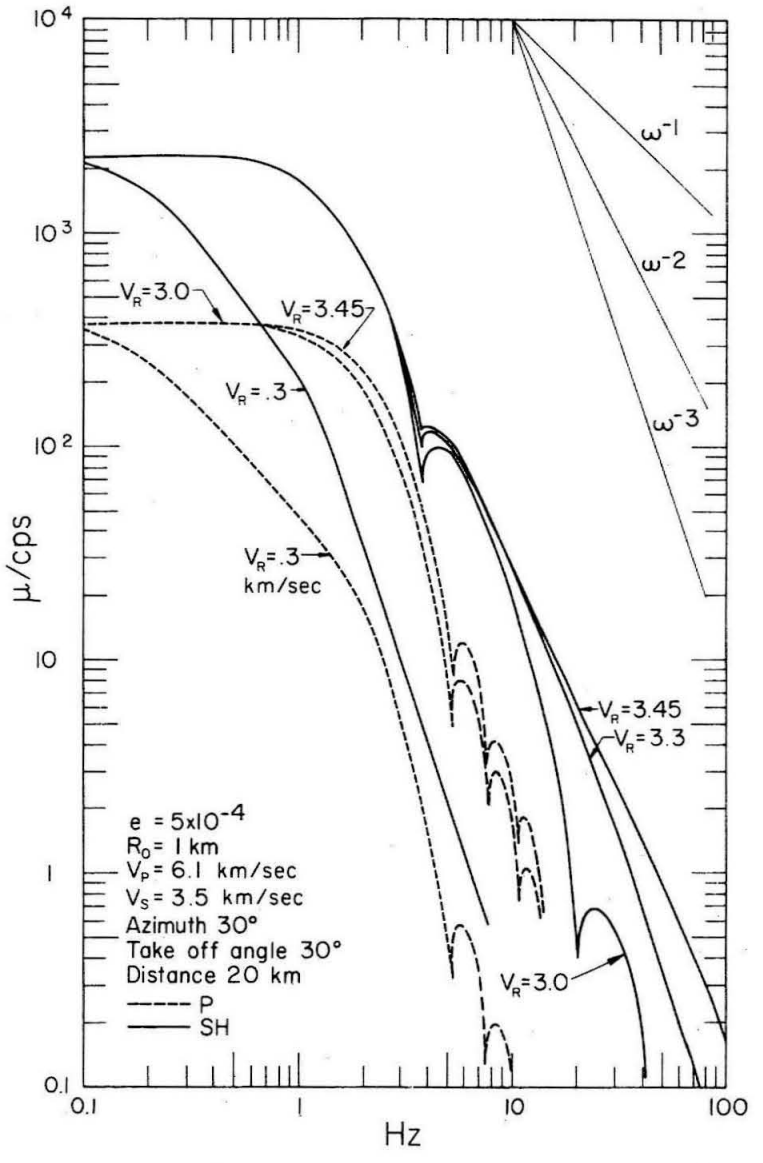

Figure VII-1-1. Effect of rupture velocity on the displacement spectrum. Case of a stationary rupture with equilateral growth.

that the dependence of the spectra on V_R is nonlinear. As the rupture velocity becomes slow, we note the development of an intermediate frequency range, where the spectrum has approximately a slope of -1, before it steepens to -3 at higher frequencies. There is clearly no simple scaling law of these curves as a function of V_R ; in fact, one wonders whether a "corner frequency" may be usefully defined. If f_o is such a corner frequency, then according to the results of section IV-5, we have

$$2\pi f_o = \left(\frac{9 V_R V^2_{(p,s)}}{R_o^3} \right)^{1/3} . \qquad \text{(VII-1-1)}$$

We may therefore compute the following values of f_o , in hertz

	P-spectrum	S-spectrum
V_R = 3. km/sec	1.6	1.1
V_R = .3 km/sec	0.74	0.51

It is clear that (VII-1-1) yields the intersection of the high frequency asymptote with the long-period level. Should one insist in defining a corner frequency in all cases, this is a self-consistent way to do it. However, it is doubtful that such a concept is very useful for low rupture velocities.

Let us point out in passing that the frequency at which the spectrum reaches its long-period asymptote apparently scales linearly

with rupture velocity. Unfortunately, this point is rather difficult to pick on theoretical spectra (figure VII-1-1), let alone on observed spectra.

Finally, we wish to comment on the observational result that S-corner frequencies are lower than P-corner frequencies. For various reasons discussed earlier, observed spectra are rather band-limited. Now, if the spectra of figure VII-1-1 were only given in the frequency band .5 cps to 10 cps, then we see that the average high frequency slope of the S-spectrum can easily be underestimated, and thus the corner frequency will be biased towards longer periods. This bias is not present for the P-spectrum, and therefore from band limited data, the difference between S- and P-corner frequencies will exhibit a tendency to be overestimated.

Let us now turn to the long-period spectral behavior. Figure VII-1-2 shows three P-wave spectra computed for R_s = 5 km, 20 km, and $R_s = \infty$. If R_s is unbounded, the long-period spectrum is flat, as we also know from Chapter IV. On the other hand, a finite value of R_s leads to a peaked spectrum. However, even when R_s = 5 km, which is two and a half source dimensions, the peak level is very nearly equal to the "flat level." And a more acceptable value of ten source dimensions yields a spectrum which is quasi-flat over almost a decade in frequency. Of course, this only corroborates the findings of section IV-5 and we shall not repeat the discussion here.

ii) Propagating rupture, unilateral growth

The model discussed so far is adequate to model the tectonic

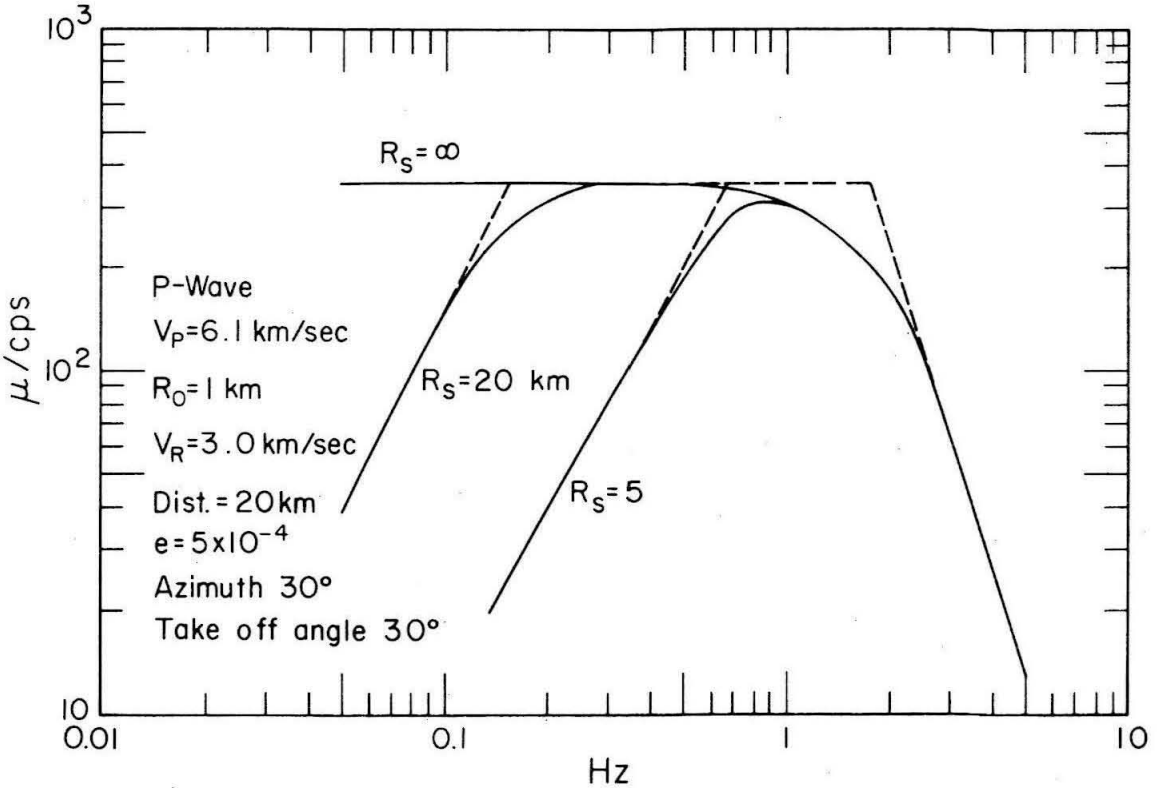

Figure VII-1-2. Effect of R_s on the long period displacement amplitude spectrum. Case of equilateral growth.

release due to underground explosions. Let us now investigate the case of a rupture growing unilaterally, since this is more appropriate to model an earthquake.

Recall first that multipoles of higher degrees are excited in addition to the fundamental quadrupole, and that their effects are essentially felt at high frequencies. Figure VII-1-3 shows how these multipoles of higher degree affect the spectra--in a particular direction. The first impression is that this effect, although clearly noticeable, is not particularly large. However, under closer scrutiny, the figure reveals that the S-spectrum character has been radically changed by the additional multipoles. Indeed, because of the rapid rate of growth chosen in this case ($V_R \simeq .98\ V_s$) the quadrupole spectrum exhibits a high frequency slope of almost -2. However, since the rupture is unilateral, the radiation field must "see" a different propagation velocity in different directions. In particular, the propagation rate in the direction indicated on the figure is certainly less than V_R . This explains why the multipoles of higher degree steepen the spectrum at high frequency. When ten multipoles are taken into account, the slope is in fact -3.

From the explanation given above, one expects this effect to be strongly dependent on azimuth; this is indeed the case, and we shall see later that this effect is very strong for back azimuths for which the azimuth makes an obtuse angle with the direction of propagation. As we pointed out in Chapter IV, one should probably add a few more multipoles (up to $\ell = 15$) in order to reach convergence. However, the computation becomes then quite lengthy, and necessitates a more

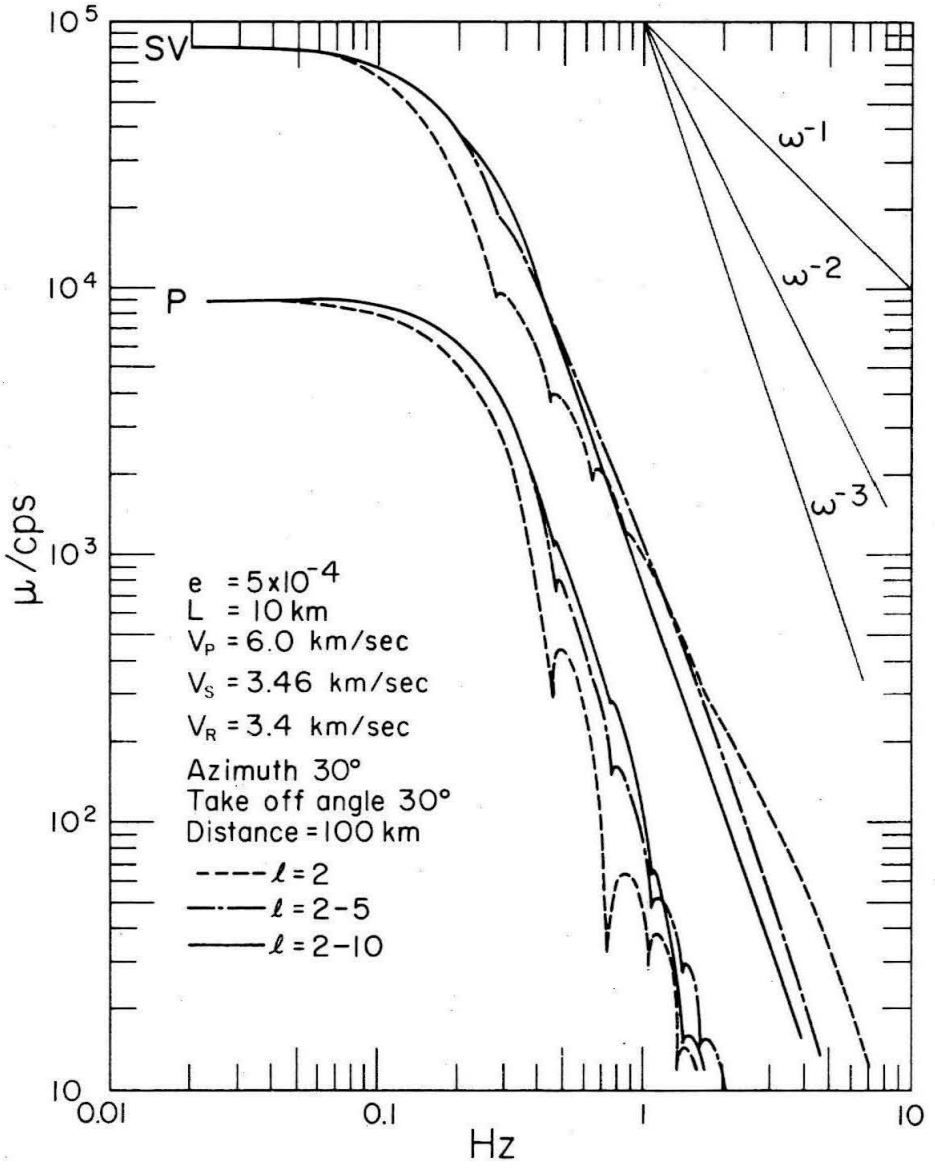

Figure VII-1-3. Effect of the multipoles of higher degree on the displacement amplitude spectrum. Case of unilateral growth.

efficient algorithm than the one we used. Convergence problems are only critical at very high frequencies, and for azimuths close to 180°, and we shall simply keep this in mind for the present discussion.

According to the analysis of section IV-5, if one wishes to define a corner frequency in that case, one should simply replace R_o by L in (VII-1-1) . This means that the corner frequency obtained at convergence should be about twice that obtained from the quadrupole only. Figure VII-1-3 seems to agree with this result reasonably well. However, here again, one expects azimuthal effects to be rather strong, and the concept of a corner frequency thereby loses some of its usefulness.

The spectra scale with V_R and R_s much in the same way as we saw earlier. Figures VII-1-4 through VII-1-6 show a variety of possible spectral shapes obtained by varying these parameters. This is shown separately for P , SV and SH spectra. Note also that these figures correspond to an azimuth and a take-off angle of 30° each. It seems at first glance that the spectral shape changes rapidly as a function of R_s and V_R . However, we should point out that if $R_s > 10L$, and if V_R is greater than, say, $V_s/3$, then the range of possible shapes is somewhat reduced. Nevertheless, there is a definite dependence of the general far-field spectral shape on the rupture velocity and the relaxation radius. The parameter V_R controls the high frequency side of the spectrum, while R_s controls the long-period side. Furthermore, unless one goes to small values of both R_s and V_R , there is little interference between these parameters; in particular, the spectra are rather insensitive to either one at

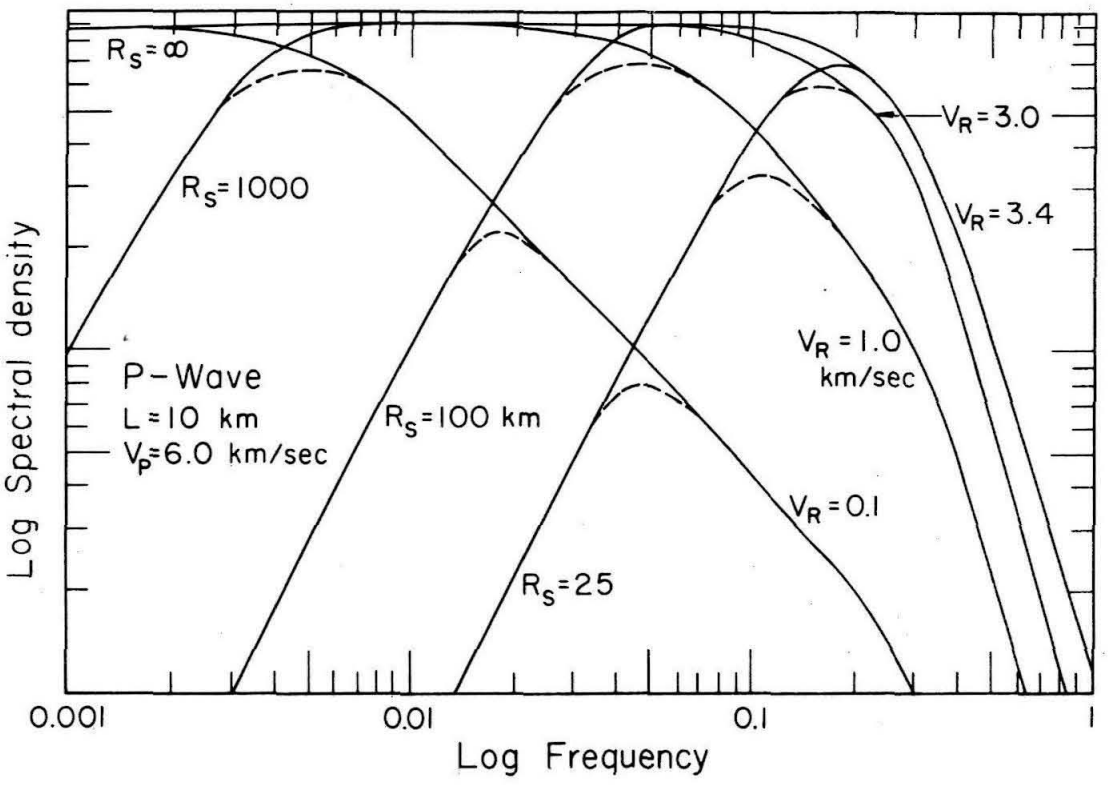

Figure VII-1-4. Effects of R_s and V_R on the global shape of the displacement amplitude spectrum. Unilateral growth. P-wave spectra.

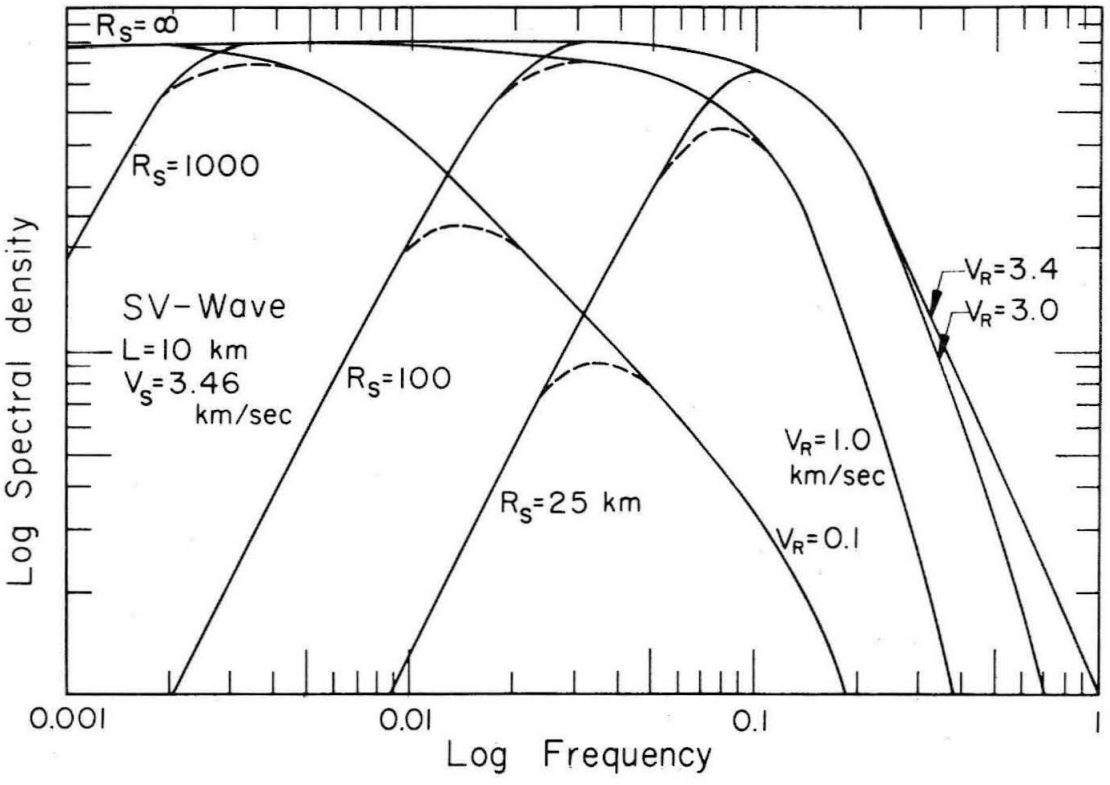

Figure VII-1-5. Same as figure VII-1-4. SV-wave spectra.

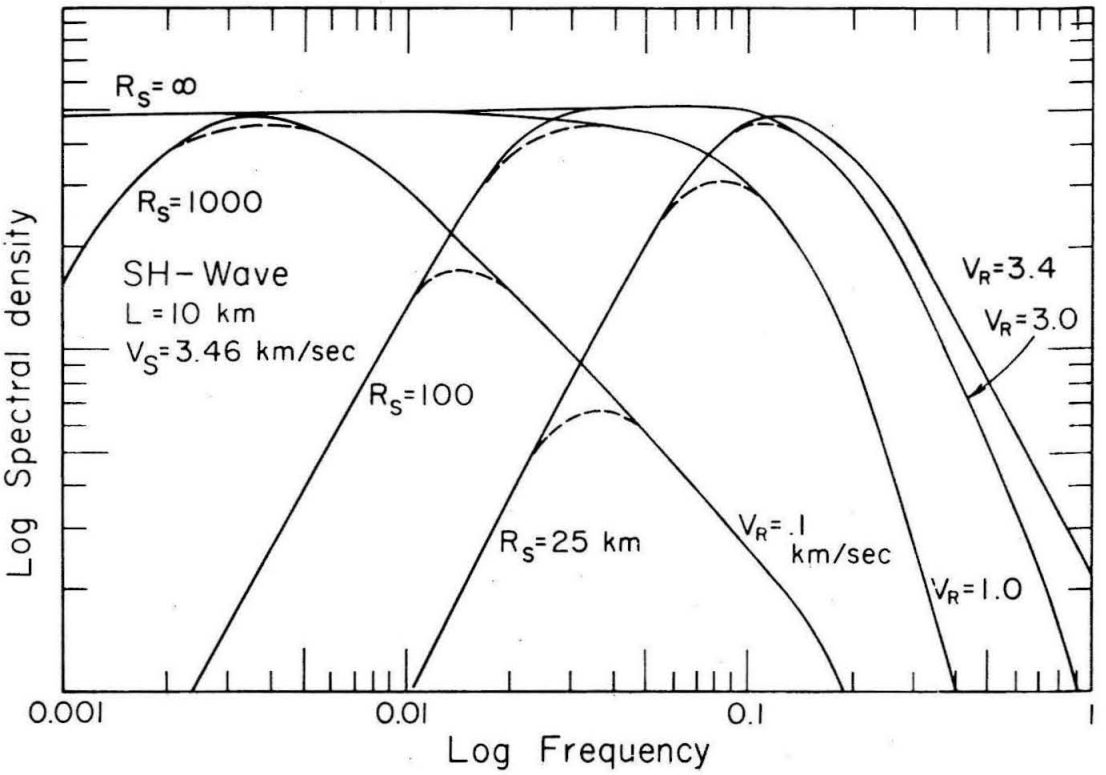

Figure VII-1-6. Same as figure VII-1-4. SH-wave spectra.

intermediate frequencies.

Much simpler is the scaling with rupture length, as shown on figure VII-1-7. To simplify the matter we assume that R_s is proportional to L, which is an acceptable assumption. The calculations are plainly in agreement with the results of Chapter IV. A change in rupture length simply results in a translation of the whole far-field spectrum. In fact, increasing L by one order of magnitude results in an increase of the peak level by three orders of magnitude, and a shift by a decade in frequency towards long periods. Thus the points A,B,C are transformed into A'B'C'. For convenience, the segment AA' was graduated in terms of length. The figure illustrates several things. First, since the average high frequency slope of the spectra tends asymptotically to -3, the scaling as a function L consists essentially in sliding the spectra along their high frequency asymptotes. This is particularly true for the P-spectrum. Now if we assume that the body wave magnitude m_b is closely related to the P-wave spectral amplitude at 1 cps, we may conclude that, at constant prestress, m_b possesses an upper bound. The S-wave magnitude, however, could be unbounded if V_R approaches V_s since the slope of the S-spectrum may be close to -2 in that case. Of course, this opens the possibility that efficient SV to P conversion near the source--for example, at the free surface--could result in large measured values of m_b. Clearly a similar analysis can be made for the surface wave magnitude M_s, which may be related to the S-spectral amplitude at 0.05 cps. We shall return to this question below.

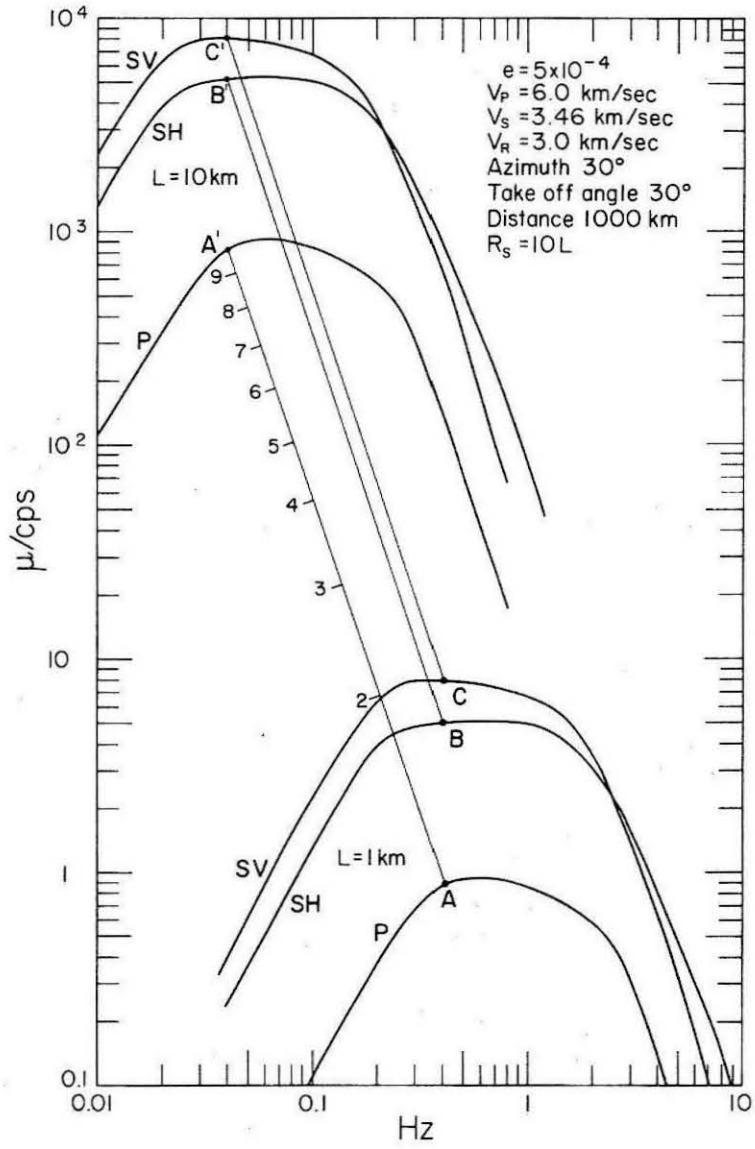

Figure VII-1-7. Scaling of the displacement spectra with rupture length.

VII-2 The near-field amplitude spectra

Discussion of the near-field spectra is somewhat less informative for several reasons. First of all, we are evaluating here a very simple model, and it is precisely in the near-field that the details of the source mechanism should be felt the most strongly. Thus near-field observations will depend very much on the fault geometry, on the history of rupture, on the complexity of the stress field (e.g., Hanks, 1973), and we do not take any of these into account. Furthermore, it is also in the near-field that most of the approximations made in Chapter IV lose some of their validity. However, we can point out several interesting general features which should hold independently of the particular model chosen.

Since near-field effects are only important at long periods, only the quadrupole term contributes to the radiation, and there is in that case no convergence problem. Let us discuss first the case of an observer lying inside the relaxation zone, that is, the case where R_s is infinite.

As we showed in Chapter IV, there is little point in talking about P- and S-waves in that case. The reason for this is clealy illustrated by figure VII-2-1. The spherical (r,θ,ϕ) components of the so-called P- and S- displacement spectra behave as ω^{-3} at long periods in that case. This is obviously unphysical since the radiated energy would be unbounded in that case. On the other hand, the total spectra--also shown on figure VII-1-2 as P+S--behave as ω^{-1} which is what should be expected for a net offset in displacement. This figure also shows that only the r component of the P-wave, and the θ and ϕ components of

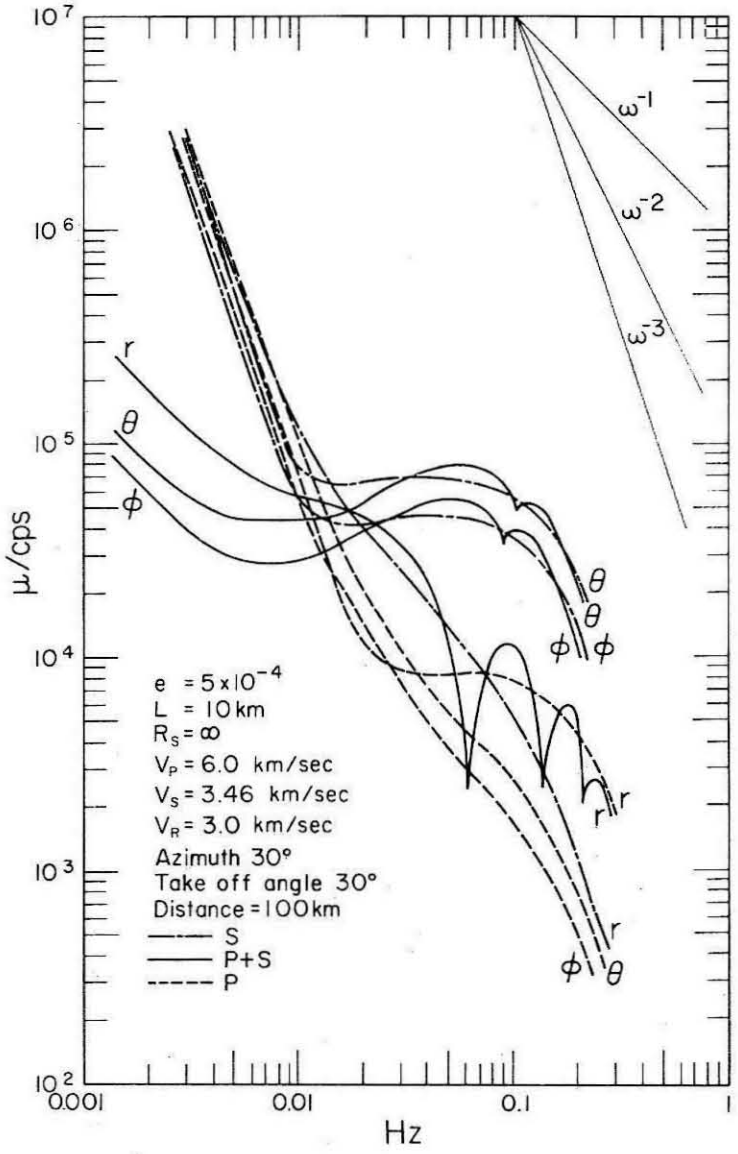

Figure VII-2-1. Near-field spectra. Case of unbounded R_s .

the S-wave--SV and SH respectively--are the only components which survive at high frequency. This means, of course, that the high frequency radiation is far-field in nature, and that no near-field effects are felt at such frequencies.

Let us also point out that near-field spectral observations can be quite complicated because of interference phenomena, which give a scalloped aspect to the spectra. In addition, for example, the θ and ϕ components of the S-spectra exhibit a quasi-flat portion at intermediate frequency, while the r component, which is pure near-field, is monotonic . On the other hand, one notices that the θ and ϕ components of total radiation are not flat but exhibit a broad peak. The shape of that peak will, of course, be azimuthally dependent since the quadrupole patterns for P, SV and SH waves are different.

Figure VII-2-2 focuses on the dependence of the near-field with hypocentral distance. Only the radial component of the P-spectrum is shown, but similar results obviously hold for other components as well. Two cases are considered: for a source length of 10 km, R_s is chosen successively at 100 km and at infinity. The most obvious effect is that the greater the distance, the longer the period at which the near-field is observed. This stems from the fact that far-field terms decay with distance as r^{-1} , while near-field terms have a faster decay of r^{-2} , r^{-3} and r^{-4} . It is interesting to note that when R_s is finite, the far-field spectrum is of course peaked, but that this peak practically disappears at short distances, due to the near-field radiation. Of course, inside the relaxation zone, only the case $R_s = \infty$ is relevant.

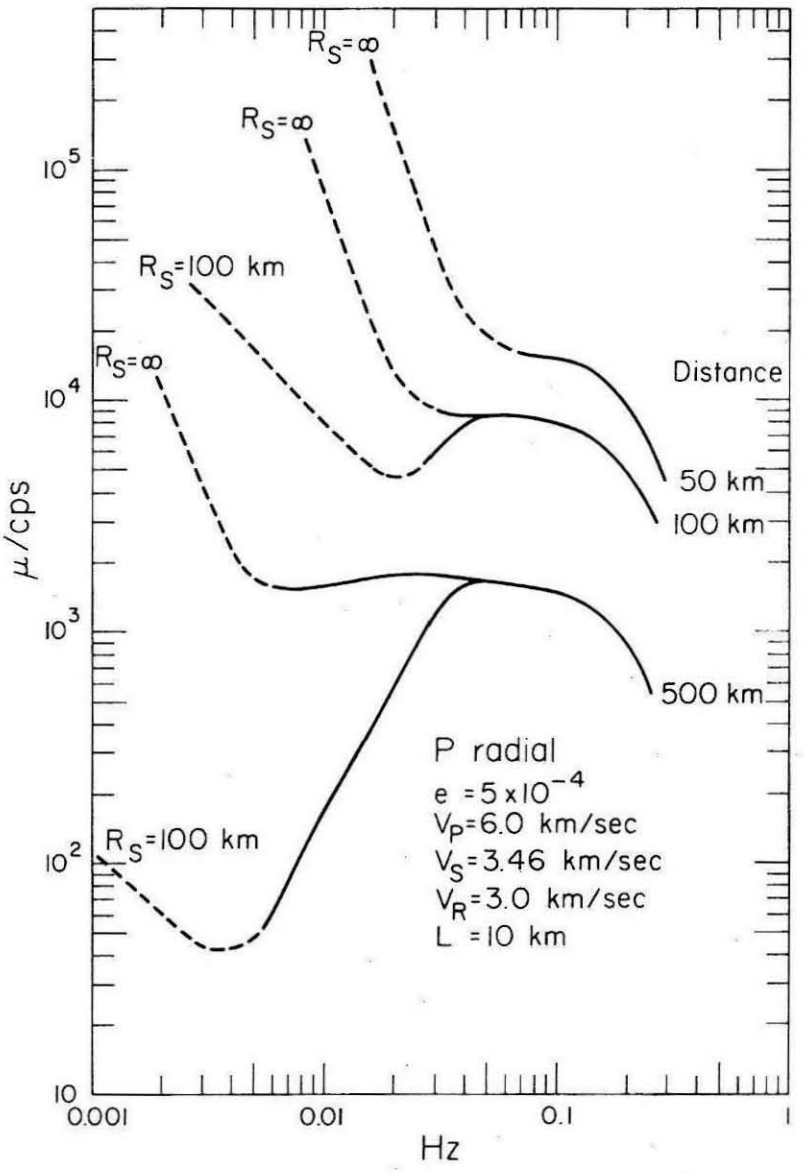

Figure VII-2-2. Dependence of the near-field on hypocentral distance.

These are the only aspects of the near-field radiation that we can usefully discuss here. More complete investigations must be undertaken on the basis of each particular event, by taking into account the details of faulting, the inhomogeneities in the vicinity in the source, etc. Such investigations have been undertaken, for example, by Hanks (1973) or Cherry, et al. (1973).

VII-3 Azimuthal effects, radiation patterns

The azimuthal dependence of the radiation fields was mentioned several times in the preceding discussion. To be complete, a description of this dependence should include a presentation of the spectra at many azimuths and many take-off angles. Similarly, three dimensional radiation patterns should be plotted on the focal sphere, using a contour representation on a stereographic projection. This is well beyond the goals of the present discussion and we shall try and show, on the basis of selected examples, how complex the radiation field really is.

i) Azimuthal dependence of the spectra

Figure VII-3-1 shows two sets of spectra computed for a propagating rupture, at the same distance, the same take-off angle, but at two complementary azimuths. The difference is striking.

First of all, there is clearly more high frequency energy radiated in the forward direction (azimuth 20°) than in the backward direction (azimuth 160°). This is accompanied by a drastic change in the character of the spectra. The spectra are indeed smooth in the forward direction and very scalloped in the backward direction. This is of course due to different interference phenomena. As we pointed out earlier, because the rupture is unilateral, the rupture velocity "seen" by the radiation field is greater in the forward direction than in the backward direction. This effect is rather more pronounced for the S-spectra than for the P-spectra, which is to be expected since V_R is closer to V_s than to V_p .

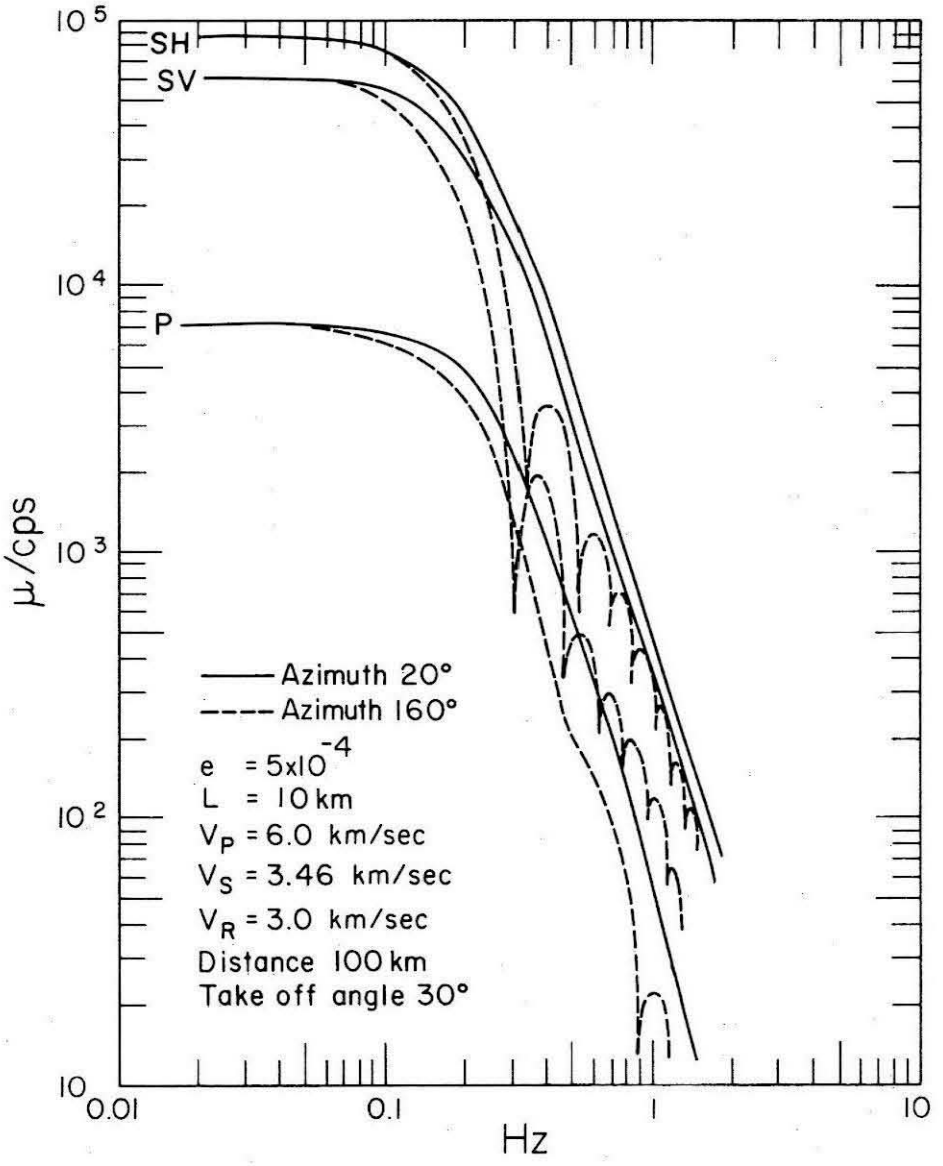

Figure VII-3-1. Azimuthal dependence of displacement spectra.

We should comment on the remark made earlier that the convergence of the multipolar expansion is slower for back azimuths. A total of ten multipoles have been added to compute the spectra of figure VII-3-1. To check the convergence of the series, we compared the partial sum of five multipoles with figure VII-3-1. The result is that convergence is practically attained with only five terms at the forward azimuth, while ten multipoles are not quite sufficient in the other case. In fact, the details of the high-frequency spectra at azimuth 160° can be slightly modified by adding a few more multipoles, particularly for frequencies higher than 0.5 cps. Our numerical experiments indicate that the spectral levels shown on this figure are a little too high, so that the average slope will be increased by the additional terms.

Figure VII-3-1 also illustrates how the "corner frequency" may depend on azimuth. No comment is needed except to emphasize once again that such a concept can only be used in a gross sense, and that a suitable averaging over all directions should be performed in evaluating it.

ii) Radiation patterns

In order to better illustrate the azimuthal dependence of the radiated field, we computed radiation patterns at periods of 20, 10, 5, and 2 seconds. These radiation patterns for P, SV, and SH waves were computed at constant take-off angle 30°, for the same model as used in figure VII-3-1 for two rupture velocities. They are given in figures VII-3-2 through VII-3-4. In addition, because of the obvious symmetry

of the source, only one half of the pattern in given in each case. The left-hand side of each figure corresponds to V_R = 3 km/sec and the right-hand side to V_R = 1 km/sec . For completeness, both amplitude and phase are shown as a function of azimuth.

The simplest patterns are obtained at long periods, where the radiation field is dominantly quadrupole in all cases, and where no effect of the rupture velocity can be noted. We note, however, a slight alteration of these patterns at a period of ten seconds, and, by comparison with figure VII-3-1, this corresponds, of course, to a period where higher degree multipoles begin to be felt. We see that the holes in the amplitude pattern are not as pronounced, the phase discontinuities not as sharp, and we also note a very slight distortion towards the direction of rupture propagation.

At shorter periods, these effects are much more pronounced, and the patterns change very rapidly with frequency. At the same time, several phenomena take place: it seems that the SH pattern at 5 seconds possesses a rather strong monopole component, while P and SV develop apparently dominant dipole components at the same period. We know that this cannot be the case since the solution used for the computation contains neither monopole nor dipole (see section IV-2). It may thus clearly be misleading to try and deduce the multipolar content of a radiation field from observations at one frequency, and one take-off angle. The converse situation is also true: for instance, a dipole could be excited such as in the solution of section IV-3, but its contribution could be negligible at some frequencies and certain directions (for instance, in the holes of the dipole spectrum).

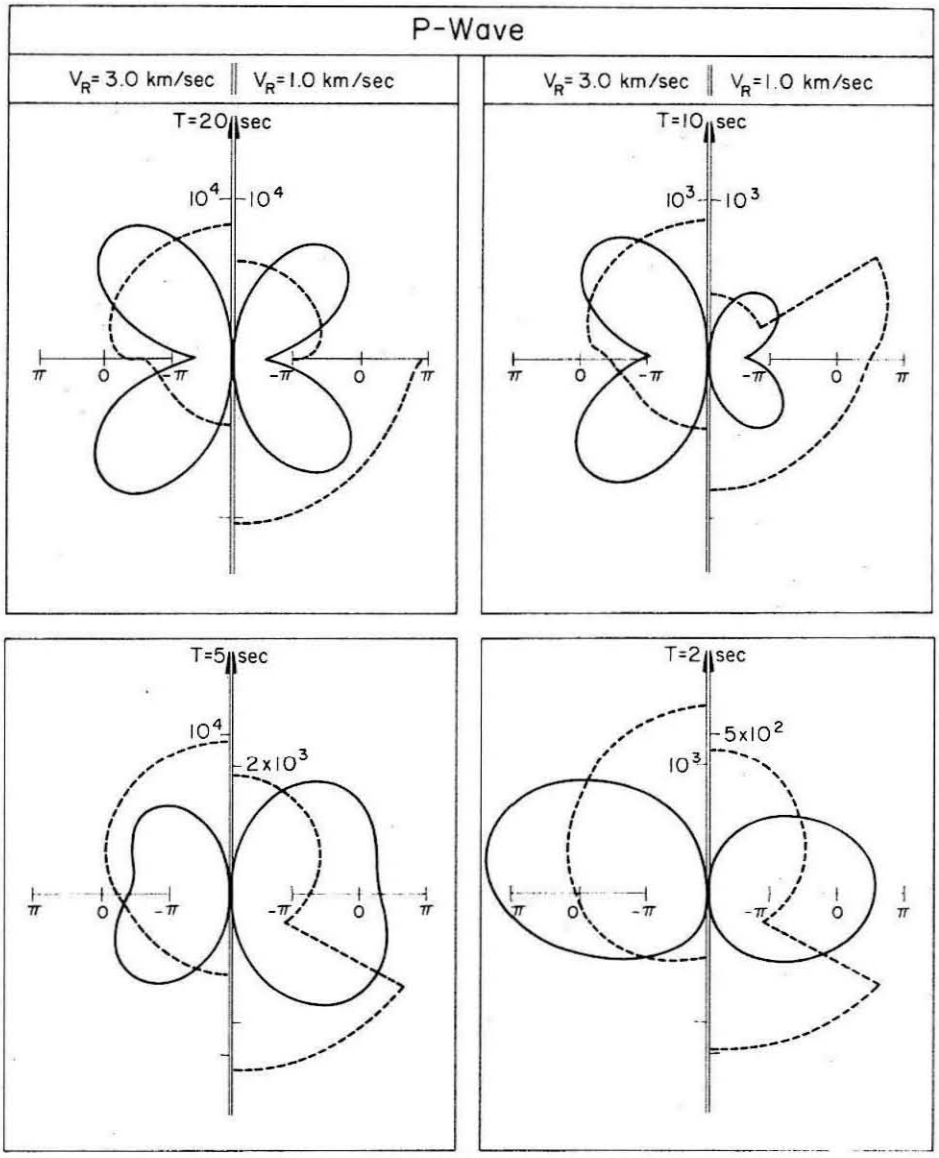

Figure VII-3-2. P-wave radiation patterns at four periods, and for two rupture velocities. Only half-patterns are shown. The solid line is the amplitude pattern; the broken line is the phase pattern.

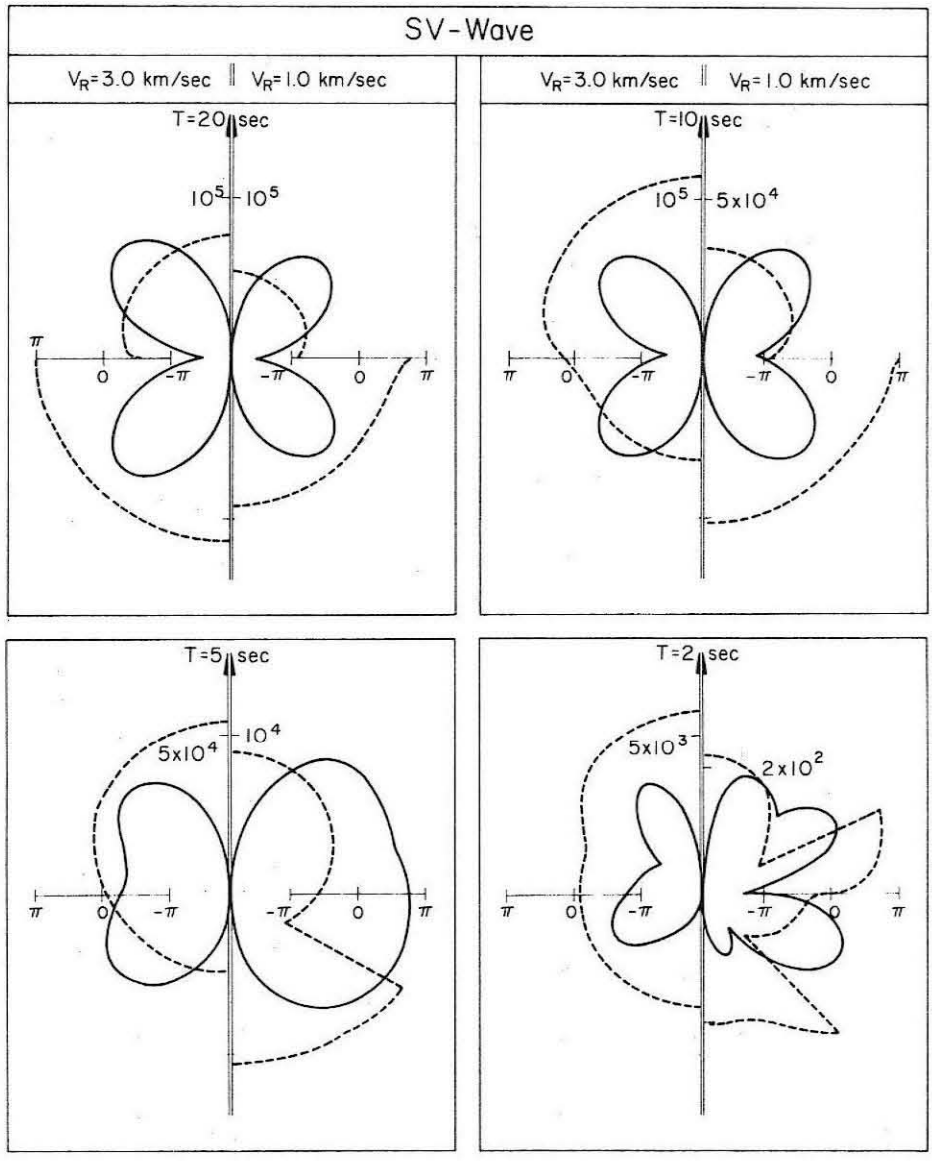

Figure VII-3-3. Same as figure VII-3-2. SV-wave.

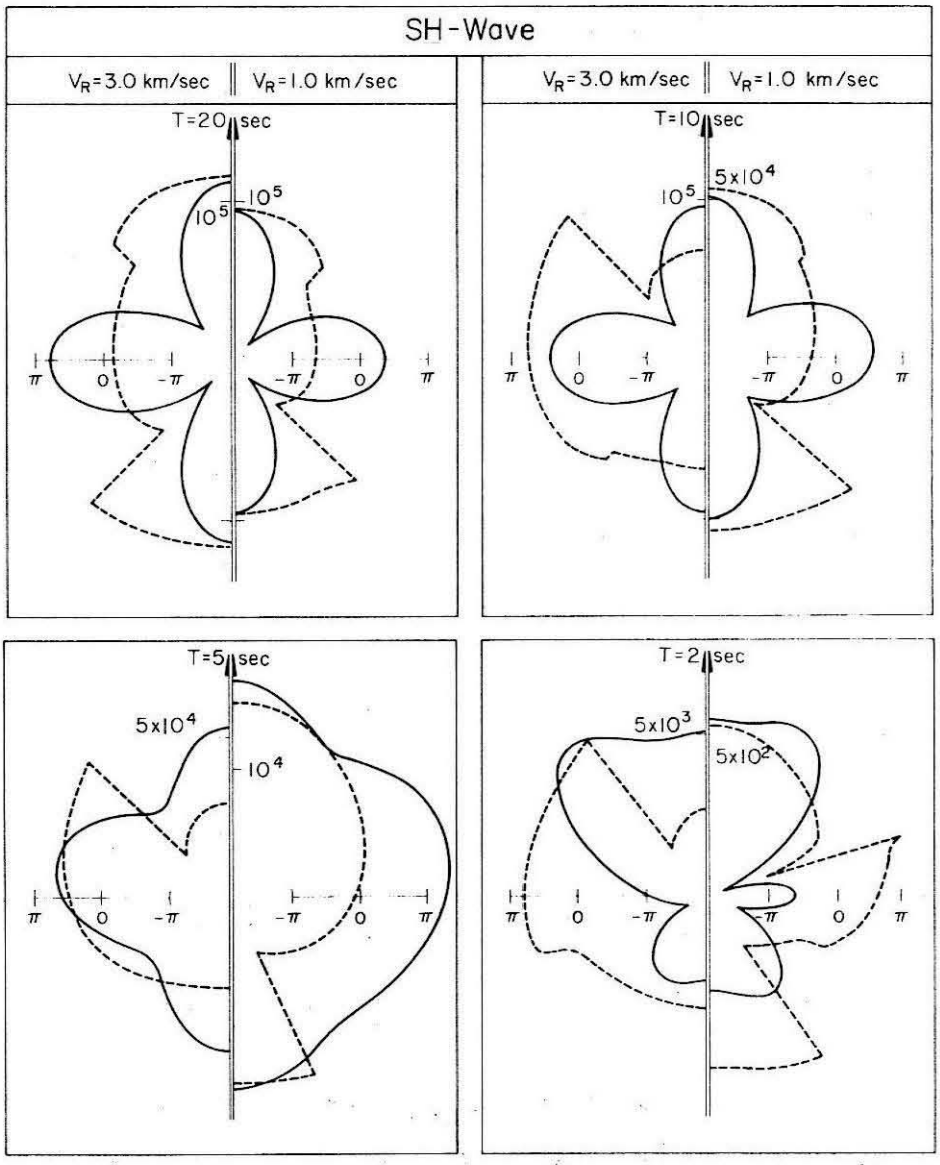

Figure VII-3-4. Same as figure VII-3-2. SH-wave.

Note that the details of the SV and SH radiation patterns at two seconds and for low rupture velocity are probably not real, and would be altered by adding a few more multipoles.

In all cases we observe that more high frequency energy is radiated in the direction of rupture propagation than in the other direction, and that this effect is stronger for higher rupture velocity. All of the short period patterns are indeed distorted in a forward direction. This was to be expected, and is consistent with similar results in electromagnetism (e.g., Stratton, 1941).

It is clear from these figures that the quadrupole is no longer dominant at high frequencies. In fact, no multipole dominates. It is fascinating to see that ten multipoles, with individual patterns of great complexity, can add up to yield such simple results. This requires a very particular combination of their amplitudes and phases, which could be easily destroyed if an error is made in the calculation. We may thus consider this simplicity as an indirect check of the correctness of our calculation.

Finally, let us note that the loss of the quadrupolar character of the radiation field--at high frequencies--does not invalidate the determination of focal mechanism from first motion data. Indeed, the direction of first motions, which is a time domain concept, is essentially controlled by the very beginning of the rupture. It cannot be associated in any way with the radiation pattern at any particular frequency, which depends on the whole time series. In fact, in order to retrieve a theoretical time series from the spectra given here, one must know the phase spectra as well. This is the object of the next section.

VII-4 The phase spectra

In order to eventually be able to retrieve time domain information from spectral results--in particular, to construct synthetic seismograms --one must know the phase spectra as well at the amplitude spectra. Because the phase is rather more sensitive than the amplitude to numerical uncertainties, we only tried in this preliminary investigation to study it for frequencies lower than 1 cps. We shall recall that convergence problems started to be important for higher frequencies (see figure VII-3-1).

Although it is sufficient to know a phase angle modulo 2π , there are a number of advantages in "unwinding" the phase spectrum. This is true in particular for purposes of interpolation, and also to study the slope of the phase spectrum as a function of frequency (group delay). We also confine ourselves to the far-field case since near-field effects may be evaluated analytically (see section IV-5).

Figure VII-4-1 shows the phase spectra for various displacement components, computed at a hypocentral distance of 100 km, or ten source dimensions. The immediate observation is that, even at such a short distance, the phase spectrum is overwhelmed by the propagation term--$k_\alpha r$. The spectra are very linear, and show very little fine structure (at least in that particular direction). The figure also shows that an additional term is present in the spectra, which depends quite strongly on the rupture velocity V_R . This is definitely a source effect, and it appears to be strong enough to be detectable in close range observations. A slow rupture velocity yields a steeper phase spectrum, and thus implies a larger group delay at the source.

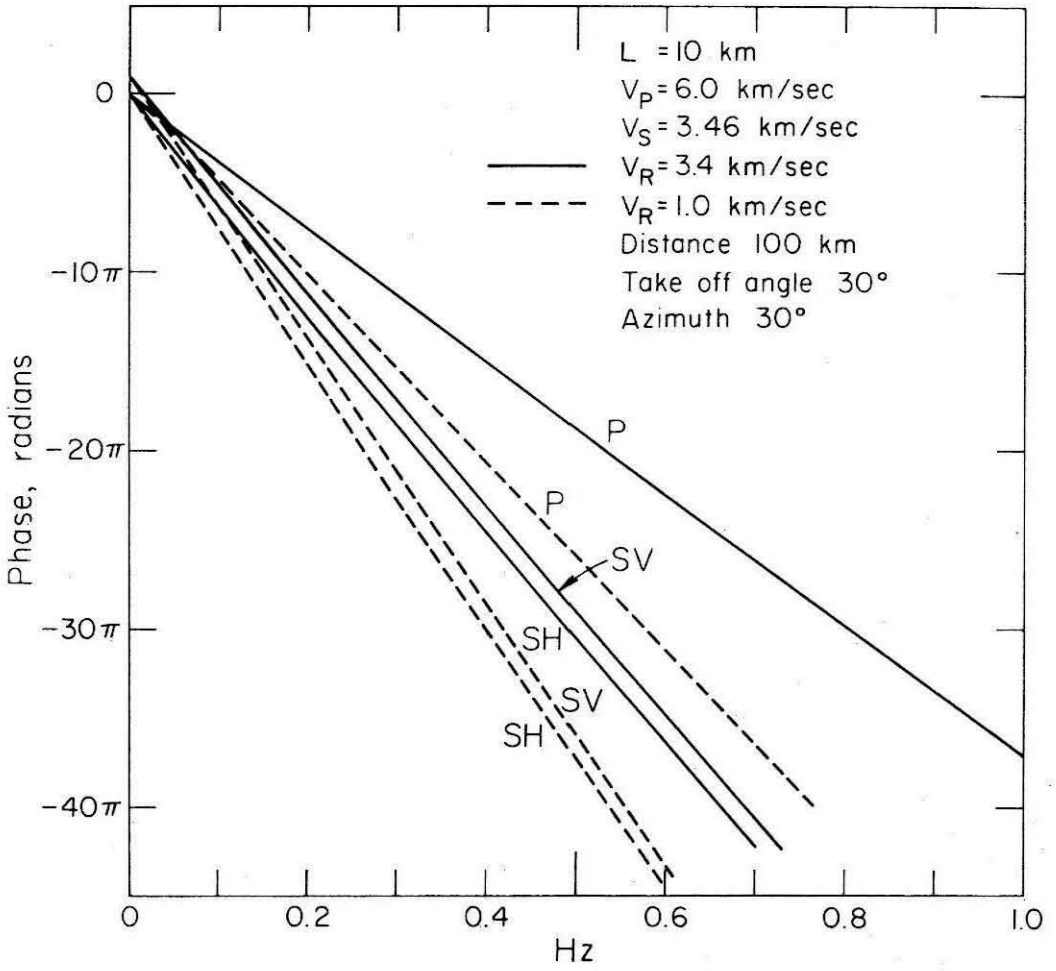

Figure VII-4-1. Far-field phase spectra computed at a distance of ten source dimensions, and for two rupture velocities.

When the propagation term $-k_\alpha r$ is removed (figure VII-4-2), one is left with the phase at the source. This is the initial phase of an equivalent multipolar point source (see Chapter V). This reduced phase spectrum is much more interesting, and yields important information about the rupture phenomenon.

First of all, the initial phase does not depend linearly on frequency. This means that our source model is inherently dispersive. As discussed in section IV-5, one defines the group delay at the source by

$$t_g(\omega) = -\frac{\partial(\text{phase})}{\partial\omega} = \frac{-1}{2}\frac{\partial(\text{phase})}{\partial f} \qquad \text{(VII-4-1)}$$

Since the steeper slopes in figure VII-4-2 occur at long periods, we deduce that long-period radiation is rather more delayed than high frequency radiation. This delay clearly increases with decreasing rupture velocity, and it is not difficult to see that the long-period group delay is of the order of L/V_R, the rupture duration. This is quite consistent with the results of section IV-5. Recall that we found the long-period delay to be $0.75\ L/V_R$ for a stationary source. We have confirmed this result on the basis of numerical calculations not shown here. For propagating sources (figure VII-4-2) we see that the delay is closer to L/V_R, and that it is slightly larger for S-waves than for P-waves at this particular azimuth.

Just as we predicted in Chapter IV, the group delay tends towards zero at high frequencies. This is especially clear for S-waves and for high rupture velocities. The group delay for P-waves does not converge

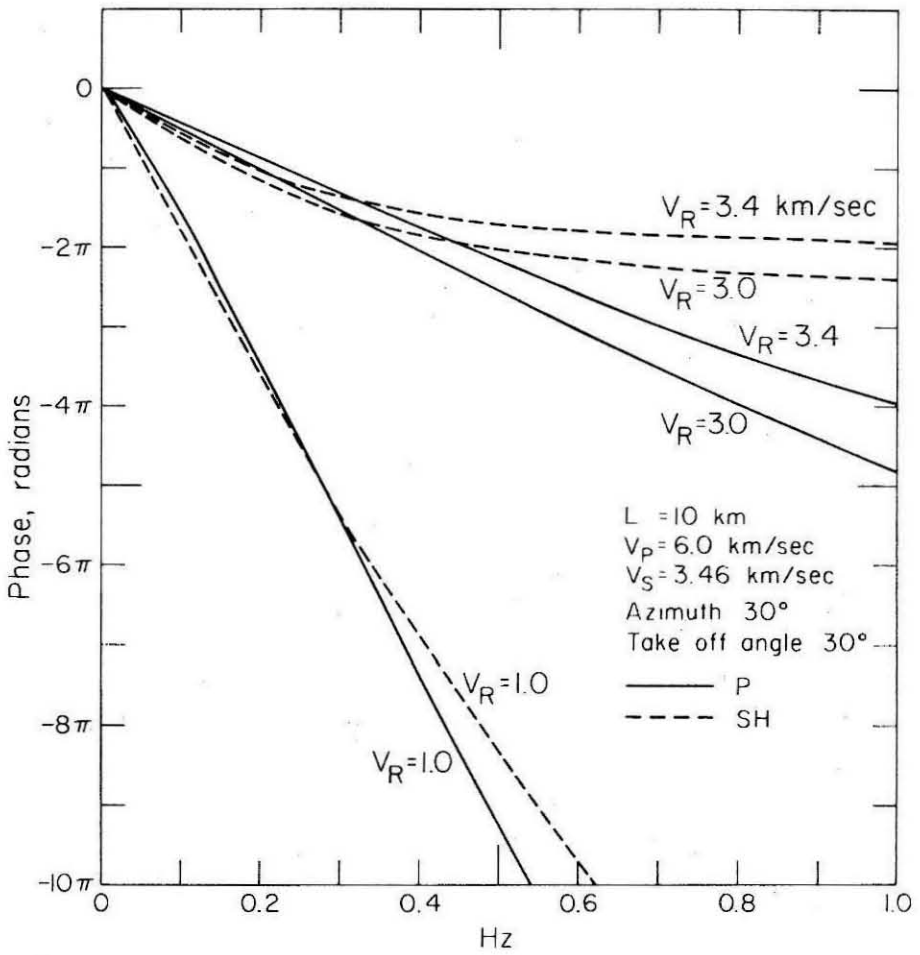

Figure VII-4-2. Far-field phase spectra corrected back to equivalent point source. Effects of rupture velocity.

to zero as rapidly, and this can be intuitively explained by noting that V_R stays rather small compared to V_p, even when it approaches V_s. As a result, our source model is less dispersive for P-waves at low to intermediate frequencies than it is for S-waves. Of course, one wonders whether this is azimuthally dependent. Figure VII-4-3 shows phase spectra (at the source) computed for three different azimuths, and at constant take-off angle. It is immediately obvious that, just as the amplitude spectra, the phase spectra become more complicated as back azimuths. The portions marked with question marks correspond to frequency bands where the phase varies extremely rapidly with frequency. Each one of these bands is associated with a hole in the amplitude spectrum, while the regions where the phase varies smoothly with frequency are to be correlated with peaks of the amplitude (see e.g., figure VII-3-1). When the phase varies rapidly, it can only be unwound by sampling it very densely. Because our frequency sampling was not dense enough, each one of the jumps shown in figure VII-4-3 is only known up to an undetermined number of full cycles (2π). Furthermore, since the holes in the amplitude spectra are due to destructive interference phenomena, these frequency bands are precisely those for which numerical noise is critical. On the other hand, and for exactly the same reason, little power is radiated in the same frequency bands, so that spectral details in such bands are not essential.

Outside the narrow frequency bands where the phase varies rapidly, one notices little azimuthal dependence of the slope. The strongest dependence is found for the P-wave, for which the group delay at the source is slightly smaller at forward azimuths than at back azimuths.

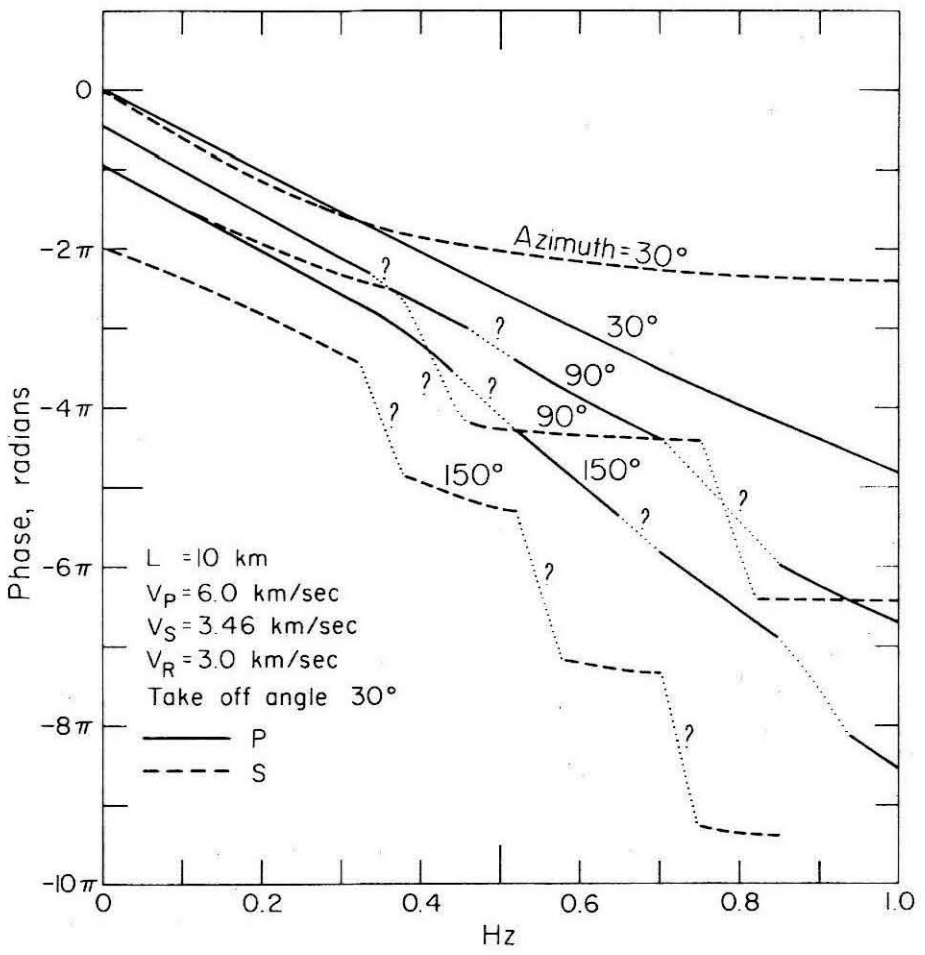

Figure VII-4-3. Far-field phase spectra corrected back to equivalent point source. Azimuthal dependence.

This is consistent with the idea advanced earlier that the radiation field "sees" a slower rupture velocity at back azimuths. Azimuthal effects seem to be smaller at long periods, which was also to be expected.

The fact that P- and S-waves may have different group delays at the source is somewhat unsettling and deserves further discussion. It seems to indicate that P- and S-waves should exhibit different apparent origin times. This effect has been called the "Z" phenomenon. The International Dictionary of Geophysics gives the following definition:

> "Z phenomenon: it has been suggested that the main P and S waves may issue from some earthquake foci at times separated by the order of some seconds. Such a separation is called the Z phenomenon, but it is now thought to be much less significant than formerly."

Observational evidence for such a discrepancy in P and S apparent origin times is relatively abundant in the seismological literature prior to 1950. For example, Jeffreys (1927) found that the linear travel time equations for the direct P- and S-waves from two British earthquakes had different constant terms by two or three seconds. The S radiation appeared to have originated earlier than the P radiation. Having observed this phenomenon in several other instances, Jeffreys (1937) concluded that the two waves both originated from the rupture zone but at different times. Gutenberg and Richter (1943) developed an explanation of the phenomenon first suggested by Reid (1918) and used later by Benioff (1938). This explanation calls for a transsonic rupture velocity, that is, such that $V_s < V_R < V_p$. If this is the case, they

argue, the first arrival of the S-wave actually comes from the point on the fault which is closest to the observer, while the P-wave first arrival comes from the point of initial rupture, hence the discrepancy in origin times. As pointed out by Bullen (1963), the concept fell into disuse and thus into obscurity after the work of Richter (1950). Richter plotted P arrival times against S-P times for several Southern California earthquakes and defined the origin time as the intercept of this curve for S-P = 0 . This method presents the advantage of yielding origin times independent of the velocity (at constant Poisson ratio), but also the procedure will hide a hypothetical Z phenomenon by a shift of the origin time. In fact, if the Z phenomenon really takes place, the origin times so obtained should be slightly too late, and thus the mean velocities deduced from them slightly too high. If one tries in turn to locate an earthquake by using this high velocity, either the solution may be difficult to find, or the hypocentral depth will be too shallow.

Figure VII-4-2 shows that no transsonic rupture velocity is required for the occurrence of the Z phenomenon. We have here a frequency dependent effect, but since we are only talking about arrival times, and since instrument responses are generally band-limited, this dependence may be neglected. From figures VII-4-2 and VII-4-3, we see that in the case V_R = 3.0 km/sec , V_s = 3.5 km/sec , the group delay for S-waves at 1 sec is practically negligible, while that for P-waves is of the order of two or three seconds. This matches Jeffreys' (1927) observations very well. Furthermore, this result is only weakly dependent on azimuth.

The phenomenon is even more pronounced for low rupture velocities. For instance, for V_R = 1.0 km/sec, figure VII-4-2 shows that at .5 cps

the S delay is 6.5 sec while the P delay is 9.5 sec, a Z phenomenon of three seconds.

To go even further along this line of discussion, one may wonder whether premonitory apparent changes in the V_p/V_s ratio before earthquakes (e.g., Whitcomb and others , 1973) could not be partly interpreted as a source effect. In order to create an apparent decrease of that ratio, one only needs to assume that the failure mechanism of small events preceding larger ones changes--for example, V_R may increase so that S-P decreases. Thus, the premonitory phenomenon would not be due to a wave propagation effect only, but also due to a change in the failure characteristics of the medium. The dilemma will be solved by obtaining conclusive data both from local and from teleseismic events. Although this is the object of much current research, we feel that the question is still open at this time. This is a vast subject, full of promising ramifications, and this is not the proper place for an extensive discussion.

Although it is probably too early to reach definitive conclusions, we suggest that the long forgotten Z phenomenon may have to be revived, and that only careful observations will prove or disprove it. Since it is rather difficult to retrieve the initial phase of the radiated fields with sufficient accuracy, we propose the following procedure: seismic records could be filtered by narrow band causal filters, and the S-P times could be plotted against frequency for several events with neighboring foci. Changes in group delays at the source from event to event might be observed in this fashion. This is, of course, subject to improvements, and further theoretical and numerical work is needed in

that respect.

Before leaving the subject, we should point out that only the curvature of the phase spectrum, as well as the slope difference between S and P, are of importance. The linear trend present in the spectrum will only yield a net shift in the origin time, which is of course impossible to retrieve from observations of arrival times only.

VII-5 Evaluation of the model

The examples given in the previous sections give a general idea of the radiation fields predicted by our model. Let us now turn to an evaluation of how this model compares with observations, and with completely numerical models. The present section does not do justice either to the flexibility of the model, or to the large body of observations currently available (e.g., Tucker, et al., 1973; Hanks, 1973). But, then again, an extensive discussion would be too voluminous to insert here.

i) Magnitude data

As mentioned earlier, the spectral shape which our model predicts, and the scaling laws presented in this chapter permit us to discuss the relationship between the body-wave magnitude m_b and the surface-wave magnitude M_s. Of course, because magnitude scales have been empirically defined from time domain observations (e.g., Richter, 1958), a quantitative comparison can only be made by computing synthetic seismograms and following the usual procedure to calculate magnitudes. However, by plotting the S-spectral amplitude at a period of 20 seconds against the P amplitude at one second as a function of source dimension, one obtains an idea of the character of the m_b/M_s curve predicted by the model. A sketch of such plots is given on figure VII-5-1, for three relaxation radii and three rupture velocities. The axes are scaled so as to correspond to the source and medium parameters used in the previous sections. The distance was kept constant and equal to 100 km.

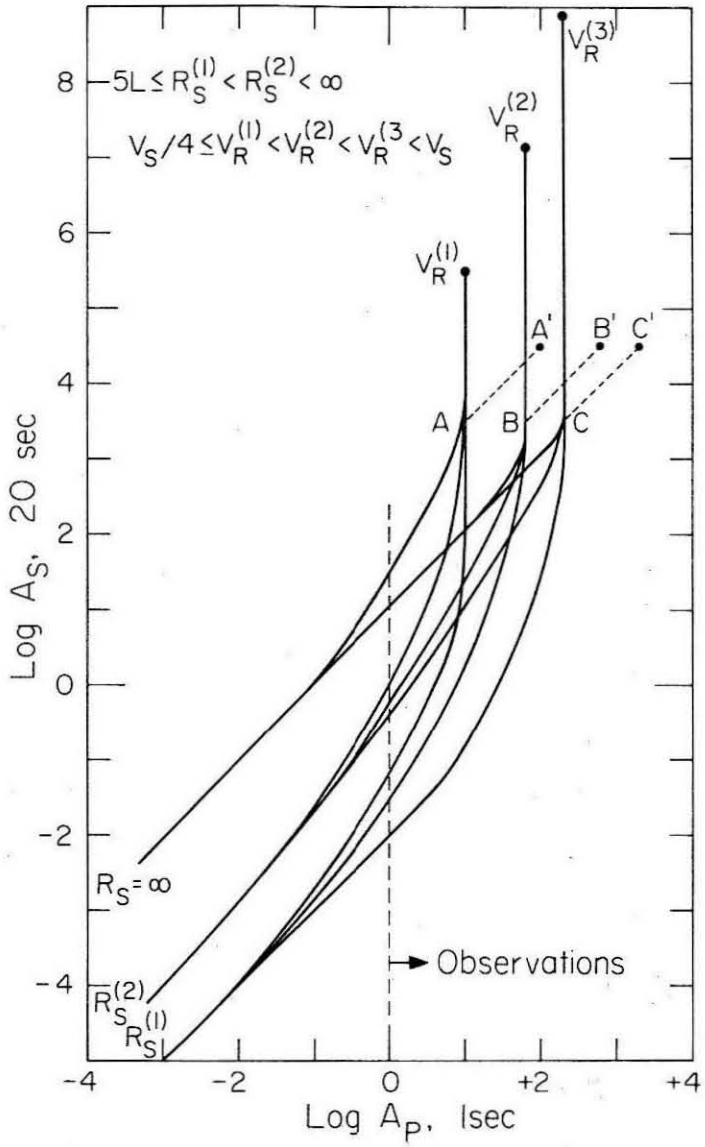

Figure VII-5-1. Plot of S spectral amplitude at 20 seconds versus P spectral amplitude at 1 second period. Simulation of m_b / M_s plots.

The low magnitude part of the graph is controlled by R_s and the large magnitude part by the rupture velocity. The net result is that a band of possible observations is defined in the $m_b - M_s$ plane, which allows for much scatter in the data. In addition, a change of the prestress yields a shift of the whole graph along a direction inclined at 45° on the axes. Since there is an observational cut-off, we do not expect to observe the lower part of the curves. Furthermore, we pointed out in Chapter IV that R_s may equal many source dimensions for small events so that the observations should cluster towards the upper limit of the zone defined in figure VII-5-1 for low magnitudes.

The diagram predicts an upper bound for both m_b and M_s, at fixed prestress. In particular, the curves bend sharply upwards when the bound on m_b is reached. The bend occurs for a fault dimension between 5 km and 10 km, depending on the rupture velocity. This corresponds to a magnitude between 5 and 6. Of course, an increase in the prestress would bring the points A,B,C to A',B',C' respectively, and this complicates the problem. The latitude offered by the three parameters V_R, R_s, and the prestress level may account for the very large scatter of the observations (Evernden, 1973, personal communication).

The character of these curves provides an explanation as to why no earthquake with local magnitude larger than 6 ½ has been observed in Southern California (Hanks, 1973, personal communication). Furthermore, observations of a large number of events with widely differing locations and depths show that the m_b/M_s diagram does indeed exhibit this character, in spite of the scatter (Evernden, 1973, personal communication).

Figure VII-5-1 shows an upper bound for M_s as well, which agrees with the observations since no earthquake with magnitude greater than 9 has ever been recorded. However, when the rupture velocity equals the shear velocity, we saw earlier that the S-spectrum has a high frequency slope of ω^{-2} and thus M_s should be unbounded. But it seems difficult to envision a rupture propagating for 700 km or 800 km at the shear velocity since this would require very high stress levels on a large regional scale.

Let us again emphasize that spectral levels are not simply related to time domain amplitudes, so that we shall confine ourselves here to this qualitative discussion.

ii) Comparison with numerical models

Cherry (1973) constructed a two dimensional fault model for which the rupture propagation is controlled by a failure criterion such as the one described in Chapter III. A minimum of plastic work is required before failure, and a dynamic friction is imposed on the rupture surface. The radiation field is calculated by combining a finite element technique with a finite difference scheme for the time dependence.

Figure VII-5-2 shows the near-field radiation obtained by Cherry at a particular station. The components x and y are measured parallel and orthogonal to the fault line respectively. Also shown on the figure is the radiation spectrum calculated from our model, using the average rupture parameters obtained by Cherry. The agreement is very good at high frequency. In particular, both models predict an average slope of ω^{-3}. On the other hand, one observes a discrepancy at long periods.

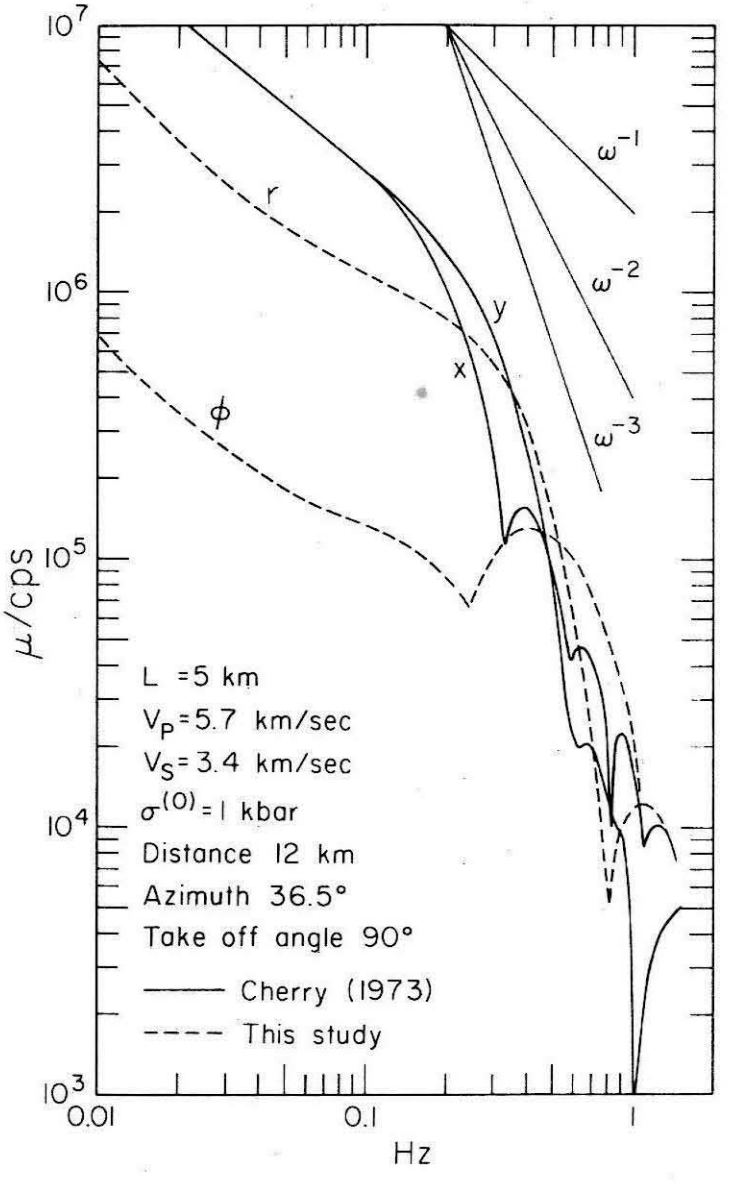

Figure VII-5-2. Comparison of spherical rupture model with results from a two-dimensional numerical finite difference code.

The field is practically radial for both models, but we predict a smaller relative long-period amplitude -- by a factor of 4 .

Recall however, that Cherry uses a two dimensional model, while we use a three dimensional one, and since the distance is about two rupture dimensions, the finiteness of the fault should not be neglected. Furthermore,Cherry assumes a significant hydrostatic pressure, while we have a pure shear prestress; it is also rather difficult to evaluate the effects due to different boundary conditions, both on the fault surface, and at large distances: Cherry "freezes" the fault when the relative velocity of the two lips vanishes--unless the shear stress exceeds the dynamic friction--and thus he may freeze the fault in an "overshot" configuration†.

In spite of the extreme differences between the two models, the agreement shown on figure VII-5-2 is still excellent. The corner frequency chosen by Cherry (1973) at .3 cps is almost exactly that predicted by our model, and since the high frequency spectra are quite comparable, it is likely that the far-field spectra would also compare favorably.

iii) The Harris Ranch earthquake of 27 October 1969

Figure VII-5-3 shows an example of spectral data compared with

---

† Cherry (1973, personal communication) overestimated his spectral levels by a factor of 2π . Thus the two models can be better reconciled, since we must then scale our prestress to 160 bars, which is of the order of his static stress drop ($\sim$ 110 bars) and his dynamic stress drop ($\sim$ 250 bars). The long-period difference is thus geometrical.

a theoretical spectrum. The data were computed by McEvilly and Johnson (1973). This is a displacement amplitude spectrum computed for the Harris Ranch earthquake of 27 October 1969. This was a magnitude 4.6 strike-slip event on the San Andreas fault system; the focal depth was 12.5 km; the epicentral distance was 1.25 km; the spectrum shown corresponds to the EW component, and the entire wave train shown on figure VII-5-4b was used to compute it. The theoretical spectrum was simply obtained by use of the scaling laws from one of the cases computed earlier. We see that a good fit is obtained for a rupture length of 1.4 km, a rupture velocity of 3.0 km/sec, a prestress of 300 bars, and a relaxation radius of about 10 fault lengths. The interaction of the incident wave with the free surface was simply taken into account by doubling the free-space amplitude.

Of course, we are not capable of reproducing the high frequency details of the spectrum, which are most likely due to surface layering, and which come from the long coda shown on figure VII-5-4b. However, the general shape of the spectrum is matched reasonably well. It is probable that the slightly high spectral amplitude predicted by the model around 1 cps could be corrected by using, for example, a slightly lower rupture velocity. The fit is good at long periods, and a finite value of R_s is required to match the marked trough at 0.1 cps. Note that the very long-period slope of the observed spectrum is steeper than ω^{-1}, which suggests that there is significant contamination by long-period noise.

There is no doubt that this fit could be improved by suitable manipulation of the fault parameters. For instance, one could try a

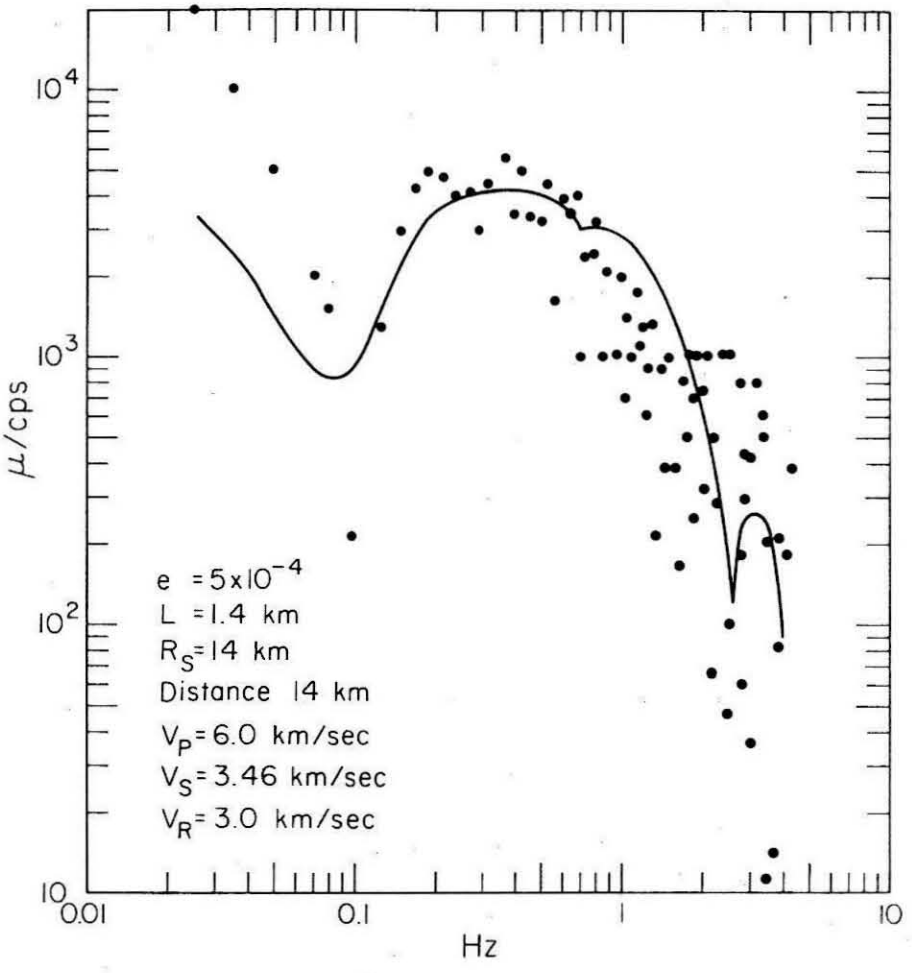

Figure VII-5-3. Comparison of observed spectrum from the Harris Ranch earthquake of 27 October 1969 with theoretical spectrum from the propagating spherical rupture model.

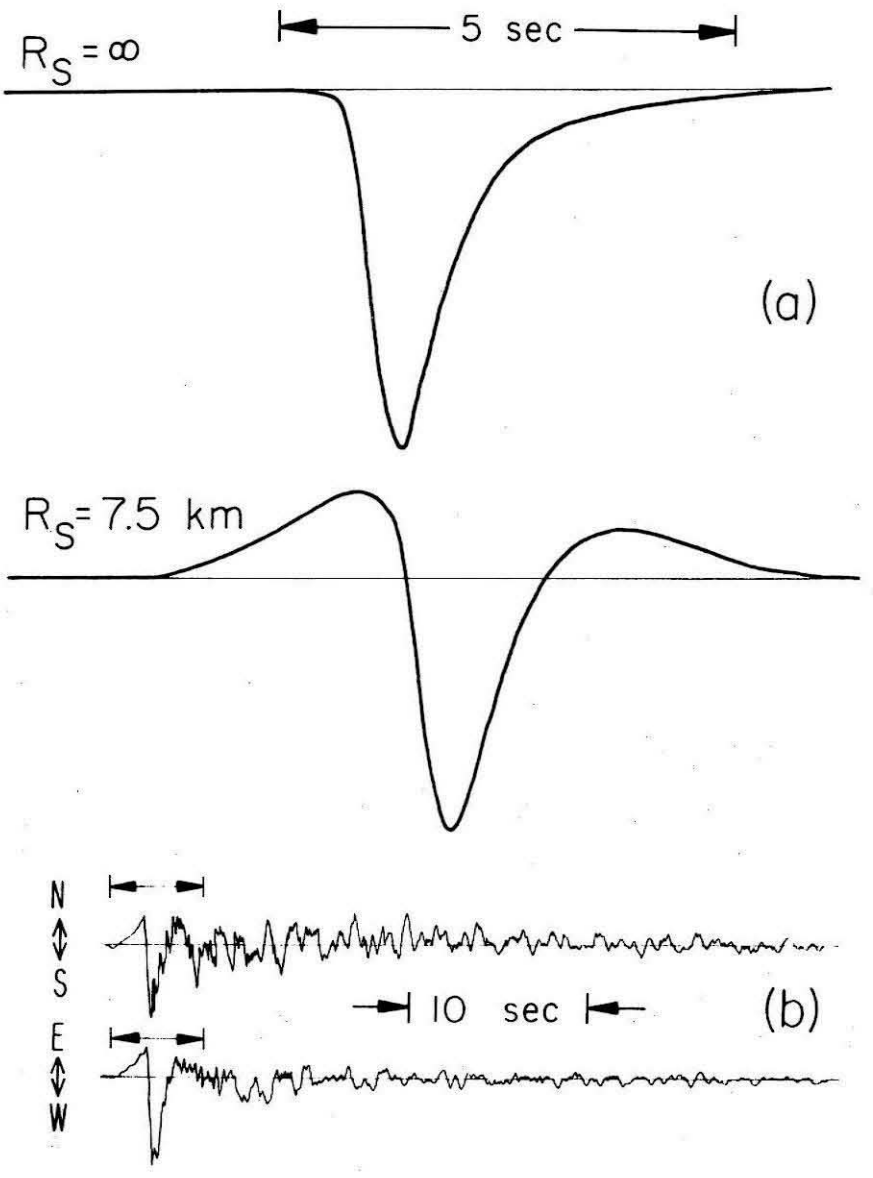

Figure VII-5-4. a) Wave forms computed for spherical rupture model with equilateral growth. b) Observed ground displacement from the Harris Ranch earthquake of 27 October 1969.

larger rupture dimension, combined with a smaller prestress, then a smaller value of R_s would be required. But the results shown here are sufficient for our present purposes. In particular, it seems that a finite value of R_s is required in order to match the long-period spectrum. The trough seen at about 0.1 cps is also present on the NS component (McEvilly and Johnson, 1973). This feature should be translated into a particular pulse shape in the time domain.

Figure VII-5-4 shows synthetic far-field pulses computed for a stationary spherical rupture of radius 750 m. When R_s is infinite, the pulse is unipolar (e.g., Molnar, et al., 1973). This is no longer the case where R_s is finite. It is easy to compare qualitatively these pulse shapes with the seismograms shown below them. McEvilly and Johnson (1973) show that these records represent essentially the ground displacement except at very long periods (tilts). It is clear that a finite value of R_s is suggested by the time domain data as well.

The rather qualitative comparisons presented above are only preliminary results in an effort to systematically compare model and observations. We should make note of the fact that Tucker and Brune (1973) observed flat spectra for many aftershocks of the San Fernando earthquake, observed at close range. Thus their data suggest that R_s should be very large compared with the fault dimensions for those events. Although any precise statement concerning the comparison of data and model would require a more complete study, we can nevertheless state that the results of this section are very encouraging.

GENERAL CONCLUSION

The present work is essentially open ended, both from the theoretical point of view and from the point of view of its applications. As we mentioned at the very beginning, even more questions are raised than are answered. Because this is the case, it is not superfluous to stress again the underlying philosophy. The failure model and the elastodynamic treatment given here are very crude and quite sophisticated at the same time. The crudeness comes from the geometry that we chose, and from the many approximations and idealizations involved in the mathematical treatment. The sophistication lies in the flexibility of the model, obtained by allowing for a sufficient number of parameters. The most appealing aspect of the model is that it can be readily generalized in many ways, and that these generalizations can be made on a physical basis. This is an enormous advantage over kinematical models which leave little place for the physics of the phenomenon.

However, it is essential to investigate all the properties of a model in its simplest form, before even thinking of generalizing it. Only through such a systematic procedure can one determine which effect is due to which cause. It is a shortcoming of very realistic and thus complex models that one cannot, in general, determine a single cause for a particular effect. Thus, as a rule, generalizations should only be implemented as they are required by the observations.

As we see it, the next step following this study will be to systematically compare the model with existing data. The results shown in the last chapter probably do not even cover all the possible features

offered by this model, and, lengthy as the procedure may be, all the details of the predicted radiation field should be investigated and evaluated against a background of data. Only then shall we be in a position to decide which model characteristic should be modified. Eventually, the comparison will lead to conclusions as to the physical conditions surrounding failure of earth materials and earthquakes. The last results shown are most encouraging and enhance our belief that the method will prove successful.

BIBLIOGRAPHY

Abramowitz, M., and Stegun, I.A., 1964, *Handbook of Mathematical Functions*. National Bureau of Standards, Applied Mathematics Series 55.

Aki, K., 1967, Scaling Law of Seismic Spectrum, *J. Geophys. Res.*, *72*, 1217.

Aki, K., 1968, Seismic Displacements near a Fault, *J. Geophys. Res.*, *73*, 5359.

Aki, K., Reasenberg, P., DeFazio, T.,and Tsai, Y.B., 1969, Near-Field and Far-Field Evidence for Triggering of an Earthquake by the BENHAM Explosion, *Bull. Seismol. Soc. Amer.*, *59*, 2197.

Alewine, R.W. III, and Jordan, T.H., 1973, Generalized Inversion of Earthquake Static Displacement Fields, *Geophys. J. Roy. Astr. Soc.*, *35*, (in press).

Alewine, R.W. III, and Jungels, P.H., 1973, Application of Stochastic Inversion Theory and the Finite Element Method to Zero-Frequency Seismology, *Geophys. J. Roy. Astr. Soc.*, (in press).

Alexander, S.S., 1963, *Surface Wave Propagation in the Western United States*, Ph.D. Thesis, California Institute of Technology.

Anderson, D.L., Minster, J.B., and Cole, D., 1973, The Effect of Oriented Cracks on Seismic Velocities, *J. Geophys Res.*, (in press).

Archambeau, C.B., 1964, *Elastodynamic Source Theory*, Ph.D. Thesis, California Institute of Technology.

Archambeau, C.B., 1968, General Theory of Elastodynamic Source Fields, *Rev. of Geophys.*, *6*, 241.

Archambeau, C.B., 1972, The Theory of Stress Wave Radiation from Explosions in Prestressed Media, *Geophys. J. Roy. Astr. Soc.*, *29*, 329.

Archambeau, C.B., J.C. Bradford, P.W. Broome, W.C. Dean, E.A. Flinn, and R.L. Sax, 1965, Data Processing Techniques for the Detection and Interpretation of Teleseismic Signals, *I.E.E.E. proceedings*, *53*, 1860.

Archambeau, C.B., and Sammis, C., 1970, Seismic Radiation from Explosions in Prestressed Media and the Measurement of Tectonic Stress in the Earth, *Rev. of Geophys.*, *8*, 473.

Arscott, F.M., 1964, *Periodic Differential Equations*, Macmillan, N.Y.

Barenblatt, G.I., 1959, Concerning Equilibrium Cracks Forming during Brittle Fracture : The Stability of Isolated Cracks, Relationships with Energetics Theories, *Appl. Math. Mech.*, *23*, 1273.

Benioff, H., 1938, The Determination of the Extent of Faulting with Application to the Long Beach Earthquake, *Bull. Seismol. Soc. Amer.*, *28*, 77.

Ben-Menahem, A., 1962, Radiation of Seismic Body Waves from a Finite Moving Source inthe Earth, *J. Geophys. Res.*, *67*, 345.

Ben-Menahem, A., 1962, An Operational Representation of the Addition Theorems for Spherical Waves, *J. of Math. and Phys.*, XLI, 201.

Ben-Menahem, A., and Singh, S.J., 1968, Multipolar Elastic Fields in a Layered Half Space, *Bull. Seismol. Soc. Amer.*, *58*, 1519.

Ben-Menahem, A., Smith, S.W., and Teng, L.T., 1965, A Procedure for Source Studies from Spectrums of Long Period Seismic Waves, *Bull. Seismol. Soc. Amer.*, *55*, 203.

Berckhemer, H., and Jacob, K.H., 1968, Investigation of the Dynamical Process in Earthquake Foci by Analysing the Pulse Shape of Body Waves, *Final Sci. Rep. AF61(052)-801, Air Force Cambridge Research Laboratories.*

Brace, W.F., and Byerlee, J.D., 1966, Stick-slip as a Mechanism for Earthquakes, *Science*, *153*, 990.

Brune, J.N., 1970, Tectonic Stress and the Spectra of Seismic Shear Waves from Earthquakes, *J. Geophys. Res.*, *75*, 4997. Corrected, 1971, *J. Geophys. Res.*, *76*, 5002.

Bullen, K., 1963, *Introduction to the Theory of Seismology*, Cambridge University Press, N.Y.

Burdick, L., and Helmberger, D.V., 1973, Time Functions Appropriate for Deep Earthquakes, (Abstract), Seismol. Soc. Amer.

Burridge, R., 1969, Spherically Symmetric Differential Equations, the Rotation Group, and Tensor Spherical Functions, *Proc. Camb. Phil. Soc.*, *65*, 1957.

Burridge, R., and Alterman, Z., 1972, The Elastic Radiation from an Expanding Spherical Cavity, *Geophys. J. Roy. Astr. Soc.*, *30*, 451.

Burridge, R., and Halliday, G.S., 1971, Dynamic Shear Cracks with Friction as Models for Shallow Focus Earthquakes, *Geophys. J. Roy. Astr. Soc.*, *25*, 261.

Burridge, R., and Knopoff, L., 1964, Body Force Equivalents for Seismic Dislocations, *Bull. Seismol. Soc. Amer.*, *54*, 1875.

Byerlee, J.D., and Brace, W.F., 1968, Stick-slip, Stable Sliding, and Earthquakes, *J. Geophys. Res.*, *73*, 6031.

Carslaw, H.S., and Jaeger, J.C., 1959, *Conduction of Heat in Solids*, Oxford, Clarendon Press.

Cherry, T., 1973, Calculation of Near-field Earthquake Ground Motion, *SSS-R-73-1759*, Systems, Science and Software, Annual Report, A.R.P.A. order nb. 2134.

Cherry, T., C.B. Archambeau, G.A. Frazier, A.J. Good, K.G. Hamilton, and D.G. Harkrider, 1972, The Teleseismic Radiation Field from Explosions, *SSS-R-72-1193*, Systems, Science and Software, Final Report, Contract nb. DASA-01-71-C-0156.

Coleman, B.D., 1964, Thermodynamics of Materials with Memory, *Arch. Rational Mech. Anal.*, *17*, 1.

Courant, R., and Hilbert, D., 1937, *Methods of Mathematical Physics*, third printing, 1966, Interscience, Wiley, N.Y.

Dahlen, F.A., 1973, Elastic Dislocation Theory for a Self-gravitating Elastic Configuration with an Initial Stress Field, *Geophys. J. Roy. Astr. Soc.*, *31*, 357.

De Hoop, A.T., 1958, *Representation Theorems for the Displacement in an Elastic Solid*, Ph. D. Thesis, Technische Hogeschool, Delft, Netherlands.

Dziewonski, A.M., and Gilbert, F.M., 1973, Temporal Variation of the Seismic Moment Tensor and the Evidence of Precursive Compression for Two Deep Earthquakes, *Nature*, (in press).

Edmonds, A.R., 1957, *Angular Momentum in Quantum Mechanics*, Princeton University Press.

Erdelyi, A., 1953, *Bateman Manuscript Project*, *Higher Transcendental Functions*, *vol. 1, 2, 3*, *Tables of Integral Transforms*, *vol. 1, 2*, McGraw and Hill.

Eshelby, J.D., 1956, The Continuum Theory of Lattice Defects, *Solid State Physics*, *3*, 79.

Eshelby, J.D., 1957, The Determination of the Elastic Field of an Ellipsoidal Inclusion, and Related Problems, *Proc. R. Soc. A241*, 376.

Ferrers, 1877, *Spherical Harmonics*, London.

Freund, L.B., 1972, Energy Flux into the Tip of an Extending Crack in an Elastic Solid, *Journal of Elasticity*, 2, 341.

Friedman, B., and Russek, J., 1954, Addition Theorems for Spherical Waves, *Quart. Appl. Math.*, *12*, 13.

Futterman, W.I., 1962, Dispersive Body Waves, *J. Geophys. Res.*, *67*, 5279.

Gel'fand, I.M., Minlos, R.A., and Shapiro, Z.Y., 1963, *Representations of the Rotation and Lorentz Groups and Their Applications*, Permagon Press, N.Y.

Gilbert, F., and Helmberger, D.V., 1972, Generalized Ray Theory for a Layered Sphere, *Geophys. J. Roy. Astr. Soc.*, *27*, 57.

Gottfried, K., 1966, *Quantum Mechanics*, Benjamin, N.Y.

Gradshteyn, I.S., and Ryshik, I.M., 1965, *Table of Integrals, Series, and Products*, Academic Press, N.Y. and London.

Griffith, A.A., 1921, The Phenomenon of Rupture and Flow in Solids, *Phil. Trans. Roy. Soc. London, Ser. A*, *221*, 163.

Griggs, D., and Handin, J., 1960, Observation on Fracture and Hypothesis of Earthquakes, *Geol. Soc. Amer. Mem. 79*, 347.

Gutenberg, B., and Richter, C.F., 1943, Apparent Origin Time of $\overline{S}$, *Bull. Seismol. Soc. Amer.*, *33*, 269.

Hanks, T.C., 1972, *A Contribution to the Determination and Interpretation of Seismic Source Parameters*, Ph. D. Thesis, California Institute of Technology.

Hanks, T.C., 1973, The Faulting Mechanism of the San Fernando Earthquake, *J. Geophys. Res.*, (in press).

Hanks, T.C., and Thatcher, W., 1972, A Graphical Representation of Seismic Source Parameters, *J. Geophys. Res.*, *77*, 4393.

Hanks, T.C., and Wyss, M., 1972, The Use of Body Wave Spectra in the Determination of Seismic Source Parameters, *Bull. Seismol. Soc. Amer.*, *62*, 561.

Harkrider, D.G., 1964, Surface Waves in Multilayered Elastic Media, I, Rayleigh and Love Waves from Sources in a Multilayered Half-Space, *Bull. Seismol. Soc. Amer.*, *54*, 627.

Harkrider, D.G., 1970, Surface Waves in Multilayered Elastic Media, II, Higher Mode Spectra and Spectral Ratios from Point Sources in Plane Layered Earth Models, *Bull. Seismol. Soc. Amer.*, *60*, 1937.

Harkrider, D.G., and Archambeau, C.B., 1973, Theoretical Rayleigh and Love Waves from Explosions in Prestressed Source Regions, (in preparation)

Haskell, N.A., 1964, Total Energy and Energy Spectral Density of Elastic Wave Radiation from Propagating Faults, *Bull. Seismol. Soc. Amer.*, *54*, 1811.

Haskell, N.A., 1966, Total Energy and Energy Spectral Density of Elastic Wave Radiation from Propagating Faults, Part 2, Statistical Source Model, *Bull. Seismol. Soc. Amer.*, *56*, 125.

Haskell, N.A., 1967, Analytic Approximation for the Elastic Radiation from a Contained Underground Explosion, *J. Geophys. Res.*, *66*, 2937.

Haskell, N.A., 1969, Elastic Displacements in the Near-field of a Propagating Fault, *Bull. Seismol. Soc. Amer.*, *59*, 865.

Helmberger, D.V., and Wiggins, R.A., 1971, Upper Mantle Structure of Mid-Western United States, *J. Geophys. Res.*, *76*, 3229.

Hobson, E.W., 1931, *The Theory of Spherical and Ellipsoidal Harmonics*, Cambridge University Press.

Ida, Y., 1970, Thermodynamic Problems Related to Growth of Magma, *J. Geophys. Res.*, *75*, 4051.

Ida, Y., 1972, Cohesive Force across the Tip of a Longitudinal-Shear Crack and Griffith's Specific Surface Energy, *J. Geophys. Res.*, *77*, 3796.

Ida, Y., 1973, Stress Concentration and Unsteady Propagation of Longitudinal-Shear Cracks, *J. Geophys. Res.*,*78*, 3418.

Ida, Y., and Aki, K., 1972, Seismic Source Time Function of Propagating Longitudinal-Shear Cracks, *J. Geophys. Res.*, *77*, 2034.

International Dictionary of Geophysics, 1967, S.K. Runcorn, Editor, Permagon Press.

James, R.W., 1969, Transformation of Spherical Harmonics under Change of Reference Frame, *Geophys. J. Roy. Astr. Soc.*, *17*, 305.

Jahnke, E., and Emde, F., 1909, *Functionentafeln*, 1945, 4th Edition, Dover, N.Y.

Jeffreys, H., 1927, On two British Earthquakes, *Mon. Not. Roy. Astr. Soc., Geophys. Suppl.*, *1*, 483.

Jeffreys, H., 1931, On the Cause of Oscillatory Movements in Seismograms, *Mon. Not. Roy. Astr. Soc., Geophys. Suppl.*, 2, 407.

Jeffreys, H., 1937, A Further Study of Near Earthquakes, *Mon. Not. Roy. Astr. Soc., Geophys. Suppl.*, 4, 196.

Jeffreys, Sir Harold, 1970, *The Earth*, 5th Edition, Cambridge U. Press.

Johnson, L.A., 1973, A Collection of Solutions to Lamb's Problem, (unpublished manuscript).

Jordan, T.H., 1972, *Estimation of the Radial Variation of Seismic Velocities and Density in the Earth*, Ph. D. Thesis, California Institute of Technology.

Julian, B.R., and Anderson, D.L., 1968, Travel Times, Apparent Velocities and Amplitudes of Body Waves, *Bull. Seismol. Soc. Amer.*, 58, 339.

Jungels, P.H., 1973, *Modeling of Tectonic Processes Associated with Earthquakes*, Ph. D. Thesis, California Institute of Technology.

Jungels, P.H., and Fazier, G.A., 1973, Finite Element Analysis of the Residual Displacements for an Earthquake Rupture: Source Parameters for the San Fernando Earthquake, *J. Geophys. Res.*, 78, 5062.

Kostrov, B.V., 1966, Unsteady Propagation of Longitudinal-Shear Cracks, *Appl. Math. Mech.*, 30, 1241.

Kupradze, V.D., 1963, *Dynamical Problems in the Theory of Elasticity*, in *Progress in Solid Mechanics*, vol III, Sneddon and Hill, North Holland, Amsterdam.

Lambert, D.G., Flinn, E.A., and Archambeau, C.B., 1972, A Comparative Study of the Elastic Wave Radiation from Earthquakes and Underground Explosions, *Geophys. J. Roy. Astr. Soc.*, 29, 403.

Landau, L., and Lifchitz, E., 1967, *Theorie de l'Elasticite*, Editions Muir, Moscou.
1951, *Theory of Elasticity*, Addison-Wesley.

Lifchitz, I., and Rosentsveig, L., 1947, in *Journal de Physique Experimentale et Theorique*, 17, 783.

Linde, A.T., and Sacks, I.S., 1971, Errors in the Spectral Analysis of Long Period Seismic Body Waves, *J. Geophys. Res.*, 76, 3326.

Linde, A.T., and Sacks, I.S., 1972, Dimensions, Energy, and Stress Release for South American Deep Earthquakes, *J. Geophys. Res.*, *77*, 1439.

Love, A.E.H., 1927, *A Treatise on the Mathematical Theory of Elasticity*, Cambridge University Press.

Love, A.E.H., 1911, *Some Problems in Geodynamics*, Dover, 1967.

Luke, Y.L., 1969, *The Special Functions and Their Approximations*, Academic Press, N.Y. and London.

Malvern, L.E., 1969, *Introduction to the Mechanics of a Continuous Medium*, Prentice-Hall.

Maruyama, T., 1963, On the Force Equivalents of Dynamical elastic Dislocations with Reference to the Earthquake Mechanism, *Bull. Earthq. Res. Inst. Tokyo*, *41*, 467.

McEvilly, T., and Johnson, L., 1973, Near-field Accelerometer Array, A.R.P.A. Technical Report nb.2, A.R.P.A. order nb. 2134.

McGinley, J.R., 1969, *A Comparison of Observed Permanent Tilts and Strains Due to Earthquakes with Those Calculated from Displacement Dislocations in Elastic Earth Models*, Ph. D. Thesis, California Institute of Technology.

Miller, W.Jr., 1964, Some Applications of the Representation of the Euclidean Group in Three-space, *Communications on Pure and Applied Mathematics*, XVII, 527.

Misner, C.W., Thorne, K.S., and Wheeler, J.A., 1973, *Gravitation*, Freeman.

Mitchell, B.J., and Helmberger, D.V., 1973, Shear Velocities at the Base of the Mantle from Observations of S and ScS, *J. Geophys. Res.*, *78*, 6009.

Mogi, K., 1971, Fracture and Flow of Rocks under Triaxial Compression, *J. Geophys. Res.*, *76*, 1255.

Molnar, P., 1971, P-wave Spectra from Underground Nuclear Explosions, *Geophys. J. Roy. Astr. Soc.*, *23*, 273.

Molnar, P., Jacob, K., and McCamy, K., 1973, Implications of Archambeau's Earthquake Source Theory for Slip on Faults, *Bull. Seismol. Soc. Amer.*, *63*, 101.

Morse, P.M., and Feshbach, H., 1953, *Methods of Theoretical Physics*, vol. I and II, McGraw and Hill.

Niazi, M., 1973, Earthquake Source Dynamics from Far-field Amplitude and Phase Spectra of Body Waves, *Geophys. J. Roy. Astr. Soc.*, (in press).

O'Connell, R.J., and Wasserburg, G.J.,1972, Dynamics of Submergence and Uplift of a Sedimentary Basin Underlain by a Phase Change Boundary, *Rev. of Geophys.*, *10*, 335.

Orowan, E., 1960, Mechanism of Seismic Faulting, in *G.S.A. memoir 79, Rock Deformation*, 323.

Phinney, R., and Burridge, R., 1973, Representation of the Elastic-Gravitational Excitation of a Spherical Earth Model by Generalized Spherical Harmonics, *Geophys. J. Roy. Astr. Soc.*, (in press).

Press, F., and Archambeau, C.B., 1962, Release of Tectonic Strain by Underground Nuclear Explosions, *J. Geophys. Res.*, *67*, 337.

Randall, M.J., 1964, On the Mechanism of Earthquakes, *Bull. Seismol. Soc. Amer.*, *54*, 1283.

Randall, M.J., 1966, Seismic Radiation from a Sudden Phase Transition, *J. Geophys. Res.*, *71*, 5297.

Randall, M.J., 1971, Elastic Multipole Theory and Seismic Moment, *Bull. Seismol. Soc. Amer.*, *61*, 1321.

Randall, M.J., 1973, Spectral Peaks and Earthquakes Source Dimension, *J. Geophys. Res.*, *78*, 2609.

Randall, M.J., 1973, Low Frequency Spectra in Seismic Waves from Explosions, *Geophys. J. Roy. Astr. Soc.*, *32*, 387.

Reid, H.F., 1918, The Starting Points of Earthquake Vibrations, *Bull. Seismol. Soc. Amer.*, *8*, 79.

Richter, C.F., 1950, Velocities of P at Short Distances, *Bull. Seismol. Soc. Amer.*, *40*, 281.

Richter, C.F., 1958, *Elementary Seismology*, Freeman.

Robinson, K., 1951, Elastic Energy of an Ellipsoidal Inclusion in an Infinite Elastic Solid, *J. Appl. Phys.*, *22*, 1045.

Sack, R.A., 1946, Extension of Griffith's Theory of Rupture to Three Dimensions, *Proc. Phys. Soc. London, 58*, 729.

Sadowsky, M.A., and Sternberg, E., 1949, Stress Concentration around a Triaxial Ellipsoidal Cavity, *J. Appl. Mech., 71*, 149.

Satô, Y., 1950, Transformation of Wave Functions Related to the Transformation of Coordinate Systems, *Bull. Earthq. Res. Inst. Tokyo, 28*, I and II.

Savage, J.C., 1966, Radiation from a Realistic Model of Faulting, *Bull. Seismol. Soc. Amer., 56*, 577.

Scholz , C., Molnar, P., and Johnson, T., 1972, Detailed Studies of Frictional Sliding and Implications for the Earthquake Mechanism, *J. Geophys. Res., 77*, 6392.

Steketee, I.A., 1958, Some Geophysical Applications of the Elasticity Theory of Dislocations, *Can. J. Phys., 36*, 1168.

Stakgold, I., 1968, *Boundary Value Problems of Mathematical Physics*, vol. I and II, Macmillan, N.Y.

Stratton, J.A., 1941, *Electromagnetic Theory*, McGraw and Hill.

Trifunac, M.D.,1973, A Three-Dimensional Dislocation Model for the San Fernando, California, Earthquake of February 9, 1971, *Bull. Seismol. Soc. Amer.*, (in press).

Trifunac, M.D., and Hudson, D.E., 1971, Analysis of the Pacoima Dam Accelerogram, San Fernando, California, Earthquake of 1971, *Bull. Seismol. Soc. Amer., 61*, 1393.

Truesdell, C., 1965, Thermodynamics of Deformation, in *Non-Equilibrium Thermodynamics, Variational Techniques and Stability*, 101, University of Chicago Press.

Truesdell, C., and Noll, W., 1965, The Non-linear Field Theories of Mechanics, in *Encyclopedia of Physics*, ed. S. Flügge, vol.3/3, Berlin, Springer Verlag.

Truesdell, C., and Toupin, R.A., 1960, The Classical Field Theories, in *Encyclopedia of Physics*, ed. S. Flügge, vol. 3/1, Berlin, Springer Verlag.

Tucker, B.E., and Brune, J.N., 1973, Seismograms, S-wave Spectra, and Source Parameters for Aftershocks of February 9, 1971, San Fernando Earthquake, Preprint.

Turnbull, L.S., 1973, Characteristics of an Ellipsoidal Volume Source in a Layered Half Space, *Trans. Amer. Geophys. Union, 54,* 366.

Usami, T., Odaka, T., and Satô, Y., 1970, Theoretical Seismograms and Earthquake Mechanism, *Bull. Earthq. Res. Inst. Tokyo, 48,* 533.

Volterra, V., 1907, Sur 1'Equilibre des Corps Elastiques Multiplement Connexes, *Ann. Ec. Norm. Sup., ser 3, 24,* 401, Paris.

Whitcomb, J.H., Garmany,J.D., and Anderson, D.L., 1973, Earthquake Prediction: Variations of Seismic Velocities before the San Fernando Earthquake, *Science, 180,* 632.

Whittaker, E.T., and Watson, G.N., 1927, *A Course of Modern Analysis,* 4th Edition, reprinted 1969, Cambridge University Press.

Wyss, M., 1970, Stress Estimates for South American Shallow and Deep Earthquakes, *J. Geophys. Res., 75,* 1529.

Wyss, M., and Brune, J.N., 1967, The Alaska Earthquake of 28 March 1964: A Complex Multiple Rupture, *Bull. Seismol. Soc. Amer.,37,* 1017.

Wyss, M., and Brune, J.N., 1968, Seismic Moment, Stress and Source Dimensions for Earthquakes in the California Nevada Region, *J. Geophys. Res.,73,* 4681.

Wyss, M., and Hanks, T.C., 1972, The Source Parameters of the San Fernando Earthquake Inferred from Teleseismic Body Waves, *Bull. Seismol. Soc. Amer., 62,*591.

Wyss, M., and Molnar, P., 1972, Source Parameters of Intermediate and Deep Focus Earthquakes in the Tonga Arc, *Phys. Earth Planet. Interiors, 6,* 279.

Yokobori, T., 1965, *Strength, Fracture and Fatigue of Materials,* Noordhoff / Groningen / The Netherlands.

APPENDICES

APPENDIX 1

REYNOLDS' TRANSPORT THEOREM FOR THE CASE OF MOVING BOUNDARIES

i) Reynolds' Transport Theorem

Considering a region of a continuum undergoing a continuous flow, we first seek a description of this flow in a fixed reference frame. For this we consider the position x of a "particle," or small volume element of the continuum, and follow it as a function of time so that

$$x_i(t) = \phi_i(X,t) \quad . \tag{A-1-1}$$

Here X is the position of the particle at some reference time t_o, $X_i = \phi_i(X,t_o)$. We shall say that x is the position, at time t, of the particle X, and for convenience we assume $t_o = 0$ without loss of generality.

Equation (A-1-1) can be viewed as a (Lagrangian) mapping, and the flow is said to be continuous if this mapping is continuous. We shall further assume that the ϕ's are sufficiently differentiable so that there exists a continuous inverse mapping

$$X_i(t) = \Phi_i(x,t) \quad . \tag{A-1-2}$$

We shall further assume that a small right-handed triad moving with the flow stays right-handed as a function of time. If the flow is also regular, thereby forbidding singular points for the mapping (A-1-1), then the jacobian $J = \det\left(\frac{\partial x}{\partial X}\right)$ will be strictly positive. The velocity field V associated with that flow is then

$$V_i(x,t) = \left(\frac{\partial \phi_i}{\partial t}\right)_X \tag{A-1-3}$$

The usual form of Reynolds' transport theorem (e.g. Malvern, 1969. sec. 5-2) expresses the material time derivative of the volume integral of an arbitrary continuous tensorial function of the flow $F(\mathbf{x},t)$. The geometry is described on figure A-1-1. The surface $S(t)$ is a material surface--i.e., moving with the flow--and is to be considered instantaneously as a control surface traversed by the flow.

We wish to evaluate the quantity $\frac{d}{dt}\iiint_{V(t)} F(\mathbf{x},t)\, d^3x = \frac{df}{dt}$ where d^3x is the volume element. The main difficulty that arises is that both the integrand and the volume of integration are time dependent. We therefore transform first the integral into an integral over a fixed volume. For this we operate the change of variable of integration (A-1-1). This change of variable is a logical one since it maps the time dependent volume $V(t)$ into its initial position $V(0)$; we thus circumvent the difficulty mentioned above. We write

$$\frac{df}{dt} = \frac{d}{dt}\int_{V(o)} F\left[\phi(\mathbf{X},t),t\right] J\, d^3X \quad . \qquad \text{(A-1-4)}$$

Here we specifically assume that $J > 0$. The volume of integration is now time independent and we can write

$$\frac{df}{dt} = \int_{V(o)} \left[\frac{dF}{dt} J + F\frac{dJ}{dt}\right] d^3X \qquad \text{(A-1-5)}$$

But, by the usual differentiation rule for a determinant, we have

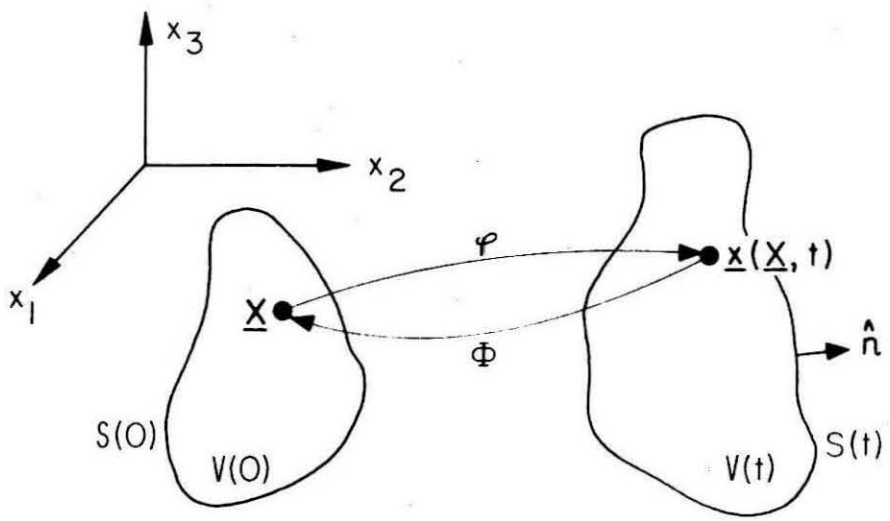

Figure A-1-1. Mappings defining the flow of a continuum, as a function of time. $V(t)$ is a material volume, moving with the flow.

$$\frac{dJ}{dt} = J_{ij} \frac{d}{dt}\left(\frac{\partial x_i}{\partial X_j}\right) = J_{ij} \frac{\partial V_i}{\partial X_j} \quad .$$

Here J_{ij} is the cofactor of the (i,j) element in J. Noting that, by simple expansion of the determinant J with respect to the jth column, $J_{ij} \frac{\partial x_k}{\partial X_j} = \delta_{ik} J$, we then write

$$\frac{dJ}{dt} = J_{ij} \frac{\partial V_i}{\partial x_k} \frac{\partial x_k}{\partial X_j} = J \delta_{ik} \frac{\partial V_i}{\partial x_k} = J \nabla_x \cdot \mathbf{V}$$

Thus (A-1-5) yields

$$\frac{df}{dt} = \int_{V(o)} \left[\frac{dF}{dt} + F \nabla_x \cdot \mathbf{V} \right] J \, d^3X$$

Or, transforming the volume of integration back to $V(t)$, we get the first form of the transport theorem.

$$\frac{d}{dt} \int_{V(t)} F(\mathbf{x},t) \, d^3\mathbf{x} = \int_{V(t)} \left[\frac{df}{dt} + F \nabla_x \cdot \mathbf{V} \right] d^3x \qquad \text{(A-1-6)}$$

Other forms are obtained by using the following relations

$$\frac{dF}{dt} = \frac{\partial F}{\partial t} + (\mathbf{V} \cdot \nabla_x) F$$

and

$$\nabla_x \cdot (F\mathbf{V}) \equiv (\mathbf{V} \cdot \nabla_x) F + F \nabla_x \cdot \mathbf{V} \quad .$$

Then

$$\frac{d}{dt} \int_{V(t)} F(\mathbf{x},t)\, d^3x = \int_{V(t)} \left[\frac{\partial F}{\partial t} + \nabla_x \cdot (F\mathbf{V}) \right] d^3x \qquad \text{(A-1-7)}$$

Or, by application of Gauss' theorem

$$\frac{d}{dt} \int_{V(t)} F(\mathbf{x},t)\, d^3x = \int_{V(t)} \frac{\partial F}{\partial t}\, d^3x + \int_{S(t)} F\, \mathbf{V} \cdot \hat{n}\, da \qquad \text{(A-1-8)}$$

The physical interpretation of (A-1-8), often used as a heuristic proof, is obvious. If $S(t)$ is instantaneously considered as a control surface then we have (e.g., Malvern, 1969)

[Rate of increase of the amount of F possessed by the material instantaneously inside S] = [rate of increase of the total amount of F inside S] + [net rate of outward flux of F carried by mass transport through S]

Because $S(t)$ is a material surface, it englobes the same mass at any time t and conservation equations can be obtained directly from (A-1-6), (A-1-7), or (A-1-8) if F is a conserved quantity (see section iv below).

ii) Generalization to the Case of Moving Boundaries

We now turn to the generalization of the transport theorem to the case of a volume $U(t)$, bounded by a surface $\Sigma(t)$, which is no longer a material surface. We shall give two derivations, the first one being somewhat more heuristic, the second one more formal.

A) First proof

Consider the flow described by (A-1-1), and a closed surface $\Sigma(t)$, surrounding a volume $U(t)$ of the continuum. We assume that $\Sigma(t)$ deforms as a function of time sufficiently smoothly so that for δt sufficiently small there exists a piecewise continuous mapping of the points of $\Sigma(t + \delta t)$ into those of $\Sigma(t)$. Obviously if such a mapping exists, it can serve to define the velocity $\mathbf{U}$ of $\Sigma(t)$ at all points of $\Sigma(t)$. The geometry is described on figure (A-1-2).

Consider the material surface $S(t)$, surrounding the volume $V(t)$, which coincides at time t with $\Sigma(t)$. Then

$$f(t) = \int_{U(t)} F(\mathbf{x},t)\, d^3x = \int_{V(t)} F(\mathbf{x},t)\, d^3x \quad . \tag{A-1-9}$$

After a small increment of time δt, we have

$$f(t + \delta t) = \int_{U(t + \delta t)} F(\mathbf{x},t)\, d^3x \quad . \tag{A-1-10}$$

But $S(t + \delta t)$ does not coincide with $\Sigma(t + \delta t)$ and we have

$$f(t + \delta t) = \int_{V(t + \delta t)} F\, d^3x + \delta t \int_{S(t + \delta t)} F\,(\mathbf{U} - \mathbf{V}) \cdot \hat{\mathbf{n}}_S\, da + 0(\delta t^2) \quad , \tag{A-1-11}$$

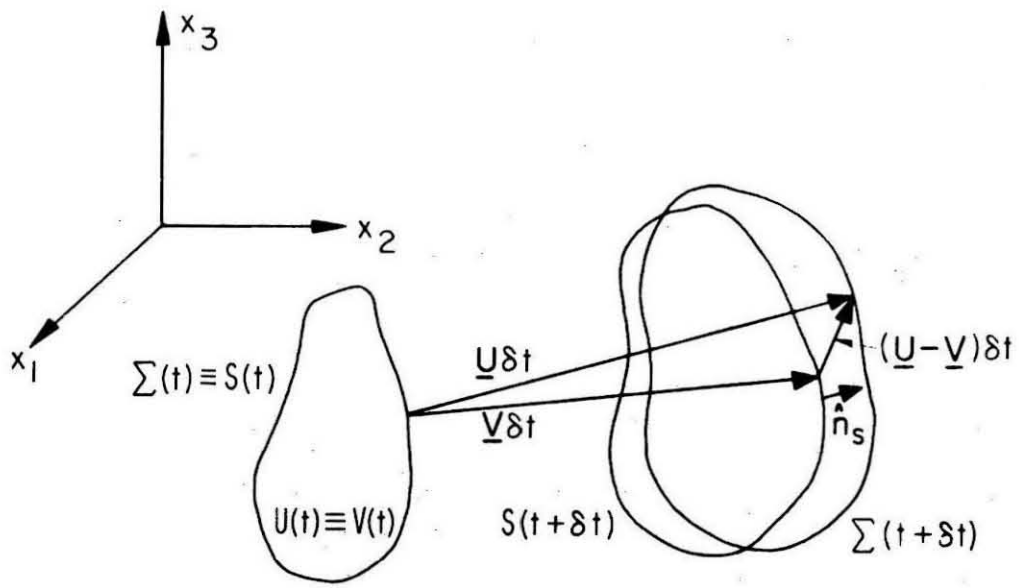

Figure A-1-2. Case of a surface $\Sigma(t)$ which is not a material surface. $\mathbf{V}$ is the material velocity, $\mathbf{U}$ the velocity of $\Sigma(t)$. $S(t)$ is a material surface coinciding with $\Sigma(t)$ at time t . $V(t)$ is bounded by $S(t)$ while $U(t)$ is bounded by $\Sigma(t)$.

where the correction term is added in order to account for the difference between the volumes $U(t + \delta t)$ and $V(t + \delta t)$.

Combining (A-1-9), (A-1-10) and (A-1-11) and defining

$$\frac{d}{dt}\int_{U(t)} F\, d^3x = \lim_{\delta t \to 0} \frac{1}{\delta t}\left[\int_{U(t+\delta t)} F\, d^3x - \int_{U(t)} F\, d^3x\right] , \tag{A-1-12}$$

we get

$$\frac{d}{dt}\int_{U(t)} F\, d^3x = \frac{d}{dt}\int_{V(t)} F\, d^3x + \int_{S(t)} F(\,\mathbf{U}-\mathbf{V}\,)\cdot \hat{\mathbf{n}}_S\, da \quad . \tag{A-1-13}$$

The transport theorem in its conventional form now applies to the first term on the right-hand side of (A-1-13); if we use (A-1-8), we obtain immediately

$$\frac{d}{dt}\int_{U(t)} F\, d^3x = \int_{V(t)} \frac{\partial F}{\partial t}\, d^3x + \int_{S(t)} F\ \ \mathbf{U}\cdot\hat{\mathbf{n}}\, da \quad ,$$

Where the material velocity $\mathbf{V}$ is no longer present. However, if we observe that at time t , the volume $V(t)$ and the material surface $S(t)$ coincide respectively with $U(t)$ and $\Sigma(t)$, we can then write

$$\frac{d}{dt}\int_{U(t)} F\, d^3x = \int_{U(t)} \frac{\partial F}{\partial t}\, d^3x + \int_{\Sigma(t)} F\ \ \mathbf{U}\cdot\hat{\mathbf{n}}\, da \quad , \tag{A-1-14}$$

which is the desired theorem. Note that (A-1-14) reduces as expected to the usual result (A-1-8) when $\mathbf{U} = \mathbf{V}$.

B) Second proof

In order to derive (A-1-14) on a more formal basis, we need to make a number of more restrictive assumptions about the volume $U(t)$. In particular, we assume that the points $\mathbf{r}_\Sigma \in \Sigma(t)$ can be described as a function of time by a mapping

$$r_{\Sigma_i}(t) = \psi_i(\mathbf{R},t) \qquad \text{(A-1-15)}$$

Here $R_i = \psi_i(\mathbf{R},0)$. However, such a mapping describing the evolution of $\Sigma(t)$ is non unique. We shall only consider here the class of surfaces $\Sigma(t)$ for which a mapping (A-1-15) can be found which is a valid description of some continuous flow. This means that we assume $\Sigma(t)$ to evolve sufficiently smoothly in time so that ψ_i can be found and defined throughout the continuum, with continuity and differentiability properties similar to those for ϕ_i . Then the value taken at $\mathbf{r}_\Sigma$ by the field

$$U_i(\mathbf{r},t) = \left(\frac{\partial \psi_i}{\partial t}\right)_R \qquad \text{(A-1-16)}$$

is defined as the velocity of $\Sigma(t)$ at $\mathbf{r}_\Sigma$. The existence of the inverse mapping

$$R_i(t) = \Psi_i(\mathbf{r}(t),t) \quad , \qquad \text{(A-1-17)}$$

is also assumed.

We now want to express $\frac{d}{dt} f(t) = \frac{d}{dt} \int_{U(t)} F \, d^3x$, and it is logical to use (A-1-1) to change the variable of integration. The mapping of the particle X through (A-1-17) can be obtained by a careful consideration of the superposition of the flows (A-1-1) and (A-1-15)--see figure A-1-3. For simplicity we shall distinguish material points X, undergoing the flow (A-1-1) and "surface" points R , undergoing the flow (A-1-15).

Consider the material point of location $\mathbf{x}(t)$ that coincides at time t with the surface point located at $\mathbf{r}(t)$. Then at that time both these points are mapped at the same location $\mathbf{X} = \Phi(\mathbf{r}, t)$ by (A-1-17). At time $t + \delta t$ the material point is located at $\mathbf{x}(t + \delta t) = \mathbf{x}(t) + \mathbf{V}\delta t$, and is still mapped into $\mathbf{X}$. But the surface point is now located at $\mathbf{r}(t + \delta t) = \mathbf{r}(t) + \mathbf{U}\delta t$. Thus at time $t + \delta t$ the surface point $\mathbf{r}(t + \delta t)$ coincides with a new material point. This last point was located <u>at time t</u> at $\mathbf{x}(t) + (\mathbf{U} - \mathbf{V})\,\delta t$ (to first order in δt). Then the surface point which was mapped at time t into $\mathbf{X}$ is now mapped into $\mathbf{X} + \mathbf{W}\delta t$, where

$$\mathbf{W} = (\mathbf{U} - \mathbf{V}) \cdot \nabla_x \Phi \qquad \text{(A-1-18)}$$

By use of the mapping (A-1-1) we have therefore reduced the original problem to the simpler equivalent problem where a surface $\Sigma_o(t)$ moves with velocity $\mathbf{W}$ through a fixed continuum (see figure (A-1-3).

This is expressed mathematically by

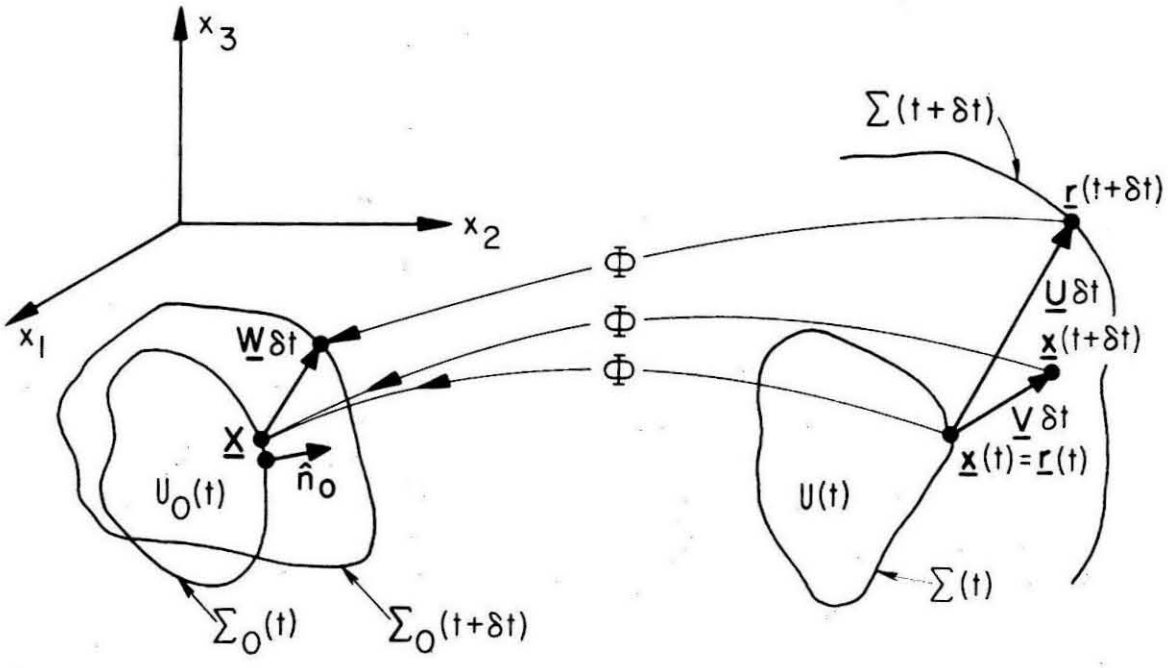

Figure A-1-3. The surface $\Sigma(t)$, bounding the volume $U(t)$, is not a material surface. Thus, if Φ is the mapping representing the flow of the medium, $\Sigma(t)$ is mapped into a time dependent surface $\Sigma_o(t)$, which has a velocity $\mathbf{W}$. $\mathbf{U}$ is the velocity of $\Sigma(t)$, $\mathbf{V}$ the velocity of the medium. Two points $\mathbf{x}$ (material point) and $\mathbf{r}$ (surface point), which coincide at time t, do not coincide any more at time $t + \delta t$.

$$\frac{df}{dt} = \frac{d}{dt} \int_{U_o(t)} F[\Phi(\mathbf{x},t),t]\ J\ d^3R$$

$$= \int_{U_o(t)} \frac{d}{dt}[FJ]\ d^3X + \int_{\Sigma_o(t)} FJ\ \ \mathbf{W}\cdot\hat{n}_o\ da \qquad \text{(A-1-19)}$$

The surface integral on the right-hand side of (A-1-19) takes into account the rate of increase of the volume U_o . Because we have defined $\mathbf{W}$ everywhere we can apply Gauss' theorem and write

$$\frac{df}{dt} = \int_{U_o(t)} \left[\frac{d}{dt}(FJ) + \frac{\partial}{\partial X_i}[FJW_i]_x\right] d^3X \qquad \text{(A-1-20)}$$

But $\frac{\partial}{\partial X_i}[FJ]_x \equiv 0$ and $\frac{\partial W_i}{\partial X_i} = \frac{\partial}{\partial X_i}(U_k - V_k)\frac{\partial \Phi_i}{\partial x_k} = \nabla_x \cdot (\mathbf{U}-\mathbf{V})$.

Using the theorem (A-1-6) in (A-1-20) we obtain immediately

$$\frac{df}{dt} = \int_{U_o(t)} \left[\frac{dF}{dt} + F\ \nabla_x \cdot \mathbf{V} + F\ \nabla_x \cdot (\mathbf{U}-\mathbf{V})\right] J\ d^3X$$

or

$$\frac{df}{dt} = \int_{U(t)} \left[\frac{dF}{dt} + F\ \nabla_x \cdot \mathbf{U}\right] d^3x \qquad \text{(A-1-21)}$$

It is then a trivial matter to transform (A-1-21) into

$$\frac{df}{dt} = \int_{U(t)} \frac{\partial F}{\partial t} + \int_{\Sigma(t)} F\mathbf{U}\cdot \hat{n}\, da \qquad \text{(A-1-22)}$$

This last equation is identical to (A-1-14), but its proof required rather stringent assumptions which were not needed for the former proof.

iii) Medium with an interior surface of discontinuity

We now turn to the case where the surface $\Sigma(t)$, of velocity $\mathbf{U}$ is a surface of discontinuity of the medium. Phase boundaries and shock fronts constitute examples of such discontinuity. The velocity of the material $\mathbf{V}$, and the flow function F are then assumed to be discontinuous across $\Sigma(t)$. For convenience, we choose the normal $\hat{n}_\Sigma$ to be such that $\mathbf{U}\cdot\hat{n}_\Sigma > 0$, i.e., $\Sigma(t)$ is now an oriented surface propagating in the direction of its positive normal. We seek to apply the transport theorem to the material volume $V(t)$ bounded by the material surface $S(t)$. As shown in figure A-1-4, the volume $V(t)$ is separated by $\Sigma(t)$ into two contiguous volumes $V_1(t)$ and $V_2(t)$, and similarly $S(t)$ is cut into two surfaces $S_1(t)$ and $S_2(t)$. We can furthermore consider $\Sigma(t)$ to be composed of two surfaces Σ_1 and Σ_2 with outer normals $-\hat{n}_\Sigma$ and $\hat{n}_\Sigma$ respectively. The transport theorem may now be applied to the two volumes $V_1(t)$ and $V_2(t)$ separately. We write

$$\frac{d}{dt}\int_{V(t)} F\, d^3x = \frac{d}{dt}\int_{V_1(t)} F\, d^3x + \frac{d}{dt}\int_{V_2(t)} F\, d^3x$$

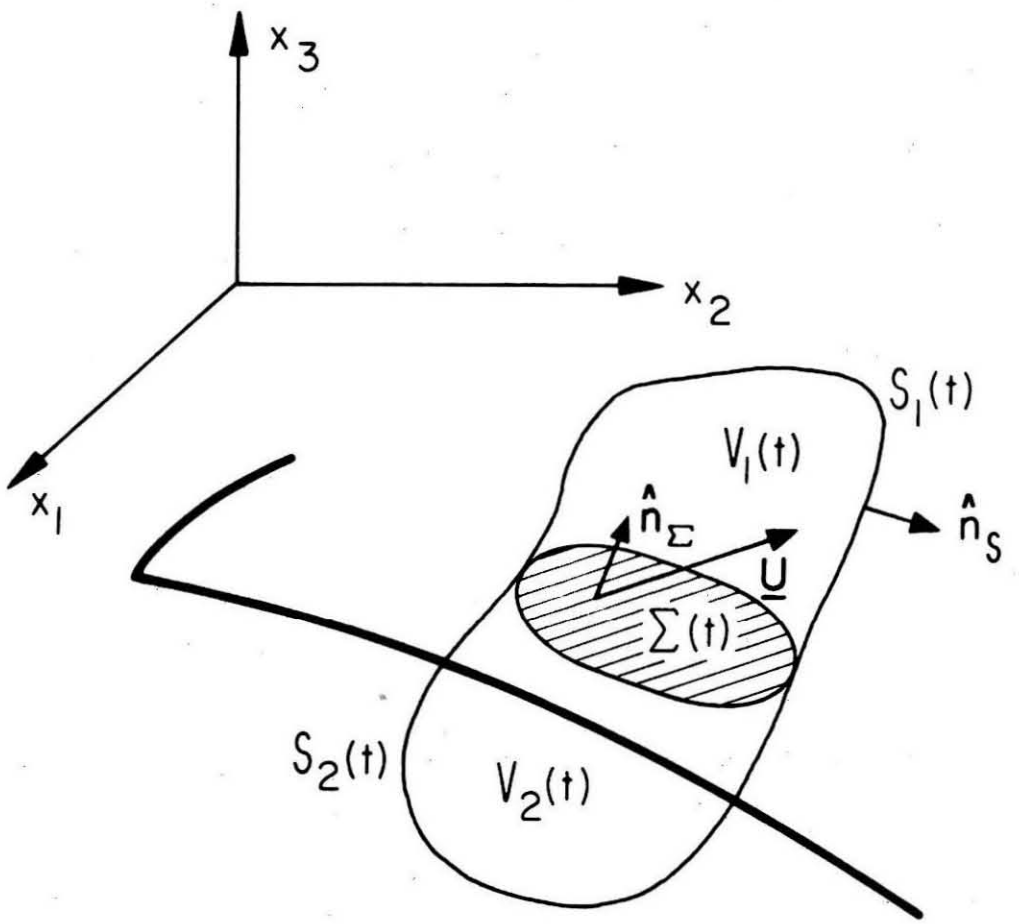

Figure A-1-4. Case of a propagating discontinuity. $\Sigma(t)$ is the surface of discontinuity, of velocity $\mathbf{U}$. $S_1(t) + S_2(t)$ is a material surface, moving with the medium.

or

$$\frac{d}{dt}\int_{V(t)} F\, d^3x = \int_{V_1(t)+V_2(t)} \frac{\partial F}{\partial t}\, d^3x + \int_{S_1(t)+S_2(t)} F\, \mathbf{V}\cdot \hat{n}_s\, da$$

$$- \int_{\Sigma_1(t)} F\, \mathbf{U}\cdot \hat{n}_\Sigma\, da + \int_{\Sigma_2(t)} F\, \mathbf{U}\cdot \hat{n}_\Sigma\, da \qquad \text{(A-1-23)}$$

The surfaces $S_1(t)$ and $S_2(t)$ are not closed surfaces and therefore we cannot apply Gauss' theorem to the surface integral over them. This can be circumvented by writing

$$\int_{S_1(t)+S_2(t)} F\, \mathbf{V}\cdot \hat{n}\, da = \int_{S_1(t)+\Sigma_1(t)} F\, \mathbf{V}\cdot \hat{n}\, da + \int_{S_2(t)+\Sigma_{2(t)}} F\, \mathbf{V}\cdot \hat{n}\, da$$

$$+ \int_{\Sigma_1(t)} F\, \mathbf{V}\cdot \hat{n}_\Sigma\, da - \int_{\Sigma_2(t)} F\, \mathbf{V}\cdot \hat{n}_\Sigma\, da$$

Here the outer normal $\hat{n}$ is defined as $-\hat{n}_\Sigma$ for $\Sigma_1(t)$ and as $\hat{n}_\Sigma$ for $\Sigma_2(t)$.

We can now apply Gauss' theorem because the surfaces $S_1(t) + \Sigma_1(t)$ and $S_2(t) + \Sigma_2(t)$ are closed, and we obtain

$$\frac{d}{dt}\int_{V(t)} F\, d^3x = \int_{V(t)} \left[\frac{\partial F}{\partial t} + \nabla_x \cdot (F\mathbf{V})\right] d^3x + \int_{\Sigma(t)} \left[\!\left[F(\mathbf{V}-\mathbf{U})\cdot \hat{n}_\Sigma \right]\!\right]_\Sigma da$$

(A-1-24)

We have introduced the notation $[\![Q]\!]_\Sigma$ to indicate the jump of the quantity Q across $\Sigma(t)$. This jump is defined as the difference of the limiting values of Q when Σ is approached from its positive side and its negative side successively. Equation (A-1-24) represents Reynolds' transport theorem in the presence of an internal boundary which is a surface of discontinuity. It is worth noting that if $\mathbf{V}-\mathbf{U}$ is tangential to $\Sigma(t)$ on both sides of Σ or if the jump vanishes, then (A-1-24) reduces to (A-1-7) , i.e., the usual theorem. This means that there is no flux of F across $\Sigma(t)$ by material transport. This is true in particular if $\mathbf{U}=\mathbf{V}$, that is when $\Sigma(t)$ is a material surface.

iv) Conservation equations

A) Away from discontinuities

The transport theorem in the form (A-1-24) expresses the conservation of the quantity F . Let $V(t)$ be bounded by a material surface, but be otherwise arbitrary. Then if $k(\mathbf{x},t)$ is the rate of production of F at the particle $\mathbf{x}$, we have

$$\frac{d}{dt}\int_{V(t)} F(\mathbf{x},t)\, d^3x = \int_{V(t)} k(\mathbf{x},t)\, d^3x \quad . \tag{A-1-25}$$

Because of the arbitrariness of $V(t)$ the equality of two integrals over $V(t)$ implies the identity of the integrands and thus, using (A-1-6) and (A-1-7) we get

$$\frac{dF(\mathbf{x},t)}{dt} + F\,\nabla_{\mathbf{x}}\cdot\mathbf{V} = k(\mathbf{x},t) \tag{A-1-26}$$

or

$$\frac{\partial F(\mathbf{x},t)}{\partial t} + \nabla_{\mathbf{x}} \cdot (F\mathbf{V}) = k(\mathbf{x},t) \quad , \tag{A-1-27}$$

which are to be satisfied at every point where the flow is regular. The specific forms taken by these equations to express conservation of mass, momentum, energy, ... etc., are given in Chapter I.

B) At discontinuities

Because of the preceeding discussion, and because (A-1-27) is satisfied at every regular point of the medium, we see that the second integral on the right-hand side of (A-1-24) must vanish identically unless $\Sigma(t)$ is a layer source for F. If $\Sigma(t)$ possesses a production rate density of F, $k_{\Sigma}(\mathbf{x},t)$, then at every point on Σ

$$\left[\!\left[F(\mathbf{V}-\mathbf{U}) \cdot \hat{n}_{\Sigma} \right]\!\right]_{\Sigma} = k_{\Sigma}(\mathbf{x},t) \quad . \tag{A-1-28}$$

This equation will yield the usual Hugoniot equations of shock wave theory. It will be particularly useful when applied to a phase boundary with the latent heat of transformation appearing on the right-hand side.

If the source density $k(\mathbf{x},t)$ is of the form $\nabla \cdot \kappa$, then by application of Gauss' theorem, and comparison with equations (A-1-23) and (A-1-24) we see that

$$k_{\Sigma}(\mathbf{x},t) = \left[\!\left[\kappa \cdot \hat{n}_{\Sigma} \right]\!\right]_{\Sigma} \quad . \tag{A-1-29}$$

This last relation is used extensively in section I-1.

APPENDIX 2

G FUNCTIONS: EVALUATION OF THE INTEGRAL

$$G(a,\mu,\nu;z) = \int_o^z e^{-at} t^{\mu} J_{\nu}(t)\, dt$$

a) A particular case

In a first step we evaluate the integral in the case

$$F(\ell;z) = G(0,-\ell+\tfrac{1}{2},\ell+\tfrac{1}{2};z)$$

In Erdelyi (B.M.P. vol. 2, p. 22, #4) we find

$$\int_o^1 x^{-\nu+1/2} J_{\nu}(xy)(xy)^{1/2}\, dx = \frac{2^{1-\nu} y^{\nu-3/2}}{\Gamma(\nu)} - y^{-1/2} J_{\nu-1}(y) \quad ,$$

therefore we write, with $u = t/z$, $t = uz$, $dt = zdu$

$$F(\ell;z) = z^{-\ell+1} \int_o^1 u^{-\ell} J_{\ell+1/2}(uz)(uz)^{1/2}\, du$$

thus, with $\nu = \ell + 1/2$

$$F(\ell;z) = z^{-\ell+1} \quad \frac{2^{-\ell+1/2} z^{\ell-1}}{\Gamma(\ell+1/2)} - z^{-1/2} J_{\ell-1/2}(z)$$

or

$$F(\ell;z) = \frac{2^{-\ell+1/2}}{\Gamma(\ell+1/2)} - \sqrt{\frac{2}{\pi}} \frac{j_{\ell-1}(z)}{z^{\ell-1}} \qquad \text{(A-2-1)}$$

From this result one deduces immediately

$$\int_a^b (r)^{-(\ell+1)} j_\ell(kr)\, r^2 dr = \frac{j_{\ell-1}(ka)}{ka^{\ell-1}} - \frac{j_{\ell-1}(kb)}{kb^{\ell-1}} \qquad \text{(A-2-2)}$$

and in an identical fashion

$$\int_a^b (r)^{-(\ell+1)} h_\ell^{(2)}(kr)\, r^2 dr = \frac{h_{\ell-1}^{(2)}(ka)}{ka^{\ell-1}} - \frac{h_{\ell-1}(kb)}{kb^{\ell-1}} \qquad \text{(A-2-3)}$$

Both of these results are used in Chapter IV in the computation of the multipole coefficients for a spherical rupture.

b) General case

We now turn to the general case and evaluate

$$G(a,\mu,\nu;z) = \int_o^z e^{-at}\, t^\mu\, J_\nu(t)\, dt \qquad \text{(A-2-4)}$$

in Abramowitz (p. 483), we find the following recursion relation

$$(a^2 + 1)\, G(a,\mu,\nu;z) = e^{-az}\, z^{\mu}\, J_{\nu+1}(z)$$

$$+ (\mu - \nu + 1)\, e^{-az}\, z^{\mu-1}\, J_{\nu}(z)$$

$$- a e^{-az}\, z^{\mu}\, J_{\nu}(z)$$

$$+ a(2\mu - 1)\; G(a,\mu-1,\nu;z)$$

$$+ [\nu^2 - (\mu-1)^2]\, G(a,\mu-2,\nu;z) \qquad \text{(A-2-5)}$$

We rewrite this relation, changing μ to $\mu+2$

$$[(\mu+1)^2 - \nu^2]\, G(a,\mu,\nu;z) = e^{-az}\, z^{\mu+2}\, J_{\nu+1}(z)$$

$$+ (\mu + 3 - \nu)\, e^{-at}\, z^{\mu+1}\, J_{\nu}(z)$$

$$- a\, e^{-az}\, z^{\mu+2}\, J_{\nu}(z)$$

$$+ a(2\mu + 3)\; G(a,\mu+1,\nu;z)$$

$$- (a^2 + 1)\, G(a,\mu+2,\nu;z) \qquad \text{(A-2-6)}$$

We shall be concerned with negative values of μ and the recursion relation (A-2-6) permits to reduce $|\mu|$ at constant a and ν . Defining

$$P(a,\mu,\nu;z) = \frac{z^{\mu+2} e^{-az}}{(\mu+1)^2 - \nu^2}$$

$$Q(a,\mu,\nu;z) = \frac{(\mu + 3 - \nu)\, z^{\mu+1} - az^{\mu+2}}{(\mu+1)^2 - \nu^2}\, e^{-az}$$

$$V(a,\mu,\nu) = \frac{a(2\mu + 3)}{(\mu+1)^2 - \nu^2}$$

$$W(a,\mu,\nu) = -\frac{a^2 + 1}{(\mu+1)^2 - \nu^2}$$

we can write

$$G(a,\mu,\nu;z) = P(a,\mu,\nu;z)\, J_{\nu+1}(z)$$

$$+ Q(a,\mu,\nu;z)\, J_{\nu}(z)$$

$$+ V(a,\mu,\nu)\, G(a,\mu+1,\nu;z)$$

$$+ W(a,\mu,\nu)\, G(a,\mu+2,\nu;z) \qquad \text{(A-2-7)}$$

By concatenation of this formula for $n-1$ successive values of μ, we can express $G(a,\mu,\nu;z)$ in terms of the same functions with two successive values of μ :

$$
\begin{array}{ll}
A_o \times & G(..,\mu,..) = P(\ ,\mu,\ )\ J_{\nu+1} + Q(\ ,\mu,\ )\ J_\nu + \\
& \qquad V(\ ,\mu,\ )\ G(\ ,\mu+1,\ ) + W(\ ,\mu,\ )\ G(\ ,\mu+2,\ ) \\
+A_1 \times & \cdots\cdots\cdots\cdots\cdots\cdots\cdots\cdots \\
\vdots & \\
+A_{n-2} \times & G(\ ,\mu+n-2,\ ) = P(\ ,\mu+n-2,\ )\ J_{\nu+1} + Q(\ ,\mu+n-2,\ )\ J_\nu + \\
& \qquad V(\ ,\mu+n-2,\ )\ G(\ ,\mu+n-1,\ ) + W(\ ,\mu+n-2,\ )\ G(\ ,\mu+n,\ )
\end{array}
$$

By summing these equalities weighted by the coefficients $A_o,\ldots,A_{n-2}$, we get

$$
G(a,\mu,\nu;z) = \sum_{i=0}^{n-2} A_i \left[P(a,\mu+i,\nu;z)\ J_{\nu+1}(z) + Q(a,\mu+i,\nu;z)\ J_\nu(z)\right]
$$

$$
+ A_{n-1}\ G(a,\mu+n-1,\nu;z)
$$

$$
+ A_{n-2}\ W(a,\mu+n-2,\nu)\ G(a,\mu+n,\nu;z) \qquad \text{(A-2-8)}
$$

where the coefficients A_i are entirely determined by the recursion

$$
\left\{
\begin{array}{l}
A_i = V(a,\mu+i-1,\nu)\ A_{i-1} + W(a,\mu+i-2,\nu)\ A_{i-2} \\
\\
A_o = 1;\ A_1 = V(a,\mu,\nu)
\end{array}
\right. \qquad \text{(A-2-9)}
$$

because of the presence of the denominator $(\mu+1)^2 - \nu^2$ in the coefficient $W(a,\mu,\nu)$, this recursion breaks down for $\mu + (n-2) + 1 = \nu$ or $n = \nu+1-\mu$.

But for the functions G we have to evaluate in Chapter IV, ν takes the constant value $\nu = \ell+1/2$ and μ varies from $-\ell+1/2$ to $\ell+3/2$. Because of the denominator appearing in the coefficients $P(a,\mu,\nu;z)$, $Q(a,\mu,\nu;z)$, $V(a,\mu,\nu)$, $W(a,\mu,\nu)$ the maximum μ for which we can apply the reduction formula (A-2-8) is $\mu = \ell-3/2$. Thus we see that for $-\ell+1/2 \leq \mu \leq \ell-3/2$ we can apply the reduction formula, and thus we need only evaluate

$$G(a,\ell-1/2,\ell+1/2;z)$$

$$G(a,\ell+1/2,\ell+1/2;z)$$

$$G(a,\ell+3/2,\ell+1/2;z)$$

that is, $G(a,m-1/2,\ell+1/2;z)$ for $\ell \leq m$. It should be noted that this is perfectly feasible in closed form. For this purpose we need to evaluate the spherical Bessel functions in closed form. It should also be noted that the case where $a = i$ is a particular one which should be integrated separately.

Recall that

$$G(a,m-1/2,\ell+1/2;z) = \sqrt{\frac{2}{\pi}} \int_0^z e^{-at}\, t^m\, j_\ell(t)\, dt \qquad \text{(A-2-10)}$$

The spherical Bessel function $j_\ell(t)$ is expressible in terms of a

finite combination of sines and cosines: we write the Hankel functions of the first and second kind as

$$h_\ell^{(1)}(t) = \frac{e^{it}}{i^{\ell+1} t} \sum_{k=0}^{\ell} (\ell+1/2,k)(-2it)^{-k}$$

$$h_\ell^{(2)}(t) = \frac{i^{\ell+1} e^{-it}}{t} \sum_{k=0}^{\ell} (\ell+1/2,k)(2it)^{-k}$$

and therefore

$$j_\ell(t) = \frac{1}{2}\left[h_\ell^{(1)}(t) + h_\ell^{(2)}(t)\right]$$

$$= \sum_{k=0}^{\ell} \frac{(\ell+1/2,k)}{(2t)^{k+1}} (-1)^{\ell+1} i^{k+\ell+1} \left[e^{it} + (-1)^{k+\ell+1} e^{-it}\right]$$

Using the following formula (Erdelyi, B.M.P. vol.1, p. 134, #5)

$$\int_o^z t^n e^{-pt}\, dt = \frac{n!}{p^{n+1}} - e^{-pz} \sum_{m=0}^{n} \frac{n!}{m!} \frac{z^m}{p^{n-m+1}}$$

and replacing a by $i\alpha$, then, with $(\ell+1/2,k) = \frac{(\ell+k)!}{k!\,\Gamma(n-k+1)}$,

we have the following results

1) $\alpha \neq 1$

a) $\ell+1 \leq m$

$$\int_o^z e^{-i\alpha t}\, t^m\, j_\ell(t)\, dt = \sum_{k=0}^{\ell} \frac{(\ell+1/2,k)}{2^{k+1}}\, (-1)^{\ell+k+m+1}\, i^{m+\ell+1} (m-k-1)!$$

$$\cdot \left(\frac{1}{(\alpha-1)^{m-k}} + \frac{(-1)^{k+\ell+1}}{(\alpha+1)^{m-k}} - \sum_{j=o}^{m-k-1} \frac{(iz)^j}{j!} \left[\frac{e^{-i(\alpha-1)z}}{(\alpha-1)^{m-k-j}} + \frac{(-1)^{k+\ell+1} e^{-i(\alpha+1)z}}{(\alpha+1)^{m-k-j}} \right] \right)$$

(A-2-11)

b) $m = \ell$

$$\int_o^z e^{-i\alpha t}\, t^\ell j_\ell(t)\, dt = \int_o^z e^{-i\alpha t}\, t^\ell j_{\ell-1}(t)\, dt$$

$$+ \frac{i(2\ell)!}{\ell!\, 2^{\ell+1}} \cdot \int_{(\alpha-1)z}^{(\alpha+1)z} \frac{e^{-it}}{t}\, dt \qquad \text{(A-2-12)}$$

We have therefore expressed the function $G(a,\mu,\nu;z)$ for the case $\nu = \ell+1/2$, $-\ell+1/2 \leq \mu \leq \ell+3/2$ in terms of a finite combination of elementary functions and an exponential integral, all of which can be evaluated by standard numerical methods.

2) $\alpha = 1$

The particular case $\alpha = 1$ is of interest since it corresponds in Chapter IV to the case where the rupture velocity equals the seismic

velocity. This may be used to model an instantaneous rupture or equivalently a shock generated rupture. However $W(a,\mu,\nu)$ vanishes in that case and from the recursion (A-2-7) we see that the only integral left after reduction is $G(i,\ell+1/2,\ell+1/2;z)$ which is a standard integral found in Abramovitz (p. 483, #11-3-9)

$$G(i,\ell+1/2,\ell+1/2;z) = \frac{e^{iz}z^{-(\ell-1/2)}}{2(\ell+1)} \left[J_{\ell+1/2}(z) - iJ_{\ell+3/2}(z)\right] \qquad \text{(A-2-13)}$$

Although equations (A-2-11) and (A-2-12) provide closed forms for the G functions, numerical experiments showed that their computation by this method becomes rapidly unstable even for low values of μ and ν . It was found empirically that the most reliable method is to evaluate them as finite Faurier transforms, using a numerical integration scheme.

APPENDIX 3

COMPUTATION OF THE INTEGRAL $I_{\ell}^{(1)}$

We defined in Chapter IV the integral

$$I_{\ell}^{(1)} = \int_{o}^{\tau_o} e^{-i\omega t_o} \frac{\partial}{\partial t_o} R^3(t_o)\, d^{\ell-2}(t_o)\, dt_o \qquad \text{(A-3-1)}$$

We shall now obtain a closed form for it in the case where $R(t_o)$ and $d(t_o)$ are polynomials of t_o. In that case, we may write

$$\frac{\partial}{\partial t_o} R^3(t_o)\, d^{\ell-2}(t_o) = \sum_{n=0}^{N} a_n t_o^n \,, \qquad \text{(A-3-2)}$$

where a_n $(n=0,\ldots,N)$ are coefficients which depend on the rupture geometry under consideration. From Erdelyi (B.M.P., vol 1, p. 134. #5) we have

$$\int_{o}^{t} t^n e^{-pt}\, dt = \frac{n!}{p^{n+1}} - e^{-pz} \sum_{m=0}^{n} \frac{n!}{m!} \frac{z^m}{p^{n-m+1}} \,. \qquad \text{(A-3-3)}$$

Then by simple substitution we get

$$I_{\ell}^{(1)}(\tau_o,\omega) = \sum_{n=0}^{N} a_n \left[\frac{n!}{(i\omega)^{n+1}} - e^{-i\omega\tau_o} \sum_{m=0}^{n} \frac{n!}{m!} \frac{(\tau_o)^m}{(i\omega)^{n-m+1}} \right] \qquad \text{(A-3-4)}$$

which is the result we sought.

APPENDIX 4

ASYMPTOTIC BEHAVIOR OF THE INTEGRALS $I_\ell^{(1)}, I_\ell^{(2)}, I_\ell^{(3)}, J_\nu^{(1)}, J_\nu^{(2)}, J_\nu^{(3)}$

When evaluating the radiation fields generated by a growing and propagating spherical rupture (Chapter IV), we expressed the dynamic multipole coefficients in terms of integrals over the source time t_o. These were

$$I_\ell^{(1)}(\omega) = \int_o^{\tau_o} e^{-i\omega t_o} \frac{d}{dt_o}\left[R^3(t_o)\, d^{\ell-2}(t_o)\right] dt_o \tag{A-4-1}$$

$$I_\ell^{(2)}(\omega) = \int_o^{\tau_o} e^{-i\omega t_o} \frac{d}{dt_o}\left[R^3(t_o)\, d^{\ell-2}(t_o)\right] \frac{j_{\ell-1}(k_\alpha V_R t_o)}{(k_\alpha V_R t_o)^{\ell-1}} dt_o \tag{A-4-2}$$

$$I_\ell^{(3)}(\omega) = \int_o^{\tau_o} e^{-i\omega t_o} \frac{d}{dt_o}\left[R^3(t_o)\, d^{\ell-2}(t_o)\right] \cdot \left[\frac{j_{\ell-1}(k_\alpha V_R t_o)}{(k_\alpha V_R t_o)^{\ell-1}} - \frac{j_{\ell-1}(k_\alpha R_s)}{(k_\alpha R_s)^{\ell-1}}\right] dt_o \tag{A-4-3}$$

and,

$$J_\nu^{(1)}(\omega) = \int_o^{\tau_o} e^{-i\omega t_o} \frac{\partial R^3(t_o)}{\partial t_o}\, j_\nu\left(k_\alpha d(t_o)\right)\, dt_o \tag{A-4-4}$$

$$J_\nu^{(2)}(\omega) = \int_o^{\tau_o} e^{-i\omega t_o} \frac{\partial R^3(t_o)}{\partial t_o}\, \frac{j_1\left(k_\alpha R(t_o)\right)}{k_\alpha R(t_o)}\, j_\nu\left(k_\alpha d(t_o)\right)\, dt_o \tag{A-4-5}$$

$$J_\nu^{(3)}(\omega) = \int_o^{\tau_o} e^{-i\omega t_o} \frac{\partial R^3(t_o)}{\partial t_o} \left[\frac{j_1(k_\alpha R(t_o))}{k_\alpha R(t_o)} - \frac{j_1(k_\alpha R_s)}{k_\alpha R_s} \right] \cdot j_\nu(k_\alpha d(t_o))\, dt_o \qquad \text{(A-4-6)}$$

The integrals $I_\ell^{(1)}, I_\ell^{(2)}, I_\ell^{(3)}$ appear in the approximate solution to the problem, while $J_\nu^{(1)}, J_\nu^{(2)}, J_\nu^{(3)}$ appear in the exact solution. Here $R(t_o)$ is the radius of the spherical rupture, $d(t_o)$ the amount of translation along the z axis, and we shall assume these functions to be polynomials of t_o. $k_\alpha = \omega/V_\alpha$ is the wave number, τ_o and R_s, the total rupture time and the relaxation radius, are constants of the problem.

We shall now investigate the long period and high frequency asymptotic behavior of these integrals.

A) Long period behavior, $\omega << 1$

In this case, we have $\omega t_o < \omega\tau_o << 1$, $k_\alpha V_R t_o < k_\alpha V_R \tau_o << 1$, and $k_\alpha R_s << 1$. Thus the following asymptotic behavior hold

$$\left.\begin{aligned} e^{-i\omega t_o} &= 1 + 0(\omega) \quad , \\ \frac{j_{\ell-1}(k_\alpha V_R t_o)}{(k_\alpha V_R t_o)^{\ell-1}} &= \frac{1}{1\cdot 3\cdot 5\ldots\cdot(2\ell-1)} + 0(\omega^2) \\ \frac{j_{\ell-1}(k_\alpha R_s)}{(k_\alpha R_s)^{\ell-1}} &= \frac{1}{1\cdot 3\cdot 5\ldots\cdot(2\ell-1)} + 0(\omega^2) \end{aligned}\right\} \qquad \text{(A-4-7)}$$

$$\left.\begin{aligned} \frac{j_{\ell-1}(k_\alpha V_R t_o)}{(k_\alpha V_R t_o)^{\ell-1}} - \frac{j_{\ell-1}(k_\alpha R_s)}{(k_\alpha R_s)^{\ell-1}} &= \frac{k_\alpha^2 (R_s^2 - V_R^2 t_o^2)/2}{1\cdot 3\cdot 5\cdots(2\ell+1)} + O(\omega^4) \\ j_\nu\left(k_\alpha d(t_o)\right) &= \frac{\left[k_\alpha d(t_o)\right]^\nu}{1\cdot 3\cdot 5\cdots(2\nu+1)} + O(\omega^{\nu+2}) \end{aligned}\right\} \quad \text{(A-4-7) (Cont.)}$$

Therefore we get immediately the following asymptotic behavior for $\omega << 1$

$$I_\ell^{(1)}(\omega) \sim R^3(\tau_o)\, d^{\ell-2}(\tau_o) \qquad \text{(A-4-8)}$$

$$I_\ell^{(2)}(\omega) \sim \frac{1}{1\cdot 3\cdot 5\cdots(2\ell-1)}\, R^3(\tau_o)\, d^{\ell-2}(\tau_o) \qquad \text{(A-4-9)}$$

$$I_\ell^{(3)}(\omega) \sim \frac{k_\alpha^2/2}{1\cdot 3\cdot 5\cdots(2\ell+1)} \int_o^{\tau_o} \left[R_s^2 - V_R^2 t_o^2\right] \frac{d}{dt_o}\left[R^3(t_o) d^{\ell-2}(t_o)\right] dt_o \qquad \text{(A-4-10)}$$

$$J_\nu^{(1)}(\omega) \sim \frac{k_\alpha^\nu}{1\cdot 3\cdot 5\cdots(2\nu+1)} \int_o^{\tau_o} d^\nu(t_o) \frac{dR^3(t_o)}{dt_o} dt_o \qquad \text{(A-4-11)}$$

$$J_\nu^{(2)}(\omega) \sim \frac{k_\alpha^\nu/3}{1\cdot 3\cdot 5\cdots(2\nu+1)} \int_o^{\tau_o} d^\nu(t_o) \frac{dR^3(t_o)}{dt_o} dt_o \qquad \text{(A-4-12)}$$

$$J_\nu^{(3)}(\omega) \sim \frac{k_\alpha^{\nu+2}/30}{1\cdot 3\cdot 5\cdots(2\nu+1)} \int_o^{\tau_o} d^\nu(t_o) \left[R_s^2 - R^2(t_o)\right] \frac{dR^3(t_o)}{dt_o} dt_o \qquad \text{(A-4-13)}$$

However, as shown in Chapter IV, the dominant terms at very long period correspond to the values $\ell = 2$ and $\nu = 0$ respectively. For these particular values we find for $\omega << 1$

$$\begin{cases} I_2^{(1)}(\omega) \sim R^3(\tau_o) \\ I_2^{(2)}(\omega) \sim R^3(\tau_o)/3 \\ I_2^{(3)}(\omega) \sim \frac{k_\alpha^2}{10} \int_o^{\tau_o} \left[R_s^2 - V_R^2 t_o^2\right] R^2(t_o)\, R'(t_o)\, dt_o \end{cases} \tag{A-4-14}$$

and

$$\begin{cases} J_o^{(1)}(\omega) \sim R^3(\tau_o) \\ J_o^{(2)}(\omega) \sim R^3(\tau_o)/3 \\ J_o^{(3)}(\omega) \sim \frac{k_\alpha^2}{10} \int_o^{\tau_o} \left[R_s^2 - R^2(t_o)\right] R^2(t_o)\, R'(t_o)\, dt_o \end{cases} \tag{A-4-15}$$

To obtain the expressions given in (A-4-14) and (A-4-15) we assumed that none of these terms vanish, that is $R_s > R(\tau_o) > 0$.

B) High frequency behavior, $\omega >> 1$

The asymptotic behavior of these integrals is more difficult to obtain in that case. We shall assume a simple case corresponding to one of the models described in Chapter IV, and computed in Chapter VII: we take $R(t_o)$ and $d(t_o)$ to be linear functions of t_o and, without loss of generality take

$$R(t_o) = d(t_o) = V_R t_o/2$$

where V_R is the rupture velocity. We know that the solutions of Chapter IV hold only for $V_R < c_\alpha$, where c_α is the wave velocity. When the rupture propagates at sonic or supersonic velocity, it must then be assumed to have been created instantaneously.

Let us first note that, if $R_s >> V_R \tau_o$, that is for a relaxation zone much larger than the rupture dimensions, the terms in R_s appearing in $I_\ell^{(3)}$ and $J_\nu^{(3)}$ are negligible. The high frequency behavior of these integrals is then independent of R_s and we have

$$\left.\begin{aligned} I_\ell^{(3)}(\omega) &\sim I_\ell^{(2)}(\omega) \\ J_\nu^{(3)}(\omega) &\sim J_\nu^{(2)}(\omega) \end{aligned}\right\} \quad \text{for} \quad \omega >> 1 \qquad \text{(A-4-16)}$$

Furthermore we know that, for $\omega >> 1$

$$\int_o^{\tau_o} e^{-i\omega\tau_o} t_o^n \, dt_o = \frac{i\tau_o^n \, e^{-i\omega\tau_o}}{\omega} + O(\omega^{-2})$$

so that we get immediately

$$I_\ell^{(1)}(\omega) = O(\omega^{-1}) \qquad \text{for} \quad \omega >> 1 \tag{A-4-17}$$

The remaining integrals may be rewritten after suitable changes of variables

$$I_\ell^{(2)}(\omega) = \frac{\ell+1}{(2k_\alpha)^{\ell+1}} \int_o^{k_\alpha V_R \tau_o} e^{-i\zeta t} \, t \, j_{\ell-1}(t) \, dt \tag{A-4-18}$$

$$J_\nu^{(1)}(\omega) = \frac{3}{8k_\alpha^3} \int_o^{k_\alpha V_R \tau_o} e^{-i\zeta t} \, t^2 \, j_\nu(t/2) \, dt \tag{A-4-19}$$

$$J_\nu^{(2)}(\omega) = \frac{3}{8k_\alpha^3} \int_o^{k_\alpha V_R \tau_o} e^{-i\zeta t} \, t \, j_1(t/2) \, j_\nu(t/2) \, dt \tag{A-4-20}$$

where $\zeta = c_\alpha / V_R$ is a number greater than one. The problem is now reduced to the study of the integrals appearing on the right-hand sides of (A-4-12) through (A-4-20) . These integrals do not have any limit as $\omega \to \infty$, and thus one cannot properly define asymptotic forms for them. Instead we separate the integral by writing

$$\int_0^{k_\alpha V_R \tau_o} = \int_0^{X} + \int_X^{k_\alpha V_R \tau_o} \qquad \text{(A-4-21)}$$

and choose X to be a fixed number, large enough so that for $t > X$ we can use the approximation

$$j_{\ell-1}(t) \simeq \frac{1}{2}\left[\frac{i^{-\ell}\, e^{it}}{t} + \frac{i^{\ell}\, e^{-it}}{t}\right]$$

This approximation may be used in the second integral on the right-hand side of (A-4-21), the first integral being now a fixed number. Consider for example the case of (A-4-18), we have

$$\int_X^{k_\alpha V_R \tau_o} e^{-i\zeta t}\, t\, j_{\ell-1}(t)\, dt \simeq \frac{i^{\ell+1}}{2}\left[(-1)^{\ell+1}\, \frac{e^{i(1-\zeta)k_\alpha V_R \tau_o} - e^{i(1-\zeta)X}}{1-\zeta} + \frac{e^{-i(1+\zeta)k_\alpha V_R \tau_o} - e^{-i(1+\zeta)X}}{1+\zeta}\right] \qquad \text{(A-4-22)}$$

We see now why we must have $\zeta \neq 1$, since this expression becomes singular for $\zeta = 1$. It is clear that this expression is of order one as $\omega \to \infty$, so that, by combination of (A-4-21) and (A-4-22) we get

$$I_{\ell}^{(2)}(\omega) \sim I_{\ell}^{(3)}(\omega) = 0(1/\omega^{\ell+1}) \quad \text{for} \quad \omega >> 1 \qquad \text{(A-4-23)}$$

Similar results are obtained for (A-4-19) and (A-4-20) by the same method. We get, after some algebra

$$\left.\begin{matrix} J_{\nu}^{(1)}(\omega) \\ J_{\nu}^{(2)}(\omega) \\ J_{\nu}^{(3)}(\omega) \end{matrix}\right\} = 0(\omega^{-3}) \quad \text{for} \quad \omega >> 1 \qquad \text{(A-4-24)}$$

If $R(t_o)$ and $d(t_o)$ are more complicated functions of t_o the analysis is still possible, but becomes more difficult. For $\zeta = 1$ the rupture grows at sonic velocity and the solution to the source problem must be obtained differently from the beginning (see e.g., Archambeau, 1972).

APPENDIX 5

COMPUTATION OF THE VECTOR DISPLACEMENT FIELD FROM THE DILATATION AND ROTATION POTENTIALS

In the frequency domain the vector displacement field is given in terms of the dilatation and rotation potentials by

$$\tilde{\mathbf{u}}(\mathbf{r},\omega) = -\frac{1}{k_p^2}\nabla\tilde{\Theta}(\mathbf{r},\omega) + \frac{2}{k_s^2}\nabla\times\tilde{\Omega}(\mathbf{r},\omega) \qquad \text{(A-5-1)}$$

The first term represents the "P wave," the second one the "S wave" radiation. Archambeau (1964, Appendix 4) showed how one obtains the curvilinear components of the vector $\mathbf{u}$ from the dilatation Θ and the cartesian (rectangular) components of the rotation Ω_i, $i = 1,2,3$. We recall his result for the case of spherical coordinates

$$\tilde{u}_r = -\frac{1}{k_p^2}\frac{\partial\tilde{\Theta}}{\partial r} - \frac{2}{k_s^2 r\sin\theta}\left\{\left(\sin\phi\sin\theta\frac{\partial}{\partial\theta} + \cos\phi\cos\theta\frac{\partial}{\partial\phi}\right)\tilde{\Omega}_1 + \left(\sin\phi\cos\theta\frac{\partial}{\partial\phi} - \cos\phi\sin\theta\frac{\partial}{\partial\theta}\right)\tilde{\Omega}_2 - \left(\sin\theta\frac{\partial}{\partial\phi}\right)\tilde{\Omega}_3\right\} \qquad \text{(A-5-2a)}$$

$$\tilde{u}_\theta = -\frac{1}{k_p^2 r}\frac{\partial\tilde{\Theta}}{\partial\theta} + \frac{2}{k_s^2 r\sin\theta}\left\{\left(\sin\theta\cos\phi\frac{\partial}{\partial\phi} + r\sin\theta\sin\phi\frac{\partial}{\partial r}\right)\tilde{\Omega}_1 + \left(\sin\theta\sin\phi\frac{\partial}{\partial\phi} - r\sin\theta\cos\phi\frac{\partial}{\partial r}\right)\tilde{\Omega}_2 + \left(\cos\theta\frac{\partial}{\partial\phi}\right)\tilde{\Omega}_3\right\} \qquad \text{(A-5-2b)}$$

$$\tilde{u}_\phi = -\frac{1}{k_p^2 r \sin\theta}\frac{\partial\tilde{\Theta}}{\partial\phi} + \frac{2}{k_s^2 r}\left\{\left(r\cos\theta\cos\phi\frac{\partial}{\partial r} - \sin\theta\cos\phi\frac{\partial}{\partial\theta}\right)\tilde{\Omega}_1\right.$$

$$+\left(r\cos\theta\sin\phi\frac{\partial}{\partial r} - \sin\theta\sin\phi\frac{\partial}{\partial\theta}\right)\tilde{\Omega}_2$$

$$\left.-\left(r\sin\theta\frac{\partial}{\partial r} + \cos\theta\frac{\partial}{\partial\theta}\right)\tilde{\Omega}_3\right\} \qquad \text{(A-5-2c)}$$

Because we used multipolar expansions to evaluate the potentials in Chapter IV, these spherical components are the most convenient ones to compute. Archambeau (1964) also gives the equivalent expressions for cartesian and cylindrical coordinates. On the other hand, having the spherical components of the vector $\tilde{\mathbf{u}}(\mathbf{r},\omega)$, one can as easily obtain its cartesian components through the orthogonal transformation

$$\begin{bmatrix}\tilde{u}_x\\ \tilde{u}_y\\ \tilde{u}_z\end{bmatrix} = \begin{bmatrix}\cos\phi\sin\theta & \cos\phi\cos\theta & -\sin\phi\\ \sin\phi\sin\theta & \sin\phi\cos\theta & \cos\phi\\ \cos\theta & -\sin\theta & 0\end{bmatrix}\begin{bmatrix}\tilde{u}_r\\ \tilde{u}_\theta\\ \tilde{u}_\phi\end{bmatrix} \qquad \text{(A-5-3)}$$

Similarly, the cylindrical components are given by

$$\begin{bmatrix}\tilde{u}_p\\ \tilde{u}_\phi\\ \tilde{u}_z\end{bmatrix} = \begin{bmatrix}\sin\theta & \cos\theta & 0\\ 0 & 0 & 1\\ \cos\theta & -\sin\theta & 0\end{bmatrix}\begin{bmatrix}\tilde{u}_r\\ \tilde{u}_\theta\\ \tilde{u}_\phi\end{bmatrix} \qquad \text{(A-5-4)}$$

In order to apply equation (A-4-2), we must find expressions for $\frac{\partial\tilde{\chi}}{\partial r}$, $\frac{\partial\tilde{\chi}}{\partial\theta}$, $\frac{\partial\tilde{\chi}}{\partial\phi}$, where $\tilde{\chi}$ is any one of the four potentials $\tilde{\Omega}_i$ $(i = 1,2,3)$, $\tilde{\Theta}$, and is given by a multipolar expansion such as

$$\tilde{\chi}(r,\omega) = \sum_{\ell=0}^{\infty} \sum_{m=0}^{\ell} Z_\ell(kr)[A_{\ell m} \cos m\phi + B_{\ell m} \sin m\phi] P_\ell^m(\cos\theta) \qquad (A\text{-}5\text{-}5)$$

Here $Z_\ell(kr)$ represents either a spherical Bessel function or a Hankel function of order ℓ. From Stratton (p. 406) we have

$$\frac{\partial}{\partial r} Z_\ell(kr) = \frac{k}{2\ell+1} [\ell Z_{\ell-1}(kr) - (\ell+1) Z_{\ell+1}(kr)] \qquad (A\text{-}5\text{-}6)$$

Similarly from Stratton (1941, p. 402) we have

$$\frac{\partial P_\ell^m(\cos\theta)}{\partial\theta} = \frac{1}{2}\left[(\ell-m+1)(\ell+m) P_\ell^{m-1}(\cos\theta) - P_\ell^{m+1}(\cos\theta)\right] \qquad (A\text{-}5\text{-}7)$$

This last formula is valid for $m = 0$, and yields $\frac{\partial P_o^o(\cos\theta)}{\partial\theta} = 0$ provided that we define

$$P_\ell^{-m}(\cos\theta) = (-1)^m \frac{(\ell-m)!}{(\ell+m)!} P_\ell^m(\cos\theta)$$

(It should be noted in that respect that the similar formula given by Jahnke and Emde (1945, p. 114) must be in error since it conflicts with

the recurrence formula given below it for $m = 0$).

We thus obtain

$$\frac{\partial \chi}{\partial r} = \sum_{\ell=0}^{\infty} \sum_{m=0}^{\ell} \frac{k}{2\ell+1} \left[\ell Z_{\ell-1}(kr) - (\ell+1) Z_{\ell+1}(kr) \right]$$

$$\cdot \left[A_{\ell m} \cos m\phi + B_{\ell m} \sin m\phi \right] P_{\ell}^{m}(\cos \theta) \qquad \text{(A-5-8)}$$

$$\frac{\partial \chi}{\partial \theta} = \sum_{\ell=0}^{\infty} \sum_{m=0}^{\ell} Z_{\ell}(kr) \left[A_{\ell m} \cos m\phi + B_{\ell m} \sin m\phi \right]$$

$$\cdot \frac{1}{2} \left[(\ell-m+1)(\ell+m) P_{\ell}^{m-1}(\cos \theta) - P_{\ell}^{m+1}(\cos \theta) \right] \qquad \text{(A-5-9)}$$

$$\frac{\partial \chi}{\partial \phi} = \sum_{\ell=0}^{\infty} \sum_{m=0}^{\ell} Z_{\ell}(kr)\, m \left[-A_{\ell m} \sin m\phi + B_{\ell m} \cos m\phi \right] P_{\ell}^{m}(\cos \theta) \qquad \text{(A-5-10)}$$

This last expression may be rewritten by using the following relations (Stratton, p. 401)

$$\frac{1}{\sin \theta} P_{\ell}^{m}(\cos \theta) = \frac{\cos \theta}{2m} \left[(\ell-m+1)(\ell+m) P_{\ell}^{m-1}(\cos \theta) + P_{\ell}^{m+1}(\cos \theta) \right]$$

$$+ \sin \theta \, P_{\ell}^{m}(\cos \theta)$$

or (Jahnke and Emde, p. 114)

$$\cot\theta\, P_\ell^m(\cos\theta) = \frac{1}{2m}\left[(\ell-m+1)(\ell+m)\, P_\ell^{m-1}(\cos\theta) + P_\ell^{m+1}(\cos\theta)\right]$$

Then specific terms appearing in (A-5-2) are

$$\cot\theta\,\frac{\partial\tilde{\chi}}{\partial\phi} = \sum_{\ell=0}^{\infty}\sum_{m=0}^{\ell} Z_\ell(kr)\left[-A_{\ell m}\sin m\phi + B_{\ell m}\cos m\phi\right]$$

$$\cdot\,\frac{1}{2}\left[(\ell-m+1)(\ell+m)\, P_\ell^{m-1}(\cos\theta) + P_\ell^{m+1}(\cos\theta)\right] \qquad \text{(A-5-11)}$$

$$\frac{1}{\sin\theta}\frac{\partial\tilde{\chi}}{\partial\phi} = \sum_{\ell=0}^{\infty}\sum_{m=0}^{\ell} Z_\ell(kr)\left[-A_{\ell m}\sin m\phi + B_{\ell m}\cos m\phi\right]$$

$$\cdot\left\{\frac{\cos\theta}{2}\left[(\ell-m+1)(\ell+m)\, P_\ell^{m-1}(\cos\theta) + P_\ell^{m+1}(\cos\theta)\right]\right.$$

$$\left. + m\sin\theta\, P_\ell^m(\cos\theta)\right\} \qquad \text{(A-5-12)}$$

These last expressions are somewhat better suited for numerical applications than (A-5-10) because of the complications occurring at $\theta = 0$ or π .

APPENDIX 6

INTERACTION OF BODY WAVES WITH A FREE SURFACE

In section III-1, we encountered the problem of the interaction of body waves with a free surface. The theory for the case of plane waves can be found in textbooks on elementary wave propagation (e.g., Richter, 1958). The closed form solution for incident plane waves is given by Cherry et al. (1972). We shall enumerate here their results without proof.

Figure A-6-1 describes the geometry. If c is the apparent velocity of the incident plane wave along the free surface, then the incidence angles for P- and S- waves are given by the equation

$$c = \frac{V_p}{\sin \theta_p} = \frac{V_s}{\sin \theta_s} \qquad \text{(A-6-1)}$$

where V_p and V_s are the P and S wave velocities respectively.

a) Incidence of SH waves

In that case at all incidences one gets a pure reflection, of reflection coefficient 1. The particle motion at the surface is in the x direction and has amplitude twice that of the incident wave.

b) Incidence of P waves

In that case we have $V_s < V_p \leq c$. The reflection coefficient (P → P) is

$$R = \frac{1}{D}\left[4\left(\frac{c^2}{V_p^2} - 1\right)^{1/2}\left(\frac{c^2}{V_s^2} - 1\right)^{1/2} - \left(\frac{c^2}{V_s^2} - 2\right)^2\right] \qquad \text{(A-6-2)}$$

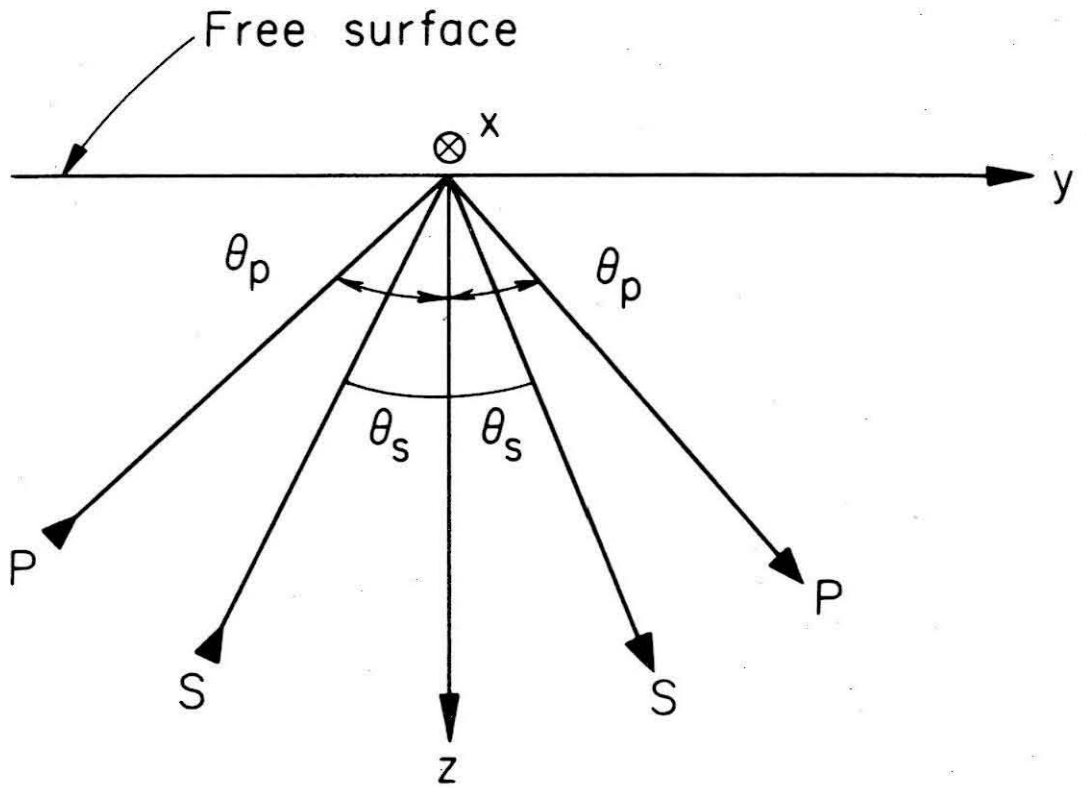

Figure A-6-1. Incidence of rays upon a free surface.

The conversion coefficient (P → SV) is

$$C = \frac{1}{D}\left[4\left(\frac{c^2}{V_p^2} - 1\right)^{1/2}\left(\frac{c^2}{V_s^2} - 2\right)\right] \qquad \text{(A-6-3)}$$

As for the particle motion at the free surface, the amplitude of the radial motion (in the y direction) for an incident P wave of amplitude 1 is

$$\text{Rad} = \frac{1}{D}\left[4\,\frac{cV_p}{V_s^2}\left(\frac{c^2}{V_p^2} - 1\right)\left(\frac{c^2}{V_s^2} - 1\right)^{1/2}\right] \qquad \text{(A-6-4)}$$

and the amplitude of vertical particle motion in that case is

$$\text{Vert} = \frac{1}{D}\left[2\,\frac{cV_p}{V_s^2}\left(\frac{c^2}{V_p^2} - 1\right)^{1/2}\left(\frac{c^2}{V_s^2} - 2\right)\right] \qquad \text{(A-6-5)}$$

In the equations (A-6-2) to (A-6-5) the quantity D is given by

$$D = 4\left(\frac{c^2}{V_p^2} - 1\right)\left(\frac{c^2}{V_s^2} - 1\right) + \left(\frac{c^2}{V_s^2} - 2\right)^2 \qquad \text{(A-6-6)}$$

c) Incidence of SV waves

For SV waves two cases arise

α) If $V_s < V_p \leq c$

then the reflection coefficient (SV → SV) is

$$R = \frac{1}{D}\left[4\left(\frac{c^2}{V_p^2} - 1\right)^{1/2}\left(\frac{c^2}{V_s^2} - 1\right)^{1/2} - \left(\frac{c^2}{V_s^2} - 2\right)^2 \right] \qquad \text{(A-6-7)}$$

where D is now given by

$$D = 4\left(\frac{c^2}{V_p^2} - 1\right)^{1/2}\left(\frac{c^2}{V_s^2} - 1\right)^{1/2} + \left(\frac{c^2}{V_s^2} - 2\right)^2 \qquad \text{(A-6-8)}$$

The conversion coefficient is then

$$C = -\frac{1}{D}\left[4\left(\frac{c^2}{V_p^2} - 1\right)^{1/2}\left(\frac{c^2}{V_s^2} - 2\right)\right] \qquad \text{(A-6-9)}$$

For an incident SV wave of amplitude 1 the radial and vertical amplitudes of particle motion at the free surface are respectively

$$\text{Rad} = \frac{1}{D}\left[2\,\frac{c}{V_s}\left(\frac{c^2}{V_s^2} - 1\right)^{1/2}\left(\frac{c^2}{V_s^2} - 2\right)\right] \qquad \text{(A-6-10)}$$

$$\text{Vert} = \frac{1}{D}\left[4\,\frac{c}{V_s}\left(\frac{c^2}{V_p^2} - 1\right)^{1/2}\left(\frac{c^2}{V_s^2} - 1\right)^{1/2} \right] \qquad \text{(A-6-11)}$$

β) If $V_s \leq c < V_p$

In that case the incidence angle is greater than the critical angle. Ray theory does not apply any longer and one must take into account the generation of Rayleigh waves. Since for practical purposes this case does not arise for the applications mentioned in section III-1, we shall omit the theory for that case. The reader will find the necessary information, for example, in Brekhovskikh (1960).

APPENDIX 7

DERIVATION OF EULER ANGLES FROM FAULT ORIENTATION PARAMETERS

As described in Chapter IV, the most convenient coordinate system to represent the radiation field from a propagating rupture is that one with the z-axis along the direction of propagation. It is shown in Chapter V how to transform the radiation field under a rotation of the reference frame, if the Euler angles are known. We now derive these Euler angles to transform the coordinate system to the local geographical system, described on figure (A-7-1). The z-axis is along the local vertical, the x-axis in a northerly direction.

The fault geometry can be described by its strike, dip, and plunge, denoted S, D, and P respectively. We choose the convention that the strike be measured counterclockwise from the North so that $-\pi \leq S \leq \pi$, or $0 \leq S \leq 2\pi$. The dip can then be measured clockwise from the horizontal by a vertical observer at the hypocenter so that $0 \leq D \leq \pi$. The same observer measures the plunge downward from the horizontal, thus $-\pi/2 \leq P \leq \pi/2$. The unit vectors $\hat{x}_G$, $\hat{y}_G$, $\hat{z}_G$ are then transformed into the unit vectors $\hat{x}_S, \hat{y}_S, \hat{z}_S$, by the (orthogonal) rotation matrix

$$T = \begin{bmatrix} -\sin S \sin D & -\sin S \cos D \cos P + \cos S \sin P & \sin S \cos D \sin P + \cos S \cos P \\ \sin D \cos S & \cos S \cos D \cos P + \sin S \sin P & -\cos S \cos D \sin P + \sin S \cos P \\ -\cos D & \sin D \cos P & -\sin D \sin P \end{bmatrix} \qquad \text{(A-7-1)}$$

The columns of T are the components of $\hat{x}_S$, $\hat{y}_S$, $\hat{z}_S$ in the $\hat{x}_G, \hat{y}_G, \hat{z}_G$,

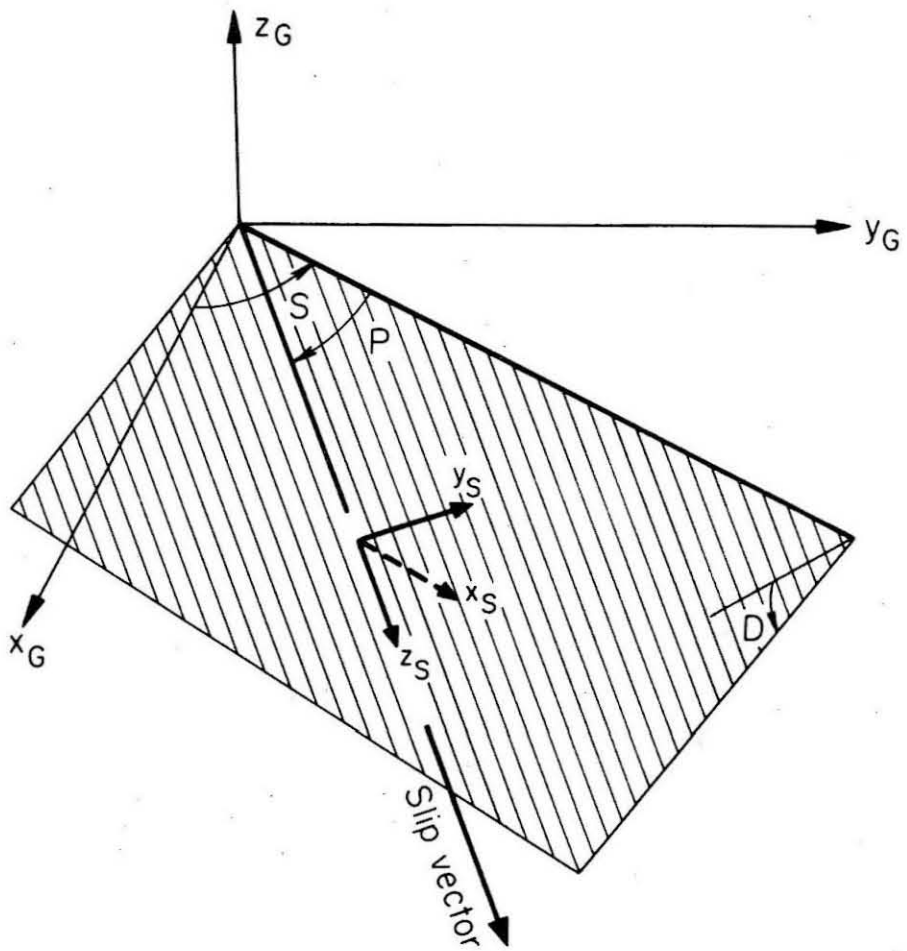

Figure A-7-1. Fault geometry relating the source coordinate system to the geographical coordinate system. S , D , P , are the strike, dip, and plunge angles respectively.

system. $\mathbf{T}$ can then be written equivalently in terms of the Euler angles Φ_1, Θ, Φ_2 described in Chapter V (figure V-2-1) - (Gelf'and, 1963). Calling the new matrix $\mathbf{R}$, we have

$$\mathbf{R} = \begin{bmatrix} \cos\Phi_1 \cos\Phi_2 - \cos\Theta \sin\Phi_1 \sin\Phi_2 & -\cos\Phi_1 \sin\Phi_2 - \cos\Theta \sin\Phi_1 \cos\Phi_2 & \sin\Theta \sin\Phi_1 \\ \sin\Phi_1 \cos\Phi_2 + \cos\Theta \cos\Phi_1 \sin\Phi_2 & -\sin\Phi_1 \sin\Phi_2 + \cos\Theta \cos\Phi_1 \cos\Phi_2 & -\sin\Theta \cos\Phi_1 \\ \sin\Phi_2 \sin\Theta & \sin\Theta \cos\Phi_2 & \cos\Theta \end{bmatrix} \tag{A-7-2}$$

Here $0 \leq \Phi_1 \leq 2\pi$, $0 \leq \Theta \leq \pi$, $0 \leq \Phi_2 \leq 2\pi$.

We obtain the relation between the fault orientation parameters and the Euler angles by simple identification of $\mathbf{T}$ and $\mathbf{R}$.

1) $T_{33} = \pm 1$.

In that case the transformation is a simple rotation of angle Φ_1 around the z-axis, thus

$$\left.\begin{array}{ll} \Phi_1 = \cos^{-1}(T_{11}) \; ; \; \Theta = \begin{cases} 0 \\ \pi \end{cases} \; ; \; \Phi_2 = 0 & \text{if } T_{21} > 0 \\ \Phi_1 = 2\pi - \cos^{-1}(T_{11}) \; ; \; \Theta = \begin{cases} 0 \\ \pi \end{cases} \; ; \; \Phi_2 = 0 & \text{if } T_{21} < 0 \end{array}\right\} \tag{A-7-3}$$

2) $T_{33} \neq \pm 1$.

Then because $0 < \Theta < \pi$

$$\Theta = \cos^{-1}(T_{33}) \tag{A-7-4}$$

$\sin\Theta = (1-T_{33}^2)^{1/2}$ is a positive quantity. Furthermore we have

$$\sin\Phi_1 = \frac{T_{13}}{\sin\Theta} \quad , \quad \cos\Phi_1 = -\frac{T_{23}}{\sin\Theta} \quad ,$$

$$\sin\Phi_2 = \frac{T_{31}}{\sin\Theta} \quad , \quad \cos\Phi_2 = \frac{T_{32}}{\sin\Theta} \quad .$$

Therefore

$$\left.\begin{aligned} \Phi_1 &= \cos^{-1}\frac{-T_{23}}{(1-T_{33}^2)^{1/2}} && \text{if } T_{13} > 0 \\ \Phi_1 &= 2\pi - \cos^{-1}\frac{-T_{23}}{(1-T_{33}^2)^{1/2}} && \text{if } T_{13} < 0 \end{aligned}\right\} \quad \text{(A-7-5)}$$

and

$$\left.\begin{aligned} \Phi_2 &= \cos^{-1}\frac{T_{32}}{(1-T_{33}^2)^{1/2}} && \text{if } T_{31} > 0 \\ \Phi_2 &= 2\pi - \cos^{-1}\frac{T_{32}}{(1-T_{33}^2)^{1/2}} && \text{if } T_{31} < 0 \end{aligned}\right\} \quad \text{(A-7-6)}$$

The Euler angles thus obtained transform the geographical coordinates into the source coordinates. The inverse rotation may be obtained by replacing the matrix T_{ij} by its transposed T_{ji} in the results above; the Euler angles for the inverse rotation are $\pi-\Phi_2$, Θ , $\pi-\Phi_1$.

APPENDIX 8

ULTRASPHERICAL FUNCTIONS AND JACOBI POLYNOMIALS

The formulae describing the transformation of multipolar expansions under rotations of the coordinate system are given in Chapter V. They involve ultraspherical functions for which we now derive a simple closed form for the cases of interest to us.

Gel'fand (1963) gives the following analytical expressions for the ultraspherical functions.

$$P_n^{m\kappa}(\mu) = F(1-\mu)^{-\frac{\kappa-m}{2}}(1+\mu)^{-\frac{\kappa+m}{2}}\frac{d^{n-\kappa}}{d\mu^{n-\kappa}}\left[(1-\mu)^{n-m}(1+\mu)^{n+m}\right] \tag{A-8-1}$$

where

$$F = \frac{(-1)^{n-m}\, i^{\kappa-m}}{2^n (n-m)!}\sqrt{\frac{(n-m)!\,(n+\kappa)!}{(n+m)!\,(n-\kappa)!}}$$

These functions possess the following symmetry properties (Gel'fand, 1963)

$$\begin{cases} P_n^{m\kappa}(\mu) = P_n^{\kappa m}(\mu) \\ P_n^{-m-\kappa}(\mu) = P_n^{m\kappa}(\mu) \end{cases} \tag{A-8-2}$$

and therefore depend only on the values of $|m+\kappa|$ and $|m-\kappa|$. One is thus led to define

$$\alpha = |m-\kappa| \quad , \quad \beta = |m+\kappa| \quad , \quad s_- = n - \frac{1}{2}(\alpha+\beta) \quad , \quad s_+ = n + \frac{1}{2}(\alpha+\beta) \quad ,$$

$$t_- = n - \frac{1}{2}(\alpha-\beta) \quad , \quad t_+ = n + \frac{1}{2}(\alpha-\beta) \quad ,$$

where all of these quantities are integers.

By identification we can rewrite (A-8-1) as

$$\mathbf{P}_n^{m\kappa}(\mu) = K(\alpha,n,s_+,s_-,t_+,t_-) \cdot (1-\mu)^{\alpha/2} (1+\mu)^{\beta/2} P_{s_-}^{\alpha\beta}(\mu) \qquad \text{(A-8-3)}$$

where K is a constant and $P_{s_-}^{\alpha\beta}(\mu)$ are the Jacobi polynomials in Erdelyi's notation

$$P_{s_-}^{\alpha\beta}(\mu) = \frac{(-1)^{s_-}}{2^{s_-} \cdot s_-!} (1-\mu)^{-\alpha} (1+\mu)^{-\beta} \frac{d^{s_-}}{d\mu^{s_-}} \left[(1-\mu)^{s_-+\alpha} (1+\mu)^{s_-+\beta} \right] \qquad \text{(A-8-4)}$$

Since the indices are integers, (A-8-4) can be rewritten in closed form

$$P_{s_-}^{\alpha\beta}(\mu) = 2^{-s_-} \sum_{j=0}^{s_-} \binom{s_-+\alpha}{j} \binom{s_-+\beta}{s_--j} (\mu-1)^{s_--j} (\mu+1)^j \qquad \text{(A-8-5)}$$

We evaluate K by simple identification

$$\frac{1}{K} = i^{\alpha} 2^{n-s_-} \sqrt{\frac{t_+!\, t_-!}{s_+!\, s_-!}} \qquad \text{(A-8-6)}$$

Equations (A-8-3), (A-8-5) and (A-8-6) are then combined to yield

$$P_n^{m\kappa}(\mu) = (-i)^{\alpha}\, 2^{-n} \sqrt{\frac{s_+!\, s_-!}{t_+!\, t_-!}} \sum_{j=0}^{s_-} \binom{s_-+\alpha}{j} \binom{s_-+\beta}{s_--j} (\mu-1)^{s_--j} (\mu+1)^{j} \cdot (1-\mu)^{\alpha/2} (1+\mu)^{\beta/2} \tag{A-8-7}$$

Equation (A-8-7) provides a closed form for the ultraspherical function which is particularly suitable for computation on digital machines.

Formula (A-8-7) is a polynomial involving few terms, especially for low degree n. It is thus particularly convenient for numerical computations in those cases. For seismological problems one is rarely interested in considering more than a few multipoles and (A-8-7) is adequate. For larger degrees and orders useful recurrence relations are given by Edmonds (1957).

APPENDIX 9

AN ADDITION THEOREM FOR SPHERICAL WAVE FUNCTIONS

The following addition theorem for spherical waves functions is used in Chapter IV to compute the radiation fields from a propagating rupture. It is used also in Chapter V to determine the transformation of multipolar expansions under translation of the coordinate system.

The proof presented here is parallel to that of Friedman and Russek (1954), but uses also some remarks given by Miller (1964). The results of Friedman and Russek are erroneous at least in one case, and so are Ben-Menahem's (1962) who recast the solution in operational form.

We define a spherical wave function by

$$Z_n(kr)\, Y_n^m(\theta,\phi) = (-1)^m \sqrt{\frac{(2n+1)(n-m)!}{4\pi\,(n+m)!}} \cdot Z_n(kr)\, P_n^m(\cos\theta)\, e^{im\phi} \qquad \text{(A-9-1)}$$

Here r , θ , ϕ are the usual spherical coordinates in the original coordinate system. θ , ϕ are the polar angles of the position vector $\mathbf{r}$. $Z_n(kr)$ is either the spherical Bessel function $j_n(kr)$ or a spherical Hankel function of the first or second kind, $h_n^{(1)}(kr)$ or $h_n^{(2)}(kr)$. Thus (A-9-1) may represent a standing wave, or an outgoing or incoming travelling wave.

Let α , β be the polar angles of the wave vector $\mathbf{k}$, then we

can write (Morse and Feshbach, 1953, p. 1466)

$$e^{i\mathbf{k}\cdot\mathbf{r}} = 4\pi \sum_{\ell=0}^{\infty} \sum_{n=-\ell}^{\ell} i^{\ell}\, j_{\ell}(kr)\, Y_{\ell}^{m}(\theta,\phi)\, \overline{Y}_{\ell}^{m}(\alpha,\beta) \qquad \text{(A-9-2)}$$

Here $\overline{Y}_{\ell}^{m}$ is the complex conjugate of Y_{ℓ}^{m}, and we have

$$Y_{\ell}^{m} = (-1)^{m}\, Y_{\ell}^{-m} \qquad \text{(A-9-3)}$$

We shall use the following integral representation for spherical waves (Friedman and Russek, 1954)

$$4\pi i^{n}\, Z_{n}(kr)\, Y_{n}^{m}(\theta,\phi) = \int_{0}^{2\pi} \int_{C} e^{i\mathbf{k}\cdot\mathbf{r}}\, Y_{n}^{m}(\alpha,\beta)\, \sin\alpha\, d\alpha d\beta \qquad \text{(A-9-4)}$$

where the integration contour C is shown on figure A-9-1 for the various cases involving $Z_{n}(kr)$ (Morse and Feshbach, 1953, p. 1467; Friedman and Russek, 1954, p. 17). Multiplying both sides of (A-9-2) by $Y_{\nu}^{\mu}(\alpha,\beta)$ and integrating over α and β according to (A-9-4) we get the following expansion

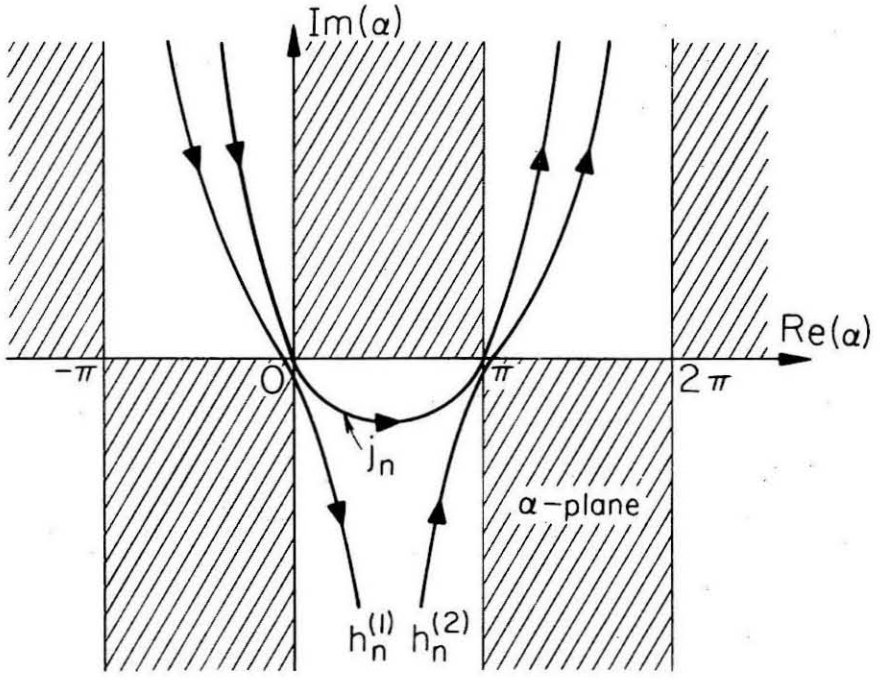

Figure A-9-1. Contours in the α-plane for the integral representation of Hankel and Bessel functions.

$$\int_o^{2\pi}\int_C Y_\nu^\mu(\alpha,\beta)\ e^{i\mathbf{k}\cdot\mathbf{r}}\ \sin\alpha\ d\alpha d\beta =$$

$$4\pi \sum_{\ell=o}^{\infty}\ \sum_{m=-\ell}^{\ell} i^\ell\ j_\ell(kr)\ Y_\ell^m(\theta,\phi) \int_o^{2\pi}\int_C \overline{Y}_\ell^{\ m}(\alpha,\beta)\ Y_\nu^\mu(\alpha,\beta)\ \sin\alpha\ d\alpha d\beta \qquad \text{(A-9-5)}$$

If now the vector $\mathbf{r}$ is written as $\mathbf{r}_1 + \mathbf{r}_2$, then

$$e^{i\mathbf{k}\cdot\mathbf{r}} = e^{i\mathbf{k}\cdot\mathbf{r}_1}\ e^{i\mathbf{k}\cdot\mathbf{r}_2} \qquad \text{(A-9-6)}$$

Equation (A-9-6) can be substituted into the integrand on the right-hand side of (A-9-4) . Friedman and Russek (1954) prove that if $|\mathbf{r}_1| < |\mathbf{r}_2|$, then $\exp(i\,\mathbf{k}\cdot\mathbf{r}_1)$ may then be replaced by use of (A-9-2) and that the infinite summation can be interchanged with the integral . Indeed they do so, but claim that in the case $|\mathbf{r}_2| < |\mathbf{r}_1|$ one only has to interchange the scalars r_1 and r_2 in the final result. This is clearly not the case; as we can see at this point, one has to interchange the <u>vectors</u> $\mathbf{r}_1$ and $\mathbf{r}_2$.

Let us assume that $|\mathbf{r}_1| < |\mathbf{r}_2|$. Then by substituting (A-9-6) into (A-9-4) , using (A-9-2) to expand $\exp(i\,\mathbf{k}\cdot\mathbf{r}_1)$, and interchanging the order of summation and integration, we obtain

$$4\pi i^n Z_n(kr)\, Y_n^m(\theta,\phi) = 4\pi \sum_{\nu=o}^{\infty} \sum_{\mu=-\nu}^{\nu} i^\nu j_\nu(kr_1)\, Y_\nu^\mu(\theta_1,\phi_1)$$

$$\cdot \int_o^{2\pi} \int_C e^{i\mathbf{k}\cdot\mathbf{r}_2}\, Y_n^m(\alpha,\beta)\, \overline{Y}_\nu^{\,\mu}(\alpha,\beta)\, \sin\alpha\, d\alpha d\beta \qquad \text{(A-9-7)}$$

We can now make use of (A-9-3) and of the expansion for a product of spherical functions (Edmonds, 1957)

$$\overline{Y}_n^{\,-m}(\alpha,\beta)\, \overline{Y}_\nu^{\,\mu}(\alpha,\beta) = \sum_{\ell,p} \left(\frac{(2n+1)(2\nu+1)(2\ell+1)}{4\pi} \right)^{1/2}$$

$$\cdot \begin{pmatrix} n & \nu & \ell \\ -m & \mu & p \end{pmatrix} Y_\ell^p(\alpha,\beta) \begin{pmatrix} n & \nu & \ell \\ 0 & 0 & 0 \end{pmatrix} \qquad \text{(A-9-8)}$$

Here the symbols appearing on the right-hand side are the usual 3-j symbols of Wigner, introduced in the theory of coupling of angular momentum vectors in quantum mechanics.

Equation (A-9-8) can be substituted into (A-9-7) and the order of summation and integration can be interchanged since the sum in (A-9-8) is a finite one. Then, using (A-9-4) whenever possible, we

get

$$Z_n(kr)\ Y_n^m(\theta,\phi) = \sum_{\nu=0}^{\infty} \sum_{\mu=-\nu}^{\nu} \sum_{\ell,p} A(n,m|\nu,\mu|\ell,p)$$

$$j_\nu(kr_1)\ Y_\nu^\mu(\theta_1,\phi_1)\ Z_\ell(kr_2)\ Y_\ell^p(\theta_2,\phi_2)$$

(A-9-9)

which is the addition theorem for spherical wave functions that we sought. The coefficient A is given by

$$A(n,m|\nu,\mu|\ell,p) = i^{\nu+\ell-n}(-1)^m[4\pi(2n+1)(2\nu+1)(2\ell+1)]^{1/2}$$

$$\cdot \begin{pmatrix} n & \nu & \ell \\ -m & \mu & p \end{pmatrix} \begin{pmatrix} n & \nu & \ell \\ 0 & 0 & 0 \end{pmatrix}$$

(A-9-10)

For the second 3-j coefficient not to vanish we need $n+\nu+\ell$ to be even (see Edmonds, 1957). In that case, we must have $p = \mu-m$, but since $|p| \leq \ell$, this means $|\mu-m| \leq \ell$. Further, from the triangular inequality we must have (Edmonds, 1957 ; Gottfried, 1966) $|n-\nu| \leq \ell \leq n+\nu$.

We can permute the first and third column in both 3-j coefficients without changing their value since $n+\ell+\nu$ is even. Then using the relation between 3-j coefficients and the Clebsch-Gordan coefficients

(Edmonds, p. 46; Gottfried, P. 220)

$$\begin{pmatrix} j_1 & j_2 & j_3 \\ m_1 & m_2 & m_3 \end{pmatrix} = (-1)^{j_1 - j_2 - m_3} (2j_3 + 1)^{-1/2} (j_1\ j_2\ m_1\ m_2 | j_3\ -m_3)$$

(A-9-11)

we eventually get

$$Z_n(kr)\ Y_n^m(\theta,\phi) = \sum_{\nu=0}^{\infty} \sum_{\mu=-\nu}^{\nu} \sum_{\ell=|n-\nu|}^{n+\nu} C(\nu,\mu,\ell|n,m)$$

$$\cdot\ j_\nu(kr_1)\ Y_\nu^\mu(\theta_1,\phi_1)\ Z_\ell(kr_2)\ Y_\ell^{m-\mu}(\theta_2,\phi_2)$$

(A-9-12)

where

$$C(\nu,\mu,\ell|n,m) = i^{\nu+\ell-n} \left(\frac{4\pi(2\nu+1)(2\ell+1)}{2n+1}\right)^{1/2}$$

$$\cdot\ (\ell\ \nu\ m-\mu\ \mu\ |\ n\ m)(\ell\ \nu\ 0\ 0\ |\ n\ 0) \qquad \text{(A-9-13)}$$

The coefficient C is non-zero only if $\ell+\nu+n$ is even. The Clebsch-Gordan coefficients appearing in (A-9-13) can be evaluated by standard recursion relations. See, for example, Edmonds (1957).

The result given by (A-9-12) and (A-9-13) is identical with that obtained by Miller (1964) in the case of standing waves.

This result is valid for $r_1 < r_2$. If the converse is true, then r_1 and r_2 are to be interchanged, and not only r_1 and r_2 as stated by Friedman and Russek (1954). Their equations (19) and (21) can hardly be correct since they do not reduce to the identity in the case of zero translation; in fact, their right-hand sides are not spherical wave expansions in all cases. Ben-Menahem (1962) used their results and his theorem suffers, therefore, from the same shortcoming. One can easily verify that (A-9-12) reduces to the identity in the case $r_1 = 0$.

One particularly interesting case is that when the translation r_1 is along the z-axis of the initial coordinate system. Then θ_1 is 0 or π , and only the terms for $\mu = 0$ remain; ϕ_1 can be taken to be zero. We have

$$Y_\nu^o(\theta_1, 0) = \sqrt{\frac{2\nu+1}{4\pi}}\, \varepsilon^\nu \qquad \text{(A-9-14)}$$

where $\varepsilon = \cos\theta_1$ is ± 1 . Noting that $\phi_2 = \phi$ in that case, we obtain

$$Z_n(kr)\, Y_n^m(\theta,\phi) = \sum_{\nu=o}^{\infty} \sum_{\ell=|n-\nu|}^{n+\nu} C_1(\nu,\ell|n,m)$$

$$\cdot\, j_\nu(kr_1)\, Z_\ell(kr_2)\, Y_\ell^m(\theta_2,\phi) \qquad \text{(A-9-15)}$$

where

$$C_1(\nu,\ell|n,m) = \varepsilon^{\nu}\, i^{\nu+\ell-n}(2\nu+1)\sqrt{\frac{2\ell+1}{2n+1}}$$

$$\cdot\ (\ell\ \nu\ m\ 0|\ n\ m)(\ell\ \nu\ 0\ 0\ |\ n\ 0) \qquad \text{(A-9-16)}$$

Note that if $r_1 = 0$, there is no translation, then $\nu = 0$ is the only term present and we have $\ell = n$, thus

$$Z_n(kr)\ Y_n^m(\theta,\phi) = C_1(0,n|n,m)\ Z_n(kr)\ Y_n^m(\theta,\phi) \qquad \text{(A-9-17)}$$

But

$$C_1(0,n|n,m) = (n\ 0\ m\ 0\ |\ n\ m)\ (n\ 0\ 0\ 0\ |\ n\ 0) = 1$$

and (A-9-17) is a proper equality. We make use of (A-9-15) in Chapter IV and in Chapter V. This result is equivalent to the one obtained by Satô (1950), who used a different approach, since the terms in the sum over ℓ in (A-9-15) vanish if $\ell \leq m$.

APPENDIX 10

3-j SYMBOLS USED IN CHAPTER IV

Vector coupling coefficients, or 3-j symbols are used in Appendix 9 in the addition theorem for spherical wave functions. This theorem is used in Chapter IV to solve the problem of a propagating spherical rupture. The table given below provides closed forms for all the 3-j symbols to be used in Chapter IV. This table is derived from the closed forms tabulated by Edmonds (1957).

a) $\underline{\nu = \ell - 2}$

$$\begin{pmatrix} \ell & \ell-2 & 2 \\ 0 & 0 & 0 \end{pmatrix} = \begin{pmatrix} \nu+2 & \nu & 2 \\ 0 & 0 & 0 \end{pmatrix} = (-1)^{\nu}(\nu+2)(\nu+1)\sqrt{\frac{6(2\nu)!}{(2\nu+5)!}}$$

$$\begin{pmatrix} \ell & \ell-2 & 2 \\ 1 & 0 & -1 \end{pmatrix} = \begin{pmatrix} \nu+2 & \nu & 2 \\ 1 & 0 & -1 \end{pmatrix} = 2(-1)^{\nu+1}(\nu+1)\sqrt{(\nu+2)(\nu+3)} \cdot \sqrt{\frac{(2\nu)!}{(2\nu+5)!}}$$

$$\begin{pmatrix} \ell & \ell-2 & 2 \\ 2 & 0 & -2 \end{pmatrix} = \begin{pmatrix} \nu+2 & \nu & 2 \\ 2 & 0 & -2 \end{pmatrix} = (-1)^{\nu}\sqrt{(\nu+1)(\nu+2)(\nu+3)(\nu+4)} \cdot \sqrt{\frac{(2\nu)!}{(2\nu+5)!}}$$

b) $\underline{\nu = \ell}$

$$\begin{pmatrix} \ell & \ell & 2 \\ 0 & 0 & 0 \end{pmatrix} = \begin{pmatrix} \nu & \nu & 2 \\ 0 & 0 & 0 \end{pmatrix} = 2(-1)^{\nu+1}\, \nu(\nu+1) \sqrt{\frac{(2\nu-2)!}{(2\nu+3)!}}$$

$$\begin{pmatrix} \ell & \ell & 2 \\ 1 & 0 & -1 \end{pmatrix} = \begin{pmatrix} \nu & \nu & 2 \\ 1 & 0 & -1 \end{pmatrix} = (-1)^{\nu} \sqrt{\nu(\nu+1)} \sqrt{\frac{6(2\nu-2)!}{(2\nu+3)!}}$$

$$\begin{pmatrix} \ell & \ell & 2 \\ 2 & 0 & -2 \end{pmatrix} = \begin{pmatrix} \nu & \nu & 2 \\ 2 & 0 & -2 \end{pmatrix} = (-1)^{\nu} \sqrt{(\nu-1)\nu(\nu+1)(\nu+2)} \sqrt{\frac{6(2\nu-2)!}{(2\nu+3)!}}$$

c) $\underline{\nu = \ell + 2}$

$$\begin{pmatrix} \ell & \ell+2 & 2 \\ 0 & 0 & 0 \end{pmatrix} = \begin{pmatrix} \nu-2 & \nu & 2 \\ 0 & 0 & 0 \end{pmatrix} = (-1)^{\nu}\, \nu(\nu-1) \sqrt{\frac{6(2\nu-4)!}{(2\,+1)!}}$$

$$\begin{pmatrix} \ell & \ell+2 & 2 \\ 1 & 0 & -1 \end{pmatrix} = \begin{pmatrix} \nu-2 & \nu & 2 \\ 1 & 0 & -1 \end{pmatrix} = 2(-1)^{\nu}\, \nu \sqrt{(\nu-1)(\nu-2)} \sqrt{\frac{(2\nu-4)!}{(2\nu+1)!}}$$

$$\begin{pmatrix} \ell & \ell+2 & 2 \\ 2 & 0 & -2 \end{pmatrix} = \begin{pmatrix} \nu-2 & \nu & 2 \\ 2 & 0 & -2 \end{pmatrix} = (-1)^{\nu} \sqrt{(\nu-3)(\nu-2)(\nu-1)\nu} \cdot \sqrt{\frac{(2\nu-4)!}{(2\nu+1)!}}$$

APPENDIX 11

BOUNDARY CONDITIONS FOR AN ELASTIC ELLIPSOIDAL INCLUSION

The boundary conditions prevailing on the boundary of an elastic ellipsoidal inclusion embedded in an infinite elastic matrix are described in Chapter VI. The system (VI-1-31) expresses the continuity of the tractions and displacements at the boundary of the inclusion.

We shall give in this Appendix the completely developed forms of these equations in ellipsoidal coordinates. The notation used here is the same as in Chapter VI. However, for simplicity, the definition of some coefficients has been changed slightly. For consistency with the results of Chapter VI, the following operations must be performed on the coefficients used below :

A_2 , A_3 , A_4 , B_2 , B_3 , B_4 must be mutiplied by $1 / km^2$.

A_5 , A_6 , A_7 , B_5 , B_6 , B_7 must be multiplied by $-k' / km^2$.

A_8 , A_9 , A_{10} , B_8 , B_9 , B_{10} must be multiplied by kk' / im^2 .
Other coefficients must be multiplied by $1 / m^2$.

The constants ν and μ are the Poisson ratio and the rigidity of the matrix respectively, and the constants ν' and μ' are those of the inclusion.

The equation expressing the continuity of the stress component $\tau_{\alpha\alpha}$ across the boundary $\alpha = \alpha_o$ may be developed as :

$$h_\alpha^2 s_\alpha \left[A_1 \frac{\partial^2 D_\alpha}{\partial \alpha^2} - B_2 \frac{\partial^2 d_\alpha}{\partial \alpha^2} \right] s_\beta d_\beta s_\gamma d_\gamma$$

$$+ h_\alpha^2 s_\alpha \left[A_3 \frac{\partial^2 s_\alpha}{\partial \alpha^2} - B_3 \frac{\partial^2 s_\alpha}{\partial \alpha^2} \right] s_\beta^2 s_\gamma^2 + h_\alpha^2 s_\alpha \left[A_4 \frac{\partial^2 C_\alpha}{\partial \alpha^2} \right.$$

$$\left. - B_4 \frac{\partial^2 c_\alpha}{\partial \alpha^2} \right] s_\beta c_\beta s_\gamma c_\gamma + h_\alpha^2 c_\alpha \left[A_5 \frac{\partial^2 D_\alpha}{\partial \alpha^2} - B_5 \frac{\partial^2 d_\alpha}{\partial \alpha^2} \right]$$

$$\cdot c_\beta d_\beta c_\gamma d_\gamma + h_\alpha^2 c_\alpha \left[A_6 \frac{\partial^2 S_\alpha}{\partial \alpha^2} - B_6 \frac{\partial^2 s_\alpha}{\partial \alpha^2} \right] s_\beta c_\beta s_\gamma c_\gamma$$

$$+ h_\alpha^2 c_\alpha \left[A_7 \frac{\partial^2 C_\alpha}{\partial \alpha^2} - B_7 \frac{\partial^2 c_\alpha}{\partial \alpha^2} \right] c_\beta^2 c_\gamma^2 + h_\alpha^2 d_\alpha \left[A_8 \frac{\partial^2 D_\alpha}{\partial \alpha^2} \right.$$

$$\left. - B_8 \frac{\partial^2 d_\alpha}{\partial \alpha^2} \right] d_\beta^2 d_\gamma^2 + h_\alpha^2 d_\alpha \left[A_9 \frac{\partial^2 S_\alpha}{\partial \alpha^2} - B_9 \frac{\partial^2 s_\alpha}{\partial \alpha^2} \right] s_\beta d_\beta s_\gamma d_\gamma$$

$$+ h_\alpha^2 d_\alpha \left[A_{10} \frac{\partial^2 C_\alpha}{\partial \alpha^2} - B_{10} \frac{\partial^2 c_\alpha}{\partial \alpha^2} \right] c_\beta d_\beta c_\gamma d_\gamma + h_\alpha^2 \left[A_{11} \frac{\partial^2 L_\alpha}{\partial \alpha^2} \right.$$

$$\left. - B_{11} \frac{\partial^2 l_\alpha}{\partial \alpha^2} \right] l_\beta l_\gamma + h_\alpha^2 \left[A_{12} \frac{\partial^2 M_\alpha}{\partial \alpha^2} - B_{12} \frac{\partial^2 m_\alpha}{\partial \alpha^2} \right] s_\beta d_\beta s_\gamma d_\gamma$$

$$+ h_\alpha^2 \left[A_{13} \frac{\partial^2 N_\alpha}{\partial \alpha^2} - B_{13} \frac{\partial^2 n_\alpha}{\partial \alpha^2} \right] n_\beta n_\gamma + h_\alpha^2 \left[A_{14} \frac{\partial^2 O_\alpha}{\partial \alpha^2} \right.$$

$$\left. - B_{14} \frac{\partial^2 o_\alpha}{\partial \alpha^2} \right] c_\beta d_\beta c_\gamma d_\gamma + h_\alpha^2 \left[A_{15} \frac{\partial^2 P_\alpha}{\partial \alpha^2} - B_{15} \frac{\partial^2 p_\alpha}{\partial \alpha^2} \right]$$

$$\cdot s_\beta c_\beta s_\gamma c_\gamma$$

$$+ h_\alpha \frac{\partial h_\alpha}{\partial \alpha} A_1 W_\alpha + \left[h_\alpha \frac{\partial h_\alpha}{\partial \alpha} s_\alpha - 2 h_\alpha^2 c_\alpha d_\alpha \right] \left[A_2 \frac{\partial D_\alpha}{\partial \alpha} \right.$$

$$\left. - B_2 \frac{\partial d_\alpha}{\partial \alpha} \right] s_\beta d_\beta s_\gamma d_\gamma + \left[h_\alpha \frac{\partial h_\alpha}{\partial \alpha} s_\alpha - 2 h_\alpha^2 c_\alpha d_\alpha \right] \left[A_3 \frac{\partial S_\alpha}{\partial \alpha} \right.$$

$$\left. - B_3 \frac{\partial s_\alpha}{\partial \alpha} \right] s_\beta^2 s_\gamma^2 + \left[h_\alpha \frac{\partial h_\alpha}{\partial \alpha} s_\alpha - 2 h_\alpha^2 c_\alpha d_\alpha \right] \left[A_4 \frac{\partial C_\alpha}{\partial \alpha} \right.$$

$$\left. - B_4 \frac{\partial c_\alpha}{\partial \alpha} \right] s_\beta c_\beta s_\gamma c_\gamma + \left[h_\alpha \frac{\partial h_\alpha}{\partial \alpha} c_\alpha + 2 h_\alpha^2 s_\alpha d_\alpha \right] \left[A_5 \frac{\partial D_\alpha}{\partial \alpha} \right.$$

$$\left. - B_5 \frac{\partial d_\alpha}{\partial \alpha} \right] c_\beta d_\beta c_\gamma d_\gamma + \left[h_\alpha \frac{\partial h_\alpha}{\partial \alpha} c_\alpha + 2 h_\alpha^2 s_\alpha d_\alpha \right] \left[A_6 \frac{\partial S_\alpha}{\partial \alpha} \right.$$

$$\left. - B_6 \frac{\partial s_\alpha}{\partial \alpha} \right] s_\beta c_\beta s_\gamma c_\gamma + \left[h_\alpha \frac{\partial h_\alpha}{\partial \alpha} c_\alpha + 2 h_\alpha^2 s_\alpha d_\alpha \right] \left[A_7 \frac{\partial C_\alpha}{\partial \alpha} \right.$$

$$\left. - B_7 \frac{\partial c_\alpha}{\partial \alpha} \right] c_\beta^2 c_\gamma^2 + \left[h_\alpha \frac{\partial h_\alpha}{\partial \alpha} d_\alpha + 2 k^2 h_\alpha^2 s_\alpha c_\alpha \right] \left[A_8 \frac{\partial D_\alpha}{\partial \alpha} \right.$$

$$\left. - B_8 \frac{\partial d_\alpha}{\partial \alpha} \right] d_\beta^2 d_\gamma^2 + \left[h_\alpha \frac{\partial h_\alpha}{\partial \alpha} d_\alpha + 2 k^2 h_\alpha^2 s_\alpha c_\alpha \right] \left[A_9 \frac{\partial S_\alpha}{\partial \alpha} \right.$$

$$\left. - B_9 \frac{\partial s_\alpha}{\partial \alpha} \right] s_\beta d_\beta s_\gamma d_\gamma + \left[h_\alpha \frac{\partial h_\alpha}{\partial \alpha} d_\alpha + 2 k^2 h_\alpha^2 s_\alpha c_\alpha \right] \left[A_{10} \frac{\partial C_\alpha}{\partial \alpha} \right.$$

$$\left. - B_{10} \frac{\partial c_\alpha}{\partial \alpha} \right] c_\beta d_\beta c_\gamma d_\gamma + h_\alpha \frac{\partial h_\alpha}{\partial \alpha} \left[A_{11} \frac{\partial L_\alpha}{\partial \alpha} - B_{11} \frac{\partial l_\alpha}{\partial \alpha} \right] l_\beta l_\gamma$$

$$+ h_\alpha \frac{\partial h_\alpha}{\partial \alpha} \left[A_{12} \frac{\partial M_\alpha}{\partial \alpha} - B_{12} \frac{\partial m_\alpha}{\partial \alpha} \right] s_\beta d_\beta s_\gamma d_\gamma + h_\alpha \frac{\partial h_\kappa}{\partial \alpha}$$

$$\cdot \left[A_{13} \frac{\partial N_\alpha}{\partial \alpha} - B_{13} \frac{\partial n_\alpha}{\partial \alpha} \right] n_\beta n_\gamma + h_\alpha \frac{\partial h_\alpha}{\partial \alpha} \left[A_{14} \frac{\partial O_\alpha}{\partial \alpha} \right.$$

$$\left. - B_{14} \frac{\partial o_\alpha}{\partial \alpha} \right] c_\beta d_\beta c_\gamma d_\gamma + h_\alpha \frac{\partial h_\alpha}{\partial \alpha} \left[A_{15} \frac{\partial P_\alpha}{\partial \alpha} - B_{15} \frac{\partial p_\alpha}{\partial \alpha} \right] s_\beta c_\beta s_\gamma c_\gamma$$

$$+ k^2 \frac{h_\beta^2}{h_\alpha} \frac{\partial h_\alpha}{\partial \beta} s_\alpha \left[A_2 D_\alpha - B_2 d_\alpha \right] s_\beta^2 c_\beta s_\gamma d_\gamma - \frac{h_\beta^2}{h_\alpha} \frac{\partial h_\alpha}{\partial \beta}$$

$$\cdot s_\alpha \left[A_3 S_\alpha - B_3 s_\alpha \right] s_\beta c_\beta d_\beta s_\gamma^2 + \frac{h_\beta^2}{h_\alpha} \frac{\partial h_\alpha}{\partial \beta} s_\alpha \left[A_4 C_\alpha \right.$$

$$\left. - B_4 c_\alpha \right] s_\beta^2 d_\beta s_\gamma d_\gamma + k^2 \frac{h_\beta^2}{h_\alpha} \frac{\partial h_\alpha}{\partial \beta} c_\alpha \left[A_5 D_\alpha - B_5 d_\alpha \right]$$

$$\cdot s_\beta c_\beta^2 c_\gamma d_\gamma - \frac{h_\beta^2}{h_\alpha} \frac{\partial h_\alpha}{\partial \beta} c_\alpha \left[A_6 S_\alpha - B_6 s_\alpha \right] c_\beta^2 d_\beta s_\gamma c_\gamma$$

$$+ \frac{h_\beta^2}{h_\alpha} \frac{\partial h_\alpha}{\partial \beta} c_\alpha \left[A_7 C_\alpha - B_7 c_\alpha \right] s_\beta d_\beta c_\beta c_\gamma^2 + k^2 \frac{h_\beta^2}{h_\alpha} \frac{\partial h_\alpha}{\partial \beta}$$

$$d_\alpha \left[A_8 D_\alpha - B_8 d_\alpha \right] s_\beta c_\beta d_\beta d_\gamma^2 - \frac{h_\beta^2}{h_\alpha} \frac{\partial h_\alpha}{\partial \beta} d_\alpha \left[A_9 S_\alpha - B_9 s_\alpha \right]$$

$$\cdot c_\beta d_\beta^2 s_\gamma d_\gamma + \frac{h_\beta^2}{h_\alpha} \frac{\partial h_\alpha}{\partial \beta} d_\alpha \left[A_{10} C_\alpha - B_{10} c_\alpha \right] s_\beta d_\beta^2 c_\gamma d_\gamma$$

$$- 2 \frac{h_\beta^2}{h_\alpha} \frac{\partial h_\alpha}{\partial \beta} \left[A_{11} L_\alpha - B_{11} l_\alpha \right] s_\beta c_\beta d_\beta l_\gamma - \frac{h_\beta^2}{h_\alpha} \frac{\partial h_\alpha}{\partial \beta}$$

$$\left[A_{12} M_\alpha - B_{12} m_\alpha \right] \left[c_\beta d_\beta^2 + k^2 s_\beta^2 c_\beta \right] s_\gamma d_\gamma - 2 \frac{h_\beta^2}{h_\alpha} \frac{\partial h_\alpha}{\partial \beta}$$

$$\cdot \left[A_{13} N_\alpha - B_{13} n_\alpha \right] s_\beta c_\beta d_\beta n_\gamma + \frac{h_\beta^2}{h_\alpha} \frac{\partial h_\alpha}{\partial \beta} \left[A_{14} O_\alpha - B_{14} o_\alpha \right]$$

$$\cdot \left[s_\beta d_\beta^2 + k^2 s_\beta c_\beta^2 \right] c_\gamma d_\gamma - \frac{h_\beta^2}{h_\alpha} \frac{\partial h_\alpha}{\partial \beta} \left[A_{15} P_\alpha - B_{15} p_\alpha \right]$$

$$\cdot \left[c_\beta^2 d_\beta - s_\beta^2 d_\beta \right] s_\gamma c_\gamma$$

$$+ k^2 \frac{h_\gamma^2}{h_\alpha} \frac{\partial h_\alpha}{\partial \gamma} s_\alpha \left[A_2 D_\alpha - B_2 d_\alpha \right] s_\beta d_\beta s_\gamma^2 c_\gamma$$

$$- \frac{h_\gamma^2}{h_\alpha} \frac{\partial h_\alpha}{\partial \gamma} s_\alpha \left[A_3 S_\alpha - B_3 s_\alpha \right] s_\beta^2 s_\gamma c_\gamma d_\gamma + \frac{h_\gamma^2}{h_\alpha} \frac{\partial h_\alpha}{\partial \gamma} s_\alpha$$

$$\cdot \left[A_4 C_\alpha - B_4 c_\alpha \right] s_\beta c_\beta s_\gamma^2 d_\gamma + k^2 \frac{h_\gamma^2}{h_\alpha} \frac{\partial h_\alpha}{\partial \gamma} c_\alpha \left[A_5 D_\alpha \right.$$

$$\left. - B_5 d_\alpha \right] c_\beta d_\beta s_\gamma c_\gamma^2 - \frac{h_\gamma^2}{h_\alpha} \frac{\partial h_\alpha}{\partial \gamma} c_\alpha \left[A_6 S_\alpha - B_6 s_\alpha \right]$$

$$\cdot s_\beta c_\beta c_\gamma^2 d_\gamma + \frac{h_\gamma^2}{h_\alpha} \frac{\partial h_\alpha}{\partial \gamma} c_\alpha \left[A_7 C_\alpha - B_7 c_\alpha \right] c_\beta^2 s_\gamma c_\gamma d_\gamma$$

$$+ k^2 \frac{h_\gamma^2}{h_\alpha} \frac{\partial h_\alpha}{\partial \gamma} d_\alpha \left[A_8 D_\alpha + B_8 d_\alpha \right] d_\beta^2 s_\gamma c_\gamma d_\gamma - \frac{h_\gamma^2}{h_\alpha} \frac{\partial h_\alpha}{\partial \gamma}$$

$$\cdot d_\alpha \left[A_9 S_\alpha - B_9 s_\alpha \right] s_\beta d_\beta c_\gamma d_\gamma^2 + \frac{R_\gamma^2}{h_\alpha} \frac{\partial h_\alpha}{\partial \gamma} d_\alpha \left[A_{10} C_\alpha \right.$$

$$\left. - B_{10} c_\alpha \right] c_\beta d_\beta s_\gamma d_\gamma^2 - 2 \frac{h_\gamma^2}{h_\alpha} \frac{\partial h_\alpha}{\partial \gamma} \left[A_{11} L_\alpha - B_{11} l_\alpha \right]$$

$$\cdot l_\beta s_\gamma c_\gamma d_\gamma - \frac{h_\gamma^2}{h_\alpha} \frac{\partial h_\alpha}{\partial \gamma} \left[A_{12} M_\alpha - B_{12} m_\alpha \right] s_\beta d_\beta \left[c_\gamma d_\gamma^2 \right.$$

$$\left. - k^2 s_\gamma c_\gamma \right] - 2 \frac{h_\gamma^2}{h_\alpha} \frac{\partial h_\alpha}{\partial \gamma} \left[A_{13} N_\alpha - B_{13} n_\alpha \right] n_\beta s_\gamma c_\gamma d_\gamma$$

$$+ \frac{R_\gamma^2}{h_\alpha} \frac{\partial h_\alpha}{\partial \gamma} \left[A_{14} O_\alpha - B_{14} o_\alpha \right] \left[s_\gamma d_\gamma^2 + k^2 s_\gamma c_\gamma^2 \right] c_\beta d_\beta$$

$$- \frac{h_\gamma^2}{h_\alpha} \frac{\partial h_\alpha}{\partial \gamma} \left[A_{15} P_\alpha - B_{15} p_\alpha \right] \left[c_\gamma^2 d_\gamma - s_\gamma^2 d_\gamma \right] s_\beta c_\beta$$

$$+ 2 h_\alpha^2 c_\alpha d_\alpha \left[\nu A_2 \frac{\partial D_\alpha}{\partial \alpha} - \nu' B_2 \frac{\partial d_\alpha}{\partial \alpha} \right] s_\beta d_\beta s_\gamma d_\gamma$$

$$+ 2 h_\alpha^2 c_\alpha d_\alpha \left[\nu A_3 \frac{\partial S_\alpha}{\partial \alpha} - \nu' B_3 \frac{\partial s_\alpha}{\partial \alpha} \right] s_\beta^2 s_\gamma^2$$

$$+ 2k_\alpha^2 c_\alpha d_\alpha \left[\nu A_4 \frac{\partial C_\alpha}{\partial \alpha} - \nu' B_4 \frac{\partial c_\alpha}{\partial \alpha} \right] s_\beta c_\beta s_\gamma c_\gamma$$

$$- 2 k_\alpha^2 s_\alpha d_\alpha \left[\nu A_5 \frac{\partial D_\alpha}{\partial \alpha} - \nu' B_5 \frac{\partial d_\alpha}{\partial \alpha} \right] c_\beta d_\beta c_\gamma d_\gamma$$

$$- 2 k_\alpha^2 s_\alpha d_\alpha \left[\nu A_6 \frac{\partial S_\alpha}{\partial \alpha} - \nu' B_6 \frac{\partial s_\alpha}{\partial \alpha} \right] s_\beta c_\beta s_\gamma c_\gamma$$

$$- 2 k_\alpha^2 s_\alpha d_\alpha \left[\nu A_7 \frac{\partial C_\alpha}{\partial \alpha} - \nu' B_7 \frac{\partial c_\alpha}{\partial \alpha} \right] c_\beta^2 c_\gamma^2$$

$$- 2 k^2 k_\alpha^2 s_\alpha c_\alpha \left[\nu A_8 \frac{\partial D_\alpha}{\partial \alpha} - \nu' B_8 \frac{\partial d_\alpha}{\partial \alpha} \right] d_\beta^2 d_\gamma^2$$

$$- 2 k^2 k_\alpha^2 s_\alpha c_\alpha \left[\nu A_9 \frac{\partial S_\alpha}{\partial \alpha} - \nu' B_9 \frac{\partial s_\alpha}{\partial \alpha} \right] s_\beta d_\beta s_\gamma d_\gamma$$

$$- 2 k^2 k_\alpha^2 s_\alpha c_\alpha \left[\nu A_{10} \frac{\partial C_\alpha}{\partial \alpha} - \nu' B_{10} \frac{\partial c_\alpha}{\partial \alpha} \right] c_\beta d_\beta c_\gamma d_\gamma$$

$$+ 2 k^2 k_\beta^2 s_\alpha \left[\nu A_2 D_\alpha - \nu' B_2 d_\alpha \right] s_\beta c_\beta^2 d_\beta s_\gamma d_\gamma$$

$$- 2 k_\beta^2 s_\alpha \left[\nu A_3 S_\alpha - \nu' B_3 s_\alpha \right] c_\beta^2 d_\beta^2 s_\gamma^2$$

$$+ 2 k_\beta^2 s_\alpha \left[\nu A_4 C_\alpha - \nu' B_4 c_\alpha \right] s_\beta c_\beta d_\beta^2 s_\gamma c_\gamma$$

$$- 2 k^2 k_\beta^2 c_\alpha \left[\nu A_5 D_\alpha - \nu' B_5 d_\alpha \right] s_\beta^2 c_\beta d_\beta c_\gamma d_\gamma$$

$$+ 2 k_\beta^2 c_\alpha \left[\nu A_6 S_\alpha - \nu' B_6 s_\alpha \right] s_\beta c_\beta d_\beta^2 s_\gamma c_\gamma$$

$$- 2 k_\beta^2 c_\alpha \left[\nu A_7 C_\alpha - \nu' B_7 c_\alpha \right] s_\beta^2 d_\beta^2 c_\gamma^2$$

$$
\begin{aligned}
&- 2k^4 h_\beta^2 d_\alpha \left[\nu A_8 D_\alpha - \nu' B_8 d_\alpha \right] s_\beta^2 c_\beta^2 d_\gamma^2 \\
&+ 2k^2 h_\beta^2 d_\alpha \left[\nu A_9 S_\alpha - \nu' B_9 s_\alpha \right] s_\beta c_\beta^2 d_\beta s_\gamma d_\gamma \\
&- 2k^2 h_\beta^2 d_\alpha \left[\nu A_{10} C_\alpha - \nu' B_{10} c_\alpha \right] s_\beta^2 c_\beta d_\beta c_\gamma d_\gamma \\
&+ 2k^2 h_\gamma^2 s_\alpha \left[\nu A_2 D_\alpha - \nu' B_2 d_\alpha \right] s_\beta d_\beta s_\gamma c_\gamma^2 d_\gamma \\
&- 2 h_\gamma^2 s_\alpha \left[\nu A_3 S_\alpha - \nu' B_3 s_\alpha \right] s_\beta^2 c_\gamma^2 d_\gamma^2 \\
&+ 2 h_\gamma^2 s_\alpha \left[\nu A_4 C_\alpha - \nu' B_4 c_\alpha \right] s_\beta c_\beta s_\gamma c_\gamma d_\gamma^2 \\
&- 2k^2 h_\gamma^2 c_\alpha \left[\nu A_5 D_\alpha - \nu' B_5 d_\alpha \right] c_\beta d_\beta s_\gamma^2 c_\gamma d_\gamma \\
&+ 2 h_\gamma^2 c_\alpha \left[\nu A_6 S_\alpha - \nu' B_6 s_\alpha \right] s_\beta c_\beta s_\gamma c_\gamma d_\gamma^2 \\
&- 2 h_\gamma^2 c_\alpha \left[\nu A_7 C_\alpha - \nu' B_7 c_\alpha \right] c_\beta^2 s_\gamma^2 d_\gamma^2 \\
&- 2k^4 h_\gamma^2 d_\alpha \left[\nu A_8 D_\alpha - \nu' B_8 d_\alpha \right] d_\beta^2 s_\gamma^2 c_\gamma^2 \\
&+ 2k^2 h_\gamma^2 d_\alpha \left[\nu A_9 S_\alpha - \nu' B_9 s_\alpha \right] s_\beta d_\beta s_\gamma c_\gamma^2 d_\gamma \\
&- 2k^2 h_\gamma^2 d_\alpha \left[\nu A_{10} C_\alpha - \nu' B_{10} c_\alpha \right] c_\beta d_\beta s_\gamma^2 c_\gamma d_\gamma \\
&=
\end{aligned}
$$

$$
\begin{aligned}
= & - \tau_{xx}^{(o)} \; k^2 m^2 h_\alpha^2 \; c_\alpha^2 d_\alpha^2 \; s_\beta^2 s_\gamma^2 \\
& - \tau_{yy}^{(o)} \; \frac{k^2 m^2}{k'^2} h_\alpha^2 s_\alpha^2 d_\alpha^2 \; c_\beta^2 c_\gamma^2 \\
& + \tau_{zz}^{(o)} \; \frac{k^2 m^2}{k'^2} h_\alpha^2 s_\alpha^2 c_\alpha^2 \; d_\beta^2 d_\gamma^2 \\
& + 2 \tau_{yz}^{(o)} \; \frac{i k m^2}{k'^2} h_\alpha^2 s_\alpha^2 c_\alpha d_\alpha \; c_\beta d_\beta c_\gamma d_\gamma \\
& + 2 \tau_{zx}^{(o)} \; \frac{i k^2 m^2}{k'} h_\alpha^2 s_\alpha c_\alpha^2 d_\alpha \; s_\beta d_\beta s_\gamma d_\gamma \\
& - 2 \tau_{xy}^{(o)} \; \frac{k^2 m^2}{k'} h_\alpha^2 s_\alpha c_\alpha d_\alpha^2 \; s_\beta c_\beta s_\gamma c_\gamma
\end{aligned}
$$

(A-11-1)

Equation (A-11-1) must be satisfied identically in β and γ on the surface of the ellipsoid $\alpha = \alpha_o$. We must therefore find all the independent functions of these variables appearing in this equation. This is done in Appendix 12.

Similarly the continuity of the component of traction $\tau_{\alpha\beta}$ on the surface of the inclusion is expressed by the following equation :

$$\left[A_2 \left(-k^2 s_\alpha^3 \frac{\partial D_\alpha}{\partial \alpha} \right) - B_2 \left(-k^2 s_\alpha^3 \frac{\partial d_\alpha}{\partial \alpha} \right) \right] s_\beta^2 c_\beta s_\gamma d_\gamma$$

$$+ \left[A_2 \left(k^2 s_\alpha \frac{\partial D_\alpha}{\partial \alpha} \right) - B_2 \left(k^2 s_\alpha \frac{\partial d_\alpha}{\partial \alpha} \right) \right] s_\beta^4 c_\beta s_\gamma d_\gamma$$

$$+ \left[A_3 \left(s_\alpha^3 \frac{\partial S_\alpha}{\partial \alpha} \right) - B_3 \left(s_\alpha^3 \frac{\partial s_\alpha}{\partial \alpha} \right) \right] s_\beta c_\beta d_\beta s_\gamma^2$$

$$+ \left[A_3 \left(-s_\alpha \frac{\partial S_\alpha}{\partial \alpha} \right) - B_3 \left(-s_\alpha \frac{\partial s_\alpha}{\partial \alpha} \right) \right] s_\beta^3 c_\beta d_\beta s_\gamma^2$$

$$+ \left[A_4 \left(-s_\alpha^3 \frac{\partial C_\alpha}{\partial \alpha} \right) - B_4 \left(-s_\alpha^3 \frac{\partial c_\alpha}{\partial \alpha} \right) \right] s_\beta^2 d_\beta s_\gamma c_\gamma$$

$$+ \left[A_4 \left(s_\alpha \frac{\partial C_\alpha}{\partial \alpha} \right) - B_4 \left(s_\alpha \frac{\partial c_\alpha}{\partial \alpha} \right) \right] s_\beta^4 d_\beta s_\gamma c_\gamma$$

$$+ \left[A_5 \left(-k^2 s_\alpha^2 c_\alpha \frac{\partial D_\alpha}{\partial \alpha} \right) - B_5 \left(-k^2 s_\alpha^2 c_\alpha \frac{\partial d_\alpha}{\partial \alpha} \right) \right] s_\beta c_\beta^2 c_\gamma d_\gamma$$

$$+ \left[A_5 \left(k^2 c_\alpha \frac{\partial D_\alpha}{\partial \alpha} \right) - B_5 \left(k^2 c_\alpha \frac{\partial d_\alpha}{\partial \alpha} \right) \right] s_\beta^3 c_\beta^2 c_\gamma d_\gamma$$

$$+ \left[A_6 \left(s_\alpha^2 c_\alpha \frac{\partial S_\alpha}{\partial \alpha} \right) - B_6 \left(s_\alpha^2 c_\alpha \frac{\partial s_\alpha}{\partial \alpha} \right) \right] c_\beta^2 d_\beta s_\gamma c_\gamma$$

$$+ \left[A_6 \left(-c_\alpha \frac{\partial S_\alpha}{\partial \alpha} \right) - B_6 \left(-c_\alpha \frac{\partial s_\alpha}{\partial \alpha} \right) \right] s_\beta^2 c_\beta^2 d_\beta s_\gamma c_\gamma$$

$$+ \left[A_7 \left(-s_\alpha^2 c_\alpha \frac{\partial C_\alpha}{\partial \alpha} \right) - B_7 \left(-s_\alpha^2 c_\alpha \frac{\partial c_\alpha}{\partial \alpha} \right) \right] s_\beta c_\beta d_\beta c_\gamma^2$$

$$+ \left[A_7 \left(c_\alpha \frac{\partial C_\alpha}{\partial \alpha} \right) - B_7 \left(c_\alpha \frac{\partial c_\alpha}{\partial \alpha} \right) \right] s_\beta^3 c_\beta d_\beta c_\gamma^2$$

$$+ \left[A_8 \left(-k^2 s_\alpha^2 d_\alpha \frac{\partial D_\alpha}{\partial \alpha} \right) - B_8 \left(-k^2 s_\alpha^2 d_\alpha \frac{\partial d_\alpha}{\partial \alpha} \right) \right] s_\beta c_\beta d_\beta d_\gamma^2$$

$$+\left[A_8\left(k^2 d_\alpha \frac{\partial D_\alpha}{\partial \alpha}\right) - B_8\left(k^2 d_\alpha \frac{\partial d_\alpha}{\partial \alpha}\right)\right] s_\beta^3 c_\beta d_\beta d_\gamma^2$$

$$+\left[A_9\left(s_\alpha^2 d_\alpha \frac{\partial S_\alpha}{\partial \alpha}\right) - B_9\left(s_\alpha^2 d_\alpha \frac{\partial s_\alpha}{\partial \alpha}\right)\right] c_\beta d_\beta^2 s_\gamma d_\gamma$$

$$+\left[A_9\left(-d_\alpha \frac{\partial S_\alpha}{\partial \alpha}\right) - B_9\left(-d_\alpha \frac{\partial s_\alpha}{\partial \alpha}\right)\right] s_\beta^2 c_\beta d_\beta^2 s_\gamma d_\gamma$$

$$+\left[A_{10}\left(-s_\alpha^2 d_\alpha \frac{\partial C_\alpha}{\partial \alpha}\right) - B_{10}\left(-s_\alpha^2 d_\alpha \frac{\partial c_\alpha}{\partial \alpha}\right)\right] s_\beta d_\beta^2 c_\gamma d_\gamma$$

$$+\left[A_{10}\left(d_\alpha \frac{\partial C_\alpha}{\partial \alpha}\right) - B_{10}\left(d_\alpha \frac{\partial c_\alpha}{\partial \alpha}\right)\right] s_\beta^3 d_\beta^2 c_\gamma d_\gamma$$

$$+\left[A_{11}\left(2 s_\alpha^2 \frac{\partial L_\alpha}{\partial \alpha}\right) - B_{11}\left(2 s_\alpha^2 \frac{\partial \ell_\alpha}{\partial \alpha}\right)\right] s_\beta c_\beta d_\beta \ell_\gamma$$

$$+\left[A_{11}\left(-2 \frac{\partial L_\alpha}{\partial \alpha}\right) - B_{11}\left(-2 \frac{\partial \ell_\alpha}{\partial \alpha}\right)\right] s_\beta^3 c_\beta d_\beta \ell_\gamma$$

$$+\left[A_{12}\left(s_\alpha^2 \frac{\partial M_\alpha}{\partial \alpha}\right) - B_{12}\left(s_\alpha^2 \frac{\partial m_\alpha}{\partial \alpha}\right)\right]\left(d_\beta^2 - k^2 s_\beta^2\right) c_\beta s_\gamma d_\gamma$$

$$+\left[A_{12}\left(-\frac{\partial M_\alpha}{\partial \alpha}\right) - B_{12}\left(-\frac{\partial m_\alpha}{\partial \alpha}\right)\right]\left(d_\beta^2 - k^2 s_\beta^2\right) s_\beta^2 c_\beta s_\gamma d_\gamma$$

$$+\left[A_{13}\left(\ell s_\alpha^2 \frac{\partial N_\alpha}{\partial \alpha}\right) - B_{13}\left(2 s_\alpha^2 \frac{\partial n_\alpha}{\partial \alpha}\right)\right] s_\beta c_\beta d_\beta n_\gamma$$

$$+\left[A_{13}\left(-2 \frac{\partial N_\alpha}{\partial \alpha}\right) - B_{13}\left(-2 \frac{\partial n_\alpha}{\partial \alpha}\right)\right] s_\beta^3 c_\beta d_\beta n_\gamma$$

$$+\left[A_{14}\left(-s_\alpha^2 \frac{\partial O_\alpha}{\partial \alpha}\right) - B_{14}\left(-s_\alpha^2 \frac{\partial o_\alpha}{\partial \alpha}\right)\right]\left(d_\beta^2 + k^2 c_\beta^2\right) s_\beta c_\gamma d_\gamma$$

$$+\left[A_{14}\left(\frac{\partial O_\alpha}{\partial \alpha}\right) - B_{14}\left(\frac{\partial o_\alpha}{\partial \alpha}\right)\right]\left(d_\beta^2 + k^2 c_\beta^2\right) s_\beta^3 c_\gamma d_\gamma$$

$$+\left[A_{15}\left(s_\alpha^2\ \frac{\partial P_\alpha}{\partial \alpha}\right)-B_{15}\left(s_\alpha^2\ \frac{\partial P_\alpha}{\partial \alpha}\right)\right]\left(c_\beta^2-s_\beta^2\right) d_\beta\, s_\gamma\, c_\gamma$$

$$+\left[A_{15}\left(-\frac{\partial P_\alpha}{\partial \alpha}\right)-B_{15}\left(-\frac{\partial P_\alpha}{\partial \alpha}\right)\right]\left(c_\beta^2-s_\beta^2\right) s_\beta^2 d_\beta^2 s_\gamma\, c_\gamma$$

$$+\left(k^2 s_\alpha^2 c_\alpha d_\alpha\right)\left[A_2 D_\alpha - B_2 d_\alpha\right] s_\beta^2 c_\beta\, s_\gamma d_\gamma$$

$$+\left(-s_\alpha^2 c_\alpha d_\alpha\right)\left[A_3 S_\alpha - B_3 s_\alpha\right] s_\beta c_\beta d_\beta\, s_\gamma^2$$

$$+\left(s_\alpha^2 c_\alpha d_\alpha\right)\left[A_4 C_\alpha - B_4 c_\alpha\right] s_\beta^2 d_\beta\, s_\gamma c_\gamma$$

$$+\left(k^2 s_\alpha c_\alpha^2 d_\alpha\right)\left[A_5 D_\alpha - B_5 d_\alpha\right] s_\beta c_\beta^2 c_\gamma d_\gamma$$

$$+\left(-s_\alpha c_\alpha^2 d_\alpha\right)\left[A_6 S_\alpha - B_6 s_\alpha\right] c_\beta^2 d_\beta\, s_\gamma d_\gamma$$

$$+\left(s_\alpha c_\alpha^2 d_\alpha\right)\left[A_7 C_\alpha - B_7 c_\alpha\right] s_\beta c_\beta d_\beta\, c_\gamma^2$$

$$+\left(k^2 s_\alpha c_\alpha d_\alpha^2\right)\left[A_8 D_\alpha - B_8 d_\alpha\right] s_\beta c_\beta d_\beta\, d_\gamma^2$$

$$+\left(-s_\alpha c_\alpha d_\alpha^2\right)\left[A_9 S_\alpha - B_9 s_\alpha\right] c_\beta d_\beta^2 s_\gamma d_\gamma$$

$$+\left(s_\alpha c_\alpha d_\alpha^2\right)\left[A_{10} C_\alpha - B_{10} c_\alpha\right] s_\beta d_\beta^2 c_\gamma d_\gamma$$

$$+\left(-2 s_\alpha c_\alpha d_\alpha\right)\left[A_{11} L_\alpha - B_{11} l_\alpha\right] s_\beta c_\beta d_\beta\, l_\gamma$$

$$+\left(-s_\alpha c_\alpha d_\alpha\right)\left[A_{12} M_\alpha - B_{12} m_\alpha\right]\left(d_\beta^2-k^2 s_\beta^2\right) c_\beta s_\gamma d_\gamma$$

$$+ (-2 s_\alpha c_\alpha d_\alpha) [A_{13} N_\alpha - B_{13} n_\alpha] s_\beta c_\beta d_\beta n_\gamma$$

$$+ (s_\alpha c_\alpha d_\alpha) [A_{14} O_\alpha - B_{14} o_\alpha] (d_\beta^2 + k^2 c_\beta^2) s_\beta c_\gamma d_\gamma$$

$$+ (-s_\alpha c_\alpha d_\alpha) [A_{15} P_\alpha - B_{15} p_\alpha] (c_\beta^2 - s_\beta^2) d_\beta s_\gamma c_\gamma$$

$$+ A_1 s_\beta c_\beta d_\beta W_\alpha$$

$$+ \left[A_2 s_\alpha \frac{\partial D_\alpha}{\partial \alpha} - B_2 s_\alpha \frac{\partial d_\alpha}{\partial \alpha}\right] s_\beta^2 c_\beta d_\beta^2 s_\gamma d_\gamma$$

$$+ \left[A_3 s_\alpha \frac{\partial S_\alpha}{\partial \alpha} - B_3 s_\alpha \frac{\partial s_\alpha}{\partial \alpha}\right] s_\beta^3 c_\beta d_\beta s_\gamma^2$$

$$+ \left[A_4 s_\alpha \frac{\partial C_\alpha}{\partial \alpha} - B_4 s_\alpha \frac{\partial c_\alpha}{\partial \alpha}\right] s_\beta^2 c_\beta^2 d_\beta s_\gamma c_\gamma$$

$$+ \left[A_5 c_\alpha \frac{\partial D_\alpha}{\partial \alpha} - B_5 c_\alpha \frac{\partial d_\alpha}{\partial \alpha}\right] s_\beta c_\beta^2 d_\beta^2 c_\gamma d_\gamma$$

$$+ \left[A_6 c_\alpha \frac{\partial S_\alpha}{\partial \alpha} - B_6 c_\alpha \frac{\partial s_\alpha}{\partial \alpha}\right] s_\beta^2 c_\beta^2 d_\beta s_\gamma c_\gamma$$

$$+ \left[A_7 c_\alpha \frac{\partial C_\alpha}{\partial \alpha} - B_7 c_\alpha \frac{\partial c_\alpha}{\partial \alpha}\right] s_\beta c_\beta^3 d_\beta c_\gamma^2$$

$$+ \left[A_8 d_\alpha \frac{\partial D_\alpha}{\partial \alpha} - B_8 d_\alpha \frac{\partial d_\alpha}{\partial \alpha}\right] s_\beta d_\beta^3 c_\beta d_\gamma^2$$

$$+ \left[A_9 d_\alpha \frac{\partial S_\alpha}{\partial \alpha} - B_9 d_\alpha \frac{\partial s_\alpha}{\partial \alpha}\right] s_\beta^2 c_\beta d_\beta^2 s_\gamma d_\gamma$$

$$+ \left[A_{10} d_\alpha \frac{\partial C_\alpha}{\partial \alpha} - B_{10} d_\alpha \frac{\partial c_\alpha}{\partial \alpha}\right] s_\beta c_\beta^2 d_\beta^2 c_\gamma d_\gamma$$

$$+\left[A_{11}\frac{\partial L_\alpha}{\partial\alpha}-B_{11}\frac{\partial l_\alpha}{\partial\alpha}\right]s_\beta c_\beta d_\beta\, l_\beta l_\gamma$$

$$+\left[A_{12}\frac{\partial M_\alpha}{\partial\alpha}-B_{12}\frac{\partial m_\alpha}{\partial\alpha}\right]s_\beta^2 c_\beta d_\beta^2 s_\gamma d_\gamma$$

$$+\left[A_{13}\frac{\partial N_\alpha}{\partial\alpha}-B_{13}\frac{\partial n_\alpha}{\partial\alpha}\right]s_\beta c_\beta d_\beta\, n_\beta n_\gamma$$

$$+\left[A_{14}\frac{\partial O_\alpha}{\partial\alpha}-B_{14}\frac{\partial o_\alpha}{\partial\alpha}\right]s_\beta c_\beta^2 d_\beta^2 c_\gamma d_\gamma$$

$$+\left[A_{15}\frac{\partial P_\alpha}{\partial\alpha}-B_{15}\frac{\partial p_\alpha}{\partial\alpha}\right]s_\beta^2 c_\beta^2 d_\beta s_\gamma c_\gamma$$

$$+\left[A_2(1-2\nu)s_\alpha\frac{\partial D_\alpha}{\partial\alpha}-B_2(1-2\nu')s_\alpha\frac{\partial d_\alpha}{\partial\alpha}\right](-s_\alpha^2+s_\beta^2)c_\beta d_\beta^2 s_\gamma d_\gamma$$

$$+\left[A_3(1-2\nu)s_\alpha\frac{\partial S_\alpha}{\partial\alpha}-B_3(1-2\nu')s_\alpha\frac{\partial s_\alpha}{\partial\alpha}\right](-s_\alpha^2+s_\beta^2)s_\beta c_\beta d_\beta s_\gamma^2$$

$$+\left[A_4(1-2\nu)s_\alpha\frac{\partial C_\alpha}{\partial\alpha}-B_4(1-2\nu')s_\alpha\frac{\partial c_\alpha}{\partial\alpha}\right](-s_\alpha^2+s_\beta^2)c_\beta^2 d_\beta s_\gamma c_\gamma$$

$$+\left[A_5(1-2\nu)c_\alpha\frac{\partial D_\alpha}{\partial\alpha}-B_5(1-2\nu')c_\alpha\frac{\partial d_\alpha}{\partial\alpha}\right](s_\alpha^2-s_\beta^2)s_\beta d_\beta^2 c_\gamma d_\gamma$$

$$+\left[A_6(1-2\nu)c_\alpha\frac{\partial S_\alpha}{\partial\alpha}-B_6(1-2\nu')c_\alpha\frac{\partial s_\alpha}{\partial\alpha}\right](s_\alpha^2-s_\beta^2)s_\beta^2 d_\beta s_\gamma c_\gamma$$

$$+\left[A_7(1-2\nu)c_\alpha\frac{\partial C_\alpha}{\partial\alpha}-B_7(1-2\nu')c_\alpha\frac{\partial c_\alpha}{\partial\alpha}\right](s_\alpha^2-s_\beta^2)s_\beta c_\beta d_\beta c_\gamma^2$$

$$+\left[A_8(1-2\nu)k^2 d_\alpha\frac{\partial D_\alpha}{\partial\alpha}-B_8(1-2\nu')k^2 d_\alpha\frac{\partial d_\alpha}{\partial\alpha}\right](s_\alpha^2-s_\beta^2)s_\beta c_\beta d_\beta d_\gamma^2$$

$$+\left[A_9(1-2\nu)k^2 d_\alpha\frac{\partial S_\alpha}{\partial\alpha}-B_9(1-2\nu')k^2 d_\alpha\frac{\partial s_\alpha}{\partial\alpha}\right](s_\alpha^2-s_\beta^2)s_\beta^2 c_\beta s_\gamma d_\gamma$$

$$+\left[A_{10}(1-2\nu)k^2 d_\alpha \frac{\partial c_\alpha}{\partial \alpha} - B_{10}(1-2\nu')k^2 d_\alpha \frac{\partial c_\alpha}{\partial \alpha}\right](s_\alpha^2 - s_\beta^2)\, s_\beta c_\beta^2 c_\gamma d_\gamma$$

$$+\left[A_2(1-2\nu)k^2 c_\alpha d_\alpha D_\alpha - B_2(1-2\nu')k^2 c_\alpha d_\alpha^2\right](s_\alpha^2 - s_\beta^2)\, s_\beta^2 c_\beta s_\gamma d_\gamma$$

$$+\left[A_3(1-2\nu)\, c_\alpha d_\alpha S_\alpha - B_3(1-2\nu')\, c_\alpha d_\alpha s_\alpha\right](-s_\alpha^2 + s_\beta^2)\, s_\beta c_\beta d_\beta s_\gamma^2$$

$$+\left[A_4(1-2\nu)\, c_\alpha d_\alpha C_\alpha - B_4(1-2\nu')\, c_\alpha^2 d_\alpha\right](s_\alpha^2 - s_\beta^2)\, s_\beta^2 d_\beta s_\gamma c_\gamma$$

$$+\left[A_5(1-2\nu)\, k^2 s_\alpha d_\alpha D_\alpha - B_5(1-2\nu')\, k^2 s_\alpha d_\alpha^2\right](-s_\alpha^2 + s_\beta^2)\, s_\beta c_\beta^2 c_\gamma d_\gamma$$

$$+\left[A_6(1-2\nu)\, s_\alpha d_\alpha S_\alpha - B_6(1-2\nu')\, s_\alpha^2 d_\alpha\right](s_\alpha^2 - s_\beta^2)\, c_\beta^2 d_\beta s_\gamma c_\gamma$$

$$+\left[A_7(1-2\nu)\, s_\alpha d_\alpha C_\alpha - B_7(1-2\nu')\, s_\alpha c_\alpha d_\alpha\right](-s_\alpha^2 + s_\beta^2)\, s_\beta c_\beta d_\beta c_\gamma^2$$

$$+\left[A_8(1-2\nu)\, k^4 s_\alpha c_\alpha D_\alpha - B_8(1-2\nu')k^4 s_\alpha c_\alpha d_\alpha\right](-s_\alpha^2 + s_\beta^2)\, s_\beta c_\beta d_\beta d_\gamma^2$$

$$+\left[A_9(1-2\nu)\, k^2 s_\alpha c_\alpha S_\alpha - B_9(1-2\nu')\, k^2 s_\alpha^2 c_\alpha\right](s_\alpha^2 - s_\beta^2)\, c_\beta d_\beta^2 s_\gamma d_\gamma$$

$$+\left[A_{10}(1-2\nu)\, k^2 s_\alpha c_\alpha C_\alpha - B_{10}(1-2\nu')k^2 s_\alpha c_\alpha^2\right](-s_\alpha^2 + s_\beta^2)\, s_\beta d_\beta^2 c_\gamma d_\gamma$$

$$=$$

$$-k^2 m^2 (s_\alpha^2 - s_\beta^2)\, s_\alpha c_\alpha d_\alpha\, s_\beta c_\beta d_\beta\, s_\gamma^2\, \tau_{xx}^{(0)}$$

$$-\frac{k^2 m^2}{k'^2}(s_\alpha^2 - s_\beta^2)\, s_\alpha c_\alpha d_\alpha\, s_\beta c_\beta d_\beta\, c_\gamma^2\, \tau_{yy}^{(0)}$$

$$+\frac{k^2m^2}{k'^2}\left(s_\alpha^2-s_\beta^2\right)s_\alpha c_\alpha d_\alpha s_\beta c_\beta d_\beta\; c_\gamma^2\;\tau_{zz}^{(0)}$$

$$+\left(-\frac{ik^2m^2}{k'^2}\right)\left(s_\alpha d_\alpha^2 s_\beta c_\beta^2 c_\gamma d_\gamma + s_\alpha c_\alpha^2 s_\beta d_\beta^2 c_\gamma d_\gamma\right)\cdot\left(s_\alpha^2-s_\beta^2\right)\tau_{yz}^{(0)}$$

$$+\left(\frac{ik^2m^2}{k'}\right)\left(c_\alpha d_\alpha^2 s_\beta^2 c_\beta s_\gamma d_\gamma + s_\alpha^2 c_\alpha c_\beta d_\beta^2 s_\gamma d_\gamma\right)\cdot\left(s_\alpha^2-s_\beta^2\right)\tau_{zx}^{(0)}$$

$$+\left(-\frac{k^2m^2}{k'}\right)\left(c_\alpha^2 d_\alpha s_\beta^2 d_\beta s_\gamma c_\gamma + s_\alpha^2 d_\alpha c_\beta^2 d_\beta s_\gamma c_\gamma\right)\cdot\left(s_\alpha^2-s_\beta^2\right)\tau_{xy}^{(0)}$$

(A-11-2)

The remarks made earlier about equation (A-11-1) apply here as well. Note that equation (A-11-2) was divided through by the factor $h_\alpha h_\beta / q_\gamma^2$. The equation expressing the continuity of $\tau_{\alpha\gamma}$ is simply obtained from (A-11-2) by interchanging β and γ everywhere.

We turn now to the equation expressing the continuity of the normal component of displacement u_α. We shall denote by Δ the trace of the prestress, that is

$$\Delta = \tau_{xx}^{(0)} + \tau_{yy}^{(0)} + \tau_{zz}^{(0)} \qquad \text{(A-11-3)}$$

The developed equation reads :

$$\frac{1}{2\mu} A_1 + \left\{ \left[s_\alpha \frac{\partial D_\alpha}{\partial \alpha} - (3-4\nu)\, c_\alpha d_\alpha D_\alpha \right] \frac{A_2}{2\mu} + \left[R^2 s_\alpha^2 c_\alpha + (3-4\nu')\, c_\alpha d_\alpha^2 \right] \frac{B_2}{2\mu'} \right\} s_\beta d_\beta s_\gamma d_\gamma$$

$$+ \left\{ \left[s_\alpha \frac{\partial S_\alpha}{\partial \alpha} - (3-4\nu)\, c_\alpha d_\alpha S_\alpha \right] \frac{A_3}{2\mu} - \left[s_\alpha c_\alpha d_\alpha - (3-4\nu')\, s_\alpha c_\alpha d_\alpha \right] \frac{B_3}{2\mu'} \right\} s_\beta^2 s_\gamma^2$$

$$+ \left\{ \left[s_\alpha \frac{\partial C_\alpha}{\partial \alpha} - (3-4\nu)\, c_\alpha d_\alpha C_\alpha \right] \frac{A_4}{2\mu} + \left[s_\alpha^2 d_\alpha + (3-4\nu')\, c_\alpha^2 d_\alpha \right] \frac{B_4}{2\mu'} \right\} s_\beta c_\beta s_\gamma c_\gamma$$

$$+ \left\{ \left[c_\alpha \frac{\partial D_\alpha}{\partial \alpha} + (3-4\nu)\, s_\alpha d_\alpha D_\alpha \right] \frac{A_5}{2\mu} + \left[R^2 s_\alpha c_\alpha^2 - (3-4\nu')\, s_\alpha d_\alpha^2 \right] \frac{B_5}{2\mu'} \right\} c_\beta d_\beta c_\gamma d_\gamma$$

$$+ \left\{ \left[c_\alpha \frac{\partial S_\alpha}{\partial \alpha} + (3-4\nu)\, s_\alpha d_\alpha S_\alpha \right] \frac{A_6}{2\mu} - \left[c_\alpha^2 d_\alpha + (3-4\nu')\, s_\alpha^2 d_\alpha \right] \frac{B_6}{2\mu'} \right\} s_\beta c_\beta s_\gamma c_\gamma$$

$$+ \left\{ \left[c_\alpha \frac{\partial C_\alpha}{\partial \alpha} + (3-4\nu)\, s_\alpha d_\alpha C_\alpha \right] \frac{A_7}{2\mu} - \left[-s_\alpha c_\alpha d_\alpha + (3-4\nu')\, s_\alpha c_\alpha d_\alpha \right] \frac{B_7}{2\mu'} \right\} c_\beta^2 c_\gamma^2$$

$$+\left\{\left[d_\alpha \frac{\partial D_\alpha}{\partial \alpha} + k^2(3-4\nu)\, s_\alpha c_\alpha D_\alpha\right]\frac{A_8}{2\mu} - \left[-k^2 s_\alpha c_\alpha d_\alpha + k^2(3-4\nu')\, s_\alpha c_\alpha d_\alpha\right]\frac{B_8}{2\mu'}\right\} d_\beta^2 d_\gamma^2$$

$$+\left\{\left[d_\alpha \frac{\partial S_\alpha}{\partial \alpha} + k^2(3-4\nu)\, s_\alpha c_\alpha S_\alpha\right]\frac{A_9}{2\mu} - \left[c_\alpha d_\alpha^2 + k^2(3-4\nu')\, s_\alpha^2 c_\alpha\right]\frac{B_9}{2\mu'}\right\} s_\beta d_\beta s_\gamma d_\gamma$$

$$+\left\{\left[d_\alpha \frac{\partial C_\alpha}{\partial \alpha} + k^2(3-4\nu)\, s_\alpha c_\alpha C_\alpha\right]\frac{A_{10}}{2\mu} - \left[-s_\alpha d_\alpha^2 + k^2(3-4\nu')\, s_\alpha c_\alpha^2\right]\frac{B_{10}}{2\mu'}\right\} c_\beta d_\beta c_\gamma d_\gamma$$

$$+\left\{\left[\frac{\partial L_\alpha}{\partial \alpha}\right]\frac{A_{11}}{2\mu} - \left[2 s_\alpha c_\alpha d_\alpha\right]\frac{B_{11}}{2\mu'}\right\} l_\beta l_\gamma$$

$$+\left\{\left[\frac{\partial M_\alpha}{\partial \alpha}\right]\frac{A_{12}}{2\mu} - \left[c_\alpha d_\alpha^2 - k^2 s_\alpha^2 c_\alpha\right]\frac{B_{12}}{2\mu'}\right\} s_\beta d_\beta s_\gamma d_\gamma$$

$$+\left\{\left[\frac{\partial N_\alpha}{\partial \alpha}\right]\frac{A_{13}}{2\mu} - \left[2 s_\alpha c_\alpha d_\alpha\right]\frac{B_{13}}{2\mu'}\right\} n_\beta n_\gamma$$

$$+\left\{\left[\frac{\partial O_\alpha}{\partial \alpha}\right]\frac{A_{14}}{2\mu} + \left[s_\alpha d_\alpha^2 + k^2 s_\alpha c_\alpha^2\right]\frac{B_{14}}{2\mu'}\right\} c_\beta d_\beta c_\gamma d_\gamma$$

$$+\left\{\left[\frac{\partial P_\alpha}{\partial \alpha}\right]\frac{A_{15}}{2\mu} - \left[c_\alpha^2 d_\alpha - s_\alpha^2 d_\alpha\right]\frac{B_{15}}{2\mu'}\right\} s_\beta c_\beta s_\gamma c_\gamma$$

$$= -k^2 m^2 s_\alpha c_\alpha d_\alpha \left(\frac{\tau_{xx}^{(0)}}{2\mu} - \frac{\sigma\Delta}{2\mu(1+\sigma)}\right) s_\beta^2 s_\gamma^2$$

$$+\frac{\ell^2 m^2}{k'}\, c_\alpha^2 d_\alpha\, \frac{\tau_{xy}^{(0)}}{2\mu}\, s_\beta c_\beta s_\gamma c_\gamma$$

$$-\frac{im^2}{k'}\, c_\alpha d_\alpha^2\, \frac{\tau_{xz}^{(0)}}{2\mu}\, s_\beta d_\beta s_\gamma d_\gamma$$

$$-\frac{\ell^2 m^2}{k'}\, s_\alpha^2 d_\alpha\, \frac{\tau_{xy}^{(0)}}{2\mu}\, s_\beta c_\beta s_\gamma c_\gamma$$

$$+\frac{\ell^2 m^2}{k'^2}\, s_\alpha c_\alpha d_\alpha \left(\frac{\tau_{yy}^{(0)}}{2\mu} - \frac{\sigma\Delta}{2\mu(1+\sigma)} \right) c_\beta^2 c_\gamma^2$$

$$-\frac{im^2}{k'^2}\, s_\alpha d_\alpha^2\, \frac{\tau_{yz}^{(0)}}{2\mu}\, c_\beta d_\beta c_\gamma d_\gamma$$

$$+\frac{i\ell^2 m^2}{k'}\, s_\alpha^2 c_\alpha\, \frac{\tau_{xz}^{(0)}}{2\mu}\, s_\beta d_\beta s_\gamma d_\gamma$$

$$-\frac{i\ell^2 m^2}{k'^2}\, s_\alpha c_\alpha^2\, \frac{\tau_{yz}^{(0)}}{2\mu}\, c_\beta d_\beta c_\gamma d_\gamma$$

$$-\frac{m^2}{k'^2}\, s_\alpha c_\alpha d_\alpha \left(\frac{\tau_{zz}^{(0)}}{2\mu} - \frac{\sigma\Delta}{2\mu(1+\sigma)} \right) d_\beta^2 d_\gamma^2$$

(A-11-4)

This equation was divided through by h_α . Finally we express the continuity of the component u_β of the displacement field by the equation :

$$\Big\{ \left(-k^2 s_\alpha D_\alpha\right) A_2 - \left(-k^2 s_\alpha d_\alpha\right) \frac{\nu}{\nu'} B_2 + \Big[k^2 (3-4\nu) \cdot d_\alpha S_\alpha \Big] A_9 - \Big[k^2 (3-4\nu') \frac{\nu}{\nu'} s_\alpha d_\alpha \Big] B_9 + \left(-k^2 M_\alpha\right) A_{12} - \left(-k^2 m_\alpha\right) \frac{\nu}{\nu'} B_{12} \Big\} s_\beta^2 c_\beta s_\gamma d_\gamma$$

$$+ \Big\{ \Big[-(3-4\nu) s_\alpha D_\alpha \Big] A_2 - \Big[-(3-4\nu') \frac{\nu}{\nu'} s_\alpha d_\alpha \Big] B_2 + \left(d_\alpha S_\alpha\right) A_9 - \left(s_\alpha d_\alpha\right) \frac{\nu}{\nu'} B_9 + M_\alpha A_{12} - m_\alpha \frac{\nu}{\nu'} B_{12} \Big\} c_\beta d_\beta^2 s_\gamma d_\gamma$$

$$+ \Big\{ \left(-s_\alpha C_\alpha\right) A_4 - \left(-s_\alpha c_\alpha\right) \frac{\nu}{\nu'} B_4 + \Big[(3-4\nu) c_\alpha S_\alpha \Big] A_6 - \Big[(3-4\nu') \frac{\nu}{\nu'} c_\alpha s_\alpha \Big] B_6 - P_\alpha A_{15} + P_\alpha \frac{\nu}{\nu'} B_{15} \Big\} s_\beta^2 d_\beta s_\gamma c_\gamma$$

$$+ \Big\{ \Big[-(3-4\nu) s_\alpha C_\alpha \Big] A_4 - \Big[-(3-4\nu') \frac{\nu}{\nu'} s_\alpha c_\alpha \Big] B_4 + \left(c_\alpha S_\alpha\right) A_6 - \left(s_\alpha c_\alpha\right) \frac{\nu}{\nu'} B_6 + P_\alpha A_{15} - P_\alpha \frac{\nu}{\nu'} B_{15} \Big\} c_\beta^2 d_\beta s_\gamma c_\gamma$$

$$+ \Big\{ \left(-k^2 c_\alpha D_\alpha\right) A_5 - \left(-k^2 c_\alpha d_\alpha\right) \frac{\nu}{\nu'} B_5 + \Big[k^2 (3-4\nu) d_\alpha C_\alpha \Big] A_{10} - \Big[k^2 (3-4\nu') \frac{\nu}{\nu'} c_\alpha d_\alpha \Big] B_{10} - k^2 O_\alpha A_{14} + k^2 O_\alpha \frac{\nu}{\nu'} B_{14} \Big\} \cdot s_\beta c_\beta^2 c_\gamma d_\gamma$$

$$+ \Big\{ \Big[(3-4\nu) c_\alpha D_\alpha \Big] A_5 - \Big[(3-4\nu') \frac{\nu}{\nu'} c_\alpha d_\alpha \Big] B_5 - d_\alpha C_\alpha A_{10}$$

$$+ c_\alpha d_\alpha \frac{\mu}{\mu'} B_{10} - O_\alpha A_{14} + o_\alpha \frac{\mu}{\mu'} B_{14} \Big\} s_\beta d_\beta^2 c_\gamma d_\gamma$$

$$+ \Big\{ \Big[-2(1-2\nu) s_\alpha S_\alpha \Big] A_3 - \Big[-2(1-2\nu') \frac{\mu}{\mu'} s_\alpha^2 \Big] B_3$$

$$+ \Big[-2(1-2\nu) c_\alpha C_\alpha \Big] A_7 - \Big[-2(1-2\nu') \frac{\mu}{\mu'} c_\alpha^2 \Big] B_7$$

$$+ \Big[-2k^4 (1-2\nu) d_\alpha D_\alpha \Big] A_8 - \Big[-2k^4 (1-2\nu') d_\alpha^2 \frac{\mu}{\mu'} \Big] B_8$$

$$+ 2L_\alpha A_{11} - 2\ell_\alpha \frac{\mu}{\mu'} B_{11} + 2N_\alpha A_{13} - 2n_\alpha \frac{\mu}{\mu'} B_{13} \Big\}$$

$$\cdot s_\beta c_\beta d_\beta s_\gamma^2$$

$$+ \Big\{ \Big[2(1-2\nu) c_\alpha C_\alpha \Big] A_7 - \Big[2(1-2\nu') \frac{\mu}{\mu'} c_\alpha^2 \Big] B_7$$

$$+ \Big[2k^2 (1-2\nu) d_\alpha D_\alpha \Big] A_8 - \Big[2k^2 (1-2\nu') \frac{\mu}{\mu'} d_\alpha^2 \Big] B_8$$

$$+ (-2P_1 L_\alpha) A_{11} - (-2P_1 \ell_\alpha) \frac{\mu}{\mu'} B_{11} + (-2P_2 N_\alpha) A_{13}$$

$$- (-2P_2 n_\alpha) \frac{\mu}{\mu'} B_{13} \Big\} s_\beta c_\beta d_\beta$$

$$=$$

$$- k^2 m^2 \left(\tau_{xx}^{(0)} - \frac{\sigma \Delta}{1+\sigma} \right) s_\alpha^2 s_\beta c_\beta d_\beta s_\gamma^2$$

$$+ \frac{k^2 m^2}{k^{12}} \tau_{xy}^{(0)} s_\alpha c_\alpha c_\beta^2 d_\beta s_\gamma c_\gamma$$

$$
\begin{aligned}
&- \frac{i m^2}{k'} \tau^{(0)}_{xz} \, s_\alpha d_\alpha \, c_\beta d_\beta^2 \, s_\gamma d_\gamma \\
&- \frac{k^2 m^2}{k'} \tau^{(0)}_{xy} \, s_\alpha c_\alpha \, s_\beta^2 d_\beta \, s_\gamma c_\gamma \\
&+ \frac{k^2 m^2}{k'^2} \left(\tau^{(0)}_{yy} - \frac{\sigma \Delta}{1+\sigma} \right) c_\alpha^2 \, s_\beta c_\beta d_\beta \, c_\gamma^2 \\
&- \frac{i m^2}{k'^2} \tau^{(0)}_{yz} \, c_\alpha d_\alpha \, s_\beta d_\beta^2 \, c_\gamma d_\gamma \\
&+ \frac{i k^2 m^2}{k'} \tau^{(0)}_{xz} \, s_\alpha d_\alpha \, s_\beta^2 c_\beta \, s_\gamma d_\gamma \\
&- \frac{i k^2 m^2}{k'^2} \tau^{(0)}_{yz} \, c_\alpha d_\alpha \, s_\beta c_\beta^2 \, c_\gamma d_\gamma \\
&- \frac{m^2}{k'^2} \left(\tau^{(0)}_{zz} - \frac{\sigma \Delta}{1+\sigma} \right) d_\alpha^2 \, s_\beta c_\beta d_\beta \, d_\gamma^2
\end{aligned}
$$

(A-11-5)

This equation was divided through by the factor $-h_\alpha / 2\mu$. The corresponding equation for the component u_γ of the displacement field is simply obtained by interchanging β and γ in (A-11-5). The reduction of the equations given in this Appendix is done by applying the formulae of Appendix 12, and by following the algorithm given at the end of it.

APPENDIX 12

SOLUTION FOR THE STATIC ELLIPSOIDAL INCLUSION

The boundary conditions expressed in Appendix 11 are to be satisfied identically in β and γ on the inclusion boundary $\alpha = \alpha_o$. This appendix contains the necessary formulae to reduce these equations. General formulae are given which include 1) identities between the Jacobi elliptic functions; 2) first and second derivatives of the Lamé functions of the first and second kind, of the metric coefficients, and of the Lamé products; 3) useful identities to reduce some of the expressions encountered in reducing the equations; 4) a list of the independent functions of β and γ found in each one of the four equations of Appendix 11; and 5) a flow chart of the reduction algorithm.

i) General identities between Jacobi elliptic functions

These identities can be found in the literature (e.g., Whittaker and Watson, 1927), Arscott (1964), Erdelyi (1953).

$$s_\alpha^2 + c_\alpha^2 = 1$$

$$k^2 s_\alpha^2 + d_\alpha^2 = 1$$

$$d_\alpha^2 - k^2 c_\alpha^2 = k'^2$$

$$k^2 s_\gamma^2 s_\beta^2 - \frac{k^2}{k'^2} c_\beta^2 c_\gamma^2 + \frac{1}{k'^2} d_\beta^2 d_\gamma^2 = 1$$

$$s_\beta^2 + s_\gamma^2 = (1+k^2)\, s_\beta^2 s_\gamma^2 - \frac{1}{k'^2}\, c_\beta^2 c_\gamma^2 + \frac{1}{k'^2}\, d_\beta^2 d_\gamma^2$$

$$(1 - k^2 s_\beta^2 s_\gamma^2)\, s_{\beta+\gamma} = s_\beta c_\gamma d_\gamma + s_\gamma c_\beta d_\beta$$

$$(1 - k^2 s_\beta^2 s_\gamma^2)\, c_{\beta+\gamma} = c_\beta c_\gamma - s_\beta s_\gamma d_\beta d_\gamma$$

$$(1 - k^2 s_\beta^2 s_\gamma^2)\, d_{\beta+\gamma} = d_\beta d_\gamma - k^2 s_\beta s_\gamma c_\beta c_\gamma$$

ii) Derivatives appearing in the equation

a) Lamé functions of the first kind

$$Ec_0^0 = 1 \qquad \frac{d\, Ec_0^0}{d\alpha} = 0 \qquad \frac{d^2 Ec_0^0}{d\alpha^2} = 0$$

$$Ec_1^0 = d_\alpha \qquad \frac{d\, d_\alpha}{d\alpha} = -k^2 s_\alpha c_\alpha$$

$$\frac{d^2 d_\alpha}{d\alpha^2} = -k^2 c_\alpha^2 d_\alpha + k^2 s_\alpha^2 d_\alpha$$

$$Ec_1^1 = s_\alpha \qquad \frac{d\, s_\alpha}{d\alpha} = c_\alpha d_\alpha$$

$$\frac{d^2 s_\alpha^2}{d\alpha} = -s_\alpha d_\alpha^2 - k^2 s_\alpha c_\alpha^2$$

$$Es_1^1 = c_\alpha \qquad \frac{d\, c_\alpha}{d\alpha} = -s_\alpha d_\alpha$$

$$\frac{d^2 c_\alpha}{d\alpha^2} = -c_\alpha d_\alpha^2 + k^2 s_\alpha^2 c_\alpha$$

$Ec_2^0 = \ell_\alpha$

$$\frac{d\ell_\alpha}{d\alpha} = 2 s_\alpha c_\alpha d_\alpha$$

$$\frac{d^2\ell_\alpha}{d\alpha^2} = 2 c_\alpha^2 d_\alpha^2 - 2 s_\alpha^2 d_\alpha^2 + 2k^2 s_\alpha^2 c_\alpha^2$$

$Ec_2^1 = m_\alpha$

$$\frac{dm_\alpha}{d\alpha} = c_\alpha d_\alpha^2 - k^2 s_\alpha c_\alpha^2$$

$$\frac{d^2 m_\alpha}{d\alpha^2} = -s_\alpha d_\alpha^3 - 2k^2 s_\alpha c_\alpha^2 d_\alpha - k^2 c_\alpha^3 d_\alpha + 2k^2 s_\alpha^2 d_\alpha c_\alpha$$

$Ec_2^2 = n_\alpha$

$$\frac{dn_\alpha}{d\alpha} = 2 s_\alpha c_\alpha d_\alpha$$

$$\frac{d^2 n_\alpha}{d\alpha^2} = 2 c_\alpha^2 d_\alpha^2 - 2 s_\alpha^2 d_\alpha^2 - 2k^2 s_\alpha^2 c_\alpha^2$$

$Es_2^1 = o_\alpha$

$$\frac{do_\alpha}{d\alpha} = -s_\alpha d_\alpha^2 - k^2 s_\alpha c_\alpha^2$$

$$\frac{d^2 o_\alpha}{d\alpha^2} = -c_\alpha d_\alpha^3 + 2k^2 s_\alpha^2 c_\alpha d_\alpha - k^2 c_\alpha^3 d_\alpha + 2k^2 s_\alpha^2 d_\alpha c_\alpha$$

$Es_2^2 = p_\alpha$

$$\frac{dp_\alpha}{d\alpha} = c_\alpha^2 d_\alpha - s_\alpha^2 d_\alpha$$

$$\frac{d^2 p_\alpha}{d\alpha^2} = -2 s_\alpha d_\alpha^2 c_\alpha - k^2 s_\alpha c_\alpha^3 - 2 s_\alpha c_\alpha d_\alpha^2 + k^2 s_\alpha^3 c_\alpha$$

b) Lamé functions of the second kind

The first derivatives are obtained in terms of the wronskian between Lamé functions of the first and second kind. The second derivatives are obtained directly by writing Lamé's equation.

We define the wronskian by

$$W_\lambda(z) = \lambda(z)\,\frac{d\Lambda}{dz} - \Lambda(z)\,\frac{d\lambda}{dz}$$

Then

$$\begin{cases} \dfrac{\partial D_\alpha}{\partial \alpha} = \dfrac{W_d - k^2 s_\alpha c_\alpha D_\alpha}{d_\alpha} \\ \dfrac{\partial^2 D_\alpha}{\partial \alpha^2} = k^2\left[s_\alpha^2 - c_\alpha^2\right] D_\alpha \end{cases}$$

$$\begin{cases} \dfrac{\partial S_\alpha}{\partial \alpha} = \dfrac{W_s + c_\alpha d_\alpha S_\alpha}{s_\alpha} \\ \dfrac{\partial^2 S_\alpha}{\partial \alpha^2} = -\left[d_\alpha^2 + k^2 c_\alpha^2\right] S_\alpha \end{cases}$$

$$\begin{cases} \dfrac{\partial C_\alpha}{\partial \alpha} = \dfrac{W_c - s_\alpha d_\alpha C_\alpha}{c_\alpha} \\ \dfrac{\partial^2 C_\alpha}{\partial \alpha^2} = -\left[d_\alpha^2 - k^2 s_\alpha^2\right] C_\alpha \end{cases}$$

$$\begin{cases} \dfrac{\partial L_\alpha}{\partial \alpha} = \dfrac{W_\ell + 2 s_\alpha c_\alpha d_\alpha L_\alpha}{\ell_\alpha} \\ \dfrac{\partial^2 L_\alpha}{\partial \alpha^2} = \left(6k^2 s_\alpha^2 - 2/P_1\right) L_\alpha \end{cases}$$

$$\begin{cases} \dfrac{\partial M_\alpha}{\partial \alpha} = \dfrac{W_m - c_\alpha (k^2 s_\alpha^2 - d_\alpha^2) M_\alpha}{s_\alpha d_\alpha} \\ \dfrac{\partial^2 M_\alpha}{\partial \alpha^2} = \left[-4 k^2 c_\alpha^2 - d_\alpha^2 + k^2 s_\alpha^2 \right] M_\alpha \end{cases}$$

$$\begin{cases} \dfrac{\partial N_\alpha}{\partial \alpha} = \dfrac{W_n + 2 s_\alpha c_\alpha d_\alpha N_\alpha}{n_\alpha} \\ \dfrac{\partial^2 N_\alpha}{\partial \alpha} = \left[6 k^2 s_\alpha^2 - 2/P_2 \right] N_\alpha \end{cases}$$

$$\begin{cases} \dfrac{\partial O_\alpha}{\partial \alpha} = \dfrac{W_o - \left[s_\alpha d_\alpha^2 + k^2 s_\alpha c_\alpha^2 \right] O_\alpha}{c_\alpha d_\alpha} \\ \dfrac{\partial^2 O_\alpha}{\partial \alpha^2} = -\left[d_\alpha^2 + k^2 c_\alpha^2 - 4 k^2 s_\alpha^2 \right] O_\alpha \end{cases}$$

$$\begin{cases} \dfrac{\partial P_\alpha}{\partial \alpha} = \dfrac{W_p + \left(c_\alpha^2 d_\alpha - s_\alpha^2 d_\alpha \right) P_\alpha}{s_\alpha c_\alpha} \\ \dfrac{\partial^2 P_\alpha}{\partial \alpha^2} = -\left[4 d_\alpha^2 + k^2 c_\alpha^2 - k^2 s_\alpha^2 \right] P_\alpha \end{cases}$$

c) Functions of the metric coefficients

We have the following definitions.

$$h_\alpha = \frac{1}{km\, q_\beta q_\gamma} \qquad h_\beta = \frac{i}{km\, q_\gamma q_\alpha} \qquad h_\gamma = \frac{-1}{km\, q_\alpha q_\beta}$$

$$q_\alpha = \left(s_\beta^2 - s_\gamma^2 \right)^{1/2} \qquad q_\beta = \left(s_\alpha^2 - s_\gamma^2 \right)^{1/2} \qquad q_\gamma = \left(s_\alpha^2 - s_\beta^2 \right)^{1/2}$$

Then we have to compute the following expressions

$$h_\beta^2 = - \frac{h_\alpha^2 \, q_\beta^2}{q_\alpha^2} \qquad h_\gamma^2 = \frac{h_\alpha^2 \, q_\gamma^2}{q_\alpha^2}$$

$$\frac{\partial h_\alpha}{\partial \alpha} = - s_\alpha c_\alpha d_\alpha \frac{h_\alpha}{q_\beta^2} - s_\alpha c_\alpha d_\alpha \frac{h_\alpha}{q_\gamma^2}$$

$$\frac{\partial h_\alpha}{\partial \beta} = s_\beta c_\beta d_\beta \frac{h_\alpha}{q_\gamma^2}$$

$$\frac{\partial h_\alpha}{\partial \gamma} = s_\gamma c_\gamma d_\gamma \frac{h_\alpha}{q_\beta^2}$$

$$\frac{\partial h_\beta}{\partial \alpha} = - s_\alpha c_\alpha d_\alpha \frac{h_\beta}{q_\gamma^2}$$

$$\frac{\partial h_\beta}{\partial \beta} = s_\beta c_\beta d_\beta \frac{h_\beta}{q_\gamma^2} - s_\beta c_\beta d_\beta \frac{h_\beta}{q_\alpha^2}$$

$$\frac{\partial h_\beta}{\partial \gamma} = s_\gamma c_\gamma d_\gamma \frac{h_\beta}{q_\alpha^2}$$

$$\frac{\partial h_\gamma}{\partial \alpha} = - s_\alpha c_\alpha d_\alpha \frac{h_\gamma}{q_\beta^2}$$

$$\frac{\partial h_\gamma}{\partial \beta} = - s_\beta c_\beta d_\beta \frac{h_\gamma}{q_\alpha^2}$$

$$\frac{\partial h_\gamma}{\partial \gamma} = s_\gamma c_\gamma d_\gamma \frac{h_\gamma}{q_\alpha^2} + s_\gamma c_\gamma d_\gamma \frac{h_\gamma}{q_\beta^2}$$

$$h_\alpha \frac{\partial h_\alpha}{\partial \alpha} = - s_\alpha c_\alpha d_\alpha h_\alpha^2 \frac{q_\alpha^2}{q_\beta^2 q_\alpha^2} - s_\alpha c_\alpha d_\alpha h_\alpha^2 \frac{q_\alpha^2}{q_\gamma^2 q_\alpha^2}$$

$$\frac{h_\beta^2}{h_\alpha} \frac{\partial h_\alpha}{\partial \beta} = - s_\beta c_\beta d_\beta h_\alpha^2 \frac{q_\beta^2}{q_\gamma^2 q_\alpha^2}$$

$$\frac{h_\gamma^2}{h_\alpha} \frac{\partial h_\alpha}{\partial \gamma} = s_\gamma c_\gamma d_\gamma h_\alpha^2 \frac{q_\gamma^2}{q_\beta^2 q_\alpha^2}$$

These equations are purposely left unsimplified because these are the most convenient forms when reducing the boundary condition equations.

d) Lamé products, and ellipsoidal surface harmonics.

We define the following ellipsoidal surface harmonics and their derivatives

1) $Sc_0^0 = 1$

$$\frac{\partial Sc_0^0}{\partial \beta} = \frac{\partial Sc_0^0}{\partial \gamma} = \frac{\partial^2 Sc_0^0}{\partial \beta^2} = \frac{\partial^2 Sc_0^0}{\partial \gamma^2} = \frac{\partial^2 Sc_0^0}{\partial \beta \partial \gamma} = 0$$

2) $Sc_1^0 = d_\beta d_\gamma$

$$\frac{\partial Sc_1^0}{\partial \beta} = - k^2 s_\beta c_\beta d_\gamma$$

$$\frac{\partial Sc_1^0}{\partial \gamma} = -k^2 d_\beta s_\gamma c_\gamma$$

$$\frac{\partial^2 Sc_1^0}{\partial \beta \partial \gamma} = k^4 s_\beta c_\beta s_\gamma c_\gamma$$

$$\frac{\partial^2 Sc_1^0}{\partial \beta^2} = -k^2 c_\beta^2 d_\beta d_\gamma + k^2 s_\beta^2 d_\beta d_\gamma$$

$$\frac{\partial^2 Sc_1^0}{\partial \gamma^2} = -k^2 d_\beta c_\gamma^2 d_\gamma + k^2 d_\beta s_\gamma^2 d_\gamma$$

3) $Sc_1^1 = s_\beta s_\gamma$

$$\frac{\partial Sc_1^1}{\partial \beta} = c_\beta d_\beta s_\gamma$$

$$\frac{\partial Sc_1^1}{\partial \gamma} = s_\beta c_\gamma d_\gamma$$

$$\frac{\partial^2 Sc_1^1}{\partial \beta \partial \gamma} = c_\beta d_\beta c_\gamma d_\gamma$$

$$\frac{\partial^2 Sc_1^1}{\partial \beta^2} = -s_\beta d_\beta^2 s_\gamma - k^2 s_\beta c_\beta^2 s_\gamma$$

$$\frac{\partial^2 Sc_1^1}{\partial \gamma^2} = -s_\gamma d_\gamma^2 s_\beta - k^2 s_\gamma c_\gamma^2 s_\beta$$

4) $Ss_1^1 = c_\beta c_\gamma$

$$\frac{\partial Ss_1^1}{\partial \beta} = -s_\beta d_\beta c_\gamma$$

$$\frac{\partial Sc_1^1}{\partial \gamma} = -c_\beta s_\gamma d_\gamma$$

$$\frac{\partial^2 Sc_1^1}{\partial \beta \partial \gamma} = s_\beta d_\beta s_\gamma d_\gamma$$

$$\frac{\partial^2 Sc_1^1}{\partial \beta^2} = -c_\beta d_\beta^2 c_\gamma + k^2 s_\beta^2 c_\beta c_\gamma$$

$$\frac{\partial^2 Sc_1^1}{\partial \gamma^2} = -c_\beta c_\gamma d_\gamma^2 + k^2 c_\beta s_\gamma^2 c_\gamma$$

5) $Sc_2^0 = (s_\beta^2 - P_1)(s_\gamma^2 - P_1) = l_\beta l_\gamma$

$$\frac{\partial Sc_2^0}{\partial \beta} = 2 s_\beta c_\beta d_\beta (s_\gamma^2 - P_1)$$

$$\frac{\partial Sc_2^0}{\partial \gamma} = 2 (s_\beta^2 - P_1) s_\gamma c_\gamma d_\gamma$$

$$\frac{\partial^2 Sc_2^0}{\partial \beta \partial \gamma} = 4 s_\beta c_\beta d_\beta s_\gamma c_\gamma d_\gamma$$

$$\frac{\partial^2 Sc_2^0}{\partial \beta^2} = \left(2 c_\beta^2 d_\beta^2 - 2 s_\beta^2 d_\beta^2 - 2 k^2 s_\beta^2 c_\beta^2\right)(s_\gamma^2 - P_1)$$

$$\frac{\partial^2 Sc_2^0}{\partial \gamma^2} = \left(2 c_\gamma^2 d_\gamma^2 - 2 s_\gamma^2 d_\gamma^2 - 2 k^2 s_\gamma^2 c_\gamma^2\right)(s_\beta^2 - P_1)$$

6) $Sc_2^1 = s_\beta d_\beta s_\gamma d_\gamma = m_\beta m_\gamma$

$$\frac{\partial Sc_2^1}{\partial \beta} = c_\beta^2 d_\beta^2 s_\gamma d_\gamma - k^2 s_\beta^2 c_\beta s_\gamma d_\gamma$$

$$\frac{\partial Sc_2^1}{\partial \gamma} = s_\beta d_\beta c_\gamma d_\gamma^2 - k^2 s_\beta d_\beta s_\gamma^2 c_\gamma$$

$$\frac{\partial^2 Sc_2^1}{\partial \beta \partial \gamma} = \left(c_\beta d_\beta^2 - k^2 s_\beta c_\beta^2\right)\left(c_\gamma d_\gamma^2 - k^2 s_\gamma^2 c_\gamma^2\right)$$

$$\frac{\partial^2 Sc_2^1}{\partial \beta^2} = \left(-s_\beta d_\beta^3 - 2k^2 s_\beta c_\beta^2 d_\beta - k^2 c_\beta^3 d_\beta + 2k^2 s_\beta^2 d_\beta c_\beta\right) s_\gamma d_\gamma$$

$$\frac{\partial^2 Sc_2^1}{\partial \gamma^2} = s_\beta d_\beta \left(-s_\gamma d_\gamma^3 - 2k^2 s_\gamma c_\gamma^2 d_\gamma - k^2 c_\gamma^3 d_\gamma + 2k^2 s_\gamma^2 d_\gamma c_\gamma\right)$$

7) $Sc_2^2 = \left(s_\beta^2 - P_2\right)\left(s_\gamma^2 - P_1\right)$ see Sc_2^0

8) $Ss_2^1 = c_\beta d_\beta c_\gamma d_\gamma = o_\beta o_\gamma$

$$\frac{\partial Ss_2^1}{\partial \beta} = \left(-s_\beta d_\beta^2 - k^2 s_\beta c_\beta^2\right) c_\gamma d_\gamma$$

$$\frac{\partial Ss_2^1}{\partial \gamma} = \left(-s_\gamma d_\gamma^2 - k^2 s_\gamma c_\gamma^2\right) c_\beta d_\beta$$

$$\frac{\partial^2 Ss_2^1}{\partial \beta \partial \gamma} = \left(-s_\beta d_\beta^2 - k^2 s_\beta c_\beta^2\right)\left(-s_\gamma d_\gamma^2 - k^2 s_\gamma c_\gamma^2\right)$$

$$\frac{\partial^2 Ss_2^1}{\partial \beta^2} = \left(-c_\beta d_\beta^3 + 2k^2 s_\beta^2 c_\beta d_\beta - k^2 c_\beta^3 d_\beta + 2k^2 s_\beta^2 c_\beta d_\beta\right) c_\gamma d_\gamma$$

$$\frac{\partial^2 Ss_2^1}{\partial \gamma^2} = c_\beta d_\beta \left(-c_\gamma d_\gamma^3 + 2k^2 s_\gamma^2 c_\gamma d_\gamma - k^2 c_\gamma^3 d_\gamma + 2k^2 s_\gamma^2 c_\gamma d_\gamma\right)$$

9) $Ss_2^2 = s_\beta c_\beta s_\gamma c_\gamma = p_\beta p_\gamma$

$$\frac{\partial Ss_2^2}{\partial \beta} = \left(c_\beta^2 d_\beta - s_\beta^2 d_\beta\right) s_\gamma c_\gamma$$

$$\frac{\partial Ss_2^2}{\partial \gamma} = s_\beta c_\beta \left(c_\gamma^2 d_\gamma - s_\gamma^2 d_\gamma\right)$$

$$\frac{\partial^2 Ss_2^2}{\partial \beta \partial \gamma} = \left(c_\beta^2 d_\beta - s_\beta^2 d_\beta\right)\left(c_\gamma^2 d_\gamma - s_\gamma^2 d_\gamma\right)$$

$$\frac{\partial^2 Ss_2^2}{\partial \beta^2} = \left(-2 s_\beta c_\beta d_\beta^2 - k^2 s_\beta c_\beta^3 - 2 s_\beta c_\beta d_\beta^2 + k^2 s_\beta^3 c_\beta\right) s_\gamma c_\gamma$$

$$\frac{\partial^2 Ss_2^2}{\partial \gamma^2} = \left(-2 s_\gamma c_\gamma d_\gamma^2 - k^2 s_\gamma c_\gamma^3 - 2 s_\gamma c_\gamma d_\gamma^2 + k^2 s_\gamma^3 c_\gamma\right) s_\beta c_\beta$$

Clearly, some of the expressions given above could be simplified and rewritten in a more elegant form. One must remember, however, that there is little point in doing this until one knows which independent functions of β and γ one wishes to appear. The equations listed above are particularly useful to determine the various symmetries of the displacements and stresses of the problem (see Chapter VI).

iii) Identities used in reducing the equations.

The identities given below were proven as they were needed in the process of reducing the boundary condition equations of Appendix 11. Their specific purpose is the following : the left-hand side is in all cases a particular quantity encountered during the reduction process, and the right-hand side is written in such a way so as to make specific

functions of β and γ appear explicitly. These functions must be some of the independent functions of β and γ described later in the Appendix.

1) $$\left[q_\gamma^4 s_\gamma^2 c_\gamma^2 - q_\beta^4 s_\beta^2 c_\beta^2 \right] f(\beta,\gamma) =$$
$$\left[q_\alpha^2 q_\beta^2 q_\gamma^2 (c_\alpha^2 - s_\alpha^2) + s_\alpha^2 c_\alpha^2 (q_\gamma^4 - q_\beta^4) \right] f(\beta,\gamma)$$

2) $$\left[q_\gamma^4 s_\gamma^2 d_\gamma^2 - q_\beta^4 s_\beta^2 d_\beta^2 \right] f(\beta,\gamma) =$$
$$\left[q_\alpha^2 q_\beta^2 q_\gamma^2 (d_\alpha^2 - k^2 s_\alpha^2) + s_\alpha^2 d_\alpha^2 (q_\gamma^4 - q_\beta^4) \right] f(\beta,\gamma)$$

We shall drop the arbitrary function $f(\beta,\gamma)$ for the remaining identities.

3) $$q_\gamma^4 c_\gamma^2 d_\gamma^2 - q_\beta^4 c_\beta^2 d_\beta^2 = - q_\alpha^2 q_\beta^2 q_\gamma^2 (d_\alpha^2 + k^2 c_\alpha^2) + c_\alpha^2 d_\alpha^2 (q_\gamma^4 - q_\beta^4)$$

4) $$q_\gamma^2 s_\gamma^4 - q_\beta^2 s_\beta^4 = - s_\alpha^2 q_\alpha^2 (s_\beta^2 + s_\gamma^2) + s_\beta^2 s_\gamma^2 q_\alpha^2$$

5) $$q_\gamma^2 s_\beta^2 - q_\beta^2 s_\gamma^2 = s_\alpha^2 q_\alpha^2 - q_\alpha^2 (s_\beta^2 + s_\gamma^2)$$

6) $$q_\gamma^2 s_\gamma^2 - q_\beta^2 s_\beta^2 = - s_\alpha^2 q_\alpha^2$$

7) $q_\beta^2 q_\gamma^4 c_\gamma^2 - q_\beta^4 q_\gamma^2 c_\beta^2 = - c_\alpha^2 q_\alpha^2 q_\beta^2 q_\gamma^2$

8) $q_\beta^2 q_\gamma^4 d_\gamma^2 - q_\beta^4 q_\gamma^2 d_\beta^2 = - d_\alpha^2 q_\alpha^2 q_\beta^2 q_\gamma^2$

9) $q_\beta^2 q_\gamma^4 s_\gamma^2 - q_\beta^4 q_\gamma^2 s_\beta^2 = - s_\alpha^2 q_\alpha^2 q_\beta^2 q_\gamma^2$

10) $q_\beta^2 q_\gamma^4 s_\beta^2 c_\gamma^2 d_\gamma^2 - q_\beta^4 q_\gamma^2 s_\gamma^2 c_\beta^2 d_\beta^2 =$

$$q_\alpha^2 q_\beta^2 q_\gamma^2 \left(\frac{1}{k'^2} d_\alpha^2 c_\beta^2 c_\gamma^2 - \frac{1}{k'^2} c_\alpha^2 d_\beta^2 d_\gamma^2 \right)$$

11) $q_\beta^2 q_\gamma^4 c_\beta^2 s_\gamma^2 d_\gamma^2 - q_\beta^4 q_\gamma^2 s_\beta^2 d_\beta^2 c_\gamma^2 =$

$$q_\alpha^2 q_\beta^2 q_\gamma^2 \left(k'^2 d_\alpha^2 s_\beta^2 s_\gamma^2 - s_\alpha^2 d_\beta^2 d_\gamma^2 \right)$$

12) $q_\beta^2 q_\gamma^4 s_\gamma^2 c_\gamma^2 d_\beta^2 - q_\beta^4 q_\gamma^2 s_\beta^2 c_\beta^2 d_\gamma^2 =$

$$q_\alpha^2 q_\beta^2 q_\gamma^2 \left(- k'^2 c_\alpha^2 s_\beta^2 s_\gamma^2 - s_\alpha^2 c_\beta^2 c_\gamma^2 \right)$$

13) $q_\gamma^4 c_\gamma^2 d_\gamma^2 s_\gamma^2 \ell_\beta - q_\beta^4 c_\beta^2 d_\beta^2 s_\beta^2 \ell_\gamma =$

$$- q_\alpha^2 q_\beta^2 q_\gamma^2 \left\{ (d_\alpha^2 + k^2 c_\alpha^2)(1 - P_1 k^2 s_\alpha^2) s_\beta^2 s_\gamma^2 \right.$$

$$- \frac{P_1}{k'^2} k^2 c_\alpha^2 (d_\alpha^2 - k^2 s_\alpha^2) c_\beta^2 c_\gamma^2$$

$$\left. + \frac{P_1}{k'^2} d_\alpha^2 (c_\alpha^2 - s_\alpha^2) d_\beta^2 d_\gamma^2 \right\} +$$

$$+ (q_\gamma^4 - q_\beta^4) \Big\{ c_\alpha^2 d_\alpha^2 (1 - P_1 \ell^2 s_\alpha^2) s_\beta^2 s_\gamma^2$$

$$+ P_1 \frac{\ell^2}{\ell^{12}} s_\alpha^2 c_\alpha^2 d_\alpha^2 \quad c_\beta^2 c_\gamma^2$$

$$- \frac{P_1}{\ell^{12}} \quad s_\alpha^2 c_\alpha^2 d_\alpha^2 \quad d_\beta^2 d_\gamma^2 \Big\}$$

$$14) \; q_\gamma^4 c_\gamma^2 d_\gamma^2 s_\gamma^2 n_\beta - q_\beta^4 c_\beta^2 d_\beta^2 s_\beta^2 n_\gamma =$$

[replace P_1 by P_2 in 13)]

iv) Reduction of the boundary condition equations.

We now turn to the problem of solving the equations of Appendix 11. These equations must be satisfied identically in β and γ for $\alpha = \alpha_o$. We list below all the terms appearing in these equations, and give their expressions in terms of independent functions of β and γ . Each one of these independent functions gives rise to a separate equation since its coefficient must be equal to the coefficient of the same function on the right-hand side of the boundary condition equation. The circled numbers indicate the number of the equation generated by each particular term.

a) Continuity of $\tau_{\alpha\alpha}$.

There are 12 independent functions of β and γ in (A-11-1) , which are :

$$h_\alpha^2 \, s_\beta \, d_\beta \, s_\gamma \, d_\gamma \qquad (1)$$

$$h_\alpha^2 \, s_\beta \, c_\beta \, s_\gamma \, c_\gamma \qquad (2)$$

$$h_\alpha^2 \, c_\beta \, d_\beta \, c_\gamma \, d_\gamma \qquad (3)$$

$$h_\alpha^2 \, s_\beta^2 \, s_\gamma^2 \qquad (4)$$

$$h_\alpha^2 \, c_\beta^2 \, c_\gamma^2 \qquad (5)$$

$$h_\alpha^2 \, d_\beta^2 \, d_\gamma^2 \qquad (6)$$

$$h_\alpha \frac{\partial h_\alpha}{\partial \alpha} \, s_\beta \, d_\beta \, s_\gamma \, d_\gamma \qquad (7)$$

$$h_\alpha \frac{\partial h_\alpha}{\partial \alpha} \, s_\beta \, c_\beta \, s_\gamma \, c_\gamma \qquad (8)$$

$$h_\alpha \frac{\partial h_\alpha}{\partial \alpha} \, c_\beta \, d_\beta \, c_\gamma \, d_\gamma \qquad (9)$$

$$h_\alpha \frac{\partial h_\alpha}{\partial \alpha} \, s_\beta^2 \, s_\gamma^2 \qquad (10)$$

$$h_\alpha \frac{\partial h_\alpha}{\partial \alpha} \, c_\beta^2 \, c_\gamma^2 \qquad (11)$$

$$h_\alpha \frac{\partial h_\alpha}{\partial \alpha} \quad d_\beta^2 d_\gamma^2 \qquad (12)$$

All the other terms in (A-11-1) can be expressed as linear combinations involving these 12 independent functional forms. We have

$$h_\alpha^2 \ell_\beta \ell_\gamma = h_\alpha^2 \left\{ (1-P_1)(1-k^2 P_1)\, s_\beta^2 s_\gamma^2 \,(4) - \frac{P_1(k^2 P_1 - 1)}{k'^2}\, c_\beta^2 c_\gamma^2 \,(5) + \frac{P_1(P_1-1)}{k'^2}\, d_\beta^2 d_\gamma^2 \right\}$$

$$h_\alpha^2 n_\beta n_\gamma = h_\alpha^2 \{ \text{replace } P_1 \text{ by } P_2 \}$$

$$h_\alpha \frac{\partial h_\alpha}{\partial \alpha} \ell_\beta \ell_\gamma = h_\alpha \frac{\partial h_\alpha}{\partial \alpha} \left\{ (1-P_1)(1-k^2 P_1)\, s_\beta^2 s_\gamma^2 \,(10) - \frac{P_1(k^2 P_1 - 1)}{k'^2}\, c_\beta^2 c_\gamma^2 \,(11) + \frac{P_1(P_1-1)}{k'^2}\, d_\beta^2 d_\gamma^2 \,(12) \right\}$$

$$h_\alpha \frac{\partial h_\alpha}{\partial \alpha} n_\beta n_\gamma = (\text{replace } P_1 \text{ by } P_2)$$

$$h_\alpha \frac{\partial h_\alpha}{\partial \alpha} = h_\alpha \frac{\partial h_\alpha}{\partial \alpha} \left\{ k^2 s_\beta^2 s_\gamma^2 \,(10) - \frac{k^2}{k'^2}\, c_\beta^2 c_\gamma^2 \,(11) + \frac{1}{k'^2}\, d_\beta^2 d_\gamma^2 \,(12) \right\}$$

We shall not indicate the equation numbers any longer.

$$\frac{h_\gamma^2}{h_\alpha}\frac{\partial h_\alpha}{\partial \gamma} s_\beta d_\beta s_\gamma^2 c_\gamma + \frac{h_\beta^2}{h_\alpha}\frac{\partial h_\alpha}{\partial \beta} s_\beta^2 c_\beta s_\gamma d_\gamma =$$

$$h_\alpha^2 (c_\alpha^2 - s_\alpha^2) s_\beta d_\beta s_\gamma d_\gamma + h_\alpha \frac{\partial h_\alpha}{\partial \alpha}\frac{s_\alpha c_\alpha}{d_\alpha} s_\beta d_\beta s_\gamma d_\gamma$$

$$\frac{h_\gamma^2}{h_\alpha}\frac{\partial h_\alpha}{\partial \gamma} s_\beta c_\beta s_\gamma^2 d_\gamma + \frac{h_\beta^2}{h_\alpha}\frac{\partial h_\alpha}{\partial \beta} s_\beta^2 d_\beta s_\gamma c_\gamma =$$

$$h_\alpha^2 (d_\alpha^2 - k^2 s_\alpha^2) s_\beta c_\beta s_\gamma c_\gamma + h_\alpha \frac{\partial h_\alpha}{\partial \alpha}\frac{s_\alpha d_\alpha}{c_\alpha} s_\beta c_\beta s_\gamma c_\gamma$$

$$\frac{h_\gamma^2}{h_\alpha}\frac{\partial h_\alpha}{\partial \gamma} c_\beta d_\beta s_\gamma c_\gamma^2 + \frac{h_\beta^2}{h_\alpha}\frac{\partial h_\alpha}{\partial \beta} s_\beta^2 c_\beta^2 c_\gamma d_\gamma =$$

$$h_\alpha^2 (c_\alpha^2 - s_\alpha^2) c_\beta d_\beta c_\gamma d_\gamma + h_\alpha \frac{\partial h_\alpha}{\partial \alpha}\frac{s_\alpha c_\alpha}{d_\alpha} c_\beta d_\beta c_\gamma d_\gamma$$

$$\frac{h_\gamma^2}{h_\alpha}\frac{\partial h_\alpha}{\partial \gamma} s_\beta^2 s_\gamma c_\gamma d_\gamma + \frac{h_\beta^2}{h_\alpha}\frac{\partial h_\alpha}{\partial \beta} s_\beta c_\beta d_\beta s_\gamma^2 =$$

$$h_\alpha^2 (d_\alpha^2 + k^2 c_\alpha^2) s_\beta^2 s_\gamma^2 + h_\alpha \frac{\partial h_\alpha}{\partial \alpha}\frac{c_\alpha d_\alpha}{s_\alpha} s_\beta^2 s_\gamma^2$$

$$\frac{h_\gamma^2}{h_\alpha}\frac{\partial h_\alpha}{\partial \gamma} c_\beta^2 s_\gamma c_\gamma d_\gamma + \frac{h_\beta^2}{h_\alpha}\frac{\partial h_\alpha}{\partial \beta} s_\beta c_\beta d_\beta c_\gamma^2 =$$

$$h_\alpha^2 (d_\alpha^2 - k^2 s_\alpha^2) c_\beta^2 c_\gamma^2 + h_\alpha \frac{\partial h_\alpha}{\partial \alpha}\frac{s_\alpha d_\alpha}{c_\alpha} c_\beta^2 c_\gamma^2$$

$$\frac{h_\gamma^2}{h_\alpha}\frac{\partial h_\alpha}{\partial \gamma} d_\beta^2 s_\gamma c_\gamma d_\gamma + \frac{h_\beta^2}{h_\alpha}\frac{\partial h_\alpha}{\partial \beta} s_\beta c_\beta d_\beta d_\gamma^2 =$$

$$h_\alpha^2 (c_\alpha^2 - s_\alpha^2) d_\beta^2 d_\gamma^2 + h_\alpha \frac{\partial h_\alpha}{\partial \alpha}\frac{s_\alpha c_\alpha}{d_\alpha} d_\beta^2 d_\gamma^2$$

$$\frac{h_\gamma^2}{h_\alpha}\frac{\partial h_\alpha}{\partial \gamma} \ell_\beta s_\gamma c_\gamma d_\gamma + \frac{h_\beta^2}{h_\alpha}\frac{\partial h_\alpha}{\partial \alpha} s_\beta c_\beta d_\beta \ell_\gamma =$$

$$- h_\alpha^2 \Big\{ (d_\alpha^2 + k^2 c_\alpha^2)(1 - P_1 k^2 s_\alpha^2) s_\beta^2 s_\gamma^2$$

$$- P_1 \frac{k^2}{k'^2} c_\alpha^2 (d_\alpha^2 - k^2 s_\alpha^2) c_\beta^2 c_\gamma^2$$

$$+ P_1 \frac{1}{k'^2} d_\alpha^2 (c_\alpha^2 - s_\alpha^2) d_\beta^2 d_\gamma^2 \Big\}$$

$$+ h_\alpha \frac{\partial h_\alpha}{\partial \alpha} \Big\{ \frac{c_\alpha d_\alpha}{s_\alpha} (1 - P_1 k^2 s_\alpha^2) s_\beta^2 s_\gamma^2$$

$$+ P_1 \frac{k^2}{k'^2} s_\alpha c_\alpha d_\alpha c_\beta^2 c_\gamma^2$$

$$- P_1 \frac{1}{k'^2} s_\alpha c_\alpha d_\alpha d_\beta^2 d_\gamma^2 \Big\}$$

For n_β and n_γ change P_1 to P_2.

$$\frac{h_\gamma^2}{h_\alpha}\frac{\partial h_\alpha}{\partial \gamma} s_\beta d_\beta c_\gamma d_\gamma^2 + \frac{h_\beta^2}{h_\alpha}\frac{\partial h_\alpha}{\partial \beta} c_\beta d_\beta^2 s_\gamma d_\gamma =$$

$$- h_\alpha^2 (d_\alpha^2 + k^2 c_\alpha^2) s_\beta d_\beta s_\gamma d_\gamma + h_\alpha \frac{\partial h_\alpha}{\partial \alpha}\frac{c_\alpha d_\alpha}{s_\alpha} s_\beta d_\beta s_\gamma d_\gamma$$

$$\frac{h_\gamma^2}{h_\alpha}\frac{\partial h_\alpha}{\partial \gamma} s_\beta c_\beta c_\gamma^2 d_\gamma + \frac{h_\beta^2}{h_\alpha}\frac{\partial h_\alpha}{\partial \beta} c_\beta^2 d_\beta s_\gamma c_\gamma =$$

$$- h_\alpha^2 \left(d_\alpha^2 + k^2 c_\alpha^2 \right) s_\beta c_\beta s_\gamma c_\gamma + h_\alpha \frac{\partial h_\alpha}{\partial \alpha} \frac{c_\alpha d_\alpha}{s_\alpha} s_\beta c_\beta s_\gamma c_\gamma$$

$$\frac{h_\gamma^2}{h_\alpha}\frac{\partial h_\alpha}{\partial \gamma} c_\beta d_\beta s_\gamma d_\gamma^2 + \frac{h_\beta^2}{h_\alpha}\frac{\partial h_\alpha}{\partial \beta} s_\beta d_\beta^2 c_\gamma d_\gamma =$$

$$h_\alpha^2 \left(d_\alpha^2 - k^2 s_\alpha^2 \right) c_\beta d_\beta c_\gamma d_\gamma + h_\alpha \frac{\partial h_\alpha}{\partial \alpha} \frac{s_\alpha d_\alpha}{c_\alpha} c_\beta d_\beta c_\gamma d_\gamma$$

$$h_\gamma^2 s_\beta d_\beta s_\gamma c_\gamma^2 d_\gamma + h_\beta^2 s_\beta c_\beta^2 d_\beta s_\gamma d_\gamma = - h_\alpha^2 c_\alpha^2 s_\beta d_\beta s_\gamma d_\gamma$$

$$h_\gamma^2 s_\beta c_\beta s_\gamma c_\gamma d_\gamma^2 + h_\beta^2 s_\beta c_\beta d_\beta^2 s_\gamma c_\gamma = - h_\alpha^2 d_\alpha^2 s_\beta c_\beta s_\gamma c_\gamma$$

$$h_\gamma^2 c_\beta d_\beta s_\gamma^2 c_\gamma d_\gamma + h_\beta^2 s_\beta^2 c_\beta d_\beta c_\gamma d_\gamma = - h_\alpha^2 s_\alpha^2 c_\beta d_\beta c_\gamma d_\gamma$$

$$h_\gamma^2 s_\beta^2 c_\gamma^2 d_\gamma^2 + h_\beta^2 c_\beta^2 d_\beta^2 s_\gamma^2 = h_\alpha^2 \left(\frac{d_\alpha^2}{k'^2} c_\beta^2 c_\gamma^2 - \frac{c_\alpha^2}{k'^2} d_\beta^2 d_\gamma^2 \right)$$

$$h_\gamma^2 c_\beta^2 s_\gamma^2 d_\gamma^2 + h_\beta^2 s_\beta^2 d_\beta^2 c_\gamma^2 = h_\alpha^2 \left(k'^2 d_\alpha^2 s_\beta^2 s_\gamma^2 - s_\alpha^2 d_\beta^2 d_\gamma^2 \right)$$

$$h_\gamma^2 d_\beta^2 s_\gamma^2 c_\gamma^2 + h_\beta^2 s_\beta^2 c_\beta^2 d_\gamma^2 = h_\alpha^2 \left(- k'^2 c_\alpha^2 s_\beta^2 s_\gamma^2 - s_\alpha^2 c_\beta^2 c_\gamma^2 \right)$$

Since the same functions of β and γ appear on the right-hand side of (A-11-1), this equation is thus equivalent to a system of 12 equations in which β and γ do not appear any more, and where $\alpha = \alpha_o$.

b) Continuity of $\tau_{\alpha\beta}$ and $\tau_{\alpha\gamma}$.

There are 11 independent functions of β and γ which appear in (A-11-2), and they are

$$s_\beta^2 c_\beta s_\gamma d_\gamma \qquad (13)$$

$$c_\beta d_\beta^2 s_\gamma d_\gamma \qquad (14)$$

$$s_\beta^2 d_\beta s_\gamma c_\gamma \qquad (15)$$

$$c_\beta^2 d_\beta s_\gamma c_\gamma \qquad (16)$$

$$s_\gamma c_\gamma d_\gamma \qquad (17)$$

$$s_\beta^3 c_\gamma d_\gamma \qquad (18)$$

$$s_\beta c_\beta d_\beta s_\gamma^2 \qquad (19)$$

$$s_\beta c_\beta d_\beta \qquad (20)$$

$$s_\beta^4 c_\beta s_\gamma d_\gamma \qquad (21)$$

$$s_\beta^4 d_\beta s_\gamma c_\gamma \qquad (22)$$

$$s_\beta^5 \; c_\gamma \, d_\gamma \qquad (23)$$

$$s_\beta^3 \, c_\beta \, d_\beta \, s_\gamma^2 \qquad (24)$$

$$s_\beta^3 \; c_\beta \, d_\beta \qquad (25)$$

The decomposition of any term figuring in (A-11-2) in terms of these 11 functions is elementary in that case and can be omitted. Recall that the equation expressing the continuity of $\tau_{\alpha\gamma}$ is simply obtained from (A-11-2) by interchanging β and γ . The independent functions of β and γ figuring in that equation are thus obtained by interchanging β and γ in the above expressions. However, since the α dependence of the equations is the same in both cases, and since β and γ are not present in the final system, one can verify that the systems for $\tau_{\alpha\beta}$ and $\tau_{\alpha\gamma}$ are identical, and therefore redundant.

c) Continuity of u_α .

There are 6 independent functions of β and γ in (A-11-4), which are given below.

$$s_\beta \, d_\beta \, s_\gamma \, d_\gamma \qquad (26)$$

$$s_\beta \, c_\beta \, s_\gamma \, c_\gamma \qquad (27)$$

$$c_\beta \, d_\beta \, c_\gamma \, d_\gamma \qquad (28)$$

$s_\beta^2 s_\gamma^2$ (29)

$c_\beta^2 c_\gamma^2$ (30)

1 (31)

$d_\beta^2 d_\gamma^2$ is expressed in terms of 29-30-31

Since no other term appears in (A-11-4), no further discussion is necessary.

d) Continuity of u_β and u_γ .

These two components of displacement yield identical systems, just as the corresponding tractions do. There are 8 independent functions of β and γ in (A-11-5), which are found to be

$s_\beta^2 c_\beta \; s_\gamma d_\gamma$ (32)

$c_\beta d_\beta^2 \; s_\gamma d_\gamma$ (33)

$s_\beta^2 d_\beta \; s_\gamma c_\gamma$ (34)

$c_\beta^2 d_\beta \; s_\gamma c_\gamma$ (35)

$s_\beta c_\beta^2 \; c_\gamma d_\gamma$ (36)

$$s_\beta d_\beta c_\gamma d_\gamma \qquad (37)$$

$$s_\beta c_\beta d_\beta s_\gamma^2 \qquad (38)$$

$$s_\beta c_\beta d_\beta \qquad (39)$$

In that case again, no further discussion is required.

v) Reduction of the system (1) through (39)

We are now in the presence of a system of 39 linear equations in the 29 unknowns $A_1,\ldots,A_{15},B_2,\ldots,B_{15}$. (B_1 does not appear in the equations of Appendix 11.) We shall now describe the algorithm which leads to a reduction of this system.

First of all, the system of equations naturally separates itself into four systems which are

System A: Equations 1,7,13,14,21,26,32,33 .

Unknowns $A_2,A_9,A_{12},B_2,B_9,B_{12}$.

Data $\tau_{xz}^{(o)}$

System B: Equations 2,9,15,16,22,27,34,35 .

Unknowns $A_4,A_6,A_{15},B_4,B_6,B_{15}$.

Data $\tau_{xy}^{(o)}$

System C: Equations 3,10,17,18,23,28,36,37 .

Unknowns $A_5, A_{10}, A_{14}, B_5, B_{10}, B_{14}$.

Data $\tau_{yz}^{(o)}$

System D: Equations 4,5,6,8,11,12,19,20,24,25,29,30,31,38,39 .

Unknowns $A_1, A_3, A_7, A_8, A_{11}, A_{13}, B_3, B_7, B_8, B_{11}, B_{13}$.

Data $\tau_{xx}^{(o)}$, $\tau_{yy}^{(o)}$, $\tau_{zz}^{(o)}$.

For example, the first subsystem--System A--is reduced by the following operations:

a) By addition and subtraction of (32) and (33), we get (32-1) and (33-1) which are simpler

b) (26) may be simplified by substituting (7) into it. This yields (26-1)

c) Subtract (14) from (13) to get (13-1)

d) Subtract (1) from (14) to get (14-1)

e) Subtract (14) from (21) to get (21-1)

At this point it should be easy to see that

f) (7) and (14-1) can be combined to yield (13-1)

g) (7) and (21-1) can be combined to yield (13-1)

h) (33-1) and (26-1) can be combined to yield (32-1)

Three of the eight equations are thus redundant. We are left with five equations for six unknowns. However, with a little effort it can be seen that the elementary internal displacement solution with coefficient B_{12} can be expressed as a linear combination of those with coefficients

B_2 and B_9 . We can thus choose $B_{12} = 0$. The 5×5 system obtained in this fashion can then be rewritten in a more elegant fashion and is given in Chapter VI. Systems B and C are reduced in exactly the same fashion. The algebra is more difficult for System D, but proceeds from the same principles.

The final results are given in Chapter VI; they are in the form of three 5×5 systems and one 9×9 system.

APPENDIX 13

CALCULATION OF WRONSKIANS OF LAMÉ FUNCTIONS

Let $\lambda(z)$ be a Lamé function of the first kind. Then as pointed out in Chapter VI, one can associate to $\lambda(z)$ a Lamé function of the second kind by the integral relation

$$\Lambda(z) = C\,\lambda(z) \int_{ik'}^{z} \frac{du}{\lambda^2(z)} \tag{A-13-1}$$

The normalization factor C may be chosen so that $\Lambda(z) = \lambda(z)$ for a particular value $z = \alpha$. Then we have

$$C = \left[\int_{ik'}^{\alpha} \frac{du}{\lambda^2(z)} \right]^{-1} \tag{A-13-2}$$

and also

$$C = W_{\lambda}(\alpha) = \Lambda'(\alpha)\,\lambda(\alpha) - \Lambda(\alpha)\,\lambda'(\alpha) \tag{A-13-3}$$

The wronskians appearing in equations (VI-1-32) through (VI-1-35) can be computed by (A-13-2), in which we set $\alpha = \alpha_o$.

We denote the incomplete elliptic integral of the second kind by

$$E(z) = \int_{o}^{z} dn^2\, u\, du \tag{A-13-4}$$

We define

$$a_o = \alpha_o - ik' = \mathrm{Re}(\alpha_o)$$

Here α is the first of the ellipsoidal coordinates defined in section VI-1.

The calculation of the wronskians does not present any major difficulty. We shall use integrals given by Gradshteyn and Ryshik (1965, p. 630), and by Whittaker and Watson (1927, p. 516). Then, adopting the notation of section VI-1,

$$\frac{1}{W_\alpha} = a_o \tag{A-13-5}$$

$$\frac{1}{W_s} = a_o - E(a_o) \tag{A-13-6}$$

$$\frac{1}{W_c} = a_o - \frac{1}{k'^2} E(a_o) + \frac{dn\ \alpha_o}{k'^2\ sn\ \alpha_o\ cn\ \alpha_o} \tag{A-13-7}$$

$$\frac{1}{W_d} = \frac{1}{k'^2} E(a_o) - \frac{cn\ \alpha_o}{k'^2\ sn\ \alpha_o\ dn\ \alpha_o} \tag{A-13-8}$$

$$\frac{1}{W_m} = \frac{k^2}{W_d} + \frac{1}{W_s} \tag{A-13-9}$$

$$\frac{1}{W_o} = \frac{1}{k'^2\ W_c} - \frac{k^2}{k'^2\ W_d} \tag{A-13-10}$$

$$\frac{1}{W_p} = \frac{1}{W_s} + \frac{1}{W_c} \tag{A-13-11}$$

$$\frac{1}{W_\ell} = \frac{-1}{2\ \mathrm{sn}\ \alpha_o\ \mathrm{cn}\ \alpha_o\ \mathrm{dn}\ \alpha_o \left(\mathrm{sn}^2\ \alpha_o - P_1\right)}$$

$$- \frac{(3P_1-1)\ k^2-k'^2}{2P_1\ k'^2}\ \frac{1}{W_c} + \frac{1}{2P_1}\ \frac{1}{W_s} + \frac{k^4(3P_1-1)}{2P_1\ k'^2}\ \frac{1}{W_d} \tag{A-13-12}$$

where $$P_1 = \frac{1}{1+k^2 - \sqrt{1-k^2k'^2}}$$

W_n can be obtained by changing P_1 in (A-13-12) to

$$P_2 = \frac{1}{1+k^2 + \sqrt{1-k^2k'^2}}$$

Equations (A-13-5) through (A-13-8) yield results which are identical with those of Sadowsky and Sternberg (1949). However, (A-13-12) cannot be reconciled with the Lamé function of the second kind given by these authors. Although (A-13-12) may be rewritten in a form similar to that given by Sadowsky and Sternberg, we have been unable to achieve complete agreement, in spite of repeated efforts to do so.